

Wednesday

Program subject to change until 12/16/2019.



105TH Scientific Assembly and Annual Meeting December 1-6 | McCormick Place, Chicago







SPDL40

Body Imaging Case Challenge (Case-based Competition)

Wednesday, Dec. 4 7:15AM - 8:15AM Room: E451B



AMA PRA Category 1 Credit ™: 1.00 ARRT Category A+ Credit: 0

Participants

Sayf A. Al-Katib, MD, Royal Oak, MI (*Presenter*) Nothing to Disclose Monisha Shetty, MD, Royal Oak, MI (*Presenter*) Nothing to Disclose

For information about this presentation, contact:

monisha.shetty @beaumont.edu

Sayf.Al-Katib@beaumont.edu

Special Information

This interactive session will use RSNA Diagnosis Live™. Please bring your charged mobile wireless device (phone, tablet or laptop) to participate.

LEARNING OBJECTIVES

1) Engage in a friendly, fast-paced, interactive body imaging unknown case competition. 2) Review presentation and imaging pearls of uncommon diagnoses of the chest, abdomen and pelvis. 3) Monitor individual and team performance in real-time by answering a spectrum of questions types using the RSNA Diagnosis Live platform. 4) Analyze personal results of the competition by way of a self-assessment report sent via email.





SPSC40

Controversy Session: Incidental Pancreatic Cyst Management

Wednesday, Dec. <u>4</u> 7:15AM - 8:15AM Room: E350

GI

AMA PRA Category 1 Credit ™: 1.00 ARRT Category A+ Credit: 1.00

Participants

Desiree E. Morgan, MD, Birmingham, AL (*Moderator*) Institutional Research Grant, General Electric Company; Consultant, General Electric Company

William W. Mayo-Smith, MD, Boston, MA (Moderator) Nothing to Disclose

For information about this presentation, contact:

dmorgan@uabmc.edu

LEARNING OBJECTIVES

1) Understand the variability among expert published recommendations for follow up of incidentally discovered pancreatic cysts. 2) Develop basic knowledge of potential cyst malignant transformation. 3) Summarize the ACR incidental pancreatic cyst management algorithm and apply recommendations for cyst follow up relevant to clinical practice.

Sub-Events

SPSC40A Incidental Pancreatic Cyst Risks: The Facts

Participants

Koenraad J. Mortele, MD, Boston, MA (Presenter) Nothing to Disclose

SPSC40B Pancreatic Cyst Management Algorithms: The Mess

Participants

Atif Zaheer, MD, Baltimore, MD (Presenter) Nothing to Disclose

LEARNING OBJECTIVES

1) Understand the natural history of Intraductal papillary mucinous neoplasms (IPMNs). 2) Understand the importance of surveillance and intervention of the cystic lesions of the pancreas due to their malignant potential. 3) Discuss different management algorithms and how they relate to the natural history of the disease.

ABSTRACT

Cystic lesions of the pancreas are a common finding on routine imaging and due to the pre-cancerous nature of some of these lesions, there is a dire need of standard guidelines for surveillance. There are multiple surveillance algorithms suggested by different groups such as the American College of Gastroenterology, Fukuoka guidelines etc. that vary with their level of aggressiveness for intervention. The goal is to discuss management algorithms as they relate to the natural history of the pre-cancerous cystic lesions (IPMNs) of the pancreas.

SPSC40C ACR Pancreatic Cyst Guidelines: The Summary

Participants

Desiree E. Morgan, MD, Birmingham, AL (*Presenter*) Institutional Research Grant, General Electric Company; Consultant, General Electric Company

LEARNING OBJECTIVES

1) Understand the patterns of recommendations, based on level of potential risk for biologically significance, in the ACR white paper on incidental pancreatic cysts. 2) Know which imaging features described in the ACR recommendations are associated with increased risk for malignancy during surveillance for incidentally detected pancreatic cysts.

SPSC40D Should ACR Guidelines Be Followed-YES

Participants Elizabeth M. Hecht, MD, New York, NY (*Presenter*) Nothing to Disclose

For information about this presentation, contact:

ehecht@columbia.edu

LEARNING OBJECTIVES

1) Debate the pros and cons of applying the ACR guidelines in clinical practice.

ABSTRACT

While the risk of malignancy is low for small incidentally discovered asymptomatic pancreatic cysts, no one wants to miss a cancer.

Yet, surveillance can be costly for patients and the healthcare system. The ACR management guidelines published in 2017 provided algorithms intended to help the radiologist and care providers but there are competing guidelines.

SPSC40E Should ACR Guidelines Be Followed-NO

Participants

David M. Hough, MD, Rochester, MN (Presenter) Nothing to Disclose

LEARNING OBJECTIVES

Debate the pros and cons of applying ACR guidelines in clinical practice

ABSTRACT

It is beneficial to have practice guidelines to improve quality and uniformity in management of incidental pancreatic cysts. However there are competing guidelines, and compelling reasons why the ACR recommendations may not be appropriate to your practice.

SPSC40F Q&A





SPSH40

Hot Topic Session: Mass Casualty Incidents-When Disaster Strikes

Wednesday, Dec. 4 7:15AM - 8:15AM Room: E451A

ER

AMA PRA Category 1 Credit ™: 1.00 ARRT Category A+ Credit: 1.00

Participants

Ferco H. Berger, MD, Toronto, ON (Moderator) Speaker, Siemens AG

For information about this presentation, contact:

fhberger@gmail.com

Sub-Events

SPSH40A The Situation Room: A Survival Guide for MCI

Participants Ronald M. Bilow, MD, Houston, TX (*Presenter*) Nothing to Disclose

For information about this presentation, contact:

ronald.m.bilow@uth.tmc.edu

LEARNING OBJECTIVES

1) Understand the difference between standard imaging department operations and during a disaster situation. 2) Obtain a basic understanding of disaster response planning considerations specific to radiology services.

ABSTRACT

In the face of disaster, imaging services remains an important component of emergent patient care. It is sometimes, erroneously, assumed that radiology departments, particular level one trauma centers, will handle the patient surge by simply performing their normal work at decreased throughput time. This is not only impossible, but many of the 'normal' steps in registering patients, entering examination requests and myriad other steps in the chain of events leading from patient needs to final results will be altered. Additionally, the traditional key players in providing services under disaster conditions make many false assumptions regarding how radiology departments can or are able to operate. This presentation will highlight some of the concepts one must consider in developing a viable disaster preparedness and response plan, as well as how to gain acceptance by other institutional services at the planning level.

SPSH40B Beyond Broken Bones: Non-trauma MCI and the Impact on Medical Imaging

Participants

Jamlik-Omari Johnson, MD, Atlanta, GA (Presenter) Nothing to Disclose

SPSH40C Global Disaster Response and Serving Regions with Scarce Resources

Participants Berndt P. Schmit, MD, Tucson, AZ (*Presenter*) Nothing to Disclose

For information about this presentation, contact:

bschmit@radiology.arizona.edu

LEARNING OBJECTIVES

1) Infrastructure and logistical challenges to implementing advanced radiology in the austere setting. 2) Cultural and political issues with providing services in another country. 3) Importance of local ownership and stakeholders for success.

ABSTRACT

There are a myriad of unique challenges to building radiology capacity in an austere setting whether created by poverty or disaster. Experiences with build sustainable radiology in the developing world will be shared including: finding and developing local partnerships, assessing and designing clinical programs, building vendor relationships, donor relationship and equipment issues, value stream and service line thinking, maintenance and engineering support, training and teaching local resources.







MSRT41

ASRT@RSNA 2019: Myth? Legend? Super Tech? The Radiologist Assistant Explained (Interactive Session)

Wednesday, Dec. 4 8:00AM - 9:00AM Room: N230B

ОТ

AMA PRA Category 1 Credit ™: 1.00 ARRT Category A+ Credit: 1.00

Participants

Wesley Shay, Trumbull, CT (Presenter) Nothing to Disclose

LEARNING OBJECTIVES

1) Define the role of the Radiologist Assistant. 2) Identify areas of growth for the Radiologist Assistant. 3) Compare the Radiologist Assistant to other providers. 4) Recommend the Radiologist Assistant be utilized in their department.

ABSTRACT

As radiologic technologists with advanced training in radiological procedures, image assessment, patient management and assessment, Radiologist Assistants (RAs) are physician extenders specifically designed for the medical imaging environment. RAs practice under the supervision of the radiologist: to perform non-invasive and invasive medical imaging procedures; evaluate, manage, and educate patients; communicate radiologist findings with other members of the healthcare team; and act as patient navigators for the imaging department. Due to RAs' specialized education and training, they maximize efficiency and workflow, provide quality patient care, and maintain high standards of radiation safety.







PI-RADS Hands-on Workshop (Interactive Session)

Wednesday, Dec. 4 8:00AM - 10:00AM Room: E450A



AMA PRA Category 1 Credits ™: 2.00 ARRT Category A+ Credits: 2.25

Participants

Jelle O. Barentsz, MD, PhD, Nijmegen, Netherlands (*Moderator*) Nothing to Disclose Jelle O. Barentsz, MD, PhD, Nijmegen, Netherlands (*Coordinator*) Nothing to Disclose Baris Turkbey, MD, Bethesda, MD (*Presenter*) Research support, Koninklijke Philips NV; Royalties, Invivo Corporation; Investigator, NVIDIA Corporation Roel D. Mus, MD, Nijmegen, Netherlands (*Presenter*) Nothing to Disclose Antonio C. Westphalen, MD, Medina, WA (*Presenter*) Nothing to Disclose Daniel J. Margolis, MD, New York, NY (*Presenter*) Nothing to Disclose Daniel J. Margolis, MD, PhD, Gent, Belgium (*Presenter*) Nothing to Disclose Joseph J. Busch, MD, Chattanooga, TN (*Presenter*) Nothing to Disclose Prasad R. Shankar, MD, Ann Arbor, MI (*Presenter*) Nothing to Disclose Leonardo K. Bittencourt, MD, PhD, Rio de Janeiro, Brazil (*Presenter*) Nothing to Disclose Silvia D. Chang, MD, Vancouver, BC (*Presenter*) Nothing to Disclose William J. Weadock, MD, Ann Arbor, MI (*Presenter*) Nothing to Disclose

For information about this presentation, contact:

Vibeke.Loegager@regionh.dk

Roel.Mus@radboudumc.nl

djm9016@med.cornell.edu

turkbeyi@mail.nih.gov

LKAYAT@gmail.com

pshankar@med.umich.edu

jelle.barentsz@radboudumc.nl

Special Information

Participants will review cases on their own devices and answer questions. The cases will then be reviewed by the presenters. Note: this activity is best done on a laptop or tablet. Although phones will work, their small size limits optimal image view.

LEARNING OBJECTIVES

1) Understand and how to use the PI-RADS v2.1 Category Assessment to detect and localize significant prostate cancer for both peripheral and transitional zone. 2) Recognize benign pathology like prostatitis and BPH and to differentiate these from significant prostate cancers.

ABSTRACT

You need to bring your own laptops or tablets, as in this 'Hands-on Workshop' you will review multi-parametric MRI cases with various prostatic pathology using your own laptop or tablet. Though a Cloud-connection (RadPix) your device will serve as a dedicated prostate-MRI workstation through which you can analyse 20 cases. This activity is best done on a laptop or tablet. Although phones and small tablets will work, their small size limits optimal image viewing. Focus will be on the overall assessment of PI-RADS v2.1 category. You will be interactively teached how to score the probability of the presence of a significant prostate in patients with elevated PSA or other suspicion to have prostate cancer. All 20 cases are from daily practice, and have various levels of difficulty. They include easy and difficult significant cancers, inflammation, BPH, and most common pitfalls. Internationally renowned teachers will guide you during your PI-RADS v2.1 scoring process. You will be able to ask them all question you have on prostate mp-MRI, from acquisition to diagnosis to MR-biopsy. Prior to this course you need to download a digital course book at http://bit.ly/prostate2019. This digital pdf-course book includes all the cases and will guide you during the course through the various cases.

Active Handout:Roel Dirk Mus

http://abstract.rsna.org/uploads/2019/16002001/Active RC507.pdf





MSCP41

Case-based Review of Pediatric Radiology (Interactive Session)

Wednesday, Dec. 4 8:30AM - 10:00AM Room: E450B



AMA PRA Category 1 Credits ™: 1.50 ARRT Category A+ Credit: 1.75

Participants

Edward Y. Lee, MD, Boston, MA (Director) Nothing to Disclose

LEARNING OBJECTIVES

1) Review clinical presentations of congenital and acquired pediatric disorders. 2) Discuss optimal imaging techniques for assessing various pediatric disorders. 3) Learn characteristic imaging findings of congenital and acquired pediatric disorders.

Sub-Events

MSCP41A Pediatric Brain Disorders

Participants Noor A. Al Khori, MD, Doha, Qatar (*Presenter*) Nothing to Disclose

For information about this presentation, contact:

nalkhori@sidra.org

LEARNING OBJECTIVES

1) Review imaging features of a few disorders. 2) Review relevant clinical features, pathophys, and associations. 3) Review the role of various imaging modalities in diagnosis and management.

MSCP41B Pediatric Vascular Disorders

Participants

Jared R. Green, MD, Chicago, IL (Presenter) Nothing to Disclose

ABSTRACT

During this interactive session, vascular anomalies cases will be presented allowing the learners to recognize the imaging findings and to understand the importance of performing US and MR for diagnosis. Key points will be discussed to avoid misdiagnosis.

MSCP41C Pediatric Abdominal Disorders

Participants

Grace S. Phillips, MD, Seattle, WA (Presenter) Nothing to Disclose

LEARNING OBJECTIVES

1) To describe the imaging appearance of various pediatric abdominal tumors and tumor-like conditions. 2) To discuss an appropriate imaging algorithm for pediatric abdominal masses. 3) To highlight specific imaging and patient characteristics that help to narrow the differential diagnosis.

ABSTRACT

During this interactive session, pediatric abdominal disorder cases will be presented allowing the learners to recognize and describe the imaging features of various diagnostic entities. Key points will be discussed to avoid misdiagnosis.

MSCP41D Pediatric Pelvic Disorders

Participants

Domen Plut, MD, Ljubljana, Slovenia (Presenter) Nothing to Disclose

ABSTRACT

During this case-driven, interactive session, pediatric pelvic disorders will be presented allowing the participants to recognize and describe the imaging features of various diagnostic entities.







MSES41

Essentials of GI Imaging

Wednesday, Dec. 4 8:30AM - 10:00AM Room: S100AB

GI

AMA PRA Category 1 Credits ™: 1.50 ARRT Category A+ Credit: 1.75

Sub-Events

MSES41A Acute Left Lower Quadrant Pain

Participants Jennifer W. Uyeda, MD, Boston, MA (*Presenter*) Consultant, Allena Pharmaceuticals, Inc

MSES41B Biliary Interventions

Participants Paula Novelli, MD, Pittsburgh, PA (*Presenter*) Nothing to Disclose

For information about this presentation, contact:

novellipm2@upmc.edu

LEARNING OBJECTIVES

1) Describe imaging workup and diagnostic strategies for evaluating bile duct pathology including benign and malignant strictures, iatrogenic bile duct injury, biliary complications of liver transplant, stone disease. 2) Apply the essentials of periprocedural care including sedation and analgesia. 3) Understand techniques for accessing the biliary tree and strategies for percutaneous management of bile duct pathology. 4) Know how to manage complications of percutaneous biliary intervention.

MSES41C Congenital Abnormalities of Biliary Tree

Participants Giuseppe Brancatelli, MD, Palermo, Italy (*Presenter*) Speaker, Bayer AG; Travel support, Bracco Group

For information about this presentation, contact:

gbranca@yahoo.com

LEARNING OBJECTIVES

1) To review the etiology of congenital abnormalities of the biliary tree. 2) To describe the characteristic radiological features with pathologic correlation. 3) To discuss the advantages and limitations of current imaging techniques for the differential diagnosis of these conditions.

MSES41D Imaging Diagnosis and Staging of Cholangiocarcinoma

Participants

Celso Matos, MD, Lisbon, Portugal (Presenter) Nothing to Disclose

For information about this presentation, contact:

celso.matos@fundacaochampalimaud.pt

LEARNING OBJECTIVES

1) Describe imaging workup and diagnostic strategies for evaluating cholangiocarcinoma. 2) Recognize imaging patterns of massforming, periductal-infiltrating and intraductal-growing cholangiocarcinoma. 3) Discuss differential diagnosis.

ABSTRACT

Cholangiocarcinoma is a primary malignant tumor originating from the bile duct epithelium with a broad spectrum of imaging patterns and clinical manifestations.CT and MRI are the most commonly used imaging modalities. They are used alone or in combination with endoscopy techniques to detect, characterize, stage, and assess resectability. In this lecture an overview of the different imaging patterns allowing to achieve those aims will be presented and discussed.







MSRO41

BOOST: Pediatric-Case-based Multidisciplinary Review (Interactive Session)

Wednesday, Dec. 4 8:30AM - 10:00AM Room: S103CD



AMA PRA Category 1 Credits ™: 1.50 ARRT Category A+ Credit: 1.75

Participants

Michael S. Gee, MD, PhD, Boston, MA (*Presenter*) Nothing to Disclose Shannon A. MacDonald, MD, Boston, MA (*Presenter*) Nothing to Disclose Camilo Jaimes Cobos, MD, Boston, MA (*Presenter*) Nothing to Disclose Dave Ebb, MD, Boston, MA (*Presenter*) Nothing to Disclose

LEARNING OBJECTIVES

1) Explain imaging anatomy relevant to pediatric cancer staging and treatment. 2) Develop a search pattern for relevant oncologic anatomy on CT and MRI for pediatric patients with cancer.

ABSTRACT

None.





MSSR41

RSNA/ESR Sports Imaging Symposium: Upper Extremity Sports Injuries (Interactive Session)

Wednesday, Dec. 4 8:30AM - 10:00AM Room: E350



AMA PRA Category 1 Credits ™: 1.50 ARRT Category A+ Credit: 1.75

FDA Discussions may include off-label uses.

Participants

Andrew J. Grainger, MD, Leeds, United Kingdom (*Moderator*) Consultant, Levicept Ltd; Director, The LivingCare Group; Laura W. Bancroft, MD, Venice, FL (*Moderator*) Nothing to Disclose

For information about this presentation, contact:

laurabancroftmd@gmail.com

LEARNING OBJECTIVES

1) To appreciate common patterns of athletic injury in the shoulder and wrist. 2) To become familiar with the techniques available and imaging appearances of shoulder and wrist athletic injury. 3) To consolidate the knowledge gained from the session with interactive cases of upper limb athletic injury.

Sub-Events

MSSR41A Shoulder Injuries in the Throwing Athlete

Participants

Lynne S. Steinbach, MD, San Francisco, CA (Presenter) Nothing to Disclose

LEARNING OBJECTIVES

1) To understand the biomechanics of throwing forces as they relate to the shoulder. 2) To become familiar with rotator cuff, labroligamentous, and osseous abnormalities caused by overhead sports.

ABSTRACT

Overhead throwing athletes develop significant abnormalities as a result of acquired adaptations to the extremes of motion in the dominant shoulder. These abnormalities may eventually result in an inability to throw with the same velocity, the so-called "dead arm" syndrome. These abnormalities involve tendons, ligaments, labrum, muscles, nerves, vessels, and bones. This presentation will review the biomechanics of throwing forces as they relate to the shoulder. The MR imaging characteristics of the resultant abnormalities in the labroligamentous structures and the rotator cuff will also be highlighted. As a prototype, the throwing motion in baseball occurs over a period of approximately 2 seconds and is divided into six stages: wind up, cocking, early and late acceleration, deceleration, and follow through. The late cocking, acceleration, and deceleration phases produce the greatest stress on the glenohumeral joint structures. As with other throwing sports, the superior labrum and rotator cuff are often affected by these extreme forces.

MSSR41B Soft Tissue Wrist Injury in the Athlete

Participants

Christian W. Pfirrmann, MD, MBA, Forch, Switzerland (Presenter) Nothing to Disclose

LEARNING OBJECTIVES

1) To learn about the patterns of injury seen at the wrist in athletes. 2) To understand the advantages and disadvantages of different modalities for imaging the athlete's wrist. 3) To recognize the imaging appearances of cartilage and ligamentous injury at the wrist.

ABSTRACT

Wrist injuries account for 5 % of sports injuries. In the young athlete, fracturesare the most common injuries. The hand and wrist are the most common sitesfor fracture in the young athlete. Physeal injuries are typical overuse injuries ingymnasts. Chronic stress reactions with a widening of the growth plate areseen in the distal radial and less common in the ulnar growth plate. Injuries tothe TFCC in the athlete occur in acute trauma and with overuse. TFCC injuriesare an important cause for ulnar-sided wrist pain. The differential diagnosisincludes ulnar styloid impaction syndrome, ulnar impingement syndrome andtenosynovitis of the extensor carpi ulnaris tendon. Injury to the interosseousligaments may lead to carpal instability. Chronic injury of the intrinsic orextrinsic ligaments of the wrist may cause ganglion cyst formation.

MSSR41C Interactive Case Discussion

Participants

Christian W. Pfirrmann, MD, MBA, Forch, Switzerland (*Presenter*) Nothing to Disclose Lynne S. Steinbach, MD, San Francisco, CA (*Presenter*) Nothing to Disclose

LEARNING OBJECTIVES

1) To appreciate pathologic and normal developmental changes in skeletally immature throwing athletes, especially around the physis. 2) To consolidate the knowledge gained from the session with interactive cases of upper limb athletic injury as it relates to the skeletally immature throwing athlete.

ABSTRACT

The first part of this interactive session will show some cases of pathologic and normal developmental changes around the physis of shoulders of skeletally immature throwing athletes. The second part of this intercactive sessions will show and diuscuss cases with athletic unjuries about the wrist.





Occupational Lung Disease (Interactive Session)

Wednesday, Dec. 4 8:30AM - 10:00AM Room: N226



AMA PRA Category 1 Credits ™: 1.50 ARRT Category A+ Credit: 1.75

Participants

Cristopher A. Meyer, MD, Madison, WI (Moderator) Investor, Elucent Medical; Consultant, NIOSH Certified B-reader

Special Information

This interactive session will use RSNA Diagnosis Live™. Please bring your charged mobile wireless device (phone, tablet or laptop) to participate.

LEARNING OBJECTIVES

1) State the radiographic and CT findings of silicosis, CWP, and asbestos-related lung disease. 2) Always consider beryllium exposure when faced with an interstitial lung disease with features of sarcoidosis. 3) Describe the importance of expiratory imaging in the identification of small airway disease. 4) Identify clues to exposure history when interpreting HRCTs for interstitial lung disease.

ABSTRACT

Despite increased safety measures, workers remain at risk for occupational exposures. Silicosis, coal workers' pneumoconiosis, and asbestos-related lung disease continue to affect workers because of ongoing exposures in the workplace, long latency between exposure and disease, and changes in mining techniques. Immune-mediated diseases such as chronic hypersensitivity pneumonitis and chronic beryllium disease may also result from workplace exposure. Airway-centered occupational lung diseases are often the subtlest and may required expiratory imaging for recognition. This session will review these categories of occupational lung disease and conclude with a case-based session that emphasizes specific findings that may alert the interpreting radiologist to the possibility of occupational lung disease when faced with an unknown HRCT for interstitial lung disease.

Sub-Events

RC501A Classic Dusts: Asbestos, Silica, and Coal

Participants

Jeffrey P. Kanne, MD, Madison, WI (Presenter) Research Consultant, PAREXEL International Corporation;

For information about this presentation, contact:

jkanne@uwhealth.org

RC501B Occupational Lung Disease: The Other Guys (Beryllium, Hard Metal, Aluminum, Siderosis)

Participants

Sudhakar N. Pipavath, MD, Seattle, WA (Presenter) Scientific Advisory Board, Boehringer Ingelheim GmbH

RC501C Airway-related Interstitial Lung Disease and Emerging Occupational Lung Disease

Participants

Christian W. Cox, MD, Rochester, MN (Presenter) Nothing to Disclose

RC501D HRCT Patterns of Occupational Lung Disease: Case-based

Participants

Cristopher A. Meyer, MD, Madison, WI (Presenter) Investor, Elucent Medical; Consultant, NIOSH Certified B-reader

For information about this presentation, contact:

cmeyer2@uwhealth.org







ABR and RRC Updates

Wednesday, Dec. 4 8:30AM - 10:00AM Room: N229

ED

AMA PRA Category 1 Credits ™: 1.50 ARRT Category A+ Credit: 0

Sub-Events

RC502A ABR Update

Participants Valerie P. Jackson, MD, Tucson, AZ (*Moderator*) Nothing to Disclose Brent J. Wagner, MD, West Reading, PA (*Presenter*) Nothing to Disclose Vincent P. Mathews, MD, Hartland, WI (*Presenter*) Nothing to Disclose

LEARNING OBJECTIVES

1) Describe the value of ABR board certification. 2) Review the expectations of the public regarding board certification. 3) Describe ABR's OLA program for diagnostic radiology. 4) Discuss advantages of longitudinal assessment over traditional MOC examinations.

RC502B RRC Update

Participants Janet E. Bailey, MD, Ann Arbor, MI (*Presenter*) Nothing to Disclose Felicia Davis, Chicago, IL (*Presenter*) Nothing to Disclose

LEARNING OBJECTIVES

1) Identify opportunities for improved understanding of ACGME Radiology RRC processes, procedures, and policies. 2) Describe updates to the Common Program Requirements. 3) Discuss the ACGME Milestones 2.0 with focus on key features and changes.







Rapid Fire: 80 Cardiac Cases in 80 Minutes

Wednesday, Dec. 4 8:30AM - 10:00AM Room: E353B



AMA PRA Category 1 Credits ™: 1.50 ARRT Category A+ Credit: 1.75

Participants

Charles S. White, MD, Reisterstown, MD (Moderator) Nothing to Disclose

For information about this presentation, contact:

cwhite@umm.edu

LEARNING OBJECTIVES

1) Show rapid fire cardiac cases.

Sub-Events

RC503A Thoracic Vascular: 20 Cases

Participants Sachin S. Saboo, MD, FRCR, San Antonio, TX (*Presenter*) Nothing to Disclose

LEARNING OBJECTIVES

1) Describe key imaging features of twenty interesting thoracic vascular cases. 2) Assess significance of these imaging findings with respect to management.

RC503B Cardiothoracic Oncology: 20 Cases

Participants

Phillip M. Young, MD, Rochester, MN (Presenter) Consultant, Arterys Inc

For information about this presentation, contact:

young.phillip@mayo.edu

LEARNING OBJECTIVES

1) Review a variety of cardiothoracic oncologic diseases. 2) Discuss role of imaging in guiding workup and therapy. 3) Review role of imaging in advanced planning and treatment monitoring.

RC503C Pericardium: 20 Cases

Participants

Seth J. Kligerman, MD, Denver, CO (*Presenter*) Speakers Bureau, Boehringer Ingelheim GmbH; Author, Reed Elsevier; Consultant, IBM Corporation

LEARNING OBJECTIVES

1) Review various acute and chronic inflammatory conditions that involve the pericardium on CT and MRI. 2) Show various benign and malignant masses that involve the pericardial on CT and MRI. 3) Discuss differential diagnosis and methods of differentiation.

RC503D Coronary Arteries and Myocardium: 20 Cases

Participants

Jacobo Kirsch, MD, Miami, FL (Presenter) Nothing to Disclose

LEARNING OBJECTIVES

1) To review the imaging manifestations of common and uncommon ischemic and non-ischemic cardiac pathologies.





Musculoskeletal Series: MRI of Elbow, Wrist, and Hand

Wednesday, Dec. 4 8:30AM - 12:00PM Room: S406A



AMA PRA Category 1 Credits [™]: 3.00 ARRT Category A+ Credits: 3.50

FDA Discussions may include off-label uses.

Participants

Bruce B. Forster, MD, Vancouver, BC (*Moderator*) Stockholder, Canada Diagnostic Centres; Travel reimbursement, Sectra AB Bethany U. Casagranda, DO, Pittsburgh, PA (*Moderator*) Nothing to Disclose Linda Probyn, MD, Toronto, ON (*Moderator*) Nothing to Disclose Tetyana A. Gorbachova, MD, Huntingdon Valley, PA (*Moderator*) Nothing to Disclose

For information about this presentation, contact:

bethany.casagranda@ahn.org

LEARNING OBJECTIVES

1) To familiarize the audience with imaging diagnosis of common pathologies involving the elbow, wrist and hand, including abnormalities affecting tendons and ligaments in the setting of trauma.

Sub-Events

RC504-01 MRI of Elbow Ligament Injuries

Wednesday, Dec. 4 8:30AM - 8:50AM Room: S406A

Participants

Kirkland W. Davis, MD, Madison, WI (Presenter) Author with royalties, Reed Elsevier; Editor with royalties, Reed Elsevier

For information about this presentation, contact:

kdavis@uwhealth.org

LEARNING OBJECTIVES

1) Demonstrate normal anatomy of the principle ligaments of the elbow. 2) Understand imaging options when assessing for elbow ligament injury. 3) Identify partial and complete tears of the principle ligaments of the elbow.

RC504-02 MRI of Elbow Tendon Injuries

Wednesday, Dec. 4 8:50AM - 9:10AM Room: S406A

Participants

Soterios Gyftopoulos, MD, Scarsdale, NY (Presenter) Nothing to Disclose

For information about this presentation, contact:

Soterios.Gyftopoulos@nyumc.org

LEARNING OBJECTIVES

1) Review the important elbow tendon anatomy. 2) Review the imaging options available to evaluate elbow tendon pathology. 3) Describe the imaging appearances of the clinically relevant tendon pathology that occurs at the elbow.

RC504-03 Associated Radiological Findings in Patients with Ulnar Collateral Ligament Injuries of the First Metacarpophalangeal Joint

Wednesday, Dec. 4 9:10AM - 9:20AM Room: S406A

Participants

Sebastian Manneck, MD, Basel, Switzerland (*Presenter*) Nothing to Disclose Anna Hirschmann, MD, Basel, Switzerland (*Abstract Co-Author*) Nothing to Disclose

PURPOSE

To evaluate the frequency of concomitant volar plate avulsion in patients with ulnar collateral ligament (UCL) tear of the first metacarpophalangeal (MCP) joint indicating extensive injury.

METHOD AND MATERIALS

Patients with radiographs and MR images of the thumb obtained between January 2014 and November 2018 were selected through a retrospective search of our PACS database for the keywords "UCL injury" and "thumb" in the radiological report. Twenty-five

patients with an injury at the UCL of the first MCP joint on radiographs and MRI were then retrospectively assessed for a concomitant injury at the palmar structures by two musculoskeletal radiologists independently. Descriptive statistics were used to report the imaging interpretation. Wilcoxon and kappa statistics were calculated (P-value < 0.05).

RESULTS

24% [6]/16% [4](Reader1/Reader2) partial tears and 48% [12]/60% [15] (R1/R2) complete tears of the UCL were evident on MRI. UCL avulsion fractures were seen more frequently on MRI (28% [7]/16% [4]; R1/R2) compared to radiographs 12% [3]; (P=0.046; 0.317). Volar plate injuries were evident in 12% [3]/ 8% [2] on radiographs and in 80% [20]/76% [19] (R1/R2) on MRI (P =0.0001). Dislocation of the UCL >= 3 mm, as an indication for surgery, was evident in 8% [2] on radiographs and 40% [10] /56% [14] (R1/R2) on MRI (P=0.005). Ten/11 patients (R1/R2) with a dislocated UCL tear showed a concomitant volar plate injury (100 %/ 79%) as opposed to 10/8 patients (R1/R2) with non-displaced UCL-tears (66 %/ 72%). No injury to the dorsal ligament complex was seen. Interrater-agreement was 1.0/0.444 for UCL and 0.783/0.566 for palmar plate injuries on radiographs/MRI.

CONCLUSION

UCL and palmar plate injuries commonly coexist and radiographs underestimate the severity of injury. MR images show more subtle abnormalities.

CLINICAL RELEVANCE/APPLICATION

MRI is advocated in patients with suspected UCL tears to assess concomitant volar capsulo-ligamentous injuries. Accurate diagnosis of first MCP-joint injury can significantly impact treatment strategy and clinical outcome to prevent from developing persistent pain and chronic instability.

RC504-04 High-Resolution 3D Cone-Beam CT with a New Prototype of a Twin Robotic X-Ray System in Wrist Imaging: Comparison of Image Quality to Third-Generation Dual-Source CT

Wednesday, Dec. 4 9:20AM - 9:30AM Room: S406A

Participants

Tobias Gassenmaier, MD, Wurzburg, Germany (*Presenter*) Nothing to Disclose Andreas Kunz, MD, Wurzburg, Germany (*Abstract Co-Author*) Nothing to Disclose Carsten H. Gietzen, MD, Wuerzburg, Germany (*Abstract Co-Author*) Research Grant, Siemens AG Andreas M. Weng, Wuerzburg, Germany (*Abstract Co-Author*) Nothing to Disclose Thorsten A. Bley, MD, Wuerzburg, Germany (*Abstract Co-Author*) Nothing to Disclose Jan P. Grunz, MD, Wuerzburg, Germany (*Abstract Co-Author*) Research Grant, Siemens AG

PURPOSE

To evaluate image quality of a prototype version for cone-beam computed tomography (CBCT) of a twin robotic X-ray system in wrist imaging compared to a 3rd gen. dual-source CT (DSCT).

METHOD AND MATERIALS

16 cadaveric human wrists were examined with a not commercially available prototype version for CBCT of the above mentioned Xray system and a conventional 3rd gen. DSCT. Images were acquired with a standard-dose (SD) and low-dose (LD) protocol with matched radiation doses between systems (16 cm CTDIvol = 13.8 mGy in SD and 3.3 mGy in LD protocol). Two independent, blinded radiologists assessed overall image quality (IQ) in axial, coronal and sagittal MPRs utilizing a seven-point Likert scale (1 - very poor, [...], 7 - excellent IQ). Interrater reliability was assessed with the intraclass correlation coefficient (ICC; absolute agreement, 2way random-effects model). For objective analysis of IQ, the number of pixels within the highest (representing trabecula) and lowest (representing fatty bone marrow) 20% of grey values were quantified within a region of interest measurement in cancellous bone. High pixel numbers within the defined ranges were considered to indicate higher spatial resolution with good trabecular contrast.

RESULTS

In general, subjective IQ in CBCT was superior to dose-equivalent DSCT scans (all p<=0.030 for SD and p<0.001 for LD). For instance, median subjective IQ values for coronal MPRs were 7/7 (Reader 1 / Reader 2) in CBCT vs. 6/6 in DSCT with the SD protocol and 5/6 in CBCT vs. 3/3 in DSCT with the LD protocol. Single measure ICC was 0.936 (95% confidence interval, 0.897-0.961; p<0.001), indicating good to excellent reliability. Objective image analysis revealed higher pixel counts within the defined ranges when comparing CBCT to DSCT in both the SD (median 1744 pixels [IQR 1345 - 2237] vs. 1240 [657 - 1762]; p=0.001) and LD protocol (904 [577 - 1533] vs. 697 [486 - 1110]; p=0.013), indicating better delineation of trabecula in CBCT.

CONCLUSION

The new prototype version of the twin robotic X-ray system's CBCT mode provides superior image quality regarding delineation of trabecula at standard and low dose levels compared to dose-equivalent scan protocols on 3rd gen. DSCT.

CLINICAL RELEVANCE/APPLICATION

With improved image quality compared to 3rd gen. DSCT the new CBCT mode of the multifunctional X-ray system appears highly promising for 3D wrist imaging in vivo and may well hold potential for dose reduction.

RC504-05 Evaluation of the Ulnar Nerve with Shear-Wave Elastography: A Potential Sonographic Method for the Diagnosis of Ulnar Neuropathy

Wednesday, Dec. 4 9:30AM - 9:40AM Room: S406A

Participants

Sujin Kim, MD, Seoul, Korea, Republic Of (*Presenter*) Nothing to Disclose Guen Young Lee, Seongnam, Korea, Republic Of (*Abstract Co-Author*) Nothing to Disclose Ara Ko, MD, Seoul, Korea, Republic Of (*Abstract Co-Author*) Nothing to Disclose Jiyun Oh, Seoul, Korea, Republic Of (*Abstract Co-Author*) Nothing to Disclose Seok-min Jeong, Seoul, Korea, Republic Of (*Abstract Co-Author*) Nothing to Disclose

For information about this presentation, contact:

jaywony@gmail.com

PURPOSE

The aim of this study was to verify if shear-wave elastography (SWE) can be used to differentiate ulnar neuropathy at the cubital tunnel from asymptomatic ulnar nerve or medial epicondylitis and to determine a cut-off value for this parameter accurately identifying patient with ulnar neuropathy

METHOD AND MATERIALS

This study included 10 patients with ulnar neuropathy at the cubital tunnel, which was confirmed with electromyography (3 women, 7 men; mean age, 51.9 years), 10 patients with medial epicondylitis (5 women, 5 men; mean age, 56.1 years), and 37 patients with asymptomatic ulnar nerve and lateral epicondylitis (21 women, 16 men; 54.0 years). Each patient was subjected to SWE of the ulnar nerve at three levels: in the cubital tunnel and at the distal upper arm, and proximal forearm.

RESULTS

Patients with ulnar neuropathy in the cubital tunnel (mean, 66.8kPa) presented with significantly greater ulnar nerve stiffness in the cubital tunnel than the controls with medial epicondylitis (mean, 21.2kPa, P=0.015) or lateral epicondylitis (mean, 33.9kPa, P=0.040). There are no statistically significant differences of ulnar nerve stiffness at the distal upper arm and the proximal forearm between patients and controls. Ulnar nerve stiffness of 31kPA provide 100% specificity, 80.0% sensitivity, 100% positive predictive value and 83.3% negative predictive value for the differentiation between ulnar neuropathy and medial epicondylitis.

CONCLUSION

SWE seems to be a reliable and simple quantitative adjunct test to support the diagnosis of ulnar neuropathy at the cubital tunnel, especially to differentiate ulnar neuropathy at the cubital tunnel from medial epicondylitis.

CLINICAL RELEVANCE/APPLICATION

SWE seems to be a reliable and simple quantitative adjunct test to differentiate ulnar neuropathy at the cubital tunnel from medial epicondylitis.

RC504-06 MRI of Ulnar-sided Wrist Pain

Wednesday, Dec. 4 9:40AM - 10:00AM Room: S406A

Participants

Bruce B. Forster, MD, Vancouver, BC (Presenter) Stockholder, Canada Diagnostic Centres; Travel reimbursement, Sectra AB

For information about this presentation, contact:

bruce.forster@vch.ca

LEARNING OBJECTIVES

1) Understand the anatomy relevant to wrist/hand, with respect to ulnar sided wrist pain (USWP). 2) Appreciate the advantages and disadvantages of imaging modalities in workup of USWP. 3) List the common imaging features of causative pathologies of USWP, including Kienbock's disease, ulnocarpal abutment, TFCC pathology, hook of hamate fracture, and ECU pathology.

RC504-07 MRI of Radial-sided Wrist Pain

Wednesday, Dec. 4 10:30AM - 10:50AM Room: S406A

Participants Bethany U. Casagranda, DO, Pittsburgh, PA (*Presenter*) Nothing to Disclose

For information about this presentation, contact:

bethany.casagranda@ahn.org

LEARNING OBJECTIVES

1) Identify relevant wrist anatomy. 2) Describe physical exam tactics. 3) Develop differential diagnosis. 4) Identify imaging findings of each differential including osseous and soft tissue trauma, arthritis, Wartenberg's syndrome, De Quervain's tenosynovitis, lateral antebrachial cutaneous nerve neuritis and intersection syndrome.

RC504-08 Direct Visualization of Finger Pulley Injuries at 7T MRI: An Ex Vivo Feasibility Study

Wednesday, Dec. 4 10:50AM - 11:00AM Room: S406A

Participants

Rafael Heiss, Erlangen, Germany (*Presenter*) Speakers Bureau, Siemens AG Alexander Librimir, Erlangen, Germany (*Abstract Co-Author*) Nothing to Disclose Christoph Lutter, Bamberg, Germany (*Abstract Co-Author*) Nothing to Disclose Frank W. Roemer, MD, Erlangen, Germany (*Abstract Co-Author*) Officer, Boston Imaging Core Lab, LLC; Research Director, Boston Imaging Core Lab, LLC; Shareholder, Boston Imaging Core Lab, LLC Michael Uder, MD, Erlangen, Germany (*Abstract Co-Author*) Nothing to Disclose Rolf Janka, MD, PhD, Erlangen, Germany (*Abstract Co-Author*) Nothing to Disclose Volker Schoffl, Bamberg, Germany (*Abstract Co-Author*) Nothing to Disclose Armin Nagel, DiplPhys, Heidelberg, Germany (*Abstract Co-Author*) Nothing to Disclose Thomas Bayer, MD, Bamberg, Germany (*Abstract Co-Author*) Nothing to Disclose

PURPOSE

To evaluate feasibility of 7T magnetic resonance imaging (MRI) for direct visualization of the finger flexor pulleys A2, A3 and A4

before and after artificial pulley injury in an ex-vivo model and to correlate results with anatomical preparations.

METHOD AND MATERIALS

30 fingers from 10 human cadavers were examined before and after iatrogenic pulley disruption with a 7T imaging protocol, which is comparable to a clinical protocol lasting 15 minutes. Images were assessed by two experienced radiologists for the presence and location of finger pulley lesions. Image quality was evaluated according a 4-point Likert scale from not evaluable to excellent. Macroscopic and histopathological preparation was used as gold standard for comparing findings with MRI. Diagnostic performance was assessed using sensitivity and specificity.

RESULTS

Mechanically induced finger flexor pulley lesions were detected with a sensitivity of 100% and a specificity of 98%. Finger flexor A2, A3 and A4 pulley lesions were detected at the radial and ulnar, as well as in the middle parts of the finger pulley in 33.3% each. In 62.5% of all pulley lesions a dislocation and intercalation of the pulley stump in between the flexor tendon and finger phalanges was observed. The average Likert score for direct visualization of pulleys before rupture was 2.67 and after rupture creation 2.79, meaning a very good image quality in average.

CONCLUSION

7T MRI enables direct visualization and characterization of traumatic pulley lesions with definition of rupture morphology, detection of complicated lesions and evaluation of small pulleys such as A3 and A4.

CLINICAL RELEVANCE/APPLICATION

Direct 7T visualization allows pre-surgical evaluation of pulley injuries and is able to characterize complex pulley injuries including those exhibiting stump dislocations, even for small pulleys.

RC504-09 A Multimodality Census of Carpal Coalitions

Wednesday, Dec. 4 11:00AM - 11:10AM Room: S406A

Participants

Alessandra J. Sax, MD, Philadelphia, PA (*Presenter*) Nothing to Disclose William B. Morrison, MD, Philadelphia, PA (*Abstract Co-Author*) Consultant, AprioMed AB Patent agreement, AprioMed AB Consultant, Zimmer Biomet Holdings, Inc Consultant, Samsung Electronics Co, Ltd Consultant, Medical Metrics, Inc Aleksandr Rozenberg, MD, Philadelphia, PA (*Abstract Co-Author*) Nothing to Disclose Adam C. Zoga, MD,MBA, Philadelphia, PA (*Abstract Co-Author*) Nothing to Disclose

For information about this presentation, contact:

alisax87@gmail.com

PURPOSE

Coalition in the wrist is less common than the foot, but still encountered routinely. Although frequently incidental, they can also be a primary or secondary source of pain. To date, few series have been conducted to establish the prevalence and morphology of carpal coalitions. We endeavored to create the largest known study to date detailing the configurations and imaging features of carpal coalitions across multiple imaging modalities.

METHOD AND MATERIALS

A report database from upper extremity x-ray, CT, and MRI exams was retrospectively mined for the word 'coalition'. Studies were reviewed by 2 MSK radiologists. Configurations, ordering indication, and pathology across the coalition were logged. Pathology potentially related to the coalition was observed and the relative risks were calculated.

RESULTS

Of the 430 x-rays, lunotriquetral coalition was most prevalent in 88%, capitohamate in 7%, scapholunate in 2%, hamate-pisiform in 1%, trapezoid-capitate in 1%, with single occurrences in other locations. 71% of x-rays were ordered for recent injury (within 1 month), 29% for non-traumatic pain. Of the 114 MRIs, lunotriquetral coalition was most common in 83%, capitohamate in 2%, hamate-pisiform in 3%, trapezoid-capitate in 6%, and 6% at an os styloideum or os trapezoideum secundareum. 35% of MRIs were ordered for recent injury, 65% for non-traumatic pain. Degenerative changes across the coalition occurred in 33% of MRIs. There was a significant increased risk of triscaphe arthritis, (23% of MRIs, relative risk (RR) 3.09, 95% confidence interval (CI) 1.36-7.04). 43% of exams involved extensor tendons (RR 1.23, 95% CI .79-1.93). Extensor tears (13%, RR 10.11, 95% CI 1.61-63.49), specifically the extensor carpi ulnaris (10%, RR 7.58, 95% CI 1.17-48.94) were the most significant. A scapholunate tear was present in 24% (RR 1.61, 95% CI .85-3.07). Flexor compartment tendinosis was present in 24% (RR 1.61, 95% CI .85-3.07).

CONCLUSION

While carpal coalitions are relatively infrequent, some cause variations in biomechanical stability and can be symptomatic. Radiologists should be familiar with the most common coalitions including lunotriquetral and capitohamate as well as less common locations, morphologic variations, and imaging findings associated with carpal coalitions.

CLINICAL RELEVANCE/APPLICATION

Recognizing carpal coalition and associated pathology is important as it may be directly or indirectly responsible for patients' symptoms.

RC504-10 Clinical and Cost-Effectiveness Implications of Utilizing Immediate Acute Magnetic Resonance Imaging (MRI) in the Management of Patients with Suspected Scaphoid Fracture and Negative Initial Radiographs: Results From a Randomized Clinical Trial

Wednesday, Dec. 4 11:10AM - 11:20AM Room: S406A

Sanjay Vijayanathan, MBBS, Harrow, United Kingdom (*Abstract Co-Author*) Nothing to Disclose Davina Mak, MBBS, BSC, Middlesex, United Kingdom (*Presenter*) Nothing to Disclose Alireza Zavareh, MD, FRCR, Bristol, United Kingdom (*Abstract Co-Author*) Nothing to Disclose Amanda Isaac, MBChB, FRCR, Rickmansworth, United Kingdom (*Abstract Co-Author*) Nothing to Disclose Bharti Malhotra, MBA, London, United Kingdom (*Abstract Co-Author*) Nothing to Disclose Laura Hunter, London, United Kingdom (*Abstract Co-Author*) Nothing to Disclose Janet Peacock, PhD, London, United Kingdom (*Abstract Co-Author*) Nothing to Disclose James Shearer, PhD, London, United Kingdom (*Abstract Co-Author*) Nothing to Disclose Vicky J. Goh, MBBCh, Chalfont St Giles, United Kingdom (*Abstract Co-Author*) Nothing to Disclose Paul McCrone, London, United Kingdom (*Abstract Co-Author*) Nothing to Disclose Sam Gidwani, London, United Kingdom (*Abstract Co-Author*) Nothing to Disclose

For information about this presentation, contact:

tiago.rua@kcl.ac.uk

PURPOSE

Given the limited accuracy of radiographs on presentation to the Emergency Department (ED), the management of suspected scaphoid fractures remains clinically challenging and an economic burden to healthcare systems. This trial evaluated the clinical and cost-effectiveness implications of using immediate Magnetic Resonance Imaging (MRI) as an add-on test during the ED attendance for patients with negative findings on the initial radiographs.

METHOD AND MATERIALS

A pragmatic, randomized, single-center trial compared the use of immediate MRI for patients presenting to the ED with suspected scaphoid fractures against standard care with radiographs only. Participants' use of health services was estimated from primary care and secondary care databases and questionnaires at baseline, 3 and 6 months post-recruitment. Costs were compared using generalized linear models and combined with quality-adjusted life years (QALYs) to estimate cost-effectiveness.

RESULTS

A total of 136 participants were recruited based on 1:1 ratio, block randomization methods (mean age 37 years; 57% male; 79% full-time employed). 6.2% (4/65, control group) and 10% (7/67, intervention group) of participants sustained scaphoid fractures (p=0.37). 7.7% (5/65, control group) and 22% (15/67, intervention group) of participants had other fractures diagnosed (p=0.019). The use of MRI increased the diagnostic accuracy both in the diagnosis of scaphoid fracture (100.0% vs 93.8%) and any other fracture (98.5% vs 84.6%). Mean (SD) cost per participant up to 3 months post-recruitment was £542.4 (£855.2) for the control group and £368.4 (£338.6) for the intervention, leading to a cost difference of £174 (95% CI -£30 to £378, p=0.094). The cost difference per participant at 6 months increased to £266 (95% CI £3.3 to £528, p=0.047). The MRI intervention dominated standard care costing less and achieving more QALY gains, presenting a probability of 96% and 100% of being cost-effective at month 3 and 6 considering traditional willingness-to-pay thresholds.

CONCLUSION

The use of immediate MRI in the management of participants with suspected scaphoid fracture and negative radiographs led to significant cost-savings whilst improving and expediting the pathway's diagnostic accuracy.

CLINICAL RELEVANCE/APPLICATION

The immediate use of MRI in the management of suspected scaphoid fractures should be included as part of standard of care as an add-on test for patients with negative radiographs.

RC504-11 MRI of Thumb Injuries

Wednesday, Dec. 4 11:20AM - 11:40AM Room: S406A

Participants

Linda Probyn, MD, Toronto, ON (Presenter) Nothing to Disclose

For information about this presentation, contact:

linda.probyn@sunnybrook.ca

LEARNING OBJECTIVES

1) Describe relevant normal anatomy of the thumb including tendons, ligaments and pulleys. 2) Explain common pathologies related to thumb injuries, including tendon, ligament and osseous injuries. 3) Compare other imaging modalities and how they can be complimentary to assist in diagnosing injuries of the thumb.

RC504-12 MRI of Finger Injuries

Wednesday, Dec. 4 11:40AM - 12:00PM Room: S406A

Participants

Tetyana A. Gorbachova, MD, Huntingdon Valley, PA (Presenter) Nothing to Disclose

For information about this presentation, contact:

gorbacht@einstein.edu

LEARNING OBJECTIVES

1) Recognize normal osseous and soft tissue anatomy of the fingers on MRI. 2) Describe various types of finger injuries and their clinical and treatment implications. 3) Identify common pitfalls in diagnosis of finger injuries on MRI.





Neuroradiology Series: Stroke

Wednesday, Dec. 4 8:30AM - 12:00PM Room: N228



AMA PRA Category 1 Credits ™: 3.25 ARRT Category A+ Credits: 4.00

Participants

Max Wintermark, MD, Lausanne, Switzerland (*Moderator*) Consultant, More Health; Consultant, Magnetic Insight; Consultant, icoMetrix NV; Consultant, Nines; Consultant, Subtle Medical; Consultant, Nous; Pamela W. Schaefer, MD, Boston, MA (*Moderator*) Nothing to Disclose

For information about this presentation, contact:

pschaefer@partners.org

LEARNING OBJECTIVES

1) To become familiar with evidence, advantages and challenges of CT based stroke imaging work up. 2) Improve knowledge of thrombectomy technique for ischemic stroke treatment. 3) Understand and apply aspiration thrombectomy, stent retriever thrombectomy, and combined approaches for ischemic stroke treatment.4) Describe and recognize the most common complications following thrombectomy for ischemic stroke treatment. 5) Understand the variance and penetrance of EVT across the world. 6) To understand the primary and potential future roles of magnetic resonance imaging in stroke diagnosis, prognostication, and treatment monitoring.

Sub-Events

RC505-01 CT-Based Imaging Workshop in Acute Ischemic Stroke: Evidence and Practical Pearls

Wednesday, Dec. 4 8:30AM - 9:00AM Room: N228

Participants

Achala S. Vagal, MD, Mason, OH (Presenter) Research Grant, Cerovenus

RC505-02 Location-Specific Alberta Stroke Program Early CT Score (ASPECTS) Paradigm in the Cohort of Acute Ischemic Stroke Patients

Wednesday, Dec. 4 9:00AM - 9:10AM Room: N228

Participants

Seyed Mohammad Seyedsaadat, MD, Rochester, MN (*Presenter*) Nothing to Disclose Waleed Brinjikji, MD, Rochester, MN (*Abstract Co-Author*) Nothing to Disclose JoAnna Schaafsma, Toronto, ON (*Abstract Co-Author*) Nothing to Disclose John C. Benson, MD, Rochester, MN (*Abstract Co-Author*) Nothing to Disclose Ian T. Mark, MD, Rochester, MN (*Abstract Co-Author*) Nothing to Disclose Eric Polley, PhD, Rochester, MN (*Abstract Co-Author*) Nothing to Disclose Sapna Rawal, MD, Toronto, ON (*Abstract Co-Author*) Nothing to Disclose Timo Krings, MD, PhD, Toronto, ON (*Abstract Co-Author*) Nothing to Disclose Alejandro A. Rabinstein, MD, Rochester, MN (*Abstract Co-Author*) Nothing to Disclose David F. Kallmes, MD, Rochester, MN (*Abstract Co-Author*) Nothing to Disclose Consultant, General Electric Company Consultant, Medtronic plc Consultant, Johnson & Johnson

For information about this presentation, contact:

Seyedsaadat.SeyedMohammad@mayo.edu

PURPOSE

Despite the importance of the occlusion site in predicting the outcome of acute ischemic stroke (AIS) patients, ASPECTS does not adjust the weight of the ten sub-regions based on their impact on patient's outcome. This study was performed in a cohort of AIS patients to determine the predictive value of each ASPECTS sub-region.

METHOD AND MATERIALS

In this retrospective, multi-center study, clinical and neuroimaging data of AIS patients who presented within the first 24 hours of symptom onset and underwent embolectomy from 2014 to 2018 was collected. Three expert neuroradiologists reviewed baseline non-contrast head CT scans to score early ischemic changes based on ASPECTS. Logistic regression analysis was performed to find the essential ASPECTS sub-regions in predicting the 3-month outcome of AIS patients.

RESULTS

Among a total of 353 patients, 214 patients had a 3-month poor outcome (mRS>2). Eighty one percent of patents with M4 infarct, 79% of Caudate, and 77% of those with M5 had poor outcomes (Figure 1). Univariate analysis showed significantly higher rate of poor outcome than favorable outcome in patients with infarction in Insula (68% vs. 32%; p-value=0.005), Caudate (79.49% vs.

20.51%; p-value=0.013), M2 (73.3% vs. 26.7%; p-value=0.023), M4 (81.5% vs. 18.5%, p-value=0.015), and M5 (76.9% vs. 23.1%, p-value= 0.022). Logistic regression analysis showed that infarction in M4 (OR: 2.93; 95%CI: 1.09- 9.43), Caudate (OR: 3.27; 95%CI: 1.33-8.45), and Insula (OR: 1.75; 95%CI: 1.08- 2.85) are significant predictors of 3-months poor outcome.

CONCLUSION

Infarction of Caudate, M4, and Insula are strongly associated with poor outcomes in patients with AIS. Our findings are consistent with similar studies that suggested an unequal impact of brain topography on the outcomes of AIS patients.

CLINICAL RELEVANCE/APPLICATION

Developing modified ASPECTS based on the proper weighting of each ten ASPECTS brain region seems to be a more accurate tool than the current ASPECTS for predicting the outcome of AIS patients.

RC505-03 Prognostic Value of Dual-Energy CT-based Detection of Distal Microemboli Following Stroke Thrombectomy

Wednesday, Dec. 4 9:10AM - 9:20AM Room: N228

Participants

Dylan Wolman, MD, Stanford, CA (*Presenter*) Nothing to Disclose Matthew B. Gologorsky, BS, Stanford, CA (*Abstract Co-Author*) Nothing to Disclose Max Wintermark, MD, Lausanne, Switzerland (*Abstract Co-Author*) Consultant, More Health; Consultant, Magnetic Insight; Consultant, icoMetrix NV; Consultant, Nines; Consultant, Subtle Medical; Consultant, Nous; Jeremy J. Heit, MD,PhD, Stanford, CA (*Abstract Co-Author*) Consultant, Medtronic plc; Consultant, Terumo Corporation; Scientific Advisory Board, iSchemaView, Inc; Medical Advisory Board, iSchemaView, Inc

PURPOSE

Endovascular thrombectomy (ET) is an effective treatment for stroke due to large-vessel occlusion (LVO). Revascularization after ET stroke predicts good long-term neurologic outcomes. Current measures of revascularization, such as the modified thrombolysis in cerebral infarction score (mTICI), do not capture the location or number of residual microemboli (RME). We determined whether dual-energy CT (DECT) detects and localizes RME following ET and if RME presence predicts poorer outcomes.

METHOD AND MATERIALS

DECT following ET was prospectively performed in all patients who did not undergo MRI over one year. Two unblinded readers scored DECT for RME presence and location (Figure 1A-B). Manual ROI labels were placed at the treated vascular segment, within the contralateral control vessel (or M1 segment for basilar LVO), and at the site of putative RME on conventional appearing 120-kVp (standard) CT series, low-kVp weighted DECT series (Q34s), and virtual non-contrast (VNC) and iodine map (IM) reconstructions. Primary outcome measure was a good functional outcome (modified Rankin Scale [mRS] score 0-2) at 90-days. Pairwise Wilcoxon rank-sum and chi-square tests were performed to assess the discriminatory capabilities of DECT versus standard CT and to assess for correlation between 90-day neurologic outcomes and the site of detected RME, respectively.

RESULTS

Twenty-nine patients were included. DECT was performed 6 hrs (IQR 5-10) after ET. Successful revascularization was achieved in 27 (93% TICI 2b-3) patients. Twenty patients (69%) had RME on post-ET DSA, and DECT identified RME in 19/20 (95%) patients. Analysis of ROI attenuation values demonstrated that Q34s, VNC, and IM series differentiated RME from control vessels (P=0.004-0.01), while standard series could not (P=0.31). Good neurologic outcomes were achieved in 12/19 (63%) patients with RME versus 9/10 (90%) patients without RME. The proximity of RME detected on post-ET DECT inversely correlated with 90-day mRS scores in the anterior circulation (P=0.028).

CONCLUSION

Postinterventional DECT detects RME, the location of which may provide prognostic value.

CLINICAL RELEVANCE/APPLICATION

RME presence and location may offer additional prognostic information following ET.

RC505-04 Value of CT Perfusion for Morphologic Outcome Prediction in Acute Ischemic Cerebellar Stroke

Wednesday, Dec. 4 9:20AM - 9:30AM Room: N228

Participants

Matthias P. Fabritius, MD, Munich, Germany (*Abstract Co-Author*) Nothing to Disclose Paul Reidler, MD, Munich, Germany (*Abstract Co-Author*) Nothing to Disclose Kolja M. Thierfelder, MD, Munich, Germany (*Abstract Co-Author*) Nothing to Disclose Daniel Puhr-Westerheide, MD, Munich, Germany (*Abstract Co-Author*) Nothing to Disclose Stefan Maurus, MD, Munich, Germany (*Presenter*) Nothing to Disclose Philipp M. Kazmierczak, MD, Munchen, Germany (*Abstract Co-Author*) Nothing to Disclose Wolfgang G. Kunz, MD, Munich, Germany (*Abstract Co-Author*) Grant, Medtronic plc

For information about this presentation, contact:

matthias.fabritius@med.uni-muenchen.de

PURPOSE

The diagnosis of ischemic cerebellar stroke is challenging due to non-specific symptoms and very limited accuracy of commonly applied computed tomography (CT) imaging. Advances in CT perfusion imaging provide increasing value in the detection of posterior circulation stroke, but the prognostic value remains unclear. We aimed to identify imaging parameters that predict morphologic outcome in cerebellar stroke patients using advanced CT including whole-brain CT perfusion (WB-CTP).

METHOD AND MATERIALS

We selected all subjects with cerebellar WB-CTP pertusion deticits and follow-up-confirmed cerebellar infarction from a consecutive cohort with suspected stroke who underwent WB-CTP. Posterior-circulation-Acute-Stroke-Prognosis-Early-CT-Score (pc-ASPECTS) was determined on non-contrast CT (NCCT), CT angiography source images (CTA-SI) and on parametric WB-CTP maps. The cerebellar perfusion deficit volumes on all maps as well as the final infarction volume (FIV) on follow-up imaging were quantified. Uni- and multivariate regression analyses were performed.

RESULTS

Sixty patients fulfilled the inclusion criteria. pc-ASPECTS on CTA-SI (β , -9.239; 95% Confidence Interval [CI], -14.220 to -4.259; p<0.001) and CBF deficit volume (β , 0.886; 95% CI, 0.684-1.089; p<0.001) were significantly associated with FIV in univariate linear regression analysis. The association of CBF deficit volume (β , 0.830; 95% CI, 0.605-1.055; p<0.001) was confirmed in a multivariate linear regression model adjusted for age, sex, pc-ASPECTS on NCCT and CTA-SI and the National Institutes of Health Stroke Scale (NIHSS) score on admission. No other clinical or imaging parameters were associated with the cerebellar stroke FIV (p>0.05). Due to the relevant frequencies of concomitant brainstem and supratentorial involvement, clinical outcome evaluation was not feasible.

CONCLUSION

In contrast to NCCT and CTA, WB-CTP imaging contains prognostic information for morphologic outcome in patients with acute cerebellar stroke.

CLINICAL RELEVANCE/APPLICATION

As clinical assessment of the severity of cerebellar stroke is often difficult and limited, more objective imaging parameters like WB-CTP might potentially support clinical decision-making, and hence facilitate clinical trial design by identifying real ischemic target lesions and excluding stroke mimics, which may otherwise confound results in the low NIHSS clinical trial setting.

RC505-05 MRI in Stroke and Cerebrovascular Disease

Wednesday, Dec. 4 9:30AM - 10:00AM Room: N228

Participants

Seena Dehkharghani, MD, New York, NY (Presenter) Nothing to Disclose

RC505-06 Hot Topic Panel: Is CT-perfusion Now the Standard of Care for Stroke?

Wednesday, Dec. 4 10:10AM - 10:40AM Room: N228

Participants

Achala S. Vagal, MD, Mason, OH (*Presenter*) Research Grant, Cerovenus Seena Dehkharghani, MD, New York, NY (*Presenter*) Nothing to Disclose Jeremy J. Heit, MD, PhD, Stanford, CA (*Presenter*) Consultant, Medtronic plc; Consultant, Terumo Corporation; Scientific Advisory Board, iSchemaView, Inc; Medical Advisory Board, iSchemaView, Inc Johanna M. Ospel, MD, Basel, Switzerland (*Presenter*) Nothing to Disclose

RC505-07 Neurointerventional Stroke Treatment: Techniques and Complications

Wednesday, Dec. 4 10:40AM - 11:10AM Room: N228

Participants

Jeremy J. Heit, MD, PhD, Stanford, CA (*Presenter*) Consultant, Medtronic plc; Consultant, Terumo Corporation; Scientific Advisory Board, iSchemaView, Inc; Medical Advisory Board, iSchemaView, Inc

RC505-08 Deep Learning-Based Penumbra Estimation Using DWI and ASL for Acute Ischemic Stroke Patients

Wednesday, Dec. 4 11:10AM - 11:20AM Room: N228

Participants

Yuan Xie, Stanford, CA (*Abstract Co-Author*) Nothing to Disclose Yannan Yu, Palo Alto, CA (*Presenter*) Nothing to Disclose Jiahong Ouyang, Stanford, CA (*Abstract Co-Author*) Research support, General Electric Company Charles Huang, Palo Alto, CA (*Abstract Co-Author*) Nothing to Disclose Enhao Gong, PhD, Menlo Park, CA (*Abstract Co-Author*) Stockholder, Subtle Medical Soren Christensen, Stanford, CA (*Abstract Co-Author*) Nothing to Disclose Maarten Lansberg, Stanford, CA (*Abstract Co-Author*) Nothing to Disclose Greg Zaharchuk, MD, PhD, Stanford, CA (*Abstract Co-Author*) Research Grant, General Electric Company; Research Grant, Bayer AG; Stockholder, Subtle Medical

PURPOSE

In acute ischemic stroke, estimating the penumbra, or region at-risk of infarction in the absence of reperfusion, is important to determine whether the patient is likely to benefit from treatment. The current gold standard for penumbra is based on the time-to-peak of the residue function (Tmax) map, which is reconstructed from bolus contrast perfusion weighted imaging (PWI), where tissue with a Tmax > 6s is generally considered to represent penumbra. We demonstrate that a deep learning model can predict the penumbra region based on non-contrast DWI and ASL-CBF images.

METHOD AND MATERIALS

60 patients were identified retrospectively from a multi-center stroke study. All patients underwent 3T MR imaging at baseline, with DWI, PWI, and ASL (either single post-label delay [2000 ms, 1.5T] or multidelay [700-3000 ms, 3T]). DWI images were acquired with TR/TE 4000/77.5ms and b=1000s/mm2. Penumbra mask was calculated using RAPID software using a criterion of Tmax > 6s (version 4.5.1, iSchemaView, Menlo Park, CA, USA) and used as ground truth. A residual deep convolutional neural network with a U-Net architecture was constructed using DWI, ADC maps, and ASL-CBF as input with Tmax>6s segmentations as ground truth. The model's output is an image where each voxel ranges between 0 and 1, representing the probability of the voxel being included in penumbra. 5-fold cross validation was used to evaluate the model performance. Assessments included receiver-operator

characteristic metrics (area-under-the-curve [AUC]), Dice score, precision, recall, specificity, and penumbra volume at optimal threshold.

RESULTS

The model produced a voxel-based AUC of 0.873, and a per-subject AUC of 0.86 ± 0.06 . At the prediction threshold yielding best performance, the Dice score was 0.40 ± 0.18 , the precision was 0.42 ± 0.17 , recall was 0.44 ± 0.23 , and specificity was 0.94 ± 0.03 . Mean absolute volume difference from ground truth was 33 ± 28 ml.

CONCLUSION

Using information available in ASL and DWI scans, a deep learning model can estimate the size and location of the penumbra without the use of contrast agents.

CLINICAL RELEVANCE/APPLICATION

Using deep learning, an acute stroke patient's penumbra region can be accurately outlined with diffusion weighted imaging (DWI) and cerebral blood flow map from arterial spin labeling (ASL-CBF), providing a quicker and non-contrast way to evaluate the potential benefit of thrombectomy treatment.

RC505-09 Correlation of National Incidence and Outcomes of Ischemic Strokes and Distribution of Joint Commission Certified Advanced Stroke Centers and CAST Certified Physicians to Perform Endovascular Therapies

Wednesday, Dec. 4 11:20AM - 11:30AM Room: N228

Participants

Neena A. Davisson, MD, Decatur, GA (*Presenter*) Nothing to Disclose Laura K. Findeiss, MD, Atlanta, GA (*Abstract Co-Author*) Nothing to Disclose Richard Duszak JR, MD, Atlanta, GA (*Abstract Co-Author*) Nothing to Disclose Danny Hughes, PhD, Reston, VA (*Abstract Co-Author*) Nothing to Disclose Nima Kokabi, MD, Atlanta, GA (*Abstract Co-Author*) Research support, Sirtex Medical Ltd

For information about this presentation, contact:

dneena@emory.edu

PURPOSE

To determine whether the geographic distribution of Committee on Advanced Subspecialty Training (CAST) certified physicians and Joint Commission (JC) certified Comprehensive Stroke Centers (CSCs) correlate with the regional incidence and outcomes of ischemic stroke.

METHOD AND MATERIALS

Using the Centers for Disease Control and Prevention Interactive Atlas of Heart Disease and Stroke, the national incidence of ischemic stroke death for patients 35-75 years of age was identified at state-level. Rates of admission and outcomes of ischemic stroke in the Medicare population were also calculated. Using the same tool, the national distribution of JC CSCs was identified. Additionally, the national distribution of 2019 CAST certified physicians, as published by the Society of Neurological Surgery, was overlaid. Pearson Correlation (r) was performed between stroke hospitalization rates and outcomes with the number of JC CSCs and CAST physicians.

RESULTS

The average nationwide ischemic stroke hospitalization rate in the Medicare population in 2013-2015 was 10.4 per 1000 beneficiaries and the average ischemic stroke death rate in patients 35-75 years of age in 2014-2016 was 4.8 per 100,000. States with the highest stroke hospitalization rates (12.2 to 13.9 per 1000 beneficiaries) and stroke death rates (6.7 to 20 per 100,000 beneficiaries) were located mainly in the Southeast. JC CSCs (n=134) are located in 37 states and the District of Columbia with a predominance in the Northeast. CAST physicians (n=171) are located in 33 states with a predominance in the Northeast. There was no correlation between location of CAST physicians and stroke hospitalization rates or death rates with r = -0.01 and r = -0.01, respectively (p's>0.05). There was no correlation between JC CSCs and stroke hospitalization rates or death rates with r = -0.16 and r = 0.08, respectively (p's>0.05).

CONCLUSION

There is no correlation between the geographic location of CAST physicians or JC certified CSCs and the incidence and outcomes of ischemic stroke. More strategic planning is necessary to ensure the needs of communities are met, with sufficient availability of physicians and CSCs capable of treating ischemic strokes endovascularly.

CLINICAL RELEVANCE/APPLICATION

CAST physicians and JC CSCs are not strategically distributed where the incidence of ischemic stroke is highest. Efforts should be made to optimize availability of thrombectomy-capable physicians in these areas.

RC505-10 Understanding the Variance of Decision Making in Acute Stroke Based on the Principles of Neuroeconomics

Wednesday, Dec. 4 11:30AM - 12:00PM Room: N228

Participants

Johanna M. Ospel, MD, Basel, Switzerland (Presenter) Nothing to Disclose

LEARNING OBJECTIVES

To understand current endovascular treatment practice patterns of physicians across different specialties and countriesTo learn about current real-life endovascular treatment decision-making in the absence of clear evidenceTo explore factors that influence endovscular treatment decision-making and possible thought processes behind these factors





The Radiology Hearing Loss and Tinnitus

Wednesday, Dec. 4 8:30AM - 10:00AM Room: E353C



AMA PRA Category 1 Credits ™: 1.50 ARRT Category A+ Credit: 1.75

Sub-Events

RC506A Temporal Bone Anatomy

Participants

Caroline D. Robson, MBChB, Boston, MA (Presenter) Author with royalties, Reed Elsevier;

LEARNING OBJECTIVES

1) Become familiar with normal temporal bone anatomy. 2) Use optimal imaging planes on CT to assess anatomy. 3) Develop indication based temporal bone MR protocols. 4) Recognize normal developmental variants. 5) Identify anatomic variants that pose surgical hazards.

Active Handout:Caroline Diana Robson

http://abstract.rsna.org/uploads/2019/19000239/Active RC506A.pdf

RC506B Conductive Hearing Loss

Participants Suresh K. Mukherji, MD, Carmel, IN (*Presenter*) Nothing to Disclose

LEARNING OBJECTIVES

1) Define conductive hearing loss. 2) Review the anatomy of the middle ear. 3) Describe common pathology that results in conductive hearing loss.

ABSTRACT

This talk with introduce the audience to the concept of conductive hearing loss. The talk with define conductive hearing loss, review the anatomy of the middle ear and discuss common pathologies that cause conductive hearing loss. The session will end by providing the audience with a "checklist" of findings that should be commented in the report for patients with conductive hearing loss.

RC506C Sensorineural Hearing Loss

Participants

Jan W. Casselman, MD, PhD, Brugge, Belgium (Presenter) Consultant, Koninklijke Philips NV; Speaker, QR srl

For information about this presentation, contact:

jan.casselman@azsintjan.be

LEARNING OBJECTIVES

1) To understand what sensorineural hearing loss is. 2) To become familiar with the most frequent pathologies causing sensorineural hearing loss in children and adults. 3) To learn which imaging techniques are best suited to detect the different causes of sensorineural hearing loss.

ABSTRACT

In this course the meaning of sensorineural hearing loss will be explained and also how it can be distinguished clinically from conductive or mixed hearing loss. The most frequent causes of sensorineural hearing loss that can be detected in children and adults will be discussed. The pathologies causing sensorineural hearing loss can be located at the level of the inner ear, internal auditory canal and cerebellopontine angle or along the audtiory pathways. Finally the best suited imaging techniques to detect sensorineural hearing loss will be discussed.

RC506D Tinnitus

Participants C. Douglas Phillips, MD, New York, NY (*Presenter*) Nothing to Disclose

For information about this presentation, contact:

dphillips@med.cornell.edu

LEARNING OBJECTIVES

Understand the distinction between objective and subjective tinnitus.
 Be able to discuss primary tinnitus and its significance.
 Describe the imaging findings of common entities associated with tinnitus.
 Discuss some current research into the mechanisms

ABSTRACT

Tinnitus is a very common problem in the US and is a source of diminished enjoyment of life and leisure due to the incessant nature of the disease. There are associations that can increase the potential diagnosis of an etiologic factor for tinnitus, including associations with hearing loss, a subjective nature of the tinnitus, and exposure to certain toxins as well as environmental conditions. We will discuss the various forms of tinnitus and who should be imaged in the setting of tinnitus, as well as describe imaging findings associated with tinnitus.







Emergency Ultrasound Pitfalls and Pearls

Wednesday, Dec. 4 8:30AM - 10:00AM Room: E451B



AMA PRA Category 1 Credits ™: 1.50 ARRT Category A+ Credit: 1.75

Participants

Leslie M. Scoutt, MD, Essex, CT (Moderator) Speaker, Koninklijke Philips NV

For information about this presentation, contact:

leslie.scoutt@yale.edu

LEARNING OBJECTIVES

1) Describe pearls and pitfalls in ultrasound evaluation of patients presenting with right upper quadrant pain with a focus on hepatobiliary pathology. 2) Discuss how to avoid mistakes in the ultrasound assessment of common pediatric emergencies. 3) Discuss pearls and pitfalls in ultrasound assessment of gynecologic emergencies.

ABSTRACT

As part of the series focused on the role of imaging in the emergency department, this course will focus on the role of ultrasound in the assessment of clinically suspected hepatobiliary pathology, pathology commonly encounteres and more specific to the pediatric population and gynecological emergencies. The goal of the presentations will be to focus on pearls so that the audience will learn how to best and most successfully use ultrasound and thereby avoid a more costly CT and the risks of radiation exposure and iodinate contrast. However, common pitfalls will also be addressed so that the audience learns how to avoid mistakes as well as when ultrasound is not adequate for complete patient evaluation and further imaging should be recommended. While ultrasound is often the first study ordered, one needs to learn 'when to hold 'em, and when to fold 'em' to do what is best for patient care.

Sub-Events

RC508A Hepatobiliary Ultrasound: Pearls and Pitfalls

Participants Leslie M. Scoutt, MD, Essex, CT (*Presenter*) Speaker, Koninklijke Philips NV

For information about this presentation, contact:

leslie.scoutt@yale.edu

LEARNING OBJECTIVES

1) Discuss the ultrasound findings of acute cholecystitis. 2) Describe the ultrasound appearance of complicated or advanced cholecystitis. 3) Discuss the role of ultrasound in the evaluation of obstruction of the biliary track.

RC508B Pediatric Ultrasound

Participants Susan D. John, MD, Houston, TX ($\ensuremath{\textit{Presenter}}\xspace$) Nothing to Disclose

For information about this presentation, contact:

susan.d.john@uth.tmc.edu

LEARNING OBJECTIVES

1) Perform effective ultrasound examinations for pediatric gastrointestinal conditions. 2) Avoid pitfalls of US of the GI tract in children by using best practices. 3) Recognize potentially confusing US findings in various pediatric conditions.

RC508C Non-Obstetrical Gynecologic Ultrasound

Participants Ana P. Lourenco, MD, Foxboro, MA (*Presenter*) Nothing to Disclose

For information about this presentation, contact:

alourenco@lifespan.org

LEARNING OBJECTIVES

1) Detect a variety of causes of acute female pelvic pain at ultrasound, including but not limited to torsion, hemorrhagic cysts, pelvic inflammatory disease, ovarian hyperstimulation, IUD complications, as well as various non-gynecologic etiologies. 2) Describe potential sonographic pearls and pitfalls in gynecologic ultrasound.





Useful Applications of Gastrointestinal Tract Imaging

Wednesday, Dec. 4 8:30AM - 10:00AM Room: S402AB

GI

AMA PRA Category 1 Credits ™: 1.50 ARRT Category A+ Credit: 1.75

Sub-Events

RC509A Esophageal Imaging: GERD and Beyond

Participants David J. Disantis, MD, Jacksonville, FL (*Presenter*) Nothing to Disclose

For information about this presentation, contact:

djdisantis@gmail.com

LEARNING OBJECTIVES

1) Perform a dual phase esophagram. 2) Recognize the types of pathology that can be diagnosed with esophagography.

ABSTRACT

Swallowing studies and esophagrams remain the most frequently performed gastrointestinal fluoroscopic studies. This presentation offers a step-by-step guide for performing a high quality dual phase esophagram, with examples of the types of pathology that can be detected using these techniques.

RC509B Imaging Following Bariatric Procedures

Participants

Laura R. Carucci, MD, Midlothian, VA (Presenter) Nothing to Disclose

For information about this presentation, contact:

laura.carucci@vcuhealth.org

LEARNING OBJECTIVES

1) Recognize the expected postoperative radiologic appearance following commonly performed bariatric surgical procedures for morbid obesity, in particular the Roux-en-Y gastric bypass, gastric band and gastric sleeve. 2) Describe and recognize common complications and potential pitfalls on imaging studies following these bariatric procedures.

RC509C State-of-the-Art MR Enterography

Participants

Seong Ho Park, MD, Seoul, Korea, Republic Of (Presenter) Research Grant, Central Medical Service Co, Ltd

For information about this presentation, contact:

parksh.radiology@gmail.com

LEARNING OBJECTIVES

1) Explain how to obtain MR enterography images with adequate quality. 2) Describe MR enterography findings in Crohn's patients according to current interpretive guidelines.

RC509D Optimizing Your CT Colonography Service

Participants

Judy Yee, MD, Bronx, NY (*Presenter*) Research Grant, EchoPixel, Inc; Research Grant, Koninklijke Philips NV; Research Grant, General Electric Company

For information about this presentation, contact:

jyee@montefiore.org

LEARNING OBJECTIVES

1) Compare CT colonography to other colorectal cancer screening tests. 2) Understand the latest techniques for performing low radiation dose CT colonography. 3) Identify methods for time-efficient interpretation. 4) Describe the current status of CT colonography for colorectal cancer screening and diagnosis.





Ultrasound in the First Trimester of Pregnancy

Wednesday, Dec. 4 8:30AM - 10:00AM Room: S401CD



AMA PRA Category 1 Credits ™: 1.50 ARRT Category A+ Credit: 1.75

LEARNING OBJECTIVES

1) Describe the typical appearances of a tubal ectopic pregnancy. 2) List findings that suggest an interstitial ectopic pregnancy. 3) Differentiate a spontaneous abortion in progress from a cervical ectopic pregnancy. 4) Recommend the appropriate follow up for early pregnancies of unknown location (PUL) identified on transvaginal sonography. 5) Differentiate with certainty a failed pregnancy from a pregnancy suspicious for but not diagnostic of failed pregnancy based on the sonographer finding. 6) Diagnose ectopic pregnancy and identify its location. 7) Recognize normal fetal anatomy in the first trimester and differentiate the normal fetus from an abnormal fetus. 8) Predict the sex of the developing fetus during the first trimester and understand the importance of sex determination in some conditions. 9) Recognize 'must know' major anomalies evident in first trimester. 10) Understand the role of first trimester sex designation. 11) Evaluate first trimester assessment of multiple pregnancies.

Sub-Events

RC510A Ectopic Pregnancy

Participants Mindy M. Horrow, MD, Philadelphia, PA (*Presenter*) Spouse, Employee, Merck & Co, Inc

For information about this presentation, contact:

horrowm@einstein.edu

LEARNING OBJECTIVES

1) Describe the typical appearances of a tubal ectopic pregnancy. 2) List findings that suggest an interstitial ectopic pregnancy. 3) Differentiate a spontaneous abortion in progress from a cervical ectopic pregnancy.

RC510B Abnormal Early Intrauterine Pregnancies

Participants Carol B. Benson, MD, Boston, MA (*Presenter*) Nothing to Disclose

For information about this presentation, contact:

cbenson@bwh.harvard.edu

LEARNING OBJECTIVES

1) Recommend the appropriate follow up for early pregnancies of unknown location (PUL) identified on transvaginal sonography. 2) Differentiate with certainty a failed pregnancy from a pregnancy suspicious for but not diagnostic of failed pregnancy based on the sonographer finding. 3) Diagnose ectopic pregnancy and identify its location. 4) Recognize normal fetal anatomy in the first trimester and differentiate the normal fetus from an abnormal fetus. 5) Predict the sex of the developing fetus during the first trimester and understand the importance of sex determination in some conditions.

ABSTRACT

During this session, findings in early pregnancy on transvaginal ultrasound will be discussed including pregnancies of unknown location (PUL), intrauterine pregnancies of uncertain viability (IPUV), and ectopic pregnancy. Criteria for definitive diagnosis of failed pregnancy will be reviewed, as will sonographic findings suspicious for but not diagnostic of failed pregnancy. Diagnosis of ectopic pregnancy will be discussed, including sonographic findings and determination of the location of the ectopic pregnancy. In addition, sonographic evaluation of the fetus during the first trimester will be presented with attention to the early diagnosis of some fetal malformation and the importance of sex determination for some conditions.

Active Handout:Carol Beer Benson

http://abstract.rsna.org/uploads/2019/18000742/Active RC510B.pdf

RC510C First Trimester Anomalies, Sex, and Other Things

Participants Kalesha Hack, MD, FRCPC, Toronto, ON (*Presenter*) Nothing to Disclose

For information about this presentation, contact:

kalesha.hack@sunnybrook.ca

LEARNING OBJECTIVES

1) Recognize 'must know' major anomalies evident in first trimester. 2) Understand the role of first trimester sex designation. 3) Evaluate first trimester assessment of multiple pregnancies.

ABSTRACT

This refresher course will review the major anomalies which must be recognized in the later half of first trimester. We will also discuss the role of assessment of external genitalia in first trimester and what key features should be documented in the assessment in twin gestation.





Update on Radionuclide Therapies

Wednesday, Dec. 4 8:30AM - 10:00AM Room: S504CD



AMA PRA Category 1 Credits ™: 1.50 ARRT Category A+ Credit: 1.75

FDA Discussions may include off-label uses.

Sub-Events

RC511A New Guidelines for I-131 Therapy of Thyroid Cancer

Participants Don C. Yoo, MD, Lexington, MA (*Presenter*) Consultant, inviCRO, LLC

For information about this presentation, contact:

donyoo@brown.edu

LEARNING OBJECTIVES

1) Describe why thyroid cancer is increasing. 2) Review guidelines for the use of I-131 in the treatment of thyroid cancer. 3) Review the controversies in thyroid cancer treatment.

ABSTRACT

The purpose of this educational activity is to review the reasons why the incidence of thyroid cancer has risen so rapidly over the last 40 years and discuss the role of radioiodine ablation in patients with thyroid cancer. Issues that will be discussed include controversies in the extent of thyroid surgery and the appropriate use of radioiodine ablation in patients with thyroid cancer which is controversial in low risk and intermediate risk patients. The incidence of thyroid cancer in the United States has almost tripled since the early 1970s with unchanged mortality principally due to overdiagnosis. The extent of surgery performed for thyroid cancer is controversial especially in small cancers but only patients with complete thyroidectomy are candidates for radioiodine ablation. Recently lower doses of I-131 have been shown to be effective for radioiodine ablation of remnant thyroid tissue after thyroidectomy. High risk patients will benefit from radioiodine ablation with decreased recurrence and improved mortality. Radioiodine ablation in low risk patients is very controversial and has not been shown to improve mortality.

RC511B Lu177-DOTATATE Therapy for Neuroendocrine Tumors

Participants

Erik S. Mittra, MD, PhD, Portland, OR (Presenter) Nothing to Disclose

LEARNING OBJECTIVES

1) Understand the background and role of Peptide Receptor Radionuclide Therapy (PRRT) for neuroendocrine tumors (NETs). 2) Review the latest publications on the subject. 3) Understand how to perform this therapy and future directions.

RC511C Hepatic Artery Infusion Therapy with Y90 Microspheres

Participants

Charles Y. Kim, MD, Raleigh, NC (Presenter) Consultant, Medtronic plc; Consultant, Humacyte; Consultant, Galvani

LEARNING OBJECTIVES

1) Review range of malignancies treated with Y90 microsphere infusion. 2) Discuss the types of Y90 therapy and dosimetric considerations. 3) Describe the procedures and technical steps involved in Y90 therapy. 4) Recognize pertinent scintigraphic findings associated with Y90 therapy.

ABSTRACT

Intra-arterial Yttrium-90 (Y90) therapy is an important treatment modality for a variety of hepatic tumors. While numerous types of embolotherapies are employed by interventional radiologists for treatment of cancer, Y90 therapy is unique in its multimodality and multi-procedural nature. Not only does this treatment effect rely on deposited ionizing radiation therapy, but scintigraphic imaging is also an integral component of treatment. Two types of Y90 therapies are available, made by two different manufacturers. The differences between the two types are subtle, but there are differences in administration and manufacturer-recommended dosimetric calculation. These various differences will be highlighted. Y90 therapy is comprised of several steps and is frequently subclassified into a 'planning' phase and 'treatment' phase. In the planning phase, detailed angiographic imaging is performed to delineate arterial anatomy , determine tumoral distributions, and redistribute vascular flow if indicated. Scintigraphic imaging is an integral component of this planning phase, in order to help identify angiographically occult arterial anomalies, confirm appropriate infusion site, and to quantify the hepatopulmonary shunt fraction. From this information, as well as other factors, the appropriate treatment doses can be determined. In the treatment phase(s), the Y90 dose is administered to the appropriate portions of the liver with subsequent scintigraphic imaging for confirmation.





Vascular Series: MR Angiography-New Techniques and Their Application

Wednesday, Dec. 4 8:30AM - 12:00PM Room: S503AB



AMA PRA Category 1 Credits ™: 3.00 ARRT Category A+ Credits: 3.50

FDA Discussions may include off-label uses.

Participants

Thomas K. Foo, PhD, Niskayuna, NY (Moderator) Employee, General Electric Company

Martin R. Prince, MD,PhD, New York, NY (*Moderator*) Patent agreement, General Electric Company; Patent agreement, Hitachi, Ltd; Patent agreement, Siemens AG; Patent agreement, Koninklijke Philips NV; Patent agreement, Nemoto Kyorindo Co, Ltd; Patent agreement, Bayer AG; Patent agreement, Lantheus Medical Imaging, Inc; Patent agreement, Bracco Group; Patent agreement, Mallinckrodt plc; Patent agreement, Guerbet SA; Patent agreement, Toshiba Corporation

Tim Leiner, MD, PhD, Utrecht, Netherlands (Moderator) Speakers Bureau, Koninklijke Philips NV Research Grant, Bayer AG

For information about this presentation, contact:

map2008@med.cornell.edu

thomas.foo@ge.com

LEARNING OBJECTIVES

1) Understand the latest MR Angiography methods. 2) Identify optimal approaches to using MR Angiography techniques throughout the body. 3) Appraise the strengths and weaknesses of various MR approaches to vascular imaging.

Sub-Events

RC512-01 K-Space Options for Improving MRA

Wednesday, Dec. 4 8:30AM - 9:00AM Room: S503AB

Participants

Walter F. Block, PhD, Madison, WI (*Presenter*) Stockholder and Co-founder, TherVoyant; Research support, General Electric Company;

For information about this presentation, contact:

wfblock@wisc.edu

LEARNING OBJECTIVES

1) Understand basic strategies used in MR Angiography to subsample the MR raw data space (k-space) to improve the temporal and spatial performance parameters of MRA. 2) Learn how spatial resolution, temporal resolution, and SNR performance are linked. 3) Learn the difference between an acquisition method's temporal footprint and temporal frame rate.

ABSTRACT

MR Angiography is hampered by MR's need to acquire data in an alternative domain (k-space) with a relative lack of sensors (receivers) relative to CT and US, where thousands of detectors can be active at once. To capture the human vascular system at the temporal and spatial resolution necessary to answer important diagnostic questions, clinical MRA pulse sequences sub-sample the k-space acquisition space in a myriad of ways that tradeoff performance in spatial resolution, temporal resolution, and SNR. The presentation will highlight the general classes of these methodologies, which usually acquire lower spatial frequency data more often than higher spatial frequencies (variable k-space density). Often these k-space acquisition strategies are paired with a reconstruction methodology that iteratively works to generate the mostly likely image reconstruction possible for the given subsampled k-space data. The presentation will discuss the assumptions that all these methodologies make and ways physicians can assess the effects these assumptions may make on clinical decision-making.

RC512-02 Added Value of MRI-Based Vascular Calcification Visualization for the Assessment of Arterial Stenosis in Patients with Lower-Extremity Peripheral Artery Disease Undergoing Non-Contrast Quiescent Interval Slice-Selective (QISS) MRA

Wednesday, Dec. 4 9:00AM - 9:10AM Room: S503AB

Participants

Akos Varga-Szemes, MD, PhD, Charleston, SC (*Presenter*) Research Grant and Travel Support, Siemens AG Research Consultant, Elucid Bioimaging

Megha Penmetsa, Charleston, SC (Abstract Co-Author) Nothing to Disclose

Thomas M. Todoran, MD, Charleston, SC (*Abstract Co-Author*) Research Consultant, Medtronic plc; Research Consultant, General Electric Company

Pal Suranyi, MD, PhD, Charleston, SC (*Abstract Co-Author*) Nothing to Disclose Stephen R. Fuller, Charleston, SC (*Abstract Co-Author*) Nothing to Disclose Andreas Fischer, MD, Charleston, SC (*Abstract Co-Author*) Nothing to Disclose Robert R. Edelman, MD, Evanston, IL (*Abstract Co-Author*) Research support, Siemens AG; Royalties, Siemens AG Ioannis Koktzoglou, PhD, Evanston, IL (*Abstract Co-Author*) Research support, Siemens AG U. Joseph Schoepf, MD, Charleston, SC (*Abstract Co-Author*) Research Grant, Astellas Group; Research Grant, Bayer AG; Research Grant, Bracco Group; Research Grant, Siemens AG; Research Grant, Heartflow, Inc; Research support, Bayer AG; Consultant, Elucid BioImaging Inc; Research Grant, Guerbet SA; Consultant, HeartFlow, Inc; Consultant, Bayer AG; Consultant, Siemens AG; ; ;

For information about this presentation, contact:

schoepf@musc.edu

PURPOSE

This study sought to investigate the added value of prototype proton density weighted, in-phase 3D stack-of-stars (PDIP-SOS) MRI-based calcification visualization on the diagnostic accuracy of detecting peripheral artery disease (PAD) using non-contrast quiescent interval slice-selective (QISS) MRA.

METHOD AND MATERIALS

Twenty-six patients (70±8 years) with suspected PAD, referred for lower extremity CTA prior to digital subtraction angiography (DSA), were prospectively enrolled for a same-day 1.5T or 3T MRI. PDIP-SOS MRI and QISS MRA were acquired covering the iliofemoral run-off. Two readers rated image quality (4-point scale) and graded stenosis (>=50%) on QISS-MRA without and with the visualization of calcification. Sensitivity and specificity were calculated using DSA as reference. Intra-arterial calcium was quantified using ImageJ (NIH) and compared between MRI and non-contrast CT (NCCT) using paired t-test, Pearson's correlation and Bland-Altman analysis.

RESULTS

Overall subjective image quality ratings were significantly higher for CTA compared to MRA (4.0 [3.0-4.0] and 3.0 [3.0-4.0]; p=0.0369) with good to excellent inter-reader agreement (all ICCs >0.746). The sensitivity and specificity of QISS MRA, QISS MRA with PDIP-SOS, and CTA for the detection of >=50% stenosis were 85.4%, 92.2%, 90.2% and 90.3%, 93.2%, 94.2%, respectively. Calcification was visualized by PDIP-SOS and NCCT in 123 (59.4%) and 126 (60.8%) vascular segments, respectively (p=0.2500). Quantification of calcification showed statistically significant differences between PDIP-SOS and NCCT (80.6±31.2mm3 vs 88.0±29.8mm3; p=0.0002) with high correlation (r=0.77, p<0.0001) and moderate mean of differences (-7.4mm3) between the techniques.

CONCLUSION

PDIP-SOS MRI increases the accuracy of non-contrast QISS MRA in patients evaluated for PAD. This combined protocol may prove especially useful for the comprehensive assessment of vascular anatomy prior to interventional procedure planning.

CLINICAL RELEVANCE/APPLICATION

The visualization and quantification of vascular calcification by MRI may prove especially useful for the comprehensive assessment of vascular anatomy prior to interventional procedure planning.

RC512-03 Radial Self-Navigated Native MRA in Comparison to Conventional Navigator-Gated Contrast-Enhanced MRA of the Thoracic Aorta in an Aortic Patient Collective

Wednesday, Dec. 4 9:10AM - 9:20AM Room: S503AB

Participants

Martina Roxane Correa Londono, MD, Bern, Switzerland (*Presenter*) Nothing to Disclose Verena Obmann, MD, Cleveland Heights, OH (*Abstract Co-Author*) Nothing to Disclose Nino Trussardi, Bern, Switzerland (*Abstract Co-Author*) Nothing to Disclose Davide Piccini, Erlangen, Germany (*Abstract Co-Author*) Employee, Siemens AG Michael Ith, Bern, Switzerland (*Abstract Co-Author*) Nothing to Disclose Hendrik von Tengg-Kobligk, MD, Bern, Switzerland (*Abstract Co-Author*) Research Grant, W. L. Gore & Associates, Inc Bernd Jung, Freiburg, Germany (*Abstract Co-Author*) Nothing to Disclose

For information about this presentation, contact:

martina.correa-londono@insel.ch

PURPOSE

The non-enhanced balanced steady state with free precession MRA technique has been shown to provide high diagnostic image quality of thoracic aortic disease.

METHOD AND MATERIALS

In this retrospective study, 92 patients were enrolled, 31 patients received a native MRA (mean age 63.9 years) and 61 patients a CE-MRA (mean age 63.1 years). Scan time was recorded and image quality with respect to vessel contrast, vessel sharpness and artifact level was assessed in three thoracic aortic segments: aortic root/ascending aorta, aortic arch and descending aorta. Imaging protocol: Native MRA based on an ECG-triggered self-navigated prototype 3D radial bSSFP sequence (TE=1.83 ms; TR=3.6 ms) was acquired with an inherent isotropic FOV of 250 mm and spatial resolution of 1.3 mm. A ECG-triggered first-pass CE-MRA (TE=1.33 ms; TR=3.4 ms) with navigator respiration control was acquired with a FOV of $340 \times 255 \times 83$ mm and a spatial resolution of $1.4 \times 1.3 \times 1.3$ mm with 0.1 ml/kg body weight gadobenate dimeglumine at a flow rate of 0.4 ml/s. To measure the inter-rater agreement the weighted Cohen's kappa coefficient (κ) was calculated. To assess statistical differences between the two MRA sequences, first the Fisher's Exact test and than the Mann-Whitney-U test were applied.

RESULTS

The overall diagnostic image quality of native MRA was superior at all areas analyzed, compared to the CE-MRA (p<0.001, p<0.001, p=0.005, respectively). A detailed analysis of how the presence of foreign materials like sternal cerclage or artificial heart valves deteriorates image quality for different MRA methods is of interest for future analysis. Scan time of the non CE-MRA was significantly reduced, mean 05:56 ±01:32 min vs. 08:51± 02:57 min in the CE-MRA (p<0.001).

CONCLUSION

In conclusion diagnostic image quality of the entire thoracic aorta including the aortic root can be obtained without administration of contrast media offering a benefit in potential side effects of contrast media, especially in patients with impaired renal function or by avoiding deposition of Gd in the body in general. In addition this superior image quality is gained within a faster scan time, a valuable feature in daily radiological routine.

CLINICAL RELEVANCE/APPLICATION

Superior diagnostic image quality of the entire thoracic aorta can be obtained without contrast media and within a faster scan time, a highly valuable feature in daily routine.

RC512-04 Reproducibility of High-Resolution DANTE-Prepared 3D FLASH MRI in Serial Studies of Atherosclerotic Femoral Arteries

Wednesday, Dec. 4 9:20AM - 9:30AM Room: S503AB

Participants

Yuting Wang, Chengdu, China (*Presenter*) Nothing to Disclose Xinke Liu, Beijing, China (*Abstract Co-Author*) Nothing to Disclose Henrik Haraldsson, PhD, San Francisco, CA (*Abstract Co-Author*) Nothing to Disclose Chengcheng Zhu, San Francisco, CA (*Abstract Co-Author*) Nothing to Disclose Megan Ballweber, San Francisco, CA (*Abstract Co-Author*) Nothing to Disclose Warren J. Gasper, San Francisco, CA (*Abstract Co-Author*) Nothing to Disclose David A. Saloner, PhD, San Francisco, CA (*Abstract Co-Author*) Nothing to Disclose

For information about this presentation, contact:

wangyuting_330@163.com

PURPOSE

To evaluate the reproducibility of high-resolution MR imaging of atherosclerotic femoral arteries in serial follow-up scans, and calculate the sample size needed for future longitudinal studies.

METHOD AND MATERIALS

Ten patients with known femoral artery atherosclerosis were imaged with a 3D isotropic FLASH sequence with DANTE-prepared black blood contrast. Studies were acquired at baseline, within 1 week and 1 month. Five of these patients were also scanned at 6 months. Using internal fiducials strict registration of arterial segment levels was obtained. Total vessel area, lumen area, wall area and wall volume were measured to assess atheroma in the wall. Measurements were compared among the scans repeated at different timepoints. Agreement was measured by the intraclass correlation coefficient (ICC). Measurement error was quantified by pairwise slice-based/ patient-based coefficient of variance (CV) as defined by pooled variance/mean. Sample sizes needed to detect 5% and 10% changes in vessel area/volume were calculated using 80% power and 5% significance level.

RESULTS

The measurement of vessel area, lumen area, wall area and wall volume showed excellent agreement among repeated scans, with ICCs ranging from 0.97 to 0.99 for 3 scans, and 0.96 to 0.99 for 4 scans. Relatively small interscan measurement errors were observed. The slice-based CVs for the vessel area, lumen area and wall area were 5.0%, 6.8%, 8.4%, and the patient-based CV for volume measurement was 5.9% among 3 scans. Similar results were observed for patients who had 4 scans, with above-mentioned CVs of 5.5%, 6.6%, 9.4% and 7.2% respectively. These results indicate to compare treatment efficacy for two strategies for treatment of femoral artery atherosclerosis, it would be necessary to recruit 89 subjects if differences in wall area/volume changes were 5%, and 22 subjects if the differences were 10%.

CONCLUSION

High resolution DANTE-FLASH MRI is useful for quantifying atherosclerotic vessel area and volume of femoral arteries with low variability among serial repeated scans. Volume measurement tends to be more reproducible than vessel wall area measurements.

CLINICAL RELEVANCE/APPLICATION

High resolution DANTE-FLASH MRI is useful for quantifying atherosclerotic vessel area and volume of femoral arteries, and measuring the corresponding changes due to therapeutic effects.

RC512-05 4D Flow MRA

Wednesday, Dec. 4 9:30AM - 10:00AM Room: S503AB

Participants

Shreyas S. Vasanawala, MD, PhD, Palo Alto, CA (*Presenter*) Research collaboration, General Electric Company; Consultant, Arterys Inc; Consultant, Inkspace; Research Grant, Bayer AG;

LEARNING OBJECTIVES

1) To know components required to implement clinically 4D flow. 2) To know types of clinically relevant data that can be extracted from 4D flow. 3) Become familiar with applications of 4D flow for MRA.

ABSTRACT

4D flow is a time resolved volumetric phase contrast MRI technique. This presentation will cover essential components required to implement 4D flow in a clinical setting, review types of clinically relevant data that can be extracted from 4D flow, and present several approaches to integrating 4D flow into clinical MRI protocols. Essential components include a pulse sequence and postprocessing software. Data that can be extracted includes blood flow, cardiovascular function, and anatomy. Protocols can be greatly simplified with 4D flow, enabling a decoupling of image acquisition and interpretation, thereby enhancing efficiency of patient, technologist, and radiologist time. Representative thoracic and abdominal applications will be presented.

RC512-06 Non-Contrast MRA

Wednesday, Dec. 4 10:30AM - 11:00AM Room: S503AB

Participants

Robert R. Edelman, MD, Evanston, IL (Presenter) Research support, Siemens AG; Royalties, Siemens AG

For information about this presentation, contact:

redelman999@gmail.com

LEARNING OBJECTIVES

1) Explore rationale for non-contrast MR angiography. 2) Discuss techniques for optimized non-contrast MR-based vascular imaging in clinical practice, including advantages and limitations. 3) Review current evidence for clinical utility in comparison to contrast-enhanced MRA and CT angiography.

ABSTRACT

Non-contrast MRA techniques offer a viable alternative to CTA and contrast-enhanced MRA (CEMRA) for cross-sectional vascular imaging without the risks or costs associated with contrast agent administration. They can evaluate the renal and peripheral arteries with image quality and accuracy that is competitive with CTA. Recently developed non-contrast neurovascular imaging techniques can substantially outperform legacy 2D and 3D time-of-flight MRA, providing image quality that approaches that of CEMRA. In addition to the use of non-contrast MRA for depiction of the vascular lumen, high-resolution non-Cartesian 3D MRI can now show vessel wall calcifications comparably to CT. This information (hitherto unavailable using MRI) can be critical to the planning of interventional vascular procedures. The anatomic information provided by non-contrast MRA can also be efficiently complemented with hemodynamic information that is not available from CTA using phase contrast and ASL-based approaches.

RC512-07 Free-Breathing Fast Low-Angle Shot Quiescent-Interval Slice-Selective MR Angiography for Improved Detection of Vascular Stenoses in the Pelvis and Abdomen

Wednesday, Dec. 4 11:00AM - 11:10AM Room: S503AB

Participants

Akos Varga-Szemes, MD, PhD, Charleston, SC (*Presenter*) Research Grant and Travel Support, Siemens AG Research Consultant, Elucid Bioimaging

Emily A. Aherne, MBBCh, FFR(RCSI), New York, NY (Abstract Co-Author) Nothing to Disclose

U. Joseph Schoepf, MD, Charleston, SC (*Abstract Co-Author*) Research Grant, Astellas Group; Research Grant, Bayer AG; Research Grant, Bracco Group; Research Grant, Siemens AG; Research Grant, Heartflow, Inc; Research support, Bayer AG; Consultant, Elucid BioImaging Inc; Research Grant, Guerbet SA; Consultant, HeartFlow, Inc; Consultant, Bayer AG; Consultant, Siemens AG; ; ; Thomas M. Todoran, MD, Charleston, SC (*Abstract Co-Author*) Research Consultant, Medtronic plc; Research Consultant, General Electric Company

Ioannis Koktzoglou, PhD, Evanston, IL (Abstract Co-Author) Research support, Siemens AG

Robert R. Edelman, MD, Evanston, IL (Abstract Co-Author) Research support, Siemens AG; Royalties, Siemens AG

For information about this presentation, contact:

redelman999@gmail.com

PURPOSE

Balanced steady-state free precession (bSSFP)-based quiescent-interval slice-selective (QISS) magnetic resonance angiography (MRA) is accurate for the non-contrast evaluation of peripheral artery disease (PAD); however, drawbacks include the need for breath-holding and sensitivity to off-resonance artifacts. The purpose of this study was to evaluate the image quality and diagnostic accuracy in the pelvis and abdomen of free-breathing fast low-angle shot (FLASH)-based QISS techniques in comparison to standard QISS in patients with PAD, using computed tomographic angiography (CTA) as the reference.

METHOD AND MATERIALS

Twenty-seven patients (69±10 years, 17 men) with PAD were enrolled in this IRB approved, HIPAA compliant prospective study between April and December 2018. Patients underwent non-contrast MRA using standard bSSFP-based QISS and prototype free-breathing radial-FLASH and Cartesian-FLASH-based QISS at 3T. A subset of patients (n=22) also underwent CTA as the reference standard. Nine arterial segments per patient were evaluated spanning the abdomen, pelvis, and upper thigh regions. Objective (signal intensity ratio (SIR) and relative standard deviation (SD)) and subjective image quality (4-point scale) and stenosis (>50%) were evaluated by two readers and compared using one-way analysis of variance, Wilcoxon and McNemar tests, respectively.

RESULTS

A total of 179 vascular segments were available for analysis by all QISS techniques. No significant difference was observed among bSSFP, radial-FLASH, and Cartesian-FLASH-based techniques in SIR (p=0.428) and relative SD (p=0.220). Radial-FLASH-based QISS demonstrated the best image quality (p<0.0001) and the highest inter-reader agreement ($\kappa=0.721$). The sensitivity values of bSSFP, radial-FLASH, and Cartesian-FLASH-based QISS for the detection of >50% stenosis were 76.0%, 84.0%, and 80.0%, respectively, while specificity values were 97.6%, 94.0%, and 92.8%, respectively. Moreover, FLASH-based QISS consistently reduced off-resonance artifacts compared to the bSSFP-based approach.

CONCLUSION

Free-breathing FLASH-based QISS MRA techniques provide improved image quality and sensitivity, high specificity, and reduced offresonance artifacts for vascular stenosis detection in the abdomen and pelvis.

CLINICAL RELEVANCE/APPLICATION

FLASH-based QISS MRA provides improved image quality, accuracy and reduced off-resonance artifacts, thereby enhancing the utility of QISS for the non-contrast evaluation of PAD.

RC512-08 Advanced Fresh Blood Imaging (FBI) Using Centric ky-kz Trajectory with a New Exponential

Refocusing Flop Angle

Wednesday, Dec. 4 11:10AM - 11:20AM Room: S503AB

Participants

Mitsue Miyazaki, PhD, La Jolla, CA (*Presenter*) Employee, Canon Medical Systems Corporation Masaaki Umeda, Otawara, Japan (*Abstract Co-Author*) Employee, Canon Medical Systems Corporation Yoshimori Kassai, MS, Otawara, Japan (*Abstract Co-Author*) Employee, Canon Medical Systems Corporation Lijun Zhang, Beijing, China (*Abstract Co-Author*) Employee, Canon Medical Systems Corporation Cheng Ouyang, La Jolla, CA (*Abstract Co-Author*) Nothing to Disclose Sheronda Statum, La Jolla, CA (*Abstract Co-Author*) Nothing to Disclose Won C. Bae, PhD, La Jolla, CA (*Abstract Co-Author*) Nothing to Disclose Katsumi Nakamura, MD, Kitakyushu, Japan (*Abstract Co-Author*) Nothing to Disclose Christine B. Chung, MD, Solana Beach, CA (*Abstract Co-Author*) Nothing to Disclose

For information about this presentation, contact:

mimiyazaki@ucsd.edu

PURPOSE

To advance fresh blood imaging (FBI) in peripheral non-contrast MR angiography (NC-MRA) using a new centric ky-kz trajectory with an exponential flop angle to reduce specific absorption rate (SAR) and tremendous reduction in scan time.

METHOD AND MATERIALS

FBI utilizes a physiological signal difference between systolic and diastolic triggered images. The centric ky-kz trajectory is implemented in FBI (cFBI), acquiring multiple slice-encodings (SEs) and phase-encodings (PEs) per TR; whereas, standard FBI acquires one SE per TR. By applying exponential flop angle (eFA), cFBI enables reduction of SAR. The design of eFA has high flop angles (Hflop) at the center of k space (about 36 lines or more) for bright blood imaging and exponentially decreasing flop angles at periphery of k space to reduce SAR. Having about 36-line Hflop of 180 deg is required to ensure depiction of bright blood; imaging of cFBI was performed maintaining Hflop and varying low flop angles (Lflop), Hflop/Lflop of 180/180, 180/90, 180/60, 180/30 and 180/1 deg. Parameters are: for all lower flop <180 (TR of 2RR intervals) and constant (180/180) flop (TR of 3RR intervals due to SAR), TEeff of 60 ms, 1NAQ, 320x320 matrix, 100 1.4-mm slices, FOV of 40x40 cm, parallel imaging of 3, and resolution of 0.63(PE)x0.63(RO)x 0.7(SE) mm after interpolation. All exteriments were performed using a 3T clinical system on healthy volunteers (5 males, 24-68 yo).

RESULTS

The scan time of cFBI was reduced to about 1/2 to 1/3 (1:30-2:00 min) by acquiring multiple SEs and PEs data compared to standard FBI. The Hflop/Lflop of 180/180 deg. causes lengthen of TR due to high SAR and longer scan time. Regarding artifacts, standard FBI often causes N/2 artifacts in the PE direction that degrade image quality; whereas, cFBI minimizes N/2 artifacts. As shown in Fig. 1, image quality of all 5 images was evaluated all 'excellent' without any N/2 artifacts.

CONCLUSION

Advanced cFBI with eFA enables high resolution quality NC-MRA images with fast acquisition without major artifacts like N/2 artifacts. Compared to standard FBI, cFBI reduces the scan time to 1/3 to 1/2, opening a possibility of scanning entire peripheral vasculature in 5 to 6 mins.

CLINICAL RELEVANCE/APPLICATION

This study demonstrates tremendous scan time reduction in centric ky-kz FBI (cFBI) with eFA compared to standard FBI. This advanced cFBI enables obtaining quality NC-MRA images without N/2 artifacts seen in standard FBI.

RC512-09 Low-Dose Contrast-Enhanced MR Angiography of the Lower Extremities at 3T with Dynamic 3 Station Imaging

Wednesday, Dec. 4 11:20AM - 11:30AM Room: S503AB

Participants

Guenther K. Schneider, MD, PhD, Homburg, Germany (*Abstract Co-Author*) Research Grant, Siemens AG; Speakers Bureau, Siemens AG; Speakers Bureau, Bracco Group; Research Grant, Bracco Group;

Tobias Woerner, MD, Homburg, Germany (Presenter) Nothing to Disclose

Arno Buecker, MD, Homburg, Germany (*Abstract Co-Author*) Consultant, Bracco Group Speaker, Bracco Group Consultant, Medtronic plc Speaker, Medtronic plc Research Grant, Novartis AG Research Grant, GlaxoSmithKline plc Research Grant, Biotest AG Research Grant, OncoGenex Pharmaceuticals, Inc Research Grant, Bristol-Myers Squibb Company Research Grant, Eli Lilly & Company Research Grant, Pfizer Inc Research Grant, F. Hoffmann-La Roche Ltd Research Grant, sanofi-aventis Group Research Grant, Merrimack Pharmaceuticals, Inc Research Grant, Sirtex Medical Ltd Research Grant, Concordia Healthcare Corp Research Grant, AbbVie Inc Research Grant, Takeda Pharmaceutical Company Limited Research Grant, Merck & Co, Inc Research Grant, Affimed NV Research Grant, Bayer AG Research Grant, Johnson & Johnson Research Grant, Seattle Genetics, Inc Research Grant, Onyx Pharmaceuticals, Inc Research Grant, Synta Pharmaceuticals Corp Research Grant, Siemens AG Research Grant, iSYMED GmbH Research Grant, Abbott Laboratories Co-founder, Aachen Resonance GmbH

Paul S. Raczeck, MD, Homburg, Germany (Abstract Co-Author) Nothing to Disclose

For information about this presentation, contact:

dr.guenther.schneider@uks.eu

PURPOSE

In our study we evaluated the diagnostic performance of lower extremity MR Angiography in patients with suspected lower limb atherosclerotic disease using a three-station dynamic MRA approach.

METHOD AND MATERIALS

10 consecutive adult nations perceptating diagnostic imaging of the lower limb arteries for suspected athemscleratic disease

underwent MRA at 3 T. Imaging was performed by acquiring a three-station dynamic MRA using a TWIST-sequence. For each station a 3ml contrast medium bolus (Gd-HP-DO3A / Prohance) was injected (1.5ml/sec) each followed by a 20 ml saline flush. Images were retrospectively reviewed and evaluated with regard to image quality and visualization of arterial segments; severity of stenosis; and presence of venous contamination. 16 patients underwent subsequent DSA yielding 256 artery segments for correlation between MRI and DSA.

RESULTS

Dynamic three station low dose CE-MRA at 3T allows for diagnostic, dynamic imaging in every vessel territory of the lower limb even in patients with advanced arteriosclerotic disease. Diagnostic performance based on the vessel segments both evaluated by CE MRA and DSA for > 50 % stenosis demonstrated a sensitivity of 93.55% [84.3 -98.2% (95%-CI)] and specifity of 98.51% [95.7-99.8%(95%-CI)] for CE-MRA; For vessel occlusion sensitivity was 93.1% [77.23 -99.15 % (95%-CI] and specifity of 99.13% [96.91 - 99.89%](95%-CI)]. No studies were rated non-diagnostic due to venous overlay, since always an optimal 3D-dataset from dynamic imaging could be chosen.

CONCLUSION

With a total of only 9 ml ProHance (corresponding to 0.05 mmol/kg BW in a 90 kg patient resp. 0.06 mmol/kg in a 75 kg patient) three station dynamic CE MRA of the lower extremity is possible.Advantages of this approach include the possibility to look at the optimal time of arterial enhancement of each leg separately and the possibility of avoiding venous contamination of images. Time for each dataset typically is approximately 5 sec. to allow for a high enough spatial resolution, nevertheless this temporal resolution is enough to achieve a solely arterial image.

CLINICAL RELEVANCE/APPLICATION

Regarding the discussion on safety of Gd-based contrast agents the lowest possible dose should be used in any indication for CE MRI. Our study shows the feasibility of low dose CE MRA with a macrocyclic contrast agent only using a total of 9 ml of a 0.5 M contrast agent for the evaluation of the complete run-off vessels.

RC512-10 Phase Contrast MRA: Technology Advances and Impact of High Performance Gradients

Wednesday, Dec. 4 11:30AM - 12:00PM Room: S503AB

Participants

Thomas K. Foo, PhD, Niskayuna, NY (Presenter) Employee, General Electric Company

For information about this presentation, contact:

thomas.foo@ge.com

LEARNING OBJECTIVES

1) To know the impact on gradient performance on phase-contrast velocity imaging 2) To know how phase-velocity noise, vascular signal-to-noise ratio, and sequence echo time (TE) impacts the measurement of flow volume 3) To know how high-performance gradients with 3-4x the maximum gradient amplitude and 2.5-4.0x the maximum slew rate impacts phase-contrast MRA and 4D Flow.

ABSTRACT

With increasing capability in gradient amplitude to 80 mT/m, the echo time (TE) can be reduced. However, in whole-body systems, there is still a limitation of peripheral nerve stimulation as to how fast the gradient amplitudes can be switched. With the development of new high-performance head-only gradient systems, maximum gradient amplitudes of 3-4x and maximum slew rates of 2.5-4.0x can be achieved. This benefits phase-contrast MRA, especially for low-velocity encoding values (VENC) for slow flow, as in the CSF.





Pediatric Series: Pediatric Radiology

Wednesday, Dec. 4 8:30AM - 12:00PM Room: S405AB



AMA PRA Category 1 Credits ™: 3.25 ARRT Category A+ Credits: 4.00

FDA Discussions may include off-label uses.

Participants

Heather J. Bray, MD, Vancouver, BC (*Moderator*) Nothing to Disclose Ibtissem Bellagha SR, MD, El Manar, Tunisia (*Moderator*) Nothing to Disclose Nancy R. Fefferman, MD, New York, NY (*Moderator*) Nothing to Disclose Paul S. Babyn, MD, Saskatoon, SK (*Moderator*) Nothing to Disclose

Sub-Events

RC513-01 Imaging of Pediatric Breast Masses

Wednesday, Dec. 4 8:30AM - 8:50AM Room: S405AB

Participants Teresa Chapman, MD,MA, Seattle, WA (*Presenter*) Nothing to Disclose

For information about this presentation, contact:

Teresa.chapman@seattlechildrens.org

LEARNING OBJECTIVES

1) Recognize normal glandular tissue of the pediatric patient. 2) Apply appropriate management recommendations to breast ultrasound findings of a girl with a palpable abnormality. 3) Provide an appropriate differential diagnosis for a solid tissue finding in the pediatric breast.

RC513-02 Findings on Serial MRI Following Esophageal Button Battery Removal: Correlation with Clinical Outcomes

Wednesday, Dec. 4 8:50AM - 9:00AM Room: S405AB

Participants

Erica Riedesel, MD, Atlanta, GA (*Presenter*) Nothing to Disclose Matthew Santore, MD, Atlanta , GA (*Abstract Co-Author*) Nothing to Disclose Carey G. Sauer, MD, Atlanta , GA (*Abstract Co-Author*) Nothing to Disclose Ann Schecter, MD, Atlanta , GA (*Abstract Co-Author*) Nothing to Disclose Edward J. Richer, MD, Atlanta, GA (*Abstract Co-Author*) Nothing to Disclose Adina L. Alazraki, MD, Atlanta, GA (*Abstract Co-Author*) Nothing to Disclose

For information about this presentation, contact:

erica.riedesel@choa.org

PURPOSE

Recent reports of increased morbidity and mortality in pediatric patients following esophageal button battery impaction have prompted national clinical practice guidelines from NASPGHAN which advocate use of cross-sectional imaging to assess for associated vascular or airway injury. The purpose of this study is to review serial MRI findings following endoscopic removal of esophageal button battery.

METHOD AND MATERIALS

Radiology reports from 2018 were searched for terms 'battery' and 'button battery.' Patient demographics, endoscopic findings, imaging, and clinical follow-up were reviewed in EMR. Focused evaluation of MRI findings was performed by 4 attending pediatric radiologists.

RESULTS

12 patients with MRI following endoscopic removal of esophageal battery per NASPGHAN guidelines were identified with a total of 31 MRI studies. Esophageal mucosal injury and submucosal edema/enhancement was seen on initial MRI in all cases regardless of level of esophageal injury or time of battery exposure. Mucosal findings were persistent on serial MRI in all but 2 cases. Esophageal findings on MRI were concordant with esophagram in all cases. Extensive mediastinal edema was seen on initial MRI in all cases and persistent on serial MRI. Vascular and airway changes were seen on initial MRI in 71% (5/7) of patients with proximal esophageal injury with resolution on serial MRI. 1 patient developed contained esophageal leak. No patients developed tracheoesophageal (TE) or aortoenteric (AE) fistula.

Extensive mediastinal edema was seen in all cases following button battery removal, suggesting this finding alone carries little sensitivity or specificity. Structural changes to mediastinal vessels and airway, reported to implicate higher risk of developing TE and AE fistula, were seen in all cases of proximal esophageal injury, however resolved on serial MRI and no pateints in our cohort developed these complications.

CLINICAL RELEVANCE/APPLICATION

Recent NASPGHAN guidelines advocate use of cross-sectional imaging following button battery ingestion, however little has been reported on clinical impact of imaging findings. This is the largest cohort of patients with serial MRI following esophageal button battery removal to be reported, however our study remains limited by small sample size. Further multiinstitutional and multidisciplinary studies are needed to correlate clinical and imaging findings to further guide practices.

RC513-03 Role of Imaging in Evaluating the Complications of Hematopoietic Stem Cell Transplantation in Pediatric Patients in an Indian Setup

Wednesday, Dec. 4 9:00AM - 9:10AM Room: S405AB

Participants

Murali K. Logudoss, MBBS, MD, Chennai, India (*Presenter*) Nothing to Disclose Rasheed Arafath, MBBS, Chennai, India (*Abstract Co-Author*) Nothing to Disclose Amarnath Chellathurai, MD, FRCR, Chennai, India (*Abstract Co-Author*) Nothing to Disclose Rakesh Prasad, DMRD, MBBS, Chennai, India (*Abstract Co-Author*) Nothing to Disclose Anand N. Parimalai, MD, Chennai , India (*Abstract Co-Author*) Nothing to Disclose Shilpa Vijayasekar, MBBS, Chennai, India (*Abstract Co-Author*) Nothing to Disclose

For information about this presentation, contact:

drlmkmdrd@gmail.com

PURPOSE

The purpose of this study is to analyze the imaging spectrum of complications of Hematopoietic Stem Cell Transplant in pediatric patients.

METHOD AND MATERIALS

It's a prospective observational study involving 328 pediatric patients who had various malignancies and underwent HSCT in our institution from 2015- 2018. The complications were classified based on the time lines of HSCT 1. Pre-engraftment (<30 days) 2. Early post-transplantation period (30-100) 3. Late post-transplantation period (>100 days) The complications were also classified based on system of involvement and into infective and non infective causes. Radiograph, CT, sputum and blood cultures, specific viral and fungal markers and other relevant investigations were performed in these patients to confirm the diagnosis.

RESULTS

Out of the 328 patients almost 300 patients developed some sort of complication following HSCT. 162 patients developed complications in the Pre-engraftment phase, 81 patients had complications in Early post-transplantation period and 40 patient had complications in Late post-transplantation period. Pulmonary complications were the most common and were present in 90 patients. Pulmonary infection was the most common in all three phases and the commonest organisms included Klebsiella, CMV and aspergillus. Non infective pulmonary complications included Diffuse alveolar haemorrhage, Organising pneumonia, aspiration pneumonitis, ARDS and Graft versus host disease. GIT complications include Colitis, Acute gastroenteritis , Sinosoidal obstruction syndrome, Hepato renal syndrome, Acalculous cholecystitis, Bowel aspergillosis and pancreatitis. GUT complications included Hemorrhagic cystitis. CNS complications PRES, Cerebral infarct, SAH, Otitis media, encephalitis, Sinusitis & Orbital cellulitis, Cerebral infarct , ICH and Viral leukoencephalopathy. Several multiple system complications including graft rejection, GVHD, Septicipemia and Multi Organ Dysfuction were also noted.

CONCLUSION

Post HSCT patients are prone for several complications dependent on the immune status and time line of transplant. The role of imaging is in early detection and narrowing the differentials in patients having post transplant complications.

CLINICAL RELEVANCE/APPLICATION

85 of the total 328 patients in our study died because of the complications of HSCT. Early radiological identification of the complications of HSCT helps in effective treatment of these pediatric patients especially in a county like India with low infection control.

RC513-04 Accuracy of Craniocervical Measurements for Identifying Partial or Complete Craniocervical Ligament Injuries in Pediatric Patients

Wednesday, Dec. 4 9:10AM - 9:20AM Room: S405AB

Participants

Nicholas M. Beckmann, MD, Houston, TX (*Presenter*) Nothing to Disclose Suresh Cheekatla, MBBS, Houston, TX (*Abstract Co-Author*) Nothing to Disclose Chunyan Cai, Houston, TX (*Abstract Co-Author*) Nothing to Disclose O. C. West, MD, Houston, TX (*Abstract Co-Author*) Royalties, Reed Elsevier

For information about this presentation, contact:

Nicholas.M.Beckmann@uth.tmc.edu

PURPOSE

1. Assess accuracy of CT measurements of craniocervical alignment in identifying pediatric patients with craniocervical ligament injury 2. Assess CT soft tissue findings in pediatric patients with craniocervical ligament injuries

METHOD AND MATERIALS

Retrospective review of 48 patients <=16 years old with craniocervical ligament injuries and CT of the cervical spine. Injured patients classified as partial (PD) or complete (CD) disruption of ligaments at craniocervical junction. Patients assessed for craniocervical soft tissue findings and craniocervical alignment using previously described measurements. Comparison of craniocervical measurements in PD and CD groups was made with 2:1 age & gender matched pairs control cohort. Accuracy of measurements was assessed by ROC curves with calculation of area under curve (AUC).

RESULTS

For CD (n=27), C1-C2 distance (AUC=0.90, 95%CI=0.83-0.97), atlanto-occipital distance (AUC=0.95-0.98, 95%CI=0.90-1.00), and basion-dens distance (AUC=0.90, 95%CI=0.82-0.98) had excellent accuracy diagnosing injury. Powers ratio (AUC=0.85, 95%CI=0.76-0.94) had good, basion-posterior axial line (AUC=0.74, 95%CI=0.61-0.86) fair, and atlantodental distance (AUC=0.69, 95%CI=0.57-0.82) poor accuracy. For PD (n=21), basion-dens distance (AUC=0.75, 95%CI=0.62-0.88) had fair accuracy diagnosing injury. Powers ratio (AUC=0.63, 95%CI=0.47-0.79), C1-C2 distance (AUC=0.60, 95%CI=0.45-0.75), atlantodental distance (AUC=0.55, 95%CI=0.39=0.71), atlanto-occipital distance (AUC=0.63-0.65, 95%CI=0.47-0.81), and basion-posterior axial line (AUC=0.60, 95%CI=0.44-0.76) all had poor accuracy. 81% (n=22) of CD and 38% (n=8) of PD patients had non-concentric atlanto-occipital joints. 100% of CD patients had >=1 soft tissue finding and 81% (n=22) had >=2 findings. 73% (n=16) of PD patients had >=1 soft tissue finding. 86% (n=18) of PD patients had non-concentric atlanto-occipital joints and/or soft tissue findings.

CONCLUSION

Measurements of craniocervical alignment have poor accuracy identifying craniocervical ligament injuries not resulting in complete craniocervical dissociation. Recognizing soft tissue injury and non-concentric atlanto-occipital joints can help identify craniocervical injuries on CT.

CLINICAL RELEVANCE/APPLICATION

In pediatric patients, clinicians should rely more on soft tissue findings and non-concentric atlanto-occipital joints than craniocervical measurements to diagnose craniocervical injury on CT.

RC513-05 Comparison of Ferumoxytol and Gadolinium Chelate-Enhanced MRI for Assessment of Sarcomas in Children and Adolescents

Wednesday, Dec. 4 9:20AM - 9:30AM Room: S405AB

Awards

Trainee Research Prize - Fellow

Participants

Florian Siedek, MD, Stanford, CA (*Presenter*) Nothing to Disclose Anne M. Muehe, MD, Stanford, CA (*Abstract Co-Author*) Nothing to Disclose Ashok Joseph Theruvath, MD, Stanford, CA (*Abstract Co-Author*) Nothing to Disclose Raffi S. Avedian, MD, Redwood City, CA (*Abstract Co-Author*) Nothing to Disclose Sheri Spunt, Palo Alto, CA (*Abstract Co-Author*) Nothing to Disclose Kristina E. Hawk, MD,PhD, Stanford, CA (*Abstract Co-Author*) Nothing to Disclose Tie Liang, PhD, Stanford, CA (*Abstract Co-Author*) Nothing to Disclose Crystal R. Farrell, MD, Grand Rapids, MI (*Abstract Co-Author*) Nothing to Disclose Heike E. Daldrup-Link, MD, Palo Alto, CA (*Abstract Co-Author*) Nothing to Disclose

For information about this presentation, contact:

f.siedek@gmail.com

PURPOSE

To compare Ferumoxytol- (Fe) and Gadolinium-chelate (Gd) enhanced MRI scans for assessment of bone and soft tissue sarcomas in pediatric and adolescent patients.

METHOD AND MATERIALS

We retrospectively enrolled 22 pediatric and adolescent patients (16 males, 6 females; mean age 15.3 ± 5 years) with biopsy proven bone or soft tissue sarcoma, who underwent pre-treatment Fe- and Gd-MRI with an interval of 4 weeks or less. MRI sequences included T1-spinecho (SE), fat saturated T2-fast SE (FSE) and T1-LAVA sequences. 3D tumor volumes on Gd- and Fe-MRI scans were compared with Bland-Altman analysis. Signal-to-noise ratios (SNR) and contrast-to-noise ratios (CNR) of tumor, marrow, muscle and vessels were compared with Wilcoxon signed-rank test. In addition, 4 radiologists independently scored 15 qualitative parameters which were compared with Kendall's Tau correlation and McNemar's tests.

RESULTS

Tumor volume measurements agreed significantly on Fe-MRI and Gd-MRI with correlation coefficients of 1, 0.99, 0.99 on T1-SE, T2-FSE and T1-LAVA sequences, respectively. Gd-MRI showed significantly higher tumor SNR compared to Fe-MRI (p<0.01) on T1-LAVA sequences. Fe-MRI showed significantly higher vessel SNR (p=0.01) and marrow SNR (p=0.04) compared to Gd-MRI on T1-LAVA sequences. Also, Fe-MRI showed significantly higher marrow SNR (p=0.02) and tumor-to-marrow SNR and CNR (both p=0.04) compared to Gd-MRI on T1-LAVA sequences. Also, Fe-MRI showed significantly higher marrow SNR (p=0.02) and tumor-to-marrow SNR and CNR (both p=0.04) compared to Gd-MRI on T1-SE sequences. Semiquantitative scores revealed a significant agreement between Gd-MRI and Fe-MRI for cortical destruction (1.0), pathological fracture (1.0), tumor extension in epiphysis, metaphysis and diaphysis (0.92, 1.0, 1.0), joint invasion (0.92), presence of extraosseous soft tissue (0.89) and skip lesions (1.0). T1-enhancement of peri-tumoral edema was significantly more frequent on Gd-MRI compared to Fe-MRI (p<0.01). Neurovascular bundle involvement and potential tumor thrombus were assessed with significantly higher confidence on Fe-MRI (p<0.01).

CONCLUSION

Fe-MRI provides equal assessment of the extent of sarcomas in bone and soft tissue compartments compared to Gd-MRI. Fe-MRI provides improved evaluation of neurovascular involvement or tumor thrombus.

CLINICAL RELEVANCE/APPLICATION

Considering concerns about brain Gd-deposition, Fe-MRI is a clinically available alternative. Ferumoxytol provides lasting vascular/tissue enhancement for combined local and whole-body tumor staging.

RC513-06 Comparison of Whole Body Diffusion Weighted MRI and 18F-FDG PET/MRI for Therapy Response Assessment of Pediatric Tumors: A Prospective, Non-Randomized Multi-Center Study

Wednesday, Dec. 4 9:30AM - 9:40AM Room: S405AB

Participants

Ashok Joseph Theruvath, MD, Stanford, CA (*Presenter*) Nothing to Disclose Florian Siedek, MD, Stanford, CA (*Abstract Co-Author*) Nothing to Disclose Anne M. Muehe, MD, Stanford, CA (*Abstract Co-Author*) Nothing to Disclose Julian Kirchner, Dusseldorf, Germany (*Abstract Co-Author*) Nothing to Disclose Lale Umutlu, MD, Essen, Germany (*Abstract Co-Author*) Consultant, Bayer AG Heike E. Daldrup-Link, MD, Palo Alto, CA (*Abstract Co-Author*) Nothing to Disclose

For information about this presentation, contact:

atheruva@stanford.edu

PURPOSE

Ionizing radiation-free whole-body diffusion-weighted magnetic resonance imaging (WB-DW MRI) can detect malignant tumors in children with high sensitivity. However, assessing tumor therapy response often requires tumor metabolism information, measured by 18F-fluoro-deoxyglucose positron emission tomography (18F-FDG PET). Here, we investigated if ionizing radiation-free WB-DW MRI can predict chemotherapy response of pediatric tumors, using simultaneously acquired 18F-FDG PET scans and clinical outcomes as the standard of reference.

METHOD AND MATERIALS

Sixty-two pediatric patients and young adults with extra-cerebral solid tumors underwent simultaneous WB-DW MRI and 18F-FDG PET/MRI before and after induction chemotherapy. We measured minimum tumor apparent diffusion coefficients (ADCmin) and maximum standardized uptake values (SUVmax) of up to six target lesions per patient and assessed tumor therapy response according to tumor-specific response criteria (Lugano or PERCIST). We evaluated differences in ADCmin and SUVmax between responders and non-responders using Wilcoxon tests, and agreements between WB-DW MRI- and 18F-FDG PET/MRI-based tumor response classifications with Krippendorff's alpha statistics. This study is registered with ClinicalTrials.gov (NCT01542879).

RESULTS

We found significant agreement between treatment response categories on WB-DW MRI and 18F-FDG PET/MRI after induction chemotherapy (A=0.91). Predictions of clinical response were not significicantly different (p=0.58) using change in SUVmax (0.90; 95% CI: 0.81-0.97) and ADCmin (0.83; 95% CI: 0.55-0.99). We found discordant results between PET and MRI response assessments in seven patients who received their interim scan in the early post-treatment phase. In these patients, chemotherapy-induced changes in tumor metabolism preceded changes in proton diffusion. Sensitivity and specificity for tumor therapy response assessment, respectively, were 94% and 100% for 18F-FDG PET/MRI; as well as 93% and 100% for WB-DW MRI.

CONCLUSION

WB-DW MRI can provide a radiation-free approach to assess therapy response of solid pediatric tumors. In some patients, tumor response on early post-treatment WB-DW MRI lags behind the response on 18F-FDG PET/MRI.

CLINICAL RELEVANCE/APPLICATION

WB-DW MRI can be used for therapy response assessments of pediatric tumors that typically undergo follow-up imaging at 8-12 weeks after the start of chemotherapy.

RC513-07 Cervical Lymphadenopathy in Children: A Diagnostic Tree Analysis Model Based on US and Clinical Findings

Wednesday, Dec. 4 9:40AM - 9:50AM Room: S405AB

Participants

Ji Eun Park, Seongnam, Korea, Republic Of (*Presenter*) Nothing to Disclose Young Jin Ryu, MD, Seongnam, Korea, Republic Of (*Abstract Co-Author*) Nothing to Disclose Ji Young Kim, MD, Seongnam, Korea, Republic Of (*Abstract Co-Author*) Nothing to Disclose

PURPOSE

To establish a diagnostic tree analysis (DTA) model based on ultrasonography (US) imaging findings and clinical characteristics for differential diagnosis of cervical lymphadenopathy in children.

METHOD AND MATERIALS

Total 242 patients (131 boys and 111 girls; mean age, 11.2 ± 0.3 years; range, 1 month-18 years) with pathologically confirmed Kikuchi disease (KD) (n = 127), Reactive hyperplasia (RH) (n = 64), lymphoma (n = 24), and suppurative lymphadenitis (SL) (n = 27) who underwent neck US were included. US images of lymph nodes were retrospectively reviewed with regards to location, number, distribution, size, echogenicity, margin, presence of necrosis, calcification, perinodal fat hyperechogenicity, and loss of fatty hilum. Clinical information including age, sex, cervical tenderness, erythema, heat sense, fever, hepatomegaly, splenomegaly, history of antibiotics, and laboratory results were collected. The patients were randomly divided into training (70%, 167/242) and validation (14%, 75/242) datasets to assess diagnostic performance of the DTA model. The DTA model was created using a classification and regression tree algorithm on the basis of US imaging findings and clinical findings.

RESULTS

In the DTA model, perinodal fat hyperechogenicity, loss of fatty hilum, and echogenicity of the lymph nodes (homogeneous or

heterogeneous) were found to be significant predictors in the diagnostic algorithm for differential diagnosis of cervical lymphadenopathy while any clinical findings were not. The overall accuracies were 86.2% and 82.7% in training and validation datasets. The accuracy of KD, RH, lymphoma and SL was 92.2%, 80.4%, 62.5%, and 86.2% in the training dataset, and 91.9%, 61.1%, 75.0%, and 91.7% in the validation dataset, respectively.

CONCLUSION

The presence of perinodal fat hyperechogenicity, heterogeneity of echotexture and loss of fatty hilum were significant ultrasonographic findings in the DTA for differential diagnosis of cervical lymphadenopathy in children.

CLINICAL RELEVANCE/APPLICATION

The DTA model based on US imaging findings may be useful for differential diagnosis of cervical lymphadenopathy in children.

RC513-08 Sonography of the Pediatric Neck

Wednesday, Dec. 4 9:50AM - 10:10AM Room: S405AB

Participants

Janet R. Reid, MD, Philadelphia, PA (Presenter) Nothing to Disclose

For information about this presentation, contact:

reidj@email.chop.edu

LEARNING OBJECTIVES

1) List the top three neck masses in each of three age categories: infants, young children and adolescents. 2) Discuss helpful sonographic features to distinguish benign reactive from malignant lymph nodes in children. 3) Identify the most common locations and imaging features for congenital cystic neck masses.

RC513-09 Adnexal Pathology in Children: Beyond Ovarian Masses

Wednesday, Dec. 4 10:20AM - 10:40AM Room: S405AB

Participants

Ting Y. Tao, MD, PhD, Saint Louis, MO (Presenter) Nothing to Disclose

For information about this presentation, contact:

taoty@slu.edu

LEARNING OBJECTIVES

1) Develop an imaging approach to adnexal pathology in children. 2) Expand differential diagnoses of pediatric adnexal pathology beyond neoplastic ovarian masses. 3) Identify clinical features of non-neoplastic adnexal pathology.

RC513-10 Whole-Body MR Imaging and MR-Guided Biopsy in Initial Diagnosis and Follow-Up of Pediatric Malignancies: Comparison with Other Imaging Modalities and Evaluation of Tumor Response to Treatment

Wednesday, Dec. 4 10:40AM - 10:50AM Room: S405AB

Participants

Guenther K. Schneider, MD, PhD, Homburg, Germany (*Presenter*) Research Grant, Siemens AG; Speakers Bureau, Siemens AG; Speakers Bureau, Bracco Group; Research Grant, Bracco Group;

Tobias Woerner, MD, Homburg, Germany (Abstract Co-Author) Nothing to Disclose

Paul S. Raczeck, MD, Homburg, Germany (Abstract Co-Author) Nothing to Disclose

Arno Buecker, MD, Homburg, Germany (*Abstract Co-Author*) Consultant, Bracco Group Speaker, Bracco Group Consultant, Medtronic plc Speaker, Medtronic plc Research Grant, Novartis AG Research Grant, GlaxoSmithKline plc Research Grant, Biotest AG Research Grant, OncoGenex Pharmaceuticals, Inc Research Grant, Bristol-Myers Squibb Company Research Grant, Eli Lilly & Company Research Grant, Pfizer Inc Research Grant, F. Hoffmann-La Roche Ltd Research Grant, sanofi-aventis Group Research Grant, Merrimack Pharmaceuticals, Inc Research Grant, Sirtex Medical Ltd Research Grant, Concordia Healthcare Corp Research Grant, AbbVie Inc Research Grant, Takeda Pharmaceutical Company Limited Research Grant, Merck & Co, Inc Research Grant, Affimed NV Research Grant, Bayer AG Research Grant, Johnson & Johnson Research Grant, Seattle Genetics, Inc Research Grant, Onyx Pharmaceuticals, Inc Research Grant, Synta Pharmaceuticals Corp Research Grant, Siemens AG Research Grant, iSYMED GmbH Research Grant, Abbott Laboratories Co-founder, Aachen Resonance GmbH

Peter Fries, MD, Homburg, Germany (Abstract Co-Author) Research Grant, Guerbet SA

For information about this presentation, contact:

dr.guenther.schneider@uks.eu

PURPOSE

82 pediatric oncologic patients underwent evaluation of whole body MRI as the sole staging andfollow-up procedure including lung imaging. When necessary biopsy of tumors was performed under MR guidance for histologic proof of primary tumors or for proof of recurrence or metastases. Results were compared with established staging procedures as PET, MIBG or bone scintigraphy, CT and ultrasound.

METHOD AND MATERIALS

409 whole body MR examinations in 82 patients were performed on a 1.5 T (Siemens, Aera) or a 3 T(Siemens, VIDA) scanner. 25 lymphoma, 39 solid tumors including neuro-, nephro- and hepatoblastoma as well as 18 pts. with different types of sarcoma were evaluated. MR protocol included T1w sequences pre and post CM (0,05 mmol/kg BW MultiHance) and in the hepatobliary phase. DWI were acquired during free breathing and transversal T2w-TSE sequences and a composed coronal whole-body STIR-sequence completed the whole body imaging. When necessary, additional sequences to allow for local staging of soft-tissue- or bonetumors

were performed. If indicated MR-guided biopsy of tumors / metastases or recurrent disease was performed to acquire tissue samples.

RESULTS

Differences between MRI and CT were seen regarding the higher number of small lung metastases detected (< 3mm) on CT. Advantages for WB-MRI were seen in follow-up of diffuse T-cell Lymphoma, in which MRI could show PET-negative residual disease under chemotherapy and in staging of sarcoma. Recurrent disease in 2 Hodgkin- and 4 Non-Hodgkin-Lymphoma was diagnosed primarily by WB-MRI at follow-up examinations. Similarly MRI facilitated detection of recurrent tumors and restaging in solid tumors, especially in Ewing-sarcoma. DDX between therapy associated bone marrow-changes, bone infarcts and recurrent disease or mets was also facilitated by MRI.

CONCLUSION

WB-MRI can correctly stage and diagnose a variety of malignant tumors in pediatric patients and allows foraccurate patient management during therapy and follow-up including MR-guided biopsy. Advantages of established imaging methods were only seen for detection of small lung metastases on pulmonary CT, however differences did not result in a change of patient management.

CLINICAL RELEVANCE/APPLICATION

This study evaluates the potential of state of the art whole body MR imaging in staging and follow-up ofpediatric patients including MR guided biopsy, to allow for complete work-up of disease without radiationexposure.

RC513-11 Comparison of Magnetic Resonance Imaging Appendix Measurements in Children with and without Acute Appendicitis

Wednesday, Dec. 4 10:50AM - 11:00AM Room: S405AB

Participants

Eric L. Tung, MD, Providence, RI (*Presenter*) Nothing to Disclose Rama S. Ayyala, MD, Providence, RI (*Abstract Co-Author*) Nothing to Disclose Grayson L. Baird, PhD, Providence, RI (*Abstract Co-Author*) Nothing to Disclose Cassandra M. Sams, MD, Providence, RI (*Abstract Co-Author*) Nothing to Disclose Thaddeus W. Herliczek, MD, Westport, MA (*Abstract Co-Author*) Nothing to Disclose Hale Wills, MD, Providence, RI (*Abstract Co-Author*) Nothing to Disclose David W. Swenson, MD, Providence, RI (*Abstract Co-Author*) Nothing to Disclose

For information about this presentation, contact:

EricTung34@gmail.com

PURPOSE

Rapid, non-contrast MRI has been reported as accurate for diagnosing acute appendicitis at specialized pediatric hospitals, but there remains a dearth of evidence-based, MRI-specific criteria upon which the diagnosis should be established. Our goal was to improve current MRI-specific diagnostic criteria for pediatric appendicitis through comparison of normal and abnormal appendixrelated measurements.

METHOD AND MATERIALS

Our human-factors experimental design included 123 studies from children (4-18 years) with suspected acute appendicitis who underwent rapid, non-contrast MRI following equivocal US exams from January 2014 to December 2017. A positive diagnosis of acute appendicitis was defined as resolution of acute abdominal pain after surgical or medical appendicitis-specific intervention. All exams were graded independently and blinded to clinical data by two fellowship-trained pediatric radiologists. Complete experimental block design was used to determine the performance characteristics of individual diagnostic criteria. Data were modeled using generalized mixed modeling with SAS/GLIMMIX. The study was powered equally for sensitivity and specificity.

RESULTS

MRI had a sensitivity of 89% (95% CI 79-93%) and specificity of 98% (CI 94-99%). The mean appendix diameter of negative cases and positive cases was 6.2mm (CI 5.9-6.6) and 10.5mm (CI 10.0-11.2), respectively (p<0.001). Using ROC analysis and Youden Criterion for appendix diameter, an ROC of 0.92 was achieved, and an optimal cut-off of 8.0mm was identified (sensitivity and specificity of 85% and 84%, respectively). A wall thickness cutoff of >=2mm was optimal (sensitivity and specificity of 70% and 89%, respectively). Appendix intraluminal fluid-fluid level had a sensitivity and specificity of 27% and 100%, respectively. Periappendiceal fluid had a sensitivity and specificity of 75% and 91%, respectively.

CONCLUSION

Appendix diameter is a strong predictor of acute appendicitis with an optimal MRI cutoff of 8.0mm. Other individual diagnostic criteria including appendix wall thickness of >=2mm, appendix intraluminal fluid-fluid level, and peri-appendiceal fluid have high specificity but relatively low sensitivity. When considering these diagnostic criteria in aggregate, rapid MRI without contrast is accurate in evaluation of suspected pediatric acute appendicitis.

CLINICAL RELEVANCE/APPLICATION

Rapid, non-contrast MRI is an accurate and radiation-free evaluation for pediatric acute appendicitis that requires aggregate assessment of several diagnostic criteria. To our knowledge, this is the largest study to date that evaluates the performance of individual MRI-specific features of pediatric appendicitis.

RC513-12 Configuration and Size of the Residual Intussusception Mass May Be Useful for Differentiating False Failure from Truly Failed Air Reduction for Ileocolic Intussusception

Wednesday, Dec. 4 11:00AM - 11:10AM Room: S405AB

Participants Hae Won Kim, MD, Seoul, Korea, Republic Of (*Abstract Co-Author*) Nothing to Disclose Tae Yeon Jeon, MD, Seoul, Korea, Republic Of (*Presenter*) Nothing to Disclose Saelin Oh, Seoul, Korea, Republic Of (*Abstract Co-Author*) Nothing to Disclose So-Young Yoo, Seoul, Korea, Republic Of (*Abstract Co-Author*) Nothing to Disclose Ji Hye Kim, MD, Seoul, Korea, Republic Of (*Abstract Co-Author*) Nothing to Disclose

For information about this presentation, contact:

hathorjeon@gmail.com

PURPOSE

To determine clinical and radiologic parameters enabling reliable differentiation of false failure from truly failed air reduction in children with intussusceptions.

METHOD AND MATERIALS

Between January 2003 and May 2018, we reviewed 373 procedures of fluoroscopic air reduction for ileocolic intussusceptions (324 patients under 18 years of age; mean age, 2.3 years). Using a consensus approach, two pediatric radiologists evaluated fluoroscopic images during air reduction and classified all procedures according to the radiologic criteria: successful (SR) versus failed results (FR). Cases with FR, which include a remaining intussusception mass and no air reflux into the terminal ileum, were divided into true failure group and false failure group based on clinical outcome or surgical records. Clinical and radiologic data were analyzed, including demographics, laboratory, ultrasound, and fluoroscopic findings. The t-test, Mann-Whitney U test, or Fisher's exact test were used for comparison and discriminating power was calculated by standardized mean difference (SMD).

RESULTS

Of 373 procedures, 264 (71%) were SR and 109 (29%) were FR. All 264 cases with SR were true successful air reduction. Of 109 cases with FR, 40 (37%) were true failure group and 69 (63%) were false failure group. The symptom of bloody stool, the presence of pathologic lead points, US findings including the presence of entrapped fluid, free peritoneal fluid, and decreased blood flow of the bowel were more common in true failure group than in false failure group (P<.05; SMD<0.8). At fluoroscopy, all cases with FR showed residual masses around the ileocecal valve. The size of mass was larger in true failure group than in false failure group (P<.001; SMD=2.5). All except one (98%) of true failure group had residual masses with protruded configuration, whereas 88% (61/69) of false failure group showed the indented configuration of the mass (P<.001; SMD=3.4).

CONCLUSION

Only 37% of cases with FR were proved to be truly failed air reduction. Recognition of a residual mass configuration in combination with measurement of its size can be used to differentiate false failure from truly failed air reduction in children with intussusceptions.

CLINICAL RELEVANCE/APPLICATION

Accurate diagnosis of failed air reduction for ileocolic intussusception allows optimal clinical management and prevents unnecessary delayed repeated enema attempts or futile surgery.

RC513-13 Identifying Unilateral and Circumferential Hyperechoic Periappendiceal Fat Improves Specificity for the Sonographic Diagnosis of Appendicitis in Pediatric Patients

Wednesday, Dec. 4 11:10AM - 11:20AM Room: S405AB

Participants Ryan H. Penticuff, MD, Stanford, CA (*Presenter*) Nothing to Disclose Eric W. Olcott, MD, Palo Alto, CA (*Abstract Co-Author*) Nothing to Disclose R. Brooke Jeffrey Jr, MD, Stanford, CA (*Abstract Co-Author*) Nothing to Disclose

For information about this presentation, contact:

rhpent2@stanford.edu

PURPOSE

To test the hypothesis that unilateral and circumferential types of hyperechoic periappendiceal fat are specific sonographic indicators of appendicitis in pediatric patients.

METHOD AND MATERIALS

Appendiceal sonograms of 271 consecutive pediatric patients (ages, 1-18 years; January, 2016 - November, 2017) with suspected appendicitis were retrospectively evaluated to determine the appendiceal mean outer diameter (MOD) and categorize hyperechoic periappendiceal fat as one of three mutually exclusive types (0, none; type 1, spanning <180° of the appendiceal circumference, termed 'unilateral'; type 2, spanning >=180° of the appendiceal circumference, termed 'circumferential'). Histopathologic reports and 6-week clinical follow-up served as reference standards for the diagnosis of appendicitis. Statistical methods included univariable and multivariable regression, the McNemar test, and receiver operating characteristic (ROC) analysis.

RESULTS

Appendicitis was present in 107 patients of whom 16.8%, 43.0% and 26.2% had fat type 0, 1 and 2, respectively. Fat types 1 and 2 each were significantly associated with appendicitis in multivariable regression; fat type 0 was strongly negatively associated and excluded from further evaluation. Fat type 1 and fat type 2 each significantly increased specificity and positive predictive value to 100.0% in patients with diagnostically equivocal MODs of 6-8mm as well as those with MOD >=6 mm, compared to MOD alone (P<0.001). Fat type 1 or fat type 2 increased the probability of appendicitis over MOD alone for MOD values of 6-12 mm, with greater effect at lower MOD values.

CONCLUSION

Unilateral and circumferential types of hyperechoic periappendiceal fat are each specific sonographic indicators of appendicitis in pediatric patients with MOD 6-8 mm and patients with MOD >=6 mm.

CLINICAL RELEVANCE/APPLICATION

Improved specificity in the sonographic diagnosis of appendicitis is a clinically worthwhile goal, particularly for patients with maximum outer diameters (MOD) of 6-8mm in which diagnosis is equivocal when based on MOD alone.

RC513-14 Limited Ultrasound for Appendicitis

Wednesday, Dec. 4 11:20AM - 11:30AM Room: S405AB

Participants Saba Sadeghi, Toronto, ON (*Presenter*) Nothing to Disclose Nikan Behboodpour, Toronto, ON (*Abstract Co-Author*) Nothing to Disclose Paymun Pezeshkpour, North York, ON (*Abstract Co-Author*) Nothing to Disclose Afsaneh Amirabadi, PhD, Toronto, ON (*Abstract Co-Author*) Nothing to Disclose Michael R. Aquino, MD, MS, Toronto, ON (*Abstract Co-Author*) Co-author, Reed Elsevier

For information about this presentation, contact:

mike.r.aquino@gmail.com

PURPOSE

Limited abdominal US performed for suspected appendicitis requires less time to complete but is associated with the risk of missing clinically significant extra-intestinal findings. The objective of this study is to determine the frequency and clinical significance of non-bowel-related findings identified on full abdominal US performed in pediatric emergency department patients for suspected acute appendicitis.

METHOD AND MATERIALS

Retrospective single center study. Reports of abdominal-pelvic US performed at an academic children's hospital in patients in whom there was suspicion of appendicitis were reviewed. Studies performed between 17:00 and 07:59 hours on patients <18-years-old between June 2013, and January 2017, were included in the study. To be included, the study indication had to specifically denote a suspicion for appendicitis. Patients with known pre-existing conditions were excluded.

RESULTS

A total of 1709 patients (mean age 9 years; 53% male and 47% female) were included. US results for appendicitis were positive, negative, and equivocal in 67%, 27%, and 7%, respectively. There were 418 extra-intestinal findings identified on 342/1709 (20%) full abdominal US exams. The most common findings were: ovarian cyst 13 (11 hemorrhagic), splenomegaly 23, pelviectasis 22, increased periportal echogenicity in the liver 84, increased pancreatic parenchymal echogenicity 5, bladder debris 53, and gallbladder contraction 5. Diagnoses requiring immediate management included: ovarian torsion 3, liver abscess 1, biliary tree dilatation 3. Congenital findings were identified involving the: uterus 3 and kidneys 16, including 3 urachal remnants. A total of 6 masses were found: 2 ovarian, 2 hemangiomas (1 hepatic and 1 splenic), and 2 gallbladder polyps.

CONCLUSION

Extra-intestinal findings involving the solid abdominal organs and female reproductive organs were common on full abdominal-pelvic US performed for suspected acute appendicitis and could potentially be missed on limited US. Findings included acute diagnoses that required immediate management (ovarian torsion and liver abscess) but these were rare. Congenital abnormalities were most often related to the kidneys.

CLINICAL RELEVANCE/APPLICATION

Ultrasound for appendicitis limited to the bowel or right lower quadrant may miss clinically significant acute and congenital findings.

RC513-15 Diagnosing Appendicitis: Imaging and Hospital Charge Trends Over 15 Years

Wednesday, Dec. 4 11:30AM - 11:40AM Room: S405AB

Participants

Shireen Hayatghaibi, MA, MPH, Houston, TX (Presenter) Nothing to Disclose

Andrew T. Trout, MD, Cincinnati, OH (*Abstract Co-Author*) Author, Reed Elsevier; Author, Wolters Kluwer nv; Research Grant, Canon Medical Systems Corporation; Board Member, Joint Review Committee on Educational Programs in Nuclear Medicine Technology; Speakers Bureau, Reed Elsevier; Speakers Bureau, iiCME

Jonathan R. Dillman, MD, MSc, Cincinnati, OH (*Abstract Co-Author*) Research Grant, Siemens AG; Research Grant, Guerbet SA; Travel support, Koninklijke Philips NV; Research Grant, Canon Medical Systems Corporation; Research Grant, Bracco Group

For information about this presentation, contact:

sehayatg@texaschildrens.org

PURPOSE

To assess diagnostic imaging utilization and associated imaging charge trends for pediatric appendicitis at U.S. children's hospitals between 2004 and 2018.

METHOD AND MATERIALS

This retrospective study used data from the Pediatric Health Information System (PHIS) database, managed by the Children's Hospital Association. Pediatric patients (age range: 0-17 years, mean= 9.6 years) who underwent appendectomy at one of 44 children's hospitals from January 1, 2004 through September 30, 2018 were included. Patients were identified using ICD-10 (International Classification of Diseases, 10th Revision) codes K35.2, K35.3, K35.80, K35.89, K37 and K36. Patient demographics, imaging performed (related to the diagnosis of appendicitis, including CT, ultrasound, MRI, and radiography), and imaging charges were analyzed. Mean patient total imaging charges were calculated by year and were adjusted by the consumer pricing index for 2018.

The final study population consisted of 91,804 patients with 131,454 imaging procedures. From 2004 to 2018, CT utilization decreased from 42.2% (2490/5901) to 19.1% (1,433/7,486), p<0.001. In contrast, ultrasound (US) utilization increased from 25.7% (1515/5901) to 62.5% (4,677/7,486), p<0.001. Radiography utilization decreased from 32% (1,889/5,901) to 16.2% (1,215/7,486), p<0.001. MRI use increased, though utilization remained low from 0.1% (7/5,901) to 2.2% (163/7,486), p<0.001. Mean number of imaging exams per patient increased with 1.35 in 2004, 1.37 in 2008, 1.39 in 2013 and 1.43 in 2018. Mean number of imaging exams per patient was 1.02 for patients with a CT, 1.29 for patients with an US, and 2.09 for patients with an MRI as part of their encounter. Patient mean charges varied, \$3,017 in 2004, \$4,125 in 2008 (absolute increase of \$1,108), \$3,389 in 2013 (absolute decrease \$351).

CONCLUSION

There has been a significant shift in imaging of children with appendicitis over 15 years in the U.S., as the use of CT has decreased and US use has increased. While US is a less costly modality (patient perspective), the mean number of imaging exams per patient has increased (with US), therefore patient imaging charges have not decreased.

CLINICAL RELEVANCE/APPLICATION

Trend from CT to US suggests the emphasis in imaging of pediatric appendicitis has been on radiation exposure reduction without substantial attention to broader questions of efficiency and cost.

RC513-16 Imaging of Pediatric GI Bleeding

Wednesday, Dec. 4 11:40AM - 12:00PM Room: S405AB

Participants

Summer L. Kaplan, MD, MS, Philadelphia, PA (Presenter) Nothing to Disclose

For information about this presentation, contact:

kaplans2@email.chop.edu

LEARNING OBJECTIVES

1) List common etiologies of GI bleeding in children. 2) Apply the appropriate imaging tests depending on suspected etiology. 3) Recommend vascular intervention when appropriate.





Interventional Series: Reproductive Health Interventions

Wednesday, Dec. 4 8:30AM - 12:00PM Room: S105AB



AMA PRA Category 1 Credits ™: 3.25 ARRT Category A+ Credits: 3.75

FDA Discussions may include off-label uses.

Participants

Paul J. Rochon, MD, Aurora, CO (*Moderator*) Speaker, Penumbra, Inc; Speakers Bureau, C. R. Bard, Inc; Speaker, Cook Group Incorporated; Advisory Board, Medtronic plc; Speaker, Medtronic plc

Theresa M. Caridi, MD, Washington, DC (*Moderator*) Medical Advisory Board, Boston Scientific Corporation; Consultant, Boston Scientific Corporation; Medical Advisory Board, Embolx, Inc; Consultant, Embolx, Inc; Research Grant, Embolx, Inc; Shareholder, Embolx, Inc; Speakers Bureau, Terumo Corporation; Medical Advisory Board, Varian Medical Systems, Inc;

For information about this presentation, contact:

Theresa.m.caridi@gunet.georgetown.edu

Sub-Events

RC514-01 Prostate Embolization: Technical Considerations

Wednesday, Dec. 4 8:30AM - 8:45AM Room: S105AB

Participants

Jafar Golzarian, MD, Minneapolis, MN (*Presenter*) Officer, EmboMedics Inc; Consultant, Boston Scientific Corporation; Consultant, Medtronic plc; Consultant, Guerbet SA;

For information about this presentation, contact:

golzarian@umn.edu

LEARNING OBJECTIVES

1) Discuss about complex anatomy and collateral pathway. 2) Review tips and tricks accessing prostate artery. 3) Discuss best use of embolic materials.

RC514-02 Prostate Embolization: Outcomes

Wednesday, Dec. 4 8:45AM - 9:00AM Room: S105AB

Participants

Jafar Golzarian, MD, Minneapolis, MN (*Presenter*) Officer, EmboMedics Inc; Consultant, Boston Scientific Corporation; Consultant, Medtronic plc; Consultant, Guerbet SA;

LEARNING OBJECTIVES

1) Understand indications and contraindications to prostatic artery embolization. 2) Understand the selection of patients who are ideally suited for prostatic artery embolization. 3) Become familiar with embolic materials used in PAE. 4) Identify and anticipate complications related to PAE. 5) Understand and interpret the existing literature on PAE and how this would translate into setting expectations for the procedure in a clinical setting. 6) Become familiar with the basic techniques of PAE.

RC514-03 Benign Prostate Hyperplasia: Advantages of MR Angiography (MRA)-Guided Prostate Artery Embolization (PAE)

Wednesday, Dec. 4 9:00AM - 9:10AM Room: S105AB

Participants

Thomas J. Vogl, MD, PhD, Frankfurt, Germany (*Presenter*) Nothing to Disclose Annette Zinn I, Frankfurt, Germany (*Abstract Co-Author*) Nothing to Disclose Elsayed M. Elhawash, BMedSc,MS, Frankfurt am Main, Germany (*Abstract Co-Author*) Nothing to Disclose Nagy N. Naguib, MD, MSc, Frankurt, Germany (*Abstract Co-Author*) Nothing to Disclose

For information about this presentation, contact:

T.Vogl@em.uni-frankfurt.de

PURPOSE

To evaluate advantages of MR angiography (MRA)-guided prostate artery embolization (PAE) and to correlate preinterventional MRI findings and analysis of the prostatic artery (PA) with clinical outcomes, intervention time and radiation exposure.

METHOD AND MATERIALS

This study includes 32 patients (mean: 64 ± 7.62 ; range 47-80). Clinical success was evaluated through the International Prostate Symptom Score (IPSS) and Quality of Life (QoL) before and after PAE. To identify PA origin, MRA reconstruction with maximum intensity projection (MIP) and three-dimensional reconstruction was performed. Mean intervention time was 95.88 minutes, mean fluoroscopy time was 30.2 minutes, mean dose area product was 29,365.21 μ Gym² and mean entrance dose was 1,614.01 mGy.

RESULTS

The retrospectively evaluated data documented a clinical success in 72.7% of patients with a highly significant reduction in IPSS (p<0.0001; mean 9.67 points). Analysis of PA origin via MRA was sufficient in 30 patients (90.1%) and a significant reduction of the intervention time (p=0.030) and the dose area product was detected.

CONCLUSION

MRA-guided PAE is a feasible and safe treatment option and significantly improves the IPSS and QoL scores. It reduces procedure time and radiation exposure for patients and interventional radiologists.

CLINICAL RELEVANCE/APPLICATION

MRA guidance in PAE is feasible and reduces procedure time and radiation exposure

RC514-04 Uterine Fibroid Embolization: Techniques

Wednesday, Dec. 4 9:10AM - 9:25AM Room: S105AB

Participants

Theresa M. Caridi, MD, Washington, DC (*Presenter*) Medical Advisory Board, Boston Scientific Corporation; Consultant, Boston Scientific Corporation; Medical Advisory Board, Embolx, Inc; Consultant, Embolx, Inc; Research Grant, Embolx, Inc; Shareholder, Embolx, Inc; Speakers Bureau, Terumo Corporation; Medical Advisory Board, Varian Medical Systems, Inc;

LEARNING OBJECTIVES

1) Familiarize the audience with the techniques of Uterine Fibroid Embolization. 2) Learn indications/contraindications for the procedure. 3) Understand procedural techniques ad outcomes/complications. 4) Understand periprocedural care.

RC514-05 Magnetic Resonance-Guided Focused Ultrasound Surgery (MRgFUS) Ablate Adenomyosis Combined with Gonadotropin-Releasing Hormone Agonist: A Clinical Study

Wednesday, Dec. 4 9:25AM - 9:35AM Room: S105AB

Participants

Yaoqu Huang, MD, Foshan, China (Presenter) Nothing to Disclose

For information about this presentation, contact:

doctorhyq@163.com

PURPOSE

To investigate the clinical efficacy of magnetic resonance-guided focused ultrasound surgery (MRgFUS) ablation for adenomyosis after gonadotropin-releasing hormone agonist (GnRH-a) pretreatment.

METHOD AND MATERIALS

From May 2017 to April 2018, twenty patients with symptomatic adenomyosis were underwent MRgFUS treatment. Before MRgFUS ablation, all patients were pretreated with GnRH-a. After ablation, the short-term clinical efficacy were assessed.

RESULTS

After GnRH-a therapy, the average volumes of the uterus and adenomyosis were reduced 48.3% and 47.9%, respectively, and the average signal intensity(SI) ratio of adenomyotic lesions decreased by 29.2%. After MRgFUS ablation, contrast-enhanced MRI showed an average nonperfused volume (NPV) ratio of 82.4±11.5%. Nine patients (45.0%) had 15 class A or B complications according to the Society of Interventional Radiology. Three months after MRgFUS treatment, the volumes of the uterus and adenomyosis were reduced by 20.4% and 36.9%, respectively, compared with baseline. Compared with baseline, the dysmenorrhea scores and PBAC scores significantly decreased at 3 months and 6 months after MRgFUS treatment.

CONCLUSION

MRgFUS ablation is feasible, safe and effective for patients with adenomyosis. GnRH-a pretreatment can significantly decrease the SI and volume of adenomyotic lesions and may create favorable conditions for subsequent MRgFUS ablation.

CLINICAL RELEVANCE/APPLICATION

GnRH-a pretreatment can create favorable conditions for subsequent MRgFUS treatment, it is recommended that MRgFUS combined with GnRH-a as a recommended protocol for adenomyosis ablation.

RC514-06 Uterine Fibroid Embolization: Outcomes

Wednesday, Dec. 4 9:35AM - 9:50AM Room: S105AB

Participants

Theresa M. Caridi, MD, Washington, DC (*Presenter*) Medical Advisory Board, Boston Scientific Corporation; Consultant, Boston Scientific Corporation; Medical Advisory Board, Embolx, Inc; Consultant, Embolx, Inc; Research Grant, Embolx, Inc; Shareholder, Embolx, Inc; Speakers Bureau, Terumo Corporation; Medical Advisory Board, Varian Medical Systems, Inc;

For information about this presentation, contact:

Theresa.m.caridi@gunet.georgetown.edu

LEARNING OBJECTIVES

1) Define the expected technical and clinical outcomes for UFE; what percentages we provide to our patients. 2) Distinguish urban myths versus actual challenges in UFE on topics such as expected fertility and outcomes for various fibroid locations. 3) Understand the most recent data regarding UFE outcomes and comparison to surgical treatments for fibroids. 4) Identify areas for further UFE outcomes investigation.

RC514-07 The Treatment of Submucosal Uterine Fibroids by Using Magnetic Resonance-Guided Focused Ultrasound Surgery (MRgFUS): The Evaluation of Efficacy and Safety in 3-Year Prospective Study

Wednesday, Dec. 4 9:50AM - 10:00AM Room: S105AB

Participants

Flavia Cobianchi Bellisari, MD, Laquila , Italy (*Presenter*) Nothing to Disclose Sonia Iafrate, Laquila, Italy (*Abstract Co-Author*) Nothing to Disclose Ilaria Capretti, Laquila, Italy (*Abstract Co-Author*) Nothing to Disclose Ester Cannizzaro, MD, L'Aquila, Italy (*Abstract Co-Author*) Nothing to Disclose Federica de Matteis, Laquila , Italy (*Abstract Co-Author*) Nothing to Disclose Francesco Arrigoni, L'Aquila , Italy (*Abstract Co-Author*) Nothing to Disclose Margherita Di Luzio, L'Aquila, Italy (*Abstract Co-Author*) Nothing to Disclose Sara Mascaretti, Laquila , Italy (*Abstract Co-Author*) Nothing to Disclose Carlo Masciocchi, MD, L'Aquila, Italy (*Abstract Co-Author*) Nothing to Disclose

For information about this presentation, contact:

sonia.iafrate87@gmail.com

PURPOSE

This study aimed to evaluate clinical efficacy and safety of Magnetic Resonance-guided Focused Ultrasound (MRgFUS) in the treatment of sub-mucosal uterine fibroids in a 3-year prospective study

METHOD AND MATERIALS

Twenty patients affected by sub-mucosal uterine fibroids were treated by MRgFUS (age range 23-54 years), from December 2013 to January 2016. The patients were studied with MRI and classified according to the FIGO staging system. Non-perfused volumes (NPVs) were measured immediately after MRgFUS to calculate the treated area on the c.e. T1-weighed sequences (MRI). The Uterine Fibroid Symptoms and Quality of Life Questionnaire (UFS-QOL) was used to assess the patients' Symptom Severity Scores (SSS) before and after 3 year post-treatment

RESULTS

After MRgFUS treatment, a mean NPV extension of 90,5 % was observed. At follow-up studies up to 3-year, 9 out of 20 patients showed progressive reduction of the uterine volume with regularization of the uterine wall, 11 out of 20 patients showed significant reduction of fibroid volume (about 87%). Each patient was treated during one session. All the patients reported improvement in the UFS-QOL symptoms severity score, when compared with the pre-treatment score. No severe adverse events were observed

CONCLUSION

The results obtained from this study showed that MRgFUS could be safely and effectively used to ablate sub-mucosal uterine fibroids and to improve clinical symptomatology and morphology of uterus

CLINICAL RELEVANCE/APPLICATION

Efficacy and safety of MRgFUS

RC514-08 Treatment of Type 2 and 3 Uterine Fibroids with MR-Guided Focused Ultrasound Surgery: Study of 248 Fibroids

Participants

Ritu M. Kakkar, MBBS, DMRD, Mumbai, India (*Abstract Co-Author*) Nothing to Disclose Shrinivas B. Desai, MD, Mumbai, India (*Presenter*) Nothing to Disclose

For information about this presentation, contact:

riturupesh@gmail.com

PURPOSE

To evaluate the role of Magnetic Resonance guided Focussed Ultrasound Surgery (MRgFUS) in treatment of type 2 and 3 uterine fibroids by evaluating post treatment non perfused volume .To evaluate difference in treatment energies and duration of treatment as compared to type 1 fibroids

METHOD AND MATERIALS

248 symptomatic fibroids enhancing type 2 and 3 (T2 iso and hyperintense) uterine fibroids in 104 Indian women , were selected for study after approval from ethics committee following .Pre treatment baseline MRI with contrast was performed and fbroids were classified on basis of T2 signal intensity .Fibroids were classified as Type 1 - hypointense to muscle ,Type 2 - isointense to muscle and type 3- hyperintense to muscle .Treatment was performed on a 1.5-T whole-body system (Signa; GE Healthcare) in the ExAblate 2000 (InSightec) device, using nominal spot protocol .The mean energies ranged between 3500-4200J,while the duration of treatment was 3.5 to 4 hours .Pretreatment fibroid volumes and post treatment non perfused volumes were calculated.

RESULTS

The mean volume of fibroids before treatment was 127 cc with SD, 71.22 cc.The post treatment contrast enhanced images showed

Wednesday, Dec. 4 10:00AM - 10:10AM Room: S105AB

that the volume of fibroid that was nonperfused was 92.21 cc (mean) with SD of 44.12 cc. The average percentage NPV of the total fibroid volume was 72.44 % with a SD of 5.60%. The mean energies used in the treatment ranged between 3500-4200 J, which is 15 -16 % higher than type 1 fibroids 2000-3000J. The average duration of treatment was 3.5 -4 hours ,1.4 times higher than type 1 fibroids.78% patients has no significant adverse effects. Skin burn with blisters were seen 2% patients. Post treatment leg pain was seen 10% patients immediaterly after treatment

CONCLUSION

MRgFUS is a non invasive technology providing good treatment and volume reduction in patients with T2 iso and hyperintense fibroids ,with acceptable adverse effect profile inspite of higher energies used

CLINICAL RELEVANCE/APPLICATION

MRgFUS can be considered treatment of T2 iso and hyperintense fibroids and can used as an alternative to Uterine artery embolization and in patients not willing for surgery

RC514-09 High-intensity Focused Ultrasound in the Treatment of Uterine Fibroids

Wednesday, Dec. 4 10:10AM - 10:25AM Room: S105AB

Participants

Alexander H. Lam, MD, Orange, CA (Presenter) Nothing to Disclose

LEARNING OBJECTIVES

1) Become aware of the indications/contraindications for HIFU, procedural steps, outcomes/complications, and periprocedural care.

ABSTRACT

The purpose of this lecture is to discuss High Intensity Focused Ultrasound (HIFU) in the treatment of uterine fibroids.

RC514-10 Pelvic Congestion Syndrome

Wednesday, Dec. 4 10:25AM - 10:40AM Room: S105AB

Participants

Gloria M. Salazar, MD, Boston, MA (Presenter) Consultant, Medtronic plc

For information about this presentation, contact:

gmsalazar@partners.org

LEARNING OBJECTIVES

Describe different categories of Pelvic Venous Disorders.
 Identify relevant venous anatomy for proper clinical evaluation.
 Establish proper clinical evaluation of patients.
 Define treatment strategies optimized for different patients' clinical presentation.
 Understand different interventional treatments and their potential complications.

ABSTRACT

Pelvic Venous Disorders include descriptors of different conditions associated with pelvic venous hypertension resulting in chronic pelvic pain. It could be associated with ovarian vein reflux and/or venous compression syndromes. In some patients, it is associated with internal iliac vein reflux and varicose veins of the legs, as well as May-Thurner Syndrome. The management of chronic pelvic pain is best achieved with a multidisciplinary approach that involves gynecology, pain management, physical therapy, psychological therapy, and interventional radiology. We will review the literature supporting the diagnosis & treatment of these conditions, highlight the differential diagnosis and other therapies that are often required and describe the technical approaches to ovarian vein embolization, internal iliac vein embolization and left internal iliac stenting.

RC514-11 Contraceptive Implant Migration and Removal

```
Wednesday, Dec. 4 10:55AM - 11:10AM Room: S105AB
```

Participants

Paul J. Rochon, MD, Aurora, CO (*Presenter*) Speaker, Penumbra, Inc; Speakers Bureau, C. R. Bard, Inc; Speaker, Cook Group Incorporated; Advisory Board, Medtronic plc; Speaker, Medtronic plc

For information about this presentation, contact:

paul.rochon@ucdenver.edu

LEARNING OBJECTIVES

1) To recognize the risks and complications associated with contraceptive implant placement and removal. 2) To apply image guided techniques for complex removal of contraceptive implants.

RC514-12 Post-partum Hemorrhage

Wednesday, Dec. 4 11:10AM - 11:25AM Room: S105AB

Participants Matthew A. Brown, MD, Aurora, CO (*Presenter*) Nothing to Disclose

For information about this presentation, contact:

matthew.a.brown@ucdenver.edu

LEARNING OBJECTIVES

1) Learner should be able to understand the role of embelization alongside standard ebstatrical therapy for past parties

1) Learners should be able to understand the role of embolization alongside standard obstetrical therapy for post partial hemorrhage (PPH). 2) Learners should be able to understand the technique and embolic materials used for treatment of PPH.

RC514-13 Uterine Artery Embolization for Abnormal Uterine Bleeding in the Setting of Retained Products of Conception

Wednesday, Dec. 4 11:25AM - 11:35AM Room: S105AB

Participants

Kaitlin A. Carrato, MD, Washington, DC (Presenter) Nothing to Disclose

James B. Spies, MD, Washington, DC (Abstract Co-Author) Nothing to Disclose

Theresa M. Caridi, MD, Washington, DC (*Abstract Co-Author*) Medical Advisory Board, Boston Scientific Corporation; Consultant, Boston Scientific Corporation ; Medical Advisory Board, Embolx, Inc; Consultant, Embolx, Inc; Research Grant, Embolx, Inc; Shareholder, Embolx, Inc; Speakers Bureau, Terumo Corporation; Medical Advisory Board, Varian Medical Systems, Inc;

PURPOSE

Retained products of conception (RPOC) can cause significant abnormal uterine bleeding after delivery or abortion, which can be difficult to distinguish from a uterine arteriovenous malformation (AVM) as both show hypervascularity on imaging. There is limited data regarding the efficacy and outcomes of uterine artery embolization (UAE) as a treatment option for RPOC without subsequent intervention. The purpose of this study is to report the outcomes of patients treated with UAE for RPOC.

METHOD AND MATERIALS

A single-center retrospective review was performed of 5 patients from October 2012 to August 2018 who underwent UAE for suspected RPOC versus uterine AVM and were ultimately found on angiogram to have RPOC. Outcomes included technical success, cessation of bleeding, complications and need for subsequent procedures.

RESULTS

Of the 5 patients with abnormal uterine bleeding, 2 had vaginal delivery, 2 had spontaneous abortions and 1 had a D&C. All 5 had transvaginal ultrasound diagnoses, 2 with RPOC vs. AVM and 3 with RPOC. Two patients had subsequent pelvic MRI, one of which was diagnosed with AVM and the other with AVM vs. RPOC. All 5 patients underwent uterine artery angiogram with diagnosis of hypervascular RPOC (no AVM present) followed by UAE with immediate technical success. None of the patients had abnormal uterine bleeding post-procedure. None of the patients required further procedures, although one patient underwent a planned D&C for removal of RPOC following UAE. No complications were reported.

CONCLUSION

The diagnosis of uterine RPOC versus AVM can be difficult with noninvasive imaging alone and definitive uterine artery angiogram may be needed before instrumentation is considered. Furthermore, in this series of patients at a single US institution, UAE has been a safe and effective standalone treatment option for patients with abnormal uterine bleeding related to RPOC.

CLINICAL RELEVANCE/APPLICATION

Retained products of conception have detrimental consequences such as abnormal uterine bleeding. This study reports clinical outcomes from a US institution's experience with UAE for treatment of RPOC.

RC514-14 Investigation of the Relationship between Magnetic Resonance Imaging Performance and Outcome of Uterine Artery Embolization in Patients with Adenomyosis

Wednesday, Dec. 4 11:35AM - 11:45AM Room: S105AB

Participants

Siqi Hu, Guangzhou , China (*Presenter*) Nothing to Disclose Wenbo Guo, PhD, Guangzhou, China (*Abstract Co-Author*) Nothing to Disclose Rui Zheng, Guangzhou, China (*Abstract Co-Author*) Nothing to Disclose Dan Zeng, Guangzhou, China (*Abstract Co-Author*) Nothing to Disclose Tingting Wan, Guangzhou, China (*Abstract Co-Author*) Nothing to Disclose

PURPOSE

To evaluate the safety and effectiveness of uterine artery embolization (UAE) applied to adenomyosis in short-term (6 months) follow-up. And to investigate the relationship between magnetic resonance imaging (MRI) performance and outcome of UAE in patients with adenomyosis.

METHOD AND MATERIALS

Between 2009-2016, 73 patients with adenomyosis who underwent bilateral UAE were retrospectively analyzed. These patients were divided into three groups according to the distribution and characteristics of T1WI and T2WI signal intensity (SI) of adenomyosis lesions on MRI. Type I: high SI on both T2WI and T1WI; Type II: high SI only on T2WI; Type III: no high SI on neither T2WI or T1WI (SI equal to that of rectus abdominis). Followed-up review lasted 12 months after UAE. Improvements in dysmenorrhea and menorrhagia were evaluated based on the symptom relief criteria.

RESULTS

The proportion of type 1, 2, 3 in preoperative MRI were 31.5% (n=23), 50.7% (n=37), 17.8% (n=13). Sixty-one of the 73 patients with dysmenorrhea (83.6%) reported improvement, fifty-seven of the 73 patients with menorrhagia (78.1%) reported improvement after UAE in 12 months. The effective rate of dysmenorrhea for type I, II, III were 73.9%(17/23),89.2%(33/37),84.6%(11/13) (p=0.62), respectively. The effective rate of menorrhagia for type I, II, III were 69.6%(16/23),78.4%(29/37),92.3%(12/13) (p=0.16).

CONCLUSION

Patients with adenomyosis who underwent UAE showed a favorable short-term control of dysmenorrhea and menorrhagia. But there was no statistically significant on prognosis between three types on MRI.

CLINICAL RELEVANCE/APPLICATION

To investigate whether the different preoperative MRI findings in patients with adenomyosis can predict the prognosis of UAE

RC514-15 Gender Differences in Peripheral Vascular Disease

Wednesday, Dec. 4 11:45AM - 12:00PM Room: S105AB

Participants

Kristofer M. Schramm, MD, Aurora, CO (Presenter) Nothing to Disclose

LEARNING OBJECTIVES

To describe trends in female vascular disease.
 To review barriers to female access to care and treatment of vascular disease.
 To establish differences in outcomes in open and endovascular repair of female vascular disease.







BI-RADS Interactive Challenge (Interactive Session)

Wednesday, Dec. 4 8:30AM - 10:00AM Room: E451A



AMA PRA Category 1 Credits ™: 1.50 ARRT Category A+ Credit: 1.75

Participants

Carol H. Lee, MD, Guilford, CT (Moderator) Nothing to Disclose

For information about this presentation, contact:

zuleyml@upmc.edu

Special Information

This interactive session will use RSNA Diagnosis Live™. Please bring your charged mobile wireless device (phone, tablet or laptop) to participate.

LEARNING OBJECTIVES

1) Identify cases for which the BI-RADS assessment may be unclear. 2) Apply the appropriate BI-RADS descriptors and categories to breast imaging studies.

Sub-Events

RC515A Mammography

Participants Carol H. Lee, MD, Guilford, CT (*Presenter*) Nothing to Disclose

LEARNING OBJECTIVES

1) Identify areas of confusion in applying BI-RADS to mammograms. 2) Assess instances of inappropriate BI-RADS assessment to mammograms. 3) Apply appropriate descriptors and assessment categories to mammograms.

RC515B Ultrasound

Participants

Paula B. Gordon, MD, Vancouver, BC (*Presenter*) Stockholder, OncoGenex Pharmaceuticals, Inc ; Stockholder, Volpara Health Technologies Limited; Scientific Advisory Board, Real Imaging Ltd; Scientific Advisory Board, DenseBreast-info, Inc; Scientific Advisor, Dense Breasts Canada

LEARNING OBJECTIVES

1) Show interesting cases that include ultrasound images will be shown; audience participation will be invited.

RC515C MRI

Participants Wendy B. Demartini, MD, Stanford, CA (*Presenter*) Nothing to Disclose

LEARNING OBJECTIVES

1) Recognize and describe clinically relevant findings. 2) Apply appropriate assessment categories. 3) Use interpretation strategies that improve diagnostic performance.





Paid Family/Parental Leave in Radiology with a Focus on Private Practice: A Panel Discussion (In Conjunction with the American Association for Women Radiologists)

Wednesday, Dec. 4 8:30AM - 10:00AM Room: S404CD

HP

AMA PRA Category 1 Credits ™: 1.50 ARRT Category A+ Credit: 1.75

Participants

Elizabeth K. Arleo, MD, New York, NY (Moderator) Editor, Reed Elsevier

Nina E. Kottler, MD, MS, Sydney, Australia (*Presenter*) Partner, Radiology Partners; Stockholder, Radiology Partners Catherine J. Everett, MD, New Bern, NC (*Presenter*) Shareholder, Radiology Partners; President, Eidetico Radiology Solutions Annie Sartor, San Francisco, CA (*Presenter*) Nothing to Disclose Kamran Ali, MD, Wichita, KS (*Presenter*) Nothing to Disclose

For information about this presentation, contact:

catherine.everett@radpartners.com

ela9033@med.cornell.edu

laurabancroftmd@gmail.com

kamrad9898@yahoo.com

LEARNING OBJECTIVES

1) Explain the 1993 Family Leave Act, its scope and its limitations. 2) Present the case for paid family/parental leave. 3) Discuss challenges and strategies for implementing paid family/parental leave in radiology private practices.





Emerging Technology: Dual-energy and Spectral CT Update 2019

Wednesday, Dec. 4 8:30AM - 10:00AM Room: S505AB

CH CT GI MK NR

AMA PRA Category 1 Credits ™: 1.50 ARRT Category A+ Credit: 1.75

FDA Discussions may include off-label uses.

Participants

Savvas Nicolaou, MD, Vancouver, BC (*Moderator*) Institutional research agreement, Siemens AG; Stockholder, Canada Diagnostic Centres

For information about this presentation, contact:

savvas.nicolaou@vch.ca

LEARNING OBJECTIVES

1) Briefly review the principles of Dual Energy CT/Spectral imaging. 2) Review virtual non-contrast imaging, iodine mapping, 3 material decomposition, and monoenergetic imaging. 3) Review cases demonstrating abdominal organ perfusion and oncologic applications in the abdomen. 4) To outline novel applications of dual energy CT in assessing bone marrow edema, gout, ligament/tendon analysis and metal artifact reduction. 5) To outline novel techniques using Dual Energy CT in pulmonary embolism, cardiac ischemia assessment. 6) Review DECT/spectral imaging applications in the brain.

Sub-Events

RC517A How to Successfully Implement a Dual-energy CT in Your Practice?

Participants

Nicolas Murray, MD, Vancouver, BC (Presenter) Nothing to Disclose

LEARNING OBJECTIVES

1) To learn the tips and tricks to make a dual-energy CT implementation successful. 2) To recognize the potential barriers in implementation of dual-energy CT in your practice.

RC517B Practical Multi-energy Applications of the Cardiothoracic System

Participants

Prabhakar Rajiah, MD, FRCR, Dallas, TX (Presenter) Royalties, Reed Elsevier

LEARNING OBJECTIVES

1) To describe the different implementations of multi-energy CT technology. 2) To discuss the updates on the utility of multienergy CT in cardiothoracic imaging. 3) To review the applications of multi-energy CT in cardiothoracic imaging.

RC517C Novel and Emerging Neuroradiology Multi-energy Applications

Participants

Aaron D. Sodickson, MD, PhD, Boston, MA (*Presenter*) Institutional research agreement, Siemens AG; Speaker, Siemens AG; Speaker, General Electric Company

For information about this presentation, contact:

asodickson@bwh.harvard.edu

LEARNING OBJECTIVES

1) Review Dual Energy CT fundamentals and post-processing applications. 2) Demonstrate the utility of Dual Energy CT to add value in neuro imaging, including pathology detection, lesion characterization, diagnostic confidence, and reduced length-of-stay.

RC517D Dual-energy/Spectral CT of the Abdomen: Making a Difference

Participants

Desiree E. Morgan, MD, Birmingham, AL (*Presenter*) Institutional Research Grant, General Electric Company; Consultant, General Electric Company

LEARNING OBJECTIVES

1) Apply strategies of dual energy CT for streamlined characterization of incidentally detected intra-abdominal abnormalities such as hepatic steatosis, adrenal adenomas, and renal lesions. 2) Develop and utilize post processing techniques that improve detection and identification of clinically relevant imaging features of abdominal tumors. 3) Understand limitations and compare workflow differences among major dual/multienergy scanning systems for abdominal applications.

Participants Fabio Becce, MD, Lausanne, Switzerland (*Presenter*) Research Consultant, Horizon Pharma USA, Inc; Confidentiality Agreement, MARS Bioimaging Ltd

LEARNING OBJECTIVES

1) Comprehend the basic principles and technical aspects of dual- and multi-energy CT when imaging the musculoskeletal system. 2) Apply dual-energy CT when assessing various musculoskeletal disorders, from crystal-related arthropathies to bone marrow edema. 3) Identify potential new applications of dual-energy CT in musculoskeletal imaging, such as CT arthrography and ironrelated disorders.







Metabolic Tumor Imaging: Current and Beyond

Wednesday, Dec. 4 8:30AM - 10:00AM Room: S501ABC



AMA PRA Category 1 Credits ™: 1.50 ARRT Category A+ Credit: 1.75

FDA Discussions may include off-label uses.

Participants

Marius E. Mayerhoefer, MD, PhD, Vienna, Austria (Moderator) Speaker, Siemens AG; Research support, Siemens AG

For information about this presentation, contact:

marius.mayerhoefer@meduniwien.ac.at

LEARNING OBJECTIVES

Learn about he new PET tracers and they new potential clinical applications.
 Review the added value of PET/MRI in oncology.
 Learn about the current and future applications of hyperpolarised MRI.

Sub-Events

RC518A PET Tracers: Which Ones Will Be Next to Make it to Clinical Practice?

Participants

Jan Grimm, MD, PhD, New York, NY (Presenter) Nothing to Disclose

LEARNING OBJECTIVES

1) To have an appreciation for some of the latest PET tracers in clinical research in oncology. 2) Understand the PET and radiotherapy agents currently FDA approved and those undergoing the approval process. 3) Understand the next generation of PET tracers and molecular imaging agents that could be the next standard-of-care imaging probes.

RC518B PET/MRI: The Added Value in Oncology

Participants

Hebert Alberto Vargas, MD, Cambridge, United Kingdom (Presenter) Nothing to Disclose

LEARNING OBJECTIVES

1) To understand the concept of value in imaging and how it relates to PET/MR technology. 2) To discuss the need for research specifically geared toward assessing the value of PET/MRI in oncology.

RC518C Hyperpolarized MRI: Current and Future Applications

Participants

Ferdia A. Gallagher, PhD, FRCR, Cambridge, United Kingdom (*Presenter*) Research support, General Electric Company; Research support, GlaxoSmithKline plc

For information about this presentation, contact:

fag1000@cam.ac.uk

LEARNING OBJECTIVES

1) To explore the role of metabolism in cancer development. 2) To understand how these changes in metabolism can be exploited using hyperpolarized 13C-pyruvate. 3) To review the current evidence for hyperpolarized carbon-13 imaging in oncology. 4) To understand potential clinical applications for hyperpolarized carbon-13 imaging. 5) To consider the role of new hyperpolarized molecules in oncology.

ABSTRACT

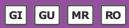
There is increasing evidence to support a role for metabolism in tumor development; for example, deregulation of cellular energetics is now considered to be one of the key hallmarks of cancer. Changes in tumor metabolism over time are now known to be early biomarkers of successful response to chemotherapy and radiotherapy. There are a number of imaging methods that have been used to probe cancer metabolism: the most widely available is 18F-fluorodeoxyglucose (FDG), an analogue of glucose, used in PET. Hyperpolarized carbon-13 MRI (13C-MRI) is an emerging molecular imaging technique for studying cellular metabolism, particularly in the field of oncology. This method allows non-invasive measurements of tissue metabolism in real-time. To date, the most promising probe used in conjunction with hyperpolarized MRI has been 13C-labelled pyruvate: pyruvate is metabolized into lactate in normal tissue in the absence of oxygen, but in tumors this occurs very rapidly even in the presence of oxygen. Results from many animal models have shown that there is a reduction in the metabolism of pyruvate following successful treatment with chemotherapy. Tumor lactate labelling has also been shown to correlate with the grade of some tumor types. There are now a small number of sites performing human hyperpolarized carbon-13 MRI imaging. This talk will discuss the progress that has been made in this field within the area of oncology and potential clinical applications.





MR Image Guidance Radiotherapy

Wednesday, Dec. 4 8:30AM - 10:00AM Room: E353A



AMA PRA Category 1 Credits ™: 1.50 ARRT Category A+ Credit: 1.75

FDA Discussions may include off-label uses.

Participants

Kathryn J. Fowler, MD, San Diego, CA (*Moderator*) Consultant, 12 Sigma Technologies; Researcher, Nuance Communications, Inc; Contractor, Midamerica Transplant Services; ;

For information about this presentation, contact:

k1fowler@ucsd.edu

LEARNING OBJECTIVES

1) Review MR imaging staging for gynecological cancers. 2) Discuss acquisition parameters and recommended sequences for evaluation. 3) Evaluate techniques for evaluating treatment response. 4) Emerging techniques. 5) Recognize the role of MR guided SBRT for borderline resectable and locally advanced pancreas tumors. 6) Recognize the role of MR guided SBRT for intra-abdominal oligometastatic tumors. 7) Identify adaptive workflow strategies to increase physician utilization and clinic efficiency. 8) Identify why MRI-guided radiation therapy has the potential to improve treatment outcomes in the management of pelvic malignancies. 9) Differentiate between rules for safe dose escalation during non-adaptive stereotactic body radiation therapy (SBRT) versus adaptive MRI-guided SBRT. 10) Develop an MRI-guided adaptive treatment flow for the management of cervical cancer. 11) recognize the unique challenges of implementing MRI-guided radiation therapy workflows. 12) develop procedures for safe and efficient delivery of online adaptive radiation therapy. 13) understand the common sources of dosimetric errors in MRI-guided radiation therapy.

Sub-Events

RC520A MR Imaging Requirements for Gastrointestinal/Gynecological Tumors

Participants

Rebecca Rakow-Penner, MD, PhD, San Diego, CA (Presenter) Research Grant, General Electric Company

For information about this presentation, contact:

rrakowpenner@ucsd.edu

LEARNING OBJECTIVES

1) Review MR imaging staging for gynecological cancers. 2) Discuss acquisition parameters and recommended sequences for evaluation. 3) Evaluate techniques for evaluating treatment response. 4) Emerging techniques.

RC520B Role of MR-guided RT for Abdominal Tumors

Participants

Hyun Kim, MD, Saint Louis, MO (*Presenter*) Research Grant and Speakers Bureau, Varian Medical Systems, Inc; Research Grant and Speakers Bureau, ViewRay, Inc

For information about this presentation, contact:

kim.hyun@wustl.edu

LEARNING OBJECTIVES

1) Recognize the role of MR guided SBRT for borderline resectable and locally advanced pancreas tumors. 2) Recognize the role of MR guided SBRT for intra-abdominal oligometastatic tumors. 3) Identify adaptive workflow strategies to increase physician utilization and clinic efficiency.

RC520C Role of MR-guided RT for Pelvic Tumors

Participants

Lorraine Portelance, MD, Miami, FL (*Presenter*) Advisory Committee, Sirtex Medical Ltd; Advisory Board, BTG International Ltd; Moderator, ViewRay, Inc

For information about this presentation, contact:

lportelance@med.miami.edu

LEARNING OBJECTIVES

1) Identify why MRI-guided radiation therapy has the potential to improve treatment outcomes in the management of pelvic malignancies. 2) Differentiate between rules for safe dose escalation during non-adaptive stereotactic body radiation therapy

(SBRT) versus adaptive MRI-guided SBRT. 3) Develop an MRI-guided adaptive treatment flow for the management of cervical cancer.

RC520D Practical Aspects and Workflow for MR-guided Radiotherapy

Participants

Olga Green, PhD, St. Louis, MO (Presenter) Speaker, ViewRay, Inc

For information about this presentation, contact:

ogreen@wustl.edu

LEARNING OBJECTIVES

1) recognize the unique challenges of implementing MRI-guided radiation therapy workflows. 2) develop procedures for safe and efficient delivery of online adaptive radiation therapy. 3) understand the common sources of dosimetric errors in MRI-guided radiation therapy.





Practical Aspects of MR

Wednesday, Dec. 4 8:30AM - 10:00AM Room: E351



AMA PRA Category 1 Credits ™: 1.50 ARRT Category A+ Credit: 1.75

FDA Discussions may include off-label uses.

Participants

Matthew A. Bernstein, PhD, Rochester, MN (*Coordinator*) Former Employee, General Electric Company; Intellectual property, General Electric Company

LEARNING OBJECTIVES

1) Understand basic aspects of MR Safety in the clinical environment, including how to avoid projectile incidents and manage patients with implanted devices. Understand the differences between MR Safe, MR Conditional, and MR Unsafe. 2) Understand the origin of MR artifacts that commonly occur in clinical practice. Acquire techniques to reduce or eliminate these artifacts. 3) Understand the basics of MR Siting and Acceptance testing. Review environmental factors such as vibration and moving metal. Review tests that can be performed after the MRI system is installed to verify its proper operation.

Sub-Events

RC521A MR Safety

Participants Robert E. Watson JR, MD, PhD, Rochester, MN (*Presenter*) Nothing to Disclose

For information about this presentation, contact:

Watson.robert16@mayo.edu

LEARNING OBJECTIVES

1) Provide a general framework about essential elements of MR safety, to include a) risks associated with the main magnetic field, radiofrequency field, and time varying gradient fields; b) MRI zones I, II, III, IV; c) MRI safe, MRI conditional, and MRI unsafe device labeling; d) Quenches; e) Patient screening and ferromagnetic detection; and f) management of patients with implanted devices.

RC521B MR Artifacts and How to Solve Them

Participants

Xiaohong J. Zhou, PhD, Chicago, IL (*Presenter*) Owner, Medical Physics Services; Consultant, Horizon Medical Physics Services; Consultant, General Electric Company; Consultant, Rush University; Advisor, Chinese Academy of Sciences; Consultant, Chinese Academy of Sciences; Reviewer, American College of Radiology; Royalties, Reed Elsevier

For information about this presentation, contact:

xjzhou@uic.edu

LEARNING OBJECTIVES

1) Recognize common artifacts in MR images. 2) Understand the root cause of the artifacts. 3) Describe the strategies to reduce or remove the artifacts.

RC521C MR Site Planning and Acceptance Testing

Participants

Lisa C. Lemen, PhD, Cincinnati, OH (Presenter) Consultant, General Electric Company; Consultant, Johnson & Johnson

LEARNING OBJECTIVES

1) Describe environmental factors which may impact the site selection or planning, including potential sources of vibration and moving metal. 2) Review a preliminary site layout for potential problems, including necessary support areas and access routes. 3) List environmental and system tests that can be performed after the MRI system is installed to verify its proper operation.







Machine Learning for Radiotherapy Applications

Wednesday, Dec. 4 8:30AM - 10:00AM Room: E352



AMA PRA Category 1 Credits ™: 1.50 ARRT Category A+ Credit: 1.75

Participants

Jayashree Kalpathy-Cramer, MS, PhD, Portland, OR (*Moderator*) Research support, General Electric Company; Research support, F. Hoffmann-La Roche Ltd;

Sub-Events

RC522A Deep Learning for Image Segmentation, Analysis and Reconstruction

Participants

Jonas Teuwen, MSc, PhD, Nijmegen, Netherlands (Presenter) Nothing to Disclose

For information about this presentation, contact:

jonas.teuwen@radboudumc.nl

LEARNING OBJECTIVES

1) Learn about the types of clinical problems which are best suited for deep learning solutions. 2) Learn about the current state-ofthe-art deep learning technology in the analysis and segmentation of medical images, and learn about the advantages of reconstructing images using deep learning technology. 3) Being able to critically estimate the impact and assess the applicability of newly developed deep learning technology.

ABSTRACT

Deep learning has recently attracted much interest from the medical community, mainly due the successful application to problems which were previously considered to be purely within the human realm. The availability of an ever growing amount of medical images, and the increasing availability of affordable computation resources allows to apply deep learning technologies to many different problems. However, the scope of problems for which deep learning currently performs on par or outperforms humans is rather narrow. The required human and financial effort makes it important to be able to determine clinical problems where deep learning could bring an advantage. After this refresher course, you will be aware of the state-of-the-art in deep learning for image segmentation, analysis and reconstruction. You will be able to critically assess the impact and applicability of deep learning technology in radiation oncology and be able to find future clinical opportunities.

RC522B Machine Learning Tumor Classification

Participants

Jayashree Kalpathy-Cramer, MS, PhD, Portland, OR (*Presenter*) Research support, General Electric Company; Research support, F. Hoffmann-La Roche Ltd;

LEARNING OBJECTIVES

1) Learn about applications of machine learning including radiomics and deep learning in classifying tumor sub-types. 2) Learn about risk stratification using machine learning of MR and CT images. 3) Understand the challenges when applying machine learning to tumor analysis. 4) Review best practices for applying machine learning in cancer imaging.

ABSTRACT

Machine learning has shown great potential for a range of applications in oncology from diagnosis to therapy planning and response assessment. Large repositories of clinical and imaging data typicially available at most institutions can be be used to train and validate models. We will discuss the use of machine learning including radiomics and deep learning for the analysis of CT and MR imaging in a variety of cancer types for risk stratification, radiogenomics and response assessment.

RC522C Machine Learning for Automated Treatment Planning

Participants

Carlos E. Cardenas, PhD, Houston, TX (Presenter) Research Grant, Varian Medical Systems, Inc

LEARNING OBJECTIVES

1) Learning about treatment planning problems which are suited to machine learning solutions. 2) Learn how deep learning approaches are being used to automated treatment planning. 3) Be able to discuss how machine learning tools can be safely introduced into clinical practice.





ACR Accreditation Updates II

Wednesday, Dec. 4 8:30AM - 10:00AM Room: S502AB

PH

AMA PRA Category 1 Credits ™: 1.50 ARRT Category A+ Credit: 1.75

Participants

Heidi A. Edmonson, PhD, Rochester, MN (Moderator) Nothing to Disclose

LEARNING OBJECTIVES

1) Learn new and updated information for the ACR breast x-ray imaging accreditation program. 2) Become familiar with the requirements for the ACR ultrasound accreditation program, including data acquisition methods and common deficiencies. 3) Understand how to prepare for an ACR site visit.

Sub-Events

RC523A ACR Breast X-Ray Imaging Accreditation Update

Participants

Eric A. Berns, PhD, Lone Tree, CO (Presenter) Nothing to Disclose

LEARNING OBJECTIVES

1) Understand the ACR Mammography accreditation program requirements. 2) Understand the 2D and DBT recent changes. 3) Review frequently asked questions on the program. 4) Present resources for personnel and facilities undergoing accreditation.

RC523B ACR US Accreditation Update

Participants Zheng Feng Lu, PhD, Chicago, IL (*Presenter*) Nothing to Disclose

LEARNING OBJECTIVES

1) Understand ACR ultrasound accreditation requirements. 2) Describe the methods and tools for ultrasound QA/QC with an explanation of common deficiencies. 3) List key resources for ACR ultrasound accreditation.

Active Handout: Zheng Feng Lu

http://abstract.rsna.org/uploads/2019/18001931/Active RC523B.pdf

RC523C ACR Accreditation: Preparing for a Site Visit

Participants Heidi A. Edmonson, PhD, Rochester, MN (*Presenter*) Nothing to Disclose

For information about this presentation, contact:

edmonson.heidi@mayo.edu

LEARNING OBJECTIVES

1) Identify key elements of an ACR Accreditation Program. 2) Understand what data to prepare for an ACR Site Visit. 3) Improve departmental organization for continual accreditation readiness.

Active Handout: Heidi A. Edmonson

http://abstract.rsna.org/uploads/2019/18001932/Active RC523C.pdf







The Literary Radiologist: Writing Our Patients, Our Experiences, Our History

Wednesday, Dec. 4 8:30AM - 10:00AM Room: S504AB

ОТ

AMA PRA Category 1 Credits ™: 1.50 ARRT Category A+ Credit: 1.75

Participants

Bruce J. Hillman, MD, Wake Forest, NC (Moderator) Royalties, Oxford University Press; Royalties, Lyons Press; Royalties, University Press of New England

For information about this presentation, contact:

bjh8a@virginia.edu

laurabancroftmd@gmail.com

LEARNING OBJECTIVES

 Overcome barriers that have made you hesitant to write about yourself, your experiences with patients, and what it means to you to be a radiologist.
 Express and receive constructive criticism about your own and others' creative writing as a means to improving your writing skills.
 Read your writing aloud and in public to gain confidence that what you write is interesting to others.
 Make an effort to publish your writing.

Sub-Events

RC524A How Creative Writing Informs Our Work as Physicians

Participants

Bruce J. Hillman, MD, Wake Forest, NC (*Presenter*) Royalties, Oxford University Press; Royalties, Lyons Press; Royalties, University Press of New England

For information about this presentation, contact:

bjh8a@virginia.edu

ABSTRACT

Beginning long before Arthur Conan Doyle modeled his fictional detective Sherlocke Holmes on his medical school professor, Joseph Bell, to the pennings of poet William Carlos Williams, to contemporary authors like novelist Abraham Verghese and essayist Atul Gewande, many physicians have found that their professional training and experiences uniquely inform their writing. Conversely, writing creatively helps clarify their thinking about their patients and medical practices. This program will feature three radiologists who believe that writing creatively enriches their personal and professional lives. While the presenters will introduce topics as wide-ranging as their motivation, their sources of encouragement, and their efforts to publish their work, we hope for a highly interactive ninety minutes. We encourage attendees to comment, relate their own writing experiences, and read brief examples of their work. At least a month prior to the RSNA Annual Meeting, each faculty member will post on a Web site samples of their writing to help initiate a conversation with each other and the audience.

RC524B The Radiologist and the Patient: Writing the Patient Narrative

Participants

Stephen D. Brown, MD, Boston, MA (Presenter) Nothing to Disclose

RC524C Riding the Fire: Writing Our Experiences

Participants

David C. Levin, MD, Philadelphia, PA (Presenter) Consultant, HealthHelp, LLC Board Member, Outpatient Imaging Affiliates, LLC

RC524D Here's Looking at You: Writing Our History

Participants

Bruce J. Hillman, MD, Wake Forest, NC (*Presenter*) Royalties, Oxford University Press; Royalties, Lyons Press; Royalties, University Press of New England





Radiomics: Promise and Challenges

Wednesday, Dec. 4 8:30AM - 10:00AM Room: S102CD



AMA PRA Category 1 Credits ™: 1.50 ARRT Category A+ Credit: 1.75

Participants

Sandy Napel, PhD, Stanford, CA (*Coordinator*) Medical Advisory Board, Fovia, Inc; Scientific Advisor, EchoPixel, Inc; Scientific Advisor, RADLogics, Inc

For information about this presentation, contact:

snapel@stanford,edu

LEARNING OBJECTIVES

1) Appreciate the motivation and scientific premise of quantitative image analysis (radiomics). 2) Learn about the role of computerextracted hand-engineered radiomics and deep learning in quantitative radiomics and machine learning. 3) Understand the role of quantitative radiomics in multi-omics cancer discovery studies and development of predictive models for precision medicine. 4) Learn about the motivation and methodology of A.I. technologies in Radiology. 5) Learn about the existing and future potential role of radiologic AI with other -omics data for precision medicine. 6) Learn about open-source informatics developments. 7) To understand some of the challenges in radiomics and radiogenomics and the crucial role of statistics in the study design and evaluation, to gain an understanding of the additional challenges brought along by the increasingly popular use of deep learning in radiomics, and to learn about the role of publicly available datasets and how to leverage challenges organized in the field.

Sub-Events

RC525A An Overview of Radiomics

Participants

Maryellen L. Giger, PhD, Chicago, IL (*Presenter*) Advisor, Qlarity Imaging; Stockholder, Hologic, Inc; Shareholder, Quantitative Insights, Inc; Shareholder, QView Medical, Inc; Co-founder, Quantitative Insights, Inc; Royalties, Hologic, Inc; Royalties, General Electric Company; Royalties, MEDIAN Technologies; Royalties, Riverain Technologies, LLC; Royalties, Mitsubishi Corporation; Royalties, Canon Medical Systems Corporation

For information about this presentation, contact:

m-giger@uchicago.edu

LEARNING OBJECTIVES

1) Appreciate the motivation and scientific premise of quantitative image analysis (radiomics). 2) Learn about the role of computerextracted hand-engineered radiomics and deep learning in quantitative radiomics and machine learning. 3) Understand the role of quantitative radiomics in multi-omics cancer discovery studies and development of predictive models for precision medicine.

RC525B From Radiomics to Radiogenomics

Participants

Hugo Aerts, PhD, Boston, MA (Presenter) Stockholder, Sphera Inc

LEARNING OBJECTIVES

1) Learn about the motivation and methodology of A.I. technologies in Radiology. 2) Learn about the existing and future potential role of radiologic AI with other -omics data for precision medicine. 3) Learn about open-source informatics developments.

RC525C Challenges for Radiomics and Radiogenomics

Participants

Karen Drukker, PhD, Chicago, IL (Presenter) Nothing to Disclose

For information about this presentation, contact:

kdrukker@uchicago.edu

LEARNING OBJECTIVES

1) To understand some of the challenges in radiomics and radiogenomics and the crucial role of statistics in the study design and evaluation. 2) To gain an understanding of the additional challenges brought along by the increasingly popular use of deep learning in radiomics. 3) To learn about the role of publicly available datasets and how to leverage challenges organized in the field.







Radiologist Peer-Review and Peer Learning: Options and Implementation Strategies in Academic and Private Practices

Wednesday, Dec. 4 8:30AM - 10:00AM Room: S104A



AMA PRA Category 1 Credits ™: 1.50 ARRT Category A+ Credit: 1.75

Participants

Jay K. Pahade, MD, Southport, CT (Moderator) Consultant, General Electric Company

LEARNING OBJECTIVES

1) To provide a brief review on radiologist peer review history, practices and discuss implementation of a department wide peer learning conference. 2) To review methods and strategies for successful peer learning program implementation in a private radiology practice. 3) To review methods and strategies for successful peer learning program implementation in an academic radiology department. 4) To allow open discussion with audience members on the pro's and con's of current peer review practices and changes to expect in the future.

Sub-Events

RC527A Radiologist Peer Review and Peer-learning Options, Best Practices, and Future Directions: Guide on Implementing Programs in Private Practice

Participants

Eric K. Bode, MD, Colorado Springs, CO (Program Committee Staff) Nothing to Disclose

LEARNING OBJECTIVES

already submitted

RC527B Radiologist Peer Review and Peer-learning Options, Best Practices, and Future Directions: Academic Radiology Departments

Participants

Ramin Khorasani, MD, Roxbury Crossing, MA (Presenter) Nothing to Disclose





Protocol Optimization and Artifacts in MRI (Interactive Session)

Wednesday, Dec. 4 8:30AM - 10:00AM Room: N227B

MR

AMA PRA Category 1 Credits ™: 1.50 ARRT Category A+ Credit: 1.75

Sub-Events

RC529A How to Build an Efficient MRI Workflow

Participants

Steven S. Raman, MD, Santa Monica, CA (*Presenter*) Consultant, Johnson & Johnson; Consultant, Bayer AG; Consultant, Merck & Co, Inc; Consultant, Amgen Inc; Consultant, Profound Medical Inc

LEARNING OBJECTIVES

1) Understand the components of an MRI workflow Understand customer needs. 2) Develop a culture of quality. 3) Develop a culture of ongoing disruption. 4) Develop feedback loops to improve quality of key personnel. 5) Develop ongoing PQI metrics.

ABSTRACT

In this talk, we will discuss how to develop an innovative, efficient and flexible MRI workflow that maximizes image quality, mimizes imaging time, improves technologist performance, develops a culture of quality and innovation, and improves the patient and referring physician experience.

RC529B Optimized Abdominal MRI Protocol

Participants

Scott B. Reeder, MD, PhD, Madison, WI (Presenter) Nothing to Disclose

LEARNING OBJECTIVES

1) Understand emerging strategies for optimized liver MRI protocols.2) Describe at least three examples of optimized liver MRI protocols.3) Be familiar with the challenges with implementing liver MRI protocols.

RC529C Optimized Prostate MRI Protocol

Participants

Aytekin Oto, MD, Chicago, IL (*Presenter*) Research Grant, Koninklijke Philips NV; Research Grant, Guerbet SA; Research Grant, Profound Medical Inc; Medical Advisory Board, Profound Medical Inc; Consultant, IBM Corporation; ; ;

For information about this presentation, contact:

oto@uchicago.edu

LEARNING OBJECTIVES

1) Review the critical sequences of multi-parametric prostate MR protocol and their added values to the interpretation. 2) Illustrate the impact of different technical approaches on image quality of different sequences. 3) Provide different options for optimized prostate MR protocol.

RC529D Optimized Female Pelvis MRI Protocol

Participants

Stephanie Nougaret, MD, Montpellier, France (Presenter) Nothing to Disclose

LEARNING OBJECTIVES

1) To discuss the technical and practical requirements for optimizing female pelvis MRI. 2) To become familiar with the optimal female pelvis MRI protocols. 3) To discuss the recent technological innovations in MR female pelvis imaging.

RC529E Top 10 MRI Artifacts

Participants

Mustafa R. Bashir, MD, Cary, NC (*Presenter*) Research Grant, Siemens AG; Research Grant, NGM Biopharmaceuticals, Inc; Research Grant, Madrigal Pharmaceuticals, Inc; Research Grant, Metacrine, Inc; Research Grant, Pinnacle Clinical Research; Research Grant, ProSciento Inc; Research Grant, Carmot Therapeutics; Research Grant, 1Globe Health Institute; Research Consultant, ICON plc;

LEARNING OBJECTIVES

1) To describe common artifacts in body MRI and strategies to mitigate them.

ABSTRACT

Artifacts are unavoidable in abdominal MRI. As pressure mounts to use shorter, more time-efficient protocols, fewer redundant sequences are available in a typical MRI protocol, and the diagnostic impact of artifacts may be increased. This discussion will

focus on common artifacts encountered in clinical practice and methods to minimize their effects on diagnostic interpretation. Printed on: 10/29/20







Why Diversity and Inclusion Matter: Beyond Gender and Ethnicity

Wednesday, Dec. 4 8:30AM - 10:00AM Room: S403B

LM

AMA PRA Category 1 Credits ™: 1.50 ARRT Category A+ Credit: 1.75

Participants

Yoshimi Anzai, MD, Salt Lake City, UT (Moderator) Nothing to Disclose

LEARNING OBJECTIVES

1) To learn what comes to our mind when you hear a word "diversity". 2) To understand the fundamental value of diverse society or organization. 3) To discuss how we embrace diversity to enrich our culture.

ABSTRACT

We have discussed many years or even decades that radiology lacks diversity. We are far from gender equity in radiology in the United States. Leaders in each academic institution are eager to recruit diverse future physician workforce to meet the goal of departmental or organizational diversity goal. We are so busy paying attention to such statistics, we often forget to remind ourselves why. Why we care about Diversity? Why diversity matters? Beyond gender, race, or sexual orientation, there are over twenty social identities that are used to characterize people, ie. married, smoker, tall, skinny, blond, democrat, and so on. Stereotyping is labeling people based on certain superficial appearance, which brings prejudice and premature judgment about people without deeply understanding each other. Studies have shown that more diverse organizations or having women or ethnic minority in the board grow faster and have better problem-solving skills than more homogeneous organizations. By working together with people who do not look like yourself, we foster more inclusive and empathetic culture, sparks creativity and innovation, and encourage "outside of the box" thinking within the organization.

Sub-Events

RC532A Why Diversity Matters

Participants

Yoshimi Anzai, MD, Salt Lake City, UT (Presenter) Nothing to Disclose

LEARNING OBJECTIVES

1) To understand real benefits of creating diverse organization. 2) To demonstrate how a diverse team outperform a non-diverse team. 3) To learn the impact of diversity and inclusion to the organizational culture.

RC532B Pipeline and Mentorship

Participants

Paul J. Rochon, MD, Aurora, CO (*Presenter*) Speaker, Penumbra, Inc; Speakers Bureau, C. R. Bard, Inc; Speaker, Cook Group Incorporated; Advisory Board, Medtronic plc; Speaker, Medtronic plc

LEARNING OBJECTIVES

1) To learn the strengths and weaknesses of pipeline in diversity and inclusion.

RC532C Program Directors' Role in Embracing Diversity and Inclusion

Participants

Carolynn M. DeBenedectis, MD, Natick , MA (Presenter) Nothing to Disclose

For information about this presentation, contact:

carolynn.debenedectis2@umassmemorial.org

LEARNING OBJECTIVES

1) To identify what groups are considered underrepresented in radiology. 2) Discuss why diversity and inclusion is so important for radiology's future. 3) Learn what program directors can do to reach out to these groups in order to foster their interest in radiology.

RC532D Multi-generational Workforce and Inclusive Culture

Participants

Carolyn C. Meltzer, MD, Atlanta, GA (Presenter) Nothing to Disclose

For information about this presentation, contact:

cmeltze@emory.edu

LEARNING OBJECTIVES

1) To understand the intersectionality of generational issues and diversity in the workplace. 2) Discuss the importance of unifying

mission, values, and strategy in creating an inclusive culture. 3) To explore the competitive advantage of cultivating an inclusive culture in radiology.

RC532E Q&A







Vertebral Augmentation (Hands-on)

Wednesday, Dec. 4 8:30AM - 10:00AM Room: E260



AMA PRA Category 1 Credits ™: 1.50 ARRT Category A+ Credit: 1.75

Participants

A. Orlando Ortiz, MD, MBA, Bronx, NY (Presenter) Nothing to Disclose

Bassem A. Georgy, MD, San Diego, CA (*Presenter*) Consultant, Merit Medical Systems, Inc; Consultant, Medtronic plc; Stockholder, Spine Solutions, Inc; ;

Allan L. Brook, MD, Bronx , NY (Presenter) Nothing to Disclose

Todd S. Miller, MD, White Plains, NY (Presenter) Nothing to Disclose

Afshin Gangi, MD, PhD, Strasbourg, France (Presenter) Consultant, AprioMed AB

Stefano Marcia, MD, Cagliari, Italy (*Presenter*) Consultant, Techlamed Srl; Consultant, Vexim SA; Consultant, Spineart; Consultant, Stryker Corporation;

Amish H. Doshi, MD, New York, NY (Presenter) Speaker, Merit Medical Systems, Inc

For information about this presentation, contact:

ortizo@nychhc.org

abrook@montefiore.org

LEARNING OBJECTIVES

Discuss appropriate algorithms for patient selection. 2) Review anatomic and technical considerations for vertebral augmentation.
 Present an update of the recent advances in vertebral augmentation including sacroplasty. 4) Emphasize safety issues and how to avoid complications. 5) Understand the applications of vertebral augmentation in osteoporotic and neoplastic spine pathology. 6) Update participants with respect to advances in equipment and biomaterials.

ABSTRACT

1. Patient selection for vertebral augmentation Indications and Contraindications 2. New devices and techniques in vertebral augmentation 3. Vertebral augmentation for osteoporotic and pathologic vertebral compression fractures 4. Sacroplasty (sacral augmentation) 5. Complications avoidance 6. Efficacy Vertebral augmentation is an image-guided (fluoroscopy or CT) percutaneous procedure in which a bone needle is inserted into a painful osteoporotic or pathologic fracture within the spinal axis. Biopsy, cavity creation or lesion ablation may then be performed under imaging guidance depending on the nature of the pathology that is being treated. Subsequently a radioopaque implant, usually an acrylic bone cement, is carefully injected into the vertebra or sacral ala under imagining guidance, These procedures have been shown to provide pain relief by stabilizing the fractured vertebra or sacral. As with any other invasive procedure, they carry a small risk (<<1%) of complication including bleeding, infection, neurovacular injury, or cement embolus. Appropriate patient seleciton and a detailed understanding of the technical aspects of the procedure along with active clinical patient follow-up are paramount to a successful outcome. This workshop will utilize short lectures, case examples and interactive audience participation in order to further explore critical topics in vertebral augmentation.





RC552

Liver Elastography (Hands-on)

Wednesday, Dec. 4 8:30AM - 10:00AM Room: E264



AMA PRA Category 1 Credits ™: 1.50 ARRT Category A+ Credit: 1.75

FDA Discussions may include off-label uses.

Participants

Richard G. Barr, MD, PhD, Campbell, OH (Presenter) Consultant, Siemens AG; Consultant, Koninklijke Philips NV; Research Grant, Siemens AG; Research Grant, SuperSonic Imagine; Speakers Bureau, Koninklijke Philips NV; Research Grant, Bracco Group; Speakers Bureau, Siemens AG; Consultant, Canon Medical Systems Corporation; Research Grant, Esaote SpA; Research Grant, BK Ultrasound; Research Grant, Hitachi, Ltd Nitin G. Chaubal, MD, MBBS, Thane, India (Presenter) Nothing to Disclose Chander Lulla, MD, MBBS, Mumbai, India (Presenter) Nothing to Disclose Mirko D'Onofrio, MD, Verona, Italy (Presenter) Speaker, Bracco Group Speaker, Siemens AG Consultant, Siemens AG Speaker, Hitachi, Ltd Carlo Filice, MD, Pavia, Italy (Presenter) Research Grant, Shenzhen Mindray Bio-Medical Electronics Co, Ltd; Research Grant, Hitachi, Ltd; Research Grant, Esaote SpA; Research Grant, Canon Medical Systems Corporation; Speaker, Shenzhen Mindray Bio-Medical Electronics Co, Ltd Vito Cantisani, MD, Roma, Italy (Presenter) Speaker, Canon Medical Systems Corporation; Speaker, Bracco Group; Speaker, Samsung Electronics Co, Ltd; Fabrizio Calliada, MD, Pavia, Italy (Presenter) Research Grant, Canon Medical Systems Corporation; Speakers Bureau, Hitachi, Ltd; Speakers Bureau, Shenzhen Mindray Bio-Medical Electronics Co, Ltd Ann E. Podrasky, MD, Miami, FL (Presenter) Speakers Bureau, Siemens AG Michelle L. Robbin, MD, Birmingham, AL (Presenter) Consultant, Koninklijke Philips NV; ; Hisham A. Tchelepi, MD, Los Angeles, CA (Presenter) Nothing to Disclose Norihisa Yada, MD, Kyoto, Japan (Presenter) Nothing to Disclose Laura Maiocchi, MD, Pavia, Italy (Presenter) Nothing to Disclose Patrick Warren, MD, Columbus, OH (Presenter) Nothing to Disclose Maija Radzina, MD, PhD, Riga, Latvia (Presenter) Speaker, Canon Medical Systems Corporation Anil Chauhan, MD, Minneapolis, MN (Presenter) Nothing to Disclose Giovanna Ferraioli, MD, Pavia, Italy (Presenter) Speaker, Koninklijke Philips NV; Speaker, Hitachi, Ltd; Speaker, Canon Medical Systems Corporation; Speaker, Shenzhen Mindray Bio-Medical Electronics Co, Ltd Cheng Fang, MBBS, FRCR, London, United Kingdom (Presenter) Nothing to Disclose Giuseppe Schillizzi, Roma, Italy (Presenter) Nothing to Disclose Daniele Fresilli, Roma, Italy (Presenter) Nothing to Disclose Vladimir Mitkov, MD, Moscow, Russia (Presenter) Speaker, Canon Medical Systems Corporation; Speaker, General Electric Company; Speaker, Koninklijke Philips NV; Speaker, Siemens AG; Speaker, Sonoscape Co, Ltd; Speaker, SuperSonic Imagine; Spouse, Speaker, Canon Medical Systems Corporation; Spouse, Speaker, General Electric Company; Spouse, Speaker, Koninklijke Philips NV; Spouse, Speaker, Siemens AG; Spouse, Speaker, Sonoscape Co, Ltd; Spouse, Speaker, SuperSonic Imagine; Daniela Elia, Roma, Italy (Presenter) Nothing to Disclose Guzman I. Lopardo Villarino, MD, Buenos Aires City, Argentina (Presenter) Nothing to Disclose Giorgia Polti, Rome, Italy (Presenter) Nothing to Disclose Eleonora Polito, Rome, Italy (Presenter) Nothing to Disclose Yana Solskaya, MD, Riga, Latvia (Presenter) Nothing to Disclose Olga Guiban, Rome, Italy (Presenter) Nothing to Disclose Patrizia Pacini, Rome, Italy (Presenter) Nothing to Disclose Adrian K. Lim, MD, FRCR, London, United Kingdom (Presenter) Luminary, Canon Medical Systems Corporation; Grant, Koninklijke Philips NV; Speakers Bureau, Siemens AG For information about this presentation, contact: thaneultrasound@gmail.com riaclinic@gmail.com

mradzina@gmail.com

vito.cantisani@uniroma1.it

yana.solskaya@gmail.com

Chengfang@nhs.net

vv@mitkov.ru

LEARNING OBJECTIVES

1) Improve basic knowledge and skills relevant to clinical practice in Liver elastography of the participants. 2) Teach how to practice liver elastography. 3) Show live how to do a proper examination, providing tips and tricks and updating current knowledge on different techniques. 4) Practical hands-on and slide presentation with key messages will be used.





RC553

The RSNA Technology Stack for Semantics and Reporting: RadLex, RadElement and RadReport

Wednesday, Dec. 4 8:30AM - 10:00AM Room: S103AB



AMA PRA Category 1 Credits ™: 1.50 ARRT Category A+ Credit: 1.75

Participants

Marta E. Heilbrun, MD, Salt Lake City, UT (Moderator) Nothing to Disclose

Sub-Events

RC553A The LOINC/RSNA Radiology Playbook: A Unified Terminology for Radiology Procedures

Participants

Daniel J. Vreeman, MS, Indianapolis, IN (*Presenter*) President, Blue Sky Premise, LLC; Investigator, bioMérieux; Investigator, Becton, Dickinson and Company

LEARNING OBJECTIVES

1) Explain the purpose and scope of the LOINC terminology standard. 2) Identify and select the key tools for implementing codes from the LOINC/RSNA Radiology Playbook. 3) Understand the development process for the LOINC/RSNA Radiology Playbook.

RC553B What is RadLex?

Participants

Kenneth C. Wang, MD, PhD, Ellicott City, MD (Presenter) Co-founder, DexNote, LLC

LEARNING OBJECTIVES

1. Define the characteristics of terminologies and ontologies. 2. Describe the scope of RadLex content and its applications. 3. Compare several tools for using RadLex.

RC553C RadPath Correlation Using RadLex

Participants

Ross W. Filice, MD, Washington, DC (*Presenter*) Co-founder, DexNote LLC; Research Grant, NVIDIA Corporation; Advisor, BunkerHill Health, Inc

For information about this presentation, contact:

ross.w.filice@gunet.georgetown.edu

LEARNING OBJECTIVES

1) Learn how the RadLex ontology can be used to automatically correlate radiology reports with pathology outcomes.

RC553D What is radelement.org?

Participants

Marc D. Kohli, MD, San Francisco, CA (Presenter) Nothing to Disclose

LEARNING OBJECTIVES

1) Define a common data element. 2) Describe how common data elements can be used to improve interoperability for interpretation. 3) Describe how common data elements are structured/organized.

RC553E Building Clinically Useful CDEs

Participants Victoria Chernyak, MD,MS, Bronx, NY (*Presenter*) Consultant, Bayer AG

For information about this presentation, contact:

vichka17@hotmail.com

LEARNING OBJECTIVES

1) To review advantages common data elements (CDE) offer for clinical reporting, computer-assisted reporting and image annotation. 2) To describe development of CDE based on ACR Assist RADS modules.

RC553F What is the RSNA Template Library?

Participants Marta E. Heilbrun, MD, Salt Lake City, UT (*Presenter*) Nothing to Disclose

For information about this presentation, contact:

marta.heilbrun@emory.edu

LEARNING OBJECTIVES

1) Understand the goals and intent behind the RSNA Template Library. 2) Appreciate the submission and review process for the templates in the library. 3) Explore opportunities to use the library to support data mining and AI initiatives.







RC554

Deep Learning in Radiology: How Do We Do It?

Wednesday, Dec. 4 8:30AM - 10:00AM Room: S406B



AMA PRA Category 1 Credits ™: 1.50 ARRT Category A+ Credit: 1.75

Participants

Luciano M. Prevedello, MD, MPH, Dublin, OH (Moderator) Nothing to Disclose

LEARNING OBJECTIVES

1) Learn what Deep Learning is and how it may be applied to Radiology. 2) Understand the challenges and benefits of creating a laboratory dedicated to machine learning in Radiology. 3) Be exposed to several applied examples of Deep Learning in Radiology at different institutions.

Sub-Events

RC554A Ohio State University Experience

Participants

Luciano M. Prevedello, MD, MPH, Dublin, OH (Presenter) Nothing to Disclose

LEARNING OBJECTIVES

1) Describe the existing infrastructure to handle pixel and non pixel data at our institution for translational research in machine learning. 2) Learn some applications of Deep Learning in Radiology through examples.

RC554B Stanford University Experience

Participants

Curtis P. Langlotz, MD,PhD, Menlo Park, CA (*Presenter*) Stockholder, Nines.ai; Advisory Board, Nines.ai; Stockholder, whiterabbit.ai; Advisory Board, whiterabbit.ai; Stockholder, Galileo CDS, Inc; Advisory Board, Galileo CDS, Inc; Stockholder, Bunker Hill, Inc; Board of Directors, Bunker Hill, Inc; Research Grant, General Electric Company; Research Grant, Siemens AG; Research Grant, Koninklijke Philips NV; Research Grant, Alphabet Inc

LEARNING OBJECTIVES

1) Consider the types of clinical problems that are best suited to machine learning solutions. 2) Understand how 'deep' neural networks work, and the technology and people needed for a successful program. 3) Learn about the type of work performed by an artificial intelligence laboratory focused on medical imaging and computer vision. 4) Analyze the key technologies needed to create large annotated training data sets. 5) Analyze how to select AI applications for your practice.

RC554C Mayo Clinic Rochester Experience

Participants

Bradley J. Erickson, MD, PhD, Rochester, MN (*Presenter*) Board of Directors, VoiceIt Technologies, LLC; Stockholder, VoiceIt Technologies, LLC; Board of Directors, FlowSigma, LLC; Officer, FlowSigma, LLC; Stockholder, FlowSigma, LLC

For information about this presentation, contact:

bje@mayo.edu

LEARNING OBJECTIVES

1) Describe Mayo experience with deep learning radiomics technology.







RCA41

Image to 3D Prints: How 3D Printing Works (Hands-on)

Wednesday, Dec. 4 8:30AM - 10:00AM Room: S401AB

IN

AMA PRA Category 1 Credits ™: 1.50 ARRT Category A+ Credit: 1.75

Participants

Beth A. Ripley, MD, PhD, Seattle, WA (*Presenter*) Nothing to Disclose Tatiana Kelil, MD, San Francisco, CA (*Presenter*) Nothing to Disclose Dmitry Levin, Seattle, WA (*Presenter*) Nothing to Disclose Anish Ghodadra, MD, Pittsburgh, PA (*Presenter*) Advisory Board, axial3D Limited

For information about this presentation, contact:

bethannripley@gmail.com

LEARNING OBJECTIVES

1) Describe optimal CT and MRI protocols for 3D printing. 2) Explain basic software requirements for converting DICOM images to 3D-printable .STL (standard tessellation language) files. 3) Recognize some common 3D printing artifacts. 4) Apply basic 3D printed model post-processing techniques learned during the session, including UV curing and support material removal.







RCC41

Technologies for Creating Educational Content and Teaching Files

Wednesday, Dec. 4 8:30AM - 10:00AM Room: S403A



AMA PRA Category 1 Credits ™: 1.50 ARRT Category A+ Credit: .50

Participants

Harprit S. Bedi, MD, Wellesley, MA (Moderator) Nothing to Disclose

Sub-Events

RCC41A Podcasting and Screencasting for Teaching

Participants Mahesh M. Thapa, MD, Seattle, WA (*Presenter*) Nothing to Disclose

RCC41B ePublishing

Participants Michael L. Richardson, MD, Seattle, WA (*Presenter*) Nothing to Disclose

For information about this presentation, contact:

mrich@uw.edu

LEARNING OBJECTIVES

Be familiar with pros and cons of ePublishing in general.
 Be aware of several free ePublishing programs and where to find them.
 Be aware of the ramifications of digital rights management and book pricing.
 Know how to convert an eBook into a physical paper book as needed.

RCC41C Incorporating the iPad in Resident Education: Using Mobile Technology to Improve the Way We Teach

Participants

Harprit S. Bedi, MD, Wellesley, MA (Presenter) Nothing to Disclose







MSRT42

ASRT@RSNA 2019: 3D Printing from the Radiologic Technologist's Point of View

Wednesday, Dec. 4 9:20AM - 10:20AM Room: N230B

IN

AMA PRA Category 1 Credit ™: 1.00 ARRT Category A+ Credit: 1.00

Participants

R. G. Linke, ARRT, Omaha, NE (Presenter) Nothing to Disclose

For information about this presentation, contact:

3d@childrensomaha.org

LEARNING OBJECTIVES

1) To better understand the specific uses of 3D printing in a hospital setting and the impact it has on patient care. 2) To learn of the technologist role in 3D printing in a healthcare setting. 3) Learn some of the techniques required to develop anatomical models.

ABSTRACT

3D printing is a new modality in the making within the field of Radiology. As with any modality the Radiolgic Technologist will and should play a key role. From image acquisition to the final 3D print the technologist is paramount in creating and sustaining a successful 3D printing program.





MSCP42

Case-based Review of Pediatric Radiology (Interactive Session)

Wednesday, Dec. 4 <u>10:30AM - 12:00PM Room: E450B</u>

CH GI MK NR PD

AMA PRA Category 1 Credits ™: 1.50 ARRT Category A+ Credit: 1.75

Participants

Edward Y. Lee, MD, Boston, MA (Director) Nothing to Disclose

Sub-Events

MSCP42A Pediatric Spine Disorders

Participants Amna A. Kashgari, MD, Riyadh, Saudi Arabia (*Presenter*) Nothing to Disclose

For information about this presentation, contact:

drakashgari@gmail.com

LEARNING OBJECTIVES

Review normal development of the spinal column and spinal neuralaxis.
 Describe in the imaging finding in spondylodysplasias.
 Review spinal Dysraphism classification.

ABSTRACT

The normal development and variations of the pediatric spinal column will be discused. Differentiating acquired from congenital spine and spinal cord pathologies using a case based approach.

MSCP42B Pediatric Pulmonary Disorders

Participants

Abbey Winant, MD, Boston, MA (*Presenter*) Spouse, Research Grant, Bristol-Myers Squibb Company; Spouse, Research Grant, Novartis AG; Spouse, Research Consultant, Tango Therapeutics

ABSTRACT

Congenital and acquired pediatric pulmonary cases will be presented. Discussion will include: 1) description of the imaging features for each condition, 2) tips for differentiating between conditions with similar imaging findings, 3) up-to-date recommendations for management and follow-up for each condition.

MSCP42C Pediatric Gastrointestinal Disorders

Participants Emilio Inarejos Clemente, MD, Barcelona, Spain (*Presenter*) Nothing to Disclose

For information about this presentation, contact:

emilioinarejos@gmail.com

LEARNING OBJECTIVES

1) Identify the most relevant imaging findings for each entity. 2) Define imaging key features of each condition to establish a correct diagnosis. 3) State a reasonable differential diagnosis of each case.

ABSTRACT

Congenital and acquired pediatric gastrointestinal cases will be explained. Each case will include a brief overview with its corresponding differential diagnosis.

MSCP42D Pediatric Musculoskeletal Disorders

Participants Michael Francavilla, MD, Philadelphia, PA (*Presenter*) Nothing to Disclose

For information about this presentation, contact:

francavilm@email.chop.edu

ABSTRACT

A series of pediatric musculoskeletal cases will be presented to illustrate: 1- Characteristic appearances of lower extremity MSK disorders 2- Neoplasms favoring the tibia 3- Hip disorders characteristic of children







MSES42

Essentials of Breast Imaging

Wednesday, Dec. 4 10:30AM - 12:00PM Room: S100AB

BR

AMA PRA Category 1 Credits ™: 1.50 ARRT Category A+ Credit: 1.75

Sub-Events

MSES42A Abbreviated Breast MRI: How to Get Started

Participants Christiane K. Kuhl, MD, Aachen, Germany (*Presenter*) Nothing to Disclose

For information about this presentation, contact:

ckuhl@ukaachen.de

MSES42B Localization of Non-palpable Breast Lesions: 2019

Participants

Laurie R. Margolies, MD, New York, NY (*Presenter*) Research Consultant, FUJIFILM Holdings Corporation; Research Consultant, Imago Corporation

For information about this presentation, contact:

laurie.margolies@mountsinai.org

LEARNING OBJECTIVES

1) Identify multiple methods to localize non-palpable breast lesions. 2) Compare wire and seed localization techniques. 3) Assess the pros and cons of different localization techniques.

ABSTRACT

Screen detected breast findings often undergoe image directed biopsy and when required subsequent localization and excision. Various methods for localization of non-palpable breast findings have been developed since the birth of screening mammography and include wire localizations, radioactive and non-radioactive seed localizations. This presentation will discuss the need for, the history of and the various localization methods available to today's breast imager.

MSES42C Biopsy and Perioperative Management of Breast Lesions

Participants

Eva M. Fallenberg, MD, Munich, Germany (*Presenter*) Research Grant, Bayer AG; Research Grant, Siemens AG; Research Grant, General Electric Company; Speaker, Siemens AG; Speaker, General Electric Company; Speaker, Bayer AG; Speaker, Guerbet SA;

LEARNING OBJECTIVES

1) Develop an understanding of the impact/rational of correct local staging for operation and systemic therapy decisions. 2) Differentiate advantages and disadvantages of different imaging modalities for local staging and will be able to choose the adequate one. 3) Identify the most appropriate biopsy method in the assessment of unclear or suspicious breast lesions in an individual patient.

MSES42D Digital Breast Tomosynthesis in a Diagnostic Algorithm

Participants

Dragana Djilas-Ivanovic, MD, PhD, Novi Sad, Serbia (Presenter) Nothing to Disclose







MSRO42

BOOST: Lymphoma-Case-based Multidisciplinary Review (Interactive Session)

Wednesday, Dec. 4 10:30AM - 12:00PM Room: S103CD



AMA PRA Category 1 Credits ™: 1.50 ARRT Category A+ Credit: 1.75

Participants

Chelsea C. Pinnix, MD, PhD, Houston, TX (*Moderator*) Research Grant, Merck & Co, Inc; Consultant, Global One Inc; Speaker, International Journal of Radiation Oncology, Biology & Physics Jurgen Rademaker, MD, New York, NY (*Presenter*) Nothing to Disclose Yolanda D. Tseng, MD, Seattle, WA (*Presenter*) Nothing to Disclose

LEARNING OBJECTIVES

1) Case-based review of staging and treatment response in lymphoma. 2) Discuss imaging findings in lymphoma and their clinical significance (PET, CT, MRI). 3) Describe the management of patients with lymphoma, including the role of imaging and radiation treatment options.

ABSTRACT

Management of lymphoma continues to evolve in the setting of improved imaging, pathologic understanding of this heterogeneous disease, systemic therapy, and radiotherapy techniques. This interactive, multi-disciplinary session is geared to general radiologists and radiation oncologists with the goal to provide clinically relevant, up-to-date knowledge and skills in evaluating and treating these patients. Through cases, we will review common manifestations of Hodgkin and non-Hodgkin lymphoma and imaging features of these lymphomas that are important for workup, staging, and assessment of treatment response. Cases will be used to walk participants through the management of common lymphomas with a focus on the role of radiotherapy.





MSSR42

RSNA/ESR Sports Imaging Symposium: Lower Extremity Sports Injuries (Interactive Session)

Wednesday, Dec. 4 10:30AM - 12:00PM Room: E350



AMA PRA Category 1 Credits ™: 1.50 ARRT Category A+ Credit: 1.75

Participants

Andrew J. Grainger, MD, Leeds, United Kingdom (*Moderator*) Consultant, Levicept Ltd; Director, The LivingCare Group; Laura W. Bancroft, MD, Venice, FL (*Moderator*) Nothing to Disclose

For information about this presentation, contact:

laurabancroftmd@gmail.com

LEARNING OBJECTIVES

1) To appreciate common patterns of athletic injury in the knee. 2) To become familiar with the techniques available and imaging appearances of knee, foot and ankle athletic injury. 3) To consolidate the knowledge gained from the session with interactive cases of lower limb athletic injury.

Sub-Events

MSSR42A Sports-related Injuries of the Knee: What Does the Orthopedic Surgeon Need to Know?

Participants

Theodore T. Miller, MD, New York, NY (Presenter) Nothing to Disclose

LEARNING OBJECTIVES

1) To be able to describe features of meniscal tears, ACL tears, and cartilage abnormalities that should be included in the MRI report. 2) To be able to recognize common sports-related injury patterns of the knee.

MSSR42B Multimodality Imaging of the Foot and Ankle Injuries in the Athlete

Participants

Andrew J. Grainger, MD, Leeds, United Kingdom (Presenter) Consultant, Levicept Ltd; Director, The LivingCare Group;

LEARNING OBJECTIVES

1) To appreciate the different and often contributory roles that imaging modalities have in the foot and ankle. 2) To recognize the most common ligamentous and tendon injuries in the ankle. 3) To understand how common patterns of injury relate to the mechanisms involved.

ABSTRACT

Abstract: Ankle injuries are common in many sports and the complicated anatomy of the ankle joint can be challenging the reporting radiologist. The ankle joint itself is a synovial hinge joint, but important movement for ankle function also occurs at the joints of the hind and midfoot which are also susceptible to injury. In addition to conventional radiographs, CT, MRI and ultrasound all have important roles to play in the diagnosis of foot and ankle injuries in the athlete. The ligamentous and tendon structures about the ankle are generally superficial in nature and readily amenable to assessment with ultrasound where assessment can be enhanced due to the dynamic capabilities of the technique. While MRI also demonstrates these structures, it has advantages for assessing deeper joint structures such as the chondral surfaces and bones. The complex 3d anatomy of the foot and ankle means that conventional radiographs can struggle to demonstrate bone injury which means CT also has an important role to play. This lecture will focus on the use of these imaging modalities for the assessment of acute and chronic ligamentous and tendon injury. Emphasis will be put on the mechanisms of injury and how they determine the resultant patterns of injury and the imaging appearances.

MSSR42C Interactive Case Discussion

Participants

Andrew J. Grainger, MD, Leeds, United Kingdom (*Presenter*) Consultant, Levicept Ltd; Director, The LivingCare Group; Theodore T. Miller, MD, New York, NY (*Presenter*) Nothing to Disclose

LEARNING OBJECTIVES

1) To appreciate common patterns of athletic injury in the knee. 2) To become familiar with the techniques available and imaging appearances of the knee, foot and ankle athletic injury. 3) To consolidate the knowledge gained from the session with interactive cases of lower limb athletic injury.

ABSTRACT

Cases will be presented with the opportunity for audience response highlighting and consolidating ideas presented in the preceding lecture. Abstract for that Lecture: Ankle injuries are common in many sports, and the complicated anatomy of the ankle joint can be challenging the reporting radiologist. The ankle joint itself is a synovial hinge joint, but the important movement for ankle function also occurs at the joints of the hind and midfoot which are also susceptible to injury. In addition to conventional

radiographs, CT, MRI and ultrasound all have important roles to play in the diagnosis of foot and ankle injuries in the athlete. The ligamentous and tendon structures about the ankle are generally superficial in nature and readily amenable to assessment with ultrasound where assessment can be enhanced due to the dynamic capabilities of the technique. While MRI also demonstrates these structures, it has advantages for assessing deeper joint structures such as the chondral surfaces and bones. The complex 3d anatomy of the foot and ankle means that conventional radiographs can struggle to demonstrate bone injury which means CT also has an important role to play. This lecture will focus on the use of these imaging modalities for the assessment of acute and chronic ligamentous and tendon injury. Emphasis will be put on the mechanisms of injury and how they determine the resultant patterns of injury and imaging appearances.





RCA42

Getting Stuff Done: A Hands-on Technology Workshop to Enhance Personal Productivity (Hands-on)

Wednesday, Dec. 4 10:30AM - 12:00PM Room: S401AB

IN

AMA PRA Category 1 Credits ™: 1.50 ARRT Category A+ Credit: 1.75

Participants

Puneet Bhargava, MD, Shoreline, WA (*Moderator*) Editor, Reed Elsevier Matthew B. Morgan, MD, Sandy, UT (*Presenter*) Consultant, Reed Elsevier Puneet Bhargava, MD, Shoreline, WA (*Presenter*) Editor, Reed Elsevier Amanda Lackey, MD, Springfield, MO (*Presenter*) Nothing to Disclose Tarun Pandey, MD, FRCR, Little Rock, AR (*Presenter*) Nothing to Disclose

For information about this presentation, contact:

bhargp@uw.edu

LEARNING OBJECTIVES

1) Introduce the concept of 'Getting Things Done.' Learn the concepts of Inbox Zero and other email management techniques. 2) Using tools such as note-taking applications, citation and password managers. 3) Using self-inquiry techniques, review how to make meaningful and powerful changes in how we engage with technology.





RCC42

Preparing your Radiology Practice and IT Department for Big Data

Wednesday, Dec. 4 10:30AM - 12:00PM Room: S406B



AMA PRA Category 1 Credits ™: 1.50 ARRT Category A+ Credit: 1.75

Participants

Paul J. Chang, MD, Chicago, IL (*Moderator*) Co-founder, Koninklijke Philips NV; Researcher, Koninklijke Philips NV; Researcher, Bayer AG; Advisory Board, Bayer AG; Advisory Board, Aidoc Ltd; Advisory Board, EnvoyAI; Advisory Board, Inference Analytics; Advisory Board, Subtle Medical

For information about this presentation, contact:

pchang@radiology.bsd.uchicago.edu

LEARNING OBJECTIVES

1) The potential of applying 'Big Data' approaches to radiology will be discussed. 2) The participant will be introduced to the importance of developing a comprehensive IT architecture and capability beyond the EMR in order to effectively use 'Big Data' and AI tools. 3) Strategies for preparing IT for 'Big Data' and AI will be discussed.

ABSTRACT

Current and near future requirements and constraints will require radiology practices to continuously improve and demonstrate the value they add to the enterprise. Merely 'managing the practice' will not be sufficient; groups will be required to compete in an environment where the goal will be measurable improvements in efficiency, productivity, quality, and safety. This will require optimally leveraging IT enabled business intelligence, analytics, and data driven workflow. In many ways, this challenge can be described as a 'Big Data' problem, requiring the application of newer 'Big Data' and AI approaches and tools. Unfortunately, many have discovered that an 'EMR centric' IT perspective may severely limit the ability for the enterprise to maximally leverage these newer tools to create differentiable value. This session will provide an introduction to the importance of developing a comprehensive architectural strategy to augment the existing EMR to more effectively consume 'Big Data' and AI tools.

Sub-Events

RCC42A Getting Your IT Infrastructure Ready for Big Data and AI

Participants

Paul J. Chang, MD, Chicago, IL (*Presenter*) Co-founder, Koninklijke Philips NV; Researcher, Koninklijke Philips NV; Researcher, Bayer AG; Advisory Board, Bayer AG; Advisory Board, Aidoc Ltd; Advisory Board, EnvoyAI; Advisory Board, Inference Analytics; Advisory Board, Subtle Medical

For information about this presentation, contact:

pchang@radiology.bsd.uchicago.edu

LEARNING OBJECTIVES

1) The potential of applying "Big Data" and noSQL approaches to radiology will be discussed. 2) The participant will be introduced to the importance of developing a comprehensive IT architecture and capability beyond the EMR in order to effectively use "Big Data" tools. 3) Strategies for preparing IT for business intelligence and analytics will be discussed.

ABSTRACT

Current and near future requirements and constraints will require radiology practices to continuously improve and demonstrate the value they add to the enterprise. Merely 'managing the practice' will not be sufficient; groups will be required to compete in an environment where the goal will be measurable improvements in efficiency, productivity, quality, and safety. This will require optimally leveraging IT enabled business intelligence, analytics, and data driven workflow. In many ways, this challenge can be described as a "Big Data" problem, requiring the application of newer "Big Data" approaches and tools. Unfortunately, many have discovered that an "EMR centric" IT perspective may severely limit the ability for the enterprise to maximally leverage these newer tools to create differentiable value. This session will provide an introduction to the importance of developing a comprehensive architectural strategy to augment the existing EMR to more effectively consume "Big Data" approaches and fully leverage business intelligence and analytics.

RCC42B NoSQL Approaches: Beyond the Traditional Relational Database

Participants

Paul J. Chang, MD, Chicago, IL (*Presenter*) Co-founder, Koninklijke Philips NV; Researcher, Koninklijke Philips NV; Researcher, Bayer AG; Advisory Board, Bayer AG; Advisory Board, Aidoc Ltd; Advisory Board, EnvoyAI; Advisory Board, Inference Analytics; Advisory Board, Subtle Medical

For information about this presentation, contact:

pchang@radiology.bsd.uchicago.edu

LEARNING OBJECTIVES

1) The distinction between the traditional relational (SQL) database and "NoSQL" approaches will be discussed. 2) The attendees will be given a basic introduction to how "NoSQL" tools, such as Hadoop, MapReduce, MongoDB can be complementary to existing approaches. 3) NoSQL applications and their relevance to radiology will be discussed.

ABSTRACT

Current and near future requirements and constraints will require radiology practices to continuously improve and demonstrate the value they add to the enterprise. Merely 'managing the practice' will not be sufficient; groups will be required to compete in an environment where the goal will be measurable improvements in efficiency, productivity, quality, and safety. This will require optimally leveraging IT enabled business intelligence, analytics, and data driven workflow. These approaches will require the ability to consume and utilize all available enterprise data, including unstructured reports, multimedia objects, etc. Other industries have realized that traditional IT approaches, such as the relational (SQL) database, cannot optimally address these 'difficult' data objects. Many outside of the medical domain have successfully augmented traditional approaches by newer 'Big Data' and 'NoSQL' methodologies, such as Hadoop, MapReduce, MongoDB, etc. In this session, an introduction to these newer tools will be presented.





SPAI41

RSNA AI Deep Learning Lab: Segmentation

Wednesday, Dec. 4 10:30AM - 12:00PM Room: AI Showcase, North Building, Level 2, Booth 10342



AMA PRA Category 1 Credits ™: 1.50 ARRT Category A+ Credit: 1.75

Participants

George L. Shih, MD, New York, NY (Presenter) Consultant, MD.ai, Inc; Stockholder, MD.ai, Inc;

Special Information

In order to get the best experience for this session, it is highly recommended that attendees bring a laptop with a keyboard, a decent-sized screen, and the latest version of Google Chrome. Additionally, it is recommended that attendees have a basic knowledge of deep learning programming and some experience running a Google CoLab notebook. Having a Gmail account is also helpful. Here are instructions for creating and deleting a Gmail account.

ABSTRACT

This session will focus on the use of deep learning methods for image segmentation, applied to the challenge of CT or MR brain segmentation. While focused on this particular problem, the concepts should generalize to other organs and image types.





SSK01

Breast Imaging (Tomosynthesis Screening)

Wednesday, Dec. 4 10:30AM - 12:00PM Room: E451B

BR

AMA PRA Category 1 Credits ™: 1.50 ARRT Category A+ Credit: 1.75

Participants

Sarah M. Friedewald, MD, Chicago, IL (*Moderator*) Consultant, Hologic, Inc; Research Grant, Hologic, Inc; Catherine S. Giess, MD, Wellesley, MA (*Moderator*) Nothing to Disclose

Sub-Events

SSK01-01 Interval Breast Cancer Following Use of Digital Breast Tomosynthesis in a Population-Based Screening Program for Breast Cancer

Wednesday, Dec. 4 10:30AM - 10:40AM Room: E451B

Participants

Tone Hovda, MD, Drammen, Norway (*Presenter*) Nothing to Disclose Solveig S. Hofvind, Oslo, Norway (*Abstract Co-Author*) Nothing to Disclose

For information about this presentation, contact:

tone.hovda@vestreviken.noSolveig.hofvind@kreftregisteret.no

PURPOSE

To compare rates and characteristics of interval breast cancer among women screened with digital breast tomosynthesis in combination with synthetic mammograms (DBT) and women screened with standard digital mammography (DM), in a population-based screening program for breast cancer.

METHOD AND MATERIALS

The national screening program for breast cancer is population-based, offering women aged 50-69 biennial mammographic screening. Our study population included 94,075 women screened 2014-2015; 35,303 women screened with DBT (study group) and 58,772 women screened with DM (control group). The rates of screen-detected breast cancer were 9.4/1000 and 6.1/1000, respectively. The women in the study population were followed for interval breast cancer two years after their screening examination. Rates and histopathological data (tumor type, histologic grade, diameter, lymph node status and ER/PR/Her2/Ki67 status) were analyzed. We used chi-square test and t-test to test for statistical significance. A p-value of <0.001 was considered statistically significant after the Bonferroni correction.

RESULTS

We observed an interval breast cancer rate of 2.0/1000 (68/35,303) in the study group and 1.5 (88/58,772) in the control group (p=0.115). No statistical significant differences were observed in histopathological tumor characteristics between the study and the control group.

CONCLUSION

Despite of a higher rate of screen-detected breast cancer among women screened with DBT compared with DM, we observed no statistical significant differences in rates or histopathological tumor characteristics of interval breast cancer between the groups.

CLINICAL RELEVANCE/APPLICATION

Despite an increased rate of screen-detected breast cancer for screening with DBT compared with DM shown in studies, no difference in rates of interval breast cancer was observed.

SSK01-02 Interval Cancers after Tomosynthesis plus Digital Mammography or Digital Mammography Breast Cancer Screening: The Reggio Emilia Tomosynthesis Randomized Trial

Wednesday, Dec. 4 10:40AM - 10:50AM Room: E451B

Participants

Valentina Iotti, MD, Reggio Emilia, Italy (*Presenter*) Speaker, General Electric Company; Travel support, General Electric Company Cinzia Campari, Reggio Emilia, Italy (*Abstract Co-Author*) Nothing to Disclose Paolo Giorgi Rossi, Reggio Emilia, Italy (*Abstract Co-Author*) Nothing to Disclose Andrea Nitrosi, PhD, Reggio Emilia, Italy (*Abstract Co-Author*) Nothing to Disclose Chiara Coriani, Reggio Emilia, Italy (*Abstract Co-Author*) Nothing to Disclose Manuela Pescarolo, Reggio Emilia, Italy (*Abstract Co-Author*) Nothing to Disclose Sabrina Caffarri, Reggio Emilia, Italy (*Abstract Co-Author*) Nothing to Disclose Vladimiro Ginocchi, Reggio Emilia, Italy (*Abstract Co-Author*) Nothing to Disclose Rita Vacondio, Reggio Emilia, Italy (*Abstract Co-Author*) Nothing to Disclose Pierpaolo Pattacini, Reggio Emilia, Italy (*Abstract Co-Author*) Nothing to Disclose

For information about this presentation, contact:

valentina.iotti@ausl.re.it

PURPOSE

The RETomo trial was a two-arm test-and-treat randomized controlled trial comparing digital breast tomosynthesis (DBT) plus digital mammography (DM) versus DM alone for breast cancer screening. We present interim analysis on interval cancers after the first round.

METHOD AND MATERIALS

Women (45-70 yo) presenting for a screening mammography, and previously screened with DM, were asked to participate and, if willing, randomised to the experimental arm (DBT+DM) or to the control arm (DM), both with two projections and double reading (NCT02698202). Women were assessed according to the decision at DBT+DM. Detection rate, recall rate, and interval cancer are reported. All women were followed up to 30 months from recruitment or up to second round.

RESULTS

From March 2014 to March 2016, 9779 women were recruited to the DM+DBT arm of the study, and 9787 women were recruited to the DM arm. Recall rate was 3.5% in both experimental and control arm; detection rate, including ductal carcinoma in situ (DCIS), was 8.6 per 1000 (84) and 4.5 per 1000 (44), respectively (relative detection rate 1.68, confidence interval [CI]: 1.22-2.30). Interval cancers were 17 in both arms, corresponding to an overall rate of 1.8/1000 (95% CI 1.1-2.9), including 1 DCIS in the DM+DBT arm and 2 in the DM arm. Among women younger than 50yo, followed with annual mammography, the interval cancers were 2 (rate of 0.7/1000; 95% CI 0.1-2.4) and 6 (rate of 2.1/1000; 95% CI 0.8-4.5) in the experimental and control arm, respectively.

CONCLUSION

These are the first results from a randomised trial reporting interval cancer intervals after DM+DBT compared to DM alone screening. The introduction of DBT to DM in screening strongly increased the detection rate, but had no impact on interval cancer rate, suggesting that screen detected and interval cancers come from different populations of lesions with different growth speed, but also imkplying that high sensitivity can lead to overdiagnosis.

CLINICAL RELEVANCE/APPLICATION

Our results suggest caution in introducing DBT in screening before health benefits have been demonstrated. Only pooling data on advanced cancer incidence and mortality from all ongoing trials can answer.

SSK01-03 Early Performance Measures Among Women Screened with DBT after a Prior DBT or a Prior DM, in a National Screening Program

Wednesday, Dec. 4 10:50AM - 11:00AM Room: E451B

Participants

Solveig S. Hofvind, Oslo, Norway (*Presenter*) Nothing to Disclose Anders S. Danielsen, Oslo, Norway (*Abstract Co-Author*) Nothing to Disclose Hildegunn S. Aase, MD, Bergen, Norway (*Abstract Co-Author*) Nothing to Disclose Cecilia Sandvik, Bergen, Norway (*Abstract Co-Author*) Nothing to Disclose Tone K. Neraas, Bergen, Norway (*Abstract Co-Author*) Nothing to Disclose Ingfrid H. Haldorsen, MD, Bergen, Norway (*Abstract Co-Author*) Nothing to Disclose

For information about this presentation, contact:

solveig.hofvind@kreftregisteret.no

PURPOSE

To investigate performance measures among women screened with digital breast tomosynthesis including synthesized mammography (DBT) after prior screening in a randomized controlled trial (RCT) with either DBT or standard digital mammography (DM).

METHOD AND MATERIALS

TB-2 (Tomosynthesis in X) is a prospective cohort study offering DBT to all women attending the screening unit in X. TB-2 is being performed in the consecutive screening round of TB-1, a RCT evaluating DBT versus DM. The studies are being performed as a part of BreastScreen Y, a population based program offering mammographic screening to women aged 50-69 biennially. During the first year of TB-2 (2018), 4657 women were screened with DBT after DBT, and 4659 with DBT after DM. Frequencies and proportions of consensus, recall, screen-detected breast cancer (invasive and ductal carcinoma in situ), and positive predictive values of recalls (PPV-1) and biopsies (PPV-2) were analyzed. One-sided Z tests were used to test whether the proportions within the DBT after DBT arm differed from those observed within the DBT after DM arm. A p-value of <0.05 was considered statistically significant

RESULTS

A total of 8.3% (387/4757) of the DBT after DBT screening exams were discussed at consensus compared to 8.5% (397/4759) for DBT after DM (p=0.36). The percentage of recalled women was 4.5% (211/4547) for DBT after DBT versus 5.0% (232/4758) for DBT after DM, (p=0.15). The number of breast cancers was 0.69% (32/4757) for DBT after DBT and 1.03% (48/4759) for DBT after DM (p=0.0364). PPV-1 and 2 were 20.7% (48/232) and 38.1% (48/126) for DBT after DBT, and 15.2% (32/221) and 20.7% (32/101) for DBT after DM (PPV-1: p=0.07; PPV-2: p=0.16).

CONCLUSION

Screening with DBT after DM yielded a high number of screen-detected breast cancers, which is in keeping with results from previous studies. Whether this increased detection is beneficial for women and society remains unclear.

CLINICAL RELEVANCE/APPLICATION

DBT detected more breast cancer than standard DM. Further studies investigating the tumor characteristics and aggressiveness of

these extra cancers are needed to offer women personalized treatment.

SSK01-04 Implementation of Digital Breast Tomosynthesis (DBT) in a Large Academic Oncology Center: Analysis of Screening Mammography Performance Metrics

Wednesday, Dec. 4 11:00AM - 11:10AM Room: E451B

Participants

Sona A. Chikarmane, MD, Newtonville, MA (*Presenter*) Nothing to Disclose Laila R. Cochon, MD,MSc, Boston, MA (*Abstract Co-Author*) Nothing to Disclose Ronilda Lacson, MD, PhD, Brookline, MA (*Abstract Co-Author*) Nothing to Disclose Ramin Khorasani, MD, Roxbury Crossing, MA (*Abstract Co-Author*) Nothing to Disclose Catherine S. Giess, MD, Wellesley, MA (*Abstract Co-Author*) Nothing to Disclose

For information about this presentation, contact:

schikarmane@partners.org

PURPOSE

To evaluate screening mammography performance metrics of digital breast tomosynthesis (DBT) compared to 2D full field digital mammography (FFDM) in patients' with prior history of breast cancer at a large academic oncology center.

METHOD AND MATERIALS

This HIPAA compliant, retrospective study consisted of consecutive female patients with a personal history of breast cancer treated with lumpectomy with or without radiation or mastectomy who underwent screening FFDM from October 2014-September 2016 or screening DBT from February 2017-December 2018 at an academic oncology center. An institutional breast cancer registry identified cancer diagnoses. Primary outcomes of recall rate (RR), cancer detection rate (CDR), and positive predictive value (PPV1) were compared between FFDM and DBT groups. Natural language processing was used to obtain patient and image characteristics including breast density, current or prior imaging findings from the most recent prior imaging examination, and BI-RADS category of the current screening examination.

RESULTS

There were 7282 examinations in the FFDM cohort and 4913 examinations in the DBT cohort during their study periods. Screening mammography performance metrics for FFDM included 9.7% (704/7282) recall rate, 6.3% (44/704) PPV1, and 6.0/1000 (44/7282) CDR and for DBT included 7.5% (369/4913) recall rate, 7.0% (26/369) PPV1 and 5.3/1000 (26/4913) CDR. There was a significant decrease in RR with DBT (p=0.0004) but no significant change in PPV1 (p=0.61) or CDR (p=0.59) between groups.

CONCLUSION

In patients' with a personal history of breast cancer, DBT significantly reduced recall rates while maintaining CDR and PPV1s.

CLINICAL RELEVANCE/APPLICATION

Integration of DBT in screening of breast cancer survivors can reduce recall rates while maintaining other screening mammography performance metrics.

SSK01-05 Digital Breast Tomosynthesis Slab Thickness: Impact on Reader Performance and Interpretation Time

Wednesday, Dec. 4 11:10AM - 11:20AM Room: E451B

Participants

Akshat C. Pujara, MD, Ann Arbor, MI (Presenter) Institutional Grant, General Electric Healthcare

Annette I. Joe, MD, Farmington Hills, MI (*Abstract Co-Author*) Institutional Grant, General Electric Company; Investigator, General Electric Company

Stephanie K. Patterson, MD, Ann Arbor, MI (Abstract Co-Author) Nothing to Disclose

Colleen H. Neal, MD, Ann Arbor, MI (Abstract Co-Author) Nothing to Disclose

Mitra Noroozian, MD, Ann Arbor, MI (Abstract Co-Author) Institutional Grant, General Electric Company; Investigator, General Electric Company

Heang-Ping Chan, PhD, Ann Arbor, MI (Abstract Co-Author) Research collaboration, General Electric Company; Institutional Grant, General Electric Company;

Mark A. Helvie, MD, Ann Arbor, MI (*Abstract Co-Author*) Institutional Grant, General Electric Company; Institutional Grant, IBM Corporation

Katherine E. Maturen, MD, Ann Arbor, MI (Abstract Co-Author) Royalties, Reed Elsevier; Royalties, Wolters Kluwer nv; ;

For information about this presentation, contact:

apujara@med.umich.edu

PURPOSE

To evaluate the impact of digital breast tomosynthesis (DBT) slab thickness on reader performance and interpretation time.

METHOD AND MATERIALS

This IRB-approved, HIPAA compliant prospective reader study was performed at an NCI-Designated Cancer Center. Four fellowshiptrained breast imagers (R1-R4) interpreted 122 DBT patient exams containing standard MLO and CC views with no prior exams or clinical history. Cases were presented using a standard protocol (10 mm slabs, 1 mm planes, synthetic 2D) and an experimental protocol (6 mm slabs, synthetic 2D) with a crossover design and 6-week washout period between sessions. Interpretation times were harvested from the workstation. Comparisons were made using t-tests or non-parametric tests for continuous variables, chisquare tests or Fisher's exact tests for categorical variables, and ROC curves for diagnostic performance.

RESULTS

Eleven exams were unilateral. Among 233 breasts, mammographic findings and final diagnoses included 45 masses (25 IDC, 1 DCIS,

19 benign), 22 groups of calcifications (3 IDC, 9 DCIS, 10 benign), 18 architectural distortions (11 IDC, 3 ILC, 1 DCIS, 3 benign), 14 asymmetries (2 IDC, 12 benign), and no finding in 134. Intrareader differences for observed findings were not significantly different between standard and experimental protocols (p>0.83). For detection of malignancy, area under the ROC curve (with 95% CI) was similar using standard and experimental protocols for all 4 readers: R1 [0.71 (0.65, 0.77) vs 0.69 (0.61, 0.76); p=0.81], R2 [0.82 (0.73, 0.90) vs 0.79 (0.70, 0.87); p=0.69], R3 [0.86 (0.79, 0.92) vs 0.90 (0.85, 0.96); p=0.52], and R4 [0.80 (0.71, 0.88) vs 0.82 (0.75, 0.90); p=0.79]. Mean reduction in interpretation time using the experimental protocol was 0.45 minutes or 11.2% (4.0 + 1.7 min vs 3.6 + 1.5 min; p<0.0001), and was statistically significant for 3/4 readers (p<0.005).

CONCLUSION

An experimental DBT reconstruction protocol using 6 mm slabs without 1 mm planes was associated with similar perception of specific findings and unchanged overall diagnostic performance compared with the standard protocol, and required less interpretation time.

CLINICAL RELEVANCE/APPLICATION

DBT is associated with longer interpretation time than 2D mammography. As DBT use increases, alternate reconstructions may help shorten interpretation time while maintaining reader performance.

SSK01-06 Effect of Age, Race and Screening Frequency on Recall Rates by Screening Mammogram Modality: Findings from a Learning Health System

Wednesday, Dec. 4 11:20AM - 11:30AM Room: E451B

Participants

Nila H. Alsheik, MD, Park Ridge, IL (*Abstract Co-Author*) Nothing to Disclose Michael Behling, Boston, MA (*Abstract Co-Author*) Employee, OM1, Inc Gregory Donadio, Boston, MA (*Abstract Co-Author*) Employee, OM1 Anna Lafontant, Boston, MA (*Abstract Co-Author*) Employee, OM1, Inc Melinda R. Talley, MD, Sioux Falls, SD (*Abstract Co-Author*) Nothing to Disclose Scott Pohlman, MSc, BEng, Cambridge, MA (*Abstract Co-Author*) Employee, Hologic, Inc Kathleen Troeger, Marlborough, MA (*Abstract Co-Author*) Employee, Hologic, Inc Vandana Menon, MD,PhD, Cambridge, MA (*Abstract Co-Author*) Employee, OM1 Emily F. Conant, MD, Philadelphia, PA (*Presenter*) Grant, Hologic, Inc; Consultant, Hologic, Inc; Grant, iCAD, Inc; Consultant, Advisory Panel, iCAD, Inc; Speaker, iiCME

For information about this presentation, contact:

chitchcock@om1.com

PURPOSE

Health systems seeking to maximize screening efficiency and optimize effectiveness need to balance the benefits of screening mammography (cancer detection) with recall and false positive rates. This analysis examines the effect of age, race and screening frequency on recall rates in a large US cohort.

METHOD AND MATERIALS

A big data platform was used to integrate EMR, RIS, and tumor registry data into a learning health system. This analysis included 575,180 screens from 257,597 women, performed 2015-2017, at 58 facilities across 3 large healthcare organizations. Women were defined as 2+ screens if they had 2 or more screens that were at least 9 months apart. Women were defined as 1-screen if they had no evidence of a screening mammogram in the one year prior to and at any time after the first observed exam; women with index screening mammograms within 12 months of the end of the study period were excluded. Women in 1-screen cohort include both prevalent and incident exams and thus represent screeners without an apparent recent prior exam. EMR records were used to identify women as either African American (AA), Caucasian (C), Asian (A) or Other (O).

RESULTS

Nearly a quarter of the women (N=57,418; 22.3%) met criteria for 1-screen and 200,179 for 2+ screens. Recall rates were significantly higher among women with 1-screen compared to 2+ screens, both overall and within each age and race category. There was a dramatic decrease in recall rate in the 2+ screen group vs the 1-screen group, particularly for DBT vs DM, after adjustment for age, breast density and institution (p<0.01), across all races (except O) and ages: 2+ screen groups (AA:7.00 vs 7.78%, C:7.38 vs 7.61%, A:7.33 vs 8.90%, O:6.75 vs 7.25%, Overall=7.31 vs 7.68%) vs 1-screen (AA:15.28 vs 18.14%, C: 15.43 vs 17.33%, A: 16.43 vs 21.64%, O:12.45 vs 15.45%, Overall=15.33 vs 17.62%).

CONCLUSION

While age and race are strong determinants of recall rates, screening frequency and screening modality have an even greater total impact. Initiatives to encourage compliance with annual screening mammography in women ages 40 and older, particularly with DBT, may help health systems optimize breast cancer screening programs while minimizing harms.

CLINICAL RELEVANCE/APPLICATION

Adherence to routine screening, and use of digital breast tomosynthesis, reduces recall rates and minimizes potential harms associated with screening mammography, across all strata of age and race.

SSK01-07 How to Resolve Tomosynthesis-Detected Architectural Distortion to Avert Biopsy

Wednesday, Dec. 4 11:30AM - 11:40AM Room: E451B

Participants Ingolf Karst, MD, Chicago, IL (*Presenter*) Nothing to Disclose Nadine Gottschalk, MD, Chicago, IL (*Abstract Co-Author*) Nothing to Disclose Katherine E. Conlon, MD, San Francisco, CA (*Abstract Co-Author*) Nothing to Disclose Sara Michael, MD, Chicago, IL (*Abstract Co-Author*) Nothing to Disclose Ellen B. Mendelson, MD, Chicago, IL (*Abstract Co-Author*) Advisory Board, Delphinus Medical Technologies, Inc; Speaker, Siemens

For information about this presentation, contact:

ikarst@nmh.org

PURPOSE

Architectural distortion (AD) is a feature raising suspicion of malignancy. Superimposed tissue may obscure AD on 2D, that is unmasked on a 1-mm DBT slice. After conversion to DBT, our recalls for AD have increased. With concern for overdetection, our purpose was to investigate how DBT detected AD can potentially be resolved on diagnostic examinations to avoid biopsy.

METHOD AND MATERIALS

After IRB approval, our proprietary database was used to map imaging findings (IF) that prompted a recall (11/2014-01/2017). Then we compared 3 month before and after transition to DBT. To study AD after transition, we identified all DBT screening-recalled diagnostic studies with AD as the main IF. Two breast imagers reviewed examinations to determine whether AD was seen on one or both DBT screening views, had US correlatives, and was resolved on diagnostic. For all biopsied AD, path reports were reviewed. For all resolved AD, FN rate w/in a 2 year timeframe were determined.

RESULTS

Comparing 10,387 screens before with 11,170 after transition to DBT, AD recalls accounted for a relative increase of 45.6%. After transition, we identified 40 cases w/ AD as the main IF recommended for biopsy. 15/40 (38%) screen-detected ADs, were one view only (7 CC and 8 MLO), and 7/15 (47%) w/ US correlates. Histologies were: 2 (5%) ILC, gr. 1 (1 w/ US corr.); 1 (2%) DCIS, gr. 2; 13 (32%) RSs, 6/13 (46%) w/ US corr. and 2 (15%) RS with atypias (1 w/ ADH and FEA, and 1 w/ FEA and LCIS); and 18 (45%) benign histologies of fibrosis, sclerosing adenosis, columnar cell change, apocrine metaplasia, and PASH. 6/13 (46%) RSs were excised with no upgrades. Classic LCIS was found in 2 cases. None of the diagnostic resolved cases were FN in a 2 year time period.

CONCLUSION

An increase in AD-recalled screening cases after transition to DBT may result from greater conspicuity of AD on DBT. No cancers were found in one-view-only AD w/o an US correlate. Fibrosis may be a possible concordant response to inflammation or trauma explaining subtle AD perceived on DBT. In diagnostic AD resolved cases no FN were found. With increasing DBT experience, breast imagers may need to reevaluate the management of AD to judge the need for biopsy, to determine concordance, and possibly to influence a decrease in FP while maintaining CDR.

CLINICAL RELEVANCE/APPLICATION

Determining the ways how to resolve DBT detected AD on diagnostic examinations may decrease the biopsy rate without affecting CDR.

SSK01-08 Screening Downstages Breast Cancer at Detection for Most Women but Some Need More Intensive Screening Regimen

Wednesday, Dec. 4 11:40AM - 11:50AM Room: E451B

Participants

Alexander B. Sevrukov, MD, Philadelphia, PA (*Presenter*) Nothing to Disclose Kimberly Klinger, MD, MS, Philadelphia, PA (*Abstract Co-Author*) Nothing to Disclose Lisa M. Zorn, MD, Cherry Hill, NJ (*Abstract Co-Author*) Nothing to Disclose Chandni Bhimani, DO, Voorhees, NJ (*Abstract Co-Author*) Nothing to Disclose Theresa J. Kaufman, DO, Villanova, PA (*Abstract Co-Author*) Nothing to Disclose Jason Shames, MD, Philadelphia, PA (*Abstract Co-Author*) Nothing to Disclose Annina N. Wilkes, MD, Philadelphia, PA (*Abstract Co-Author*) Nothing to Disclose Susan K. Dewyngaert, MD, Philadelphia, PA (*Abstract Co-Author*) Nothing to Disclose Lydia Liao, MD, PhD, Philadelphia , PA (*Abstract Co-Author*) Nothing to Disclose

For information about this presentation, contact:

Alexander.sevrukov@jefferson.edu

PURPOSE

To explore clinical and imaging characteristics of screening detected vs. symptomatic female breast cancer.

METHOD AND MATERIALS

We included 231 consecutive female breast cancer (BC) cases: 142 screening detected and 89 symptomatic BC (lump 81%, focal pain 9%, nipple discharge 6%, skin changes 4% cases) between April 2017 and March 2018. All screening mammography employed Digital Breast Tomosynthesis (DBT). Diagnostic mammography used DBT and Full-field Digital Mammography. Diagnostic ultrasound was performed as appropriate. BC was diagnosed via ultrasound-guided or DBT-guided vacuum-assisted core needle biopsy (CNB). Demographic, imaging and pathology (CNB and surgical) data were collected and analyzed using the independent samples T-test and Pearson Chi-square.

RESULTS

Women with screening detected BC were not significantly (p=ns) different from women with symptomatic BC in the following: Age (mean age, 62.8 vs. 61.3 years), Mammographically dense breasts (49% vs. 55%). Compared with symptomatic BC, cases of screening detected BC had a significant (p<.05) association with: Smaller invasive tumors (13.5 vs. 24.2 mm) and more minimal cancers (60% vs. 18%), Lower grade tumors (32% vs. 13% G1; 33% vs. 47% G3), Fewer node positive cases (11% vs. 49%), Longer interval from prior mammogram (33 vs. 17.7 months), Prior mammogram within past 11-24 months (70% vs. 21%). Women older than 40 years with symptomatic BC were more likely to have never had a mammogram compared to those with screening detected BC (36% vs. 1.4%, p<.05). 17% of symptomatic BC were diagnosed within 10 months of a prior negative mammogram (interval BC). Interval BC had a tendency to be larger and higher grade compared with all other cancers, however the differences

did not reach statistical significance due to a small sample size.

CONCLUSION

Screening detected BC had more favorable prognostic features than symptomatic BC, and the latter was associated with a shorter interval from a prior mammogram, including interval BC diagnosis.

CLINICAL RELEVANCE/APPLICATION

Routine screening DBT allows for detection of majority of BC at an earlier stage prior to symptoms. However, 17% of symptomatic BC diagnosed as interval BC (within 10 months of negative DBT) suggests that certain women may benefit from more intensive screening regimen. Further sudy of this population is warranted.

SSK01-09 The Potential Impact on Dose When Digital Breast Tomosynthesis (DBT) is Used in the Diagnostic Workup of Asymmetric Densities at Screening Assessment

Wednesday, Dec. 4 11:50AM - 12:00PM Room: E451B

Participants

Nisha Sharma, MBChB, Leeds, United Kingdom (*Presenter*) Nothing to Disclose Laura Hargreaves, Leeds, United Kingdom (*Abstract Co-Author*) Nothing to Disclose Barbara Dall, MBBCh, Leeds, United Kingdom (*Abstract Co-Author*) Nothing to Disclose Isobel Haigh, Leeds, United Kingdom (*Abstract Co-Author*) Nothing to Disclose Yan Chen, Nottingham, United Kingdom (*Abstract Co-Author*) Nothing to Disclose Michelle A. McMahon, FRCR, MBBS, Leeds, United Kingdom (*Abstract Co-Author*) Nothing to Disclose

For information about this presentation, contact:

nisha.sharma2@nhs.net

PURPOSE

Digital Breast Tomosynthesis (DBT) as a screening tool has improved the cancer detection rate and reduced the false positive rate. We wanted to assess the impact of DBT on dose when assessing asymmetric densities.

METHOD AND MATERIALS

All women recalled following an abnormal screening mammogram were asked to participate. All had triple assessment performed which involves clinical examination, additional mammographic views and targeted ultrasound of the breast and a biopsy if required. Performed between 13/11/2015 and 29/07/2016, this was an IRB approved prospective study. The DBT study was read within 6 weeks of the assessment clinic. The number of additional mammographic views and dose in mGy was recorded. The dose of the DBT examination was recorded. Statistical analysis: Dose was analysed in a mixed design, 2 x 2 ANOVA looking at dose with and without DBT (within cases).

RESULTS

1,470 women attended for screening assessment and 835 women consented to take part. 810 cases had complete data on dose & screening outcome. 248 cases were recalled for an asymmetric density in 247 women. 11 cancers were identified. There was a significant effect of the use of DBT, F(1,246) = 69.17, p < .0001, $\omega = .53$ (within cases): mean dose without DBT (M = 8.0, SD = 5.3) was higher than with DBT (M = 5.9, SD = 3.0). There was an interaction between the use of DBT and whether or not a biopsy was taken F(1,246) = 12.96, p < .0001, $\omega = .22$. When a biopsy was taken but Tomosynthesis/Ultrasound investigation indicated a biopsy was not necessary, mean dose was also higher without DBT (M = 11.1, SD = 7.3) than dose with DBT (M = 5.5, SD = 1.6). However, when a biopsy was taken that Tomosynthesis/Ultrasound investigation agreed should have taken place, there was no significant difference in dose without DBT (M = 9.8, SD = 5.5) and dose with DBT (M = 9.1, SD = 5.1). The reduction in the number of films used, associated with the use of DBT, was 4.3 (SD = 2.1).

CONCLUSION

DBT in assessment has the potential to reduce the dose and number of additional mammographic images required in the diagnostic work up of asymmetric densities.

CLINICAL RELEVANCE/APPLICATION

DBT in the diagnostc work up of asymmetric densities results in a reduction in the dose and number of biopsies performed.





SSK02

Breast Imaging (Ultrasound)

Wednesday, Dec. 4 10:30AM - 12:00PM Room: E450A



AMA PRA Category 1 Credits ™: 1.50 ARRT Category A+ Credit: 1.75

FDA Discussions may include off-label uses.

Participants

Jung Min Chang, MD, Seoul, Korea, Republic Of (*Moderator*) Nothing to Disclose Michael A. Cohen, MD, Atlanta, GA (*Moderator*) Nothing to Disclose

Sub-Events

SSK02-01 A Novel Imaging Biomarker for Monitoring Response to Neoadjuvant Chemotherapy

Wednesday, Dec. 4 10:30AM - 10:40AM Room: E450A

Participants

Neb Duric, PhD, Novi, MI (*Abstract Co-Author*) Officer, Delphinus Medical Technologies, Inc Cuiping Li, PhD, Plymouth, MI (*Abstract Co-Author*) Delphinus Medical Technologies, Inc Mark Sak, PhD, Novi, MI (*Abstract Co-Author*) Employee, Delphinus Medical Technologies, Inc Peter J. Littrup, MD, Rochester Hills, MI (*Abstract Co-Author*) Founder, CryoMedix, LLC Research Grant, Galil Medical Ltd Research Grant, Endo International plc Consultant, Delphinus Medical Technologies, Inc Rachel F. Brem, MD, Washington, DC (*Presenter*) Board of Directors, iCAD, Inc; Board of Directors, Dilon Technologies, Inc; Stock options, iCAD, Inc; Stockholder, Dilon Technologies, Inc; Consultant, Dilon Technologies, Inc; Consultant, ClearCut Medical Ltd; Consultant, Delphinus Medical Technologies, Inc

For information about this presentation, contact:

nduric@delphinusmt.com

PURPOSE

PET and MRI studies have shown that imaging biomarkers can be used to characterize response of tumors to Neoadjuvant chemotherapy (NAC) and predict pathological outcomes. However, serial PET and MRI exams are time consuming, carry high cost and are associated with risks such as exposure to Gadolinium or radiation. Our previous studies have shown that tissue sound speed, derived from ultrasound tomography (UST) measurements, is an imaging biomarker that can be used to track tumor changes in the breast. Since ultrasound is relatively inexpensive, the purpose of this study was to evaluate sound speed as a reliable and cost-effective imaging biomarker for assessing NAC.

METHOD AND MATERIALS

Twenty-one patients undergoing neo-adjuvant chemotherapy for invasive breast cancer, were serially examined with UST throughout their treatment. The two parameters measured were the volume (V) and the volume averaged sound speed (VASS) of the tumor. Response curves of VASS and V were plotted for each study participant. Pathology results were used to classify participants as complete or partial responders based on whether they achieved complete pathologic response (pCR) or not. The response curves were then averaged together within each group. The trend in the data was assessed by determining the Spearman correlation coefficient for changes in VASS and V. A t-test was used to determine if the response curves were statistically different between the two groups.

RESULTS

In the partial response group, VASS and V showed a gradual change with time while the complete response group showed a much steeper change with time (Figure 1). The difference between the two groups was significant (p<0.01) for all parameters. Furthermore, large drops in V and VASS in the first 3 weeks of treatment appeared to be predictive of pCR, though this finding was not prospective.

CONCLUSION

Our study demonstrates that UST can be used to monitor NAC and that the partial vs complete responders could be separated based on how V and VASS changed with time. A future larger study will test the predictive power of UST prospectively.

CLINICAL RELEVANCE/APPLICATION

UST has potential for non-invasive, rapid identification of partial vs complete responders in women undergoing NAC without the use of either a radiotracer or gadolinium. Clinical decision making would improve by transitioning non-responders to alternative treatment quickly and by demonstrating effective response to NAC.

SSK02-02 Precision Imaging: Early Ultrasound Evaluation (US) to Identify Excellent Responders to Neoadjuvant Chemotherapy (NAC) in Patients (pts) with Triple Negative Breast Cancer (TNBC)

Wednesday, Dec. 4 10:40AM - 10:50AM Room: E450A

Participants Beatriz E. Adrada, MD, Houston, TX (Presenter) Nothing to Disclose Rosalind P. Candelaria, MD, Houston, TX (Abstract Co-Author) Nothing to Disclose Kenneth Hess, PhD, Houston, TX (Abstract Co-Author) Nothing to Disclose Stacy Moulder, MD, Houston, TX (Abstract Co-Author) Research funded, AstraZeneca PLC Research funded, F. Hoffmann-La Roche Ltd Research funded, Oncothyreon Research funded, Novartis AG Research funded, Merck KGaA Lumarie Santiago, MD, Houston, TX (Abstract Co-Author) Nothing to Disclose Vicente Valero, MD, Houston, TX (Abstract Co-Author) Nothing to Disclose Elsa M. Arribas, MD, Houston, TX (Abstract Co-Author) Scientific Advisory Board, Volumetric Biotechnologies, Inc; Stockholder, Volumetric Biotechnologies, Inc Tanya W. Moseley, MD, Houston, TX (Abstract Co-Author) Consultant, Hologic, Inc Deanna L. Lane, MD, Houston, TX (Abstract Co-Author) Nothing to Disclose Marion E. Scoggins, MD, Houston, TX (*Abstract Co-Author*) Institutional Research Grant, General Electric Company H. Carisa Le-Petross, MD, FRCPC, Houston, TX (*Abstract Co-Author*) Nothing to Disclose David A. Spak, MD, Houston, TX (Abstract Co-Author) Nothing to Disclose Monica L. Huang, MD, Houston, TX (Abstract Co-Author) Nothing to Disclose Jennifer Litton, Houston, TX (Abstract Co-Author) Nothing to Disclose Alistair M. Thompson, Dundee, United Kingdom (Abstract Co-Author) Nothing to Disclose Jason White, Houston, TX (Abstract Co-Author) Nothing to Disclose Gary J. Whitman, MD, Houston, TX (Abstract Co-Author) Nothing to Disclose Jessica W. Leung, MD, Houston, TX (Abstract Co-Author) Scientific Advisory Board, Subtle Medical Wei T. Yang, MD, Houston, TX (Abstract Co-Author) Royalties, Reed Elsevier Gaiane M. Rauch, MD, PhD, Houston, TX (Abstract Co-Author) Nothing to Disclose

For information about this presentation, contact:

Beatriz, Adrada@mdanderson.org

PURPOSE

TNBC is a heterogeneous disease with distinct molecular subtypes that convey diverse clinical behavior and response to chemotherapy. The aim of this study is to determine if early US after two cycles of NAC has the potential to identify excellent responders to standard NAC averting need for costly genomic profiling and selecting patients with lower likelihood to achieve pathologic complete response (pCR) for targeted therapeutic trials.

METHOD AND MATERIALS

107 patients enrolled in "A randomized triple Negative Breast Cancer Enrolling Trial to Confirm Molecular Profiling Improves Survival" (ARTEMIS; NCT02276443) had US with three-dimensional measurements at baseline and after 2 cycles of Adriamycin-based NAC. Pathologic response was assessed at the time of surgery after completing anthracycline/taxane-based NAC. The relationship between pCR and primary tumor volume reduction (PTVR) by US was evaluated using recursive partitioning and ROC analysis.

RESULTS

Overall, 40% (43/107) of pts achieved pCR. Recursive partitioning showed that in patients with PTVR after 2 cycles >=73% pCR was 23/31 (74%). If the PTVR was < 73%, only 20/76 (26%) pts had pCR. In pts with <73% PTVR, the baseline volumetric size of the primary tumor (BTVS) further influenced pCR. If BTVS was < 35cm, 32% (19/59) had pCR, and if >=35 cm, only 6% had pCR (1/17) (P < 0.0001). The percentage of TVR after 2 cycles was also predictive of pCR (AUC = 0.79, 95% CI = 0.70, 0.88, p < 0.0001).

CONCLUSION

Early US exam after 2 cycles can identify the subgroup of TNBC with excellent response to standard NAC. Reduction in percent tumoral volume may predict patients with higher likehood to achieve pCR. An exploratory cut point of 73% PTVR will be tested in a validation study.

CLINICAL RELEVANCE/APPLICATION

Early US exam after 2 cycles can identify the subgroup of TNBC with excellent response to standard NAC, eliminating need for expensive genomic profiling and avoiding toxicity of investigational targeted therapy.

SSK02-03 Predicting Pathologic Complete Response with Ultrasound Tumor Characteristics in Triple Negative **Breast Cancer Patients**

Wednesday, Dec. 4 10:50AM - 11:00AM Room: E450A

Participants

Rosalind P. Candelaria, MD, Houston, TX (Presenter) Nothing to Disclose Kenneth Hess, PhD, Houston, TX (Abstract Co-Author) Nothing to Disclose Deanna L. Lane, MD, Houston, TX (Abstract Co-Author) Nothing to Disclose Lumarie Santiago, MD, Houston, TX (Abstract Co-Author) Nothing to Disclose Stacy Moulder, MD, Houston, TX (Abstract Co-Author) Research funded, AstraZeneca PLC Research funded, F. Hoffmann-La Roche Ltd Research funded, Oncothyreon Research funded, Novartis AG Research funded, Merck KGaA Wei T. Yang, MD, Houston, TX (Abstract Co-Author) Royalties, Reed Elsevier Alastair Thompson, Houston, TX (Abstract Co-Author) Nothing to Disclose Gaiane M. Rauch, MD, PhD, Houston, TX (Abstract Co-Author) Nothing to Disclose Monica L. Huang, MD, Houston, TX (Abstract Co-Author) Nothing to Disclose Elsa M. Arribas, MD, Houston, TX (Abstract Co-Author) Scientific Advisory Board, Volumetric Biotechnologies, Inc; Stockholder, Volumetric Biotechnologies, Inc Marion E. Scoggins, MD, Houston, TX (Abstract Co-Author) Institutional Research Grant, General Electric Company

Tanya W. Moseley, MD, Houston, TX (*Abstract Co-Author*) Consultant, Hologic, Inc H. Carisa Le-Petross, MD, FRCPC, Houston, TX (*Abstract Co-Author*) Nothing to Disclose David A. Spak, MD, Houston, TX (*Abstract Co-Author*) Nothing to Disclose Gary J. Whitman, MD, Houston, TX (*Abstract Co-Author*) Nothing to Disclose Jessica W. Leung, MD, Houston, TX (*Abstract Co-Author*) Scientific Advisory Board, Subtle Medical Vicente Valero, MD, Houston, TX (*Abstract Co-Author*) Nothing to Disclose Senthil Damodaran, Houston, TX (*Abstract Co-Author*) Nothing to Disclose Jennifer Litton, Houston, TX (*Abstract Co-Author*) Nothing to Disclose Jason White, Houston, TX (*Abstract Co-Author*) Nothing to Disclose Beatriz E. Adrada, MD, Houston, TX (*Abstract Co-Author*) Nothing to Disclose

For information about this presentation, contact:

rcandelaria@mdanderson.org

PURPOSE

To investigate which pretreatment and midtreatment ultrasound breast tumor characteristics are predictive of pathologic complete response (pCR) status in triple negative breast cancer (TNBC) patients treated with neoadjuvant chemotherapy

METHOD AND MATERIALS

As a substudy of an active, single-institution, IRB-approved clinical trial of Stage I-III TNBC patients, this imaging analysis included the first 125 patients who underwent surgery. Ultrasound was performed on all patients before (pretreatment) and after (midtreatment) completion of four cycles of AC (Adriamycin and cyclophosphamide) chemotherapy. Patients subsequently received taxane-based chemotherapy or an investigational therapy as guided by midtreatment response. Review of ultrasound images was performed while blinded to pathology results (i.e., pCR versus non-pCR) from definitive surgery. Tumor size was based on the largest dimension on ultrasound. Tumors with a nonmass finding of abnormal, altered echotexture compared to surrounding breast tissue were described as 'infiltrative'. The appearance of the tumor at midtreatment was designated as 'mass', 'architectural distortion', 'flat tumor bed', or 'clip only/no visible tumor bed'. Midtreatment response pattern was described as 'complete', 'concentric shrinkage', 'fragmented', 'stable' or 'progression'. Logistic regression analyses were performed with p values less than 0.05 considered statistically significant.

RESULTS

Mean patient age was 53 years, range 27-77. Fifty-five of 125 patients (44%) achieved pCR while 70 of 125 (56%) had non-pCR. On pretreatment ultrasound, tumors that were <= 5 cm in size (p=0.029) or tumors that did not have an associated infiltrative/nonmass appearance (p=0.0081) were more likely to achieve pCR. On midtreatment ultrasound, tumors which no longer had the appearance of a space-occupying mass (p<0.0001) or tumors that showed a complete or concentric shrinkage response pattern were more likely to result in pCR (p=0.010).

CONCLUSION

Ultrasound pretreatment tumor size, associated nonmass/infiltrative component assessed at pretreatment, midtreatment tumor appearance and tumor response pattern at midtreatment are variables that may be useful to predict pCR in TNBC.

CLINICAL RELEVANCE/APPLICATION

Ultrasound can be an accessible, informative tool during pretreatment and midtreatment to identify TNBC patients who are less likely to achieve pCR and may benefit from investigational therapies.

SSK02-04 Screening Ultrasonography-Detected Category 4A Breast Masses with a Decision-Making Support Software Based on Deep Learning as an Alternative to Biopsy

Wednesday, Dec. 4 11:00AM - 11:10AM Room: E450A

Participants

Sooyeon Kim, MD, Seoul, Korea, Republic Of (*Presenter*) Nothing to Disclose Jung Min Chang, MD, Seoul, Korea, Republic Of (*Abstract Co-Author*) Nothing to Disclose Jung Hyun Yoon, MD, Seoul, Korea, Republic Of (*Abstract Co-Author*) Nothing to Disclose Eun-Kyung Kim, MD, Seoul, Korea, Republic Of (*Abstract Co-Author*) Nothing to Disclose Ji Soo Choi, MD, PhD, Seoul, Korea, Republic Of (*Abstract Co-Author*) Nothing to Disclose Boo-Kyung Han, MD, PhD, Seoul, Korea, Republic Of (*Abstract Co-Author*) Nothing to Disclose

For information about this presentation, contact:

imchangjm@gmail.com

PURPOSE

To evaluate the additional value of a decision-making support software based on deep learning (S-DetectTM) in B-mode ultrasonography (US) for analyzing screening US-detected breast masses.

METHOD AND MATERIALS

This Institutional Review Board approved retrospective review of three institutional databases identified 246 women (median age: 45 years; range 20-83 years) with clinically and mammographically occult screening US-detected breast masses scheduled for biopsy. The masses were examined by an ultrasound machine (RS80A with Prestige, Samsung Medison, Co., Ltd.) equipped with S-DetectTM. BI-RADS final assessment categories on B-mode, and the quantitative scores of each descriptor on a continuous scale of 0 to 1 on S-DetectTM were collected. The area under the receiver operating characteristic curves (AUCs) of each descriptor of S-DetectTM were analyzed, and the added values of combining S-DetectTM to B-mode with respect to AUCs, sensitivity, and positive predictive value (PPV) were assessed.

RESULTS

Among 246 breast masses, 205 were benign and 41 were malignant (30 IDC, 7 DCIS, 2 ILC, 1 mucinous, 1 adenoid cystic carcinoma). There were 205 category 4A, 20 category 4B, 14 category 4C, and 7 category 5. The PPVs for category 4A, 4B, 4C,

and 5 on B-mode alone were 6.8%, 40.0%, 85.7%, and 100%, respectively. In differentiating benign and malignant masses using the S-DetectTM software, quantitative scores of not-circumscribed margin, irregular shape, and not-parallel orientation showed higher AUC values (0.754-0.800) than those of echogenicity and posterior features (0.544-0.692). Furthermore, by downgrading BI-RADS 4A masses with a not-circumscribed margin score < 0.000228, irregular shape score < 0.031686, or not-parallel orientation score < 0.00092 to BI-RADS 3, 50 false-positive biopsies could be avoided, without losing sensitivity. The PPV of category 4A increased to 9.0% after adding quantitative information.

CONCLUSION

The quantitative scores of not-circumscribed margin, irregular shape, and not-parallel orientation were important in analyzing USdetected masses, and adding this information to B-mode US could decrease unnecessary benign biopsies.

CLINICAL RELEVANCE/APPLICATION

The quantitative values measured by S-DetectTM of the morphological characteristics of masses on B-mode could decrease falsepositive biopsies caused by screening US, although validation is needed.

SSK02-05 Added Value of Vascular Index Using Superb Microvascular Imaging for Evaluation of Breast Masses: Comparison with Grayscale Ultrasound

Wednesday, Dec. 4 11:10AM - 11:20AM Room: E450A

Participants

Bora Yoon III, MD,MD, Seoul, Korea, Republic Of (*Presenter*) Nothing to Disclose Eun Young Chae, Seoul, Korea, Republic Of (*Abstract Co-Author*) Nothing to Disclose Hak Hee Kim, MD, Seoul, Korea, Republic Of (*Abstract Co-Author*) Nothing to Disclose Joo Hee Cha, MD, Seoul, Korea, Republic Of (*Abstract Co-Author*) Nothing to Disclose Hee Jung Shin, MD, Seoul, Korea, Republic Of (*Abstract Co-Author*) Grant, General Electric Company Woo Jung Choi, MD, Seoul, Korea, Republic Of (*Abstract Co-Author*) Nothing to Disclose

For information about this presentation, contact:

chaeey@amc.seoul.kr

PURPOSE

The purpose of this study is to evaluate the added value of vascular index using superb microvascular imaging for evaluation of breast masses in comparison with grayscale ultrasound (US).

METHOD AND MATERIALS

This prospective study was approved by the institutional review board, and informed consent was obtained. Between August 2018 and December 2018, a total of 70 breast masses (36 malignant and 34 benign) in consecutive 70 patients were evaluated with grayscale US and superb microvascular imaging (SMI). Two breast radiologists analysed grayscale US alone and combination of grayscale US and SMI using BI-RADS scale. They also independently measured the vascular index based on SMI. Diagnostic performance of grayscale US alone and combination of grayscale US and SMI was reported and compared. Vascular index was compared between benign and malignant masses and the optimal cut-off value was determined. We also assessed the interobserver variability in imaging analyses and vascular index between radiologists.

RESULTS

Interobserver variability in imaging analyses and vascular index was almost perfect (range of intraclass correlation coefficients, 0.932-0.947). Vascular index was higher among the malignant breast masses than benign lesions, with statistical significance (P<0.001). The optimal cut-off value of vascular index in discriminating between malignant and benign breast masses was 2.95 with a sensitivity of 86.1% and a specificity of 91.2%. The diagnostic performance of grayscale US alone and combination of grayscale US and SMI were 0.824 and 0.912 for reader 1 (P=0.028), and 0.795 and 0.853 for reader 2 (P=0.101), respectively.

CONCLUSION

Vascular index using SMI showed better diagnostic performance in distinguishing malignant from benign breast masses, with high interobserver variability.

CLINICAL RELEVANCE/APPLICATION

Our study indicates that the combined use of grayscale US and SMI with vascular index can improve the characterization of breast masses.

SSK02-06 Can We Learn Easier Breast Tumor Differentiation with Quantitative Speed-of-Sound Biomarkers? Comparison of Deep Learning of B-mode and Speed-of-Sound Images Using Conventional Ultrasound

Wednesday, Dec. 4 11:20AM - 11:30AM Room: E450A

Participants

Sergio J. Sanabria, PhD,MENG, Zurich, Switzerland (*Presenter*) Nothing to Disclose Lisa Ruby, MD, Zurich, Switzerland (*Abstract Co-Author*) Nothing to Disclose Katharina Martini, Zurich, Switzerland (*Abstract Co-Author*) Nothing to Disclose Konstantin Dedes, Zurich, Switzerland (*Abstract Co-Author*) Nothing to Disclose Denise Vorburger, Zurich, Switzerland (*Abstract Co-Author*) Nothing to Disclose Thomas Frauenfelder, MD, Zurich, Switzerland (*Abstract Co-Author*) Nothing to Disclose Marga B. Rominger, MD, Wettenberg, Germany (*Abstract Co-Author*) Nothing to Disclose

For information about this presentation, contact:

PURPOSE

Speed of Sound (SoS) is a quantitative diagnostic biomarker (meters per second) which correlates with tissue microstructure. Current SoS systems are dedicated and require breast immersion in a water bath. Our purpose is to obtain SoS maps from a conventional pulse-echo ultrasound (US) system, and to use a deep learning software (DLS), based on SoS texture, to correctly classify benign and malignant breast tissues.

METHOD AND MATERIALS

As part of an on-going HIPPA-compliant study, 27 women with histologically proven solid breast lesions (13 carcinoma, 14 benign) were examined. SoS were compared with 308 healthy breast segments in 106 women without abnormal findings. A laptop US system with a linear probe was used for B-mode and SoS-US imaging (UF-760 AG, Fukuda Denshi). Local phase aberrations in intrinsic reflections (speckle) of breast tisuse were measured with images acquired from different angular directions, and SoS images were reconstructed. SoS and B-mode texture was analyzed with a DLS (ViDi Suite v2.0.) trained with 60% of the images, and classification accuracy was evaluated in the remaining images.

RESULTS

A significant SoS increase (p<0.001) is observed in malignant lesions (carcinoma) with respect to benign lesions (79% fibroadenoma, 21% other). A SoS increase cut-off value of 42 m/s provided Accuracy (Ac) =81.5% for malignant/benign lesion differentiation, and Ac=96.0% for carcinoma and breast segments without lesions of different ACR densities (64% a&b, 36% c&d). The SoS differences between benign lesions and lesion-free segments were not significant (p>0.05). In comparison SoS texture analysis with DLS achieves Ac=83.4% for differentiation of benign/malignant lesion, Ac=99.0% for malignant lesion/lesion-free segments and Ac=98.0% for benign lesion/lesion-free. In comparison, B-mode DLS for the same region of interest respectively achieved Ac=50%, Ac=100%, Ac=100%. Malignant lesions that were not correctly classified with a SoS cut-off (e.g. a mucinosis carcinoma) were correctly classified with SoS DLS.

CONCLUSION

DLS of quantitative SoS maps improves differentiation of breast tumors with respect to a single cut-off value. For a reduced lesion dataset, DLS texture analysis of SoS was superior to B-mode ultrasound.

CLINICAL RELEVANCE/APPLICATION

Breast cancer differentiation with B-mode ultrasound is currently based on subtle geometric and texture features, which require extensive sonographic training experience or large lesion datasets for machine learning. On the other hand, SoS-US is a quantitative imaging modality, which provides an objective lesion assessment with reduced training data (or even a single image). The integration on SoS-US as an add-on feature on clinical ultrasound systems has potential to improve and facilitate breast diagnostics.

SSK02-07 Analysis of the Preoperative Axillary Ultrasound in 685 Women with T1 Breast Cancer: Can We Move Away from Sentinel Lymph Node Biopsy in Women with Early Breast Cancer?

Wednesday, Dec. 4 11:30AM - 11:40AM Room: E450A

Participants

Anna Rotili, MD, Milan, Italy (*Presenter*) Nothing to Disclose Filippo Pesapane, MD, Milan, Italy (*Abstract Co-Author*) Nothing to Disclose Silvia Penco, Milan, Italy (*Abstract Co-Author*) Nothing to Disclose Maria Pizzamiglio, Milan, Italy (*Abstract Co-Author*) Nothing to Disclose Brunella Di Nubila, Milan, Italy (*Abstract Co-Author*) Nothing to Disclose Enrico Cassano, Milano, Italy (*Abstract Co-Author*) Nothing to Disclose Daniela Lepanto, Milan, Italy (*Abstract Co-Author*) Nothing to Disclose Giuseppe Viale, Milan, Italy (*Abstract Co-Author*) Nothing to Disclose Viviana Galimberti, Milan, Italy (*Abstract Co-Author*) Nothing to Disclose Paolo Veronesi, Milan, Italy (*Abstract Co-Author*) Nothing to Disclose

For information about this presentation, contact:

filippo.pesapane@unimi.it

PURPOSE

The involvement of axillary lymph nodes is critical for appropriate treatment of breast cancer, and its evaluation is currently a hot topic of controversy across breast units. We aim to evaluate the negative predictive value (NPV) and specificity of axillary ultrasound (AUS) in the exclusion of metastatic axillary lymph node in study participants with early breast cancer.

METHOD AND MATERIALS

Preoperative AUS was performed in women with T1 breast cancer, enrolled in our Institute, as a part of a multicenter randomized prospective trial. NPV and specificity were calculated for different histologic groups: all histologic evidence of tumor including micrometastases and isolated tumoral cells (ITC), then only those with metastases, and next only those with metastases >3 mm.

RESULTS

Preoperative AUS in 685 consecutive study participants (mean age: 49±10 years) resulted in 33/685 (4.8%) of false positive and 53/343 (15.5%) of false negative, which is reduced to 28/343 (8.1%) excluding ITC and micrometastases and to 17/343 (4.9%) considering only metastases >3 mm. Overall NPV was 597/650 (92%, 95%CI, 90-94%) including all cases of positivity to histopathological examination. Excluding ITC and micrometastases, the NPV was 620/650 (95%%, 95%CI, 94-97%). Finally, including metastases that can be detected by AUS (namely, metastases >3 mm) alone, the NPV was 628/650 (97%, 95%CI, 95-98%). Specificity of AUS in our population was 628/685 (95%, 95%CI, 93-97%).

CONCLUSION

Our results show that in women with early breast cancer, the AUS may represent an effective, non-invasive diagnostic tool for axillary staging. Considering the high NPV and specificity, AUS allows to select those women who could benefit from observation

alone as a treatment approach.

CLINICAL RELEVANCE/APPLICATION

Currently, the oncological community moves away from sentinel lymph nodes biopsy and our results confirmed the role of AUS as a non-invasive, low-cost, easily available and accurate modality for preoperative staging of the axilla, in women with early breast cancer.

SSK02-08 Adjunctive Automated Breast Ultrasound Has Better Diagnostic Performance for Breast Cancer than Hand-Held Ultrasound

Wednesday, Dec. 4 11:40AM - 11:50AM Room: E450A

Participants

Mengmeng Jia, Beijing, China (*Presenter*) Research support, General Electric Company Xiang Zhou, Beijing, China (*Abstract Co-Author*) Nothing to Disclose Anhua Li, Guangzhou, China (*Abstract Co-Author*) Nothing to Disclose Lingyun Bao, MD, Hangzhou, China (*Abstract Co-Author*) Nothing to Disclose Peifang Liu, MD, PhD, Tianjin, China (*Abstract Co-Author*) Nothing to Disclose Yaqing Chen, PhD, Shanghai, China (*Abstract Co-Author*) Nothing to Disclose You-Lin Qiao, Beijing, China (*Abstract Co-Author*) Nothing to Disclose

For information about this presentation, contact:

mmjiacicams@126.com

PURPOSE

Adjunctive ultrasonography improves diagnosis of breast cancer. Automated breast ultrasound system(ABUS) can overcome the operator dependency and lack of standardization of Hand-held ultrasound(HHUS). We aimed to evaluate and compare the clinical value of adding HHUS or ABUS to mammography(MG) in the diagnostic workflow of breast cancer among Chinese women.

METHOD AND MATERIALS

1266 female outpatients aged 40 to 69 years old were enrolled in this hospital-based multi-center study. All the women underwent HHUS, ABUS and MG, Breast Imaging-Reporting and Data System(BI-RADS) was used to imaging interpretation and mammographic breast density assessment. Lesions classified as BI-RADS 4 or 5 by any of three modalities were defined as suspicious findings and were referred to biopsy for diagnosis. Clinical performance of different strategy was compared in terms of sensitivity, specificity and area under the curve(AUC) of receiver operating characteristics, using McNemar's test and nonparametric Z test.

RESULTS

323 breast cancer cases were detected in our study. 958 out of 1266 women were classified as having dense breast. Increased sensitivity and AUC as well as decreased specificity were observed when adding HHUS or ABUS to MG(all P<0.001). Compared with the combination of MG and HHUS, the combination of MG and ABUS had almost same sensitivity (0.988v.s. 0.985, p=1.000), higher specificity (0.876 v.s. 0.857, p=0.003) and higher AUC(0.932 v.s. 0.921, p=0.018). Same trend was observed when HHUS or ABUS was only added to women with dense breast(p=1.000, 0.004 and 0.011, respectively). In addition, compared with adding ABUS to all participants, adding ABUS to women with dense breast decreased the sensitivity(0.969 v.s. 0.988, p=0.031) while increased the specificity (0.884 v.s. 0.876, p=0.008), leading to a nonsignificant increase in AUC(0.927 v.s. 0.932, p=0.213).

CONCLUSION

Adding ultrasonography to MG can improve breast cancer diagnosis. Adjunctive ABUS have significant better diagnostic performance compared with adjunctive HHUS.

CLINICAL RELEVANCE/APPLICATION

The sensitivity of mammography in women with dense breast is limited in clinical practice. Adding ulrtasonography, especially ABUS, can improve diagnosis, and overcome the operator dependency.

SSK02-09 Efficiency of Technologist-Performed Hand-Held Whole Breast Ultrasound for Screening Women with Dense Breast Tissue

Wednesday, Dec. 4 11:50AM - 12:00PM Room: E450A

Participants

Liane E. Philpotts, MD, Madison, CT (*Presenter*) Consultant, Hologic, Inc Liva Andrejeva-Wright, MD, New Haven, CT (*Abstract Co-Author*) Nothing to Disclose Madhavi Raghu, MD, Cheshire, CT (*Abstract Co-Author*) Nothing to Disclose Melissa A. Durand, MD, Chester, CT (*Abstract Co-Author*) Nothing to Disclose Laura S. Sheiman, MD, Southport, CT (*Abstract Co-Author*) Nothing to Disclose Laura J. Horvath, MD, New Haven, CT (*Abstract Co-Author*) Nothing to Disclose Paul H. Levesque, MD, Madison, CT (*Abstract Co-Author*) Nothing to Disclose Tamara Y. Carroll, MD, New Haven, CT (*Abstract Co-Author*) Nothing to Disclose Maryam Etesami, MD, New Haven, CT (*Abstract Co-Author*) Nothing to Disclose Reni S. Butler, MD, Madison, CT (*Abstract Co-Author*) Nothing to Disclose Jaime L. Geisel, MD, Monroe, CT (*Abstract Co-Author*) Consultant, QView Medical, Inc Regina J. Hooley, MD, Weston, CT (*Abstract Co-Author*) Consultant, Hologic, Inc

For information about this presentation, contact:

liane.philpotts@yale.edu

PURPOSE

Technologist-performed hand-held screening whole breast ultrasound (WBUS) has been performed at our institution since 2009 in

women with dense breast tissue. With new federal breast density notification legislation in the United States, more facilities will be interested in offering this service to patients. The purpose of this study was to understand the workflow details around this practice in terms of time requirement for both technologists and radiologists and final outcome of cases.

METHOD AND MATERIALS

For a one month period (2/1/19 - 2/28/19) WBUS performed following a normal tomosynthesis screening mammogram at four sites (tertiary cancer center and 3 out-patient satellite offices) were prospectively recorded. Twenty-seven mammography technologists cross-trained in breast sonography performed all exams. Dedicated breast radiologists were present on-site to check cases and rescan if necessary. Technologists recorded images of four quadrants, the retroarerolar area, and axilla as well as documented any findings of interest. Data recorded for each exam included technologist scanning time, need for re-check by radiologist, radiologist scanning time, reason for re-check, and final BI-RADS score. Technologists identifiers were not recorded to reduce bias.

RESULTS

616 exams were performed: 602 bilateral and 14 unilateral. The average scanning time for bilateral exams was 12.5 minutes (range 4-34), and for unilateral exams was 5.1 (range 2-7). A re-check was performed in 67 cases (10.8%) and radiologist scanning time averaged 3.3 minutes (range 1-10). Reasons for re-check included complicated cyst/fibrocystic changes (18), mass/masses (13), normal fibroglandular tissue/artifact (12), suspicious mass (5), scars/prior biopsy (4), prominent lymph nodes (3), fat necrosis (1), recheck prior finding (1), implant rupture (1), improved image capture (1) and unrecorded (8). Final BI-RADS was BI-RADS 1/2: 96.6%, BI-RADS 3: 2.6%, BI-RADS 4/5: 0.8%.

CONCLUSION

Technologist-performed hand-held WBUS is time efficient, requiring just over 12 minutes scanning time per case. As the majority of cases are normal and do not require re-check, radiologist time involvement is minimal.

CLINICAL RELEVANCE/APPLICATION

Technologist-performed hand-held WBUS is an efficient method to provide adjuvant screening to women with dense breast tissue.







Cardiac (Coronary Atherosclerosis)

Wednesday, Dec. 4 10:30AM - 12:00PM Room: E351



AMA PRA Category 1 Credits ™: 1.50 ARRT Category A+ Credit: 1.75

Participants

Jill E. Jacobs, MD, New York, NY (Moderator) Nothing to Disclose

Suhny Abbara, MD, Dallas, TX (Moderator) Royalties, Reed Elsevier; Institutional research agreement, Koninklijke Philips NV; Institutional research agreement, Siemens AG

Yeon Hyeon Choe, MD, PhD, Seoul, Korea, Republic Of (Moderator) Nothing to Disclose

Sub-Events

SSK03-01 Calcium Scoring in Denoised Ultra-Low Dose Chest CT

Wednesday, Dec. 4 10:30AM - 10:40AM Room: E351

Participants

Edith M. Marom, MD, Tel Aviv, Israel (Presenter) Speaker, Bristol-Myers Squibb Company; Speaker, Boehringer Ingelheim GmbH; Speaker, Merck & Co, Inc; Officer, Voxellence ; ; ; ; Michael Green, MSc, Tel Aviv, Israel (Abstract Co-Author) Nothing to Disclose Eli Konen, MD, Tel Hashomer, Israel (*Abstract Co-Author*) Nothing to Disclose Nahum Kiryati, PhD, Tel Aviv, Israel (*Abstract Co-Author*) Nothing to Disclose

Arnaldo Mayer, PhD, Los Gatos, CA (Abstract Co-Author) Nothing to Disclose

For information about this presentation, contact:

edith.marom@gmail.com

PURPOSE

To assess the effect of a denoising method (D) for ultra low-dose CT (ULDCT) on calcium scoring.

METHOD AND MATERIALS

52 consented patients, referred for an outpatient chest CT, underwent 2 scans: a normal dose CT (NDCT), 120 kVp and automatic current modulation, with or without contrast media, immediately followed by an ULDCT, 120 kvp and fixed current at 10 mA for bmi <29 and 20 mA for bmi>=29. Consecutively, each ULDCT was denoised using a locally-consistent non-local-mean (LCNLM) algorithm to obtain a high signal to noise ratio (SNR) version of the ULDCT. The LCNLM algorithm leverages large databases of image patches extracted from high-SNR chest CT scans to denoise ULDCTs while enforcing local spatial consistency to preserve fine details and structures in the image. Blinded to all clinical information, a chest radiologist separately assessed the NDCT, ULDCT, and denoised ULDCT (D), documented findings, assigned an Agatston score for each of the scans and classified the severity of the calcifications in the coronary arteries (H). To account for the influence of strong dose reduction on Agatston scores, a 2nd order polynomial correction function between ULDCT and NDCT Agatston scores was computed and applied in a leave-one-out cross-validation scheme to each case. The same was done between ULDCT and D scores. The correction function was applied to the ULDCT and D scores obtained in the experiments.

RESULTS

Using ULDCT reduced the radiation for patients with a BMI > 29 by an average of 93% and for those with a BMI of up to 29 by an average of 96%. For patients with a BMI > 29 the average effective radiation dose for ULDCT was 0.41 mSv, whereas for those with a BMI of up to 29 it was 0.24mSv. All 14 patients with severe calcifications (Agatston>400) were classified correctly in the denoised ULDCT, while only 12 were classified as severe in the ULDCT. Also, all 6 patients with moderate calcifications (100<=Agatston<=400) were classified correctly in both ULDCT and the denoised ULDCT.

CONCLUSION

Interpretation of ULDCT may cause errors in calcium scoring, but implementation of the LCNLM algorithm for denoising improves ULDCT images so that calcium scoring results are similar to those obtained in normal dose scans.

CLINICAL RELEVANCE/APPLICATION

Denoising ULDCT with the LCNLM algorithm enables correct calcium scoring with dose reductions greater than 90%.

SSK03-02 Individualized Coronary Artery Calcium Scoring at Any Tube Voltage Using a kVp-independent **Reconstruction Kernel**

Wednesday, Dec. 4 10:40AM - 10:50AM Room: E351

Participants

Pooyan Sahbaee, Mount Pleasant, SC (*Abstract Co-Author*) Employee, Siemens AG Bernhard Schmidt, PhD, Forchheim, Germany (*Abstract Co-Author*) Employee, Siemens AG Akos Varga-Szemes, MD, PhD, Charleston, SC (*Abstract Co-Author*) Research Grant and Travel Support, Siemens AG Research

Consultant, Elucid Bioimaging

Dante Giovagnoli, MMedSc, MS, Charleston, SC (Abstract Co-Author) Nothing to Disclose

Andreas Fischer, MD, Charleston, SC (Abstract Co-Author) Nothing to Disclose

Richard Bayer, Charleston, SC (*Abstract Co-Author*) Institutional Research support, Bayer AG; Institutional Research support, HeartFlow, Inc; Institutional Research support, Siemens AG

U. Joseph Schoepf, MD, Charleston, SC (*Abstract Co-Author*) Research Grant, Astellas Group; Research Grant, Bayer AG; Research Grant, Bracco Group; Research Grant, Siemens AG; Research Grant, Heartflow, Inc; Research support, Bayer AG; Consultant, Elucid BioImaging Inc; Research Grant, Guerbet SA; Consultant, HeartFlow, Inc; Consultant, Bayer AG; Consultant, Siemens AG; ; ; Christian Tesche, MD, Dortmund, Germany (*Abstract Co-Author*) Nothing to Disclose

For information about this presentation, contact:

schoepf@musc.edu

PURPOSE

Low kV-scanning lowers radiation at many CT applications, yet is not currently used for coronary artery calcium scoring (CACS) as the Agatston convention is defined at 120kV. We prospectively investigated an automated tube voltage selection (ATVS)-based protocol, using a software-based correction algorithm and a kVp-independent kernel, for the accurate derivation of Agatston calcium scores from cardiac CT data acquired at any kV-level.

METHOD AND MATERIALS

With IRB approval, 24 patients (50% male, 60.2 ± 10.5 years) underwent conventional clinical CACS at 120 kVp and an additional research CACS acquisition using an individualized, body habitus-adjusted tube voltage between 70 and 130 kVp, based on the ATVS selection. Datasets of the additional CACS scans were reconstructed using a kVp-independent kernel that enables using the Agatston scoring convention without changing the weighting threshold of 130 HU, regardless of the original tube voltage chosen for image acquisition. Agatston scores and radiation dose estimates derived from the different ATVS-based coronary calcium scoring studies were compared with the standard acquisition at 120 kVp.

RESULTS

Median Agatston scores derived from the standard 120 kVp, 28.5 (IQR, 0.25 - 346.3), and the patient-tailored kVp-independent protocol, 32.1 (IQR, 0 - 348.7), showed no significant differences (p = 0.17). We found an excellent correlation for Agatston scores derived from the two different protocols with a Pearson's correlation coefficient of r = 0.99. Additionally, 96% of patients were classified into the same risk category (0, 1-10, 11-100, 101-400, or >400) using the patient-tailored kVp-independent protocol. The CT dose-length-product was 27.7 ± 8.6 mGy×cm using ATVS protocol and 30.0 ± 8.3 mGy×cm using the standard 120 kVp protocol, resulting in a significantly lower effective radiation dose with the kV-independent approach (0.39 ± 0.12 mSv vs. 0.42 ± 0.11 mSv) (p < 0.001).

CONCLUSION

ATVS-based CACS using a kVp-independent kernel enables Agatston calcium scoring in excellent correlation compared to the standard 120 kVp scanning. Additionally, radiation dose parameters were significantly reduced using the ATVS-based protocol.

CLINICAL RELEVANCE/APPLICATION

Using the ATVS with a kVp-independent reconstruction kernel allows the CACS protocol to be individualized to each patient, resulting in an optimal compromise between radiation dose and high diagnostic reliability.

SSK03-03 Smoking, but Not Other Risk Factors, Predicts High-Risk Plaque in Low Calcium Score 1-99 AU: Implications for Patient Management

Wednesday, Dec. 4 10:50AM - 11:00AM Room: E351

Participants

Thomas Senoner, Innsbruck, Austria (*Abstract Co-Author*) Nothing to Disclose Gerlig Widmann, Innsbruck, Austria (*Abstract Co-Author*) Nothing to Disclose Fabian Plank, MD, Innsbruck, Austria (*Abstract Co-Author*) Nothing to Disclose Wolfgang Dichtl, MD, Innsbruck, Austria (*Abstract Co-Author*) Nothing to Disclose Gudrun Feuchtner, MD, Innsbruck, Austria (*Presenter*) Nothing to Disclose

For information about this presentation, contact:

Gudrun.Feuchtner@i-med.ac.at

PURPOSE

The American Heart Association 2018 cholesterol guidelines recommend statin therapy in patients with a coronary calcium score (CCS) >100 AU as Class IIa, while in low CCS (1-99 AU), an "individual risk estimation" is adviced, leaving the clinician in a greyzone for decision making. High-risk plaque criteria are novel promising coronary computed tomography angiography (CTA) biomarkers for prection of major cardiac events.Hence, the objective of this study was to define predictors of high-risk plaque by coronary computed tomography (CCTA) in patients with a low CCS.

METHOD AND MATERIALS

6473 low-to-intermediate ASCVD-risk patients (60±12.51 years; 40.11% females) who underwent CCTA and CCS were prospectively enrolled. CCTA analysis included (1) stenosis severity CADRADS 0-4 and (2) high-risk plaque (HRP) criteria: low attenuation plaque (LAP) quantified by HU, napkin-ring (NR), spotty calcifications (SC) or positive remodeling (PR). Multiple multivariate binary logistic regression models were created for prediction of the different HRP-criteria by the major risk factors (nicotine, arterial hypertension, positive family history, dyslipidemia, diabetes mellitus).

997 patients had a low CCS (age 60.6 \pm 9.3, 40.12% female), among them 279 (28%) smokers. 35.6% of smokers had at least one HRP (min.2 criteria) versus only 26.9% of non-smokers (p=0.014). NRS was found more often in smokers (16.2% vs 9.2%, p=0.04). On multivariate linear regression, smoking but not the other risk factors predicted HRP (OR 1.56; 95% CI 1.10-2.20; p=0.012), napkin-ring (OR 2.05; 95% CI 1.12-3.74, p=0.02) and PR (OR 1.81; 95% CI 1.18-2.77 p= 0.006). There was a trend between LAP<30 HU and diabetes (p=0.09), and LAP<60 HU and <90 HU with dyslipidemia (p=0.069; p=0.035, respectively), but there was no correlation of any other risk factors with any other HRP criteria.

CONCLUSION

Active smoking predicts the presence of high-risk plaque, especially napkin-ring and positive remodeling in patients with a CCS between 1 and 99 AU, but not the other major cardiovascular risk factors.

CLINICAL RELEVANCE/APPLICATION

Although a CCS between 1-99 AU categorizes these patients as low-risk, a history of smoking should incite the physician to further investigate whether the patient has high-risk plaque, and manage LDL more restrictively, e.g by initiating or intensifying statin treatment, and/or aiming a lower target LDL.

SSK03-04 Coronary Calcium Scoring at 100 kV with Tin Filtration Using a kV-independent Reconstruction Kernel

Wednesday, Dec. 4 11:00AM - 11:10AM Room: E351

Participants

Christian Tesche, MD, Dortmund, Germany (*Presenter*) Nothing to Disclose Vincenzo Vingiani, MD, Castellammare di Stabia, SC (*Abstract Co-Author*) Nothing to Disclose Simon S. Martin, MD, Charleston, SC (*Abstract Co-Author*) Institutional Research support, Siemens AG Andres Abadia, Charleston, SC (*Abstract Co-Author*) Nothing to Disclose Andreas Fischer, MD, Charleston, SC (*Abstract Co-Author*) Nothing to Disclose Akos Varga-Szemes, MD, PhD, Charleston, SC (*Abstract Co-Author*) Research Grant and Travel Support, Siemens AG Research Consultant, Elucid Bioimaging Pooyan Sahbaee, Mount Pleasant, SC (*Abstract Co-Author*) Employee, Siemens AG Bernhard Schmidt, PhD, Forchheim, Germany (*Abstract Co-Author*) Employee, Siemens AG Rock Savage, Charleston, SC (*Abstract Co-Author*) Nothing to Disclose U. Joseph Schoepf, MD, Charleston, SC (*Abstract Co-Author*) Research Grant, Astellas Group; Research Grant, Bayer AG; Research Grant, Bracco Group; Research Grant, Siemens AG; Research Grant, Heartflow, Inc; Research support, Bayer AG; Consultant, Elucid BioImaging Inc; Research Grant, Guerbet SA; Consultant, HeartFlow, Inc; Consultant, Bayer AG; Consultant, Siemens AG; ; ;

For information about this presentation, contact:

schoepf@musc.edu

PURPOSE

This study aimed to investigate the feasibility of a protocol for coronary artery calcium scoring (CACS) at 100 kV with tin filtration (Sn100 kV) to provide accurate Agatston scores, as well asses its potential for radiation dose reduction, using a software-based correction algorithm and a kV-independent kernel compared to the standard 120 kV acquisition.

METHOD AND MATERIALS

With IRB approval, we analyzed image data of 114 patients (66 men, 61.8 ± 9.6 years) who underwent a clinically-indicated CACS acquisition using the standard 120 kV protocol and an additional Sn100 kV CACS scan, as part of a research study. Datasets of the Sn100 kV scans were reconstructed using a kV-independent kernel. The kV-independent kernel produced images with Hounsfield unit (HU) values equivalent to 120 kV for bone and calcium. This enables Agatston scoring without changing the original weighting threshold of 130 HU, regardless of the original tube voltage chosen for image acquisition. The Agatston scores and radiation dose values were calculated and compared between the two different protocols.

RESULTS

Median Agatston scores derived from the standard 120 kV and the Sn100 kV protocol with the kV-independent kernel were 24.7 (IQR, 0-171.1) and 21.4 (IQR, 0-173.8), respectively, without significant differences (P = 0.18). We found an excellent correlation for Agatston scores derived from the two different protocols with a Pearson's correlation coefficient of r = 0.99. The dose-length-product was 11.4 ± 4 mGycm using the Sn100 kV and 50.4 ± 24.9 mGycm using the standard 120 kV protocol (P < 0.01), resulting in a significantly lower effective radiation dose by 77% (0.16 ± 0.06 mSv vs. 0.7 ± 0.35 mSv, P < 0.01) for scanning at Sn100 kV. Additionally, 99% of patients were classified into the same risk category (0, 1-10, 11-100, 101-400, or >400) using the Sn100 kV protocol.

CONCLUSION

CACS at Sn100 kV using the kV-independent kernel is feasible and shows a high correlation compared to standard 120 kV scanning. Furthermore, the radiation dose was significantly reduced using the low-kV protocol.

CLINICAL RELEVANCE/APPLICATION

The use of a Sn100 kV protocol with a kV-independent kernel allows for a significant reduction of the radiation dose to the patient and simultaneously achieves a high diagnostic reliability.

SSK03-05 Determining Calcifications in Coronary Arteries Using Non-Gated Chest CT with 256-Detector Row in Comparison with Dedicated Calcium-Scoring CT

Wednesday, Dec. 4 11:10AM - 11:20AM Room: E351

Participants

Yuhuan Chen, MD, Beijing, China (*Abstract Co-Author*) Employee, inferVISION Jianying Li, Beijing, China (*Abstract Co-Author*) Employee, General Electric Company Taiping He, Xianyang, China (*Abstract Co-Author*) Nothing to Disclose

Matt Deng, PhD, Philadelphia, PA (Presenter) Employee, Infervision Inc

For information about this presentation, contact:

Chenyuhuan0528@163.com

PURPOSE

To investigate the reliability and accuracy of determining coronary artery calcifications (CAC) using non-contrast, non-gated chest CT with 256-detector row.

METHOD AND MATERIALS

This was an institutional review board approved study and all participants gave written informed consent. A total of 1318 patients for chest examination were enrolled to undergo both non-gated chest CT and dedicated calcium-scoring CT (CSCT) on a 256-detector row CT scanner. The chest CT was scanned in fast-helical mode with 8cm collimation, 0.28s rotation speed and pitch 0.992:1 to cover entire chest. CSCT used single prospective ECG-triggered cardiac axial mode with 0.28s rotation speed covering only the heart. Both scans used 120kV and automatic tube current modulation for obtaining a preset noise index of 20HU at 2.5cm slice thickness.Two reviewers evaluated the subjective image quality of the ungated chest CT in terms of the detection and display of calcifications in coronary arteries. CAC scores (Agatston, Mass and Volume) were determined using both image sets and were statistically compared.

RESULTS

It took less than 0.5s to cover the heart in the ungated chest CT and all cardiac images were acceptable for detecting and displaying calcifications in coronary arteries. Sensitivity and specificity of non-gated chest CT for determining positive CAC was 94.8% (182/192) and 100%, respectively. The agreement in assessing the quantitative Agatston, Volume and Mass scores between the non-gated chest CT and CSCT was almost perfect, with the Intra-class correlation coefficient (ICC) values of 0.998, 0.999 and 0.999, respectively. Additionally, there was a good agreement in CAC quantification between the non-gated chest CT and dedicated CSCT with small coefficient of variation: Mass score (9.0%), Volume score (9.5%) and Agatston score (12.6%).

CONCLUSION

non-gated chest CT with 256-detector row is a reliable imaging mode for detecting and quantifying calcifications in coronary arteries and the calcium mass score is the most accurate parameter compared with dedicated calcium-scoring CT.

CLINICAL RELEVANCE/APPLICATION

Non-gated chest CT on a 256-detector row CT with fast scan speed may be used to reliably detect and quantify calcifications in the coronary arteries.

SSK03-06 Deep Learning-Based Automated CT Coronary Artery Calcium Scoring

Wednesday, Dec. 4 11:20AM - 11:30AM Room: E351

Participants

Simon S. Martin, MD, Charleston, SC (Presenter) Institutional Research support, Siemens AG Marly van Assen, MSc, Charleston, SC (Abstract Co-Author) Nothing to Disclose Saikiran Rapaka, PhD, Princeton, NJ (Abstract Co-Author) Employee, Siemens AG Todd Hudson, MS, Charleston, SC (Abstract Co-Author) Nothing to Disclose Andreas Fischer, MD, Charleston, SC (Abstract Co-Author) Nothing to Disclose Akos Varga-Szemes, MD, PhD, Charleston, SC (Abstract Co-Author) Research Grant and Travel Support, Siemens AG Research Consultant, Elucid Bioimaging Pooyan Sahbaee, Mount Pleasant, SC (Abstract Co-Author) Employee, Siemens AG Chris Schwemmer, Erlangen, Germany (Abstract Co-Author) Employee, Siemens AG Mehmet A. Gulsun, Princeton, NJ (Abstract Co-Author) Employee, Siemens AG Serkan Cimen, Istanbul, Turkey (Abstract Co-Author) Nothing to Disclose Puneet Sharma, Princeton, NJ (Abstract Co-Author) Research Director, Siemens AG Andres Abadia, Charleston, SC (Abstract Co-Author) Nothing to Disclose Vincenzo Vingiani, MD, Castellammare di Stabia, SC (Abstract Co-Author) Nothing to Disclose Thomas J. Vogl, MD, PhD, Frankfurt , Germany (Abstract Co-Author) Nothing to Disclose U. Joseph Schoepf, MD, Charleston, SC (Abstract Co-Author) Research Grant, Astellas Group; Research Grant, Baver AG; Research Grant, Bracco Group; Research Grant, Siemens AG; Research Grant, Heartflow, Inc; Research support, Bayer AG; Consultant, Elucid BioImaging Inc; Research Grant, Guerbet SA; Consultant, HeartFlow, Inc; Consultant, Bayer AG; Consultant, Siemens AG; ; ;

For information about this presentation, contact:

schoepf@musc.edu

PURPOSE

As the determination of coronary artery calcium scores (CACS) is labor-intensive and time-consuming, a more automated workflow is desirable to reduce the need for human interaction. The purpose of this study was to evaluate an artificial intelligence (AI)-based automated coronary artery calcium scoring application for electrocardiogram (ECG)-gated non-contrast cardiac computed tomography (CT).

METHOD AND MATERIALS

We analyzed a fully automated calcium scoring application that is composed of multiple deep learning models, including voxel segmentation and computing the likelihood of a voxel being coronary calcium. The software automatically identifies the coronaries and calcified lesions, whereas aortic plaques are excluded from the calculations using a model for aorta segmentation. This algorithm was trained on about 2000 annotated ECG-gated cardiac CT scans. Then, the application was evaluated on 511 consecutive patients (mean age, 56.4±10.2 years; 211 men) undergoing dedicated calcium scoring CT. Results were compared to CACS obtained via standard manual assessment by independent cardiovascular imagers.

CACS values revealed no significant differences between the automated algorithm and the reference standard (P=0.282). CACS using the automated application showed an excellent correlation with the reference standard (Pearson, r=0.97). In addition, the fully automated software classified 476 of 511 (93.2%) patients into the same risk category (0, 1-10, 11-100, 101-400, or >400) as the human observers, whereas 35 (6.8%) patients were misclassified into a different category. Overall, 15 (2.9%) patients were downgraded to a lower category and 20 (3.9%) patients were upgraded to a higher category.

CONCLUSION

AI-based automated calcium scoring for non-contrast ECG-triggered cardiac CT shows high accuracy when compared to manually obtained reference scores. The use of this fully automated software application may reduce the need for human user interaction and interpretation time.

CLINICAL RELEVANCE/APPLICATION

The use of this AI-based fully automated software application may reduce the need for manual input and interpretation time and thus enhance workflow efficiencies for this growing CT application.

SSK03-07 Deep Learning for Calcium Scoring in Radiotherapy Treatment Planning CT Scans in Breast Cancer Patients

Wednesday, Dec. 4 11:30AM - 11:40AM Room: E351

Participants

Sanne G. van Velzen, MSc, Utrecht , Netherlands (*Presenter*) Nothing to Disclose Nikolas Lessmann, MSc, Nijmegen, Netherlands (*Abstract Co-Author*) Nothing to Disclose Marleen J. Emaus, MD, Utrecht , Netherlands (*Abstract Co-Author*) Nothing to Disclose H van Den Bongard, Utrecht , Netherlands (*Abstract Co-Author*) Nothing to Disclose Helena Verkooijen, Utrecht, Netherlands (*Abstract Co-Author*) Nothing to Disclose Ivana Isgum, PhD, Utrecht, Netherlands (*Abstract Co-Author*) Nothing to Disclose Ivana Isgum, PhD, Utrecht, Netherlands (*Abstract Co-Author*) Research Grant, Pie Medical Imaging BV Research Grant, 3mensio Medical Imaging BV Research Grant, Koninklijke Philips NV

For information about this presentation, contact:

s.g.m.vanvelzen@umcutrecht.nl

PURPOSE

Cardiovascular disease (CVD) is an important cause of mortality in breast cancer patients. Coronary artery calcification (CAC) and thoracic aorta calcification (TAC) are strong and independent risk factors for CVD and can be detected and quantified in radiotherapy treatment planning (RTTP) CT. Manual quantification of CAC and TAC is a tedious and time-consuming task. Therefore, we evaluated the performance of an AI system, developed for automatic calcium scoring in low-dose chest CT, in RTTP CT.

METHOD AND MATERIALS

We included 1409 breast cancer patients (age 56±7 years), who participated in the UMBRELLA cohort and underwent a RTTP CT (Philips Brilliance Big Bore CT, 120kVp, no ECG-triggering, no contrast, 3.0mm slice thickness). In a first step, CAC and TAC were manually annotated in these scans. In a second step, a deep learning algorithm was applied for automated detection of CAC and TAC. A baseline system was trained with 1181 low-dose chest CTs (all major CT vendors, 120/140kVp, no ECG-triggering, no contrast, 1.0-3.0mm slice thickness) from the National Lung Screening Trail (NLST). A RTTP-specific system was trained with the NLST scans and additionally 568 RTTP scans. The remaining 841 RTTP scans were used for evaluation. CAC was quantified as Agatston and volume scores; TAC as volume scores only. Agatston score was stratified into five risk categories: 0, 1-10, 11-100, 101-400, >400. Reproducibility between manual and automatic scores was evaluated with linearly weighted κ (categories) and Intraclass Correlation Coefficient (ICC, volume scores).

RESULTS

For the baseline system, ICCs were 0.85 (95% CI 0.83-0.87) and 0.98 (0.97-0.98) for CAC and TAC volumes, respectively. ICCs for the RRTP-specific system improved to 0.92 (0.91-0.93) and 0.99 (0.98-0.99) for CAC and TAC volumes, respectively. The baseline and RTTP-specific systems achieved a κ of 0.85 (0.80-0.90) and 0.89 (0.85-0.93).

CONCLUSION

An AI system trained on low-dose chest CTs allows accurate automatic CAC and TAC scoring in RTTP CT, which improves further upon RTTP-specific training.

CLINICAL RELEVANCE/APPLICATION

Accurate, fully automatic CVD risk assessment in breast cancer patients from readily available RTTP scans allows cost-effective identification of patients who may benefit from preventive treatment.

SSK03-08 Preliminary Exploration and Analysis of Coronary Artery Plaque Characteristics in HIV-Infected Patients Based on Radiomics

Wednesday, Dec. 4 11:40AM - 11:50AM Room: E351

Participants

Peijie Li, Zhengzhou , China (*Presenter*) Nothing to Disclose Yonggao Zhang, MD, Zheng Zhou , China (*Abstract Co-Author*) Nothing to Disclose Jianbo Gao, MD, Zhengzhou, China (*Abstract Co-Author*) Nothing to Disclose Li Qihua, Beijing, China (*Abstract Co-Author*) Nothing to Disclose Qingxia Zhao, Zhengzhou , China (*Abstract Co-Author*) Nothing to Disclose Marco Francone, MD,PhD, Rome, Italy (*Abstract Co-Author*) Nothing to Disclose Yan Jia, Beijing, China (*Abstract Co-Author*) Nothing to Disclose Jingjing Cui, Beijing, China (*Abstract Co-Author*) Nothing to Disclose Shaohua Hua, PhD, Zhengzhou, China (*Abstract Co-Author*) Nothing to Disclose

For information about this presentation, contact:

18790670639@163.com

PURPOSE

To analyze the difference of coronary artery plaque characteristics between HIV infected patients and non-infected patients by using radiomics technique, and screen the features related to different types of plaques.

METHOD AND MATERIALS

From March 2017 to March 2019, 206 patients (97 HIV infected patients and 109 uninfected patients) with positive coronary artery plaque confirmed by coronary computed tomography angiography(CCTA) were included in this study. The plaque types were artificially divided into calcium plaque, non-calcified plaque and mixed plaque by two experienced radiologists, and the regions of interest (ROI) were manually drawn on the CCTA images. 1029 radiomics features were automatically extracted from each plaque. The minimum redundancy and maximum correlation features were selected using analysis of variance(ANOVA) and the least absolute shrinkage and selection operator (LASSO) method of 10-fold cross-validation, and two-sample t-test was also performed to disply the difference of the selected features.

RESULTS

A total of 364 plaques including 58 (71), 34 (43) and 79 (79) patients with calcified plaques, mixed plaques and non-calcified plaques respectively in the HIV-infected group (non-infected group) were analyzed. The mixed plaques were significantly different between the two groups, and the clustering effect of calcified plaques and non-calcified plaques were poor. 24 radiomics features of mixed plaques were selected by ANOVA and LASSO, and the coefficients in the LASSO method were shown in Fig. a. The selected features of mixed plaques from HIV-infected group was significantly different from the non-infected group by t-test (all p values<0.05). Hierarchical clustering was used in order to display the differences of the selected features between HIV-infected group and non-infected group, and the radiomics heat map was shown in Fig. b.

CONCLUSION

Radiomics features showed significant difference between HIV-infected and non-infected patients with coronary artery mixed plaque. But no significant difference between calcium plaque and non-calcified plaque were found.

CLINICAL RELEVANCE/APPLICATION

HIV infection may affect the formation of mixed coronary plaque in patients, suggesting that patients with HIV infection of coronary heart disease may need different treatment methods.

SSK03-09 Calcium Scoring on Emergency Aortic Dissection CT Scans: A Missed Opportunity for Radiologists to Impact Clinical Management of Acute Chest Pain Patients

Wednesday, Dec. 4 11:50AM - 12:00PM Room: E351

Participants

Duan Chen, MD, Bronx, NY (*Abstract Co-Author*) Nothing to Disclose Alison R. Schonberger, MD, Bronx, NY (*Presenter*) Nothing to Disclose Kenny Ye, Bronx, NY (*Abstract Co-Author*) Nothing to Disclose Jeffrey M. Levsky, MD, PhD, Bronx, NY (*Abstract Co-Author*) Nothing to Disclose

PURPOSE

CT aortography (CTAo) is routinely performed in the emergency setting for acute chest pain patients. Previous studies show that the diagnostic yield of CTAo is very low. Most patients are sent home shortly after a negative scan without directed cardiovascular follow up. This study assesses these patients' long term clinical outcomes and investigates the potential prognostic value of coronary artery calcium (CAC) scoring from CTAo.

METHOD AND MATERIALS

A cohort of patients who received emergency CTAo from 2007-2012 was assembled using a quality-improvement medical record survey tool. The time period allowed for long term follow up (5-10 years). Clinical events included death, aortic dissection (AD), myocardial infarction (MI), cerebrovascular accident (CVA), and pulmonary embolism (PE). Visual CAC scores were computed from original images utilizing a validated, 12-point ordinal method. Kaplan-Meier Estimator and Cox regression were used for survival analysis.

RESULTS

1662 patients had CTAo, of which 599 (36%) had at least one subsequent documented clinical event (227 [13.7%] deaths, 86 [5.2%] AD, 119 [7.2%] MI, 96 [5.8%] CVA, 71 [4.3%] PE). Survival analysis showed a strong association between CAC score and mortality with hazard ratios (HR) increasing with higher CAC scores when age and gender were included as covariates. Eight year mortality for patients without coronary calcium (CAC of 0) was 13%, for those with low calcium (CAC 1-3) was 25% (HR 1.88), for those with moderate calcium (CAC 4-6) was 41% (HR 2.74), and for those with high calcium (CAC 7-12) was 57% (HR 3.68). CAC scores were highly predictive of major adverse cardiac events - MI, CVA, and death (p<2e-16). CAC score, however, was neither predictive of occurrence of PE (p=0.98) nor AD (p=0.24). AD and PE occurred earlier (median 517 and 578 days) than major cardiovascular events (medians 852-1191 days).

CONCLUSION

CAC scores in patients undergoing CTAo strongly predict long-term all-cause mortality and major adverse cardiovascular events. Including a CAC score in CT aortogram reports has a potential role in directing subsequent patient management by highlighting high risk patients for cardiovascular risk assessment and treatment.

CLINICAL RELEVANCE/APPLICATION

Visual CAC scores from emergency CT aortograms can provide additional value by identifying patients with high long-term cardiovascular risk who may benefit from aggressive risk factor management.

Printed on: 10/29/20





SSK04

Science Session with Keynote: Cardiac (Great Vessels)

Wednesday, Dec. 4 10:30AM - 12:00PM Room: E352



AMA PRA Category 1 Credits ™: 1.50 ARRT Category A+ Credit: 1.75

Participants

Daniel Ocazionez-Trujillo, MD, Houston, TX (*Moderator*) Nothing to Disclose Tina D. Tailor, MD, Durham, NC (*Moderator*) Nothing to Disclose

Sub-Events

SSK04-01 Cardiac Keynote Speaker: Imaging of Aortitis

Wednesday, Dec. 4 10:30AM - 10:50AM Room: E352

Participants

Daniel Ocazionez-Trujillo, MD, Houston, TX (Presenter) Nothing to Disclose

SSK04-03 Ascending Aortic Diameter, Pulmonary Artery to Ascending Aorta Ratio, and Cardiovascular Death in the National Lung Screening Trial (NLST)

Wednesday, Dec. 4 10:50AM - 11:00AM Room: E352

Participants

Yasuka Kikuchi, MD, Boston, MA (*Abstract Co-Author*) Nothing to Disclose John Sukumar Aluru, MBBS,MS, Quincy, MA (*Presenter*) Nothing to Disclose Sarah Mercaldo, PhD, Boston, MA (*Abstract Co-Author*) Nothing to Disclose Jana Taron, MD, Tuebigen, Germany (*Abstract Co-Author*) Nothing to Disclose Borek Foldyna, MD, Boston, MA (*Abstract Co-Author*) Nothing to Disclose Udo Hoffmann, MD, Boston, MA (*Abstract Co-Author*) Nothing to Disclose Udo Hoffmann, MD, Boston, MA (*Abstract Co-Author*) Research Grant, Kowa Company, Ltd ; Research Grant, Abbott Laboratories; Research Grant, HeartFlow, Inc; Research Grant, AstraZeneca PLC; Michael T. Lu, MD, Boston, MA (*Abstract Co-Author*) Grant, NVIDIA Corporation; Institutional Research Grant, Kowa Company, Ltd ; Institutional Research Grant, AstraZeneca PLC

PURPOSE

Older heavy smokers undergoing lung cancer screening CT are at high risk of cardiovascular (CV) death. Ascending aortic (Ao) diameter and a pulmonary artery to Ao diameter (PA/Ao) ratio >=1 have been associated with death in non-lung screening populations. We sought to determine normal ranges for Ao diameter and PA/Ao ratio and their association with CV death in heavy smokers from the National Lung Screening Trial (NLST).

METHOD AND MATERIALS

In 994 randomly selected NLST participants having non-contrast non-ECG gated low-dose lung screening CT, Ao and PA diameters were measured at the level of the PA bifurcation. Uni- and multivariable Cox regression models were used to estimate hazard ratios (HR) for Ao diameter and PA/Ao ratio >=1 for CV death. Multivariable models were adjusted for age, sex, smoking status, and body surface area. Inter-observer reproducibility for Ao diameter and PA/Ao ratio were assessed in 30 participants by 2 independent observers.

RESULTS

In 994 participants (age 61.5 ± 5.2 yr; 43% female), 2% (20/994) suffered CV death over median follow up of 6.7 years. Mean Ao diameter was 34.0 ± 3.7 mm. Ao diameter was significantly associated with CV death (CV death; 36.6 ± 4.3 mm vs. no CV death; 34.0 ± 3.7 mm, p=0.007), with an unadjusted HR of 2.5 per 5 mm increase (95% CI: 1.6-3.7, p<0.001). Ao diameter remained an independent predictor of CV death after adjustment (adjusted HR; 2.5 per 5mm increase, 95% CI: 1.2-3.7, p=0.009). The mean PA/Ao ratio was 0.8 ± 0.1 . In unadjusted analysis, there was borderline significant association between PA/Ao ratio >=1 with CV death (10% (2/20) vs. 2% (24/972), p=0.037 and unadjusted HR 4.3 (0.99-18, p=0.052). After adjustment, there was insufficient evidence to suggest a PA/Ao ratio >=1 is associated with CV death (HR 1.3, 0.18-10.3, p=0.78). Inter-observer reproducibility for Ao diameter and PA/Ao ratio was good (ICC: 0.95 and 0.91).

CONCLUSION

Greater Ao diameter, but not greater PA/Ao ratio, was associated with CV death after adjusting for risk factors.

CLINICAL RELEVANCE/APPLICATION

Larger ascending aortic diameter is a risk factor for cardiovascular death in persons having lung screening CT.

SSK04-04 Assessment of Disease Activity in Takayasu Arteritis: A Quantitative Study with Computed Tomography Angiography

Participants Baojin Chen, MD, Jinan, China (*Presenter*) Nothing to Disclose Ximing Wang, MD, Jinan, China (*Abstract Co-Author*) Nothing to Disclose Shuo Zhao, Jinan, China (*Abstract Co-Author*) Nothing to Disclose

PURPOSE

Identifying disease activity in Takayasu arteritis (TAK) is challenging. The aim of this study was to investigate the value of quantitative characterization with computed tomography angiography in the assessment of disease activity in patients with TAK.

METHOD AND MATERIALS

We retrospectively analyzed the data on 162 aortic CT angiography from 140 TAK patients. Patients were categorized based on disease activity according to National Institutes of Health criteria into two groups: active disease group (n = 65) and inactive disease group (n = 97).

RESULTS

Patients with active TAK had a thicker wall compared with patients with inactive TAK ($5.2 \pm 2.4 \text{ mm vs}$. $2.5 \pm 0.8 \text{ mm}$, p < 0.001). The ratio of mural CT attenuation over that of the paravertebral muscle was higher in active TAK than in inactive TAK ($1.5 \pm 0.3 \text{ vs}$. 1.1 ± 0.2 , p < 0.001). Given a thickness cutoff of 3.3 mm, sensitivity for active-phase TAK was 83.1%, specificity 89.7%, positive predictive value 84.4%, and negative predictive value 88.8%. With enhancement ratio cutoff of 1.2, sensitivity for active-phase TAK was 89.2%, specificity 76.3%, positive predictive value 71.6%, and negative predictive value 91.3%. In receiver-operating characteristic curves comparison, wall thickness and enhancement ratio were superior to C-reactive protein and erythrocyte sedimentation rate for determining active phase disease (p < 0.05).

CONCLUSION

Quantitative characterization with CT angiography was a useful tool to assess disease activity in TAK patients. Arterial wall thickness and enhancement have a high sensitivity and specificity for detecting TAK activity.

CLINICAL RELEVANCE/APPLICATION

Takayasu Arteritis (TAK) is a primary granulomatous large vessel vasculitis, affecting predominantly young women with substantial morbidity and mortality. Assessment of disease activity is crucial in the management of TAK. We analyzed the data on 162 aortic CT angiography from 140 TA patients. We described the quantitative utility of wall thickness and enhancement in the discrimination of active and inactive TAK and proposed a cutoff value for wall thickness and enhancement ratio. This will provide a quantitative reference, giving more valuable information to discriminate better active inflammation from quiescent disease, thereby aiding the decision to clinical management.

SSK04-05 Comparison of a Novel Compressed Sense Accelerated 3D Non-Contrast Modified REACT MRA with Standard Contrast-Enhanced MRA in Patients with Connective Tissue Diseases or Other Aortic Pathologies

Wednesday, Dec. 4 11:10AM - 11:20AM Room: E352

Participants

Lenhard Pennig, MD, Cologne, Germany (*Presenter*) Nothing to Disclose Anton Wagner, MD, Cologne, Germany (*Abstract Co-Author*) Nothing to Disclose Kilian Weiss, PhD, Hamburg, Germany (*Abstract Co-Author*) Employee, Koninklijke Philips NV Simon Lennartz, MD, Cologne, Germany (*Abstract Co-Author*) Institutional Research Grant, Koninklijke Philips NV David C. Maintz, MD, Koln, Germany (*Abstract Co-Author*) Nothing to Disclose Tilman Hickethier, MD, Cologne, Germany (*Abstract Co-Author*) Nothing to Disclose Claas P. Naehle, MD, Bonn, Germany (*Abstract Co-Author*) Nothing to Disclose Alexander C. Bunck, Koln, Germany (*Abstract Co-Author*) Nothing to Disclose Jonas Doerner, MD, Cologne, Germany (*Abstract Co-Author*) Nothing to Disclose

For information about this presentation, contact:

Lenhard.pennig@uk-koeln.de

PURPOSE

Patients with connective tissue diseases (CTD) require repetitive vascular imaging such as magnetic resonance angiography (MRA). Potential effects of gadolinium retention are ambiguous. This study investigated the use of a novel Compressed SENSE (Philips Healthcare) accelerated (factor 10) ECG- and respiratory-triggered 3D modified Relaxation-Enhanced Angiography without Contrast and Triggering (REACT) (non-CE-MRA) in comparison to standard non-ECG-triggered 3D contrast-enhanced MRA (CE-MRA) for imaging of the thoracic aorta.

METHOD AND MATERIALS

Retrospective analysis independently conducted by two radiologists in 30 patients with CTD (25 of 30 patients) or other aortic diseases on non-CE- and CE-MRA using a manual (Multiplanar-Reconstruction, MPR; Agfa HealthCare) and a semiautomatic (Advanced Vessel Analysis, AVA; Philips Healthcare) measurement tool on seven dedicated points (inner edge): Aortic annulus, aortic sinus, sinotubular junction, mid-ascending aorta, high-ascending aorta, aortic isthmus, descending aorta. Image quality was evaluated on a four-point scale and evaluation time for each measurement technique was noted (min).

RESULTS

There was a high agreement (r>0.9) and no significant interobserver difference between non-CE-MRA and CE-MRA using both tools with smaller differences for non-CE- than CE-MRA. However, descending aorta showed the highest difference without being clinically significant (mean 2.21% between non-CE- and CE-MRA using MPR). For non-CE-MRA, average acquisition time was 6:34 min. Non-CE-MRA showed significant better image quality from aortic annulus to mid-ascending aortae (p<0.05), at the distal points, no significant difference was noted (p>0.05). Regarding time requirement, no statistical significance was found between both measurement techniques (p=0.08).

CONCLUSION

Compressed SENSE accelerated (factor 10) 3D modified REACT allows for fast and reliable imaging of the thoracic aorta using a manual and semiautomatic measurement approach with higher image quality in the aortic root and mid-ascending aorta than CE-MRA without contrast agent and its disadvantages. This is of particular relevance for patients requiring repetitive imaging.

CLINICAL RELEVANCE/APPLICATION

Patients with connective tissue diseases require repetitive vascular imaging. Therefore, modified non-CE-MRA REACT may be an alternative since it lacks the disadvantages of contrast agent and shows high diagnostic accuracy.

SSK04-06 Inter-Examination Reproducibility of Phase-Specific Systolic Aorta Segmentation: 4D Flow MRI in Healthy Volunteers

Wednesday, Dec. 4 11:20AM - 11:30AM Room: E352

Participants

Joe F. Juffermans, MSc, Leiden, Netherlands (*Presenter*) Nothing to Disclose Jos Westenberg, PhD, Leiden, Netherlands (*Abstract Co-Author*) Nothing to Disclose Pieter J. van Den Boogaard, Leiden, Netherlands (*Abstract Co-Author*) Nothing to Disclose Roel L. van der Palen, MSc, Leiden, Netherlands (*Abstract Co-Author*) Nothing to Disclose Arno A. Roest, Leiden, Netherlands (*Abstract Co-Author*) Nothing to Disclose Hildo J. Lamb, MD, PhD, Leiden, Netherlands (*Abstract Co-Author*) Nothing to Disclose

For information about this presentation, contact:

J.F.Juffermans@lumc.nl

PURPOSE

Hemodynamic aorta parameters can be derived from 4D flow MRI and requires lumen segmentation. The aim of this study was to determine the inter-examination reproducibility of phase-specific aorta segmentation of 4D flow MRI in healthy volunteers.

METHOD AND MATERIALS

Ten volunteers (26.5±2.6years) underwent 4D flow MRI at 3T MRI (Ingenia, Philips Healthcare) twice. The 4D flow acquisition parameters were: respiratory navigator-gated, retrospective ECG-gated, velocity encoding: 200cm/s, isotropic spatial resolution: 2.5mm, temporal resolution: 35.1-36.1ms and field of view: 350x250x75mm. Thoracic aorta was segmented at five systolic phases using CAAS MR 4D flow v1.1 (Pie Medical Imaging). By positioning six perpendicular planes on the segmentation's centerline the aorta was divided into five segments; proximal and distal ascending aorta, aortic arch, proximal and distal descending aorta (pAAo, dAAO, AoA, pDAo and dDAo respectively). To evaluate the inter-examination variability the image analysis was performed for both 4D flow examinations. Finally, the centerline length (CL) and mean diameter (MD) were determined for each segment using an inhouse developed tool. The paired T-test (TT), absolute mean difference (DIFF), coefficient of variation (COV) and interclass correlation coefficient (ICC) were calculated between both examinations.

RESULTS

The TT showed no significant (p<0.05) group difference between both examinations, except for AoA MD at the fifth phase (p=0.03). The inter-examination analysis showed for MD low DIFF (0.1-1.2mm), low COV (1.6-8.8%), with good-to-excellent ICC (0.78-0.99) over all phases, excluding pAAo which had moderate-to-good ICC (0.53-0.77). For CL low DIFF (0.0-1.6mm), intermediate-to-low COV (7.5-15.2%) with good-to-strong ICC (0.71-0.91) were found over all phases, excluding pAAo which had a poor ICC (0.36-0.48).

CONCLUSION

In general, for MD and CL a good-to-excellent reproducibility was found for all segments and phases, except for pAAo. This observation can be explained by ease-of-use image analysis within the applied software, resulting in DIFF well below the spatial acquisition resolution. The reduced reproducibility of pAAo is most likely related to pronounced systolic stretching and lumen distension in the ascending aorta.

CLINICAL RELEVANCE/APPLICATION

Good-to-excellent inter-examination reproducibility of phase-specific aorta segmentation based on 4D flow MRI was found in healthy volunteers.

SSK04-07 A 3D Deep Convolutional Neural Network for Automatic Segmentation and Measurement of Type B Aortic Dissection

Wednesday, Dec. 4 11:30AM - 11:40AM Room: E352

Participants

Tong Y. Yu, Beijing, China (*Abstract Co-Author*) Nothing to Disclose Bin Lu, MD, Beijing, China (*Abstract Co-Author*) Nothing to Disclose Wei J. Yong, Beijing, China (*Abstract Co-Author*) Nothing to Disclose Jiang Q. Xiao, Beijing, China (*Abstract Co-Author*) Nothing to Disclose Zhou F. Liao, Beijing, China (*Abstract Co-Author*) Nothing to Disclose Yang Gao, Beijing, China (*Abstract Co-Author*) Nothing to Disclose Ning Guo, Beijing, China (*Abstract Co-Author*) Nothing to Disclose Jian Liu, Beijing, China (*Abstract Co-Author*) Nothing to Disclose

PURPOSE

This study aimed to develop an automatic aorta segmentation and measurement method based on 3D convolutional neural network in aortic computed tomography angiography (CTA) of the patient with type B aortic dissection (TBAD).

METHOD AND MATERIALS

149 patients with TBAD underwent CTA at initial presentation were consecutively included in this study. Areas and volumes of true and false lumen were measured at eight levels relevant to preoperative planning and postoperative evaluation with the centerline technique based on automatic centerline analysis and vessel straightening. The measurements of three blinded radiologists as the standard references. Deep learning based on 3D Unet combined intersection over union tracing algorithm was used for automatic lumen segmentation. Splitting the data into training set and test set (87% VS 13%) randomly. Data between the test set and standard reference were compared using Bland-Altman and paired Student t test. Reliability of measurement was determined using intra-class correlation analyses and the excellent agreement was defined as an ICC coefficient of > 0.8.

RESULTS

The proposed model achieved a mean dice similarity score of 0.948, 0.941 and 0.963 for the true lumen, false lumen and entire aorta respectively. Measurement derived from the proposed model showed excellent agreement with the reference standard, with mean difference 0.0620 ± 0.6715 , 95% limits of agreement -0.0119 to 0.1358. Correlation coefficient between deep learning and standard reference was 0.997 (P < 0.001), and ICC coefficient was 0.999. As for manual method, however, mean difference was 0.3881 \pm 2.0769 with statistical significance (P = 0.001), 95% limits of agreement 0.1596 to 0.6165. Correlation coefficient between manual method and standard reference was 0.975 (P < 0.001), and ICC coefficient was 0.987. Proposed deep learning method was more efficient (3.16 \pm 0.47min) than radiologists (2 \pm 0.4h) in generating the centerlines and measurement on each case (P<0.01).

CONCLUSION

This study showed that our proposed model had good accuracy in automatic segmentation of the aorta and time saving. The accuracy and repeatability of the quantitative parameters measurement were better than manual measurement results.

CLINICAL RELEVANCE/APPLICATION

With deep learning, the accurate, uniform and efficient measurement of aorta in CTA can be obtained, can benefit individualized preoperative planning and predict survival risk in the future.

SSK04-08 Sexual Dimorphism in the Association between Coronary Plaque Burden and Ascending Aorta 4D Deformation

Wednesday, Dec. 4 11:40AM - 11:50AM Room: E352

Participants

Ahmed H. Hamimi, MD, Bethesda, MD (*Presenter*) Nothing to Disclose Ahmed Abdelfadeel, Bethesda, MD (*Abstract Co-Author*) Nothing to Disclose Jatin R. Matta, Bethesda, MD (*Abstract Co-Author*) Nothing to Disclose Khaled Z. Abd-Elmoniem, PhD, Bethesda, MD (*Abstract Co-Author*) Nothing to Disclose Ahmed M. Gharib, MBChB, Bethesda, MD (*Abstract Co-Author*) Nothing to Disclose

PURPOSE

To develop and implement automatic 4D deformation analysis for Ascending Aorta (AA) and investigate the significance of sex difference on the association between AA deformation and coronary plaque burden as measured by Coronary Computerized Tomography Angiography (CCTA). The purpose is to provide an objective estimation for the 4D AA image-based surrogates of the plaque burden in asymptomatic subjects with low/intermediate risk (Framingham score (FrS) of coronary artery diseases (CAD).

METHOD AND MATERIALS

CCTA was obtained in 50 asymptomatic adults after signing informed consent. FrS, coronary calcification, and plaque burden score were obtained for all subjects. Automatic in-house AA 4D deformation algorithm and analysis were performed to assess time to peak distensibility (TPD). Univariable and multivariable generalized nonlinear regression modeling were performed to investigate the association of FrS, and TPD, with coronary plaque burden (segment involvement score (SIS) >5). Receiver Operator Curves (ROC) and Area Under the Curve (AUC) were obtained for FrS, TPD and combined for the detection of SIS>5.

RESULTS

Males subjects (n=31) were age and BMI matched to the female subjects. TPD individually, was significant predictor of SIS > 5 (regression coefficient (β = -0.15034), P-value = 0.008). Additionally, sex was a significant effect modifier of TPD, with a stronger statistically significant association with women (β = -0.0311, P-value = 0.030). ROC showed significant improvement (p=0.001) in the performance of FrS when combined with TPD for the detection of SIS>5.

CONCLUSION

In low/intermediate CAD risk asymptomatic women, there is strong association between TPD and substantial of coronary plaque burden beyond and independent of tradition CAD risk factors. AA 4D deformation analysis may supplement traditional risk scores for CAD risk stratification in women. This is in line with previous studies that demonstrated the suboptimal performance of CAD risk score models for women compared to men.

CLINICAL RELEVANCE/APPLICATION

AA 4D deformation analysis (also attainable by other imaging modalities) can be used as an independent surrogate for subclinical atherosclerosis in low /intermediate FrS asymptomatic women. This method reduces subjectivity for CCTA analysis as an additional quantitative objective measurement for CAD risk stratification, life style modification and therapy of CAD particularly in women.

SSK04-09 Dual-Energy CT in Patients with Suspect Acute Pulmonary Embolism: A Diagnostic Accuracy Systematic Review and Meta-Analysis

Wednesday, Dec. 4 11:50AM - 12:00PM Room: E352

Participants

Moreno Zanardo, MSc, San Donato Milanese, Italy (*Presenter*) Nothing to Disclose Caterina B. Monti, MD, Milano, Italy (*Abstract Co-Author*) Nothing to Disclose Simone Schiaffino, MD, Bogliasco, Italy (*Abstract Co-Author*) Nothing to Disclose

Andrea Cozzi, MD, Uboldo, Italy (*Abstract Co-Author*) Nothing to Disclose Francesco Sardanelli, MD, San Donato Milanese, Italy (*Abstract Co-Author*) Speakers Bureau, Bracco Group Advisory Board, Bracco Group Research Grant, Bayer AG Advisory Board, General Electric Company Reserach Grant, General Electric Company Speakers Bureau, Siemens AG Reserach Grant, Real Imaging Ltd

Francesco Secchi, MD, PhD, Milano, Italy (Abstract Co-Author) Nothing to Disclose

For information about this presentation, contact:

francesco.secchi@unimi.it

PURPOSE

To review the diagnostic performance of dual-energy CT (DECT) in diagnosing acute pulmonary embolism (PE).

METHOD AND MATERIALS

No IRB approval was needed, the study protocol was registered on PROSPERO and reported according to PRISMA. In February 2019, a systematic search was performed on MEDLINE/EMBASE, for articles reporting the diagnostic performance of DECT in diagnosing acute PE. Pooled sensitivity, specificity, positive and negative likelihood ratios (LR) and diagnostic odds ratio (DOR) were calculated according to the approach by Reitsma. A summary receiver operating characteristics (sROC) curve was constructed. Data were reported as estimate and 95% confidence interval (CI). The pooled effective radiation dose for the chest was calculated using the random effect model and the impact of year of publication was evaluated through meta-regression analysis. Risk of publication bias was assessed using the Egger test.

RESULTS

Of 159 initially retrieved articles, 14 studies were identified, including 23 independent study parts, for a total of 993 patients. Patients' median age ranged from 40 to 68 years. Twelve studies used a dual-tube/dual-detector DECT, while 2 used rapid-kV switching DECT. Lower voltages ranged from 80 to 100 kVp, while high voltages ranged from 135 to 140 kVp. Pooled sensitivity was 84.1% (95% CI 78.3-88.6%), pooled specificity was 88.6% (95% CI 83.9-92.1%), positive LR was 7.52 (95% CI 5.21-10.60), negative LR was 0.18 (95% CI 0.13-0.25), DOR was 42.8 (95% CI 24.2-70.3). The sROC curve had an area under the curve of 0.93. Effective radiation dose to the chest showed high heterogeneity (I2=97%), and its pooled estimate was 4.52 mSv (95% CI 3.68-5.36 mSv). At meta-regression analysis, year of publication did not significantly impact on radiation dose (coefficient .152, P=.703). A significant risk of publication bias was found (Egger's test reporting P=.006).

CONCLUSION

The diagnostic performance of DECT in acute PE is substantially comparable to that of single-energy CT, in presence of a comparable effective radiation dose to the chest.

CLINICAL RELEVANCE/APPLICATION

DECT may be used instead of single-energy CT in patients with suspect of acute PE. This may be especially useful, since DECT has been shown to provide more information with regards to lung ventilation and tissue characterization than single-energy CT, thus leading to a more accurate, comprehensive evaluation of the lungs.

Printed on: 10/29/20





SSK05

Chest (Lung Cancer Screening)

Wednesday, Dec. 4 10:30AM - 12:00PM Room: N229



AMA PRA Category 1 Credits ™: 1.50 ARRT Category A+ Credit: 1.75

FDA Discussions may include off-label uses.

Participants

Jane P. Ko, MD, New York, NY (*Moderator*) Research collaboration, Siemens AG Jo-Anne O. Shepard, MD, Boston, MA (*Moderator*) Editor with royalties, Reed Elsevier

Sub-Events

SSK05-01 Cancer Risk in Subsolid Nodules in the National Lung Screening Trial

Wednesday, Dec. 4 10:30AM - 10:40AM Room: N229

Participants Mark M. Hammer, MD, Saint Louis, MO (*Presenter*) Nothing to Disclose Lauren Palazzo, Boston, MA (*Abstract Co-Author*) Nothing to Disclose Chung Yin Kong, PhD, Boston, MA (*Abstract Co-Author*) Nothing to Disclose Andetta R. Hunsaker, MD, Sudbury, MA (*Abstract Co-Author*) Nothing to Disclose

For information about this presentation, contact:

mmhammer@bwh.harvard.edu

PURPOSE

Subsolid nodules, comprising pure ground glass (GGN) and part-solid (PSN) nodules, have a high risk of indolent malignancy. Lung-RADS management guidelines are based on expert opinion and lack independent validation. The purpose of this study is to evaluate Lung-RADS for its ability to estimate the malignancy rates of subsolid nodules, using nodules from the National Lung Screening Trial (NLST). Lung-RADS was also compared to the NELSON trial volumetric classification.

METHOD AND MATERIALS

Two hundred nodules from each of the following categories were selected from the NLST: GGN < 10 mm, GGN <= 10 mm, and PSN > 6 mm. A thoracic radiologist reviewed the baseline and follow-up CT images and measured the nodules. The primary outcome for each nodule was the development of a cancer in the same lobe. Analyses were weighted by the higher prevalence of the GGN < 10 mm category. Nodules were classified by either the Lung-RADS or NELSON trial systems.

RESULTS

A total of 434 nodules were true subsolid nodules. At baseline, Lung-RADS 2 comprised 282 (73%) of nodules, with a malignancy rate of 3%, greater than the reported 1% in the Lung-RADS document (p=0.0081). The malignancy rate for GGN < 10 mm (1.5%) was significantly smaller than that for GGN measuring 10 - 19 mm (7%), p=0.02. Lung-RADS 3 comprised 89 nodules (17%), with a malignancy rate of 13%, greater than the reported 2% in the Lung-RADS document (p<0.001). The area under the receiver operating characteristic curve for Lung-RADS at baseline was 0.715, compared to 0.668 for NELSON.

CONCLUSION

Subsolid nodules in Lung-RADS categories 2 and 3 have a higher risk of malignancy than reported, and GGN 10 - 19 mm have a risk that is closer to Lung-RADS 3 than Lung-RADS 2. There does not appear to be an advantage to using volumetric (NELSON) compared to linear measurement (Lung-RADS) classification schemes.

CLINICAL RELEVANCE/APPLICATION

The malignancy risk of subsolid Lung-RADS 2 and 3 nodules in lung cancer screening is higher than expected, which may require revision of management guidelines.

SSK05-02 Are We on the Same (Web) Page for Lung Cancer Screening? A Comprehensive Content Analysis of United States Lung Cancer Screening Program Websites

Wednesday, Dec. 4 10:40AM - 10:50AM Room: N229

Participants

Staci Gagne, MD, Boston, MA (*Abstract Co-Author*) Nothing to Disclose
Efren J. Flores, MD, Boston, MA (*Abstract Co-Author*) Nothing to Disclose
Shaunagh McDermott, FFR(RCSI), Boston, MA (*Abstract Co-Author*) Nothing to Disclose
Melissa C. Price, MD, Boston, MA (*Abstract Co-Author*) Nothing to Disclose
Milena Petranovic, MD, Boston, MA (*Abstract Co-Author*) Nothing to Disclose
Florian J. Fintelmann, MD, Boston, MA (*Abstract Co-Author*) Consultant, Jounce Therapeutics, Inc; Research support, BTG International Ltd

Justin Stowell, MD, Boston, MA (*Abstract Co-Author*) Nothing to Disclose Dexter Mendoza, MD, Boston, MA (*Abstract Co-Author*) Nothing to Disclose Brent P. Little, MD, Boston, MA (*Presenter*) Author, Reed Elsevier; Editor, Reed Elsevier; Royalties, Reed Elsevier

For information about this presentation, contact:

blittle@partners.org

PURPOSE

To assess the scope and quality of patient educational content of United States Lung Cancer Screening (LCS) program websites.

METHOD AND MATERIALS

A Google searches for "lung cancer screening", "low dose CT screening", and "lung screening" performed September 15, 2018 yielded 269 LCS program websites. 258 unique websites were equally divided and randomly assigned to 9 Thoracic Radiologists for analysis. Each radiologist reviewed text, images, videos, and PDF attachments for a random subset of sites using a standardized checklist. All main landing pages for LCS sites, along with linked pages from the institution directly dealing with LCS were included in the analysis. Information on links external to the LCS institution were not included in the content analysis. Content areas for which websites were analyzed included (1) LCS eligibility criteria, (2) monetary costs and insurance coverage, (3) benefits and (4) risks of lung cancer screening.

RESULTS

While most sites mentioned eligibility for screening (98%), 13% reported ages 55-74, 42% ages 55-77, 17% ages 55-80, and 19% gave multiple ranges. A quarter of websites did not address monetary costs of screening; out-of-pocket costs as a result of screening were rarely mentioned. Many (93%) mentioned the possibility of early detection of lung cancer and the use of low-dose CT, but 39% of sites did not mention the magnitude of the benefit, and 47% made no mention of the U.S. National Lung Cancer Screening Trial. More than half of the websites (53%) did not address any risks related to screening. Categories of risks discussed included radiation (38%), false positives (37%), and further tests (40%). Fewer sites included false negatives (20%), overdiagnosis (12%), procedural complications (10%), and anxiety/worry (20%).

CONCLUSION

There is inconsistency in the information provided to patients about lung cancer screening. Stated ages for eligibility, while commonly reported, vary widely. Health care costs are a large concern for many and yet a quarter of webpages do not address cost. In addition, the majority of LCS sites fail to address the risks of screening.

CLINICAL RELEVANCE/APPLICATION

Radiology practices should increase efforts to offer updated, standardized LCS information on websites to improve public knowledge of this imaging-based cancer screening tool and help alleviate some patient concerns.

SSK05-03 Lung Cancer Screening in NLST Eligibles: Tailoring Annual Low-Dose Computed Tomography by Post-Test Risk Stratification

Wednesday, Dec. 4 10:50AM - 11:00AM Room: N229

Participants

Mario Silva, MD, Parma, Italy (*Presenter*) Consultant, F. Hoffmann-La Roche Ltd; Speakers Bureau, F. Hoffmann-La Roche Ltd; Speakers Bureau, Boerhinger Ingelheim GmbH

Gianluca Milanese, MD, Parma, Italy (Abstract Co-Author) Nothing to Disclose

Federica Sabia, Milan, Italy (Abstract Co-Author) Nothing to Disclose

Colin Jacobs, PhD, Nijmegen, Netherlands (*Abstract Co-Author*) Research Grant, MeVis Medical Solutions AG; Royalties, MeVis Medical Solutions AG; Research Grant, Thirona

Bram van Ginneken, PhD, Nijmegen, Netherlands (*Abstract Co-Author*) Stockholder, Thirona; Co-founder, Thirona; Royalties, Thirona; Research Grant, Varian Medical Systems, Inc; Royalties, Varian Medical Systems, Inc; Research Grant, Canon Medical Systems Corporation; Royalties, Canon Medical Systems Corporation; Research Grant, Siemens AG;

Mathias Prokop, PhD, Nijmegen, Netherlands (*Abstract Co-Author*) Speakers Bureau, Bracco Group Speakers Bureau, Bayer AG Research Grant, Canon Medical Systems Corporation Speakers Bureau, Canon Medical Systems Corporation Research Grant, Siemens AG Speakers Bureau, Siemens AG Departmental spinoff, Thirona Departmental licence agreement, Varian Medical Systems, Inc Cornelia M. Schaefer-Prokop, MD, Amersfoort, Netherlands (*Abstract Co-Author*) Researcher, Thirona; Researcher, Varian Medical Systems, Inc; Spouse, Speaker, Bracco Group; Spouse, Speaker, Bayer AG; Spouse, Speaker, Canon Medical Systems Corporation; Spouse, Speaker, Siemens AG; Spouse, Research support, Siemens AG; Spouse, Research support, Canon Medical Systems Corporation; Spouse, Researcher, Thirona; Spouse, Researcher, Varian Medical Systems, Inc

Stefano Sestini, Milan, Italy (Abstract Co-Author) Nothing to Disclose

Alfonso V. Marchiano, MD, Milan, Italy (Abstract Co-Author) Nothing to Disclose

Nicola Sverzellati, MD, Parma, Italy (*Abstract Co-Author*) Consultant, PAREXEL International Corporation; Consultant, Biomedic System; Consultant, F. Hoffmann-La Roche Ltd; Consultant, Boehringer Ingelheim GmbH; Consultant, Galapagos; Advisory Board, F. Hoffmann-La Roche Ltd; Advisory Board, Boehringer Ingelheim GmbH; Speaker, F. Hoffmann-La Roche Ltd; Speaker, Boehringer Ingelheim GmbH; Speaker, F. Hoffmann-La Roche Ltd; Speaker, Boehringer Ingelheim GmbH; Speaker, F. Hoffmann-La Roche Ltd; Speaker, Boehringer Ingelheim GmbH; Speaker, F. Hoffmann-La Roche Ltd; Speaker, Boehringer Ingelheim GmbH; Speaker, F. Hoffmann-La Roche Ltd; Speaker, Boehringer Ingelheim GmbH; Speaker, F. Hoffmann-La Roche Ltd; Speaker, Boehringer Ingelheim GmbH; Speaker, F. Hoffmann-La Roche Ltd; Speaker, Boehringer Ingelheim GmbH; Speaker, F. Hoffmann-La Roche Ltd; Speaker, Boehringer Ingelheim GmbH; Speaker, F. Hoffmann-La Roche Ltd; Speaker, Boehringer Ingelheim GmbH; Speaker, F. Hoffmann-La Roche Ltd; Speaker, Boehringer Ingelheim GmbH; Speaker, F. Hoffmann-La Roche Ltd; Speaker, Boehringer Ingelheim GmbH; Speaker, F. Hoffmann-La Roche Ltd; Speaker, Boehringer Ingelheim GmbH; Speaker, F. Hoffmann-La Roche Ltd; Speaker, Boehringer Ingelheim GmbH; Speaker, F. Hoffmann-La Roche Ltd; Speaker, Boehringer Ingelheim GmbH; Speaker, F. Hoffmann-La Roche Ltd; Speaker, Boehringer Ingelheim GmbH; Speaker, F. Hoffmann-La Roche Ltd; Speaker, Boehringer Ingelheim GmbH; Speaker, F. Hoffmann-La Roche Ltd; Speaker, Boehringer Ingelheim GmbH; Speaker, F. Hoffmann-La Roche Ltd; Speaker, F. Hoffmann-La Roch

Ugo Pastorino, Milano, Italy (Abstract Co-Author) Nothing to Disclose

For information about this presentation, contact:

mariosilvamed@gmail.com

PURPOSE

To calculate the risk of lung cancer (LC) in 1 and 3 years after baseline low-dose computed tomography (LDCT), in screenees selected by National Lung Screening Trial (NLST) criteria

METHOD AND MATERIALS

For the aim of this post-hoc analysis, screenees from a prospective lung cancer screening (LCS) trial were retrospectively selected: age>=55years, pack-years>=30.Pre-test metrics: baseline demographics, medical interview, and pulmonary function test.Post-test

metrics: retrospective LDCT reading by FDA-approved workstation for LCS, featuring computer aided diagnosis (CAD) and advanced semi-automatic algorithm for volumetric segmentation of nodule. Solid nodules were classified into 3 categories: 1)no nodule or nodule 1-112mm^3; 2)nodule 113-260mm^3; 3)nodule>260mm^3. Subsolid nodules were assigned either category 2(non-solid or part-solid nodules with solid component>5mm) or category 3(solid component>=5mm). The highest category was used for screenee-wise risk assessment. The primary outcome was LC diagnosis at 1 year or 3 years; the secondary outcome was the stage of LC. The Chi squared test was used to test the association between metrics and the primary outcome at 1 or 3 years. The risk of LC in 1 or 3 years was calculated by univariate and multivariate models

RESULTS

In 1,248 NLST-eligible screenees, LC frequency was 1.2% at 1 year and 2.3% at 3 years. At 1 year, category 3 was the only predictor of LC risk in multivariate model (odds ratio 79.84 p<0.001), confirming that early follow up by LDCT (e.g.3months) is needed for characterisation of such nodules. At 3 years, LC risk was predicted by category 2 (OR5.99 p=0.009) and 3 (OR26.55 p<001), Tiffeneau<70% (OR 2.75 p=0.024). LCS simulation with triennial screening rounds for category 1 and selective annual round for category 2 and 3 (29% in our population) showed 35% reduction of LDCT through 3 years

CONCLUSION

Annual LCS could be selectively offered to 30% of NLST eligible screenees, while longer interval might be safe in those with category 1. Validation of volumetric thresholds is granted through multiple software vendors

CLINICAL RELEVANCE/APPLICATION

LCS strategy can be optimised by tailoring annual LDCT to a minority of subjects at high risk, while longer screening intervals could be a safe strategy for low risk subjects yielding substantial reduction of LDCT burden (radiation and cost). This model is being prospectively tested in a LCS trial with LDCT every 3 years

SSK05-04 Impact of Significant Coronary Artery Calcification Reported on Lung Cancer Screening Low Dose CT

Wednesday, Dec. 4 11:00AM - 11:10AM Room: N229

Participants

Dexter Mendoza, MD, Boston, MA (Abstract Co-Author) Nothing to Disclose

Bashar Kako, Boston, MA (Abstract Co-Author) Nothing to Disclose

Subba R. Digumarthy, MD, Boston, MA (*Abstract Co-Author*) Speaker, Siemens AG; Research Grant, Lunit Inc; Researcher, Merck & Co, Inc; Researcher, Pfizer Inc; Researcher, Bristol-Myers Squibb Company; Researcher, Novartis AG; Researcher, F. Hoffmann-La Roche Ltd; Researcher, Polaris Pharmaceuticals, Inc; Researcher, Cascadia Healthcare, LLC; Researcher, AbbVie Inc; Researcher, Gradalis, Inc; Researcher, Zai Lab

Jo-Anne O. Shepard, MD, Boston, MA (Abstract Co-Author) Editor with royalties, Reed Elsevier

Brent P. Little, MD, Boston, MA (Presenter) Author, Reed Elsevier; Editor, Reed Elsevier; Royalties, Reed Elsevier

For information about this presentation, contact:

dpmendoza@partners.org

PURPOSE

Coronary artery calcification (CAC) is a common and important incidental finding in low dose CT lung cancer screening (LD-LCS). Our objective were to determine the incidence of significant coronary artery calcification (CAC) reported on LD-LCS and to determine the impact of its reporting on subsequent diagnostic and therapeutic interventions.

METHOD AND MATERIALS

In this IRB approved retrospective study, we queried our lung cancer screening database for reports of LD-LCS performed between January 2016 and September 2018. All reports with significant findings designated with the "S" modifier for any LungRADS category were reviewed, and those with the "S" modifier pertaining to significant CAC were selected. The grading of CAC was extracted from the reports and compiled into four groups: moderate, severe, other non-standard descriptors (e.g. extensive, dense, etc.), or unspecified. From the electronic medical record, we reviewed and recorded baseline clinical characteristics of included patients and subsequent changes in management that resulted from the report of significant CAC. Paired Student's t-test and Fisher's exact test were used to compare subsets of patients.

RESULTS

Out of the 3110 patients who underwent LD-LCS, 756 (24.3%) patients (mean age: 67 +/-6.4 year; M=466, 61.6%: F=290, 38.4%) were reported to have significant CAC. Of these, 236 patients (31.2%) had established, documented coronary artery disease at baseline. A change in management was noted in 155 patients (20.5%). The most common changes in management were medication regimen change (n=114/155, 73.5%), stress testing (n=65/155, 41.9%), and cardiology specialist referral (36/155, 23.2%). Percutaneous (3/155, 1.9%) and surgical (3/155, 1.9%) coronary interventions were infrequent. In those without known CAD, those whose CAC were semi-quantified as moderate, severe, or other nonstandard modifier were more likely to have a change in management compared to those whose CAC were unspecified (35% vs. 25%, p=0.02).

CONCLUSION

Coronary artery calcification is a common significant finding in LD-LCS. The reporting and semi-quantitative assessment of CAC in patients without established coronary artery disease resulted in change in management.

CLINICAL RELEVANCE/APPLICATION

Routine and standardized reporting of significant CAC found on LD-LCS has the potential to change patient management and may contribute to improved cardiovascular outcomes in this high-risk population.

SSK05-05 Interobserver Agreement for Lung-RADS Categorization in Subsolid Nodule-Enriched Lung Cancer Screening CT's

Wednesday, Dec. 4 11:10AM - 11:20AM Room: N229

Participants

Yongju Kim, MD, Seongnam, Korea, Republic Of (*Presenter*) Nothing to Disclose Jihang Kim, MD, Seongnam, Korea, Republic Of (*Abstract Co-Author*) Stockholder, Monitor Corporation; Research Grant, Seoul National University Bundabg Hospital Jungheum Cho, MD, Seongnam, Korea, Republic Of (*Abstract Co-Author*) Nothing to Disclose Kibbeum Doh, Seongnam-si, Korea, Republic Of (*Abstract Co-Author*) Nothing to Disclose Junghoon Kim, Seongnam-si, Korea, Republic Of (*Abstract Co-Author*) Nothing to Disclose Kyunghee Lee, MD, PhD, Seongnam, Korea, Republic Of (*Abstract Co-Author*) Nothing to Disclose Kyunghee Lee, MD, PhD, Seongnam, Korea, Republic Of (*Abstract Co-Author*) Research Grant, Ministry of Trade, Industry, and Energy; Research Grant, SNUBH Research Fund

Kyung Won Lee, MD, PhD, Seongnam, Korea, Republic Of (Abstract Co-Author) Nothing to Disclose

PURPOSE

To evaluate the interobserver agreement for Lung-RADS categorization in subsolid nodule-enriched low-dose screening CTs.

METHOD AND MATERIALS

A retrospective review of the low-dose screening CT reports from 2013 to 2017 using keyword search for subsolid nodules found 54 baseline CTs. A total of 162 CTs, including 108 negative screening CTs as controls, were classified into Lung-RADS categories by two fellowship-trained thoracic radiologists in a consensus manner. We randomly selected 60 scans (20 in Category 1/2 and 3, 10 in Category 4A and 4B) to ensure a balanced representation of all lung-RADS categories. Five radiologists reviewed the 60 CT scans and classified each CT scans into Lung-RADS categories. Rates of concordance, minor and major discordance were calculated, with the major discordance defined as at least six months of management discrepancy. We analyzed the agreement of five observers using Cohen's kappa statistics.

RESULTS

Averaged correct categorization was achieved by five radiologists for 60.3% (181 of 300) in all cases and 45.0% (90 of 200) in positive screens. Minor and major discordance rate was 29.7% and 10.0% in all cases and 41.5% and 13.5% in positive screens, respectively. Pairwise interobserver agreement (weighted k) was 0.535 (range, 0.353-0.686; 95% confidence interval, 0.406, 0.664).

CONCLUSION

The accuracy of radiologists in the categorization of screening CTs with subsolid nodules varied and the interobserver agreement was only moderate in the retrospective study. This inconsistency may affect management recommendations in lung cancer screening.

CLINICAL RELEVANCE/APPLICATION

Lung-RADS categorization of low-dose screening CTs with subsolid nodules varies among radiologists and the inconsistency may affect management recommendations.

SSK05-06 Update on Lung Cancer Screening Utilization: Results from the 2017 Behavioral Risk Factor Surveillance System Cross-Sectional Survey

Wednesday, Dec. 4 11:20AM - 11:30AM Room: N229

Participants

Anand K. Narayan, MD,PhD, Boston, MA (*Presenter*) Nothing to Disclose Gary X. Wang, MD,PhD, Boston, MA (*Abstract Co-Author*) Nothing to Disclose Diego Lopez, Boston, MA (*Abstract Co-Author*) Nothing to Disclose Brent P. Little, MD, Boston, MA (*Abstract Co-Author*) Author, Reed Elsevier; Editor, Reed Elsevier; Royalties, Reed Elsevier Florian J. Fintelmann, MD, Boston, MA (*Abstract Co-Author*) Consultant, Jounce Therapeutics, Inc; Research support, BTG International Ltd Jo-Anne O. Shepard, MD, Boston, MA (*Abstract Co-Author*) Editor with royalties, Reed Elsevier Justin Stowell, MD, Boston, MA (*Abstract Co-Author*) Nothing to Disclose Efren J. Flores, MD, Boston, MA (*Abstract Co-Author*) Nothing to Disclose

For information about this presentation, contact:

aknarayan@mgh.harvard.edu

PURPOSE

Lung cancer screening with low dose chest CT (LCS) reduces lung cancer mortality. Despite favorable recommendations from the USPSTF for LCS in 2013 and coverage by public and private payors since 2015, initial studies reported that only <5% of eligible patients are being screened. Despite increasing insurance coverage, public awareness, and availability of LCS nationwide, few studies have evaluated recent LCS utilization. Our purpose was to estimate LCS utilization using nationally representative cross-sectional survey data from the most recent Behavioral Risk Factor Surveillance System Survey (BFRSS) survey.

METHOD AND MATERIALS

BRFSS is a nationally representative, cross-sectional phone survey of adults in the United States. The 2017 survey included questions about LCS eligibility and utilization in 11 states (Florida, Georgia, Kentucky, Maryland, Missouri, Nevada, Oklahoma, Vermont, Wyoming, Kansas, Maine). Primary outcome was the proportion of patients ages 55-79 with at least a 30 pack year smoking history who reported undergoing LCS. Multivariable logistic regression models were used to evaluate the association between self-reported LCS usage and sociodemographic characteristics, adjusted for potential confounders and accounting for complex survey design elements.

30,362 participants were included of whom 27.8% reported at least 30 pack year smoking history. Among participants with at least a 30 pack year smoking history between the ages of 55-79, 12.2% (95% CI 10.7, 13.7) reported obtaining a chest CT scan specifically to evaluate for lung cancer. In our multiple variable analyses, age, education category, income category, health insurance status, race, marital status, and employment status were not associated with statistically significant differences in self-reported receipt of LCS (p > 0.05).

CONCLUSION

Overall, utilization of LCS remains low (12%) among eligible participants, however comparison with previously published studies suggests improvements in LCS utilization.

CLINICAL RELEVANCE/APPLICATION

LCS uptake among eligible patients is low. Provider education, public awareness campaigns, and continued improvements in health insurance coverage are required to save more lives with LDCT.

SSK05-07 Impact of Multidisciplinary Review of Lung Cancer Screening CT on LungRADS Score and Follow-Up Recommendations

Wednesday, Dec. 4 11:30AM - 11:40AM Room: N229

Participants

Michael F. Morris, MD, Scottsdale, AZ (*Presenter*) Speakers Bureau, Medtronic plc Gordon Haugland, MD, Scottsdale, AZ (*Abstract Co-Author*) Nothing to Disclose Raul Galvez-Trevino, MD, Scottsdale, AZ (*Abstract Co-Author*) Nothing to Disclose Susan Passalaqua, MD, Gilbert, AZ (*Abstract Co-Author*) Nothing to Disclose Archan Shah, Gilbert , AZ (*Abstract Co-Author*) Nothing to Disclose Raed Alalawi, Phoenix , AZ (*Abstract Co-Author*) Nothing to Disclose Jennifer Wrzesinske, Gilbert , AZ (*Abstract Co-Author*) Nothing to Disclose Stacey Rodgers, Gilbert , AZ (*Abstract Co-Author*) Nothing to Disclose Brett Broussard, Gilbert , AZ (*Abstract Co-Author*) Nothing to Disclose Ryan Macke, Gilbert , AZ (*Abstract Co-Author*) Nothing to Disclose John Breard, Gilbert , AZ (*Abstract Co-Author*) Nothing to Disclose Elbert Kuo, MD,MPH, Phoenix, AZ (*Abstract Co-Author*) Speaker, Johnson & Johnson

PURPOSE

There is evolving consensus that positive lung cancer screening CT scans should be reviewed by a multidisciplinary panel. We assessed the impact of multidisciplinary review of lung cancer screening CTs initially coded as LungRADS (LR)-3, LR-4a, or LR-4b.

METHOD AND MATERIALS

From 1/2017-12/2018, 872 patients underwent lung cancer screening CT at 4 sites within an integrated health care system. A designated radiologist at each site interpreted CTs according to LR criteria. CT scans coded as LR-3 (n=71, 8.1%), LR-4a (n=33, 3.8%), or LR-4b (n=32, 3.7%) were reviewed by a multidisciplinary team of radiologists, interventional pulmonologists, and thoracic surgeons. Following multidisciplinary review, CTs were given a final LR score and follow-up recommendations were provided.

RESULTS

136 patients were coded as LR-3, LR-4a, or LR-4b by the site radiologist. After multidisciplinary review, 23 (16.9%) patients had the LR score changed. Baseline characteristic were similar between patients with a change in LR score compared to those with no change in LR score. 12 CTs (52%) had the LR score upcoded and 11 CTs (48%) were downcoded. Reasons for change in LR coding are described in Figure 1. CT scans not following LR assessment categories were more likely to be upcoded (p=0.03), whereas findings considered to be infectious/inflammatory/scarring were more likely to be downcoded (p=0.04). After LR upcoding, follow-up recommendations were changed to biopsy (n=4), PET/CT (n=4), or 3-month follow-up CT (n=4). LR downcoding resulted in followup recommendations being changed to 6 month follow-up CT (n=6), 12 month low dose CT (n=4), and PET/CT (n=1). LR upcoding facilitated early detection of lung cancer in one patient (4.3%), whereas downcoding resulted in a potential delay in cancer diagnosis in one patient (4.3%).

CONCLUSION

Multidisciplinary review of LR-3, LR-4a, and LR-4b CTs results in LR reclassification in 16.9% of patients within an integrated health care system. Lung nodules not coded according to LR assessment categories, or CT findings ascribed to infection/inflammation/scarring, were significantly more likely to have the LR score changed. Further studies should examine the impact of multidisciplinary review on CT screening outcomes.

CLINICAL RELEVANCE/APPLICATION

Multidisciplinary review of LR-3, LR-4a, and LR-4b cases results in LR reclassification and changes to follow-up recommendations in a significant minority of cases.

SSK05-08 Variability among Expert Readers in Low-Dose CT Lung Cancer Screening: Comparison of Readings between Individual Institution and Central Review in a Nationwide Lung Cancer Screening Project

Wednesday, Dec. 4 11:40AM - 11:50AM Room: N229

Participants

Eui Jin Hwang, Seoul, Korea, Republic Of (*Presenter*) Nothing to Disclose Jin Mo Goo, MD, PhD, Seoul, Korea, Republic Of (*Abstract Co-Author*) Research Grant, INFINITT Healthcare Co, Ltd; Research Grant, DONGKOOK Pharmaceutical Co, Ltd; Soon Ho Yoon, MD, Seoul, Korea, Republic Of (*Abstract Co-Author*) Nothing to Disclose Hyae Young Kim, MD, PhD, Goyang-si, Korea, Republic Of (*Abstract Co-Author*) Nothing to Disclose Jaeyoun Yi, Seoul, Korea, Republic Of (*Abstract Co-Author*) Nothing to Disclose Yeol Kim I, Goyang-si, Korea, Republic Of (*Abstract Co-Author*) Nothing to Disclose

For information about this presentation, contact:

ken921004@hotmail.com

PURPOSE

Computer-aided detection and volumetry is known to reduce interobserver variability but its potential in a real world setting has rarely been reported. This study aimed to evaluate the variability among experts in a nationwide lung cancer screening project.

METHOD AND MATERIALS

We evaluated 1647 consecutive baseline screening CT scans obtained during one month period of December 2017 from a nationwide lung cancer screening project (K-LUCAS) in which 14 institutions participated. Chest radiologists of each institution assessed CT scans using a thin-client system equipped with semi-automated nodule segmentation and computer-aided detection software based on Lung-RADS (institutional reading). One chest radiologist retrospectively reviewed all these CT scans while minimizing modification of segmentation results and minimizing rejecting tiny nodules (central review). Reading results between institutional reading and central review were compared. Positive rates of central review using Lung-RADS and NELSON criteria were also compared.

RESULTS

The average per-case positive rate was significantly higher in central review (24.9% [410/1647; 11.1-32.7% across institutions] vs. 19.3% [319/1647; 5.6-30.0% across institutions]; P<.001). The number of detected nodules was significantly larger in central review (3.04 vs. 1.17 nodule/case; P<.001), while variability in positive rates among institutions were significantly lower in central review (coefficient of variability, 21.9% vs. 40.2%; P=.044). Manual measurements while rejecting segmentation results occurred in 1.6% (80/5008) of nodules at central review and in 17.8% (342/1920) nodules at institutional reading. Positive rate with Lung-RADS is higher (24.9%) compared with that of NELSON criteria (3.9%) but lower than indeterminate scan rate defined by NELSON criteria (33.4%) which requires additional scanning.

CONCLUSION

There is considerable variability among expert readers in reading of lung cancer screening CT mainly by discarding tiny nodules and modifying or rejecting segmentations results. NELSON criteria do not reduce the number of additional scanning in nodule management compared with Lung-RADS.

CLINICAL RELEVANCE/APPLICATION

Even in a situation where computerized tools are adopted, there is considerable variability among readers. The value of reducing variability by applying stricter rules should be further investigated.

SSK05-09 An Observer Study Comparing Radiologists with the Prize-Winning Lung Cancer Detection Algorithms from the 2017 Kaggle Data Science Bowl

Wednesday, Dec. 4 11:50AM - 12:00PM Room: N229

Participants

Colin Jacobs, PhD, Nijmegen, Netherlands (*Presenter*) Research Grant, MeVis Medical Solutions AG; Royalties, MeVis Medical Solutions AG; Research Grant, Thirona

Ernst T. Scholten, MD, PhD, Haarlemmerliede, Netherlands (Abstract Co-Author) Nothing to Disclose

Anton Schreuder, MD, Nijmegen, Netherlands (Abstract Co-Author) Nothing to Disclose

Mathias Prokop, PhD, Nijmegen, Netherlands (*Abstract Co-Author*) Speakers Bureau, Bracco Group Speakers Bureau, Bayer AG Research Grant, Canon Medical Systems Corporation Speakers Bureau, Canon Medical Systems Corporation Research Grant, Siemens AG Speakers Bureau, Siemens AG Departmental spinoff, Thirona Departmental licence agreement, Varian Medical Systems, Inc Bram van Ginneken, PhD, Nijmegen, Netherlands (*Abstract Co-Author*) Stockholder, Thirona; Co-founder, Thirona; Royalties, Thirona; Research Grant, Varian Medical Systems, Inc; Royalties, Varian Medical Systems, Inc; Research Grant, Canon Medical Systems Corporation; Royalties, Canon Medical Systems Corporation; Research Grant, Siemens AG;

For information about this presentation, contact:

·· ·· · _

colin.jacobs@radboudumc.nl

PURPOSE

The 2017 Kaggle Data Science Bowl challenge awarded 1 million dollars in prize money to develop computer algorithms for predicting, on the basis of a single low-dose screening CT scan, which individuals will be diagnosed with lung cancer within one year of the scan. Participating teams received a training set of around 1500 low-dose CT scans to develop and train their algorithms and final performance was measured on a test set of 500 scans, containing 151 lung cancer cases. Over 2000 teams submitted results. The best 10 algorithms all used deep learning and are freely available as open source code. To gain insight into how the performance of these algorithms compares to radiologists, we conducted an observer study including 11 readers who read 150 cases from the test set.

METHOD AND MATERIALS

We randomly extracted 100 benign cases and 50 lung cancer cases from the test set of the challenge. Each algorithm scored each test case with a score between 0 (low) and 1 (high) for harboring a malignancy. We developed a web-accessible workstation in which human experts could review chest CT scans. The web workstation included the common tools found in a professional medical viewing workstation. We invited 11 readers, a mix of radiologists and radiology residents, to read these 150 CT cases and assign a score between 0 (low) and 100 (high) whether the patient will develop a lung cancer within one year of the presented scan. ROC analysis was used to compare the performance of the human readers with the algorithms. The primary outcome was area under the ROC curve. 95% confidence intervals were computed by 1000 bootstrap iterations and are reported between brackets.

RESULTS

The mean area under the ROC curve for the human readers was 0.90 [0.85-0.94]. The mean area under the ROC curve for the algorithms was 0.86 [0.81-0.91]. The mean human reading time per case varied between 96 and 275 seconds.

• •

- . - - . - .

CONCLUSION

The top 10 algorithms from the Kaggle Data Science Bowl 2017 showed promising performance, but were still inferior to human readers. Future analysis will focus on understanding the strengths and weaknesses of the computer algorithms and the human readers and how these can be optimally combined.

CLINICAL RELEVANCE/APPLICATION

Fully automatic algorithms using deep learning developed in a large-scale challenge show promising performance for lung cancer detection in chest CT, but performed inferior to radiologists in this subset of the test set.

Printed on: 10/29/20





SSK06

Science Session with Keynote: Emergency Radiology (Pulmonary Emboli - Current Cutting Edge, and the Future)

Wednesday, Dec. 4 10:30AM - 12:00PM Room: S103AB



AMA PRA Category 1 Credits ™: 1.50 ARRT Category A+ Credit: 1.75

FDA Discussions may include off-label uses.

Participants

Clint W. Sliker, MD, Baltimore, MD (*Moderator*) Nothing to Disclose Michael N. Patlas, MD, FRCPC, Hamilton, ON (*Moderator*) Speaker, Springer Nature Jamlik-Omari Johnson, MD, Atlanta, GA (*Moderator*) Nothing to Disclose

Sub-Events

SSK06-01 Emergency Radiology Keynote Speaker: Pulmonary Emboli: Current Clinical Picture

Wednesday, Dec. 4 10:30AM - 10:50AM Room: S103AB

Participants

Clint W. Sliker, MD, Baltimore, MD (Presenter) Nothing to Disclose

SSK06-03 Radiation Dose, Subjective and Objective Image Quality of Two Dual-Source CT Scanners in Acute Pulmonary Embolism: A Comparative Study

Wednesday, Dec. 4 10:50AM - 11:00AM Room: S103AB

Participants

Waleed Abdellatif, MD, Vancouver, BC (*Presenter*) Nothing to Disclose Eric Esslinger, Kamloops, BC (*Abstract Co-Author*) Nothing to Disclose Kevin J. Kobes, Vancouver, BC (*Abstract Co-Author*) Nothing to Disclose Amanda Wong, Vancouver, BC (*Abstract Co-Author*) Nothing to Disclose Jennifer Powell, Vancouver, BC (*Abstract Co-Author*) Nothing to Disclose Savvas Nicolaou, MD, Vancouver, BC (*Abstract Co-Author*) Institutional research agreement, Siemens AG; Stockholder, Canada Diagnostic Centres

For information about this presentation, contact:

waleed.abdellatif@vch.ca

PURPOSE

To compare radiation dose, mean acquisition time, objective and subjective image quality of two Dual Source CT scanners in the evaluation of acute pulmonary embolism (PE), operating in dual energy mode.

METHOD AND MATERIALS

Total of 221 scans on the 2nd generation SOMATOM Definition Flash CT scanner (the Flash) and 354 scans on the 3rd generation SOMATOM Force (the Force) were included, after adjusting the acquisition parameters to be the same. In a randomized blinded design, two radiologists independently reviewed both sets of scans in two settings (5-week interval) for subjective image quality using a 5-point Likert scale. Dose length product (DLP), CTDIvol and effective dose (ED) were calculated along with objective parameters such as image noise, Signal to Noise ratio (SNR), Contrast to Noise ratio (CNR) and dose-independent Figure of Merit (FOM= CNR2/ED).

RESULTS

Mean acquisition time was significantly lower in the Force in comparison to the Flash (2.81s +/-0.1 in comparison to 9.7s +/- 0.15 [mean+/- SD] respectively; p < 0.0001) with the Force 3.4 times faster than the Flash. The mean image quality score was found to be 4.33/5 and 4/5 for the Force and the Flash respectively with statistical significance (p < 0.0001 on the unpaired t-test; 95% CI= 0.17-0.49). Interobserver reliability for image quality indicates strong agreement on both, the Force (K= 0.83, P<0.005) and the Flash-generated scans (K= 0.85, P<0.005). DLP, CTDIvol and ED were significantly lower in the Force than the Flash (175.6 +/-63.7; 5.3 +/-1.9 and 2.8 +/- 1.2 in comparison to 266 +/- 255; 7.8 +/-2.2 and 3.8 +/-4.3 [mean +/- SD] respectively). Noise was significantly lower in the Force (p<0.01). SNR, CNR and FOM were significantly higher in the Force than the Flash (33.5 +/-23.4; 29.0 +/-21.3 and 543.7 +/-1037 in comparison to 23.4 +/- 17.7; 19.4 +/- 16.0 and 170.5 +/-284.3 [mean +/- SD] respectively used for emergency patients while the Flash was used for inpatients.

CONCLUSION

Objective and subjective image quality is significantly higher on the Force with significantly lower mean acquisition time and radiation dose in comparison to the Flash.

The improved image quality and speed of the Force could be very useful in emergency radiology setting with large patient volume while maintaining lower radiation dose.

SSK06-04 Diagnostic Accuracy of Dual-Energy CT in Detection of Acute Pulmonary Embolism: A Systematic Review and Meta-Analysis

Wednesday, Dec. 4 11:00AM - 11:10AM Room: S103AB

Participants

Waleed Abdellatif, MD, Vancouver, BC (*Presenter*) Nothing to Disclose Mahmoud Ebada, Zagazig, Egypt (*Abstract Co-Author*) Nothing to Disclose Souad Alkanj, Zagazig, Egypt (*Abstract Co-Author*) Nothing to Disclose Ahmed Negida, Zagazig, Egypt (*Abstract Co-Author*) Nothing to Disclose Nicolas Murray, MD, Vancouver, BC (*Abstract Co-Author*) Nothing to Disclose Faisal Khosa, Vancouver, BC (*Abstract Co-Author*) Scholarship, Canadian Association of Radiologists Scholarship, Vancouver Coastal Health Savvas Nicolaou, MD, Vancouver, BC (*Abstract Co-Author*) Institutional research agreement, Siemens AG; Stockholder, Canada Diagnostic Centres

For information about this presentation, contact:

waleed.abdellatif@vch.ca

PURPOSE

To calculate sensitivity, specificity and diagnostic accuracy of Dual-Energy CT (DECT) in the detection of acute pulmonary embolism (PE) through meta-analysis framework (PROSPERO registration Number: CRD42019120143).

METHOD AND MATERIALS

We searched Medline (via PubMed), EBSCO, Web of Science, Scopus and the Cochrane Library for relevant published studies. We selected clinical trials assessing the accuracy of DECT in the detection of PE. Quality assessment of bias and applicability was conducted using the Quality of Diagnostic Accuracy Studies-2 tool. The sensitivity, specificity, positive likelihood ratio, negative likelihood ratio, and the diagnostic odds ratio were recorded. The summary receiver operating characteristic curve was drawn to get the Cochran Q-index and the area under the curve.

RESULTS

Seven studies with high homogeneity were included in our systematic review. The pooled sensitivity was 87.9% (95% confidence interval [CI]: 80.1- 93.4%), specificity was 93.3% (95% CI: 85.1- 97.8%), and diagnostic odds ratio was 51.59 (95% CI 17.28- 153.98). The pooled PLR was 8.72 (95% CI: 4.10- 18.54) and NLR was 0.20 (95% CI: 0.11- 0.39). Cochran-Q was 0.8794 and Area Under the Curve (AUC) was 0.9416 in the sROC curve.

CONCLUSION

DECT shows high sensitivity, specificity and diagnostic accuracy in the detection of acute PE. However, studies with larger sample size are still needed to support these findings.

CLINICAL RELEVANCE/APPLICATION

This meta-analysis shows the high diagnostic accuracy of dual energy CT (DECT) in diagnosis of acute PE. Astonishingly, a few studies have been published in the literature to discuss the value of DECT in this particular diagnosis. Hence, studies with larger sample size are still needed to support these findings.

SSK06-05 Pulmonary Embolism during Pregnancy: A 17-Year Single-Center Retrospective MDCT Pulmonary Angiography Study

Wednesday, Dec. 4 11:10AM - 11:20AM Room: S103AB

Participants

David Rotzinger, MD, Lausanne, Switzerland (*Presenter*) Nothing to Disclose Vincent Dunet, Lausanne, Switzerland (*Abstract Co-Author*) Nothing to Disclose Olivier Hugli, MD, Lausanne, Switzerland (*Abstract Co-Author*) Nothing to Disclose Reto A. Meuli, MD, PhD, Lausanne, Switzerland (*Abstract Co-Author*) Nothing to Disclose Sabine Schmidt, MD, Lausanne, Switzerland (*Abstract Co-Author*) Nothing to Disclose

For information about this presentation, contact:

david.rotzinger@chuv.ch

PURPOSE

To determine the prevalence of pulmonary embolism (PE) and alternative diagnoses in pregnant women requiring computed tomography pulmonary angiography (CTPA); to assess the evolution of qualitative image quality and radiation dose over time.

METHOD AND MATERIALS

We retrospectively included all pregnant women referred to CTPA for clinically suspected PE over 17 years. Four different scanners were successively in use during the inclusion period, starting with a 4-MDCT system, then 16-MDCT, 64-MDCT, and finally 256-MDCT. Two blinded radiologists reviewed each CTPA in consensus regarding PE, alternative diagnoses and qualitative image quality. Radiation dose metrics, associated clinical and laboratory parameters were retrieved. Subgroup comparison was performed (Wilcoxon and Kruskal-Wallis tests).

RESULTS

After the exclusion of 8 (1.7%) patients due to inadequate technical CTPA quality, we analyzed 229 patients (mean age 31.7 years) with a mean gestational age of 28±7weeks. Qualitative image quality was similar across the four different CT systems used

over time (p=0.28). Sixteen (7%) patients had PE, 69 (30.1%) had an alternative diagnosis, and 144 (62.9%) had no radiological findings. Alternative radiological diagnoses in case of PE-negative CTPA included consolidation (n=14), other pulmonary infiltrates (n=33), pleural effusion (n=29), and basal atelectasis (n=43). Gestational age, symptoms and D-dimer levels were not significantly different between patients with or without PE (all p-values >0.05). We observed a 30% decrease in radiation exposure (dose-length product) over time (p<0.001), with a concomitant 4-fold increase of examinations per year.

CONCLUSION

In pregnant women, CTPA is rarely positive for PE and more often shows alternative diagnoses than PE. The use of CTPA in pregnancy has risen notably over 17 years, but radiation dose exposure has decreased by one third over the same period without a change in qualitative image quality.

CLINICAL RELEVANCE/APPLICATION

The use of CTPA in pregnancy has steadily risen over the last 17 years, and thanks to recent technical improvements, radiation dose exposure inherent in CTPA has considerably decreased while diagnostic image quality remains identical. In pregnant women, CTPA is rarely positive for PE and more often shows alternative diagnoses than PE.

SSK06-06 Attenuation Gradients Across Thoracic Vasculature on CT Pulmonary Angiography Predict Mortality Following Pulmonary Embolism

Wednesday, Dec. 4 11:20AM - 11:30AM Room: S103AB

Participants

Andrew D. Chang, MSc, Providence, RI (*Presenter*) Nothing to Disclose Lillian Dominguez-Konicki, Providence, RI (*Abstract Co-Author*) Nothing to Disclose Gian Ignacio, Providence, RI (*Abstract Co-Author*) Nothing to Disclose Michael K. Atalay, MD, PhD, Providence, RI (*Abstract Co-Author*) Nothing to Disclose Dan Shilo, MD, Staten Island, NY (*Abstract Co-Author*) Nothing to Disclose

For information about this presentation, contact:

adchang@brown.edu

PURPOSE

Early risk stratification of pulmonary emboli (PE) has important clinical value in emergency and inpatient settings. While the PE Severity Index (PESI) is a well-validated prognostication tool for this purpose, its derivation requires multiple variables and has weak positive predictive value (PPV) in identifying high-risk patients. CT for pulmonary angiography (CTPA) captures the distribution of intravenous contrast across thoracic vasculature based on hemodynamic status. We hypothesize attenuation differences across this vasculature may be independently predictive of 30-day mortality, and improve the PPV of PESI score.

METHOD AND MATERIALS

We retrospectively identified 1000 consecutive patients who had positive CTPA studies between 1/1/2017 and 2/12/2019. The primary outcome was 30-day mortality following CTPA. Patient demographics and admission information were used to calculate PESI class. CTPA studies were performed with a fixed delay of 22 sec and injection rate of 4 cc/s. For each patient, densities (HU) were measured in the superior vena cava [SVC], main pulmonary artery [PA], left atrium [LA], and descending aorta [AO] on a single mid-thoracic transaxial slice. Density differences, PESI scores, and their combination were compared between groups.

RESULTS

We identified 1000 consecutive patients with positive CTPA studies within the study period. Compared to surviving patients (n=907, 90.8%), patients who died within 30 days (n=92, 9.2%) exhibited higher attenuation in the PA (446 ± 164 vs 377 ± 128 HU, p<0.001). The absolute density change from PA to AO (PA-AO) was associated with 30-day mortality (OR 1.002, 95%CI 1.001-1.004, p=0.001). This effect did not persist after adjusting for PESI score. With a threshold PA-AO difference of 150 HU, the combined PESI/PA-AO score had greater PPV for 30-day mortality than either independently (Combined 18.7% vs PESI 15.0% vs PA-AO 13.5%).

CONCLUSION

This study provides a simple, novel approach to identify high-risk PE patients by measuring vessel densities on a single transaxial CTPA image. Odds of high-risk PE increased with greater attenuation differences between the PT and AO, with a difference of 150 HU serving as a useful threshold that improves the predictive value of the PESI score.

CLINICAL RELEVANCE/APPLICATION

Vessel density changes on standard CTPA protocol may be used to improve identification of 30-day mortality following pulmonary embolism.

SSK06-07 Estimating Quantitative Lobar and Zonal Pulmonary Perfusion from Dual Energy CT Pulmonary Angiography: Accuracy and Applications in Pulmonary Embolism

Wednesday, Dec. 4 11:30AM - 11:40AM Room: S103AB

Participants

Ramandeep Singh, MBBS, Boston, MA (Presenter) Nothing to Disclose

Subba R. Digumarthy, MD, Boston, MA (*Abstract Co-Author*) Speaker, Siemens AG; Research Grant, Lunit Inc; Researcher, Merck & Co, Inc; Researcher, Pfizer Inc; Researcher, Bristol-Myers Squibb Company; Researcher, Novartis AG; Researcher, F. Hoffmann-La Roche Ltd; Researcher, Polaris Pharmaceuticals, Inc; Researcher, Cascadia Healthcare, LLC; Researcher, AbbVie Inc; Researcher, Gradalis, Inc; Researcher, Zai Lab

Fatemeh Homayounieh, MD, Boston, MA (Abstract Co-Author) Nothing to Disclose

Mannudeep K. Kalra, MD, Lexington, MA (*Abstract Co-Author*) Research Grant, Siemens AG; Research Grant, Riverain Technologies, LLC;

Thomas G. Flohr, PhD, Forchheim, Germany (Abstract Co-Author) Employee, Siemens AG

Bernhard Schmidt, PhD, Forchheim, Germany (Abstract Co-Author) Employee, Siemens AG

For information about this presentation, contact:

rsingh17@mgh.harvard.edu

PURPOSE

To assess accuracy and variations in lobar and zonal pulmonary perfusion on dual energy CT (DECT) pulmonary angiography in patients with and without pulmonary embolism with deep learning-based prototype and Lung AnalysisTM for automatic lung segmentation and quantitative perfusion on dual energy CT.

METHOD AND MATERIALS

Our IRB approved retrospective study included 88 adult patients (M:F=38:50; mean age= 56±19 years) who underwent DECT-PA on a 384-slice, third generation dual source CT (Siemens Somatom Force). Amongst these, 40 patients had pulmonary embolism (PE) and 48 had no PE. All CT exams were reviewed for location and distribution of PE. Transverse thin (1-1.5mm) DECT images (80kV;150kV) were exported and processed on a stand-alone prototype for automatic lung lobe segmentation (RUL, RML, RLL, LUL, LLL). The mean iodine concentration was normalized to main pulmonary artery. The mean attenuation numbers (M-HU), contrast amount (CA in mg) and normalized iodine concentration (NIC) were derived. The zonal volumes (RUZ, RMZ, RLZ, LUZ, LMZ, LLZ) and mean enhancement (M-HU) were derived from Lung Analysis (Siemens SyngoViaTM). Descriptive statistics and ANOVA were performed.

RESULTS

The deep learning-based automatic lung lobe segmentation was accurate in all DECT-PA (88;100%). Both lobar and zonal perfusions were significantly lower in patients with PE as compared to those without PE (p<0.0001). The mean M-HU, CA and NIC for PE negative and positive affected were: RUL (29,700,0.11; 23,556,0,08); RML (24,283,0.09;19,194,0.07); RLL (26,709,0.10; 20,471,0.07), LUL (26,776,0.10; 18,534,0.06) and LLL (26,628,0.09; 18,402,0.06) (p<0.0001). The zonal M-HU for PE negative and positive cases were: RUZ (32; 27), RMZ (30; 20), RLZ (29; 23), LUZ (31; 23), LMZ (29; 21) and LLZ (29; 20) (p<0.0001).

CONCLUSION

Accurate lung lobe segmentation and quantitative lobar lung perfusion can be obtained with application of deep learning-based segmentation tool on DECT pulmonary angiography.

CLINICAL RELEVANCE/APPLICATION

Quantitative parameters can improve diagnostic accuracy and may help predict patient outcome for pulmonary embolism on DECT pulmonary angiography.

SSK06-08 Can Pulmonary Embolism Rule-Out Criteria Replace the Need for D-Dimer Testing among Patients with Low Clinical Probability in the Emergency Department?

Wednesday, Dec. 4 11:40AM - 11:50AM Room: S103AB

Participants Ahmed Al Lawati, MD, Muscat, Oman (*Presenter*) Nothing to Disclose Ahmed Al Abri, MD, Al Athiba, Oman (*Abstract Co-Author*) Nothing to Disclose Rashid S. Al Umairi, MD, FRCR, Muscat, Oman (*Abstract Co-Author*) Nothing to Disclose

For information about this presentation, contact:

alumairi1@yahoo.com

PURPOSE

The Pulmonary Embolism Rule-Out Criteria (PERC) rule has been suggested as an alternative to D-dimer testing in patients with low risk in pretest Pretest probability clinical scoring systems. This study looked at whether the PERC rule could safely replace the use of D-dimer in patients suspected of PE.

METHOD AND MATERIALS

Retrospectively we reviewed 350 patients with a suspected pulmonary embolism and had computed tomography pulmonary angiography (PCTA) and a blood sample for D-dimer level taken. PERC was retrospectively calculated for all patients and the diagnostic performance of the PERC rule was compared with a standard D-dimer level in the detection of PE

RESULTS

Of the 350 patients, 56 had positive CTPA and 294 had a negative scan. In these patients, the sensitivity of the PERC rule for detecting PE was 98.2% [95% confidence interval (CI): 90.45% to 99.95%], with a negative likelihood ratio of 0.16 (95% CI: 0.02 to 1.18). However, the negative predictive value of the PERC rule was 96.97 % % (95% CI: 81.70% to 99.57%). In comparison, the sensitivity for the standard D-dimer test was 98.21%% (95% CI: 90.45% to 99.95%), with a negative likelihood ratio of 0.24 (95% CI: 0.03 to 1.73). The negative predictive value for the standard D-dimer test was 95.65 % (95% CI: 75.17% to 99.38%).

CONCLUSION

The PERC rule has a high negative predictive value for excluding PE in patients presenting with suspected PE to the emergency department.

CLINICAL RELEVANCE/APPLICATION

Pulmonary embolism (PE) is a common and potentially fatal cardiovascular emergency. Pretest probability clinical scoring systems are used to stratify patients a suspicion of pulmonary embolism into low risk and high risk for PE. Patients with low risk for PE usually undergo D-dimer testing. A negative D-dimer in this low-risk group rules out PE with a high degree of certainty because of its high sensitivity. The D-dimer is, however, a poorly specific test and positive results often lead to unnecessary radiological imaging.

SSK06-09 Machine Learning Based Prediction of Pulmonary Embolism in the Emergency Department

Wednesday, Dec. 4 11:50AM - 12:00PM Room: S103AB

Participants Salim Bader, Ramat Gan, Israel (*Presenter*) Nothing to Disclose Ehud Grossman, Ramat Gan, Israel (*Abstract Co-Author*) Nothing to Disclose Sara Apter, MD, Ganei Tikva, Israel (*Abstract Co-Author*) Nothing to Disclose Edith M. Marom, MD, Tel Aviv, Israel (*Abstract Co-Author*) Speaker, Bristol-Myers Squibb Company; Speaker, Boehringer Ingelheim GmbH; Speaker, Merck & Co, Inc; Officer, Voxellence ; ; ; ; Shelly Soffer, Tel Aviv, Israel (*Abstract Co-Author*) Nothing to Disclose Yiftach Barash, Ramat Gan, Israel (*Abstract Co-Author*) Nothing to Disclose Eli Konen, MD, Tel Hashomer, Israel (*Abstract Co-Author*) Nothing to Disclose Eyal Klang, MD, Ramat Gan, Israel (*Abstract Co-Author*) Nothing to Disclose

PURPOSE

Pulmonary embolism (PE) is a challenging diagnosis, often not recognized in timely fashion. The Wells score, based on specific anamnestic questions and clinical signs, is a known clinical decision tool for performing D-dimer blood test or CTA for suspected PE. Validation studies showed area under the curves of (AUC) of 0.75-0.80 for the Wells score. Our goal was to develop a machine-learning model for raising suspicion of PE without using specific anamnestic information or D-dimer results.

METHOD AND MATERIALS

An institutional review board granted approval for this retrospective study. We retrieved data for consecutive patients (1/2012 to 12/2018) who performed CTA in our ED for suspected PE. Clinical variables included demographics, vital signs, chief complaint, background medical history coded using ICD10 coding, chronic medications and blood tests other than D-dimer (complete blood count, chemistry panel). Number and time to previous ED visits and hospitalizations were also computed as variables. We verified PE presence in the scans using ICD10 coding. We evaluated the AUC of single variables to predict PE. We used a gradient boosting machine learning model (CatBoost) to predict PE. The model was trained on years 2012-2017 data and tested on year 2018 data. We evaluated the AUC of the model and used Youden's index to find the model's optimal sensitivity and specificity.

RESULTS

Overall, 4,701 patients were included in the study. From them, 367 patients (7.8%) were diagnosed with PE. Single variables with highest AUC for prediction of PE included: days from previous ED visit (0.69), chief complaint (0.69), oxygen saturation (0.68), Creatine Phosphokinase (CPK) (0.68), albumin (0.65), days to previous hospitalization (0.64), number of background diseases (0.63), heart rate (0.62), C reactive protein (CRP)(0.61) and number of previous hospitalizations (0.61). The machine learning model showed an AUC of 0.80 (95% CI: 0.765 - 0.845) for predicting PE. Using Youden's index, the model showed a sensitivity of 98.6% and specificity of 46.6% for predicting PE.

CONCLUSION

Readily available clinical and laboratory variables can be used to train a machine learning model for raising suspicion of PE in the ED setting with accuracy similar to the Wells score.

CLINICAL RELEVANCE/APPLICATION

Machine learning model can be used to flag patients with high probability for having PE, for performing D-dimer in these patients.

Printed on: 10/29/20





SSK07

Gastrointestinal (Focal Liver Lesions Non-HCC)

Wednesday, Dec. 4 10:30AM - 12:00PM Room: S501ABC

GI

AMA PRA Category 1 Credits ™: 1.50 ARRT Category A+ Credit: 1.75

Participants

Myeong-Jin Kim, MD, PhD, Seoul, Korea, Republic Of (*Moderator*) Research grant, Bayer Pharma AG; Honoraium, Guerbet SA, GE healthcare, Philips, and Siemens Healthineers

Victoria Chernyak, MD,MS, Bronx, NY (*Moderator*) Consultant, Bayer AG Veronica L. Cox, MD, Houston, TX (*Moderator*) Nothing to Disclose

Sub-Events

SSK07-01 Diagnostic Performance of LR-M Criteria and Imaging Spectrum of Primary Hepatic Malignancies

Wednesday, Dec. 4 10:30AM - 10:40AM Room: S501ABC

Participants

Seung-Seob Kim, MD, Seoul, Korea, Republic Of (*Presenter*) Nothing to Disclose Sunyoung Lee, Seoul, Korea, Republic Of (*Abstract Co-Author*) Nothing to Disclose Jin-Young Choi, Seoul, Korea, Republic Of (*Abstract Co-Author*) Nothing to Disclose Mi-Suk Park, MD, Seoul, Korea, Republic Of (*Abstract Co-Author*) Nothing to Disclose Myeong-Jin Kim, MD, PhD, Seoul, Korea, Republic Of (*Abstract Co-Author*) Research grant, Bayer Pharma AG; Honoraium, Guerbet SA, GE healthcare, Philips, and Siemens Healthineers

For information about this presentation, contact:

k2s0127@yuhs.ac

PURPOSE

To evaluate diagnostic performance of LR-M criteria for differentiating hepatocellular carcinoma (HCC), intrahepatic mass-forming cholangiocarcinoma (iCC), and combined hepatocellular-cholangiocarcinoma (cHCC-CC) and to compare the imaging features of each type

METHOD AND MATERIALS

In this retrospective, case-control study, 110 patients with surgically proven iCC (n=67) and cHCC-CC (n=43) between June 2013 and June 2018 were enrolled as a case group. Another 110 patients with size-matched HCC were selected as a control group. Two independent readers evaluated imaging findings of preoperative MRI based on LI-RADS version 2018 and assigned LI-RADS category without knowing postsurgical histopathology. Diagnostic performance of LR-M criteria was evaluated and imaging features of iCC, cHCC-CC, and HCC were compared.

RESULTS

In the case group, 91 patients were categorized into LR-M and 15 patients into LR-5 (83% and 14%, respectively), while 13 patients of the control group were categorized into LR-M and 88 patients into LR-5 (12% and 80%, respectively). When more than two features of LR-M criteria were present, it suggested iCC or cHCC-CC with the specificity of 94.5%. Among the case group, findings of LI-RADS major criteria were more frequently seen in patients with cHCC-CC, while those of LR-M criteria were more prominent in those with iCC. Among the lesions with peripheral arterial phase hyperenhancement, enhancing rim was evenly uniform in 38 patients with iCC (out of 52 patients, 73.1%), while 14 patients with cHCC-CC showed irregularly thickened area of enhancing rim (out of 25 patients, 56%; p=0.022).

CONCLUSION

Diagnostic performance of LR-M criteria is desirable, and combination of imaging features is helpful for differentiating LR-M from HCC. The presence of irregularly thickened area of enhancing rim may suggest cHCC-CC rather than iCC.

CLINICAL RELEVANCE/APPLICATION

The presence of more than two LR-M findings is highly suggestive of iCC or cHCC-CC. Combination of imaging features may be helpful for differentiating primary liver malignancies.

SSK07-02 Pre-Operative Prediction of MVI in Liver Primary Tumors: Value of LI-RADS v2018 in Combination with Non-LI-RADS MR Features

Wednesday, Dec. 4 10:40AM - 10:50AM Room: S501ABC

Participants

Jingbiao Chen, Guangzhou, China (*Presenter*) Nothing to Disclose Sichi Kuang, Guangzhou, China (*Abstract Co-Author*) Nothing to Disclose Sidong Xie, Guangzhou, China (*Abstract Co-Author*) Nothing to Disclose Linqi Zhang, Guangzhou, China (*Abstract Co-Author*) Nothing to Disclose Binjun He, Guangzhou, China (Abstract Co-Author) Nothing to Disclose

Ying Deng, Guangzhou, China (Abstract Co-Author) Nothing to Disclose

Hao Yang, Guangzhou, China (*Abstract Co-Author*) Nothing to Disclose Yao Zhang, Guangzhou, China (*Abstract Co-Author*) Nothing to Disclose

Kathryn J. Fowler, MD, San Diego, CA (*Abstract Co-Author*) Consultant, 12 Sigma Technologies; Researcher, Nuance Communications, Inc; Contractor, Midamerica Transplant Services; ;

Claude B. Sirlin, MD, San Diego, CA (*Abstract Co-Author*) Research Grant, Gilead Sciences, Inc; Research Grant, General Electric Company; Research Grant, Siemens AG; Research Grant, Bayer AG; Research Grant, Koninklijke Philips NV; Consultant, AMRA AB; Consultant, Fulcrum; Consultant, IBM Corporation; Consultant, Exact Sciences Corporation; Consultant, Boehringer Ingelheim GmbH; Consultant, Arterys Inc; Consultant, Epigenomics; Author, Medscape, LLC; Lab service agreement, Gilead Sciences, Inc; Lab service agreement, ICON plc; Lab service agreement, Intercept Pharmaceuticals, Inc; Lab service agreement, Shire plc; Lab service agreement, Enanta; Lab service agreement, Takeda Pharmaceutical Company Limited; Lab service agreement, Alexion Pharmaceuticals, Inc; Lab service agreement, NuSirt Biopharma, Inc

Jin Wang, MD, Guangzhou, China (Abstract Co-Author) Nothing to Disclose

PURPOSE

To investigate whether a combination of LI-RADS v2018 MR features, non-LI-RADS MR features, and AFP can pre-operatively predict microvascular invasion (MVI) in primary liver cancers.

METHOD AND MATERIALS

This retrospective single-center study was approved by our institutional review board with waived informed consent requirement. Between 2014 and 2018, 188 patients had pre-operative MRI within 1 month before hepatectomy for surgically confirmed primary liver cancers. LI-RADS and non-LI-RADS (non-smooth tumor margin, two-trait predictor, and peritumoral enhancement) MR features were retrospectively assessed by two radiologists in consensus. In patients with multifocal tumors, only the largest tumor was evaluated. LI-RADS v2018 categories were assigned based on major features. MVI was assessed by a liver pathologist on resected tumor specimens. Pre-operative AFP was recorded. Univariate and multivariate analyses were used to assess MVI predictors. Sensitivity, specificity, accuracy, positive predictive value (PPV), and negative predictive value (NPV) of a multivariate prediction model were estimated.

RESULTS

173 (92.0%) patients had hepatocellular carcinoma, 11 (5.9%) had intrahepatic cholangiocarcinoma, and 4 (2.1%) had combined hepatocellular and cholangiocarcinoma. MVI was present in 85/188 (45%) patients. Pre-operative LI-RADS categories of LR-3, LR-4, LR-5 and LR-M were assigned in 5 (2.7%), 9 (4.8%), 154 (81.9%), and 20 (10.6%) patients, respectively. LR-M (OR: 5.258, P=0.005), mosaic architecture (OR: 3.159, P=0.002), and non-smooth tumor margin (OR: 2.410, P=0.009) were independent predictors of MVI (Table 1, Figure 1). The sensitivity, specificity, accuracy, PPV, and NPV of the prediction model were 5.9%, 98.1%, 56.4%, 71.4%, and 55.8%, respectively.

CONCLUSION

This single-center, retrospective study indicated combining LR-M, mosaic architecture, and non-smooth tumor margin can predict MVI with high specificity. Multi-centric, prospective studies are needed to confirm the accuracy of the model for predicting MVI in primary liver cancers.

CLINICAL RELEVANCE/APPLICATION

This retrospective single-center study showed the potential value of combining LI-RADS v2018 and non-LI-RADS MR features in predicting MVI in primary liver cancers. Further studies are warranted.

SSK07-03 Differentiating New Hepatic Metastases from Focal Hepatopathy in Patients during Treatment for Malignancy

Wednesday, Dec. 4 10:50AM - 11:00AM Room: S501ABC

Participants

Steffen Haider, MD, New York, NY (*Presenter*) Nothing to Disclose Lyndon Luk, MD, New York, NY (*Abstract Co-Author*) Nothing to Disclose Benjamin Navot, MD, New York, NY (*Abstract Co-Author*) Nothing to Disclose Firas S. Ahmed, MBChB, MPH, New York, NY (*Abstract Co-Author*) Nothing to Disclose Simona De Michele, MD, New York, NY (*Abstract Co-Author*) Nothing to Disclose Jonathan Susman, MD, Englewood, NJ (*Abstract Co-Author*) Research Consultant, BioSphere Medical, Inc Elizabeth M. Hecht, MD, New York, NY (*Abstract Co-Author*) Nothing to Disclose

For information about this presentation, contact:

sth9053@nyp.org

PURPOSE

To differentiate between liver metastases versus benign focal hepatopathy (FH) that develops over the course of medical or surgical treatment of malignancy.

METHOD AND MATERIALS

Between 2010 and 2018, there were 1179 consecutive biopsies (1069 patients) of hepatic lesions suspicious for malignancy. 924 were True Pos, 169 True Neg (TN), 43 False Neg and 43 lost to follow up. Among the TN were 22 FHs defined as new lesions following oncologic treatment and histologically as steatosis, sinusoidal and biliary congestion/obstruction or inflammation. Cirrhotic patients, primary hepatic tumors and abscesses were excluded. Patients with FH and metastases were matched for age, malignancy-type and treatment regimen. 3 abdominal radiologists (1, 1, 3 y post-fellowship) blinded to pathology reviewed pre-biopsy MR (40 malignant: 13 FH) and CT (53: 12); 3 FH pts had both MRI and CT. A 5-point Likert scale (1: definitely benign, 5: definitely malignant) and imaging characteristics were assessed. A training data set for readers was provided to introduce a common lexicon. Univariate analyses (Chi-Sq, T-test), logistic regression and inter-rater reliability (kappa, spearman, ICC) were performed.

RESULTS

Characteristics of patients with FHs included: pancreatobiliary malignancies (68%), hepatobiliary/GI surgery or stent (77%) and chemotherapy within 1y prior to biopsy (50%). Results for MR: Likert 2.3-2.5 for FH vs 3.6-4.4 for metastases (p<.05, correlation=.49). Compared to FH, metastases were associated with multiplicity (>3 lesion/liver), larger size, arterial rimenhancement, portal venous rim-enhancement/central hypoenhancement and restricted diffusion (P< 0.05, all readers, univariate, k=.48-.81 except arterial rim k=0.22, ICC=.91). Lesion multiplicity was associated with metastasis on multivariate analysis. For CT: Likert 2.3-4.0 for FH vs 3.8-4.9 for metastases (p<.05, correlation .47-.58). Only non-spherical shape was associated with FH (p<.05, all readers, k=.33-.89 except arterial rim .08-.22, ICC .97-.99).

CONCLUSION

Multiplicity, size, enhancement and diffusion characteristics may be helpful to distinguish FH from metastases on MR whereas only non-spherical shape was helpful on CT.

CLINICAL RELEVANCE/APPLICATION

Identification of FH could increase confidence in radiologic-pathologic correlation and limit biopsies following the medical-surgical treatment of malignancy. MRI may be more helpful than CT in distinguishing FH from metastases.

SSK07-04 Does Volumetric Functional MRI Improve Fudan Clinical Prognostic Scoring System for Unresectable Intrahepatic Cholangiocarcinoma Treated with Systemic Chemotherapy?

Wednesday, Dec. 4 11:00AM - 11:10AM Room: S501ABC

Participants

Ankur Pandey, MD, Baltimore, MD (*Presenter*) Nothing to Disclose Mohammadreza Shaghaghi, MD, Baltimore, MD (*Abstract Co-Author*) Nothing to Disclose Pallavi Pandey, MD, Baltimore, MD (*Abstract Co-Author*) Nothing to Disclose Mounes Aliyari Ghasabeh, MD, Baltimore, MD (*Abstract Co-Author*) Nothing to Disclose Bita Hazhirkarzar, MD, Baltimore, MD (*Abstract Co-Author*) Nothing to Disclose Roya Rezvani Habibabadi, Baltimore, MD (*Abstract Co-Author*) Nothing to Disclose Maryam Ghadimi, MD, Baltimore, MD (*Abstract Co-Author*) Nothing to Disclose Sanaz Ameli, MD, Baltimore, MD (*Abstract Co-Author*) Nothing to Disclose Pegah Khoshpouri, MD, Baltimore, MD (*Abstract Co-Author*) Nothing to Disclose Ihab R. Kamel, MD, PhD, Baltimore, MD (*Abstract Co-Author*) Research Grant, Siemens AG

For information about this presentation, contact:

apandey9@jhmi.edu

PURPOSE

To assess the incremental value of volumetric functional MRI-derived parameters over Fudan clinical prognostic scoring system in patients with intrahepatic cholangiocarcinoma (ICCA) treated with systemic chemotherapy.

METHOD AND MATERIALS

This retrospective, HIPAA compliant and IRB approved study included 68 patients with unresectable ICCA (age, 65 ± 14 yrs; 27 men [40%]). Patients underwent systemic chemotherapy after baseline MRI (including contrast-enhanced and DWI with ADC mapping). Single largest tumor was assessed by a single experienced abdominal radiologist for anatomic and functional (viable tumor volume, percentage viable tumor volume [100 × viable tumor volume/whole tumor volume], viable tumor burden [100 × viable tumor volume, volume/whole liver volume], and ADC) parameters. Cox regression was used to identify the strongest functional predictor of overall survival. Prognostic scores were calculated for each patient using the established Fudan score (utilizing serum alkaline phosphatase level, carbohydrate antigen 19-9 level, tumor margin type, tumor size, and number of intrahepatic tumors), as well as modified Fudan score (with functional MRI parameter replacing subjective tumor margin). The performance of both the scores was measured by C-index and assessed by comparing Kaplan-Meier survival estimates in different risk groups. Predictive accuracy of both scoring systems was compared. P<0.05 was considered significant.

RESULTS

Among the volumetric functional MRI parameters, ADC (>1350x10-6mm2/s vs. <=1350) showed the strongest association with overall survival (HR, 6.0; 95% CI, 3.0-11.9; P<0.001). Both Fudan and modified Fudan score (replacing the tumor margin [subjective] with ADC [quantitative]) provided prognostic prediction with differences in OS among intermediate vs. high vs. very high-risk groups (Fudan, P=.04; modified Fudan, P=0.001). C-index of the modified Fudan score for predicting survival was 0.82 (95% CI, 0.74-0.90), higher (P=0.006) than the C-index of the original Fudan score (0.67[95% CI, 0.55-0.79]).

CONCLUSION

Supplementing Fudan model with ADC provided more accurate prognosis for ICCA patients undergoing systemic chemotherapy, improving the survival prediction performance by 15%.

CLINICAL RELEVANCE/APPLICATION

Volumetric MRI can increase accuracy of the only available prognostic scoring system for ICCA treated with systemic chemotherapy by replacing the highly subjective tumor margin with more objective ADC.

SSK07-05 Diagnostic Performance of the Liver Imaging Reporting and Data System Version 2018 for Intrahepatic Cholangiocarcinoma

Wednesday, Dec. 4 11:10AM - 11:20AM Room: S501ABC

Participants

Xianlun Zou, MD, Wuhan, China (*Presenter*) Nothing to Disclose Yaqi Shen, PhD, MD, Wuhan, China (*Abstract Co-Author*) Nothing to Disclose Zhen Li, MD, PhD, Wuhan, China (*Abstract Co-Author*) Nothing to Disclose

Daoyu Hu, Wuhan, China (Abstract Co-Author) Nothing to Disclose

For information about this presentation, contact:

zouxianlun2010@163.com

PURPOSE

To evaluate the diagnostic performance of the Liver Imaging Reporting and Data System version 2018 (LI-RADS v2018) for Intrahepatic Cholangiocarcinoma (ICC).

METHOD AND MATERIALS

A total of 78 primary liver cancer with either ICC (n = 39) or hepatocellular carcinoma (HCC) (n = 39) were retrospectively reviewed. ICCs and HCCs were one-to-one matched according to age, tumor size and background disease of liver. All the patients were at high risk for HCC according to LI-RADS v2018 and performed manetic resonance imaging (MRI) examination before surgery or biopsy. The MRI protocols included routine MRI sequences, diffusion-weighted imaging (DWI) and dynamic imaging. Two readers blinded to pathology findings independently evaluated the MR images for each lesion and assigned LI-RADS categories, scoring major and ancillary features according to LI-RADS v2018. Interobserver agreements of LI-RADS category assignment and the diagnostic performance of LI-RADS v2018 in categorizing ICC were analyzed.

RESULTS

The LI-RADS categories of the 39 IMCCs by reviewer 1 include LR-4 (n=5), LR-TIV(HCC) (n=3), LR-M (n=27) and LR-TIV(M) (n=4). In the HCC group, the LI-RADS categories by reviewer 1 include LR-4 (n=7), LR-5 (n=28), LR-TIV(HCC) (n=1) and LR-M (n=3). In the results of reviewer 2, the LI-RADS categories of ICC include LR-4 (n=4), LR-TIV(HCC) (n=2), LR-M (n=26) and LR-TIV(M) (n=7); the LI-RADS categories of HCC include LR-4 (n=3), LR-5 (n=30), LR-TIV(HCC) (n=2) and LR-M (n=4). Interobserver agreements of LI-RADS category assignment were excellent (Kappa= 0.815;95% CI:0.711-0.919;P<0.001). Regarding LR-M and LR-TIV(M) categories as positive, LR-4, LR-5 and LR-TIV(HCC) as negative, the sensitivity, specificity and accuracy of LI-RADS v2018 in categorizing ICC as LR-M or LR-TIV(M) were 79.5%, 92.3%, 85.9% (reviewer 1) and 84.6%, 89.7%, 87.2% (reviewer 2) respectively.

CONCLUSION

LI-RADS v2018 performs high sensitivity, specificity and accuracy in categorizing ICC as LR-M or LR-TIV(M). However, a small part of ICC and HCC may present atypical imaging features, resulting in wrong LI-RADS categories.

CLINICAL RELEVANCE/APPLICATION

LI-RADS v2018 performs high sensitivity, specificity and accuracy in categorizing ICC as LR-M or LR-TIV(M). However, a small part of ICC and HCC may present atypical imaging features, resulting in wrong LI-RADS categories.

SSK07-06 Gd-EOB MRI for Subtype Differentiation of Hepatocellular Adenomas

Wednesday, Dec. 4 11:20AM - 11:30AM Room: S501ABC

Participants

Timo A. Auer, MD, Berlin, Germany (Presenter) Nothing to Disclose

Uli Fehrenbach, Berlin, Germany (Abstract Co-Author) Nothing to Disclose

Christian Grieser, MD, Bremen, Germany (Abstract Co-Author) Nothing to Disclose

Tobias Penzkofer, MD, Berlin, Germany (Abstract Co-Author) Researcher, AGO; Researcher, Aprea AB; Researcher, Astellas Group; Researcher, AstraZeneca PLC; Researcher, Celgene Corporation; Researcher, Genmab A/S; Researcher, Incyte Coporation; Researcher, Lion Biotechnologies, Inc; Researcher, Takeda Pharmaceutical Company Limited; Researcher, Morphotec Inc;

Researcher, Merck & Co, Inc; Researcher, Tesaro Inc; Researcher, F. Hoffmann-La Roche Ltd;

Bernd K. Hamm III, MD, Berlin, Germany (Abstract Co-Author) Research Consultant, Canon Medical Systems Corporation; Stockholder, Siemens AG; Stockholder, General Electric Company; Research Grant, Canon Medical Systems Corporation; Research Grant, Koninklijke Philips NV; Research Grant, Siemens AG; Research Grant, General Electric Company; Research Grant, Elbit Imaging Ltd; Research Grant, Bayer AG; Research Grant, Guerbet SA; Research Grant, Bracco Group; Research Grant, B. Braun Melsungen AG; Research Grant, KRAUTH Medical KG; Research Grant, Boston Scientific Corporation; Equipment support, Elbit Imaging Ltd; Investigator, CMC Contrast AB

Timm Denecke, MD, Berlin, Germany (Abstract Co-Author) Speaker, Bayer AG Travel support, Bayer AG

For information about this presentation, contact:

timo-alexander.auer@charite.de

PURPOSE

Evaluate MRI Gd-EOB enhancement characteristics to differentiate between subtypes of hepatocellular adenomas (HCA).

METHOD AND MATERIALS

48 patients with 79 histopathologically proven HCA who underwent gadoxetic acid-enhanced MRI were enrolled (standard of reference: surgical resection). Quantitative (lesion to liver enhancement) measurements and gualitative imaging features were evaluated by two blinded radiologists. Inter-reader variability was tested. Additionally, voxel heterogeneity was evaluated using texture analysis (pyradiomics).

RESULTS

Overall, 24%(19/79) HHCA, 47%(37) IHCA, 6.5%(5) bHCA and 22.5%(18) UHCA were anayzed. In the hepatobiliary phase (hbp) 87.5%(69/79) of all adenomas were rated as hypo- to isointense. 66%(52/79) showed a heterogeneous Gd-EOB-uptake. 100% of all IHCA and 80% of all bHCA were rated with a heterogenous uptake of at least 0-25%(p<0.05) (HHCA: 26%(5/19); UHCA: 33% (6/18); p>0.05), while 63%(24/37) of all IHCA showed a heterogeneous uptake of at least 50% or more (p<0.001). Quantitative ROI based analyses showed no significant difference between the subtypes (p>0.05). Volume-based analyses showed a significant increased voxel heterogeneity for IHCA /variance of mean SI: 6465.48; p=0.038) when divided into IHCA and other (vs. 2681.8).

CONCLUSION

Gd-EOB MRI imaging has an additional value for subtype differentiation of HCA, the typical heterogeneous hbp-uptake IHCA can be identified reliably. Furthermore, when combing typical morphologic MR-appearances of the other HCA-subtypes and their Gd-EOB behavior sensitivity increases significantly.

CLINICAL RELEVANCE/APPLICATION

Potential of a noninvasive MRI subtype differentation of HCA to avoid unnessecary surgical resection and/or intervention and to provide evidence in terms of guidelines for benign liver lesions.

SSK07-07 MDCT Imaging Feature Related with Histopathologic Growth Pattern to Predict Response of Bevacizumab-Based Chemotherapy in Patients with Colorectal Liver Metastases

Wednesday, Dec. 4 11:30AM - 11:40AM Room: S501ABC

Participants

Jin Cheng, MD, Beijing, China (*Abstract Co-Author*) Nothing to Disclose Fan Chai, Beijing, China (*Presenter*) Nothing to Disclose Yinli Zhang, Beijing, China (*Abstract Co-Author*) Nothing to Disclose Nan Hong, MD, Beijing, China (*Abstract Co-Author*) Nothing to Disclose Danhua Shen, Beijing, China (*Abstract Co-Author*) Nothing to Disclose Jing Zhou, Beijing, China (*Abstract Co-Author*) Nothing to Disclose Yingjiang Ye, Beijing, China (*Abstract Co-Author*) Nothing to Disclose Yingjiang Ye, Beijing, China (*Abstract Co-Author*) Nothing to Disclose Yi Wang, MD, Beijing, China (*Abstract Co-Author*) Nothing to Disclose

For information about this presentation, contact:

chengjin@pkuph.edu.cn

PURPOSE

To investigate the performance of MDCT imaging features related with histopathological growth patterns (HGPs) in predicting response of Bevacizumab-based chemotherapy and the 1-year progression free survival (PFS) in patients with of colorectal liver metastases (CRLMs).

METHOD AND MATERIALS

The study was designed as a two-step protocol. In the first-step, between January 2007 and December 2018, patients who had chemo-naïve resected CRLMs and preoperative MDCT were included. HGPs of each resected CRLMs were retrospectively reviewed. Multivariate logistic regression based on clinical, pathological and MDCT imaging factors were used to construct a model in predicting HGPs. The second step included patients who had unresectable CRLMs and were treated with the Bevacizumab-based chemotherapy between January 2012 and January 2018. The factors related with HGPs were used to build a model to predict the objective response rate (ORR) and the 1-year PFS by multivariate analyses.

RESULTS

A total of 95 resected CRLMs with desmoplastic (n=52) and replacement (n=43) HGP lesions were assessed in the first-step study. The enhanced rim on portal venous phase (PVP) was identified as the only independent predictor in distinguishing the desmoplastic HGP with the AUC of 0.761(95%CI: 0.661-0.860, P<0.001). In the second-step study, 50 CRLM patients with Bevacizumab-based chemotherapy were included. The enhanced rim on PVP was identified as the only independent significant predictor of ORR and 1-year PFS by using the multivariable analyses.

CONCLUSION

The enhanced rim on PVP of the baseline MDCT images, which related with the desmoplastic HGP of CRLM, was identified as the independent prognostic predictor of good outcome for CRLM patients with Bevacizumab-based chemotherapy.

CLINICAL RELEVANCE/APPLICATION

The HGP of CRLMs is capable of predicting response to Bevacizumab treatment and long-term survival. However, the diagnosis of HGP could only be made via histopathological analysis and the clinical application is restricted. In this present study, the baseline MDCT imaging feature of enhanced rim on portal venous phase, related with the desmoplastic HGP, was identified as the independent prognostic predictor of good outcome for CRLM patients with Bevacizumab-based chemotherapy. This imaging feature could be a potential biomarker in patient selection of target agent treatment, as well as the outcome predicting in patient with CRLMs.

SSK07-08 Prediction of Histopathologic Growth Patterns of Colorectal Liver Metastases with a Noninvasive Imaging Method

Wednesday, Dec. 4 11:40AM - 11:50AM Room: S501ABC

Participants

Jin Cheng, MD, Beijing, China (*Presenter*) Nothing to Disclose Jingwei Wei, Beijing, China (*Abstract Co-Author*) Nothing to Disclose Yinli Zhang, Beijing, China (*Abstract Co-Author*) Nothing to Disclose Yuqi Han, Beijing, China (*Abstract Co-Author*) Nothing to Disclose Dongsheng Gu, Beijing, China (*Abstract Co-Author*) Nothing to Disclose Gongwei Wang, Beijing, China (*Abstract Co-Author*) Nothing to Disclose Nan Hong, MD, Beijing, China (*Abstract Co-Author*) Nothing to Disclose Yingjiang Ye, Beijing, China (*Abstract Co-Author*) Nothing to Disclose Jie Tian, PhD, Beijing, China (*Abstract Co-Author*) Nothing to Disclose Yi Wang, MD, Beijing, China (*Abstract Co-Author*) Nothing to Disclose

For information about this presentation, contact:

chengjin@pkuph.edu.cn

PURPOSE

This study was to predict histopathologic growth patterns (HGPs) in colorectal liver metastases (CRLMs) with radiomics model.

METHOD AND MATERIALS

Patients with chemotherapy-naive CRLMs who underwent abdominal contrast-enhanced MDCT followed by partial hepatectomy between January 2007 and January 2018 were included in this retrospective study. Hematoxylin- and eosin-stained histopathologic sections of CRLMs were reviewed, with HGPs defined according to international consensus. Lesions were divided into training and validation datasets based on date of treatment. Radiomic features were extracted from pre- and post- contrast (arterial and portal venous) phase MDCT images, with review focusing on the segmented tumor-liver interface (TLI) zones of CRLMs. Minimum redundancy maximum relevance (MRMR) and decision tree (DT) methods were used for radiomics modeling. Multivariable logistic regression analyses and ROC curves were used to assess the predictive performance of these models in predicting HGP types.

RESULTS

A total of 82 CRLMs with histopathologic-demonstrated desmoplastic (n = 54) or replacement (n = 28) HGPs were assessed. The radiomics signature consisted of 20 features of each phase selected. The fused arterial and portal venous phase radiomics signature demonstrated the best predictive performance in distinguishing between replacement and desmoplastic HGPs (AUCs of 0.962 and 0.870 in the training and validation cohorts, respectively). The radiomics model showed good discrimination (C-indices of 0.974 and 0.765 in the training and validation cohorts, respectively).

CONCLUSION

A radiomics model derived from MDCT images may effectively predict the HGP of CRLMs, thus providing a basis for prognostic stratification and therapeutic decision-making.

CLINICAL RELEVANCE/APPLICATION

1. Radiomics model derived from MDCT images may effectively predict the HGP of CRLMs.2. Radiomics can supplement radiologists' visual interpretation in morphologically similar tumors.

SSK07-09 Evaluation of Pre and Post-Treatment LI-RADS Categories as Predictors of Overall Survival in HCC Patients Undergoing Transarterial Embolization

Wednesday, Dec. 4 11:50AM - 12:00PM Room: S501ABC

Participants

William Ormiston, MBChB, Auckland, New Zealand (*Presenter*) Nothing to Disclose
Hooman Yarmohammadi, MD, New York, NY (*Abstract Co-Author*) Grant, Guerbet SA
Stephanie Lobaugh, New York, NY (*Abstract Co-Author*) Nothing to Disclose
Juliana B. Schilsky, MS, New York, NY (*Abstract Co-Author*) Nothing to Disclose
Seth S. Katz, MD, PhD, New York, NY (*Abstract Co-Author*) Nothing to Disclose
Maria D. Lagratta, MD, Rumson, NJ (*Abstract Co-Author*) Nothing to Disclose
Sara Velayati, New York, NY (*Abstract Co-Author*) Nothing to Disclose
Junting Zheng, New York, NY (*Abstract Co-Author*) Nothing to Disclose
Marinela Capanu, New York, NY (*Abstract Co-Author*) Nothing to Disclose
Richard Kinh Gian Do, MD, PhD, New York, NY (*Abstract Co-Author*) Nothing to Disclose
Richard Kluwer nv; Spouse, Data Monitoring Committee, Alk Abello

For information about this presentation, contact:

ormistonw@gmail.com

PURPOSE

LI-RADS treatment response (LR-TR) algorithm has recently been proposed for the assessment of HCC response to locoregional therapy. The aim of our study was to evaluate associations between pretreatment (preTx) and posttreatment (postTx) LR-TR categories with overall survival (OS) in patients with HCC after transarterial embolization (TAE).

METHOD AND MATERIALS

In this IRB approved retrospective single center study, consecutive patients between December 2003 and December 2017 were included if they had 1 or 2 lesions and underwent TAE +/- ablation, with no prior therapy nor subsequent liver transplantation. Two radiologists (R1 and R2) reviewed preTx and postTx imaging to assign preTx LI-RADS diagnostic and postTx LR-TR categories, with agreement measured by kappa statistics. Associations with OS were examined on preTx and postTx variables, including tumor size, preTx LR categories and LR-TR categories (Viable, Equivocal, Nonviable) using Kaplan-Meier method and Cox proportional hazard regression.

RESULTS

88 patients (median 71 yo, 71 M, 17 F) were included, the majority having a single lesion (n=79, 83.2%) and either A or B BCLC stage (n=56, 63.6%). Median OS from first embolization was 35.5 months (95%CI: 26.4 - 50.2). For both readers, preTx tumor size (Hazard ratio (HR) R1 1.099 (95% CI: 1.030-1.172), R2 1.083 (95% CI: 1.016-1.154)) and LR-TIV vs LR-5 (HR R1 3.511 (95% CI: 1.617-7.625), R2 2.174 (95% CI: 1.010-4.682)) were associated with OS (p<0.05). PostTx tumor size (HR R1 1.158 (95% CI: 1.079-1.243), R2 1.135 (95% CI: 1.054-1.223)) and LR-TR Viable vs Nonviable category (HR R1 3.181 (95% CI: 1.766-5.728), R2 2.701 (95% CI: 1.498-4.872)) were associated with OS (p<0.05). Median OS for LR-TR Viable patients were 22.91 (R1, 95% CI: 17.85-31.96) and 25.64 months (R2, 95% CI: 18.58-35.70), compared to 64.21 months (R1 and R2, 95% CI: 42.71-92.45 and 36.30-94.09, respectively) for Nonviable patients. Interreader agreements were moderate for preTx LR categories (k=0.567 95% CI: 0.359-0.775) and substantial for postTx LR-TR categories (0.691 95% CI: 0.568-0.815).

CONCLUSION

Both preTx LI-RADS categories and postTx LR-TR categories were associated with OS in HCC patients following TAE.

CLINICAL RELEVANCE/APPLICATION

 LI-RADS treatment response categories show potential as a surrogate endpoint for overall survival in HCC patients treated by transarterial embolization. Further validation is needed in larger multi-center studies.

Printed on: 10/29/20





SSK08

Gastrointestinal (Dual-energy CT)

Wednesday, Dec. 4 10:30AM - 12:00PM Room: S502AB



AMA PRA Category 1 Credits ™: 1.50 ARRT Category A+ Credit: 1.75

Participants

Avinash R. Kambadakone, MD, Boston, MA (*Moderator*) Research Grant, General Electric Company; Research Grant, Koninklijke Philips NV

Lakshmi Ananthakrishnan, MD, Irving, TX (*Moderator*) Nothing to Disclose Mark D. Kovacs, MD, Charleston, SC (*Moderator*) Nothing to Disclose

Sub-Events

SSK08-01 Extracellular Volume Quantification of Liver Using Dual-Energy CT: Utility for Prediction of Liver-Related Events in Cirrhosis

Wednesday, Dec. 4 10:30AM - 10:40AM Room: S502AB

Participants

Seong Jun Bak, MD, Jinju, Korea, Republic Of (*Presenter*) Nothing to Disclose Ji Eun Kim, MD,PhD, Jinju, Korea, Republic Of (*Abstract Co-Author*) Nothing to Disclose Kyungsoo Bae, MD, Changwon, Korea, Republic Of (*Abstract Co-Author*) Nothing to Disclose Jae Min Cho, MD, Jinju, Korea, Republic Of (*Abstract Co-Author*) Nothing to Disclose Hyun Ok Kim, Jinju, Korea, Republic Of (*Abstract Co-Author*) Nothing to Disclose

For information about this presentation, contact:

wldmsrla80@hanmail.net

PURPOSE

To determine whether quantification of liver extracellular volume fraction (fECV) using dual-energy CT allows prediction of liverrelated events (LRE) in patients with cirrhosis.

METHOD AND MATERIALS

This retrospective study included 305 patients with cirrhosis who underwent dual source dual-energy liver CT and had serum markers within 2 weeks of initial CT imaging. The fECV score was measured using iodine map of equilibrium phase images obtained 3 minutes after contrast injection at 100 kVp and Sn140 kVp. Association of fECV score and serum markers with LRE was investigated. A risk model combining fECV score (<27 versus = or >27%) and albumin level (<4 versus = or >4 g/dL) was constructed for predicting LRE.

RESULTS

Increased fECV score (odds ratio, 1.27; 95% confidence interval (CI), 1.15, 1.40) was independently associated with decompensated cirrhosis at baseline (n = 85) along with Model for End Stage Liver Disease score (odds ratio, 1.32; 95% CI, 1.07, 1.63). In patients with compensated cirrhosis, 10.5% (23 of 220) experienced LRE during a median follow-up period of 2.0 years (decompensation, n = 14; hepatocellular carcinoma, n = 9). fECV score (hazard ratio, 1.40; 95% CI, 1.22, 1.62) and albumin level (hazard ratio, 0.26; 95% CI, 0.09, 0.73) were independently predictive of LRE. Mean times to LRE in patients at high (16.5 months, n = 18), intermediate (25.6 months, n = 44), and low (30.5 months, n = 158) risk of LRE were significantly different (p < 0.0001).

CONCLUSION

The fECV score derived from dual-energy CT images allows prediction of LRE in patients with cirrhosis.

CLINICAL RELEVANCE/APPLICATION

The fECV score derived from iodine map of dual-energy CT can predict hepatic decompensation or hepatocellular carcinoma in cirrhotic patients. Dual-energy scanning is recommended as a part of liver CT during the follow-up of cirrhotic patients.

SSK08-02 Assessment of Peritoneal Carcinomatosis Using Iodine Overlays from Spectral Detector Computed Tomography

Wednesday, Dec. 4 10:40AM - 10:50AM Room: S502AB

Participants

Simon Lennartz, MD, Cologne, Germany (*Presenter*) Institutional Research Grant, Koninklijke Philips NV Karin Slebocki, Cologne, Germany (*Abstract Co-Author*) Nothing to Disclose David Zopfs, MD, Cologne, Germany (*Abstract Co-Author*) Nothing to Disclose Nuran Abdullayev, MD, Cologne, Germany (*Abstract Co-Author*) Nothing to Disclose Markus le Blanc, Cologne, Germany (*Abstract Co-Author*) Nothing to Disclose Christian Wybranski, MD, Magdeburg, Germany (*Abstract Co-Author*) Nothing to Disclose Anton Wagner, MD, Cologne, Germany (*Abstract Co-Author*) Nothing to Disclose For information about this presentation, contact:

Simon.Lennartz@uk-koeln.de

PURPOSE

Peritoneal carcinomatosis (PC) is a prognostically relevant metastatic condition which can be difficult to differentiate from postoperative peritoneal alterations, particularly in early stages. The purpose of this study was to determine whether PC could be distinguished more accurately from benign peritoneal alterations when using spectral detector CT (SDCT)-derived iodine overlays (IO) in addition to conventional images (CI) compared to CI only.

METHOD AND MATERIALS

60 oncologic patients, 30 with PC confirmed by histopathology and 30 with non-malignant peritoneal alterations confirmed by follow-up or PET-CT who received clinically indicated portal-venous phase SDCT scans of the abdomen were retrospectively included. Two experienced and two less experienced radiologists blinded towards patient group and clinical information evaluated presence of PC for each patient and rated conspicuity and diagnostic certainty for up to 5 individual lesions per patient using 5-point Likert scales. Patients were randomized and the subjective assessment was conducted in a session that comprised solely conventional images and a second one which additionally included color-coded iodine overlay images between which a latency period of 6 weeks was administered to minimize recognition bias.

RESULTS

In less experienced readers, IO led to an increased sensitivity / specificity (CI: 0.78 / 0.83 vs. CI+IO: 0.82 / 0.88) for PC. Experienced radiologists showed a higher specificity when employing IO as well, which was however accompanied with a lower sensitivity (Sensitivity / Specificity: CI: 0.92 / 0.80 vs. CI+IO: 0.73 / 0.82). In the subgroup of patients with history of abdominal surgery, the rise in specificity averaged over all readers was even higher (CI: 0.78 vs. CI+IO: 0.91). Median Likert scores for lesion conspicuity were significantly higher for the combination of CI and IO (4 (3-5)) compared to CI only (3 (3-4); p<=0.05) while diagnostic certainty was comparable (4 (3-5)).

CONCLUSION

Iodine overlays are instrumental in distinguishing benign from metastatic peritoneal lesions, particularly in patients who underwent abdominal tumor surgery and for less experienced radiologists.

CLINICAL RELEVANCE/APPLICATION

Iodine overlays should be employed as a supplement rather than a surrogate for CI and the additional information on iodine uptake should not outweigh conventional image features suggestive for PC as this might result in lower overall sensitivity.

SSK08-03 The Utility of a Dual-Energy CT Protocol for Acute GI Bleeding (AGIB) in Patients with Recent Overt GI Bleeding

Wednesday, Dec. 4 10:50AM - 11:00AM Room: S502AB

Participants

Payam Mohammadinejad, MD, Rochester, MN (*Presenter*) Nothing to Disclose Lukasz Kwapisz, Rochester, MN (*Abstract Co-Author*) Nothing to Disclose Ashish R. Khandelwal, MD, Rochester, MN (*Abstract Co-Author*) Nothing to Disclose Michael L. Wells, MD, Rochester, MN (*Abstract Co-Author*) Nothing to Disclose Adam Froemming, MD, Rochester, MN (*Abstract Co-Author*) Nothing to Disclose Jeff L. Fidler, MD, Rochester, MN (*Abstract Co-Author*) Nothing to Disclose Jay P. Heiken, MD, Rochester, MN (*Abstract Co-Author*) Nothing to Disclose Jay P. Heiken, MD, Rochester, MN (*Abstract Co-Author*) Nothing to Disclose David Bruining, MD, Rochester, MN (*Abstract Co-Author*) Nothing to Disclose David Bruining, MD, Rochester, MN (*Abstract Co-Author*) Nothing to Disclose David Bruining, MD, Rochester, MN (*Abstract Co-Author*) Research Grant, Given Imaging Ltd Consultant, Bracco Group Stephanie Hansel, MD, Rochester, MN (*Abstract Co-Author*) Research support, Medtronic plc Yong Lee, Rochester, MN (*Abstract Co-Author*) Employee, Siemens AG Cynthia H. McCollough, PhD, Rochester, MN (*Abstract Co-Author*) Research Grant, Siemens AG Joel G. Fletcher, MD, Rochester, MN (*Abstract Co-Author*) Rate, Siemens AG; Consultant, Medtronic plc; Consultant, Takeda Pharmaceutical Company Limited; Grant, Takeda Pharmaceutical Company Limited; ;

For information about this presentation, contact:

fletcher.joel@mayo.edu

PURPOSE

To examine the benefit and utility of a two-phase, dual-energy (DE) CT protocol for acute GI bleeding protocol (DE-AGIB-CT) in recent overt GI bleeding.

METHOD AND MATERIALS

Consecutive patients underwent clinically-indicated two-phase DE-AGIB-CT (arterial and portal phases). A gastroenterologist reviewed all clinical information during hospitalization (endoscopy, angio, surgery) to create the reference standard. The clinical radiologist report was used to determine site and presence of active extravasation or other findings (e.g., varices, tumor) causing GI bleeding. After reconciliation, performance of DE-AGIB-CT was estimated. To ascertain the contribution of portal phase and DE images, 3 GI radiologists evaluated all patients with active bleeding, and an equal number of negative exams chosen randomly. Radiologists rated confidence in site and imaging evidence of GI bleeding using only mixed kV arterial images, then with mixed kV portal phase images, and then with dual energy images (50 keV, iodine maps, VNC).

176 patients underwent DE-AGIB-CT for the evaluation of suspected acute GI bleeding. Reference standard identified a cause for active GI bleeding in 56 patients (31.8%). 31 DE-AGIB-CT exams were positive for active extravasation (29% colon, 26% jejunum/ ileum, 26% stomach, 19% other). The sensitivity, specificity, positive and negative predictive values of DE-AGIM for correct identification of imaging evidence of GI bleeding was 61% (95%CI:46%-74%), 91% (84%-95%), 74% (58%-86%), and 85% (78%-90%). Sensitivity of active extravasation for cause of AGIB is 30 % (18.37%-43.78%). Out of 31 cases with active contrast material extravasation, in 10 cases (33%), 2/3 radiologists increased confidence in presence of active bleeding by >= 10% by evaluating portal phase images in addition to mixed kV CTA images. Dual energy reconstructions did not increase confidence in any cases.

CONCLUSION

The sensitivity of a dedicated protocol for GI bleeding was less than previously reported, even when imaging criteria were extended beyond luminal extravasation to include identification of causes of GI bleeding. Portal phase imaging increased confidence for GI bleeding.

CLINICAL RELEVANCE/APPLICATION

Physicians should take into consideration the possibility of limited sensitivity of CTA when they rely on this modality in the diagnosis and triaging of patients with acute GI bleeding. Portal phase images improve reader confidence.

SSK08-04 Can Dual-Energy CT Replace Perfusion CT in Monitoring Tumor Therapeutic Response and Predicting Outcomes in Rabbit VX2 Liver Tumors?

Wednesday, Dec. 4 11:00AM - 11:10AM Room: S502AB

Participants

Peijie Lyu, MD, Zhengzhou, China (*Presenter*) Nothing to Disclose Yan Chen, Zhengzhou, China (*Abstract Co-Author*) Nothing to Disclose Jianbo Gao, MD, Zhengzhou, China (*Abstract Co-Author*) Nothing to Disclose

For information about this presentation, contact:

lvpeijie2@163.com

PURPOSE

To investigate whether dual-energy CT (DECT) can replace perfusion CT (PCT) for monitoring and predicting tumor response to antiangiogenic treatment in rabbit VX2 liver tumors.

METHOD AND MATERIALS

In 54 VX2 liver tumor-bearing rabbits, a optimal contrast-enhanced DECT protocol during the arterial phase (AP) and portal phase (PP) was used to reconstruct images from PCT data obtained from the same scan based on time-attenuation curves. The rabbits were randomized into the control group(n=18),low (n=20) and high dosage(n=16) treated group. The normalized iodine concentrations(nIC) and PCT parameters of tumor at different time points (baseline, 2, 4, 7, 10, and 14 days after treatment) were compared among the three groups. Animals were assessed for survival, tumour size and spread, and tumour and immunohistological markers at 14 days and after 90 days.

RESULTS

There was no statistical difference in the diagnostic performance for respondents and nonrespondents differentiation between nIC and PCT parameters at 2 days and 4 days (area under the receiver operating characteristic curve, 0.73-0.76 vs.0.83-0.86) in the treated group. Radiologic parameters including BF, PEI, nICAP and nICPP at 2 days were positively correlated with the 14-day tumor size change and immunohistological markers(All P values <0.05). The overall survival days correlated with tumors with higher baseline mean transit time values on PCT(P=0.023) but not with nIC in both AP and PP.

CONCLUSION

DECT-derived nIC enabled monitor early antiangiogenic treatment effects but could not predict outcome at the end of treatment of rabbit VX2 liver tumors as compared with PCT parameters.

CLINICAL RELEVANCE/APPLICATION

Dual-energy CT can replace perfusion CT for monitoring tumor response and predicting short-term efficacy to tumor anti-angiogenic therapy but cannot predict outcome at the end of treatment .

SSK08-05 The Influence of Liver Iron Deposition on the Quantification of the Liver-Fat Fraction Using Spectral CT Imaging and Material Decomposition Technique: A Vitro Experiment Study

Wednesday, Dec. 4 11:10AM - 11:20AM Room: S502AB

Participants

Tingting Xie JR, MD, Shenzhen, China (*Presenter*) Nothing to Disclose Ying Guo, Guangzhou, China (*Abstract Co-Author*) Nothing to Disclose Guanxun Cheng, Shenzhen, China (*Abstract Co-Author*) Nothing to Disclose

PURPOSE

Our first goal was to build in vitro liver fat-iron deposition model in order to provide a phantom for fat content quantification in study. The second goal was to investigate whether iron deposition has an effect on the quantification of the liver-fat fraction using spectral CT imaging and material decomposition technique.

METHOD AND MATERIALS

Liver-fat-iron mixture samples were prepared as described. A total of 9 samples of 3 groups of homogeneous liver-fat mixed samples with fat volume percentage of 0%, 10%, 20% and 30% were prepared (group A, B and C, added iron with iron concentration of 10,

20 and 30mg/mL, respectively). All samples were scanned on a GE Revolution CT scanner using GSI mode with rapid tube voltage switching between 80-140 kVp, and with tube current 320mA, pitch 1.375mm. After the CT scan reconstructed imaging data were processed with GSI imaging analysis software package for material decomposition and characterization. Fat concentration (on fatwater bases) measured with consistent ROIs placed in the tube center with a diameter of 8mm. Each sample was recorded at 4 different regions for average and statistical analysis. A linear regression was performed using SPSS 19.0 software to analyze the relationship between the measured fat concentration and the liver fat concent (LFC).

RESULTS

(1) We had successfully developed liver iron-fat models in vitro for fat content quantification. With the designed fat volume percentage, the gradient range covered clinical fat content in liver, and the iron concentration of 20, 30 and 40mg/mL simulated the moderate and severe liver iron overload respectively. (2) The model showed good linear relationship between the measured fat concentration and LFC. And the linear correlation equation of group A, B and C were $y=0.037+61.85(R^2 = 0.998, P=0.0.02)$, $y=0.134x+263(R^2 = 0.991, P=0.043)$, and $y=0.074x+195(R^2 = 0.998, P=0.02)$.

CONCLUSION

The presence of iron underestimated of liver fat concent by using spectral CT imaging and material decomposition technique in vitro experiment.

CLINICAL RELEVANCE/APPLICATION

This study demonstrated the feasibility of using CT spectral imaging and material decomposition techniques to precisely quantify the fat concentrations under the condition of simultaneous fat deposition and iron deposition, and the presence of iron was a confounding factor, leading to the underestimation of liver fat content.

SSK08-06 Crohn's Disease Activity Quantified by Iodine Density Obtained from Dual-Energy CT Enterography

Wednesday, Dec. 4 11:20AM - 11:30AM Room: S502AB

Participants

Bari Dane, MD, New York, NY (*Presenter*) Nothing to Disclose Sean Duenas, New York, NY (*Abstract Co-Author*) Nothing to Disclose Thomas P. O'Donnell, PhD, New York, NY (*Abstract Co-Author*) Employee, Siemens AG Justin M. Ream, MD, Dobbs Ferry, NY (*Abstract Co-Author*) Nothing to Disclose Shannon Chang, New York, NY (*Abstract Co-Author*) Nothing to Disclose Alec J. Megibow, MD, New York, NY (*Abstract Co-Author*) Consultant, Bracco Group

For information about this presentation, contact:

bari.dane@nyumc.org

PURPOSE

To assess the utility of bowel wall iodine density obtained from dual source, dual-energy CT enterography (DECTE) as a biomarker of Crohn's disease (CD) activity.

METHOD AND MATERIALS

Twenty-two patients with CD imaged with DECTE from 2/2016-5/2018 were retrospectively identified by departmental report search. Iodine maps were created with commercial software (Syngovia®). Iodine content was normalized to the aorta and then manual region of interest cursors were placed over the visibly assessed maximal and minimal iodine density segments of involved and unaffected small bowel. The maximum (Imax) and minimum iodine density (Imin) were recorded. A weighted iodine density (Iweighted) was calculated. Hounsfield units from the blended (50% 150/50% 80kVp) DE images were recorded (mixed HU). The clinical assessment of disease activity using ESR, CRP, fecal calprotectin, colonoscopy/endoscopy and surgery were the reference standard. The CD activity index (CDAI) was used as a separate additional reference standard.

RESULTS

Average Imax and Imin of affected bowel were 4.27±1.11(2.4-7.4)mg/mL and 2.71±0.51(2.2-3.9)mg/mL, respectively. Iodine density of normal-appearing small bowel was 1.40±0.26(0.9-1.9)mg/mL. The Imax and Imin of affected bowel differed significantly from normal bowel (P<0.0001). Mixed HU (101.82±27.5) also statistically differed (46.33±19.62) (P<0.0001). Significant heterogeneity in the affected segments was present on iodine maps. Using overall clinical assessment as the reference standard, all patients with Imin>2.6mg/mL, Iweighted>3.3mg/mL, or Imax>4.7mg/mL had clinically active disease. Using CDAI as the reference standard, all patients with Imin>2.7mg/mL, Iweighted>3.6mg/mL or Imax>5.4mg/mL had clinically active disease. The median effective dose was 4.64±1.68(2.03-8.12)mSv.

CONCLUSION

Iodine density obtained from DECTE highlights regions of maximal activity within affected bowel segments. An iodine density of 2mg/mL appears to be a threshold between normal bowel and those involved with active CD. Iodine density thresholds Imin>2.7mg/mL, Iweighted>3.6mg/mL and Imax>5.4mg/mL appear to indicate clinically active disease.

CLINICAL RELEVANCE/APPLICATION

Because CD activity is heterogeneous, more specific targeting of affected segments can pinpoint therapeutic intervention.

SSK08-07 Can Advanced Tumor Analysis with DECT Iodine Quantification and Radiomics Help Characterize Focal Liver Lesions?

Wednesday, Dec. 4 11:30AM - 11:40AM Room: S502AB

Participants

Fatemeh Homayounieh, MD, Boston, MA (*Presenter*) Nothing to Disclose Ramandeep Singh, MBBS, Boston, MA (*Abstract Co-Author*) Nothing to Disclose Chayanin Nitiwarangkul, MD, Bangkok, Thailand (*Abstract Co-Author*) Nothing to Disclose Bernhard Schmidt, PhD, Forchheim, Germany (Abstract Co-Author) Employee, Siemens AG

Martin U. Sedlmair, MS, Forchheim, Germany (Abstract Co-Author) Employee, Siemens AG

Felix Lades, Forchheim, Germany (Abstract Co-Author) Employee, Siemens AG

Subba R. Digumarthy, MD, Boston, MA (*Abstract Co-Author*) Speaker, Siemens AG; Research Grant, Lunit Inc; Researcher, Merck & Co, Inc; Researcher, Pfizer Inc; Researcher, Bristol-Myers Squibb Company; Researcher, Novartis AG; Researcher, F. Hoffmann-La Roche Ltd; Researcher, Polaris Pharmaceuticals, Inc; Researcher, Cascadia Healthcare, LLC; Researcher, AbbVie Inc; Researcher, Gradalis, Inc; Researcher, Zai Lab

Sanjay Saini, MD, Boston, MA (Abstract Co-Author) Nothing to Disclose

Mannudeep K. Kalra, MD, Lexington, MA (*Abstract Co-Author*) Research Grant, Siemens AG; Research Grant, Riverain Technologies, LLC;

For information about this presentation, contact:

maryam.homayounieh@gmail.com

PURPOSE

We assessed a machine learning-based Dual Energy Tumor Analysis (DECT-TA) prototype (Siemens Healthineers) for semiautomatic segmentation and radiomics analysis of benign and malignant liver lesions seen on contrast-enhanced dual-energy CT (DECT).

METHOD AND MATERIALS

Our IRB-approved study included 103 adult patients (mean age 65 ± 15 years; 53 men, 50 women) with benign (n= 60) or malignant (n= 43) hepatic lesions on contrast-enhanced dual-source DECT (Siemens Force or Flash). Most malignant lesions had histologic proof; benign lesions were either stable on follow-up CT or had characteristic benign features on MRI. Low and high kV datasets were de-identified, exported offline, and post-processed with the DECT-TA for semiautomatic segmentation of the volume and rim of each liver lesion. For each segmentation, contrast enhancement and iodine concentrations, as well as 585 radiomics features were derived for different DECT image series. Statistical analyses were performed to determine if DECT-TA radiomics can differentiate benign from malignant liver lesions.

RESULTS

Iodine concentration, normalized iodine concentrations, mean iodine in the benign and malignant lesions were significantly different (p < 0.0001 - 0.0084; AUC: 0.695 - 0.856). Iodine quantification and radiomics features from lesion rims (AUC up to 0.877) had higher accuracy for differentiating liver lesions as compared to the values from lesion volumes (AUC up to 0.856). Random forest classification yielded higher accuracy for differentiating liver lesions with both the DECT iodine quantification (AUC= 0.91) than DECT radiomics (AUC= 0.90).

CONCLUSION

The DECT-TA prototype enables accurate differentiation between benign and malignant hepatic lesions based on iodine quantification and radiomics features.

CLINICAL RELEVANCE/APPLICATION

DECT segmentation, iodine quantification and radiomics can be used for characterizing focal liver lesions.

SSK08-08 Dual-Energy CT Improves Radiologist Confidence in Diagnosing Acute Bowel Ischemia Compared with Conventional CT

Wednesday, Dec. 4 11:40AM - 11:50AM Room: S502AB

Participants

Aung Zaw Win, FRCR, MRCP, Manchester, United Kingdom (*Presenter*) Nothing to Disclose Luis S. Guimaraes, MD, PhD, Toronto, ON (*Abstract Co-Author*) Nothing to Disclose Patrik Rogalla, MD, Toronto, ON (*Abstract Co-Author*) Institutional Research Grant, Canon Medical Systems Corporation

PURPOSE

The diagnostic performance of dual-energy CT (DECT) and confidence level of radiologists making the diagnosis on DECT in suspected acute bowel ischemia (ABI) in comparison with conventional CT were assessed. CT viewing times for conventional CT and DECT were evaluated.

METHOD AND MATERIALS

This retrospective study included 89 patients with clinically suspected ABI, who underwent Dual-energy CT imaging over 4 years in a large teaching institution. Clinical, laboratory, operative and biopsy findings were recorded as reference standard. Two radiologists who were blinded to the reference standard independently assessed conventional CT images to look for ABI, and subsequently, assessed DECT images. Diagnosis, confidence levels and CT reading times for both conventional CT and DECT were compared. The readers expressed their confidence levels in assessing bowel ischemia on 5 point Likert scale.

RESULTS

ABI was detected in 13 patients among 89 patients with clinical suspicion. The confidence level of Reader 1 to make the diagnosis increased by one level in 51.3% after reviewing DECT images; increased by two levels in 10.2%, and remained the same in 35.9%. For Reader 2, the confidence level increased by one level in 29.2% of patients, increased by two levels in 5.5%, unchanged in 48.6%, and decreased by one level in 15.3%. The mean reading time for conventional CT by Reader 1 was 104.6 \pm 57.23 sec, and the mean additional time to read DECT was 63.5 \pm 38.55 sec. The corresponding CT viewing times for Reader 2 were 67.4 \pm 33.39 sec, and 51.1 \pm 28.99 sec, respectively.

CONCLUSION

DECT increases the confidence of radiologists in diagnosing ABI with comparable diagnostic accuracy and reasonable extra-viewing time, as opposed to interpreting conventional CT alone. Hence, DECT is a promising imaging technique for routine clinical use in suspected ABI.

Acute Bowel Ischemia (ABI) is a clinical emergency, warranting prompt intervention or surgery, and this study aims to assess if dual-energy CT (DECT) could play a valuable role in evaluation of ABI.

SSK08-09 Non-Invasive Assessment of Liver Cirrhosis with Multiphasic Dual Energy CT Using Iodine Quantitation: Correlation with Model of End-Stage Liver Disease Score

Wednesday, Dec. 4 11:50AM - 12:00PM Room: S502AB

Participants

Domenico Mastrodicasa, MD, Stanford, CA (*Presenter*) Nothing to Disclose Martin J. Willemink, MD,PhD, Mountain View, CA (*Abstract Co-Author*) Research Grant, American Heart Association; Research Grant, Koninklijke Philips NV; Consultant, Arterys Inc Celina Duran, Boston, MA (*Abstract Co-Author*) Nothing to Disclose Virginia Hinostroza, Stanford, CA (*Abstract Co-Author*) Nothing to Disclose Lior Molvin, Palo Alto, CA (*Abstract Co-Author*) Speakers Bureau, General Electric Company Mohamed H. Khalaf, Stanford, CA (*Abstract Co-Author*) Nothing to Disclose R. Brooke Jeffrey Jr, MD, Stanford, CA (*Abstract Co-Author*) Nothing to Disclose Bhavik N. Patel, MD, Fremont, CA (*Abstract Co-Author*) Speakers Bureau, General Electric Company; Research Grant, General Electric Company

For information about this presentation, contact:

mastro@stanford.edu

PURPOSE

To determine whether contrast-enhanced multiphasic dual-energy (DE) CT iodine quantitation correlates with severity of chronic liver disease.

METHOD AND MATERIALS

This single-center, IRB-approved and HIPAA compliant retrospective study involved 28 patients with (15M; median age, 62 (58-68) years) and 22 patients without cirrhosis (8M; median age, 67 (51-75) years) who underwent a multiphasic liver protocol DECT. All three (arterial, portal venous (PVP), and delayed) phases were performed in DE mode. Patient demographics, MELD scores, and cirrhosis diagnosis were based on electronic medical records. A radiologist obtained Iodine concentration (mg I/ml) by manually placing ROIs in the caudate, left and right hepatic lobe, aorta, common hepatic artery (CHA), and portal vein (PV) on all 3 phases. ROI size and position were constant in all phases. Absolute iodine values were divided by those from the aorta for each phase to derive normalized Iodine quantitation (I). Iodine slopes (λ) were calculated as follows: Idelayed-arterial/ time(180 seconds) and Idelayed-PVP/ time(180 seconds). Slopes were correlated with MELD scores and the area under the curve of the receiver operating characteristic (AUROC) was calculated to distinguish cirrhotic and non-cirrhotic patients.

RESULTS

Cirrhotic and non-cirrhotic patients had significantly different λ delayed-PVP for caudate ($\lambda = 1.350$ vs. 2.350, P< .0001), left ($\lambda = 1.383$ vs. 2.200, P< .004), and right ($\lambda = 1.063$ vs. 1.913, P< .0001) lobe. λ delayed-arterial were significantly different for CHA ($\lambda = 2.450$ vs. 11.250, P< .023) and PV ($\lambda = 2.750$ vs. 3.750, P= .013). A statistically significant correlation was found between MELD scores and λ delayed-PVP of caudate, left and right lobes (rho =0.340, P=.034; rho=0.393, P=.005; rho=0.368, P=.034, respectively). AUROC for caudate, left, and right lobe λ delayed-PVP in differentiating cirrhotics from non-cirrhotics were 0.794, 0.739, 0.908, respectively.

CONCLUSION

Multiphasic DECT iodine quantitation over time is significantly different between cirrhotics and non-cirrhotics and correlates with MELD score.

CLINICAL RELEVANCE/APPLICATION

Multiphasic DECT iodine quantitation could serve as a non-invasive measure of cirrhosis and disease severity with high diagnostic accuracy.

Printed on: 10/29/20





SSK09

Gastrointestinal (Colon and Appendix)

Wednesday, Dec. 4 10:30AM - 12:00PM Room: S504AB



AMA PRA Category 1 Credits ™: 1.50 ARRT Category A+ Credit: 1.75

FDA Discussions may include off-label uses.

Participants

Gaurav Khatri, MD, Irving, TX (*Moderator*) Nothing to Disclose Raquel O. Alencar, MD,PhD, Boston, MA (*Moderator*) Nothing to Disclose Harmeet Kaur, MD, Houston, TX (*Moderator*) Nothing to Disclose

Sub-Events

SSK09-01 Intravoxel Incoherent Motion Diffusion-Weighted Imaging of Primary Rectal Carcinoma: Distinguish the Malignant or Benign Lymph Node

Wednesday, Dec. 4 10:30AM - 10:40AM Room: S504AB

Participants Qiang Feng, Weifang, China (*Presenter*) Nothing to Disclose Zhijun Ma, Qingzhou, China (*Abstract Co-Author*) Nothing to Disclose

For information about this presentation, contact:

fengyixiao2002@163.com

PURPOSE

The aim of this study was to evaluate the difference between the malignant or benign lymph node by IVIM and to determine the optimal parameter of IVIM.

METHOD AND MATERIALS

We retrospectively enrolled 98 patients with pathologically proven rectal adenocarcinoma. All patients underwent routine MR examination and IVIM sequence. A total of 246 lymph nodes were harvested and subjected to histological analysis. The IVIM maps were automatically generated. The t test, Mann-Whitney U test, and receiver operating characteristic curves was used for statistical analysis.

RESULTS

All IVIM parameters demonstrated the difference between metastatic lymph nodes and the normal lymph nodes (PD<0.01; PD*=0.01; Pf<0.001). For metastatic lymph nodes, f value of poorly differentiated rectal carcinoma were lower than well/moderately differentiated carcinoma, the significant difference was found (Pf=0.03). In addition, D value of mucinous carcinoma were higher than non-mucinous carcinoma (P<0.01) and D* values were on the contrary (P<0.01). D* showed a relatively higher area under the curve (AUC)(0.905) and higher sensitivity(94.48%) and specificity(85.33%) than other percentiles for differentiation of benign or malignant lymph nodes (LNs).

CONCLUSION

The IVIM parameters may distinguish between the malignant and benign lymph node during the primary staging of rectal carcinoma. D^* appears to be a valid and promising parameter to indicate the quality of LNS.

CLINICAL RELEVANCE/APPLICATION

The IVIM parameters can demostrate the malignant or benign lymph node of primary staging of rectal carcinoma. D* is recommended as part of a MR study prior to tumor removal.

SSK09-02 Dual-Energy CT Colonography: Increasing Reader Performance and Confidence in a Spectral Colon Phantom

Wednesday, Dec. 4 10:40AM - 10:50AM Room: S504AB

Participants

Markus M. Obmann, MD, Basel, Switzerland (Presenter) Nothing to Disclose

Chansik An, MD, Seoul, Korea, Republic Of (Abstract Co-Author) Nothing to Disclose

Amanda R. Schaefer, MD, San Francisco, CA (Abstract Co-Author) Nothing to Disclose

Yuxin Sun, BS, MSc, San Francisco, CA (Abstract Co-Author) Nothing to Disclose

Judy Yee, MD, Bronx, NY (*Abstract Co-Author*) Research Grant, EchoPixel, Inc; Research Grant, Koninklijke Philips NV; Research Grant, General Electric Company

Zhen J. Wang, MD, Hillsborough, CA (*Abstract Co-Author*) Stockholder, NEXTRAST, INC; Consultant, General Electric Company Benjamin M. Yeh, MD, Hillsborough, CA (*Abstract Co-Author*) Research Grant, General Electric Company; Consultant, General Electric Company; Author with royalties, Oxford University Press; Shareholder, Nextrast, Inc; Research Grant, Koninklijike Philips NV;

Research Grant, Guerbet SA; ;

For information about this presentation, contact:

markus.obmann@usb.ch

PURPOSE

To investigate if Dual-Energy CT (DECT) improves polyp detection compared to conventional CT (CCT) at CT Colonography (CTC) for different fecal tagging levels in an anthropomorphic phantom model.

METHOD AND MATERIALS

A 30 cm diameter colon phantom containing 60 polyps of different shapes (spherical, ellipsoid, flat) and size groups (5-9 mm; 11-15 mm) was serially filled with simulated feces tagged with 4 different iodine concentrations (1.26, 2.45, 4.88, and 21 mg I/ml). The artificial colon wall, polyps, feces and surrounding fat were tailored to match the spectral properties of human tissue. Low-dose scans (CTDIvol: 4.5 mGy) were performed on a dual-layer spectral CT with and without an additional outer 6 cm fat-ring (total diameter 42 cm). The phantom was divided into 336 segments, 276 without and 60 with polyps. Two abdominal radiologists independently reviewed CCT and DECT images (40 keV monoenergetic) images to record the presence of polyps in each segment and confidence (3-point Likert-scale.) Sensitivity and specificity between CCT and DECT were compared using McNemar's test, corresponding ROC AUCs were compared using DeLong's test; reader confidence was compared using Wilcoxon test.

RESULTS

Interrater agreement was substantial (κ =0.736). Overall sensitivity was higher at DECT than for CCT (59% versus 42%, respectively, p<0.001), including scans with the fat-ring (sensitivity: 48% vs 31%, respectively, p<0.001), while overall specificity was high for both (99.6% and 99.7%, respectively). Greater fecal tagging correlated with higher sensitivity for polyp detection both CCT and DECT (lowest vs highest tagging, 11 vs 76 % and 28 vs 85%, respectively, both p<0.001). At corresponding tagging levels, DECT showed higher sensitivity and specificity, resulting in superior ROC AUCs (p<0.003 for all levels). Reader confidence increased significantly with DECT compared to CCT (1.77 vs 1.54, p<0.001).

CONCLUSION

DECT improves polyp detection sensitivity and confidence in CTC exams, especially with low level fecal tagging. Effects were seen irrespective of polyp size or shape, and for larger phantom diameter. Study of clinical DECT colonography is warranted.

CLINICAL RELEVANCE/APPLICATION

DECT improves polyp detection sensitivity and confidence in a CTC phantom. Clinical DECT CTC studies to reduce cathartic bowel preparation or to salvage suboptimal tagged exams are warranted.

SSK09-03 Role of CT Colonography and Texture Analysis in Differentiating Sigmoid Cancer versus Chronic Diverticular Disease

Wednesday, Dec. 4 10:50AM - 11:00AM Room: S504AB

Participants

Riccardo Valletta, MD, Verona, Italy (*Presenter*) Nothing to Disclose Niccolo Faccioli, MD, Verona, Italy (*Abstract Co-Author*) Nothing to Disclose Matteo Bonatti, MD, Bolzano, Italy (*Abstract Co-Author*) Nothing to Disclose Fabio Lombardo, MD, Negrar, Italy (*Abstract Co-Author*) Nothing to Disclose Elena Santi, Verona, Italy (*Abstract Co-Author*) Nothing to Disclose Micaela Tagliamonte, Bolzano , Italy (*Abstract Co-Author*) Nothing to Disclose Antonello Lucarelli, Verona, Italy (*Abstract Co-Author*) Nothing to Disclose Giancarlo Mansueto, MD, Verona, Italy (*Abstract Co-Author*) Nothing to Disclose

For information about this presentation, contact:

riccardo.valletta@gmail.com

PURPOSE

To retrospectively evaluate morphological findings of chronic diverticular disease and sigmoid carcinoma at computed tomography colonography (CTC) and to evaluate texture analysis potential in order to differentiate them.

METHOD AND MATERIALS

We included in our IRB-approved retrospective study 95 consecutive patients with histologically proven chronic diverticular disease (n = 53) or sigmoid carcinoma (n = 42). Two radiologists retrospectively analyzed CTC studies unaware of the histological diagnosis. One reader scored each exam according to presence or absence of potential discriminators (Length, Wall thickness, Shouldering phenomenon, Thickening type, Growth pattern, Diverticula, Fascia thickening, Fat tissue edema, Loco-regional lymph nodes, Mucosal pattern) and performed volumetric texture analysis on the colonic tissue in both groups.

RESULTS

The Findings that suggest carcinoma diagnosis were: absence of diverticula in the affected segment (sensitivity 87.9%; specificity 90.5%); straightened growth pattern (sensitivity 71.4%; specificity 90.9%); shouldering phenomenon (sensitivity 90.5%; specificity 81.8%); complete distortion of mucosal folds (sensitivity 95.2%; specificity 75.8%). Considering mass-like lesions, growth pattern and mucosal folds distortion lose their diagnostic value. The only morphological finding with higher diagnostic value is absence of diverticula in the examined segment; its combination with shouldering phenomenon increases carcinoma diagnosis specificity. Regarding texture analysis parameters, kurtosis (first order feature, HISTO, p<0.001), correlation (second order feature, GLCM, p=0.0037) and contrast (second order feature NGLDM, p=0.0079) resulted to be significantly different between the two groups.

CONCLUSION

Carcinoma is best differentiated from chronic diverticular disease in CTC by the absence of diverticula in the affected segment and the presence of shoulder phenomenon. Texture analysis can provide an additional tool in differentiating the two entities when

considering HISTO kurtosis, GLCM correlation and NGLDM contrast, but further studies are needed

CLINICAL RELEVANCE/APPLICATION

Distinguishing colonic carcinoma from chronic diverticular disease at CTC is fundamental due to the extremely different prognosis and treatment of the two pathologies. CTC is able to do that and texture analysis can be helpful in this diagnostic process.

SSK09-04 Use of CT Encounters to Improve Colon Cancer Screening Utilization Rates: Cross-Sectional Survey Results from the National Health Interview Survey

Wednesday, Dec. 4 11:00AM - 11:10AM Room: S504AB

Participants

Efren J. Flores, MD, Boston, MA (*Presenter*) Nothing to Disclose Diego Lopez, Boston, MA (*Abstract Co-Author*) Nothing to Disclose Randy C. Miles, MD, Boston, MA (*Abstract Co-Author*) Nothing to Disclose Avinash R. Kambadakone, MD, Boston, MA (*Abstract Co-Author*) Research Grant, General Electric Company; Research Grant, Koninklijke Philips NV Anand K. Narayan, MD,PhD, Boston, MA (*Abstract Co-Author*) Nothing to Disclose

For information about this presentation, contact:

ejflores@mgh.harvard.edu

PURPOSE

Millions of patients undergo cross-sectional imaging examinations using CT every year. These imaging encounters may represent opportunities to improve colorectal cancer screening rates with CT colonography among patients who have not received recommended colon cancer screening. Using a nationally representative cross-sectional survey, the purpose of this study was to estimate the proportion of patients who have undergone CT examinations among those who have not received recommended colon cancer screening.

METHOD AND MATERIALS

Survey respondents from the 2015 National Health Interview Survey (NHIS), a nationally representative federal cross-sectional survey, were analyzed. Participants aged 50-75 without history of colorectal cancer were included. The proportion of patients who have not received recommended colon cancer screening who underwent CT examinations was estimated. Multiple variable logistic regression analyses were performed to evaluate the association between sociodemographic characteristics and colorectal cancer screening adherence. Stata survey procedures were used with NHIS-provided sampling weights to account for complex survey sampling design and to obtain statistically valid estimates for the civilian, non-institutionalized US population.

RESULTS

13,602 survey respondents met inclusion criteria. 46.8% (45.5, 48.1) reported having ever received a CT scan and 72.1% (70.4, 73.7) of those were eligible for CRC screening. Among those who previously had CT scans, Asian race participants (OR 0.47, 95% CI - 0.31, 0.72, p = 0.001) and participants without health insurance coverage (OR 0.48, 95% CI - 0.34, 0.70, p < 0.001) had lower odds of adherence, while increasing household income (OR 1.01, 95% CI 1.00 - 1.01, p < 0.001) and education (OR 1.30, 95% CI 1.10 - 1.54, p = 0.002) were associated with higher odds of adherence. Among participants who did not receive CRC screening, 35.2% (33.3%, 37.2%) reported having a CT scan, representing an estimated 10,904,722 people across the United States.

CONCLUSION

Among patients who have not received recommended colorectal cancer screening, approximately 1 out of 3 report having undergone a CT examination.

CLINICAL RELEVANCE/APPLICATION

Radiology encounters with patients undergoing CT exams may represent opportunities to improve colorectal cancer screening rates and utilization of CT colonography across the US.

SSK09-05 Radiomics-Based LN Staging after Neoadjuvant Chemoradiotherapy in Locally Advanced Rectal Cancer by Features from the Primary Tumor and One Automatically Selected Lymph Node

Wednesday, Dec. 4 11:10AM - 11:20AM Room: S504AB

Participants

Haitao Zhu, PhD, Beijing, China (*Presenter*) Nothing to Disclose Xiao-Yan Zhang, Beijing, China (*Abstract Co-Author*) Nothing to Disclose Yan-jie Shi, Beijing, China (*Abstract Co-Author*) Nothing to Disclose Ying-shi Sun, MD,PhD, Beijing, China (*Abstract Co-Author*) Nothing to Disclose

PURPOSE

This study aims to predict N stage after neoadjuvant chemoradiotherapy (NCRT) by combining the features of primary tumor and the features of one lymph node (LN) selected through a radiomics approach.

METHOD AND MATERIALS

229 patients were included in this study, chronologically divided into the discovery cohort (n=183) and validation cohort (n=46). T2-weighted images were scanned in an oblique direction perpendicular to the intestinal tube with following parameters: repetition time (TR) = 5700 ms, echo time (TE) = 110 ms, echo number = 25, field of view (FOV) = 180 mm. 41 features were extracted from the primary tumor and all visible LNs delineated on both pre-NCRT and post-NCRT MRI images. Pathological N stage after excision is used as ground truth. The LN that has the minimum or maximum value for each feature is selected and combined with the features of primary tumor to construct a Radiomics model in the discovery cohort by logistic regression with L1 regularization. The model is tested in the validation cohort and compared with several models. The average LN number and standard deviation for one patient is 13.4±5.1 in pre-NCRT scanning and 6.7±4.1 in post-NCRT scanning. The optimal way of LN selection is by using the maximum cluster prominence. The area under receiver operative curve (AUC) is 0.840 (95%CI: 0.778-0.890) for discovery cohort and 0.864 (95%CI: 0.731-0.947) for validation cohort. For the model that only uses tumor features, AUC is 0.580 (95%CI: 0.505-0.653) for discovery cohort and 0.669 (95%CI: 0.515-0.801) for validation cohort. For the model that uses tumor features and the LN that has the largest volume, AUC is 0.801 (95%CI: 0.736-0.856) for discovery cohort and 0.839 (95%CI: 0.701-0.931) for validation cohort. For the model that uses tumor features and average LN features, AUC is 0.741 (95%CI: 0.671-0.803) for discovery cohort and 0.539 (95%CI: 0.386-0.687) for validation cohort. For subjective evaluation, AUC is 0.650 (95%CI: 0.576-0.719) for discovery cohort and 0.756 (95%CI: 0.607-0.870) for validation cohort.

CONCLUSION

Radiomics model combining tumor features and features from LN with the maximum cluster prominence shows increased accuracy in predicting LN metastasis after NCRT for locally advanced rectal cancer (LARC) patients.

CLINICAL RELEVANCE/APPLICATION

Identification of lymph node (LN) status is crucial for assigning patients with LARC to appropriate treatments.

SSK09-06 The Diagnostic Performance of MRI for Detection of Extramural Venous Invasion in Colorectal Cancer: A Systematic Review and Meta-Analysis of the Literature

Wednesday, Dec. 4 11:20AM - 11:30AM Room: S504AB

Participants

Tae-Hyung Kim, MD, Seoul, Korea, Republic Of (*Abstract Co-Author*) Nothing to Disclose Sungmin Woo, MD, Seoul, Korea, Republic Of (*Presenter*) Nothing to Disclose Sangwon Han, Seoul, Korea, Republic Of (*Abstract Co-Author*) Nothing to Disclose Chong Hyun Suh, MD, Seoul, Korea, Republic Of (*Abstract Co-Author*) Nothing to Disclose Hebert Alberto Vargas, MD, Cambridge, United Kingdom (*Abstract Co-Author*) Nothing to Disclose

For information about this presentation, contact:

kth1205@gmail.com

PURPOSE

To perform a systematic review and meta-analysis regarding the diagnostic performance of MRI for detection of extramural venous invasion (EMVI) in patients with colorectal cancer.

METHOD AND MATERIALS

MEDLINE and EMBASE were searched up to November 9th 2018. We included diagnostic accuracy studies that used MRI for EMVI detection in patients with colorectal cancer, using pathology as the reference standard. The methodological quality was assessed using QUADAS-2. Sensitivity and specificity were pooled and plotted in a hierarchical summary receiver operating characteristics plot. Meta-regression analysis using several clinically relevant covariates were performed.

RESULTS

Fourteen studies (n = 1751 patients) were included. Study quality was generally moderate. Pooled sensitivity was 0.61 (95% CI 0.49-0.71) and specificity was 0.87 (95% CI 0.79-0.92). There was substantial heterogeneity: Cochran's Q-test (p<0.01), Higgins I2 (98% and 95% for sensitivity and specificity, respectively). Publication bias was present (p = 0.01). Higher prevalence of advanced T stage, high-resolution MRI and antispasmodic drugs were significant factors affecting heterogeneity (p <0.01). Location of primary tumor, preoperative treatment status, study design, definition of reference standard, magnetic field strength, and use of functional MRI sequences were not statistically significant (p = 0.17-0.92).

CONCLUSION

MRI demonstrates moderate sensitivity and good specificity for detection of EMVI in colorectal cancer. Using high-resolution MRI may improve diagnostic performance.

CLINICAL RELEVANCE/APPLICATION

MRI demonstrates moderate sensitivity and good specificity for detection of EMVI in patients with colorectal cancer. Preoperative MRI would benefit patients with coloretal cancer for correct staging and subsequent setting of optimal treatment. Furthremore, this study would provide rationale for future studies evaluating the role of MRI-detected EMVI without pathologic confirmation.

SSK09-07 Characteristic Radiographic Patterns of Biopsy-Proven Immune-Related Colitis in Melanoma Patients Treated with Cytotoxic T-Lymphocyte Antigen-4 (CTLA-4) Inhibitors

Wednesday, Dec. 4 11:30AM - 11:40AM Room: S504AB

Participants

Alex Ruan, MD, Boston, MA (Abstract Co-Author) Nothing to Disclose

Marta Braschi Amirfarzan, MD, Burlington, MA (Presenter) Nothing to Disclose

Elizabeth I. Buchbinder, MD, Boston, MA (*Abstract Co-Author*) Advisory Board, Bristol-Myers Squibb Company; Advisory Board, Array BioPharma Inc; Advisory Board, Trieza; Advisory Board, Novartis AG

Patrick A. Ott, Boston, MA (Abstract Co-Author) Consultant, Bristol-Myers Squibb Company

Richard Thomas, MBBS, MD, Boston, MA (Abstract Co-Author) Nothing to Disclose

F. Stephen Hodi JR, MD, Boston, MA (*Abstract Co-Author*) Consultant, Bristol-Myers Squibb Company; Support, Bristol-Myers Squibb Company; Advisor, Merck & Co, Inc; Advisor, F. Hoffmann-La Roche Ltd; Support, Merck & Co, Inc; Support, F. Hoffmann-La Roche Ltd; Consultant, Novartis AG; Research support, Novartis AG; Consultant, Amgen Inc; Consultant, Merck KGaA; Consultant, sanofiaventis Group; Consultant, Takeda Pharmaceutical Company Limited; Consultant, Bayer AG; Consultant, Pfizer, Inc; Consultant, Surface; Consultant, Compass; Stockholder, Apricity; Stockholder, Pionyr; Consultant, Aduro BioTech, Inc; Stockholder, Torque; Consultant, Verastem, Inc

Osama E. Rahma, MD, Boston, MA (Abstract Co-Author) Research support, Merck & Co, Inc; Speaker, Bristol-Myers Squibb

Company; Speaker, Merck & Co, Inc; Consultant, Merck & Co, Inc; Consultant, Celgene Corporation; Consultant, Five Prime; Consultant, GlaxoSmithKline plc; Consultant, GFK; Consultant, Defined Health Inc; Consultant, F. Hoffmann-La Roche Ltd; Consultant, Puretech; Consultant, Leerink Swann & Company; Consultant, PRMA Consulting ; Pending patent, "METHODS OF USING PEMBROLIZUMAB AND TREBANANIB"

Shilpa Grover, MD, MPH, Boston, MA (Abstract Co-Author) Editor, Wolters Kluwer nv

For information about this presentation, contact:

sgrover@bwh.harvard.edu

PURPOSE

To investigate the radiographic signature of biopsy-proven immune-related colitis in patients treated with CTLA-4 inhibitors.

METHOD AND MATERIALS

We retrospectively reviewed medical records of 692 cancer patients treated at our institution who received at least 1 course of an immune checkpoint inhibitor between 2011 and 2018. Among them, 100 (14%) had biopsy-proven colitis and of those, 97 (97%) had concomitant imaging. In order to characterize the radiographic features of colitis associated with CTLA-4 inhibitors, we limited our cohort to patients treated with a CTLA-4 inhibitor who underwent at least 1 baseline and on-treatment abdominal CT. Abdominal CTs were reviewed by a single radiologist for the presence and imaging characteristics of colitis.

RESULTS

We identified 20 patients with melanoma treated with either ipilimumab (17) or tremelimumab (3) (mean age 69 yrs) who subsequently developed biopsy-proven colitis. Of those 20 patients, 18 (90%) had radiographic evidence of colitis a mean of 14.6 wks after starting CTLA-4 therapy. Radiographic patterns noted were pancolitis (10 patients, 56%), segmental colitis (7, 39%), segmental colitis associated with diverticulosis (SCAD, 6, 33%), enterocolitis (3, 17%), and enteritis alone (1, 6%); several patients had multiple features. Most common CT features of colitis included bowel wall thickening (16 patients, 89%), fluid-filled colon (14, 78%), fat stranding (14, 78%), mesenteric vessel engorgement (12, 67%), and mucosal hyperenhancement (10, 56%). Among the 6 patients with classic SCAD pattern, 3 (50%) also had concomitant involvement of the hepatic flexure, a novel radiographic finding. Colitis prompted interruption of treatment and initiation of steroids in 6 patients and steroids/infliximab in 12 patients.

CONCLUSION

CTLA-4 inhibitor mediated biopsy-proven immune-related colitis has radiographic findings ranging from segmental colitis to pancolitis on CT. Bowel wall thickening was the most prevalent finding. A subset of patients with SCAD pattern may have a predilection for involvement of the hepatic flexure, reported here for the first time. These findings should be prospectively validated in additional cohorts.

CLINICAL RELEVANCE/APPLICATION

Given the expanding role of immune checkpoint blockade including CTLA-4 inhibition, radiologists should be aware of the imaging features of immune-related colitis.

SSK09-09 Retrospective Diagnostic Model Development and Validation Study: Differentiation of Complicated from Uncomplicated Appendicitis in Adolescents and Young Adults Using CT and Clinical Predictors

Wednesday, Dec. 4 11:50AM - 12:00PM Room: S504AB

Participants

Hae Young Kim, MD,MS, Seongnam, Korea, Republic Of (*Presenter*) Nothing to Disclose Ji Hoon Park, MD,PhD, Seongnam, Korea, Republic Of (*Abstract Co-Author*) Nothing to Disclose Sung Soo Lee, Seongnam-si, Korea, Republic Of (*Abstract Co-Author*) Nothing to Disclose Jong June Jeon, Seoul, Korea, Republic Of (*Abstract Co-Author*) Nothing to Disclose Woojoo Lee, Incheon, Korea, Republic Of (*Abstract Co-Author*) Nothing to Disclose Kyoung Ho Lee, MD, Seongnam, Korea, Republic Of (*Abstract Co-Author*) Nothing to Disclose

For information about this presentation, contact:

qkfmrp860329@gmail.com

PURPOSE

To develop and validate a diagnostic model comprising CT and clinical/laboratory features for differentiation of complicated from uncomplicated appendicitis.

METHOD AND MATERIALS

This retrospective study included 1153 adolescent and young adults (mean age \pm standard deviation, 30 \pm 8 years) with suspected appendicitis on CT. We used the data from a previous pragmatic multi-center randomized controlled trial that compared 2-mSv CT and conventional-dose CT for the diagnosis of appendicitis in 20 teaching hospitals. We included 804 patients from 12 sites for model development, and 349 patients from eight sites for external validation. The outcome of interest was complicated appendicitis (perforated or gangrenous appendicitis). Complicated appendicitis was surgically or pathologically confirmed in 300 and 121 patients in the development and validation set, respectively. We constructed diagnostic models using logistic regression from candidate predictors comprising eight CT features and 13 clinical/laboratory features. The final model was selected using the Bayesian information criterion. A simplified rule was derived at a cut-off score targeting 95% sensitivity in the development set. For external validation, sensitivity and specificity were measured in the validation set, using the detailed model and its simplified rule targeting 95% sensitivity.

RESULTS

Six predictors comprising 5 CT features (contrast-enhancement defect of the appendiceal wall, abscess, periappendiceal fat stranding, appendiceal diameter, and extraluminal air) and the percentage of segmented neutrophil were included in our model. In the validation set, the sensitivity and specificity were 95.9% (90.6%, 98.6%) and 19.3% (14.4%, 25.0%) using the detailed model; and 95% (90%, 98%) and 16% (11%, 21%) using the simplified rule.

CONCLUSION

We propose highly sensitive prediction model for complicated appendicitis, which may contribute to reducing the number of unnecessary appendectomies performed for uncomplicated appendicitis.

CLINICAL RELEVANCE/APPLICATION

For physicians who are willing to attempt conservative management of appendicitis while minimizing the risk of treatment failure, our model can be used with expected percentage of false negatives to be less than 1.5%.

Printed on: 10/29/20





SSK10

Genitourinary (PI-RADS v2.0 and v2.1)

Wednesday, Dec. 4 10:30AM - 12:00PM Room: N227B

GU

AMA PRA Category 1 Credits ™: 1.50 ARRT Category A+ Credit: 1.75

FDA Discussions may include off-label uses.

Participants

Varaha Tammisetti, MD, Houston, TX (*Moderator*) Nothing to Disclose Sadhna Verma, MD, Cincinnati, OH (*Moderator*) Nothing to Disclose Nicola Schieda, MD, Ottawa, ON (*Moderator*) Nothing to Disclose

Sub-Events

SSK10-01 PIRADS Score 2 Misses Significant Prostate Cancer Foci on MRI

Wednesday, Dec. 4 10:30AM - 10:40AM Room: N227B

Participants

Katja Bogner, Nuremberg, Germany (*Presenter*) Nothing to Disclose Karl Engelhard, MD, Nuremberg, Germany (*Abstract Co-Author*) Nothing to Disclose Florian Schneider, Nurnberg, Germany (*Abstract Co-Author*) Nothing to Disclose Sajad Hamel, Nuremberg, Germany (*Abstract Co-Author*) Nothing to Disclose

For information about this presentation, contact:

Katja.Bogner@Martha-Maria.de

PURPOSE

To evaluate cancer suspected areas in multiparametric MRI (mpMRI) of the prostate which were classified as PIRADS 2 lesions using scientifically proved MRI criteria of cancer by an experienced reporting investigator

METHOD AND MATERIALS

In 2012-2017 328 out of 929 patients with suspicion of prostate cancer that underwent mpMRI were categorized as PIRADS 2 by a radiologist with more than 7 years' experience, 198 of them underwent an 18-core TRUS guided biopsy added by 3 additional samples of the MRI suspected areas. Since 2015 suspicious lesions were evaluated with respect to well-known tumor criteria in literature. In 2012-2014 suspicious lesions were retrospectively categorized as PIRADS 2. In 61 of 198 patients with PIRADS 2 score suspicious lesions were found (study group). The negative predictive value (NPV) of PIRADS 2 was assessed. Chi-square-test was performed to evaluate a possible difference between the number of significant carcinomas in patients with suspicious lesions and in men with PIRADS score 2 criteria alone.

RESULTS

In the study population cancer was found in 13 of 61 men (21%), significant cancer (Gleason score > 6 or Gleason score 6 with PSA > 10 ng/ml or tumor areas in both prostate lobes) in 10 patients (16%). 11 of 13 cancer foci showed a good correlation between the suspected areas in MRI and the biopsy sides. In the control group 25 carcinomas were detected (18%), 16 of them significant (12%). PIRADS score 2 showed a NPV for significant carcinomas of 87 % in the whole population, 84% in the study group and 88% in the control group. The number of significant carcinomas detected in the study population was not significant higher than in the control group.

CONCLUSION

PIRADS scoring provides accurate reproducible reports in interpreting prostate MRI, especially in unexperienced investigators. Reported weaknesses of the PIRADS system are the straight recommendations of interpreting the different zones of the prostate with priority to first and second line sequences in diagnosis weighting. Including proved tumor criteria in MRI as early contrast enhancing foci in the transitional zone or low signal intensity areas in the peripheral zone on T2-weighted images tends to indicate prostate carcinoma beside PIRADS criteria.

CLINICAL RELEVANCE/APPLICATION

PIRADS 2 lesions could comprise significant prostate cancer foci and should require further diagnostic assessment with additionally scientific proven tumor MRI criteria.

SSK10-02 Factors that Predict Clinically Significant Prostate Cancer Among Prostate Imaging Reporting and Data System (PI-RADSv2) Category 3 Lesions Using Histopathology as a Reference

Wednesday, Dec. 4 10:40AM - 10:50AM Room: N227B

Participants

Voraparee Suvannarerg, MD, Bangkok, Thailand (*Presenter*) Nothing to Disclose Melina Hosseiny, MD, Los Angeles, CA (*Abstract Co-Author*) Nothing to Disclose

Sohrab Afshari Mirak, MD, Los Angeles, CA (Abstract Co-Author) Nothing to Disclose

David S. Lu, MD, Los Angeles, CA (*Abstract Co-Author*) Consultant, Medtronic plc Speaker, Medtronic plc Consultant, Johnson & Johnson Research Grant, Johnson & Johnson Consultant, Bayer AG Research Grant, Bayer AG Speaker, Bayer AG Steven S. Raman, MD, Santa Monica, CA (*Abstract Co-Author*) Consultant, Johnson & Johnson; Consultant, Bayer AG; Consultant, Merck & Co, Inc; Consultant, Amgen Inc; Consultant, Profound Medical Inc

For information about this presentation, contact:

vsuvannarerg@mednet.ucla.edu

PURPOSE

This study aimed to identify clinical and magnetic resonance imaging (MRI) factors that predict clinically significant prostate cancer (CSC) in patients with Prostate Imaging Reporting and Data System version 2 (PI-RADSv2) category 3 lesions using histopathology as a reference.

METHOD AND MATERIALS

This retrospective study included 339 consecutive PI-RADSv2 category 3 lesions that were identified by multiparametric prostate 3T MRI during the January 2009 to December 2018 study period. Transitional and peripheral zone lesions were also included. Histopathologic diagnosis was determined via radical prostatectomy in 232 lesions (68.4%), and by MRI-guided biopsy in 107 lesions (31.6%). CSC was defined as a Gleason score equal to or greater than 3+4. Imaging parameters, quantitative measurement, and PI-RADSv2 category were analyzed by an experienced board-certified radiologist. Univariate and multivariate logistic regression analyses were performed to identify factors significantly associated with CSC.

RESULTS

Of the 339 included lesions, 124 (36.6%) were CSC, and 215 (63.4%) were benign or non-CSC. Univariate analysis showed prostate volume (p=0.005), prostate specific antigen density (p=0.049), UCLA score (p<0.001), mean apparent diffusion coefficient (ADC) (p<0.001), ADC ratio (p<0.001), Ktrans (p=0.012), base, mid, and apex levels (p<0.001), and index lesions (p<0.001) to be significantly associated with CSC. Multivariate analysis revealed prostate volume (logistic regression coefficient [Coef.]=-0.032, 95% confidence interval [CI]: -0.05 to -0.02, p<0.001), ADC ratio (Coef.=1.478, 95% CI: 0.83-2.13, p<0.001), apex location (Coef.=1.731, 95% CI: 0.57-2.89, p=0.003), and index lesions (Coef.=1.755, 95% CI: 1.14-2.37, p<0.001) to be independent predictors of CSC. These findings were used to develop a nomogram for assessing the probability of CSC among PI-RADSv2 category 3 lesions as shown in Figure 1.

CONCLUSION

Prostate volume, ADC ratio, apex level, and index lesions were identified as the MRI parameters and quantitative measurement factors that independently predict CSC in PI-RADSv2 category 3 lesions.

CLINICAL RELEVANCE/APPLICATION

MRI parameters and quantitative measurement factors can predict the probability of CSC in PI-RADSv2 category 3 lesions.

SSK10-03 Patients Assigned to PI-RADS Category 4 and Subsequent Targeted Negative Biopsy: How To Deal With?

Wednesday, Dec. 4 10:50AM - 11:00AM Room: N227B

Participants

Lars Schimmoeller, MD, Dusseldorf, Germany (*Presenter*) Nothing to Disclose Tim Ullrich, Duesseldorf, Germany (*Abstract Co-Author*) Nothing to Disclose Nina Laqua, Dusseldorf, Germany (*Abstract Co-Author*) Nothing to Disclose Andreas Hiester, Dusseldorf, Germany (*Abstract Co-Author*) Nothing to Disclose Christian Arsov, MD, Duesseldorf, Germany (*Abstract Co-Author*) Nothing to Disclose Gerald Antoch, MD, Dusseldorf, Germany (*Abstract Co-Author*) Nothing to Disclose

For information about this presentation, contact:

Lars.schimmoeller@med.uni-duesseldorf.de

PURPOSE

To comprehensively characterize patients assigned to MRI category PI-RADS 4 and guide clinical management in the case of negative biopsy.

METHOD AND MATERIALS

This prospectively enrolled, single center cohort study includes 931 consecutive patients after mp-MRI (T2WI,DWI,DCE) at 3T for prostate cancer detection. 193 patients with PI-RADS assessment category 4 and subsequent targeted MRI/US fusion-guided plus systematic 12-core TRUS-guided biopsy as reference standard were finally analyzed. The primary endpoint was prostate cancer (PCa) detection of MRI-subgroups in PI-RADS 4 cases (S1-S3: highly likely clinically significant PCA, overlaying prostatitis, or overlaying stromal hyperplasia). Secondary endpoints were analyses of clinical data and detection of targeted biopsy cores.

RESULTS

PCa detection rate was 62% (119/193) including 48% clinically significant PCa (csPCa; Gleason score >=3+4=7). 95% of the index lesions of MRI-subgroup S1 had PCa, whereas lesions of subgroup S3 had csPCa only in 4%. 7% of the patients targeted biopsy cores missed the csPCa index lesion. PSA density (PSAD) was significantly higher in PCa patients.

CONCLUSION

Small csPCa can reliably be detected with mp-MRI by experienced readers, but can be missed by targeted biopsy alone. Re-biopsy of PI-RADS-4-lesions within subgroup S1 is recommended after negative targeted biopsy. Negatively biopsied PI-RADS-4-lesions within subgroup S3 can be followed-up without early re-biopsy. In uncertain cases PSAD should be considered for biopsy decision.

CLINICAL RELEVANCE/APPLICATION

Re-biopsy of PI-RADS-4-lesions with negative primary biopsy might be adjusted to lesion location, image appearance and PSAD. No all patients need timely re-biopsy.

SSK10-04 Dirty Peripheral Zone in Patients with Suspicious Prostate Cancer: Evaluation with PI-RADS v2 Followed by MRI-Guided Biopsy

Wednesday, Dec. 4 11:00AM - 11:10AM Room: N227B

Participants

Beom Jun Kim, Seoul, Korea, Republic Of (*Presenter*) Nothing to Disclose Chan Kyo Kim, MD, PhD, Seoul, Korea, Republic Of (*Abstract Co-Author*) Nothing to Disclose Taein An, Seoul, Korea, Republic Of (*Abstract Co-Author*) Nothing to Disclose

For information about this presentation, contact:

chankyokim@skku.edu

PURPOSE

Interpretation of dirty peripheral zone (PZ) using PI-RADS v2 is a challenge because of unclear criteria in the term between 'indistinct' in diffusion-weighted imaging (DWI) score 2 and 'focal' in DWI scores 3-5. We aimed to investigate the detection rates of prostate cancer (PCa) in dirty PZ (dirty group) and to identify any differences between dirty and non-dirty control groups.

METHOD AND MATERIALS

266 patients (dirty group = 139; control group = 127) with suspicious PCa were enrolled in this retrospective study. All patients underwent prebiopsy 3-T MRI and subsequent MRI-guided targeted biopsy and concurrent systemic biopsy. Dirty PZ was defined as >= three lesions of wedge-shaped, ill-defined or linear hypointensity in the PZ on apparent diffusion coefficient (ADC) maps. Biopsy-based definition of clinically significant cancer (CSC) was Gleason score >= 3 + 4. Detection rates of all PCa and CSC were compared between the two groups. Inter-reader agreement for PI-RADS v2 scoring was evaluated.

RESULTS

In 266 patients, detection rates of all PCa were 41.7% for dirty group and 50.4% for control group, respectively (P = 0.157); dirty group had significant lower detection rates of CSC than control group (19.4% versus 33.1%, P = 0.011). In all 326 target lesions (dirty group = 176; control group = 150), detection rates of all PCa were 43.8% for dirty group and 50.7% for control group, respectively (P= 0.222); dirty group had significantly lower detection rates of CSC than control group (21% versus 34.7%, P = 0.0063). Regarding remote lesions from target lesions based on systemic biopsy, detection rates of all PCa and CSC in dirty group versus control group were 18.7% versus 32.8% (P = 0.027) and 26.9% versus 19.1% (P = 0.731), respectively. For PI-RADS v2 score >= 4 or not, a substantial inter-reader agreement was seen for control group ($\kappa = 0.723$), while a poor inter-reader agreement was seen for dirty group ($\kappa = 0.723$), while a poor inter-reader agreement was seen for dirty group ($\kappa = 0.723$), while a poor inter-reader agreement was seen for dirty group ($\kappa = 0.723$), while a poor inter-reader agreement was seen for dirty group ($\kappa = 0.723$), while a poor inter-reader agreement was seen for dirty group ($\kappa = 0.723$), while a poor inter-reader agreement was seen for dirty group ($\kappa = 0.063$).

CONCLUSION

In patients with suspicious PCa, dirty PZ appears to contain approximately 20% CSCs, with fewer detection rates of CSCs than non-dirty PZ. Furthermore, dirty PZ reveals a poor inter-reader agreement for PI-RADS v2 scoring.

CLINICAL RELEVANCE/APPLICATION

When performing a MRI-guided targeted biopsy, we need a cautious approach for dirty PZ because it may harbor approximately 20% CSCs. However, dirty PZ demonstrates fewer detection rates of CSCs compared with non-dirty PZ.

SSK10-05 Does the PI-RADS Prostate MRI Definition of Sextant Regions Adequately Correspond with Transrectal Ultrasound to Direct Non-Fusion TRUS Biopsy of Suspicious MRI Masses?

Wednesday, Dec. 4 11:10AM - 11:20AM Room: N227B

Participants

Timothy Miao, MD, London, ON (*Presenter*) Nothing to Disclose Beatrice Lau, London, ON (*Abstract Co-Author*) Nothing to Disclose Aaron Fenster, PhD, London, ON (*Abstract Co-Author*) License agreement, Eigen Lori Gardi, London, ON (*Abstract Co-Author*) Licensing agreement, Eigen Medical Jonathan Izawa, London, ON (*Abstract Co-Author*) Nothing to Disclose Joseph Chin, MD, London, ON (*Abstract Co-Author*) Nothing to Disclose Ashley J. Mercado, MD, London, ON (*Abstract Co-Author*) Nothing to Disclose Derek W. Cool, MD, PhD, London, ON (*Abstract Co-Author*) Nothing to Disclose

PURPOSE

To determine if prostate sextant anatomical nomenclature is consistent between multiparametric MRI (MP-MRI) and transrectal ultrasound (TRUS) biopsy.

METHOD AND MATERIALS

50 patients (age 60.9±7.2 years, prostate volume 52±29cm³, prostate specific antigen 8.0±4.2 ng/mL) underwent MR-TRUS fusion biopsy. Standard 12-core sextant biopsies were also performed purely under TRUS guidance and the biopsy core locations relative to the MP-MRI were recorded. A radiologist sectioned each MP-MRI into base, mid-gland and apex regions as defined by the Prostate Imaging Reporting and Data System version 2 (PI-RADS). Each TRUS-guided biopsy core location was compared to 3D reconstructions of the MP-MRI sextant regions to determine the length of the biopsy core located within each sector.

RESULTS

590 biopsy cores were analyzed. Only 47% (92/197) of TRUS-cores targeting the base sampled any of the MP-MRI defined base, which was significantly less than TRUS-cores targeting the mid-gland (97%, 192/199) and apical (94%, 182/194) regions (p<0.001). Sampling percentages were not significantly different between right and left-sided TRUS-biopsies of base (p=0.07), mid-

gland (p=0.7) and apical regions (p=0.6). Of the 47% of TRUS-cores targeting the base that did touch the MP-MRI defined base, only 26%±18% of the total core length was within the base region-significantly less than mean total core lengths of mid-gland (59%±24%) and apical (57%±28%) TRUS-targeted cores within their corresponding MP-MRI regions (p<0.001). A subgroup analysis of TRUS-cores targeting the base of prostate revealed fewer TRUS-cores sampling the MP-MRI defined base for prostates with volume greater than 45cm³ (n=24) compared to smaller prostates (n=26): 23%±24% versus 67%±25%, respectively (p<0.001).

CONCLUSION

The PI-RADS MP-MRI definitions of apex, mid-gland and especially base do not match standard TRUS-biopsy, particularly in the base of larger prostates. Results from this study could be used to define more TRUS relevant PI-RADS definitions of prostate sectors on MP-MRI.

CLINICAL RELEVANCE/APPLICATION

These results have implications for TRUS-guided biopsy of MP-MRI prostate lesions without software fusion assistance ("cognitive fusion"), as it may lead to inaccurate targeting.

SSK10-06 Does Compliance with PIRADSv2 Technical Requirements Guarantee Image Quality or Adequacy in Prostate mpMRI Reads? A Multi-Institution Multi-Reader Study

Wednesday, Dec. 4 11:20AM - 11:30AM Room: N227B

Participants

Jonathan J. Sackett, BS, Bethesda, MD (Presenter) Research collaboration, NVIDIA Corporation JoAnna Shih, Bethesda, MD (Abstract Co-Author) Nothing to Disclose Stephanie A. Harmon, PhD, Bethesda, MD (Abstract Co-Author) Research funded, NCI Tristan Barrett, MBBS, Cambridge, United Kingdom (Abstract Co-Author) Nothing to Disclose Mehmet Coskun, MD, Ankara, Turkey (Abstract Co-Author) Nothing to Disclose Manuel V. Madariaga Sr, MD, Santiago, Chile (Abstract Co-Author) Nothing to Disclose Jamie Marko, MD, Bethesda, MD (Abstract Co-Author) Nothing to Disclose Yan Mee Law, MBBS, Singapore, Singapore (Abstract Co-Author) Nothing to Disclose Evrim B. Turkbey, MD, Rockville, MD (Abstract Co-Author) Nothing to Disclose Sherif Mehralivand, MD, Bethesda, MD (Abstract Co-Author) Nothing to Disclose Thomas H. Sanford, Bethesda, MD (Abstract Co-Author) Research collaboration, NVIDIA Corporation Nathan S. Lay, PhD, Bethesda, MD (Abstract Co-Author) Nothing to Disclose Jeffrey R. Brender, PhD, Bethesda, MD (Abstract Co-Author) Nothing to Disclose Bradford J. Wood, MD, Bethesda, MD (Abstract Co-Author) Researcher, Koninklijke Philips NV; Researcher, Celsion Corporation; Researcher, BTG International Ltd; Researcher, Siemens AG; Researcher, XAct Robotics; Researcher, NVIDIA Corporation; Intellectual property, Koninklijke Philips NV; Intellectual property, BTG International Ltd; Royalties, Invivo Corporation; Royalties, Koninklijke Philips NV; Equipment support, AngioDynamics, Inc; Researcher, Profound Medical Inc; Researcher, Canon Medical Systems Corporation; Researcher, AstraZeneca PLC; Researcher, Exact Imaging Inc Peter L. Choyke, MD, Rockville, MD (Abstract Co-Author) License agreement, Koninklijke Philips NV; Researcher, Koninklijke Philips NV; License agreement, ScanMed; License agreement, Rakuten Medical; Researcher, Rakuten Medical; Researcher, General Electric Company; Researcher, Progenics Pharmaceuticals, Inc; Researcher, Novartis AG; ; ; ; ; Baris Turkbey, MD, Bethesda, MD (Abstract Co-Author) Research support, Koninklijke Philips NV; Royalties, Invivo Corporation; Investigator, NVIDIA Corporation

For information about this presentation, contact:

jsackett@llu.edu

PURPOSE

To determine whether compliance with PIRADSv2 technical requirements is related to perceived image quality during prostate mpMRI read outs.

METHOD AND MATERIALS

62 prostate MRI examinations including T2W and DWI from 62 different institutions acquired within the last 12 months that were consecutively referred to our center were included. 6 readers assessed images as adequate or inadequate for use in PCa detection and assessment in addition to ranking image quality on a 1-5 scale. PIRADSv2 technical requirements were synthesized into sets of 7 and 10 rules for T2W and DWI, respectively. Image compliance was assessed using DICOM metadata. Statistical analysis of survey results and image compliance was performed based on reader quality scoring (Kendall Rank Tau-b) and reader adequate scoring (Wilcoxon test for association) for T2 and DWI quality assessment.

RESULTS

52/62 (83%) T2 and 38/62 (61%) DW images were rated to be adequate by a majority of readers. Reader adequacy scores showed no significant association to any rules or combination of rules. For T2 quality, 10/62 (16%) scored as high quality (score >3) by a majority of readers and 18 studies met all 7 T2 rules. There was a weak correlation (tau-b=0.22) between compliance with PIRADSv2 technical standards and image quality for T2 which was significant(p-value=0.01). Studies following all PI-RADSv2 T2 rules achieved a higher average quality score (median avg score = 3.58 for 7/7 vs. median avg score = 3 for <7/7, p=0.012). There was no significant association for individual T2 rules. For DWI quality, 6/62 (9%) scored as high quality by a majority of readers and 4 studies met all 10 DWI rules. Analysis of DWI quality scores found no relationship with PIRADSv2 compliance.

CONCLUSION

Many prostate mpMRI images are of inadequate quality for clinical use and very few images are of high quality. This is especially true for DWI. Adherence to PIRADSv2 technical requirements doesn't necessarily increase the likelihood of having a qualitatively adequate T2W or DWI for clinical use.

CLINICAL RELEVANCE/APPLICATION

High quality MRIs are needed for PCa screening and accurate targeting in MRI guided biopsies. The PIRADSv2 Minimum Technical Standards are not a sufficient threshold to ensure quality.

SSK10-07 Head-to-Head Comparison of PI-RADS 2 versus PI-RADS 2.1: Moderate Agreement and Slight Changes in Scoring and Cancer Localization

Wednesday, Dec. 4 11:30AM - 11:40AM Room: N227B

Participants

Madhuri Rudolph, MD, Berlin, Germany (Presenter) Nothing to Disclose

Alexander D. Baur, MD, Berlin, Germany (*Abstract Co-Author*) Speaker, Bayer AG; Speaker, Uropharm AG; Reseach funded, Bayer AG Matthias Haas, Berlin, Germany (*Abstract Co-Author*) Nothing to Disclose

Patrick Asbach, MD, Berlin, Germany (Abstract Co-Author) Nothing to Disclose

Samy Mahjoub, MD, Berlin, Germany (Abstract Co-Author) Nothing to Disclose

Hannes Cash, Berlin, Germany (Abstract Co-Author) Nothing to Disclose

Bernd K. Hamm III, MD, Berlin, Germany (*Abstract Co-Author*) Research Consultant, Canon Medical Systems Corporation; Stockholder, Siemens AG; Stockholder, General Electric Company; Research Grant, Canon Medical Systems Corporation; Research Grant, Koninklijke Philips NV; Research Grant, Siemens AG; Research Grant, General Electric Company; Research Grant, Elbit Imaging Ltd; Research Grant, Bayer AG; Research Grant, Guerbet SA; Research Grant, Bracco Group; Research Grant, B. Braun Melsungen AG; Research Grant, KRAUTH Medical KG; Research Grant, Boston Scientific Corporation; Equipment support, Elbit Imaging Ltd; Investigator, CMC Contrast AB

Tobias Penzkofer, MD, Berlin, Germany (*Abstract Co-Author*) Researcher, AGO; Researcher, Aprea AB; Researcher, Astellas Group; Researcher, AstraZeneca PLC; Researcher, Celgene Corporation; Researcher, Genmab A/S; Researcher, Incyte Coporation; Researcher, Lion Biotechnologies, Inc; Researcher, Takeda Pharmaceutical Company Limited; Researcher, Morphotec Inc; Researcher, Merck & Co, Inc; Researcher, Tesaro Inc; Researcher, F. Hoffmann-La Roche Ltd;

For information about this presentation, contact:

tobias.penzkofer@charite.de

PURPOSE

Our goal was to evaluate the novel scoring system in an intra-lesion comparison to the previous version 2 with respect to scoring variability, cancer detection and usage of the new prostate segments.

METHOD AND MATERIALS

3.0 T-MRI Datasets of 200 patients with MRI/TRUS biopsy (10-core systematic and targeted biopsies) were evaluated in a blinded / randomized setting. Lesions were marked and PI-RADS 2 and PI-RADS 2.1 assessment categories were assigned by one of three experienced radiologists (>5 years of reporting prostate MRI), with at least 6 months between the reading sessions. Tumor location and histopathology results were correlated and detection rates of clinically significant PCa (csPCa; >=Gleason 3+4) were tabulated against the scores for both versions.

RESULTS

214 lesions were identified and compared, 135 (63.1%) in the peripheral zone (PZ), 79 (36.9%) in the transition zone (TZ). There was no significant difference in the median PI-RADS 2 vs. 2.1 score (Wilcoxon signed rank PZ: p=0.8 and TZ: p=0.681). Distribution of PI-RADS-scores and csPCa detection rates for PI-RADS 2 vs 2.1 were: 1: 6 vs. 18 (16.7%/11.1%), 2: 51 vs. 31 (7.8%/12.9%), 3: 28 vs. 35 (17.9%/14.7%), 4: 60 vs. 59 (47.5%/44.1%), 5: 69 vs. 71 (62.3%/62.0%). Cohen's kappa for PI-RADS 2 vs. 2.1 was 0.568 and Cohen's weighted kappa was 0.78. Separated by zones detection rates were (PZ, PI-RADS 2/2.1) 1: 33.3%/22.2%, 2: 10.0%/16.7%, 3: 16.7%/14.3%, 4: 47.2%/47.1% and 5: 65.0%/63.4% and (TZ, PI-RADS 2/2.1) 1: 0.0%/0.0%, 2: 6.5%/10.5%, 3: 20.0%/15.4%, 4: 50.0%/25.0% and 5: 58.6%/60.0%. ROC analysis of the significant cancer detection accuracy revealed an AUC of 0.718 (CI 95% 0.631-0.0.805, PI-RADS 2) and 0.702 (0.613-0.791, PI-RADS 2.1) for peripheral zone lesions and 0.806 (0.706-0.907, PI-RADS 2) and 0.803 (0.702-0.904, PI-RADS 2.1) for transition zone cancers (p>0.05 for both comparisons). The new segments (Left/Right Base PZm) were marked in 5/135 (3.7%) of the PZ lesions.

CONCLUSION

Comparing PI-RADS 2 vs. 2.1 showed slight changes in the overall scoring with more pronounced changes in the lower scores and moderate to good intra-reader agreement between the two versions. ROC-performance remained stable at a high level for both PZ and TZ and the newly added segments are used in few instances.

CLINICAL RELEVANCE/APPLICATION

PI-RADS 2.1 introduces slight changes which should not prevent an immediate application of the new version.

SSK10-08 Diagnosis of Transition Zone Prostate Cancer: Comparison of the Prostate Imaging Reporting and Data System (PI-RADS) Version 2 and Version 2.1

Wednesday, Dec. 4 11:40AM - 11:50AM Room: N227B

Participants

Ayumu Kido, Kurashiki, Japan (*Presenter*) Nothing to Disclose Tsutomu Tamada, MD,PhD, Kurashiki, Japan (*Abstract Co-Author*) Nothing to Disclose Mitsuru Takeuchi, MD, PhD, Nagoya, Japan (*Abstract Co-Author*) Nothing to Disclose Takeshi Fukunaga, Kurashiki, Japan (*Abstract Co-Author*) Nothing to Disclose Kazuya Yasokawa, Kurashiki, Japan (*Abstract Co-Author*) Nothing to Disclose Akihiko Kanki, MD, Kurashiki, Japan (*Abstract Co-Author*) Nothing to Disclose Akira Yamamoto, MD, Kurashiki, Japan (*Abstract Co-Author*) Nothing to Disclose

For information about this presentation, contact:

ttamada@med.kawasaki-m.ac.jp

PURPOSE

To address limitations in the Prostate Imaging Reporting and Data System version 2 (PI-RADS v2), including interreader reproducibility and ambiguous assessment criteria for T2-weighted imaging of the transition zone (TZ), the PI-RADS Steering Committee developed an updated version (PI.RADS v2.1) in 2019. This study aimed to compare the diagnostic performance of PI-

RADS v2 and v2.1 for detecting TZ prostate cancer (TZPC) on multiparametric prostate MRI (mpMRI).

METHOD AND MATERIALS

This retrospective study received institutional review board approval. The participants comprised 58 patients with suspected TZPC who were undergoing MRI-ultrasound fusion-guided prostate-targeted biopsy (MRGB: at least two cores per MRI-targeted lesion) for a suspected TZ lesion after 3-T mpMRI, including T2-weighted imaging and diffusion-weighted imaging. The standard of reference was MRGB-derived histopathology. A lesion with Gleason score (GS) >= 7 or with GS = 3 + 3 and tumor size >= 0.5 mL (maximum tumor diameter >= 8 mm) was considered as clinically significant PC (csPC). Two readers independently assigned each TZ lesion with a score of 1-5 for T2WI, a score of 1-5 for DWI, and the overall PI-RADS assessment category according to PI-RADS v2 and v2.1. Diagnostic performance including diagnostic sensitivity, diagnostic specificity, and area under the ROC curve (AUC) were compared between the two methods using the McNemar and Delong tests.

RESULTS

Of the 58 patients, 26 were diagnosed with csPC (GS=3+3, 9; GS=3+4, 9; GS=3+5, 1; GS=4+3, 4; GS=4+4, 3) and 32 with benign lesions. Sensitivity between both methods did not differ (100% vs. 92%, p=0.50). Specificity and accuracy were significantly higher for v2.1 than for v2 (56% vs. 25%, p=0.002 and 72% vs. 59%, p=0.039, respectively). AUC tended to be higher in v2.1 than in v2, but the difference was not significant (0.859 vs. 0.799, p=0.062). In particular, PI-RADS v2.1 led to 10 false-positive results of category 3 in PI-RADS v2 being identified as true-negative results of category 2 in PI-RADS v2.1.

CONCLUSION

These observations suggest that PI-RADS v2.1 appears preferable for evaluating TZ lesions in comparison with PI-RADS v2.

CLINICAL RELEVANCE/APPLICATION

PI-RADS v2.1 is suggested to be a more suitable method for detecting csPC in TZ before prostate biopsy. The revisions of PI-RADS have steadily achieved standardization of qualitative assessment using mpMRI for csPC in the TZ.

SSK10-09 Zoomed EPI versus Conventional EPI DWI in Prostate Imaging: Impact on PIRADS Scoring and Cancer Detection

Wednesday, Dec. 4 11:50AM - 12:00PM Room: N227B

Participants

Ivan Platzek, MD, Dresden, Germany (*Presenter*) Nothing to Disclose Angelika Borkowetz, MD, Dresden, Germany (*Abstract Co-Author*) Nothing to Disclose Christian Thomas, Dresden, Germany (*Abstract Co-Author*) Nothing to Disclose Ralf-Thorsten Hoffmann, MD, Dresden, Germany (*Abstract Co-Author*) Nothing to Disclose Verena Plodeck, MD, Dresden, Germany (*Abstract Co-Author*) Nothing to Disclose

For information about this presentation, contact:

ivan.platzek@uniklinikum-dresden.de

PURPOSE

Conventional echoplanar (EPI) diffusion-weighted imaging (DWI) is prone to susceptibility artifacts. One possible alternative is zoomed EPI DWI, which has already been shown to reduce distortion artifacts compared to conventional DWI. The aim of this study was to evaluate the impact of zoomed EPI DWI on prostate cancer detection and lesion classification in multiparametric prostate MRI.

METHOD AND MATERIALS

Seventy-two patients (mean age 65 y, age range 46 - 84 y) with suspected prostate cancer who underwent prostate MRI at 3T were included in this retrospective study. Besides T2-weighted and dynamic contrast-enhanced (DCE) sequences, each exam included both conventional EPI DWI and zoomed EPI DWI. All patients had micro-enema before prostate MRI. Lesions were classified according to PIRADS v2. All 72 patients had prostate biopsy (combined systematic prostate biopsy and TRUS-guided prostate biopsy) and 14/72 patients also underwent prostatectomy. The sensitivity and specificity of mpMRI with conventional EPI (mpMRIc) or zoomed EPI DWI mpMRIz) were evaluated and compared using receiver operating characteristic (ROC) analysis, with the histopathological workup as the standard of reference.

RESULTS

75 lesions (in 52 patients) were identified on mpMRI (PIRADS 3 or higher). 32/75 lesions (42.7%) were located in the peripheral zone. Based on mpMRIc, 43/75 lesions (57.3%) were classified as PIRADS 3, 21/75 (28.0%) as PIRADS 4 and 11/75 (14,7%) as PIRADS 5. Based on mpMRIz, 52/75 lesions (69.3%) were rated as PIRADS 3, 14/75 (18.7%) as PIRADS 4 and 9/75 (12.0%) as PIRADS 5. No lesions were detected in 20 patients; in this case, the PIRADS score was set to 2. mpMRIc had a lesion-based sensitivity of 77.8% and a specificity of 93.7%, while mpMRIz DWI had a sensitivity of 55.6% and specificity of 95.2%. The accuracy of mpMRIz was significantly lower when compared to mpMRIc (p = 0.0064).

CONCLUSION

The accuracy of mpMRI with conventional EPI DWI for prostate cancer detection is superior to the accuracy of mpMRI with zoomed EPI DWI. Zoomed EPI DWI cannot be currently recommended for routine clinical prostate examinations.

CLINICAL RELEVANCE/APPLICATION

Our study shows that diffusion restriction in prostate cancer is less pronounced on zoomed EPI DWI when compared to conventional EPI DWI with identical b-values, leading to lower PIRADS scores and lower diagnostic accuracy.

Printed on: 10/29/20





SSK11

Genitourinary (Functional Renal Imaging and Contrast Issues)

Wednesday, Dec. 4 10:30AM - 12:00PM Room: N226

GU

AMA PRA Category 1 Credits ™: 1.50 ARRT Category A+ Credit: 1.75

FDA Discussions may include off-label uses.

Participants

Hilton M. Leao Filho, MD, Sao Paulo, Brazil (*Moderator*) Nothing to Disclose Olga R. Brook, MD, Boston, MA (*Moderator*) Nothing to Disclose Harris L. Cohen, MD, Memphis, TN (*Moderator*) Nothing to Disclose

Sub-Events

SSK11-01 The Effect of Iodinated Contrast Medium Volume on Post-Contrast Acute Kidney Injury after Contrast-Enhanced CT in 3,450 Patients

Wednesday, Dec. 4 10:30AM - 10:40AM Room: N226

Participants

Martin Koci, MD, Prague 5, Czech Republic (*Presenter*) Nothing to Disclose Anna Graber-Naidich, PhD, Stanford, CA (*Abstract Co-Author*) Nothing to Disclose Dominika Sucha, MD,PhD, Utrecht, Netherlands (*Abstract Co-Author*) Nothing to Disclose Domenico Mastrodicasa, MD, Stanford, CA (*Abstract Co-Author*) Nothing to Disclose Valery L. Turner, MD, Santiago, Chile (*Abstract Co-Author*) Nothing to Disclose Xingxing S. Cheng, MD, Palo Alto, CA (*Abstract Co-Author*) Nothing to Disclose Martin J. Willemink, MD,PhD, Mountain View, CA (*Abstract Co-Author*) Research Grant, American Heart Association; Research Grant, Koninklijke Philips NV; Consultant, Arterys Inc Dominik Fleischmann, MD, Stanford, CA (*Abstract Co-Author*) Research Grant, Siemens AG

For information about this presentation, contact:

mkoci@stanford.edu

PURPOSE

Iodinated contrast medium (CM) is still considered a risk factor for post-contrast acute kidney injury (PC-AKI), particularly in patients with chronic kidney disease and diabetes. However, the impact of the volume of intravenously administered CM has not been evaluated in a large population. The purpose of this work was to determine the association between CM-volume and the incidence of PC-AKI in patients who underwent contrast-enhanced computed tomography (CECT).

METHOD AND MATERIALS

This retrospective study included all patients who underwent CECT between May 2017 and November 2018 in a large academic medical center. All patients with at least one serum creatinine (SCr) value within 7 days before, and at least one SCr value within 24-96 hours after CECT were included. The primary outcome was PC-AKI, defined as >50% or >0.3mg/dL increase in SCr 24-96 hours after CECT. Patient demographics, the 35 most relevant diagnoses (coded according to The International Classification of Diseases 10), SCr, eGFR, and administered CM volume were extracted systematically searching the hospital electronic medical record system using a structured query language (SQL). Univariable and multivariable logistic regression analyses were performed.

RESULTS

In total, 3,450 patients were included. PC-AKI occurred in 207 patients (6.0%). Administered median CM volume was 98 mL (84-124, interquartile) in non PC-AKI, and 100 mL (85-130, interquartile) in PC-AKI. Univariable analyses showed that CM-volume normalized for weight (calculated as iodine dose/body weight) was not associated with PC-AKI (p=0.172). CM volume normalized for eGFR (calculated as iodine dose/eGFR) was associated with PC-AKI (OR 1.12 {1.03-1.21}, P=0.005). Similarly, diabetes mellitus (DM), atrial fibrillation (AF), and history of cerebral infarction were associated with PC-AKI in univariable analyses (all P<0.05). In multivariable models adjusted for age, gender and race, independent associations were found for DM, AF, and history of cerebral infarction (all P<0.05), while CM-volume normalized for eGFR was not independently associated with AKI (P>0.05).

CONCLUSION

In our retrospective cohort of 3,450 patients referred for CECT, the administered CM volume was not independently associated with PC-AKI.

CLINICAL RELEVANCE/APPLICATION

Our study suggests that typical volume of intravenously administered iodinated CM does not have an independent effect on the development of PC-AKI in patients referred for CECT.

SSK11-02 Development of Imaging Biomarkers of Contrast-Induced Nephropathy Using Contrast-Enhanced Ultrasound: An Animal Study

Participants Nieun Seo, MD, Seoul, Korea, Republic Of (*Presenter*) Nothing to Disclose Hyewon Oh, Seoul, Korea, Republic Of (*Abstract Co-Author*) Nothing to Disclose Yong Eun Chung, MD, PhD, Seoul, Korea, Republic Of (*Abstract Co-Author*) Nothing to Disclose

For information about this presentation, contact:

yelv@yuhs.ac

PURPOSE

To investigate imaging biomarkers of contrast induced nephropathy (CIN) using contrast enhanced ultrasound (CEUS)

METHOD AND MATERIALS

CIN model was made by administering indomethacin (10mg/kg), L-NAME (15mg/kg), and iopamidol (1ml/kg) in Spargue-Dawley male rats. After 24 hours, CEUS was performed in CIN rats (n=6) and control rats (n=6) with 12-5 MHz linear probe. Rats were injected with 0.6 ml of Sonovue (Bracco, Milano, Italy) via tail vein using infusion pump at a rate of 300 ml/hr and CEUS was recorded for 5 minutes from contrast agent injection. Image analysis was performed using dedicated software (QLAB, Philips Medical Systems) and peak enhancement (PE), time to peak enhancement (TTP), and acceleration time (AT) was measured and compared between two groups. After CEUS, the rats were sacrificed and blood and kidney tissue were harvested. Blood urea nitrogen (BUN) and creatinine (Cr) were measured to confirm the development of CIN. Cell apoptosis markers was assessed in kidney tissue. Morphological changes of tubular cells were evaluated by transmission electron microscopy (TEM). Statistical analysis was performed using Mannwhitney test and P<0.05 was considered as statistically significant.

RESULTS

BUN and Cr was significantly elevated in CIN model (BUN/Cr, 157±41/1.6±0.5 mg/dL) compared to control (15.5±3.3/0.3±0.0 mg/dL, P<0.001). Apoptotic maker (Bax/Bcl-2 level) was significantly higher in CIN model compared to control group (P<0.01). More cells were stained with cleaved caspase-3 immunohistochemical staining, suggesting more apoptotic cells in CIN model kidney tissue. On TEM, vacuole formation and mitochondrial expansion phenomenon was detected in CIN group. In terms of CEUS parameters, PE was significantly higher in control group (median, 15.9 dB; interquartile range[IQR], 3.6) than CIN group (13.1 dB; IQR, 5.1, P=0.043). TTP was significantly shorter in control group (6.9 sec; IQR, 4.0) compared to CIN group (11.8 sec; IQR, 3.9, P=0.008). AT was also significantly shorter in control group (2.3 sec; IQR, 1.2) than CIN group (4.2 sec; IQR, 1.9, P=0.003).

CONCLUSION

CEUS parameters including PE, TTP and AT can be used as an imaging biomarker of CIN. In the case of CIN, PE was decreased and both TTP and AT was prolonged.

CLINICAL RELEVANCE/APPLICATION

CEUS parameters can be used as a biomarker for the understanding pathophysiology of CIN and the development of prevention strategies of CIN.

SSK11-03 Chemical Exchange Saturation Transfer (CEST) and Magnetization Transfer (MT) Magnetic Resonance Imaging Helps Detect Metabolic and Structural Characteristics in an Animal Model of Renal Fibrosis

Wednesday, Dec. 4 10:50AM - 11:00AM Room: N226

Participants Angin Li, Wuhan, China (*Presenter*) Nothing to Disclose Zhen Li, MD, PhD, Wuhan, China (*Abstract Co-Author*) Nothing to Disclose Daoyu Hu, Wuhan, China (*Abstract Co-Author*) Nothing to Disclose

For information about this presentation, contact:

liangin11@hust.edu.cn

PURPOSE

To investigate the value of combined chemical exchange saturation transfer (CEST) and conventional magnetization transfer imaging (MT) in detecting the metabolic and structural characteristics of renal fibrosis in rats with unilateral ureteral obstruction (UUO).

METHOD AND MATERIALS

This prospective study was approved by the Institutional Laboratory Animal Ethics Committee. Thirty-five Sprague-Dawley rats underwent UUO surgery (n = 25) or sham surgery (n = 10). The obstructed and contralateral kidneys were evaluated on days 1, 3, 5 and 7 after surgery as cross-sectional or longitudinal study. After routine MRI, CEST and MT examinations, 18F-fluorodeoxyglucose (FDG) positron emission tomography (PET) was acquired to detect glucose metabolism. Fibrosis was subsequently measured by histologic and Western blot analysis. Pearson correlation analysis was used to compare correlations between asymmetrical magnetization transfer ratio at 1.2 ppm (MTRasym(1.2ppm)) and maximum standard uptake values (SUVmax), and between magnetization transfer ratio (MTR) and a-smooth muscle actin (a-SMA).

RESULTS

MTRasym(1.2ppm) and MTR of the UUO renal cortex and medulla on day 3 and day 7 were significantly different from those of the contralateral kidneys (all P < .05). MTRasym(1.2ppm) and MTR of the UUO renal cortex and medulla on day 7 were significantly different from those of the sham-operated kidneys (all P < .05). MTRasym(1.2ppm) of UUO kidneys medulla was fairly negative correlated with SUVmax (r = -0.350, P = .021), and MTR of UUO kidneys medulla was strongly negative correlated with a-SMA (r = -0.744, P < .001).

CEST and MT could provide molecular level metabolic and structural information for comprehensive assessment of renal fibrosis in UUO rats.

CLINICAL RELEVANCE/APPLICATION

In rat models of renal fibrosis, MTRasym(1.2ppm) correlated with SUVmax, and MTR correlated with a-SMA. Extrapolation of these finding from animal models to human subjects suggested that combined chemical exchange saturation transfer (CEST) and conventional magnetization transfer (MT) might potentially provide methods for diagnosis and characterization of renal fibrosis in patients with chronic kidney disease.

SSK11-04 Diagnostic Efficiency of Magnetization Transfer (MT) Technique in Staging of Diabetic Nephropathy

Wednesday, Dec. 4 11:00AM - 11:10AM Room: N226

Awards

Trainee Research Prize - Medical Student

Participants

Jing Chen, Xianyang City, China (*Presenter*) Nothing to Disclose Xirong Zhang, Xianyang, China (*Abstract Co-Author*) Nothing to Disclose Dong Han, MD, Xianyang, China (*Abstract Co-Author*) Nothing to Disclose Qi Yang, Xianyang, China (*Abstract Co-Author*) Nothing to Disclose Yan Li, Xianyang, China (*Abstract Co-Author*) Nothing to Disclose Shaoyu Wang, Shanghai, China (*Abstract Co-Author*) Nothing to Disclose Nan Yu, MD, Xianyang, China (*Abstract Co-Author*) Nothing to Disclose

For information about this presentation, contact:

345717558@qq.com

PURPOSE

To analyze the diagnostic efficiency of magnetization transfer (MT) technique in staging of diabetic nephropathy (DN).

METHOD AND MATERIALS

48 patients with DN were enrolled as the observation group in this study, and 35 healthy volunteers as the control group. Patients with DN were staged to I-IV according to eGFRs as well as renal function parameters (UAER,Scr,BUN) as a reference standard. All subjects underwent examination on a 3.0T MRI scanner (MAGNETOM Skyra, Siemens Healthcare, Erlangen, Germany) with an 18-channel body phased-array surface coil. A 3D fast low angle shot (FLASH) sequence was scanned for two times to acquire MT data, first time with a MT saturation pulse (MTon) and second time without (MToff). For MT quantification, the magnetization transfer rate (MTR) was calculated using following equation: MTR =(MToff-MTon)×100/MToff. MTR value was measured on the MT map of each subject using the region of interest method. Multiple regions of interest are drawn and averaged in the medullitary region of the upper kidney, renal hilum, and lower pole. The difference of MTR and laboratory examination in each stage were compared using one-way AVNON. The sensitivity and specificity of MTR value in the diagnosis of diabetic nephropathy at different stages were analyzed by ROC curve.

RESULTS

The MTR value of the cortex and medulla were gradually increasing with increase of DN stage (p<0.05). After ROC analysis, the MTR values of the renal cortex and medulla had a great preformance for distinguishing healthy control group from observation group, as well as in distinguishing DN VI stage group from other three groups with the area under the curve (AUC) of 0.988 and the sensitivity and specificity of 100.0% and 97.0%. The diagnostic efficiency of MTR values in renal cortex had no difference with AUC of 0.975 with the sensitivity and specificity of 94.1% and 95.4% (Delong's test, Z = 1.696, P = 0.090).

CONCLUSION

The MTR values of the renal cortex medulla have higher diagnostic efficiency in distinguishing the staging of DN, especially in identifying patients with severe diabetic nephropathy.

CLINICAL RELEVANCE/APPLICATION

MT can provide supplementary information for clinical staging about DN.

SSK11-05 Functional MR Imaging Evaluation of Renal Allograft: Role of Blood Oxygen Level Dependent (BOLD) MRI and Diffusion-Weighted (DW) MRI

Wednesday, Dec. 4 11:10AM - 11:20AM Room: N226

Participants Nitin P. Ghonge, MD, New Delhi, India (*Presenter*) Nothing to Disclose Kushal Tayade, MBBS,DMRD, New Delhi, India (*Abstract Co-Author*) Nothing to Disclose

For information about this presentation, contact:

drnitinpghonge@gmail.com

PURPOSE

To study the role of Blood Oxygen Level Dependent [BOLD] MRI and Diffusion weighted [DW] MRI in evaluation of Renal Allografts and their ability to differentiate normal allografts, acute allograft dysfunction [AAD] and chronic allograft dysfunction[CAD] and also to understand the correlation between R2* & ADC values and clinical / biopsy parameters.

METHOD AND MATERIALS

This prospective case-control study included 50 post renal transplant patients. Patients were segregated into three different categories - Normal allograft, AAD and CAD, based on pre-determined clinical criteria. BOLD MRI and DW MRI studies were

performed. Mean R2* and ADC values were analysed by Pearson correlation and were compared across groups using Kruskal Wallis test. All tests were performed with a two-tailed type-I error rate of P <0.05. A P< 0.05 was considered statistically significant. ROC curves were drawn to evaluate the feasibility of differentiation.

RESULTS

Out of 50 patients, 23 had normal allografts, 16 had acute graft dysfunction and 11 had chronic graft dysfunction. Mean R2* values in cortex and medulla were 24 \pm 2 and 26 \pm 2 in the normal allograft group, 18 \pm 2 and 15 \pm 2 in the AAD group and 41 \pm 4 and 40 \pm 5 in the CAD group. Mean ADC values in patients in the cortex and medulla were 2.38 \pm 0.08 and 2.37 \pm 0.10 in the normal allograft group, 1.99 \pm 0.11 and 1.92 \pm 0.16 in the AAD group and 1.69 \pm 0.13 and 1.67 \pm 0.11 in the CAD group. The higher the percentage of interstitial edema and tubular atrophy(as in acute dysfunction), lower are the R2* and ADC values. The higher the percentage of interstitial fibrosis and tubular atrophy(as in chronic graft dysfunction), lower the ADC value and higher the R2* value. R2* values were significantly reduced in cortex and medulla (p value < 0.001) in AAD group.

CONCLUSION

BOLD MRI-based R2* and DW MRI-based ADC values in renal cortex and medulla significantly correlate with renal functions and biopsy findings and are likely to be useful in detection of allograft dysfunction and in differentiation of normal allograft from AAD. The role in differentiation of AAD and CAD was not found to be significant.

CLINICAL RELEVANCE/APPLICATION

BOLD MRI and DW MRI techniques are fast, non-invasive and does not require contrast injection. These functional MRI parameters [R2*and ADC] are therefore likely to emerge as useful additional imaging options for prompt diagnosis of allograft dysfunction in post renal transplant patients.

SSK11-06 Evaluation of Fourier Decomposition MRI for the Assessment of Perfusion Properties of the Human Kidney: Initial Results

Wednesday, Dec. 4 11:20AM - 11:30AM Room: N226

Participants

Alexandra Ljimani, MD, Dusseldorf, Germany (*Presenter*) Nothing to Disclose Femke Reurik, Dusseldorf, Germany (*Abstract Co-Author*) Nothing to Disclose Julia Stabinska, Dusseldorf, Germany (*Abstract Co-Author*) Nothing to Disclose Anja Lutz, Dusseldorf, Germany (*Abstract Co-Author*) Nothing to Disclose Gerald Antoch, MD, Dusseldorf, Germany (*Abstract Co-Author*) Nothing to Disclose Hans-Jorg Wittsack, Duesseldorf, Germany (*Abstract Co-Author*) Nothing to Disclose

PURPOSE

To evaluate Fourier decomposition MRI (FD) in comparison to arterial spin labeling (ASL) for the assessment of renal perfusion properties in healthy subjects and patients with unilateral renal artery stenosis (RAS) (80-90%).

METHOD AND MATERIALS

Fifteen healthy volunteers (mean age 33.0±10.1 years) and five patients with unilateral RAS (mean age 58.4±16.2 years) were examined on a 1.5 T whole-body MR-scanner (Magnetom Avanto, Siemens Healthineers AG) with a non-contrast enhanced dynamic 2D-TrueFISP sequence (TR/TE 2.06/0.89 ms, acquisition time 180 ms/image, 250 images) and FAIR-TrueFisp ASL sequence (TR/TE 4.0/2.0 ms, TI 1200 ms, 30 averages) in coronal direction. The acquisition time for FD was 1.30 min and ASL 4.16 min, respectively. No ECG or respiratory triggering was used. Image registration algorithm (fMRLung 3.0, Siemens Corporate Research) was performed to compensate the spatial variation of the renal structure. Perfusion parameter maps were calculated for FD and ASL. Perfusion values were determined over the whole organs. Renal perfusion determined by FD and ASL was calculated for healthy subjects and separated for each kidney of the RAS patients. All results were compared using the student t-test.

RESULTS

The average renal perfusion of healthy volunteers was for the right kidney FD 275,4 \pm 137,2 ml/100ml/min, ASL 277,2 \pm 159,9 ml/100ml/min and for the left kidney FD 278,1 \pm 158,1 ml/100ml/min, ASL 319,4 \pm 157,2 ml/100ml/min, respectively. There was no significant difference in renal perfusion measured by FD or ASL in healthy volunteers (p>0.05). However, significant difference in side separate renal perfusion could be measured as well by FD as by ASL of patients with unilateral RAS (p<0.05).

CONCLUSION

FD seems to be an appropriate method for rapid measurement of the renal perfusion. Due to the fast acquisition time, the perfusion measurement by FD can easily be attached to any clinical protocol. Renal perfusion measured by FD shows comparable results to the already established ASL method. Alterations of renal perfusion, as unilateral RAS, further can be detected by the new FD method. Further studies are required to determine the clinical value of FD for functional renal imaging.

CLINICAL RELEVANCE/APPLICATION

FD is novel promising approach for rapid assessment of renal perfusion and might improve functional renal MR imaging in future.

SSK11-07 Assessment of Obstructive Renal Injury with Magnetic Resonance Arterial Spin Labeling: An Experimental Study in a Rat of Unilateral Ureteral Obstruction

Wednesday, Dec. 4 11:30AM - 11:40AM Room: N226

Participants

Genwen Hu, MD, Shenzhen, China (*Presenter*) Nothing to Disclose Shuyuan Zhong, Shenzhen, China (*Abstract Co-Author*) Nothing to Disclose Xiaoting Wei, MD, MD, Shenzhen, China (*Abstract Co-Author*) Nothing to Disclose Jinsen Zou, MD, Shenzhen, China (*Abstract Co-Author*) Nothing to Disclose Zhong Yang, Shenzhen, China (*Abstract Co-Author*) Nothing to Disclose Jianmin Xu, Shenzhen, China (*Abstract Co-Author*) Nothing to Disclose

For information about this presentation, contact:

hugenwen@163.com

PURPOSE

To investigate the potential of magnetic resonance arterial spin labeling (ASL) in assessment of obstructive renal injury in a rat model of Unilateral Ureteral Obstruction (UUO).

METHOD AND MATERIALS

This study was approved by the institutional animal care and use committee. UUO was created in each left kidney of 40 rats. Eight rats from the model group (n=40) were scanned at each of the five time points (on days 1, 2, 3, 4, 5 after UUO) and then sacrificed for histological examination. Contralateral kidneys were examined as controls. Another eight rats were examined before the onset of UUO to get the baseline data. Hematoxylin-eosin, Masson and a-smooth muscle actin (a -SMA) staining assays were performed. For quantification of renal blood flow (RBF) from a 3.0T scanner, a combination of flow-alternating inversion-recovery (FAIR) labeling scheme and EPI readout was carried out with following parameters for both global (control) and slice-selective (label) inversion: TR/TE: 3000/35ms; TI: 1200ms; FOV: 60×60mm2; matrix: 76×58; slice thickness: 4mm; NSA: 10. RBF were analyzed and correlated with the histopathological results.

RESULTS

Histopathologic examination revealed renal fibrosis of obstructive renal injury on the side with UUO. RBF with ASL of the obstructive lateral kidney decreased gradually with the prolongation of obstruction. Mean RBF with ASL of the left kidney with days 1, 2, 3, 4, 5 after the UUO were 187.33 ± 31.03 , 174.83 ± 24.01 , 111.54 ± 30.03 , 91.44 ± 29.93 , 86.19 ± 22.93 ml/100g/min, respectively, while the baseline data was 292.36±16.54 ml/100g/min. The RBF with day 1 after UUO significantly decreased in comparison to the control (p< 0.01). The expression of a-SMA in renal interstitial tissue increased gradually after UUO. RBF with ASL of the obstructive lateral kidney was negatively correlated with the positive expression of a -SMA (r = -0.72, p<0.01).

CONCLUSION

In this model, obstructive renal injury in the early phase was detected with magnetic resonance ASL; the degree of renal fibrosis was correlated with the degree of decrease in RBF.

CLINICAL RELEVANCE/APPLICATION

ASL may be a new kind of noninvasive technique to show the change of RBF in the process of obstructive renal injury and even other diseases, reflecting pathophysiological changes in early stage.

SSK11-08 Non-invasive Measurements of Circadian Variations in Renal Blood Flow Linked to Urinary Output Parameters

Wednesday, Dec. 4 11:40AM - 11:50AM Room: N226

Participants

Per Eckerbom, Uppsala, Sweden (*Presenter*) Nothing to Disclose Eleanor Cox, Nottingham, United Kingdom (*Abstract Co-Author*) Nothing to Disclose Jan Weis, PhD, Uppsala, Sweden (*Abstract Co-Author*) Nothing to Disclose Charlotte Buchanan, Nottingham, United Kingdom (*Abstract Co-Author*) Nothing to Disclose Peter Hansell, PhD, Uppsala, Sweden (*Abstract Co-Author*) Nothing to Disclose Fredrik Palm, PhD, Uppsala, Sweden (*Abstract Co-Author*) Nothing to Disclose Susan Francis, PhD, Nottingham, United Kingdom (*Abstract Co-Author*) Nothing to Disclose Per Liss, MD, PhD, Uppsala, Sweden (*Abstract Co-Author*) Nothing to Disclose

For information about this presentation, contact:

per.eckerbom@radiol.uu.se

PURPOSE

In humans, numerous processes are influenced by a circadian rhythm. This also applies to the kidneys and recent years has seen a growing interest in this field. The novel MRI tehchniques Phase contrast (PC), Arterial Spin Labelling (ASL) and Blood Oxygen Level Dependent (BOLD) have made it possible to study renal perfusion and oxygenation non-invasively giving a number of advantages such as no risk for contrast induced conditions and short-time repeatability. In this study we studied total and regional renal perfusion and regional renal oxygenation over 24 hours linked to urinary output parameters in healthy volunteers.

METHOD AND MATERIALS

Sixteen healthy volunteers (8 female), mean age 23 years were repeatedly scanned at 3T using a scan protocol including PC, ASL and BOLD sequences every fourth hour for 24 hours. Subjects received a urinary catheter to measure urine output parameters (urine production, excretion of Na+, K+, protein, creatinine and urea) during the study. In each subject, both kidneys were analyzed regarding total renal blood flow, regional (cortex, outer and inner medulla) perfusion and regional oxygenation.

RESULTS

Significant circadian variations were found for total renal blood flow measured by PC MRI with increased flow from noon to midnight and thereafter decreasing flow to the morning hours. For regional renal perfusion measured by ASL no significant circadian variations could be seen although a similar pattern as for total renal blood flow was seen for cortical perfusion. For oxygenation by BOLD, no significant circadian variations could be seen. For urinary parameters significant circadian variations could be seen for urine production, excretion of Na+, K+, Creatinine and Urea, all of them showing decreasing values during the night hours. Urinary protein excretion also showed decreasing values during the night but this was not found to be statistically significant.

CONCLUSION

In this study we were able to detect circadian variations in total renal blood flow using non-invasive PC MRI. The circadian renal blood flow pattern correlated well to the circadian pattern of a number of urinary parameters also measured. For regional renal perfusion and oxygenation, no significant circadian variations could be detected.

CLINICAL RELEVANCE/APPLICATION

Knowledge of circadian variations of renal blood flow could be important for future studies/clinical applications dealing with renal blood flow alterations.

SSK11-09 Optimizing Renal CT Angiography Using 80kV and Iterative Reconstruction: Reducing Radiation Dose and Reducing Contrast Agent with Improving Image Quality

Wednesday, Dec. 4 11:50AM - 12:00PM Room: N226

Participants

Zhanli Ren, Xianyang, China (*Presenter*) Nothing to Disclose Yun Shen, PhD, Beijing, China (*Abstract Co-Author*) Employee, General Electric Company Researcher, General Electric Company Jun Gu Sr, Beijing, China (*Abstract Co-Author*) Nothing to Disclose He Taiping, MMed, Xianyang, China (*Abstract Co-Author*) Nothing to Disclose Dou Li, Xian, China (*Abstract Co-Author*) Nothing to Disclose Zhijun Hu SR, Xi'an, China (*Abstract Co-Author*) Nothing to Disclose Guangming Ma, Xianyang, China (*Abstract Co-Author*) Nothing to Disclose Chenglong Ren, Shanxi, China (*Abstract Co-Author*) Nothing to Disclose Lihua Fan, Xianyang, China (*Abstract Co-Author*) Nothing to Disclose Lanxin Zhang, Xianyang, China (*Abstract Co-Author*) Nothing to Disclose Chunyu Gu, Xianyang, China (*Abstract Co-Author*) Nothing to Disclose Bunyu Gu, Xianyang, China (*Abstract Co-Author*) Nothing to Disclose Lanxin Zhang, Xianyang, China (*Abstract Co-Author*) Nothing to Disclose Chunyu Gu, Xianyang, China (*Abstract Co-Author*) Nothing to Disclose Bunyu Gu, Xianyang, China (*Abstract Co-Author*) Nothing to Disclose Chunyu Gu, Xianyang, China (*Abstract Co-Author*) Nothing to Disclose Bung Han, MD, Xianyang, China (*Abstract Co-Author*) Nothing to Disclose Wei Gao, Xianyang, China (*Abstract Co-Author*) Nothing to Disclose

PURPOSE

To explore the application of using 80 kV and iterative reconstruction in reducing radiation dose and reducing contrast agent with improving image quality to optimize renal CT angiography.

METHOD AND MATERIALS

Seventy patients for renal CT angiography were prospectively collected and randomly divided into group A and group B. Group A used 120kV tube voltage and 600mgI/kg contrast agent, and was reconstructed with 40%ASIR. Group B used 80kV tube voltage and 350mgI/kg contrast agent, and was reconstructed with ASIR-V from 40% to 100% with 10% interval. The CT values and standard deviation (SD) of right renal artery, left renal artery were measured to calculate the signal-to-noise ratio (SNR) and contrast-to-noise ratio (CNR) for renal arteries. The image quality was subjectively scored by two experienced radiologists blindly using a 5-point system. The effective dose (ED) and total contrast agent was calculated.

RESULTS

There was no significant difference in population characteristics between the two groups (p>0.05). Group B had significantly lower contrast agent (21.74±3.08g) (reduced by 43.0%) and effective radiation dose(2.10±0.20mSv) (reduced by 67.1%) than those in group A (38.11±3.74g and $6.39\pm1.76mSv$) (p<0.001). The CT values of renal arteries in group B with any reconstructions were slightly higher than those in group A, but the difference was not statistically significant (P>0.05). Compared with 40%ASIR reconstruction in group A, the SD values of renal arteries with 60%ASIR-V to 100%ASIR-V in group B were significantly lower (p<0.001), and the SNR values with 60%ASIR-V to 100%ASIR-V and the CNR values with 70%ASIR-V to 100%ASIR-V in group B were significantly higher(P < 0.001). The subjective scores on image quality by two radiologists had excellent agreement (Kappa>0.75,P<0.05), and subjective scores with 50%ASIR-V to 100%ASIR-V in group B were significantly higher than 40%ASIR in group A, and 70%ASIR-V provided the highest subjective score.

CONCLUSION

In renal CT angiography, using 80 kV and iterative reconstruction can improve image quality and significantly reduce radiation dose and contrast agent at the same time.

CLINICAL RELEVANCE/APPLICATION

Using 80kV and iterative reconstruction can provide better image quality and lower radiation dose and contrast agent for renal CT angiography, which help to optimize the scanning protocol of renal CT angiography.

Printed on: 10/29/20





SSK12

Health Service, Policy and Research (Value, Outcomes, and Risk)

Wednesday, Dec. 4 10:30AM - 12:00PM Room: S104A



AMA PRA Category 1 Credits ™: 1.50 ARRT Category A+ Credit: 1.75

FDA Discussions may include off-label uses.

Participants

Fabian Bamberg, MD, Tuebingen, Germany (*Moderator*) Speakers Bureau, Bayer AG Speakers Bureau, Siemens AG Research Grant, Siemens AG

Hanna M. Zafar, MD, Philadelphia, PA (*Moderator*) Nothing to Disclose K. Pallav Kolli, MD, San Francisco, CA (*Moderator*) Investor, Adient Medical Inc

Sub-Events

SSK12-01 Patient-Reported Financial Toxicity in Multiple Sclerosis: Predictors and Association with Neuroimaging and Medication Non-Adherence

Wednesday, Dec. 4 10:30AM - 10:40AM Room: S104A

Participants

Gelareh Sadigh, MD, Atlanta, GA (*Presenter*) Nothing to Disclose Neil Lava, MD, Atlanta, GA (*Abstract Co-Author*) Nothing to Disclose Jeffrey Switchenko, PhD, Atlanta, GA (*Abstract Co-Author*) Nothing to Disclose Richard Duszak JR, MD, Atlanta, GA (*Abstract Co-Author*) Nothing to Disclose Elizabeth A. Krupinski, PhD, Atlanta, GA (*Abstract Co-Author*) Nothing to Disclose Carolyn C. Meltzer, MD, Atlanta, GA (*Abstract Co-Author*) Nothing to Disclose Danny Hughes, PhD, Reston, VA (*Abstract Co-Author*) Nothing to Disclose Ruth C. Carlos, MD, MS, Ann Arbor, MI (*Abstract Co-Author*) Editor, Journal of the American College of Radiology; Support, Harvey L. Neiman Health Policy Institute; In-kind support, Reed Elsevier;

For information about this presentation, contact:

gsadigh@emory.edu

PURPOSE

To assess health-related financial toxicity in multiple sclerosis (MS) patients and its impact on financial coping strategies and care non-adherence.

METHOD AND MATERIALS

Adult patients with new or established diagnoses of MS visiting an outpatient neurology clinic were prospectively recruited. Financial toxicity at study entry was measured using the Comprehensive Score for Financial Toxicity Patient-Reported Outcome Measure (COST) score (range 0-44, the lower the COST score, the worse the financial toxicity). Linear regression identified independent sociodemographic, clinical, and insurance correlates of financial toxicity. Financial coping strategies and care nonadherence within 3 months prior to study entry were assessed in those with established diagnoses.

RESULTS

A total of 242 patients were recruited (44yo [95%CI,42-45]; 77% female; 47% White), median months from diagnosis, 62 (IQR,28-120). 94% have established diagnoses; 87% with relapsing remitting MS. The mean Expanded Disability Status Scale score among participants was 1.8 (95%CI,1.5-2.1) corresponding to the ability to walk without any aid. Mean enrollee COST score was 17 (95%CI,16-18.5), with 21% having at least one emergency department visit or inpatient hospitalization in the 3 months prior to entry. In response to financial burden, 62% used at least one financial coping strategy (see fig. 1). Medication and imaging nonadherence were reported by 30% and 13% of patients. In multivariable analyses, the key correlate of lower financial toxicity (i.e. higher COST score) was higher financial self-efficacy (e.g., having more confidence in being able to manage money to last for a lifetime) (coefficient 1.27 [95%CI, 1.02-1.52]; p<0.001). COST scores correlated with health-related quality of life, financial coping strategy use and care non-adherence (p<0.001).

CONCLUSION

Patients with MS are at high risk for financial toxicity, which impacts quality of life, and results in adopting financial coping strategies and care non-adherence.

CLINICAL RELEVANCE/APPLICATION

Identifying MS patients at risk for financial toxicity will help target interventions to cope with financial burden, and may improve both quality of life and treatment adherence.

SSK12-02 Financial Burden of Advanced Imaging in Radiology (FAIR Study)

Participants

Paniz Charkhchi, MD, Ann Arbor, MI (Presenter) Nothing to Disclose

Kemi Omotoso, Ann Arbor, MI (Abstract Co-Author) Nothing to Disclose

A. Mark Fendrick, MD, Ann Arbor, MI (*Abstract Co-Author*) Consultant, Abbott Laboratories Consultant, AstraZeneca PLC Consultant, sanofi-aventis Group Consultant, F. Hoffmann-La Roche Ltd Consultant, GlaxoSmithKline plc Consultant, Merck & Co, Inc Consultant, Neocure Group LLC Consultant, Pfizer Inc Consultant, POZEN Inc Consultant, Precision Health Economics LLC Consultant, The TriZetto Group, Inc Consultant, Zanzors Speakers Bureau, Merck & Co, Inc Speakers Bureau, Pfizer Inc Researcher, Abbott Laboratories Researcher, AstraZeneca PLC Researcher, sanofi-aventis Group Researcher, Eli Lilly and Company Researcher, F. Hoffmann-La Roche Ltd Researcher, GlaxoSmithKline plc Researcher, Merck & Co, Inc Researcher, Novartis AG Researcher, Pfizer Inc

Diana M. Gomez-Hassan, MD, PhD, Ann Arbor, MI (Abstract Co-Author) Nothing to Disclose

Ruth C. Carlos, MD, MS, Ann Arbor, MI (*Abstract Co-Author*) Editor, Journal of the American College of Radiology; Support, Harvey L. Neiman Health Policy Institute; In-kind support, Reed Elsevier;

For information about this presentation, contact:

panizcharkhchi@gmail.com

PURPOSE

Imaging encounters suffer from lack of price transparency and surprise billing for patient cost share, exposing vulnerable individuals to financial harm. Financial burden contributes to medical debt and care nonadherence. Despite the need, financial fragility screening is heterogeneously implemented. We assess acceptability of financial screening and estimate financial burden among those receiving advanced imaging (CT/MRI) in outpatient imaging settings at a single institution.

METHOD AND MATERIALS

We conducted a cross sectional anonymous survey of those >=22 years receiving advanced imaging at outpatient imaging clinics (n=5). To assess financial burden, we queried imaging out of pocket cost (OOP) worry, use of financial coping strategies and care nonadherence due to medical cost. Logistic regression assessed effects of demographics, chronic disease, pretest OOP notification recall and imaging OOP worry on financial coping and care nonadherence. We included an interaction term for recall and worry.

RESULTS

97% of surveys from consecutive patients had at least one question answered (Fig. 1). 66% of respondents were comfortable answering items about financial well-being in imaging clinic. 18% recalled being notified of the OOP prior to exam. 35% used at least one financial coping strategy; key correlates: test OOP worry (OR=5.2, 95%CI=2.5-11.0), worry x recall, (OR=4.7, 95%CI=1.1-19.8) income >\$50K (OR=0.3, 95%CI=0.1-0.7), any chronic disease (OR=3.7, 95%CI=1.8-7.5). 10% reported at least one nonadherence event; correlates: test OOP worry (OR=9.6, 95%CI=3.3-28) and ACA insurance (OR=19.1, 95%CI=1.2-297).

CONCLUSION

Financial coping strategies among those who responded to financial screening is common; care non-adherence, less so. Psychological worry about OOP highly correlated with both outcomes, suggesting that screening for financial worry may identify patients at high risk for using savings or assuming debt for care. Further, OOP recall magnifies the effect of worry on financial coping. A large minority declined to answer financial questions, suggesting that screening in the imaging outpatient setting will incompletely capture financial burden in this population.

CLINICAL RELEVANCE/APPLICATION

Outpatient imaging represents an appropriate venue for implementing financial screening and referral of financially vulnerable individuals. Price transparency interventions may intensify OOP worry.

SSK12-03 Comparative Effectiveness of Active Surveillance for Localized Prostate Tumors With versus Without MRI: A Decision Analysis

Wednesday, Dec. 4 10:50AM - 11:00AM Room: S104A

Participants

Stella Kang, MD,MSc, New York, NY (*Abstract Co-Author*) Royalties, Wolters Kluwer nv Rahul D. Mali, MBBS,MPH, New York, NY (*Presenter*) Nothing to Disclose Stacy Loeb, MD,MSc, New York, NY (*Abstract Co-Author*) Consultant, Eli Lilly and Company; Consultant, General Electric Company; Consultant, Bayer AG; Consultant, Lumenis Ltd; Equity, Gilead Sciences, Inc; Travel support, sanofi-aventis Group

For information about this presentation, contact:

stella.kang@nyulangone.org

PURPOSE

To evaluate different active surveillance (AS) strategies for prostate tumors with versus without MRI by comparing quality-adjusted life expectancy (QALE) and life expectancy (LE), given non-uniform practice of surveillance.

METHOD AND MATERIALS

We constructed a state-transition cohort model to compare QALE and LE of surveillance strategies in hypothetical men aged 60 years with low-grade prostate cancer. Strategies included: 1) watchful waiting (no testing; treat symptomatic disease only); 2) PSA every 6 months and annual biopsy; 3) requisite annual MRI, annual biopsy regardless of MRI result; 4) requisite annual MRI and annual biopsy only if PI-RADS score >=3; 5) requisite annual MRI and biopsy only if PI-RADS score >=3; and 7) PSA every 6 months, MRI according to the PRIAS protocol (at years 1, 3, 7, 10, and then every 5 years), and biopsy only if PI-RADS score >=4. We incorporated age, comorbidity, misclassification of cancer grade, cancer progression risks, and ending surveillance at age 75. Sensitivity analysis assessed the impact of varying parameter values on results.

In 60-year-old men, QALE and LE were the highest and essentially equivalent in two surveillance strategies: annual MRI with biopsy of lesions with PI-RADS >=4, and annual MRI with annual biopsy regardless of MRI results (both with 22.10 quality-adjusted life years; 23.05 life years). These strategies using annual MRI yielded a benefit compared with no MRI (i.e. PSA every 6 months and annual biopsy) in terms of both QALE (+12 days) and LE (+7 days). AS extended LE compared with watchful waiting at all ages. However, AS yielded higher QALE than watchful waiting only until age 62. This age threshold was driven by increasing rates and severity of treatment complications with age, and less frequent MRI using the PRIAS schedule as well as a higher PI-RADS biopsy threshold did not extend QALE over watchful waiting.

CONCLUSION

AS with annual MRI and biopsy of only lesions with PI-RADS score >=4 yields essentially equivalent QALE and LE compared with annual MRI and biopsy in men with low-grade prostate tumors, allowing for preference-based decisions.

CLINICAL RELEVANCE/APPLICATION

In active surveillance of prostate tumors, annual MRI with a biopsy threshold of PI-RADS 4 provides similar effectiveness than more frequent biopsy, and greater effectiveness than surveillance without MRI.

SSK12-04 PET/CT Utilization of Non-Small Cell Lung Cancer at Diagnosis: Does it Impact Survival?

Wednesday, Dec. 4 11:00AM - 11:10AM Room: S104A

Participants

Rustain L. Morgan, MD, MS, Aurora, CO (*Presenter*) Nothing to Disclose Megan Eguchi, MPH, Aurora, CO (*Abstract Co-Author*) Nothing to Disclose Sruthi Yekkaluri, MPH, Aurora, CO (*Abstract Co-Author*) Nothing to Disclose Sana D. Karam, MD, PHD, Aurora, CO (*Abstract Co-Author*) Nothing to Disclose Cathy Bradley, PhD, Aurora, CO (*Abstract Co-Author*) Nothing to Disclose

PURPOSE

The type of imaging utilized to stage a patient with newly diagnosed non-small cell lung cancer impacts their cancer specific survival.

METHOD AND MATERIALS

The linked Surveillance, Epidemiology, and End Results (SEER)-Medicare database between 2007 and 2015 was used to compare patient characteristics and hospital region by initial imaging modality used for patients with non-small cell lung cancer. The primary outcome was 3-year cancer specific survival (CSS). Cox proportional hazard models adjusted for imaging, age, sex, region, education, race, cancer stage, and treatment, which were examined by backward elimination. We also explored how initial imaging use varied by patient characteristics and hospital region.

RESULTS

Thirty-six thousand, four hundred seventy one patients with newly diagnosed non-small cell lung cancer underwent initial diagnostic imaging. Of those, 24.4% (n=8,884) received CT alone as their initial imaging modality, 2.4% (n=887) underwent only PET imaging, and 71.9% (n=26,700) of the patients' initial imaging included both a PET and CT exam. In the adjusted survival models compared by initial imaging modality, patients who underwent a PET exam with or without CT had better cancer specific survival than CT alone, (hazard ratio [HR] 0.66; 95% CI 0.638-0.682; P =<0.001) (HR 0.611 95% CI 0.55-0.678; P = <0.001) respectively. The overall survival was also significantly improved with PET and diagnostic CT or PET alone (hazard ratio [HR] 0.671; 95% CI 0.651-0.692; P =<0.001) and (hazard ratio [HR] 0.604; 95% CI 0.551-0.662; P =<0.001) respectively, when compared to patients who only received CT imaging.

CONCLUSION

Among patients with non-small cell lung cancer, initial staging that included PET imaging was associated with improved three-year cancer specific and overall survival compared to initial staging with CT alone.

CLINICAL RELEVANCE/APPLICATION

Utilization of PET/CT imaging at diagnosis of non-small cell lung cancer improves survival, however approximately a quarter of patients are not receiving this imaging.

SSK12-05 Are We in Agreement? Outcomes of Pathology Results Discordant with Imaging Findings After CT-Guided Biopsy

Wednesday, Dec. 4 11:10AM - 11:20AM Room: S104A

Participants Andres Camacho, MD, Boston, MA (*Presenter*) Nothing to Disclose Andrew D. Chung, MD, Kingston, ON (*Abstract Co-Author*) Nothing to Disclose Mehmet Sari, Boston, MA (*Abstract Co-Author*) Nothing to Disclose Sujithraj Dommaraju, MBBS, Boston, MA (*Abstract Co-Author*) Nothing to Disclose Elisabeth Appel, MD, Dusseldorf, Germany (*Abstract Co-Author*) Nothing to Disclose Alexander Brook, PhD, Boston, MA (*Abstract Co-Author*) Nothing to Disclose Bettina Siewert, MD, Boston, MA (*Abstract Co-Author*) Editor, Wolters Kluwer nv; Reviewer, Wolters Kluwer nv; Muneeb Ahmed, MD, Boston, MA (*Abstract Co-Author*) Research Grant, General Electric Company Stockholder, Agile Devices, Inc Scientific Advisory Board, Agile Devices, Inc Olga R. Brook, MD, Boston, MA (*Abstract Co-Author*) Nothing to Disclose

For information about this presentation, contact:

obrook@bidmc.harvard.edu

To assess the value of radiology review meetings (RRMs) evaluating concordance between pathology results and imaging findings of CT-guided biopsy.

METHOD AND MATERIALS

In this HIPAA-compliant, IRB retrospective review, 926 consecutive unique body CT-guided biopsies performed between 01/15-12/17 were included. Weekly RRM was implemented in July 2016. 453 patients were reviewed in the RRM (prospective group), and results were classified as concordant or discordant with appropriate recommendations generated by radiology team. 473 patients not reviewed at RRMs were retrospectively classified by an abdominal imaging clinical fellow (retrospective group). Times to reintervention (TRI) and times to definitive diagnosis (TDD) were obtained for discordant cases: 49/453 (11%) in prospective (n=2, lost to follow-up) and 55/473 (12%) in retrospective group (n=5, lost to follow-up).

RESULTS

CT-guided biopsy yielded a concordant result in 89% (822/926) of the cases. Re-intervention with biopsy and surgery yielded a shorter time to the definitive diagnosis compared to clinical and imaging follow up (p<0.001). When radiologists evaluated concordance between pathology and imaging findings and recommended re-biopsy for discordant cases, the number of biopsies performed as re-intervention is increased (50%, 11/22 vs. 13%, 4/31; p=0.005). Referring physicians tend to follow recommendations for re-biopsy provided by radiologists, while when no recommendations are provided by radiologists they tend to choose imaging follow-up or surgery instead (64%, 30/47 vs. 38%, 19/50; p=0.011). Unfortunately, 49% (23/47) of the cases were discussed by the referring physician with the patient before review at weekly RRM by radiologist. This may explain why even in the prospective group clinicians did not always pursue re-biopsy even if recommended by radiologist.

CONCLUSION

Radiologists frequently recommend re-biopsy for cases with discordant findings on imaging versus pathology. In cases without radiology input, clinicians tend toward clinical and imaging follow-up instead of re-biopsy. Re-intervention with biopsy or surgery results in shorter time to diagnosis. This provides yet another reason for radiologists to be more involved in patient care.

CLINICAL RELEVANCE/APPLICATION

Radiologist's participation in pathology results review after CT-guided biopsy results in higher rate of re-biopsy for discordant cases and thus shortens average time to diagnosis.

SSK12-06 Assessing Cancer Yield and Compliance with 6-, 12-, (18-) and 24-month Follow-Up for BI-RADS 3 Lesions at Recall from Screening for Women in the National Mammography Database (NMD)

Wednesday, Dec. 4 11:20AM - 11:30AM Room: S104A

Participants

Wendie A. Berg, MD, PhD, Gibsonia, PA (*Presenter*) Nothing to Disclose Jeremy M. Berg, PhD, Gibsonia, PA (*Abstract Co-Author*) Nothing to Disclose Robert D. Rosenberg, MD, Albuquerque, NM (*Abstract Co-Author*) Nothing to Disclose Elizabeth S. Burnside, MD,MPH, Madison, WI (*Abstract Co-Author*) Research Grant, Hologic, Inc Edward A. Sickles, MD, San Francisco, CA (*Abstract Co-Author*) Nothing to Disclose Margarita L. Zuley, MD, Pittsburgh, PA (*Abstract Co-Author*) Investigator, Hologic, Inc Cindy S. Lee, MD, Garden City, NY (*Abstract Co-Author*) Nothing to Disclose

For information about this presentation, contact:

wendieberg@gmail.com

PURPOSE

Probably benign, BI-RADS 3 (BR3) assessments are reserved for specific imaging findings known to have $\leq 2\%$ likelihood of malignancy. We assessed compliance, outcome and cancer yield after BR3 assessments at 6-, 12-, (18-) and 24-month follow-up.

METHOD AND MATERIALS

This retrospective cohort HIPAA-compliant study included all women recalled from screening mammography followed by BR3 assessment at additional evaluation from 2009 to 2018, from 471 NMD facilities. Only the first BI-RADS 3 occurrences were analyzed for women \geq age 25 with no reported personal history of breast cancer with biopsy or \geq 2-yr imaging follow-up, or downgraded to BI-RADS 1 or 2 with \geq 1-yr follow-up. Outcomes were analyzed: "6-mo" visit is defined as 91-270 days after BR3 assessment; 12-mo, 271-460 days; 18-mo, 461-640 days; 24-mo, 641-820 days. Cancer yield (CY) is calculated as number of breast cancers per number of women. PPV3 is probability of breast cancer per number of biopsies performed.

RESULTS

In 65,908 women (median age 55 years; range 25-90), results from 204,439 mammograms were included. Overall biopsy rate of BR3 lesions was 10.06% (6633/65,908) with CY of 1.34% (885/65,908, 95%CI 1.25 to 1.43%), PPV3 13.3%. 612 (0.9%) women had biopsy at the initial recall/BR3 visit yielding 37 cancers. 2622 women (4.0%) had follow-up at <= 90 days: 503 (19.2%) biopsied, CY 1.41% (37/2622). 44,326 (67.3%) women had follow-up at 6-mon: 4301 (9.7%) biopsied, 653 (15.2%) cancers, CY 1.47%. 29,688 (45.0%) women had follow-up at 12-mo: 1620 (5.5%) biopsied, 301 (18.6%) cancers, CY 1.01%. 7584 (11.5%) women had follow-up at 18-mo: 417 (5.5%) biopsied, 85 (20.4%) cancers, CY 1.12%. 6948 (10.5%) women had follow-up at 24-mo: 273 (3.9%) biopsied, 46 (16.8%) cancers, CY 0.66%. CY for 21,729 cases downgraded by 6-mo and seen again by 12-mo = 0.24\%. CY for 22,629 cases downgraded by 1 yr and seen again by 24-mo = 0.26% (p < 0.0001 for all BR3 CY comparisons).

CONCLUSION

Compliance with 6-month follow-up was high at 67.2%. Overall CY for probably benign findings was 1.34%, with CY at each follow-up below accepted limit of 2%.

CLINICAL RELEVANCE/APPLICATION

In the NMD, use of BR3 assessments is appropriate, with < 2% overall cancer yield. 653/885 (73.8%) cancers were diagnosed at or before 6-mo visit. Continued imaging surveillance of BR3 is supported by malignancy rates > those of BR1 or -2 at each follow-up.

SSK12-07 Cost-Effectiveness of MRI-Guided Thrombolysis for Stroke with Unknown Time of Onset

Wednesday, Dec. 4 11:30AM - 11:40AM Room: S104A

Awards

Trainee Research Prize - Resident

Participants

Wolfgang G. Kunz, MD, Munich, Germany (*Presenter*) Grant, Medtronic plc Daniel Puhr-Westerheide, MD, Munich, Germany (*Abstract Co-Author*) Nothing to Disclose Matthias P. Fabritius, MD, Munich, Germany (*Abstract Co-Author*) Nothing to Disclose Ahmed Othman, MD, Tubingen, Germany (*Abstract Co-Author*) Nothing to Disclose Saif Afat, MD, Tuebingen, Germany (*Abstract Co-Author*) Nothing to Disclose Paul Reidler, MD, Munich, Germany (*Abstract Co-Author*) Nothing to Disclose

For information about this presentation, contact:

wolfgang.kunz@med.lmu.de

PURPOSE

In acute ischemic stroke, about 25% of patients present with unknown time of onset, which is a contraindication for intravenous thrombolysis (IVT) treatment. Among this patient group, MRI has been shown to identify patients with salvageable brain tissue. The recent WAKE-UP trial demonstrated a clinical benefit of such MRI-guided IVT administration over best supportive care (BSC). We aimed to determine the cost-effectiveness of this management strategy.

METHOD AND MATERIALS

A decision model based on Markov simulations estimated lifetime costs and quality-adjusted life years (QALY) associated with MRIguided IVT or BSC (Figure 1). The analysis was performed in a United States setting from a societal perspective. Input parameters for the model were based on most recent and best available evidence (Table 1), including outcome data from the WAKE-UP trial (Figure 2). Starting age was set to 65 years according to the median age in the trial. Probabilistic sensitivity analyses (PSA) were performed using 10,000 Monte Carlo simulations to estimate uncertainty. Incremental costs (IC), incremental effectiveness (IE), and incremental cost-effectiveness ratios (ICER) were derived. Cost-effectiveness acceptability rates were determined for varying willingness-to-pay (WTP) thresholds.

RESULTS

Based on outcome data of 503 randomized patients, the base-case analysis identified MRI-guided IVT as the strategy that resulted in incremental QALYs and cost-savings over the projected lifetime compared to BSC (IC: -\$21,481; IE: +0.62 QALYs; ICER: IVT dominant). Adjusting for all input parameter uncertainty in PSA, MRI-guided IVT was the preferred strategy with acceptability rates of >99% at all WTP thresholds ranging from \$0 to \$150,000 per QALY (Figure 3). Simulations led to 99.47% dominant/cost-saving iterations (Figure 4).

CONCLUSION

MRI-guided IVT is projected to provide long-term clinical benefit whilst also leading to long-term cost-savings in the management of stroke patients with unknown time of onset.

CLINICAL RELEVANCE/APPLICATION

Providing MRI-guided IVT in stroke with unknown onset requires dedicated infrastructure. Based on the projected health and cost benefits, investments to support such an infrastructure are justified.

SSK12-08 Cost-Effectiveness Analysis of Local Ablation and Surgery for Liver Metastases of Oligometastatic Colorectal Cancer

Wednesday, Dec. 4 11:40AM - 11:50AM Room: S104A

Participants

Matthias F. Froelich, MD, Mannheim, Germany (*Presenter*) Consultant, Smart Reporting GmbH Florian Streitparth, Berlin, Germany (*Abstract Co-Author*) Nothing to Disclose Max Seidensticker, Munich, Germany (*Abstract Co-Author*) Grant, Sirtex Medical Ltd Grant, Bayer AG Grant, Siemens AG Speaker, Sirtex Medical Ltd Speaker, Bayer AG Speaker, Siemens AG Jens Ricke, MD,PhD, Berlin, Germany (*Abstract Co-Author*) Research Grant, Sirtex Medical Ltd Research Grant, Bayer AG Wolfgang G. Kunz, MD, Munich, Germany (*Abstract Co-Author*) Grant, Medtronic plc **PURPOSE**

To evaluate the cost-effectiveness of local ablative and surgical approaches in the treatment of liver metastases of oligometastatic colorectal cancer (omCRC).

METHOD AND MATERIALS

A decision model based on Markov simulations estimated lifetime costs and quality-adjusted life years (QALY) associated with the treatment strategies radiofrequency ablation (RFA), microwave ablation (MWA), and surgical resection. A United States healthcare perspective was applied. Model input parameters were based on best available and most recent evidence (Table 1). The starting age was set to 73 years. Probabilistic sensitivity analyses (PSA) were performed using 10,000 Monte Carlo simulations to estimate model uncertainty. The percentage of cost-effective iterations was determined for different willingness-to-pay (WTP) thresholds.

RESULTS

The base-case analysis showed that surgery lead to higher costs (\$49,447.86 vs. \$42,467.97 vs. \$42,245.78) while providing best outcomes compared to RFA and MWA (8.12 vs. 6.97 vs. 8.03 QALYs). In PSA, MWA was the most cost-effective strategy for all WTP thresholds below \$80,000 per QALY. For increasing WTP thresholds, surgery showed comparable yet increasingly higher percentages of cost-effective iterations compared to MWA. Local ablation with RFA was dominated by either MWA or surgery at all

WTP thresholds.

CONCLUSION

In omCRC patients with liver metastases, treatment with MWA and surgery are estimated to provide comparable efficacy. MWA was identified as the most cost-effective strategy in intermediate resource settings and should be considered as an alternative to surgery in high resource settings.

CLINICAL RELEVANCE/APPLICATION

In case patients are eligible for local treatment as well as surgery, MWA and surgery can be offered as comparable treatment options to omCRC patients with liver metastases.

SSK12-09 Early Admission and Mortality Rates for Common Outpatient Interventional Radiology Procedures

Wednesday, Dec. 4 11:50AM - 12:00PM Room: S104A

Participants

Ammar Sarwar, MD, Boston, MA (*Presenter*) Stockholder, Agile Devices, Inc; Scientific Advisory Board, Agile Devices, Inc; Grant Support, Sirtex Medical Inc

Alexander Schin, BS, Boston, MA (Abstract Co-Author) Nothing to Disclose

Max P. Rosen, MD, MPH, Weston, MA (*Abstract Co-Author*) Stockholder, Everest Scientific Inc Consultant, PAREXEL International Corporation Stockholder, Cynvenio Biosystems, Inc Medical Advisory Board, Cynvenio Biosystems, Inc

Sharina Person, PhD, Worcester, MA (*Abstract Co-Author*) Nothing to Disclose Arlene Ash, PhD, Worcester, MA (*Abstract Co-Author*) Nothing to Disclose

Muneeb Ahmed, MD, Boston, MA (Abstract Co-Author) Research Grant, General Electric Company Stockholder, Agile Devices, Inc Scientific Advisory Board, Agile Devices, Inc

For information about this presentation, contact:

asarwar@bidmc.harvard.edu

PURPOSE

Patient outcomes for outpatient interventional radiology (IR) procedures have been reported for single institutions, but not more broadly. In this study, we use national Medicare data to evaluate early admission and mortality rates after common outpatient IR procedures.

METHOD AND MATERIALS

Working with the Center for Medicare and Medicaid (CMS) Chronic Conditions Data Warehouse (CCW) and Research Data Assistance Center, we identified and obtained all outpatient claims for interventional radiology (IR) procedures and determined 7- and 30-day readmission and crude mortality rates, for the most common IR procedures performed in 2012. One hundred percent of the national outpatient Medicare claims files were obtained from CMS. The frequency of procedures, 7 and 30-day admission rates; and 7 and 30-day crude mortality rates were determined.

RESULTS

In 2012, dialysis fistulagram and port placement (N=114,208 and 92,313) were the most commonly performed outpatient interventional radiology procedures amongst the Medicare population; they were performed nearly three times as frequently as the third most common procedure, liver biopsy (N=38,332). TIPS had the highest 7- and 30-day admission rates (14% and 42%), followed by percutaneous biliary drainage (13% and 40%). Percutaneous gastrostomy and transhepatic cholangiogram had the highest 7-day mortality rate (2% each). Three procedures had at least 10% 30-day mortality (TIPS 10%, percutaneous cholangiogram 11%, percutaneous biliary drainage 12%).

CONCLUSION

Early mortality and admission are moderately common following outpatient IR procedures. Predictive models that account for patient risk could be useful both 1) to account for differences among labs in the difficulty of their patients, and 2) to flag higher risk patients undergoing higher risk IR procedures as potential candidates for in-hospital care.

CLINICAL RELEVANCE/APPLICATION

With increasing interest in Office-Based Labs in IR practice, early admission and mortality rates should be explored as potential quality indicators for outpatient IR procedures.

Printed on: 10/29/20







SSK13

Molecular Imaging (General Subspecialties)

Wednesday, Dec. 4 10:30AM - 12:00PM Room: S505AB

MI

AMA PRA Category 1 Credits ™: 1.50 ARRT Category A+ Credit: 1.75

FDA Discussions may include off-label uses.

Participants

Kathryn A. Morton, MD, Salt Lake City, UT (Moderator) Nothing to Disclose

Sub-Events

SSK13-01 To Examine the Potential Role of 2-fluorodeoxyglucose Positron Emission Tomography Integrated with CT (FDG-PET/CT) in Monitoring IFIs and Therapy Decision-Making

Wednesday, Dec. 4 10:30AM - 10:40AM Room: S505AB

Participants

Sikandar M. Shaikh, DMRD, Hyderabad, India (Presenter) Nothing to Disclose

PURPOSE

Invasive fungal infections (IFIs) are most common in immunosuppressed patients and can be life-threatening. Inadequate or no treatment is associated with high morbidity and mortality. We examined the potential role of 2-fluorodeoxyglucose positron emission tomography integrated with CT (FDG-PET/CT) in monitoring IFIs and therapy decision-making.We also evaluated the role of baseline metabolic parameters in predicting the metabolic response.

METHOD AND MATERIALS

All patients between April 2016 and March 2019 who were diagnosed with IFIs, and underwent treatment with antifungal drugs, and who also underwent FDG-PET/CT at baseline and at one or more timepoints during treatment were retrospectively included. The patient data was reviwed for pathology, microbiology, and laboratory findings. All FDG-PET/CT scans were performed according to standardized protocols. For each scan, the global total lesion glycolysis (TLG) and metabolic volume (MV), highest maximum standardized uptake value (SUVmax), and peak standardized uptake value (SUVpeak) were determined. The role of FDG-PET/CT on monitoring antifungal therapy was assessed by looking at the clinical decision made as result of the scan. Furthermore, the added value of the baseline metabolic parameters in predicting metabolic response to the antifungal treatment was evaluated.

RESULTS

Twenty-eight patients who underwent total 98 FDG-PET/CT scans were included with a mean age of 43?±?22 years. FDG-PET/CT results altered management in 14 out of the 28 patients (50%). At the final FDG-PET/CT scan, 19 (68%) had a complete metabolic response (CMR), seven a partial response and two patients were defined as having progressive disease. Using receiver operative analysis, the cut-off value, sensitivity, specificity, and significance for the baseline TLG and MV to discriminate patients with CMR were 160, 94%, 100%, p? **CONCLUSION**

FDG-PET/CT is useful in the monitoring of IFIs resulting in management therapy change in half of the patients. Baseline TLG and MV were found to be able to predict the metabolic response to antifungal treatment.

CLINICAL RELEVANCE/APPLICATION

FDG PET-CT has potential role in the evalaution of Fungal Infections and impact on treatment.

SSK13-02 Glycosaminoglycan Chemical Exchange Saturation Transfer Imaging of the Talocrural Joint in Patients with Osteochondral Lesions and Healthy Volunteers

Wednesday, Dec. 4 10:40AM - 10:50AM Room: S505AB

Participants

Daniel B. Abrar, MD, Dusseldorf, Germany (*Presenter*) Nothing to Disclose Miriam Frenken, Dusseldorf, Germany (*Abstract Co-Author*) Nothing to Disclose Anja Lutz, Dusseldorf, Germany (*Abstract Co-Author*) Nothing to Disclose Laszlo Kasprowski, Dusseldorf, Germany (*Abstract Co-Author*) Nothing to Disclose Matthias Boschheidgen, Dusseldorf, Germany (*Abstract Co-Author*) Nothing to Disclose Gerald Antoch, MD, Dusseldorf, Germany (*Abstract Co-Author*) Nothing to Disclose Christoph Schleich, MD, Dusseldorf, Germany (*Abstract Co-Author*) Nothing to Disclose

PURPOSE

To optimize a glycosaminoglycan chemical exchange saturation transfer (gagCEST) protocol for imaging of glycosaminoglycans (GAG) at 3T and to compare gagCEST values between patients with osteochondral lesions and healthy volunteers (HV).

METHOD AND MATERIALS

Wa used Black McCannel simulations for entimization of the apaCEST protocol. Therefore, the following T1 and T2 relevation times

we used bloch-micconnersingulations for optimization of the gagcest protocol. Therefore, the following 11 and 12 relaxation times of cartilage at 3T were used: T1 = 1.2 s, T2 = 0.039 s.11 HV (age 24 ± 5 years) and 4 patients (age 32 ± 9 years) with ostheochondral lesions were examined with the optimized gagCEST protocol. In addition, T1 and T2 values were determined to evaluate, if the relaxation times used in the simulation were accurate. Sequence parameters of the gagCEST sequence were: FOV = 160 x 160 mm², slice thickness = 5 mm, TE/TR = 3.5ms/7.2ms. 25 CEST images with a frequency offset between -3 ppm and 3 ppm and one S0 image were recorded. An acquisition of an additional water saturation shift referencing sequence was applied in order to correct remaining magnetic field inhomogeneities.

RESULTS

The optimization with the Bloch-McConnel simulations showed an ideal B1 amplitude of 0.8 μ T and a pulse and interpulse duration of 300 ms. We found a mean T1 time of (0.88 ± 0.13) s and a mean T2 time of (0.033 ± 0.005) s. These values significantly differed from values used in simulation. Nevertheless, further simulations revealed the same optimal pulse sequence parameters for the CEST sequence. HVs showed a significant higher gagCEST effect compared to patients (HV: MTRasym = (1.40 ± 0.71) %; patients: MTRasym = (0.05 ± 0.28) %; p-value < 0.01).

CONCLUSION

The proposed gagCEST protocol showed good performance and could distinguish between HV and patients with ostheochondral lesions.

CLINICAL RELEVANCE/APPLICATION

Our proposed gagCEST protocol allows for further molecular investigation of cartilage at the talocrural joint in different clinical settings and larger studies.

SSK13-03 Insect Larvae in Medical Imaging: New Screening System for Gut Inflammatory Compounds Using CT, MR, and PET

Wednesday, Dec. 4 10:50AM - 11:00AM Room: S505AB

Participants

Anton G. Muller, MSc, Heuchelheim, Germany (*Presenter*) Nothing to Disclose Frank Hugo Heinz Muller, MD, Neustadt Weinstrase, Germany (*Abstract Co-Author*) Investigator, General Electric Company Michael Hentschel, PhD, Bern, Switzerland (*Abstract Co-Author*) Nothing to Disclose Marian Kampschulte, MD, Giessen, Germany (*Abstract Co-Author*) Nothing to Disclose Florian H. Leinberger, Giesen, Germany (*Abstract Co-Author*) Nothing to Disclose Tine E. Trenczek, PhD, Giessen, Germany (*Abstract Co-Author*) Nothing to Disclose

For information about this presentation, contact:

Anton.G.Mueller@med.uni-giessen.de

PURPOSE

This study aims to propose and validate CT, MR and PET imaging features of gut inflammation in the insect Manduca sexta. The Epithelial structure and intestinal innate immune response in M.sexta are functionally and mechanistically comparable to humans, making M.sexta a valuable model to study the innate part of gut inflammation. This, together with the cost-effective raring and the large, cylindrical gut of M.sexta larvae will provide a quick and easy system to screen for new effectors and inhibitors of gut inflammation for pharmaceutical purposes.

METHOD AND MATERIALS

We established contrast-enhanced CT and MR as well as FDG-PET imaging, methods firstly applied to insects, to detect gut inflammation. Bacillus thuringiensis infected animals(n=19) were used as a positive control and compared to healthy animals(n=20). The gut wall of Bt and control animals were analyzed for histopathologic evidence of inflammation via cryosections. Then, ROC curves of contrast-enhanced MR and CT gut wall thickness, proportional T1 signal and signal attenuation of the gut wall, as well as the anterior SUV Max were determined. Next, we used CT, MR, and PET to investigate if animals fed with 5% dextran sulfate sodium(n=14) showed signs of gut inflammation.

RESULTS

Control and Bt-infected animals differed significantly in each diagnostic finding. All diagnostic features were excellent or good with ROC-areas of 0.96-0.8 and correlated to each other. We propose contrast-enhanced CT gut wall thickness(sen. 92% and spec. of 100%) and MRI gut wall thickness(sen. and spec. of 90%) as key diagnostic findings of gut inflammation in M.sexta. Cryosections of animals fed with Bt showed a swollen and fragmented gut wall. Animals fed with DSS showed only significant differences in 3 of 5 features suggesting only a moderate gut inflammation. In accordance with this, Bt-fed animals showed a significantly lower survival compared to DSS fed animals(p=0.0002). Both groups showed a significantly lower survival(p=0.0001) compared to the control group. Finally, we validated the empirical CT and MRI resolution using gut phantoms and μ CT.

CONCLUSION

The M.sexta screening system allows fast screening for new effectors and inhibitors of gut inflammation and could drastically reduce vertebrate animal usage in preclinical studies.

CLINICAL RELEVANCE/APPLICATION

The investigation of inhibitors of gut inflammation helps to find new therapies for inflammatory bowel diseases.

SSK13-04 Pharmacological Activation of Human Brown Adipose Tissue is Less Effective than Cold Exposure

Wednesday, Dec. 4 11:00AM - 11:10AM Room: S505AB

Participants

Ajay Kumar, MD, PhD, Troy, MI (*Presenter*) Research Grant, Mallinckrodt plc James G. Granneman, PhD, Detroit, MI (*Abstract Co-Author*) Nothing to Disclose Otto Muzik, PhD, Detroit, MI (*Abstract Co-Author*) Nothing to Disclose

For information about this presentation, contact:

ajaykumar@wayne.edu

PURPOSE

Recent studies have shown that most adult humans have brown fat cells that could be activated via the adrenergic system. Once activated, thermogenesis in these cells could affect the body's energy balance and might be instrumental in weight management. Our objective was to test whether pharmacological stimulation of the adrenergic system using an FDA-approved beta3 agonist (Mirabegron, MRB) is as effective in increasing oxidative metabolism in brown adipose tissue (BAT) as the exposure to mild cold (i.e. non-shivering) temperature.

METHOD AND MATERIALS

Six adult lean normal subjects (3F/3M, 24.1 + 4.2 years, BMI = 23.7 + 2.5) underwent 150-water and 18F-fluorodeoxyglucose (FDG) PET/CT scans either following 1h of cold stress exposure or 3h after MRB intake. Blood flow (ml/100g/min) and glucose uptake (SUV) were calculated from PET scans at the location of supraclavicular BAT. Changes in whole body daily energy expenditure (DEE) pre and post cold/MRB was measured using indirect calorimetry. BAT oxygen consumption (MRO2, ml/100g/min) was determined and used to calculate the contribution of cold- or MRB-activated BAT to whole body DEE.

RESULTS

BAT blood flow was found to be significantly higher during cold as compared to MRB intake (16.7 + 7.7 vs. 11.7 + 6.5; p = 0.041), resulting in significantly higher BAT mass during cold (73 + 67g, vs. 53 + 50g, p = 0.048). The ratio between the amount of pharmacologically activated and cold-activated BAT mass was 0.67 + 0.24. Moreover, MRO2 in BAT was significantly higher during cold as compared to MRB intake (1.37 + 0.67 vs. 1.0 + 0.49 ml/100g/min, p = 0.044). Overall, the DEE associated with activated BAT was found to be significantly higher than the DEE linked to MRB activation (7.4 + 5.8 vs. 4.5 + 3.9 kcal/d, p = 0.047).

CONCLUSION

Our findings indicates that activation of BAT using MRB is possible, however to a lesser extent ($\sim 2/3$) than activations using mild cold exposure. As cold exposure is a more natural way to activate BAT, pharmacological activation of BAT using a beta receptor agonist with possible side effects appears to be a suboptimal method to increase DEE.

CLINICAL RELEVANCE/APPLICATION

The contribution of MRB-activated BAT to whole body energy expenditure is negligible (5 - 15 kcal/d) and as such is unlikely to contribute to weight loss in subjects that are on a chronic MRB regimen.

SSK13-05 Irisin Induces White Adipose Tissue Browning in Mice by MR Imaging In Vivo

Wednesday, Dec. 4 11:10AM - 11:20AM Room: S505AB

Participants

Yue Chen, BMedSc, Nanjing, China (*Presenter*) Nothing to Disclose Yufei Zhao, Nanjing, China (*Abstract Co-Author*) Nothing to Disclose Peng Xingui, Nanjing, China (*Abstract Co-Author*) Nothing to Disclose

For information about this presentation, contact:

chenyue_0105@163.com

PURPOSE

Our study was to evaluate the browning process of Irisin on white adipose tissue (WAT) using MR imaging in vivo.

METHOD AND MATERIALS

After cultured white adipocytes were treated by different concentrations (0, 20 and 40nM, 24 hours), immunohistochemistry and western blotting (UCP 1 and DIO 2, the specific protein of brown adipocyte) were used to evaluate the browning of white adipocyte. After intraperitoneal injection of Irisin (200ng/d each) and saline (200ul each) into female C57BLKS/J mice (n=7, 10-12w), T1 weighted imaging and chemical shift selective imaging (CSSI) were performed at pre-injection and 14 days post-injection to measure the volume of WAT and the signal-noise ratio (SNR) of WAT in selective fat imaging of CSSI. Browning of WAT in MRI were compared to reference standard by histological white adipocyte area in H&E, immunohistochemistry and western blotting.

RESULTS

Primary white adipocytes were successfully cultured and induced to mature. After the intervention of Irisin, the expression levels of UCP 1 and DIO 2 proteins in white adipocytes increased significantly with the increase of the Irisin concentration. The volume of subcutaneous, visceral and total WAT after Irisin intervention by MRI was significantly lower than that of the controls. The SNR of WAT was lower than that of control, which to indicate the lipid fraction decrease and browning of WAT after Irisin injection (Figure). The area of white adipocytes in Irisin group were significantly lower than that of the controls, and the expression levels of UCP1 and Dio2 proteins were also significantly increased.

CONCLUSION

Our study was demonstrated that MR imaging could non-invasively assess browning of WAT after Irisin intervention in mice. Irisin not only reduced the volume of WAT, but also further decreased lipid fraction of WAT.

CLINICAL RELEVANCE/APPLICATION

Irisin can play a potential role in activation of browning of WAT and can be a new therapeutic target in metabolic diseases. MR imaging will play an important monitor role in this process.

SSK13-06 Glycosaminoglycan Remodeling of Lumbar Intervertebral Discs in Elite Rowers throughout Their Annual Training Cycle

Participants Miriam Frenken, Dusseldorf, Germany (*Presenter*) Nothing to Disclose Daniel B. Abrar, MD, Dusseldorf, Germany (*Abstract Co-Author*) Nothing to Disclose Laszlo Kasprowski, Dusseldorf, Germany (*Abstract Co-Author*) Nothing to Disclose Bernd Bittersohl, MD, Bern, Switzerland (*Abstract Co-Author*) Nothing to Disclose Gerald Antoch, MD, Dusseldorf, Germany (*Abstract Co-Author*) Nothing to Disclose Christoph Schleich, MD, Dusseldorf, Germany (*Abstract Co-Author*) Nothing to Disclose

PURPOSE

To assess the glycosaminoglycan (GAG) content of lumbar intervertebral discs (IVD) in elite rowers (ER) at different stages of their annual training cycle and compared to healthy volunteers (HV) using GAG chemical exchange saturation transfer (gagCEST).

METHOD AND MATERIALS

205 lumbar IVD of 21 ER (23 ±3 years, 9 female, 11 male) and 25 HV (27 ±2 years, 13 female, 12 male) were prospectively examined with 3T magnetic resonance imaging (MRI). Standard T2 weighted (T2w) sequences were used for morphological grading according to the Pfirrmann classification. GAG content of the nucleus pulposus (NP) and annulus fibrosus was determined with gagCEST in non-degenerated discs according to Pfirrmann. ER were examined during the peak of their competition preparation (T0) and 6 months later during the peak of their post-competition recovery period (T1).

RESULTS

At T0 we found significantly higher gagCEST values in ER compared to HV (NP: 4.26 $\pm 2.37\%$ vs. 3.38 $\pm 1.72\%$, p<0.05; confidence interval (CI) 0.32%/1.44%; AF: 2.75 $\pm 1.7\%$ vs.1.961 $\pm 1.23\%$, p<0.01; CI 0.4%/1.2%). At T1 gagCEST values decreased and illustrated no significant difference compared to HV (NP: 3.55 $\pm 2.31\%$, p = 0.531, CI 0.038%/0.73%; AF: 2.31 $\pm 1.57\%$, p = 0.073, CI 0.03%/0.74%).

CONCLUSION

Compared to HV lumbar IVD of ER show significantly higher gagCEST values during the peak of their competition preparation and similar values during the recovery period, indicating a GAG remodelling effect by training.

CLINICAL RELEVANCE/APPLICATION

Physical exercise (rowing) potentially prevents molecular GAG depletion in lumbar IVD.

SSK13-07 Visceral Fat Browning in a Murine Model Detected by Z-Spectrum Imaging

Wednesday, Dec. 4 11:30AM - 11:40AM Room: S505AB

Participants

Alessandro Scotti, Chicago, IL (*Abstract Co-Author*) Nothing to Disclose Victoria Gil, Chicago, IL (*Abstract Co-Author*) Nothing to Disclose Weiguo Li, Chicago, IL (*Abstract Co-Author*) Nothing to Disclose Chong Wee Liew, Chicago, IL (*Abstract Co-Author*) Nothing to Disclose Kejia Cai, PhD, Chicago, IL (*Presenter*) Nothing to Disclose

PURPOSE

Conversion of visceral fat into brown fat (browning) is highly beneficial in reducing the risk of metabolic disease, but its study is limited by resistance to conventional browning stimuli and inadequate noninvasive imaging [1,2,3]. Here we report the successful detection of white adipose tissue browning in a transgenic mouse model by measurement of depots size and fat-water fraction (FWF) from longitudinal Z-Spectrum MRI.

METHOD AND MATERIALS

The transgenic murine model was developed by ablation of the transcriptional regulator TRIP-Br2 (TRIP-Br2 KO mice) [4] and treated IP with 1mg/Kg of ß3-AR agonist CL316,243 every day for two weeks. Age-matched wild types were treated with saline. Animals underwent MRI at a 9.4T scanner before and 4, 10 and 15 days after treatment start. The size of the perirenal depots was measured on multislice T2-weighted sequences. Z-Spectrum Imaging was performed with a CEST sequence with a single slice FSE readout. Z-spectral data were fitted to a multi-Lorentzian model including the direct saturation of both water and fat and the FWF was quantified from the fitted amplitudes in every pixel [3].

RESULTS

ROI analysis showed that the perirenal fat depots decreased in size over time in the KO mice, with volumes shrinking from 11.7±1.9mm3 before treatment to 6.9±2.4mm3 after two weeks, compared to the wild types. FWF also was found decreased in the drug treated mice compared to the control group, with differences between the groups in perirenal fat up to 15% already detectable after 4 days, and increased to 20% at ten days, but decreased at 2 weeks. The changes are consistent with increased perfusion and reduced lipid content, markers of brown-like cells activation. Also subcutaneous fat showed a sustained decrease in FWF, reaching an average of 25% at the end of the study, but with a higher variability. The different timeline of changes in the fat depots might indicate a hierarchy to the activation mechanism [5].

CONCLUSION

ZSI has proven to be able to detect browning of white adipose tissue in a murine model chronically treated with adrenergic drug.

CLINICAL RELEVANCE/APPLICATION

Visceral fat is associated with high risk of metabolic disease and is resistant to conventional browning stimuli. Monitoring its browning will be instrumental in combating epidemic metabolic diseases.

SSK13-08 Granzyme B PET Imaging to Assess Innate Immune Responses

Participants Kathleen M. Capaccione, MD,PhD, New York, NY (*Presenter*) Nothing to Disclose Andrei Molotkov, MD,PhD, New York, NY (*Abstract Co-Author*) Nothing to Disclose Mikhail Doubrovin, MD, Memphis, TN (*Abstract Co-Author*) Spouse, Consultant, ATARA Biotherapeutics Ltd Akiva Mintz, MD, PhD, Paramus, NJ (*Abstract Co-Author*) Consultant, Regeneron Pharmaceuticals, Inc

PURPOSE

Granzyme B is a serine protease released by active CD8+ T cells, macrophages and natural killer cells that facilitates granulemediated apoptosis. Prior studies have demonstrated the utility of granzyme B PET imaging of CD8+ T cells to assess adaptive immunity in response to immunotherapy. Our goal is to examine the potential of granzyme B PET imaging as a biomarker of the innate immune system, which can expand its use for imaging T-cell independent diseases as well as the initial innate immune trigger of an adaptive immune response.

METHOD AND MATERIALS

Athymic nude mice were injected in the left shoulder with lipopolysaccharide (LPS) in Matrigel to induce a T-cell independent immune response. Seventy-two hours later we injected 68Ga-NOTA-GZP as previously reported and performed PET/CT imaging one hour after injection.

RESULTS

PET-CT demonstrated specific binding of the 68Ga-NOTA-GZP at the site of LPS injection within the left shoulder when compared to control animals injected with PBS. Nonspecific uptake was also seen in the liver and the bladder, suggesting routes of elimination.

CONCLUSION

Specific 68Ga-NOTA-GZP accumulation at the site of LPS injection in T cell deficient animals supports the use of granzyme B PET imaging for innate immune responses. Future studies will examine the role of granzyme B imaging in specific disease states mediated by innate immunity.

CLINICAL RELEVANCE/APPLICATION

Granzyme B PET imaging may aide the early diagnosis and evaluation of disease progression of infection and inflammation mediated by the innate immune system.

SSK13-09 Loss of Glycosaminoglycans of Lumbar Intervertebral Discs in Patients With Ankylosing Spondylitis

Wednesday, Dec. 4 11:50AM - 12:00PM Room: S505AB

Participants

Daniel B. Abrar, MD, Dusseldorf, Germany (*Presenter*) Nothing to Disclose Miriam Frenken, Dusseldorf, Germany (*Abstract Co-Author*) Nothing to Disclose Styliani Tsiami, Herne, Germany (*Abstract Co-Author*) Nothing to Disclose Philipp Sewerin, Dusseldorf, Germany (*Abstract Co-Author*) Nothing to Disclose Laszlo Kasprowski, Dusseldorf, Germany (*Abstract Co-Author*) Nothing to Disclose Xenofon Baraliakos, MD, Herne, Germany (*Abstract Co-Author*) Nothing to Disclose Gerald Antoch, MD, Dusseldorf, Germany (*Abstract Co-Author*) Nothing to Disclose Christoph Schleich, MD, Dusseldorf, Germany (*Abstract Co-Author*) Nothing to Disclose

PURPOSE

To evaluate the glycosaminoglycan (GAG) content of lumbar intervertebral discs (IVD) in patients with ankylosing spondylitis (AS) using GAG chemical exchange saturation transfer (gagCEST).

METHOD AND MATERIALS

195 lumbar IVD of 15 patients with AS (mean age 50 \pm 10 years) and 25 healthy control patients (HC) were prospectively examined with 3 T magnetic resonance imaging (MRI). MRI protocol contained morphological T2 weighted (T2w) images to grade IVD according to the Pfirrmann classification and biochemical imaging with gagCEST to calculate a region of interest (ROI) of the nucleus pulposus (NP) and annulus fibrosus (AF). Prior to statistical testing of gagCEST effects in patients and HC, IVD were classified according to Pfirrmann.

RESULTS

Significantly lower gagCEST values of NP and AF were found in non-degenerative IVD (Pfirrmann 1 and 2) of AS patients compared to HC (NP: $1.88 \ \pm 1.21\%$ vs. $3.38 \ \pm 1.71\%$; p<0.01; confidence interval (CI): 0.89%/2.11%. AF: $1.11 \ \% \pm 1.07 \ \%$ vs. $1.96 \ \% \pm 1.23 \ \%$; p<0.01; CI 0.39%/1.3%).

CONCLUSION

GagCEST analysis of morphologically non-degenerative IVDs in T2w images showed significantly lower GAG values in patients with AS in the NP and AF compared to HC.

CLINICAL RELEVANCE/APPLICATION

Our results potentially allow for the detection of GAG loss prior to morphological degeneration.

Printed on: 10/29/20





SSK14

Musculoskeletal (Interventional)

Wednesday, Dec. 4 10:30AM - 12:00PM Room: E353A



AMA PRA Category 1 Credits ™: 1.50 ARRT Category A+ Credit: 1.75

FDA Discussions may include off-label uses.

Participants

Kenneth S. Lee, MD, Madison, WI (*Moderator*) Grant, General Electric Company; Grant, National Basketball Association; Grant, Johnson & Johnson; Research support, SuperSonic Imagine; Royalties, Reed Elsevier Adam C. Zoga, MD, MBA, Philadelphia, PA (*Moderator*) Nothing to Disclose

Sub-Events

SSK14-01 Augmented Reality and Artificial Intelligence-Based Navigation during Percutaneous Vertebroplasty

Wednesday, Dec. 4 10:30AM - 10:40AM Room: E353A

Participants

Pierre Auloge, MBBS, Reims, France (*Presenter*) Nothing to Disclose Roberto Luigi Cazzato, Strasbourg, France (*Abstract Co-Author*) Proctor, Medtronic plc Guillaume Koch, MD,MSc, Strasbourg, France (*Abstract Co-Author*) Nothing to Disclose Jean Caudrelier, MD, Strasbourg, France (*Abstract Co-Author*) Nothing to Disclose Pierre de Marini, MD, Strasbourg CEDEX, France (*Abstract Co-Author*) Nothing to Disclose Julien Garnon, MD, Strasbourg, France (*Abstract Co-Author*) Proctor, Galil Medical Ltd Afshin Gangi, MD,PhD, Strasbourg, France (*Abstract Co-Author*) Consultant, AprioMed AB

For information about this presentation, contact:

pierre.auloge@chru-strasbourg.fr

PURPOSE

To assess technical feasibility, accuracy, safety and patient radiation exposure of a novel navigational tool integrating augmented reality (AR) and artificial intelligence (AI), during percutaneous vertebroplasty of patients with vertebral compression fractures (VCFs).

METHOD AND MATERIALS

This retrospective study compared the trans-pedicular access phase of percutaneous vertebroplasty between two groups of 50 patients with symptomatic single-level VCFs. Trocar insertion was performed using AR/AI-guidance with motion-compensation in Group A, and standard fluoroscopy in Group B. Technical feasibility was recorded for Group A. Accuracy of trocar placement (distance between planned/actual trajectory on sagittal/coronal fluoroscopic-images); complications; time for trocar deployment; and radiation dose/fluoroscopy-time were recorded and compared between group A and B.

RESULTS

Technical feasibility in Group A was 100%. Time for trocar deployment was significantly longer in Group A ($642 \pm 210s$) than Group B ($336 \pm 60s$; p= 0.001). Dose-Area Product and fluoroscopy-time were significantly lower in Group A (160.9 ± 220 mGy.cm2 and 5.2 \pm 3.4) than Group B (298.2 ± 190.2 mGy.cm2 and 9.97 \pm 4.8s; p=0.019 and 0.001), respectively. Time for trocar deployment was significantly longer in Group A ($538 \pm 182s$) than Group B ($374 \pm 182s$; p= 0.001). Accuracy measures for each group are ongoing. No complications were observed in the entire population.

CONCLUSION

AR/AI-guided percutaneous vertebroplasty appears feasible, accurate and safe, and facilitates lower patient radiation exposure compared to standard fluoroscopic-guidance.

CLINICAL RELEVANCE/APPLICATION

AR/AI-guided percutaneous vertebroplasty allows lower patient/operator radiation exposure compared to standard fluoroscopic-guidance.

SSK14-02 Short and Long Term Outcomes of Image-Guided Retrocalcaneal Bursal Injections

Wednesday, Dec. 4 10:40AM - 10:50AM Room: E353A

Participants Sean Boone, MD, Bronx, NY (*Presenter*) Nothing to Disclose Robert B. Uzor, MRCS, MD, Yonkers, NY (*Abstract Co-Author*) Nothing to Disclose Elisabeth Elsinger, Bronx, NY (*Abstract Co-Author*) Nothing to Disclose Eric Walter, Bronx, NY (*Abstract Co-Author*) Nothing to Disclose Dominic Catanese, Bronx, NY (*Abstract Co-Author*) Nothing to Disclose

For information about this presentation, contact:

sboone@montefiore.org

PURPOSE

The efficacy of ultrasound (US) guided and fluoroscopically (FL) guided RC bursal steroid injections for heel pain is not well understood, and no large series or extended follow-up has been previously reported. The purpose of this retrospective review is to evaluate the short and long term outcomes of this procedure.

METHOD AND MATERIALS

After IRB approval, consecutive FL and US guided RC bursa injections were retrospectively reviewed (2013-2019). Pre-procedure US images were scored by 2 blinded MSK Radiologists in consensus for degree (scale 0-3) of Achilles tendinopathy (AT) and RC bursitis. VAS pain scores (scale 0-10) were obtained pre-procedure and 1-4 weeks post-procedure; short term response was considered excellent (7-10 point decline), good (4-6 point decline), fair (1-3 point decline), or none. Review of medical records was performed for long-term outcome evaluation. VAS response categories were analyzed using student's t-test.

RESULTS

263 injections were performed. 240 injections (167 US, 73 FL) in 194 heels had at least 6 months of follow-up (range 190-1919 days): 160 female; mean age 54.5 (range 30-86); 90 right heel. Insertional AT and RC bursitis was present in 100% (263/263) and 85% (223/263), respectively. Short term VAS pain scores were available for 75 injections. Median pre- and post-procedure pain scores were 9 (IQR 7.25 to 10) and 3 (IQR 0 to 6). A statistically significant decrease in pain scores was noted post-injection, with good/excellent response in 65% and mean change of -5.17 (95% CI -4.43, -5.90; p<0.00001). On chart review, 24 (13%) patients received repeat injection, 16 (8%) had surgery, 10 (5%) had both, and 144 (74%) had no further procedure. Four cases of Achilles rupture or high-grade tear occurred 15-79 days post- procedure.

CONCLUSION

Image-guided RC bursa injections yielded significant short term pain score reduction (p<0.00001). Subsequent Achilles high grade tear or rupture was infrequent (1.5%).

CLINICAL RELEVANCE/APPLICATION

This is the first report on both short and long-term outcomes of image-guided retrocalcaneal bursa steroid injection, and is the largest (n=240) patient cohort studied for this procedure.

SSK14-03 Safety and Efficacy of Bone Marrow Aspirate and Biopsy in Severely Thrombocytopenic Patients

Wednesday, Dec. 4 10:50AM - 11:00AM Room: E353A

Participants

James D. Stensby, MD, Columbia, MO (Presenter) Nothing to Disclose

Jeremiah R. Long, MD, Ft Belvoir, VA (Abstract Co-Author) Nothing to Disclose

Travis J. Hillen, MD, Saint Louis, MO (*Abstract Co-Author*) Consultant, Biomedical Systems Consultant, Medtronic plc Jack W. Jennings, MD, Saint Louis, MO (*Abstract Co-Author*) Speakers Bureau, Merit Medical Systems, Inc; Consultant, Merit Medical Systems, Inc; Consultant, Medtronic plc; Consultant, Galil Medical Ltd; Consultant, BTG International Ltd; Consultant, C. R. Bard, Inc

For information about this presentation, contact:

stensbyj@health.missouri.edu

PURPOSE

To assess the safety and efficacy of fluoroscopically guided drill assisted bone marrow aspirate and biopsy in severely thrombocytopenic patients.

METHOD AND MATERIALS

This retrospective study received IRB approval with a waiver of patient informed consent. From January 2013 through December 2016 a total of 739 bone marrow aspirate and biopsy (BMAB) procedures were performed at a single institution under the direct supervision of a fellowship trained musculoskeletal radiologist using fluoroscopic guidance and a drill-assisted needle. Of these patients 111 BMAB were performed in 94 patients who received a CT scan of the pelvis and biopsy site within 7 days following the BMAB. These 94 patients were subdivided based on their platelet count: severe thrombocytopenia (<20 platelets/mm3) 16 BMAB in 15 patients, average 11.8 platelets/mm3; thrombocytopenia (20-50 platelets/mm3) 16 BMAB in 15 patients, average 30.1 platelets/mm3; and control (>50 platelets/mm3) 79 BMAB in 64 patients, average 213.1 platelets/mm3. The procedure report was reviewed for sedation time, aspirate volume, and aggregate size of core biopsy specimens. The electronic medical record was reviewed for specimen adequacy; pathologic diagnosis; body mass index; pre and post procedure labs including platelet count, HGB, HCT, PT, and INR levels; post-procedural transfusion; and complications including mortality at 30 and 90 days. CT scans were independently reviewed by 2 fellowship trained radiologists for the presence or absence of subcutaneous fat stranding superficial to the biopsy site or post-procedural hematoma, graded 1 to 4. Discrepancies were resolved by consensus review.

RESULTS

There was no significant difference in diagnostic yield, CT identified post-procedural hematoma, or the hemoglobin and hematocrit levels pre and post procedure between the three groups. 6 patients (1 severely thrombocytopenic, 2 thrombocytopenic, and 2 control) were lost to follow-up. There was no significant difference in complication rate or all-cause mortality at 30 and 90 days post procedure. There was a significant difference in transfusion at 30 days with thrombocytopenic and severely thrombocytopenic patients more likely to receive transfusion.

CONCLUSION

The risks of postoperative hemorrhage or complication following image-guided BMAB are not significantly different in patients with

CLINICAL RELEVANCE/APPLICATION

Image guided BMAB is a procedure that can be safely performed in patients with severe thrombocytopenia.

SSK14-04 Utility of CT-Guided Percutaneous Rib Biopsy and Factors Affecting Diagnostic Yield

Wednesday, Dec. 4 11:00AM - 11:10AM Room: E353A

Participants

Nicholas Q. Vu, MD, Pittsburgh, PA (*Presenter*) Nothing to Disclose Andrew Cordle, MD, PhD, Wexford, PA (*Abstract Co-Author*) Nothing to Disclose Carol L. Andrews, MD, Baden, PA (*Abstract Co-Author*) Author, Reed Elsevier Qingwen Chen, Pittsburgh, PA (*Abstract Co-Author*) Nothing to Disclose Jie Yao, Pittsburgh, PA (*Abstract Co-Author*) Nothing to Disclose Jeanine Buchanich, PhD, Pittsburgh, PA (*Abstract Co-Author*) Nothing to Disclose

For information about this presentation, contact:

vun@upmc.edu

PURPOSE

To determine the utility of CT-guided percutaneous rib biopsy and factors that affect diagnostic yield

METHOD AND MATERIALS

We retrospectively reviewed percutaneous CT-guided rib biopsies performed in a large academic medical center from 2008-2017 (n=88). Patient demographics, nuclear imaging studies, CT imaging features, biopsy technique (FNA and/or core), performing radiologist, periprocedural complications and pathology results were recorded. CT imaging feature categorization included lesion matrix (sclerotic, lytic or mixed), lesion size ($>/\leq 2$ cm), presence of bony destruction, and presence of an associated soft tissue mass. Overall diagnostic yield was calculated from the number of diagnostic biopsies over total number of biopsies. Diagnostic yield was also calculated for subgroups stratified by patient demographics, technique, presence of prior nuclear imaging, CT imaging features and pathology results. All variables were compared between diagnostic and non-diagnostic samples using chi-square test. Multivariate logistic regression was performed to determine factors which predicted biopsy outcome.

RESULTS

The overall diagnostic yield was 92.0%. No complications were noted. The diagnostic yield was significantly different depending on lesion matrix (95.5% for lytic, 91.7% for mixed, and 66.7% for sclerotic, p=0.011), the presence of an associated soft tissue mass (96.7% versus 81.5%, p=0.044), and size of the lesion (97.1% versus 73.7% for larger versus smaller lesions, p=0.004). The diagnostic yield for various subgroups is listed in table 1 (See attached). Multivariate logistic regression demonstrated a statistically significant result for lesion size when adjusting for other covariates (lesion matrix, soft tissue component and prior nuclear medicine study). Biopsies of large lesions predicted a diagnostic result (Odds ratio 8.91, p=0.04).

CONCLUSION

Percutaneous rib biopsy utilizing CT-guidance is a safe and effective procedure with a high diagnostic yield. The diagnostic yield is higher for lytic than sclerotic lesions, lesions with an associated soft tissue mass, and large lesions. Multivariate analysis shows that the lesion size affects diagnostic yield. Larger lesions resulted in a higher diagnostic yield than smaller lesions.

CLINICAL RELEVANCE/APPLICATION

CT-guided percutaneous rib biopsy results in a high diagnostic yield particularly for large lytic osseous lesions with an associated soft tissue mass.

SSK14-05 Efficacy and Outcome of Repeat Epidural Steroid Injection for Partially Responded Lumbar HIVD Patients under "Wait-And-See" Policy as a Pain Management Option

```
Wednesday, Dec. 4 11:10AM - 11:20AM Room: E353A
```

Participants

Bo Ram Kim, MD, Seongnam-si, Korea, Republic Of (*Presenter*) Nothing to Disclose Joon Woo Lee, MD, PhD, Sungnam, Korea, Republic Of (*Abstract Co-Author*) Nothing to Disclose Eugene Lee, Seongnam, Korea, Republic Of (*Abstract Co-Author*) Nothing to Disclose

For information about this presentation, contact:

boram7072@gmail.com

PURPOSE

To evaluate efficacy of epidural steroid injection (ESI) under 'wait-and-see (WaS)' policy, based on 1-year clinical outcome of responded lumbar herniated intervertebral disc (HIVD) patients to initial ESI

METHOD AND MATERIALS

592 lumbar HIVD patients received steroid injection from Jan 2017 to Dec 2017 in our institution. The cohort was managed pain and follow up for 1-year under 'WaS' policy to performed repeated ESI under close observation of initial injection response without prescheduled ESI session within 3 weeks, that is performed in our routine clinical practice. 3-week and 1-year telephone interview and medical record review was conducted for residual symptom, total injection number, operating status. After excluding patients with complete response without residual pain or no response with over 70% residual symptom in 3-week pain assessment, 141 responded patients comprised our study population. We divided patients into 2 groups: WaS group (n=124) and early repeat ESI, which repeat ESI within 3weeks (early ESI, n=17) group. Evaluations of characteristics and outcome results were performed chi-squared or independent Student t-test.

RESULTS

Six patients (4.8%) of WaS group and one patient (5.9%) of early ESI group underwent operation within 1 year (P = 0.853). All operations were undergone for patients with poor response that is >=50% residual symptom. Mean 1.52±0.82 session of ESIs were performed for WaS group and 2.29±0.47 session of ESIs were performed for early ESI group during follow-up period (P=0.000). 78 patients (62.9%) of WaS group could control pain with a single ESI during 1 year, though one underwent surgery at outside hospital. Time interval between first and second ESI (97.15 vs. 15.47 days, P = 0.000) and between second and third ESI (80.43 vs. 50.40 days, P = 0.395) is longer in WaS than early ESI group.

CONCLUSION

"Wait-and-see" policy could be an effective pain management option for lumbar HIVD patients with response to initial ESI. Moreover, effective option for avoiding unnecessary repeat ESI and delaying repeat injection point.

CLINICAL RELEVANCE/APPLICATION

Intermittent ESI for responded lumbar HIVD patients under 'wait-and-see' policy could reduce medical cost and side effect related steroid injection by avoiding unnecessary repeat ESI and delaying repeat ESI point.

SSK14-06 Cryoablation for Advanced and Refractory Desmoid Tumors: A Promising Treatment?

Wednesday, Dec. 4 11:20AM - 11:30AM Room: E353A

Participants

Pierre Auloge, MBBS, Reims, France (*Abstract Co-Author*) Nothing to Disclose Roberto Luigi Cazzato, Strasbourg, France (*Abstract Co-Author*) Proctor, Medtronic plc Guillaume Koch, MD,MSc, Strasbourg, France (*Abstract Co-Author*) Nothing to Disclose Jean Caudrelier, MD, Strasbourg, France (*Abstract Co-Author*) Nothing to Disclose Pierre de Marini, MD, Strasbourg CEDEX, France (*Abstract Co-Author*) Nothing to Disclose Pramod P. Rao, MBBS, DMRD, Montreal, QC (*Abstract Co-Author*) Nothing to Disclose Julien Garnon, MD, Strasbourg, France (*Abstract Co-Author*) Nothing to Disclose Julien Garnon, MD, Strasbourg, France (*Abstract Co-Author*) Nothing to Disclose Julien Garnon, MD, Strasbourg, France (*Abstract Co-Author*) Nothing to Disclose Afshin Gangi, MD,PhD, Strasbourg, France (*Presenter*) Consultant, AprioMed AB

For information about this presentation, contact:

pierre.auloge@chru-strasbourg.fr

PURPOSE

To assess efficacy and safety of percutaneous cryoablation (CA) for advanced and refractory extraabdominal desmoid tumors

METHOD AND MATERIALS

This retrospective study reviewed 31 consecutive patients with painful desmoid tumors (EVA>5) evolving despite well-managed medical treatment treated by CA between 2007 and 2019. Pain reduction, progression free survival (PFS) (clinical or radiographics), tumor shrinkage rate (TSR) (volume of the tumor at 1 and 3 years compared to the volume before treatment) and complications were collected. Clinical efficacy of treatment was defined by VAS<3 after CA. Kaplan Meier method was used to outline PFS. Paired sample t-test was used to compare volume of tumors before treatment and at 1 year and 3 year.

RESULTS

With a median follow-up of 30 months (range 1- 98 months, IQR: 8-54), the PFS was 82.6% (CI95%: 69.2, 95.9) at 1 year and 75.7% (CI95%: 60.6, 90.8) at 3 years. Clinical efficacy of treatment was obtained for 89.6% (CI 95%: 78.6,100) of patients. Median volume of desmoid tumor before treatment was 92.4mL (range 2.1-1727.9 mL, IQR: 49.7- 298.5). TSR was 48.2% (CI95%: 37.2, 72.3; p=0.002) at 1 year and 74,4% (CI95%: 59.1, 89.8; p=0.002) at 3 year. Thermo protective measures for critical structures closed to the tumor were used in 74,2% of cases. Five patients (16.2%) required 2 sessions of CA for total control. Adverse events rate was 31.2%, the most common was oedema and temporary increase of pain in the days following CA.

CONCLUSION

CA is an effective treatment for advanced and refractory extraabdominal desmoid tumor, that induces durable responses. Safety profile is acceptable but requires a good mastery of protective measures for surrounding organs.

CLINICAL RELEVANCE/APPLICATION

Among patients with progressive, refractory and symptomatic desmoid tumors, CA is an effective treatment that induces durable responses.

SSK14-07 CT-Guided Bone Marrow Aspirations and Biopsies: Retrospective Review and Comparison with Blind Procedures

Wednesday, Dec. 4 11:30AM - 11:40AM Room: E353A

Participants

Connie Y. Chang, MD, Boston, MA (*Presenter*) Nothing to Disclose Adriana C. Moreira, MD, Porto, Portugal (*Abstract Co-Author*) Nothing to Disclose Nathaniel D. Mercaldo, Boston, MA (*Abstract Co-Author*) Employee, KBR; Spouse, Employee, KBR Jad S. Husseini, MD, Boston, MA (*Abstract Co-Author*) Nothing to Disclose Robert P. Hasserjian, MD, Boston, MA (*Abstract Co-Author*) Nothing to Disclose Robert P. Hasserjian, MD, Boston, MA (*Abstract Co-Author*) Consultant, Amgen Inc; Consultant, sanofi-aventis Group; Advisory Board, Incyte Corporation; Royalties, WebMD Health Corp; Stockholder, Abbott Laboratories; Stockholder, Bayer AG; Stockholder, Medtronic plc; Stockholder, Henry Schein Inc; Stockholder, Hologic, Inc; Stockholder, Johnson & Johnson; Stockholder, Kimberly-Clark Corporation; Stockholder, Novo Nordisk AS; Stockholder, The Procter & Gamble Company; Stockholder, sanofi-aventis Group

For information about this presentation, contact:

PURPOSE

To assess the added value, if any of performing bone marrow aspirations and biopsies with CT-guidance

METHOD AND MATERIALS

76 consecutive CT-guided and 70 blind bone marrow aspirations and biopsies performed January to October 2017 were reviewed. All CT-guided biopsies were performed with the same 11 gauge battery-power drill-assisted device. Blind biopsies were performed with either the 11 gauge battery-powered drill-assisted device or a 13 gauge manual device. Pathology reports were reviewed for adequacy of smears and biopsies (categorized as adequate, suboptimal, and not adequate), and core and core volume. Patient age, gender, and body mass index (BMI), core length, core volume, procedure diagnosis, and diagnosis were compared by T-tests with P < 0.05 considered statistically significant.

RESULTS

There was no significant difference between the age (CT: 67 ± 14 , range 26-93 years; blind: 63 ± 13 , range 23-85 years; P = 0.1), BMI (CT: 29 ± 6 , range 18-46; blind: 27 ± 5 , range 19-42; P =0.1), and biopsy site (CT 42 left ilium, 34 right ilium; blind: 27 left ilium, 41 right ilium, 2 not specified; P = 0.8) between the CT-guided and blind biopsies. The blind biopsy group (48 M, 22 F) had a higher proportion of male patients than the CT-guided biopsy group (38 M, 38 F) (P = 0.02). More CT-guided aspirate smears than blind aspirate smears were categorized as adequate (CT: 72 (97%) adequate, 2 (3%) suboptimal, 0 inadequate, 1 not obtained; blind: 58 (85%) adequate, 5 (7%) suboptimal, 5 (7%) inadequate, 2 not obtained) (P = 0.02). More CT-guided biopsy samples than blind biopsy samples were categorized as adequate (CT: 72 (95%) adequate, 4 (5%) suboptimal, 0 inadequate; blind: 54 (77%) adequate, 9 (13%) suboptimal; 7 (10%) inadequate) (P = 0.002). The CT-guided biopsies had a longer core length (CT: 1.3 ± 0.6 , range 0-3.5 mm; blind: 1.0 ± 0.5 , range 0-2.6 mm; P = 0.001) and a higher core volume (CT: 0.05 ± 0.03 , median 0.03, range 0-0.2 mm3; blind: 0.05 ± 0.05 , median 0.04, range 0-0.3 mm3; P = 0.04).

CONCLUSION

CT-guided bone marrow procedures were more likely to result in an adequate smear aspirate and biopsy sample and yielded longer cores with higher core volumes.

CLINICAL RELEVANCE/APPLICATION

CT guidance is helpful in bone marrow procedures. Further studies should be performed to study the cost effectiveness of routine CT guidance, and also to define the situations in which CT guidance should be used for marrow biopsies.

SSK14-08 Safety and Efficacy of Image Guided Radiofrequency Ablation of Genicular Nerve for Pain Management in Patients with Moderate to Severe Osteoarthritis of the Knee: Initial Single Institution Experience

Wednesday, Dec. 4 11:40AM - 11:50AM Room: E353A

Participants

Felix Gonzalez, MD, Atlanta, GA (*Presenter*) Nothing to Disclose Philip K. Wong, MD, Atlanta, GA (*Abstract Co-Author*) Nothing to Disclose Stephen Cole, MD, Atlanta, GA (*Abstract Co-Author*) Nothing to Disclose Zachary Bercu, MD, Decatur, GA (*Abstract Co-Author*) Nothing to Disclose J. David Prologo, MD, Atlanta, GA (*Abstract Co-Author*) Nothing to Disclose Janice M. Newsome, MD, Alexandria, VA (*Abstract Co-Author*) Nothing to Disclose Monica B. Umpierrez, MD, Atlanta, GA (*Abstract Co-Author*) Nothing to Disclose Adam D. Singer, MD, Atlanta, GA (*Abstract Co-Author*) Nothing to Disclose Nima Kokabi, MD, Atlanta, GA (*Abstract Co-Author*) Nothing to Disclose Nima Kokabi, MD, Atlanta, GA (*Abstract Co-Author*) Nothing to Disclose

For information about this presentation, contact:

felix.m.gonzalez@emory.edu

PURPOSE

To analyze the safety and efficacy of image-guided genicular nerve radiofrequency ablation (RFA) for the treatment of pain in nonsurgical candidates with moderate to severe knee osteoarthritis (OA)

METHOD AND MATERIALS

In an IRB approved prospective study, 44 consecutive patients with pain from moderate to severe knee OA refractory to antiinflammatory analgesia and failed multiple intraarticular lidocaine-steroid injections who underwent RFA of genicular nerves were included. All patients initially underwent anesthetic blocks of the superior medial/lateral and inferior medial genicular nerve branches and experienced great short-term pain relief of >6 points out a 10 scale. Radiofrequency ablation of the same nerve branches were performed 1-2 weeks after nerve block. Efficacy of the treatment was evaluated using the Western Ontario and McMaster Universities Osteoarthritis Index (WOMAC) and Knee Injury and Osteoarthritis Outcome Score (KOOS) to assess overall symptoms, stiffness, pain, and functional daily living pre block/ablation.

RESULTS

A total of 53 knees were treated in 44 patients. The average age of the patients was 66 +/- 15.8 years. Mean follow-up time was 2 weeks, 1 and 3 months. No procedure related complication was identified. The mean total KOOS score (out of 100) improved significantly from baseline at 26.9 to 62.7 3months post treatment (p<0.001). Sub-analysis of the pain component of the KOOS questionnaire demonstrated significant improvement in mean overall symptoms score from 14.7 to 39.6 (p<0.001). Mean stiffness score improved from 39.5 to 61 (p<0.001) and mean pain score from 26.5 to 55.3 (p<0.001). There was also significant improvement in the functional daily living limitations with mean baseline score of 27.6 and 3 month post therapy score of 53 (p<0.001). There was a greater number of patients with Grade III (n=34) and grade IV (n=10) arthritis according to the Kellgren-Lawrence classification.

CONCLUSION

Imaged-quided radiofrequency ablation of genicular nerves is a safe treatment option with good short-term outcome in patients

that do not qualify for TKA because of comorbidities with moderate to sever OA of the knee refractory to conservation treatments.

CLINICAL RELEVANCE/APPLICATION

Cooled RFA of the ginicular proves a safe way to treat knee arthritis pain.

SSK14-09 Minding the Gap: Vertebral Body Fracture Clefts and What They Mean for Post-Vertebroplasty Outcomes

Wednesday, Dec. 4 11:50AM - 12:00PM Room: E353A

Participants

Caroline M. Tomas, MD, Aurora, CO (*Presenter*) Nothing to Disclose Mary Kristen Jesse, MD, Aurora, CO (*Abstract Co-Author*) Faculty, Medtronic plc

PURPOSE

Percutaneous vertebroplasty/kyphoplasty has been documented as a safe and effective treatment for vertebral body fractures. Because cement nonunion is a documented cause of failed vertebral cement fixation, we focus on how pre;procedural fracture cleft morphology and procedural cement filling may be associated with the development of nonunion and furthermore how this may affect patient outcomes.

METHOD AND MATERIALS

Retrospective review of 296 patients (172 women, 124 men) who underwent vertebroplasty/kyphoplasty for compression fractures. Variables included pre-procedure CT/MRI cleft presence and morphology, pain improvement, underlying pathology, fracture level, morphology of cement fill, and postprocedure non-union. Statistical analysis was performed utilizing ordinal logistic regression, logistic regression, Fisher's exact, and conditional t-tests of proportions, with significance level set to 0.05.

RESULTS

Majority of patients with non-union cement fill (75%) demonstrated large cleft morphology. The presence of a fracture cleft resulted in an 4.981 odds ratio of non-union and odds of cleft presence is 5.195 times higher for non-union (95% CI: 1.636, 20.157). There was a significant association between non-union cement fill and cleft-only fill (p<0.0001). Patients with secondary osteoporosis had 2.831 higher odds of cleft (95% CI: 1.119, 7.299). Odds of cleft presence was 1.029 times higher for each one year increase in age (95% CI: 1.119, 7.299). The presence of a vertebral cleft did not significantly alter pain relief outcomes.

CONCLUSION

Because risk of cement non-union increases with increasing age, secondary osteoporosis, size of the fracture clefts, and cleft-only cement fill, we should pay special attention when these variables are present to adjust our procedure protocol and expectation. The presence of a cleft should not deter the decision to proceed with vertebroplasty/kyphoplasty, as pain relief was not significantly altered; however added attention to increasing trabecular fill during the procedure is warranted to decrease the risk of non-union.

CLINICAL RELEVANCE/APPLICATION

Advanced age, secondary osteoporosis, cleft size, and cleft-only cement fill should be considered when setting vertebroplasty protocol and expectation. Increasing trabecular fill is optimal.

Printed on: 10/29/20





Nuclear Medicine (Gastrointestinal Oncology Nuclear Medicine and PET)

Wednesday, Dec. 4 10:30AM - 12:00PM Room: E451A



AMA PRA Category 1 Credits ™: 1.50 ARRT Category A+ Credit: 1.75

Participants

Amy M. Fowler, MD, PhD, Madison, WI (Moderator) Institutional research support, General Electric Company; Author with royalties, Reed Elsevier

Steve Cho, MD, Madison, WI (Moderator) Research Grant, General Electric Company; Consultant, Advanced Accelerator Applications SA;

Sub-Events

SSK15-01 Integrated Time-Of-Flight 18F-FDG PET/MRI For Assessment of Pathologic Response to Neo-Adjuvant Chemo-Radiotherapy in Borderline Resectable Pancreatic Ductal Adenocarcinoma

Wednesday, Dec. 4 10:30AM - 10:40AM Room: E451A

Awards

Trainee Research Prize - Fellow

Participants

Ishan Garg, MBBS, Rochester, MN (Presenter) Nothing to Disclose Ananya Panda, MD, MBBS, Rochester, MN (Abstract Co-Author) Nothing to Disclose Geoffrey B. Johnson, MD, PhD, Rochester, MN (Abstract Co-Author) Research Grant, General Electric Company Research Grant, Pfizer Inc Mark Truty, Rochester, MN (Abstract Co-Author) Nothing to Disclose

Sudhakar K. Venkatesh, MD, FRCR, Rochester, MN (Abstract Co-Author) Nothing to Disclose

Jeff L. Fidler, MD, Rochester, MN (Abstract Co-Author) Nothing to Disclose

Nipun Mistry, Rochester, MN (Abstract Co-Author) Nothing to Disclose

Ajit H. Goenka, MD, Rochester, MN (Abstract Co-Author) Nothing to Disclose

PURPOSE

To determine if parameters derived from integrated time-of-flight 18F-FDG PET/MRI correlate with pathologic response after neoadjuvant chemo-radiotherapy (CRT) in patients with borderline resectable pancreatic ductal adenocarcinoma (PDAC).

METHOD AND MATERIALS

Patients with FDG-avid (SUVmax>=4) borderline resectable PDAC on baseline PET/MRI who also underwent a post-CRT PET/MRI prior to surgical resection were included. Primary tumor SUVmax, glucose-corrected SUVmax (SUVgluc), SUVmean and volumetric PET parameters (total lesion glycolysis and metabolic tumor volume) were measured using anatomic guidance from simultaneously acquired contrast-enhanced MRI. Metabolic response on PET/MRI was correlated to histologic treatment response using College of American Pathologists grading system (path grade). Complete metabolic response (CMR) defined as FDG uptake indistinguishable from surrounding background and normalization of post-CRT CA 19-9 were evaluated as surrogates of path grade 1/0 (marked or complete response).

RESULTS

34 patients (52.9% males; mean age: 62-years, range 23-80) were included. Follow-up duration was 17.6±5.7 months (mean ± SD). Pathologic response grades were either 1/0 (n=13) or 2/3 (n=21). Complete metabolic response on post-CRT PET/MRI was observed in 20 patients - 12 with path grades 1/0, and 8 with path grade 2. CMR was superior to normalization of post-CRT CA 19-9 as a surrogate for path grade 1/0 (sensitivity 92.3 v/s 66.7%; specificity 61.9 v/s 18.2%; PPV 60 v/s 40%; NPV 92.9 v/s 40%; AUC 0.77 v/s 0.42; P <0.05). Using ROC analysis, a relative change of >=50% in SUVgluc had 100% sensitivity, 61.9% specificity, 61.9% PPV and 100% NPV for path grade 1/0.

CONCLUSION

Qualitative and quantitative parameters derived from FDG PET/MRI correlate with pathologic response after neoadjuvant CRT and had better performance than normalization of post-CRT CA 19-9 as a surrogate for path grade 1/0.

CLINICAL RELEVANCE/APPLICATION

Qualitative and quantitative parameters derived from 18F-FDG PET/MRI show promise for assessment of pathologic response to CRT in patients with borderline resectable PDAC and merit evaluation in larger studies.

SSK15-02 18F-FDG PET-MR Enterography in Predicting Histological Active Disease in Ulcerative Colitis: A **Randomized Controlled Trial Using Nancy Index**

Wednesday, Dec. 4 10:40AM - 10:50AM Room: E451A

Yan Li, Essen, Germany (*Presenter*) Nothing to Disclose Benedikt M. Schaarschmidt, MD, Essen, Germany (*Abstract Co-Author*) Nothing to Disclose Lale Umutlu, MD, Essen, Germany (*Abstract Co-Author*) Consultant, Bayer AG Michael Forsting, MD, Essen, Germany (*Abstract Co-Author*) Nothing to Disclose Aydin Demircioglu, Essen, Germany (*Abstract Co-Author*) Nothing to Disclose Anna K. Koch, Essen, Germany (*Abstract Co-Author*) Nothing to Disclose Ole Martin, Duesseldorf, Germany (*Abstract Co-Author*) Nothing to Disclose Ken Herrmann, Essen, Germany (*Abstract Co-Author*) Nothing to Disclose Ken Herrmann, Essen, Germany (*Abstract Co-Author*) Nothing to Disclose Hendrik Juette, Bochum, Germany (*Abstract Co-Author*) Nothing to Disclose

Andrea Tannapfel, Bochum, Germany (*Abstract Co-Author*) Nothing to Disclose Jost Langhorst, Essen, Germany (*Abstract Co-Author*) Nothing to Disclose

For information about this presentation, contact:

yan.li@uk-essen.de

PURPOSE

To evaluate the diagnostic performance of PET-MR enterography in detecting histological active inflammation in patients with ulcerative colitis and the impact of bowel purgation on diagnostic accuracies of PET-MR parameters.

METHOD AND MATERIALS

Fifty patients were enrolled in this randomized controlled trial (clinicaltrials.gov [NCT03781284]). 40 patients were randomized in two study arms, in which bowel purgation was performed either before or after PET-MR enterography. All patients underwent ileocolonoscopy with mucosal biopsies after PET-MR within 24h. Diagnostic performance of MR morphological parameters (MRmorph), diffusion-weighted imaging (DWI) and PET in detecting histological inflammation determined by Nancy index was compared with each other and between study arms. Correlation between PET and histological inflammatory severity was calculated.

RESULTS

In study arm without previous bowel purgation, SUVmax ratio of bowel segment (relative to SUVmax of the liver) facilitated the highest specificity and diagnostic accuracy compared to MRmorph and DWI. Bowel cleansing led to markedly increased metabolic activity of bowel segments, resulting in significantly reduced specificity of PET compared to study arm without purgation (0.808 vs. 0.966, p = 0.007, respectively). Inter-observer concordance for assessing MRmorph was clearly increased after bowel cleansing (Cohen's κ : 0.847 vs. 0.665, p = 0.013, respectively), though diagnostic performance of MRmorph was not significantly improved. Our findings suggested that the change of metabolic status was mainly associated with the grade of neutrophil infiltrate and less dependent on chronic infiltrate.

CONCLUSION

PET-MR enterography was an excellent non-invasive diagnostic method in the assessment of ulcerative colitis without the need of previous bowel purgation.

CLINICAL RELEVANCE/APPLICATION

SUVmaxRatio was a reliable parameter facilitating best diagnostic operating characteristics in predicting histological active disease in patients with ulcerative colitis and no previous bowel purgation was needed for PET-MR.

SSK15-03 CT-Attenuation and FDG Uptake of Visceral Adipose Tissue Can Predict the Risk of Peritoneal Recurrence in Gastric Cancer Patients after Curative Surgical Resection

Wednesday, Dec. 4 10:50AM - 11:00AM Room: E451A

Participants

Jeong Won Lee, MD,PhD, Incheon, Korea, Republic Of (*Presenter*) Nothing to Disclose Sang Mi Lee, Cheonan, Korea, Republic Of (*Abstract Co-Author*) Nothing to Disclose

PURPOSE

CT-attenuation and FDG uptake of adipose tissue have been used as imaging parameters that reflect qualitative characteristics of adipose tissue. Given that gastric cancer grows in an adipose tissue-dominated environment, gastric cancer might have interaction with visceral adipose tissue (VAT). The purpose of this study was to investigate the prognostic significance of CT-attenuation and FDG uptake of VAT to predict recurrence-free survival (RFS), peritoneal RFS and overall survival (OS) in patients with advanced gastric cancer (AGC).

METHOD AND MATERIALS

We retrospectively enrolled 117 patients with AGC who underwent staging FDG PET/CT and subsequent curative surgical resection. CT-attenuation and FDG uptake (SUV) of VAT and maximum FDG uptake of primary tumor (SUVmaxT) were measured from PET/CT images. The relationship of VAT attenuation and SUV with clinico-histopathologic factors and survival was assessed.

RESULTS

There was a significant positive correlation between VAT attenuation and SUV (p<0.001, r=0.799). In correlation analyses, both VAT attenuation and SUV showed significant positive correlations with T stage, tumor size, and platelet-to-lymphocyte ratio (p<0.05), and patients who died during follow-up had significantly higher VAT attenuation and SUV than those who survived (p<0.05). Patients with high VAT attenuation and SUV showed significantly worse RFS, peritoneal RFS, and OS than those with low values (p<0.05). On multivariate survival analysis, VAT attenuation and SUV were remained as significant predictors for peritoneal RFS and OS after adjusting age, sex, tumor stage, and SUVmaxT (p<0.05).

CONCLUSION

CT-attenuation and FDG uptake of VAT on staging FDG PET/CT were correlated with tumor characteristics and were significant independent predictive factors for peritoneal RFS and OS in patients with AGC.

CLINICAL RELEVANCE/APPLICATION

The qualitative characteristics of visceral adipose tissue measured on FDG PET/CT could be used to predict the risk of periteoneal recurrence in patients with advanced gastric cancer after surgical resection.

SSK15-04 Standardized Uptake Values on 68Ga-DOTATATE PET/CT Predict Response to Somatostatin Analog Therapy in Gastroenteropancreatic Neuroendocrine Tumors

Wednesday, Dec. 4 11:00AM - 11:10AM Room: E451A

Participants

Hwan Lee, MD, Philadelphia, PA (Presenter) Nothing to Disclose

Jennifer R. Eads, Philadelphia, PA (*Abstract Co-Author*) Consultant, Lexicon Pharmaceuticals, Inc; Spouse, Employee, Bristol-Myers Squibb Company

Daniel Pryma, MD, Philadelphia, PA (*Abstract Co-Author*) Research Grant, Siemens AG; Research Grant, 511 Pharma; Research Grant, Progenics Pharmaceuticals, Inc; Research Consultant, Progenics Pharmaceuticals, Inc; Research Consultant, 511 Pharma; Research Consultant, Actinium Pharmaceuticals, Inc; Research Consultant, Nordic Nanovector ASA

For information about this presentation, contact:

Hwan.Lee@pennmedicine.upenn.edu

PURPOSE

68Ga-DOTATATE PET/CT provides a quantitative measure of tumor somatostatin receptor status in gastroenteropancreatic neuroendocrine tumors (GEP-NETs). We examined the ability of standardized uptake values (SUVs) on 68Ga-DOTATATE PET/CT to predict response to somatostatin analog (SSA) therapy.

METHOD AND MATERIALS

The medical records of 108 consecutive patients with grade 1-2 GEP-NETs on SSA monotherapy who received 68Ga-DOTATATE PET/CT scans at a single institution were reviewed to obtain baseline characteristics, 68Ga-DOTATATE SUVmax, and progression-free survival (PFS) data. A receiver operating characteristic curve was constructed to determine the optimal SUVmax cutoff for stratification. PFS in the high vs. low SUVmax groups was compared with Kaplan-Meier survival analysis. The effects of baseline characteristics and SUVmax on PFS were examined with univariate and multivariate Cox regression.

RESULTS

SUVmax was significantly higher (p<0.001) in pancreatic compared to gastrointestinal NETs, but did not vary with other baseline clinical, pathologic, and laboratory characteristics. Median clinical follow-up was 16 months, and PFS at 6, 12, and 18 months was $91 \pm 3\%$, $80 \pm 4\%$, and $61 \pm 6\%$, respectively. The best SUVmax cutoff of 18.35 from ROC analysis yielded sensitivity and specificity of 39% and 98%, respectively, for disease progression by 12 months (area under the curve=0.66). The low SUVmax group showed significantly shorter PFS compared to the high SUVmax group (p<0.0001) with median of 6.6 months vs. >24 months, which was reproduced in a subgroup analysis of 30 SSA naïve patients (p<0.05). On univariate analysis, high tumor grade, Ki-67, and mitotic index, as well as low SUVmax and no prior SSA therapy, were identified as predictors of early treatment failure. Only low SUVmax remained statistically significant on multivariate analysis with hazard ratio of 6.85. (95% CI: 2.10-22.34). In a subgroup analysis of 46 grade 2 patients, short PFS on SSA was again predicted by SUVmax<18.35 (p<0.01), but not with the Ki-67 cutoff value of 10% (p=0.38).

CONCLUSION

Low SUVmax on 68Ga-DOTATATE PET/CT independently predicts early failure on SSA monotherapy in grade 1-2 GEP-NET patients with high specificity.

CLINICAL RELEVANCE/APPLICATION

Based on 68Ga-DOTATATE PET/CT, clinicians can better inform patients on the expected benefit of SSA therapy, especially when access to SSA is difficult, and offer proactive discussion on alternatives.

SSK15-05 68Ga-DOTATATE PET/CT Parameters for the Early Prediction of Response to Peptide Receptor-Mediated Radionuclide Therapy (PRRT) for Metastatic Neuroendocrine Tumors (NET)

Wednesday, Dec. 4 11:10AM - 11:20AM Room: E451A

Participants

Ur Metser, MD, FRCPC, Toronto, ON (*Presenter*) Nothing to Disclose Reut Anconina, MD, Toronto, ON (*Abstract Co-Author*) Nothing to Disclose Douglas Hussey, BSC,RT, Toronto, ON (*Abstract Co-Author*) Nothing to Disclose Ravi M. Mohan, MD, DPhil, Toronto, ON (*Abstract Co-Author*) Nothing to Disclose David Green, Toronto, ON (*Abstract Co-Author*) Nothing to Disclose Amy Liu, Toronto, ON (*Abstract Co-Author*) Nothing to Disclose James Brierley, Toronto, ON (*Abstract Co-Author*) Nothing to Disclose David Laidley, MD, London, ON (*Abstract Co-Author*) Nothing to Disclose Sten Myrehaug, MD,FRCPC, Toronto, ON (*Abstract Co-Author*) Travel support, Ipsen SA Travel support, Novartis AG Speaker, Novartis AG Rosalyn Juergens, Hamilton, ON (*Abstract Co-Author*) Nothing to Disclose Rebecca Wong, Toronto , ON (*Abstract Co-Author*) Nothing to Disclose

For information about this presentation, contact:

ur.metser@uhn.ca

PURPOSE

To determine whether change in 68Ga-DOTATATE (DT) uptake at tumor sites is predictive of early response to PRRT. A secondary aim was to determine whether DT uptake in reference tissues changes after first cycle of PRRT (C1).

METHOD AND MATERIALS

There were 36 patients (20 men, 16 women; mean age, 60 yrs) with metastatic well-differentiated NETs (Ki67<30%, median Ki67, 6.6) being considered for PRRT who underwent baseline & follow-up DT PET after C1. SUVmax in reference tissues (mediastinal blood pool, liver & spleen) were recorded at baseline and after C1. Response to therapy at 4 months post 4th cycle of PRRT, assessed by RECIST 1.1, was available for 28 patients (mean time to response assessment, 10.9 mo; range 6-16). SUVmax & SULpeak were recorded in <=5 marker lesions per patient (<= 2 per organ). Response to therapy was compared to SUVmax & SULpeak at baseline, change in SUVmax and SULpeak after C1, and change in ratio of average SUVmax/ SULpeak of tumor to liver and spleen.

RESULTS

At baseline and after C1, mean SUVmax in blood pool, liver and spleen were 1.45 and 1.42 (-0.7%); 5.2 and 5.8 (+13%); and 16 and 19.4 (+28.4%), respectively. There were 15/28 (53.6%) patients with stable disease (SD), 10/28 (35.7%) with partial response (PR) and 3/28 (10.7%) with progressive disease (PD). The most predictive parameters for response were baseline SUVmax & change in SUVmax/SULpeak ratio of tumor/spleen. Baseline SUVmax for SD, PR and PD was 43.8 (range: 13.5-111.2), 43.3 (range: 11-137.7) & 26.2 (range: 16.5 - 40.2), respectively. Change in SUVmax ratio of tumor/spleen for SD, PR and PD was -24.2% (range: 11.2 [-77.1]), -33.5% (range: 7.8-[-70.8]) & -13.3% (range: 0.8-[-39.6]), respectively. Change in SULpeak ratio of tumor/spleen for SD, PR and PD was -24.4% (range: 19.9-[-76.9]), -36% (range: 0.7-[-84.8]) & -7.8% (range: 19.2-[39.3]), respectively.

CONCLUSION

There is generally an SUV increase in liver & spleen after C1, with little change in blood pool activity. Although there is significant overlap in measured parameters, likely limiting utility of early prediction of response on an individual basis, lower SUVmax at baseline and smaller decrease in SUVmax/ SULpeak tumor to spleen ratio were the most predictive parameters for early disease progression.

CLINICAL RELEVANCE/APPLICATION

There is significant overlap in measured DT-PET parameters, likely limiting utility of early prediction of response on an individual basis.

SSK15-06 Diffusion-weighted MRI (DWI) and 68Ga-DOTATATE PET/CT: Comparison of Both Modalities in Assessment of Tumor Response of Hepatic Metastases of Primary Neuroendocrine Tumor (NET) Undergoing Selective Internal Radiotherapy with 90Yttrium-microspheres

Wednesday, Dec. 4 11:20AM - 11:30AM Room: E451A

Participants

Maria Ingenerf, MD, Munich, Germany (*Presenter*) Nothing to Disclose Laura Kaiser, Munich, Germany (*Abstract Co-Author*) Nothing to Disclose Adrian Curta, MD, Munich, Germany (*Abstract Co-Author*) Nothing to Disclose Homeira Karim, Munich, Germany (*Abstract Co-Author*) Nothing to Disclose Harun Ilhan, Munich, Germany (*Abstract Co-Author*) Nothing to Disclose Jens Ricke, MD,PhD, Berlin, Germany (*Abstract Co-Author*) Research Grant, Sirtex Medical Ltd Research Grant, Bayer AG Christine Schmid-Tannwald, MD, Munich, Germany (*Abstract Co-Author*) Nothing to Disclose

PURPOSE

To compare ADC values of DWI and SUV of 68Ga-DOTATATE PET/CT in assessing treatment response in patients with liver metastases of primary NET following SIRT.

METHOD AND MATERIALS

30 patients with 80 target liver metastases of primary NET who underwent abdominal MRI with DWI and 68Ga-DOTATATE PET/CT before and after SIRT were included. Tumor size, mean ADC values of the lesions and normal liver, intralesional SUVmax and SUV mean, tumor to spleen ratio (T/S ratio), and tumor to liver ratio (T/L ratio) were measured. Tumor response to radioembolization was categorized with respect to Response Evaluation Criteria in Solid Tumors v1.1 (RECIST) on follow-up examination.

RESULTS

67/80 metastases were categorized as stable disease (SD) and 13/80 metastases as partial remission (PR). Intralesional ADCmin and ADC mean increased significantly (p< 0.006) in the group of PR and SD with a significant higher increase of ADCmin values in the PR group ($54,1 \pm 14,6 \%$ vs. $24 \pm 4,9 \%$, p= 0,02) before and after SIRT. Currently used SUV measurements showed significant decrease in the PR group (SUV max, SUVmean, T/S ratio and T/L ratio), whereas only SUV max, SUVmean, T/S ratio (max/max) decrease significantly in the SD group. Using ROC curves, SUVmean was found the best metric (AUC 0.75), however similar results were found for ADCmin (AUC 0.7).

CONCLUSION

SUV measurements of 68Ga-DOTATATE PET/CT but also ADC values on DW-MRI seem to represent a valuable, functional maker for evaluation of response to SIRT treatment of hepatic metastases in patients with primary NET and may help in assessing further therapeutic strategies.

CLINICAL RELEVANCE/APPLICATION

DW-MRI appears similar to 68Ga-DOTATATE PET/CT for quantitative response assessment in patients with hepatic metastases of NET and may be used to guide further management of patients who undergo SIRT.

SSK15-07 Tumor Volume Remains the Most Important Variable When Considering Radiomic Feature Analysis in Anal Cancer

Wednesday, Dec. 4 11:30AM - 11:40AM Room: E451A

Participants

Joe Mercer, BMBCh, BMedSc, Bolton, United Kingdom (*Presenter*) Nothing to Disclose Histesh Mistry, Manchester, United Kingdom (*Abstract Co-Author*) Nothing to Disclose

Prakash Manoharan, MRCP, FRCR, Manchester, United Kingdom (*Abstract Co-Author*) Nothing to Disclose Thomas Westwood, MBBS, Manchester, United Kingdom (*Abstract Co-Author*) Nothing to Disclose Sahithi Nishtala, MBBS, FRCR, Newcastle under Lyme, United Kingdom (*Abstract Co-Author*) Nothing to Disclose Azadeh Taheri, Manchester, United Kingdom (*Abstract Co-Author*) Nothing to Disclose Andrew Renehan, MRCS, PhD, Manchester, United Kingdom (*Abstract Co-Author*) Nothing to Disclose Mark Saunders, M20 4Bx, United Kingdom (*Abstract Co-Author*) Nothing to Disclose Rohit Kochhar, MD, Manchester, United Kingdom (*Abstract Co-Author*) Nothing to Disclose

For information about this presentation, contact:

joseph.mercer@christie.nhs.uk

PURPOSE

Anal squamous cell carcinoma is a rare disease and most cases can be effectively with chemoradiotherapy. However if locoregional relapse occurs, outcomes following surgical salvage are often poor. Novel biomarkers have the potential to help predict response to treatment and select patients for appropriate follow up pathways based on risk of relapse. We aimed to explore the potential of pre-treatment PET-CT radiomic features in predicting locoregional failure and survival in these patients.

METHOD AND MATERIALS

257 consecutive patients between Jan 2012 and Jan 2018 underwent staging PET-CT. Clinical outcomes were overall survival (OS) and locoregional relapse. Radiomic features (RFs) comprising conventional PET and CTparameters, texture and shape features were extracted using LifeX software. Unsupervised learning, usingPrinicipal Components Analysis, on those parameters was then performed to generate clusters of patients. Clinical variables and endpoints were then assessed across the clusters generated. In addition, supervised learning, using elastic net regularisation, was also performed. Multivariable clinical risk prediction models, built using standard clinical parameters, with/without RFs were assessed using concordance probability estimate (CPE), adjusted R-squared (R2) and likelihood ratio-test statistic (LRT).

RESULTS

Unsupervised learning highlighted that: (1)many of the RFs correlated to tumour size; (2) patient clusters using RFs correlated with T-Stage and MRI size thus tumour volume. The final multivariable risk prediction model with RFs contained one textural and one volume-based PET parameter (CPE = 0.76, R2=0.17, LRT = 36.7), which performed marginally better than a clinical model using tumour volume (CPE = 0.75, R2=0.14, LRT = 30.0).

CONCLUSION

Survival prediction models were enhanced by a textural feature and a volume-specific parameter identified using supervised learning. Primary tumour size remains the most important factor in predicting outcome. Challenges in accurate assessment of lesion size are well known on MRI, tumour volume can be easily assessed with appropriate PET-CT reporting software and this information should be considered in routine reporting and prediction modelling.

CLINICAL RELEVANCE/APPLICATION

Improvements in risk stratification may avoid excessively intense follow up protocols while ensuring early diagnosis of locoregional failure and the best chance of successful salvage.

SSK15-08 Intratumoral Metabolic Heterogeneity and Other Quantitative 18F-FDG PET/CT Parameters for Prognosis Prediction in Esophageal Cancer

Wednesday, Dec. 4 11:40AM - 11:50AM Room: E451A

Participants Akilan Gopal, Dallas, TX (*Presenter*) Nothing to Disclose Yin Xi, PhD, Dallas, TX (*Abstract Co-Author*) Nothing to Disclose Rathan M. Subramaniam, MD,PhD, Dunedin, New Zealand (*Abstract Co-Author*) Nothing to Disclose Daniella F. Pinho, MD, Dallas, TX (*Abstract Co-Author*) Nothing to Disclose

For information about this presentation, contact:

daniella.pinho@utsouthwestern.edu

PURPOSE

To evaluate the impact of intratumoral metabolic heterogeneity and other quantitative FDG PET/CT parameters for predicting patient outcomes in esophageal cancer.

METHOD AND MATERIALS

This IRB and HIPPA complaint retrospective study included a total of 71 patients with biopsy proven adenocarcinoma or squamous cell carcinoma of the esophagus who had a FDG PET/CT for initial staging. Automated gradient-based segmentation method was used to assess the primary tumor standardized uptake value maximum and peak (SUV max and SUV peak), metabolic tumor volume (MTV) and metabolic intratumoral heterogeneity index, calculated as the area under cumulative SUV-volume histograms (AUC-CSH), with lower AUC-CSH indexes corresponding to higher degrees of tumor heterogeneity. Patient's demographics and tumor staging were also collected. Median follow up time was 28.2±30.3 months. Overall survival (OS) and progression free survival (PFS) were calculated using univariate cox regression with the adjustment of age, gender, staging, treatment and histological grade. All pet measurements were normalized and the hazard ratios change was equivalent to one standard deviation.

RESULTS

The patients' mean age was 64±10.3 years and there were 6 patients with stage I, 11 with stage II, 31 with stage III, 21 with stage IV disease, and 2 with unknown staging. Median survival was 16.1 months. Forty-six patients died and 15 were alive as of the end of the study (for 10 patients no recent information on survival was available). Eighteen patients had recurrence as of the end of the study. Higher MTV was significantly associated with reduced PFS for every standard deviation increase (HR=0.193, 95% CI=0.052-0.711, p=0.0134). Higher AUC-CSH (lower tumor heterogeneity, homogeneous tumor) was significantly associated with increased PFS for every standard deviation increase in the area under the curve (HR=10.779, 95% CI=1.306-88.957, p=0.0272).

CONCLUSION

There was a significant association of MTV and tumor heterogeneity with progression free survival for patients with esophageal cancer.

CLINICAL RELEVANCE/APPLICATION

FDG PET/CT quantitative parameters, particularly intramural metabolic heterogeneity, can provide prognostic information on initial staging scan, potentially leading to a more personalized approach for patient's treatment.

SSK15-09 Early Utilization of SPECT/CT to Improve Localization and Reduce Time to Diagnosis and Intervention in Acute Gastrointestinal Bleeding

Wednesday, Dec. 4 11:50AM - 12:00PM Room: E451A

Participants

Gaurav Gadodia, MD, Cleveland, OH (*Presenter*) Nothing to Disclose Venkata Reddannagari, Cleveland, OH (*Abstract Co-Author*) Nothing to Disclose Karunakaravel Karuppasamy, MD,FRCR, Westlake, OH (*Abstract Co-Author*) Nothing to Disclose Priyesh J. Patel, MD, Lakewood, OH (*Abstract Co-Author*) Nothing to Disclose Ram Kishore R. Gurajala, MBBS, FRCR, Beachwood, OH (*Abstract Co-Author*) Nothing to Disclose

For information about this presentation, contact:

ggadodia7@gmail.com

PURPOSE

Approximately 2% of the admissions to the emergency department are for acute GIB, with 1 in 4 requiring immediate attention. Planar scintigraphy using Tc-99m tagged red blood cells (Tc-99m RBCs) is used as an ideal first line diagnostic option in suspected GIB due to being non-invasive and having a very high sensitivity. However, due to this high sensitivity, it is often the case that patients with positive or equivocal Tc-99m RBC scans have negative findings on CT angiography and/or catheter based angiography. These patients that continue to bleed ultimately require provocative angiograms or invasive procedures like surgery, which are risky and often also negative. This is due to a combination of low confidence of interpretation and poor localization of planar scintigraphy. We hypothesized that by utilizing hybrid SPECT/CT in cases of suspected GIB, we would be able to improve confidence of interpretation and localization of the bleed, and this was tested and proven in our institution. Yet, while we found a high negative predictive value of adding SPECT/CT, positive predictive value was still low. As it is well known that the sooner a bleed is identified, the higher chances are of successful treatment, we proposed a new protocol in which SPECT/CT is utilized earlier. Thus, the purpose of this report is to evaluate if a change in imaging protocol with early utilization of SPECT/CT can improve localization of acute GIB and decrease time to intervention, and/or eliminate unnecessary procedures.

RESULTS

In our retrospective analysis, 49 patients who underwent planar scintigraphy and hybrid SPECT/CT for suspected acute nonvariceal GIB were included. 28 of them had positive studies on nuclear imaging (planar and SPECT/CT), while 21 were negative. For confidence of interpretation, of the 20 patients that were deemed "equivocal" on planar imaging, 13 were found to be negative and 7 positive on hybrid SPECT/CT. For localization, only 6 of the 28 positive patients had a bleed that was accurately localized on planar imaging, while all 28 were accurately localized on SPECT/CT. Finally in terms of outcomes, of the 28 patients with positive studies on nuclear medicine imaging, only 6 were found to be positive on angiography or endoscopy (PPV: 21.4%). However, all 21 patients who were negative on SPECT/CT were also negative on angiography or endoscopy (NPV: 100%). In our limited experience with the new protocol in 4 cases, time to diagnosis and/or intervention has been reduced by 50%.

CONCLUSION

Our retrospective analysis previously showed that SPECT/CT improves confidence of interpretation, localization, and ultimately outcomes in the diagnosis of GIB. While the PPV of 21.4% is low, it is still higher than planar scintigraphy alone, and likely is mostly due to slow or intermittent GI bleeding that is detected by SPECT/CT but not brisk enough to be seen on subsequent testing. On the other hand, our analysis demonstrated a 100% NPV, which can be utilized to avoid further unnecessary and possibly invasive or risky tests. Furthermore, SPECT/CT eliminated "equivocal" findings which are often reported on planar scintigraphy alone, and allowed for more accurate localization in all positive cases. Due to these findings and the fact that the initial flow phase of planar scintigraphy (first minute) is comparable to the first order angiographic arterial phase, we proposed that any tests that were positive or equivocal in that first minute should have their planar imaging stopped and go directly to SPECT/CT. Thus, as opposed to 60 minutes of planar testing, these higher risk cases would have SPECT/CT imaging completed within 30 minutes of tagged RBC injection. Any that were negative on SPECT/CT would not need further provocative or invasive testing, while those that were positive would proceed directly to angiography. In our limited experience of our first 4 patients in which we have implemented this protocol, definite diagnosis (in negative cases) or intervention (in positive cases) was achieved at least 50% faster (30 minutes vs. 60+ minutes for planar plus additional SPECT/CT). Based on our findings, we propose a similar protocol be implemented in centers where GIB are evaluated and treated to improve time to diagnosis or intervention, and eliminate any unnecessary testing.

METHODS

Retrospective analysis from 2001-2014 of patients with suspected non-variceal GIB who underwent planar tagged RBC scintigraphy and hybrid SPECT/CT prior to angiogram or endoscopy/colonoscopy. Data on confidence of interpretation, localization, and outcomes were collected and analyzed. Based on the results, a new protocol was implemented at our institution as follows: all patients in whom GIB is suspected, the planar scintigraphic images are watched in the flow phase (first minute), and if there is a definite positive, probable positive, or equivocal finding, the study is stopped and a SPECT/CT is performed.

Printed on: 10/29/20





SSK16

Neuroradiology (Movement Disorders)

Wednesday, Dec. 4 10:30AM - 12:00PM Room: S401CD



AMA PRA Category 1 Credits ™: 1.50 ARRT Category A+ Credit: 1.75

FDA Discussions may include off-label uses.

Participants

Seung-Koo Lee, MD, PhD, Seoul, Korea, Republic Of (*Moderator*) Nothing to Disclose Jody L. Tanabe, MD, Aurora, CO (*Moderator*) Invited participant, GE Signa Masters 2019 Neuro Summit, General Electric Company Michael M. Zeineh, PhD, MD, Stanford, CA (*Moderator*) Research funded, General Electric Company;

Sub-Events

SSK16-01 Bi-Modality MRI Radiomics Features in Identifying Parkinson's Disease and Its Clinical Subtypes

Wednesday, Dec. 4 10:30AM - 10:40AM Room: S401CD

Participants

Xiaojun Guan, Hangzhou, China (Presenter) Nothing to Disclose Tao Guo, Hangzhou, China (Abstract Co-Author) Nothing to Disclose Cheng Zhou, Hangzhou, China (Abstract Co-Author) Nothing to Disclose Ting Gao, Hangzhou , China (Abstract Co-Author) Nothing to Disclose Victor Han, Berkeley, CA (Abstract Co-Author) Nothing to Disclose Steven Cao, Berkeley, CA (Abstract Co-Author) Nothing to Disclose Chunlei Liu, Berkeley, CA (Abstract Co-Author) Nothing to Disclose Hongjiang Wei, Shanghai, China (Abstract Co-Author) Nothing to Disclose Yuyao Zhang, Shanghai, China (Abstract Co-Author) Nothing to Disclose Min Xuan, Hangzhou, China (Abstract Co-Author) Nothing to Disclose Quanquan Gu, MD, PhD, Hangzhou, China (Abstract Co-Author) Nothing to Disclose Jingjing Wu, Hangzhou, China (Abstract Co-Author) Nothing to Disclose Peiyu Huang, Hangzhou, China (Abstract Co-Author) Nothing to Disclose Jia L. Pu, Hangzhou, China (Abstract Co-Author) Nothing to Disclose Baorong Zhang, Hangzhou, China (Abstract Co-Author) Nothing to Disclose Xiaojun Xu, Hangzhou, China (Abstract Co-Author) Nothing to Disclose Minming Zhang, Hangzhou, China (Abstract Co-Author) Nothing to Disclose

For information about this presentation, contact:

xiaojunguan1102@zju.edu.cn

PURPOSE

Due to lacking of objective biomarkers, it remains a big challenge to reach a good diagnosis for Parkinson's disease (PD). Thus, we hypothesized that, in combination with radiomics and machine-learning methods, MRI-based iron quantification and structure measurement might contribute to constructing imaging biomarker.

METHOD AND MATERIALS

245 PD patients and 170 normal controls were finally included in data analysis. All of them underwent ESWAN and high-resolution 3D T1-weighted imaging scanning. Quantitative susceptibility mapping (QSM) and R2* were processed from ESWAN data. Based on newly created age-specific QSM template, symmetrical registration technology (ANTs) was used to obtain subcortex segmentations in the individual QSM and R2* space. FSL-FIRST and ANTs-CorticalThickness methods were used to segment subcortical and cortical regions respectively. Radiomics features including histogram and GLCM features in QSM, R2* and T1 images were obtained from the segmented subcortical regions. Normalized cortical features including thickness, volume, mass and surface area were calculated. In summary, 1408 radiomics features were obtained. Random Forest (RF) algorithm was used to perform feature selection with 1000 permutation and top-20 features were selected.By inputting these top-20 features, RF classifier was constructed to classify different PD subtypes and normal controls with 1000 iterations for each test.

RESULTS

We observed that the obtained 20 features, where the mean QSM signal of bilateral substantia nigra (SN) occupied the top 2 features (the impotence were 100% for left SN and 84% for right SN), had good generalization. In the classification between PD patients and normal controls, the accuracy was 81.3%, while it was 77.4% for early PD and 81.2% for late PD. The performance to identify different motor subtypes were both 79.9%. Besides, we identically subdivided PD patients into 4 classes according to an ascending rank of UPDRS scores, and the diagnostic accuracies were 79.3%, 80.2%, 80.1% and 85% from early to late stages.

CONCLUSION

Radiomics features calculated from iron and structure images could reach a good performance of PD diagnosis. By feature selection, we confirmed that nigral iron content (mean signal) is the most important feature for PD.

CLINICAL RELEVANCE/APPLICATION

Radiomics features calculated on brain iron and structural images have good generalization ability to diagnose PD with acceptable accuracy.

SSK16-02 Diagnostic Accuracy of the Magnetic Resonance Parkinsonism Index and Midbrain-to-Pons Ratio in Differentiating Progressive Supranuclear Palsy from Parkinson's Disease and Controls

Wednesday, Dec. 4 10:40AM - 10:50AM Room: S401CD

Participants

Aman Snehil, MBBS, Mumbai, India (*Abstract Co-Author*) Nothing to Disclose Ritu M. Kakkar, MBBS, DMRD, Mumbai, India (*Abstract Co-Author*) Nothing to Disclose Shrinivas B. Desai, MD, Mumbai, India (*Presenter*) Nothing to Disclose

For information about this presentation, contact:

riturupesh@gmail.com

PURPOSE

To compare the efficacy of MRPI and M/P ratio in the diagnosis and differentiation of Progressive Supranuclear Palsy from Parkinson's disease and Controls.

METHOD AND MATERIALS

40 consecutive patients were enrolled in this study, satisfying the diagnostic criteria by the National Institute for Neurological Disorders and Stroke, and the Society for PSP (NINDS SPSP), along with 40 PD and 40 control patients. All patients were assessed using standard MR imaging protocol.Standard MPrage sequence was included .The area of midbrain ,pons was calculated on midsagittal images while diameter of MCP and SCP on parasagittal and coronal images respectively .MRPI was calculated by multiplying the pons area/midbrain area ratio by MCP width/SCP width ratio. The midbrain/pons (M/P) ratio was measured as the ratio of midbrain area to pons area.

RESULTS

Mean MRPI in PSP patients (19.1 ± 4.87) was significantly higher than that in PD patients (9.11 ± 1.6) and controls (9.21 ± 2.11). In this study, MRPI was 100% sensitive, specific, and accurate in differentiating PSP from PD and was 100% sensitive, 100% specific, and 100% accurate in differentiating PSP from controls. Positive correlation was found between the duration of disease, and MRPI in the present study. MRPI was superior to the M/P ratio in differentiating between PSP and PD patients on an individual basis. No overlapping values were observed in the PSP and PD patients.There was moderate association between outcome of NINDS SPSP Criteria for PSP cases and MRPI (Eta squared=0.03). Also, moderate association between the MRPI values of possible and probable cases of PSP (t=6.46, p>0.001).

CONCLUSION

Magnetic Resonance Parkinsonism Index is more sensitive, specific, and accurate than M/P ratio in differentiating PSP from PD in the early stages on an individual basis

CLINICAL RELEVANCE/APPLICATION

MR Parkisnons Index is a simple MRI based calculation that should routinely be included in patients with atypical Parkinsons disease and can significantly impact management and prognosis

SSK16-03 Twelve-Year Diffusion Changes in the Deep Gray Nuclei on Serial MRI in Parkinson's Disease

Wednesday, Dec. 4 10:50AM - 11:00AM Room: S401CD

Participants

Leon Q. Ooi, MENG, Singapore, Singapore (*Abstract Co-Author*) Nothing to Disclose Isabel H. Chew, BA, Singapore, Singapore (*Abstract Co-Author*) Nothing to Disclose Huihua Li, Singapore, Singapore (*Abstract Co-Author*) Nothing to Disclose Septian Hartono, Singapore, Singapore (*Abstract Co-Author*) Nothing to Disclose Chu-Ning Ann, Singapore, Singapore (*Abstract Co-Author*) Nothing to Disclose Soo Lee Lim, MS, Singapore, Singapore (*Abstract Co-Author*) Nothing to Disclose Eng King Tan, Singapore, Singapore (*Abstract Co-Author*) Nothing to Disclose Ling Ling Chan, MBBS, FRCR, Singapore, Singapore (*Presenter*) Nothing to Disclose

PURPOSE

Basal ganglia pathology has been linked to motor deterioration in Parkinson's disease (PD). Diffusion tensor imaging (DTI) interrogates deep gray nuclei (DGN) microstructure in vivo, but results from cross-sectional studies in PD have been inconsistent. We investigated temporal DTI profiles in the DGN (caudate, putamen and thalamus) over a 12-year study in relation to their clinical progression.

METHOD AND MATERIALS

PD patients and HC underwent 3 scans 6 years apart (157 subjects in total at baseline), on the same 1.5T scanner. Patients were clinically evaluated using the UPDRS and H&Y staging. The standardized protocol included DTI and structural MPRAGE sequences. The DGN were segmented through FSL FIRST. Structures were individually screened and corrected during quality assessment. The segmentation masks were resampled to the DTI space and used to sample DTI indices (FA, MD, AD, RD) from each nucleus. Statistical analysis was carried out using a generalized estimating equation (GEE) to investigate differences between HC and PD at baseline, along with their longitudinal progression, adjusting for age and sex. Additionally, the GEE was used to predict H&Y and UPDRS motor scores. Statistical significance was accepted at p < 0.05.

Longitudinal analysis revealed a more severe increase in caudal diffusivity as compared to other DGN. DGN DTI indices were significantly different between HC and PD at the 3rd timepoint. Increasing diffusivity in the caudate correlated with worsening UPDRS and H&Y scores. Putaminal diffusivity correlated with worsening H&Y scores only.

CONCLUSION

Neuronal degeneration is accompanied by decrease in FA and increase in diffusivity. However, significant nucleic DTI differences only manifest in the later stages of PD. This may be secondary to known effects of iron on DTI indices, which artifactually reverse and thence blunt expected DTI changes. The correlation between increased diffusivity and worsening motor performance suggests neuronal degeneration related to PD. This degeneration likely linked to a loss of dopaminergal neurons characteristic to PD in the caudate and putamen throughout the progression of the disease.

CLINICAL RELEVANCE/APPLICATION

Temporal changes to diffusivity suggest artefactual effects from iron deposition during early stages in PD patients. Caudate diffusivity was shown to be an effective biomarker for motor performance.

SSK16-04 Response to Deep Brain Stimulation Correlates with L-DOPA Responsiveness

Wednesday, Dec. 4 11:00AM - 11:10AM Room: S401CD

Participants

Anup K. Bhattacharya, Springfield, PA (*Presenter*) Nothing to Disclose John Pearce, Philadelphia, PA (*Abstract Co-Author*) Nothing to Disclose Mahdi Alizadeh, Philadelphia, PA (*Abstract Co-Author*) Nothing to Disclose Jennifer Muller, MS,BS, Philadelphia, PA (*Abstract Co-Author*) Nothing to Disclose Daniel Kremens, Philadelphia, PA (*Abstract Co-Author*) Nothing to Disclose Tsao Wei Liang, MD, Philadelphia, PA (*Abstract Co-Author*) Nothing to Disclose Victor Romo, MD, Philadelphia, PA (*Abstract Co-Author*) Nothing to Disclose Ashwini Sharan, MD, Philadelphia, PA (*Abstract Co-Author*) Nothing to Disclose Feroze B. Mohamed, PhD, Philadelphia, PA (*Abstract Co-Author*) Nothing to Disclose Chengyuan Wu, Philadelphia, PA (*Abstract Co-Author*) Nothing to Disclose

For information about this presentation, contact:

anupb792@gmail.com

PURPOSE

Deep brain stimulation (DBS) of the subthalamic nucleus (STN) or globus pallidus pars interna (GPi) is indicated in patients with refractory Parkinson's disease (PD) with significant motor fluctuations. While clinical characteristics facilitate patient selection, currently no objective tool to predict response to DBS exists. We examined resting state functional magnetic resonance imaging (rsfMRI) to determine the feasibility of this modality to identify early responders to DBS with minimal programming.

METHOD AND MATERIALS

Ten patients with advanced PD underwent preoperative rsfMRI under anesthesia in preparation for DBS surgery. Motor scores (UPDRS-III) were collected before and after DBS. Scans were performed on a 3T MR scanner, and images were preprocessed to correct for spatial and temporal artifacts. Regions of interest (ROIs) were defined using the Harvard-Oxford and ATAG-MNI04 basal ganglia (BG) atlases. Functional connectivity (FC) was calculated using the MATLAB®-based CONN toolbox via two-tailed bivariate correlations. Significant FC differences between patients who were good responders (> 30% improvement) following DBS versus those who were poor responders (< 30% improvement) were evaluated with an ROI-to-voxel analysis (FDR-corrected p < 0.05).

RESULTS

Patients who responded more favorably to DBS had desynchronization between the putamen and supplementary motor area (SMA) and synchronization between the lentiform nucleus with the superior frontal gyrus (SFG) (Figure 1), similar to characteristic changes seen following L-DOPA administration (p=0.0001).

CONCLUSION

Our findings show promise in the ability of rsfMRI to potentially improve patient selection and provide better pre-surgical consultation for patients regarding early prognosis from DBS.

CLINICAL RELEVANCE/APPLICATION

Resting state functional MRI (rsfMRI) can be used as an objective biomarker to identify those patients who are most likely to benefit from deep brain stimulation surgery.

SSK16-05 Functional Connectivity Patterns Predictive of Treatment Response in Deep Brain Stimulation for Dystonia

Wednesday, Dec. 4 11:10AM - 11:20AM Room: S401CD

Participants

Lela Okromelidze, MD, Jacksonville, FL (*Presenter*) Nothing to Disclose Tsuboi Takashi, MD,PhD, Gainesville, FL (*Abstract Co-Author*) Nothing to Disclose Robert Eisinger, Gainesville, FL (*Abstract Co-Author*) Nothing to Disclose Leonardo Almeida, MD, Gainesville, FL (*Abstract Co-Author*) Nothing to Disclose Matthew Burns, MD, Gainesville, FL (*Abstract Co-Author*) Nothing to Disclose Kelly Foote, MD, Gainesville, FL (*Abstract Co-Author*) Nothing to Disclose Michael Okun, MD, Gainesville, FL (*Abstract Co-Author*) Nothing to Disclose Erik H. Middlebrooks, MD, Ponte Vedra Beach, FL (*Abstract Co-Author*) Research Consultant, Varian Medical Systems, Inc; Research Support, Varian Medical Systems, Inc; Research Support, Boston Scientific Corporation

PURPOSE

Globus pallidus interna (GPi) deep brain stimulation (DBS) is an effective method of treatment for medication-refractory primary generalized and cervical dystonia. However, up to 25% of patients do not respond to DBS, mainly attributed to factors such as: variation in stimulation parameters, target selection, and lack of objective biomarker. Moreover, DBS treatment in dystonia is further complicated due to delayed improvement of dystonic symptoms after stimulation, making optimal device programming challenging. An understanding of the brain connectivity patterns that underpin positive treatment response may prove to be a valuable biomarker to improve outcomes and reduce side effects by improved DBS targeting and programming.

METHOD AND MATERIALS

Group-level analysis of 39 patients with optimized DBS of GPi for primary dystonia was performed. UDRS score percentage change from pre-surgery and six months post-surgery was the primary end point. After co-registration and normalization of post-operative CT/MRI images into standard MNI atlas space, electrode contacts were reconstructed along the lead trajectories using the PaCER algorithm with manual refinement. Volume of tissue activated (VTA) was estimated based on the final DBS programming settings. The VTA was used for seed-based connectivity analysis in each subject using a group-averaged resting-state fMRI dataset of 1000 patients from the Human Connectome Project. Group-level analysis was performed using subjects' first level rs-fMRI t-score maps correlated with percentage change in UDRS score. Controlling for family-wise error rate, statistical significance was considered as p<.001.

RESULTS

Stimulation volumes with greater connectivity to the motor network correlated with improvement in UDRS score. In particular, the primary motor cortex, supplementary motor cortex, and ventral thalamus correlated strongly with UDRS improvement. Expected regions in the motor cerebellum (including lobules IV, V, VI, and VIII) also strongly correlated with UDRS improvement.

CONCLUSION

Functional imaging is a promising tool for medication-refractory primary dystonia patients' DBS treatment planning and outcome prediction.

CLINICAL RELEVANCE/APPLICATION

Functional MRI connectivity patterns may serve as a valuable biomarker for DBS targeting and programming in patients with primary dystonia.

SSK16-06 A Deeper Impact - Using MR Guided Focused Ultrasound for the Treatment of Essential Tremor Targeting Both Thalamic Ventralis Intermidius Nucleus and the Subthalamic Zona Incerta

Wednesday, Dec. 4 11:20AM - 11:30AM Room: S401CD

Participants

Ayesha Jameel, MBBS, London, United Kingdom (*Presenter*) Research Grant, InsighTec Peter Bain, London, United Kingdom (*Abstract Co-Author*) Nothing to Disclose Dipkander Nandi, London, United Kingdom (*Abstract Co-Author*) Nothing to Disclose Brynmor Jones, MRCP, FRCR, London, United Kingdom (*Abstract Co-Author*) Nothing to Disclose Olga Kirmi, MBBS, London, United Kingdom (*Abstract Co-Author*) Nothing to Disclose Wladyslaw M. Gedroyc, MBBS, MRCP, London, United Kingdom (*Abstract Co-Author*) Research Grant, InsighTec

For information about this presentation, contact:

ayesha.jameel@nhs.net;w.gedroyc@imperial.ac.uk

PURPOSE

Essential Tremor (ET) is estimated to affect 10 million people in the United States. Magnetic Resonance guided focused ultrasound (MRgFUS) is a non-invasive treatment for ET that allows targeted thermal ablation of brain tissue under real time image guidance. Previous studies have demonstrated successful targeting of the thalamic Ventral Intermedius Nucleus (Vim) to be an effective treatment in ET; this paper describes the world's first trial using MRgFUS to target both the thalamic Vim and the subthalamic Zona Incerta (ZI).

METHOD AND MATERIALS

This prospective study enrolled 13 patients with medication refractory ET for unilateral MRgFUS procedure. Tremor severity and functional impairment were assessed at baseline and regular intervals post-treatment for 24 months, using the Clinical Rating Scale for Tremor (CRST), Quality of Life in Essential Tremor (QUEST) and Bain-Findley Spirals (BFS) scores. BFS Spirals were also collated intraoperatively: immediately pre-procedure, after targeting the Vim and after targeting the ZI. All spirals were scored by 3 blinded movement disorder Neurologists. The percentage improvement in the spiral scores after Vim ablation and after ZI ablation were compared and analysed.

RESULTS

In all patients there was successful thermal ablation of the target tissue at both Vim and ZI, with improvement in all parameters over the 24months: CRST tremor score of the treated arm 73.5% and the non-treated arm 38.4%, QUEST 38%, BFS 46.9%. The intraoperative BFS scores demonstrated the additional benefit of targeting the ZI was 21.8% - improvement after Vim lesioning 27.9% but after both Vim and ZI lesioning was 49.7%. One patient (7.69%) experienced a significant adverse event; post-treatment unilateral hemi-chorea persistent at 2 years.

CONCLUSION

Our study provides further evidence that MRgFUS is an effective curative treatment for ET and demonstrates the additional benefit of targeting the subthalamic ZI with the thalamic Vim. Furthermore improvement in the tremor scores of non-treated arm shows the positive bilateral effects of targeting the ZI.

CLINICAL RELEVANCE/APPLICATION

MRgFUS has the potential to revolutionise the treatment of movement disorders such as ET It provides an non-invasive alternative

SSK16-07 Cerebellar Atrophy and Cognitive Impairment in Friedreich Ataxia

Wednesday, Dec. 4 11:30AM - 11:40AM Room: S401CD

Participants Elena A. Vola, MD, Naples, Italy (*Presenter*) Nothing to Disclose Sirio Cocozza, MD, Naples, Italy (*Abstract Co-Author*) Speaker, sanofi-aventis Group; Speaker, Genzyme Corporation; Advisory Board, Amicus Therapeutics, Inc Teresa Costabile, Naples, Italy (*Abstract Co-Author*) Nothing to Disclose Giuseppe Pontillo, MD, Capodrise, Italy (*Abstract Co-Author*) Nothing to Disclose Maria Lieto, MD, Naples, Italy (*Abstract Co-Author*) Nothing to Disclose Camilla Russo, Napoli, Italy (*Abstract Co-Author*) Nothing to Disclose Chiara Pane, Napoli, Italy (*Abstract Co-Author*) Nothing to Disclose Francesco Sacca, Naples, Italy (*Abstract Co-Author*) Nothing to Disclose Arturo Brunetti, MD, Naples, Italy (*Abstract Co-Author*) Nothing to Disclose

For information about this presentation, contact:

elena.a.vola@gmail.com

PURPOSE

Recent studies have suggested the presence of a significant atrophy affecting the cerebellar cortex in Friedreich ataxia (FRDA) patients, an area of the brain long considered to be relatively spared by the neurodegenerative phenomena occurring in this condition. Cognitive deficits, which occurs in FRDA patients, have been associated to cerebellar volume loss in other conditions. Aim of this study was to investigate the correlation between cerebellar volume and cognition in FRDA.

METHOD AND MATERIALS

19 patients with genetically confirmed FRDA (M/F:13/6; 28.4±14.1y), along with a group of 20 healthy controls (HC) of comparable age and sex (M/F:11/9; 29.4±9.7y) were included in this study. All subjects underwent an MRI scan including a 3D-T1-weighted sequence and a neuropsychological examination mainly oriented at cognitive domain that are related to cerebellar function (i.e. visuo-perception and visuo-spatial functions, visuospatial memory and working memory). Cerebellar global and lobular volumes were computed using the Spatially Unbiased Infratentorial Toolbox (SUIT v3.2), implemented in SPM12. Furthermore, a cerebellar Voxel Based Morphometry (VBM) analysis was also carried out. Correlations between MRI metrics and clinical data were tested via partial correlation analysis, correcting for age and sex.

RESULTS

FRDA patients showed a significant reduction of the total cerebellar volume (p=0.004), significantly affecting the Lobule IX (p=0.001). At the VBM analysis, a cluster of significant reduced GM density encompassing the entire lobule IX was found (p=0.003). When correlations were probed, a direct correlation between Lobule IX volume and impaired visuo-spatial functions was found (r=0.580, p=0.02), with a similar correlation between the same altered function and results obtained at the VBM (r=0.520; p=0.03).

CONCLUSION

With two different and complementary image analysis techniques, we confirmed the presence of cerebellar volume loss in FRDA, mainly affecting the posterior lobe. In particular, Lobule IX atrophy correlate with worst performances at visuo-spatial functions, further expanding our knowledge about the physiopathology of cognitive damage in FRDA.

CLINICAL RELEVANCE/APPLICATION

In FRDA patients, a significant cerebellar atrophy is present, mainly affecting the posterior lobe and Lobule IX in particular, which also correlate with cognitive performance in the domain of visuo-spatial abilities

SSK16-08 Functional and Structural Integrity Following Focused Ultrasound Thalamotomy and Its Correlation With Tremor Relief

Wednesday, Dec. 4 11:40AM - 11:50AM Room: S401CD

Participants

Gil Zur, Haifa, Israel (*Presenter*) Nothing to Disclose Orit Lesman, MD, Haifa, Israel (*Abstract Co-Author*) Nothing to Disclose Itamar Kahn, PhD, Haifa, Israel (*Abstract Co-Author*) Nothing to Disclose Ayelet Eran, MD, Haifa, Israel (*Abstract Co-Author*) Nothing to Disclose

For information about this presentation, contact:

g_zur@rambam.health.gov.il

PURPOSE

We aim to explore the impact of MRgFUS treatment functional connectivity nd white matter integrity in tremor-related circuits and test whether tremor improvement is correlated to specific pre- or post-treatment functional responsese.

METHOD AND MATERIALS

60 patients with either essential tremor or Parkinson's disease underwent tremor and quality-of-life assessments prior to and at one and six months following focused ultrasound ablation. 21 patients underwent MRI including T1, T2-Flair and resting-state fMRI before treatment and at one day, 7-10 days, 1-3 months, and 4-12 months following it. 39 patients underwent MRI including T1, T2-Flair and diffusion tensor weighted imaging before treatment and at similiar time points to the fMRI group. Diffusivity parameters were calculated and fiber tractography measures were extracted. Changes in functional connectivity and in diffusivity parameters were assessed in different brain areas that are related to tremor.

RESULTS

Decreased functional connectivity was found between the dentate nucleus and the motor thalamus following ablation. Long term damage, was found in the ablated core and in the tract connecting the thalamus and red-nucleus. Inverse correlation was found between fractional anisotropy in the motor thalamus one day following ablation and tremor improvement in both patient groups, with lower values before treatment associated with better outcome (tremor relief) in essential tremor patients.

CONCLUSION

long-term changes in functional connectivity and white matter integrity are present following focused ultrasound thalamotomy. Regions demonstrating long-term white matter changes may be responsible for the tremor relief seen in patients, implicating these regions in the disorder's pathogenesis.

CLINICAL RELEVANCE/APPLICATION

The expected findings of this project would ultimately aid in more accurate patient selection for thalamotomy, as well as assist in further development of ET tremor treatments.

SSK16-09 Correlation between Fractional Anisotropy (FA) and Apparent Diffusion Coefficient (ADC) Changes in the Targeted Ventral Intermediate Nucleus (VIM) after MRgFUS Thalamotomy and Clinical Outcome: Preliminary Results in a Single Center

Wednesday, Dec. 4 11:50AM - 12:00PM Room: S401CD

Participants

Silvia Torlone, L'Aquila, Italy (*Presenter*) Nothing to Disclose Antonella Corridore, L'Aquila, Italy (*Abstract Co-Author*) Nothing to Disclose Milvia Martino, MS, Laquila , Italy (*Abstract Co-Author*) Nothing to Disclose Maria Valeria Marcella Micelli, Laquila , Italy (*Abstract Co-Author*) Nothing to Disclose Emanuele Tommasino, MD,MSc, Laquila , Italy (*Abstract Co-Author*) Nothing to Disclose Federico Bruno, MD, L'Aquila, Italy (*Abstract Co-Author*) Nothing to Disclose Alessia Catalucci, MD, L'Aquila, Italy (*Abstract Co-Author*) Nothing to Disclose Marco Varrassi, L'Aquila, Italy (*Abstract Co-Author*) Nothing to Disclose Francesco Arrigoni, L'Aquila , Italy (*Abstract Co-Author*) Nothing to Disclose Alessandra Splendiani, MD, L'Aquila , Italy (*Abstract Co-Author*) Nothing to Disclose Carlo Masciocchi, MD, L'Aquila, Italy (*Abstract Co-Author*) Nothing to Disclose

For information about this presentation, contact:

Torlone.silvia@gmail.com

PURPOSE

The aim of the study was to evaluate changes of Fractional Anisotropy (FA) and Apparent Diffusion Coefficient (ADC) in the Ventral Intermediate Nucleus (VIM) of the thalamus after MR-guided focused ultrasound (MRgFUS) thalamotomy and the correlation with clinical outcome.

METHOD AND MATERIALS

In the period February 2018-March 2019 we enrolled 39 patients with disabling and refractory tremor (18 Essential Tremor (ET), 21 Parkinson Disease (PD) tremor, mean age 64,6 years) who underwent to unilateral VIM ablation using MRgFUS. The MRgFUS sonications were performed using a 3-Tesla MRI (GE) and a focused ultrasound system (ExAblate Neuro, Insightec). Measurements of the FA and ADC values were performed before thalamotomy, and 1 day, 1 month and 6 months thereafter using Avantage Workstation AW4.7 (GE Healthcare). Clinical evaluation was performed using the Fahn-Tolosa-Marin Scale (FTM) for tremor before treatment, 1 day, 1 month and 6 months thereafter.

RESULTS

Treatment was effective (considerable and immediate reduction of tremor) in 38 out of 39 patients (97,4%). Changes in FA and ADC values after treatment were statistically significant. There was a statistically significant (p<0,005) positive correlation between FA values in the targeted VIM at 1 day after thalamotomy and FTM score at 6 months after treatment. There were not a statistically significant association between ADC values and clinical outcomes.

CONCLUSION

Our data have demonstrated that MRgFUS thalamotomy for treatment of ET and PD tremor results in a significant change of FA and ADC values in the target VIM. Particularly, FA values at 1 day after thalamotomy showed significant associations with clinical outcome. The limitations of this report are the small number of patients and the short follow-up period. Large randomized studies are needed to assess if FA value may be considered a possible imaging marker for early prediction of clinical outcome after MRgFUS thalamotomy for ET and PD tremor.

CLINICAL RELEVANCE/APPLICATION

MRgFUS thalamotomy for treatment of ET and PD tremor results in a significant change of FA and ADC values in the target VIM: these changes may be considered a possible imaging marker for clinical outcome and provided an important prognostic value.

Printed on: 10/29/20





SSK17

Neuroradiology (Brain Tumors 2)

Wednesday, Dec. 4 10:30AM - 12:00PM Room: S402AB

NR

AMA PRA Category 1 Credits ™: 1.50 ARRT Category A+ Credit: 1.75

FDA Discussions may include off-label uses.

Participants

Javier Villanueva-Meyer, MD, San Francisco, CA (*Moderator*) Nothing to Disclose Rivka R. Colen, MD, Houston, TX (*Moderator*) Nothing to Disclose Michael Iv, MD, Stanford, CA (*Moderator*) Nothing to Disclose

Sub-Events

SSK17-01 Clinical Trial Specific MRI Exam Cards: An IROC NCI NCTN Initiative to Harmonize Neuro-Oncology Acquisition Approaches in Multi-Institutional Clinical Trials for Improved AI Driven Quality Assurance and Analysis

Wednesday, Dec. 4 10:30AM - 10:40AM Room: S402AB

Participants

Michael V. Knopp, MD, PhD, Columbus, OH (*Presenter*) Nothing to Disclose Xiangyu Yang, PhD, Columbus, OH (*Abstract Co-Author*) Nothing to Disclose Georgy Shakirin, Cologne, Germany (*Abstract Co-Author*) Employee, Koninklijke Philips NV Huyen T. Nguyen, PhD, Columbus, OH (*Abstract Co-Author*) Nothing to Disclose Frank Thiele, Aachen, Germany (*Abstract Co-Author*) Clinical Researcher, Koninklijke Philips NV Jan Borggrefe, MD, Cologne, Germany (*Abstract Co-Author*) Speaker, Koninklijke Philips NV David Poon, BS, Columbus, OH (*Abstract Co-Author*) Nothing to Disclose Tim Sbory, BS, Columbus, OH (*Abstract Co-Author*) Nothing to Disclose Connor Nealer, Columbus, OH (*Abstract Co-Author*) Nothing to Disclose Jun Zhang, PhD, Columbus, OH (*Abstract Co-Author*) Nothing to Disclose Michael Perkuhn, MD, Cologne , Germany (*Abstract Co-Author*) Nothing to Disclose NV

For information about this presentation, contact:

knopp.16@osu.edu

PURPOSE

As the Imaging and Radiation Oncology Core (IROC) is tasked within the NCI NCTN to assure the quality of imaging performed within clinical trials, we have monitored the consistency of MR sequence parameters. While standard of care imaging should adhere to best practices such as the Brain Tumor Imaging Protocol (BTIP), tremendous variability still exists. In order to facilitate harmonization and consistent practice, we initiated this project to develop clinical trial specific MR exam cards for neuro-oncologic imaging.

METHOD AND MATERIALS

MR acquisition parameters from 4011 exam timepoints and >21K sequences obtained within 5 clinical NCTN trials of 970 different patients were reviewed. Acceptable ranges were defined for key MR sequence parameters and prototype brain clinical trial MRI exam cards developed for three MR vendor systems (GE, Philips, Siemens). An initial local feasibility assessment followed by a pilot multi-center demonstration protocol was developed. Several DLM based AI tools were explored for automated QC testing and analytics.

RESULTS

The variability and lack of adherence to all protocol expectations was extensive, which did not necessarily impact the visual read interpretation, however did impact analytical tools. Even labeling for MR sequences presented an unanticipated variability making AI tool based processing extremely burdensome. Those findings confirmed the need for radically improved MR exam card management that has been initially piloted in our local environment and is ongoing in a multi-centered pilot.

CONCLUSION

Innovative MR Exam card management is essential to improve consistency for Neuro-Oncologic imaging especially when deep learning model based AI driven analytics are to be employed. In order to utilize QA tools at the time of image generation, the benefits of proactive exam card management are readily recognizable for both standard of care and clinical trial imaging.While distributed exam card management can not yet be done in a vendor neutral way, efforts like this will idenify the benefits and needs of such capabilities.

CLINICAL RELEVANCE/APPLICATION

Proactive exam card management is necessary for both standard of care and clinical trial imaging to enable more consistent MRI

and integration of AI driven quality assurance processes.

SSK17-02 CT, Conventional and Advanced MR Imaging Descriptors for Differentiating Tumefactive Demyelinating Lesions from Gliomas and Lymphomas: Determining ADC Cut-Off Value, Degree of Correlation and Diagnostic Performance of Descriptors

Wednesday, Dec. 4 10:40AM - 10:50AM Room: S402AB

Participants

Bharath B. Das, MD, MBBS, Bangalore, India (*Presenter*) Nothing to Disclose Suman T. Prabhakar, MBBS, MD, Bangalore, India (*Abstract Co-Author*) Nothing to Disclose Prashanth Reddy, MBBS, MD, Bangalore, India (*Abstract Co-Author*) Nothing to Disclose Puneeth K. K N, MD, Mumbai, India (*Abstract Co-Author*) Nothing to Disclose Jainesh V. Dodia, MBBS, MD, Bangalore, India (*Abstract Co-Author*) Nothing to Disclose Bhavana Nagabhushana Reddy, MBBS, MD, Bengaluru, India (*Abstract Co-Author*) Nothing to Disclose Sanjaya Viswamitra, MD, Bangalore, India (*Abstract Co-Author*) Nothing to Disclose

For information about this presentation, contact:

bharathradoc@gmail.com

PURPOSE

To determine ADC cut off values for differentiating TDLs from gliomas and lymphomas To determine degree of correlation of CT and MR descriptors with tumefactive demyelinating lesions (TDLs) in comparison to gliomas and lymphomas To determine diagnostic performance of these descriptors in differentiating TDLs from gliomas and lymphomas

METHOD AND MATERIALS

Histopathology proven consecutive cases of TDL, glioma, and primary CNS lymphoma (PCNSL) from January 2012 to August 2018 were included in study, which are 28-TDLs, 107 Gliomas (HGG-66, IGG-19, LGG-22) and PCNSL 22 cases. Plain CT brain done with 128 slice scanner. MRI protocol included T1, T2, FLAIR, DWI/ADC, SWI, DSC - Perfusion, post contrast and MR spectroscopy. All cases were evaluated by 2 neuroradiologists with 5 years experience. Evaluation of CT density in lesions were done in areas which showed enhancement in MR contrast study, they were visually graded and quantified. In MRI, lesions were evaluated for marginal T2 SI, ADC quantification, oedema, mass effect, vessels within lesion, MRS and perfusion characteristics. ADC values were evaluated for significant variation between lesions and then plotted in ROC curve for cut off value. Pearson correlation coefficient was used to analyze the degree of correlation. Logistic regression with trained model was used to obtain diagnostic performance parameters.

RESULTS

ADC cut off value obtained was 775x10-6mm2/s, below which diagnosis of PCNSL or HGG to be considered. With Pearson correlation coefficient, descriptors could be orderly arranged with respect to degree of correlation irrespective of directionality. The diagnostic performance parameters obtained for differentiating TDLs from differentials are sens-85%, sp-100%, PPV-100%, NPV-96%, Accuracy 97%. These parameters and correlation coefficients are also separately tabulated for TDL vs PCNSL, TDL vs HGG.

CONCLUSION

Use of ADC cut off value, CT and MR descriptors of high degree correlation can provide specific diagnosis of TDL with high diagnostic accuracy and can be confidently differentiated from gliomas and PCNSL.

CLINICAL RELEVANCE/APPLICATION

This study describes ADC cut off values, CT and MR descriptors which aid in specific diagnosis of TDL with high diagnostic accuracy. This is of importance, as TDLs need to be differentiated from gliomas and lymphomas due to conservative steroid management of TDLs and thus avoiding un-necessary invasive surgical procedure.

SSK17-03 Predicting Glioblastoma Recurrence from Preoperative MR Scans Using Fractional Anisotropy Maps with Free Water Suppression

Wednesday, Dec. 4 10:50AM - 11:00AM Room: S402AB

Awards

Trainee Research Prize - Medical Student

Participants

Marie-Christin Metz, Munich, Germany (*Presenter*) Nothing to Disclose Miguel Molina Romero, Garching bei Munchen, Germany (*Abstract Co-Author*) Nothing to Disclose Jana Lipkova, Munich, Germany (*Abstract Co-Author*) Nothing to Disclose Friederike Liesche, Munich, Germany (*Abstract Co-Author*) Nothing to Disclose Bjoern Menze, Munchen, Germany (*Abstract Co-Author*) Nothing to Disclose Claus Zimmer, Muenchen, Germany (*Abstract Co-Author*) Nothing to Disclose Benedikt Wiestler, Munich, Germany (*Abstract Co-Author*) Nothing to Disclose

For information about this presentation, contact:

marie.metz@tum.de

PURPOSE

Diffusion tensor imaging (DTI), and in particular fractional anisotropy (FA) maps have shown promise in predicting areas of tumor recurrence in glioblastoma. However, analysis of peritumoral edema, where most recurrences occur, is impeded by free water contamination of the DTI signal. In this study we evaluated the benefit of a novel, deep learning based approach for free-water correction of DTI data for prediction of later recurrence already from the first MR scans.

METHOD AND MATERIALS

We investigated 35 glioblastoma cases from our prospective glioma cohort. The preoperative MR image as well as the first MR scan showing tumor recurrence were semi-automatically segmented into contrast-enhancing and FLAIR-hyperintense areas and nonlinearly co-registered. Free-water correction of DTI data was performed using a model based on an artificial neural network, trained with synthetically generated data, and RESTORE was employed for tensor estimation. 10th, 50th and 90th percentile of FA values (both for original and free-water corrected DTI data) were collected for areas with and without recurrence in the peritumoral edema.

RESULTS

We found significant differences in free-water corrected FA maps between areas of recurrence-free edema and areas with later tumor recurrence in all of the three percentiles with p10=0.001111, p50=0.0031 and p90<0.00001 (Wilcoxon rank-sum test). In contrast, the original FA maps only showed differences in the 90th percentile, while the 10th and 50th percentile did not differ (p90=0.0003 vs. p10=0.07515 and p50=0.079).

CONCLUSION

Free-water corrected FA maps emerge as a promising tool to better assess the peritumoral edema for tumor infiltration. After freewater correction, the FA values of regions with later tumor recurrence were significantly lower than those of pure edema. This may reflect tumor infiltration not visible in conventional imaging and may therefore reveal important information for personalized treatment decisions.

CLINICAL RELEVANCE/APPLICATION

This new approach may help to predict local tumor recurrence on baseline MR scans of glioblastoma patients which may improve surgery and radiation planning tremendously.

SSK17-04 Deep Learning-Based Discrimination between Glioblastoma versus Single Metastasis on Conventional Magnetic Resonance Images

Wednesday, Dec. 4 11:00AM - 11:10AM Room: S402AB

Participants

Ilah Shin, Seoul, Korea, Republic Of (*Presenter*) Nothing to Disclose Seung-Koo Lee, MD, PhD, Seoul, Korea, Republic Of (*Abstract Co-Author*) Nothing to Disclose Sung Soo Ahn, MD, Seoul, Korea, Republic Of (*Abstract Co-Author*) Nothing to Disclose Hwiyoung Kim, Seoul, Korea, Republic Of (*Abstract Co-Author*) Nothing to Disclose Sohi Bae, MD, Goyang-si, Korea, Republic Of (*Abstract Co-Author*) Nothing to Disclose Kyunghwa Han, PhD, Seoul, Korea, Republic Of (*Abstract Co-Author*) Nothing to Disclose Yaewon Park, MD, Seoul, Korea, Republic Of (*Abstract Co-Author*) Nothing to Disclose So Yeon Won, Seoul, Korea, Republic Of (*Abstract Co-Author*) Nothing to Disclose

For information about this presentation, contact:

ilahshin@yuhs.ac

PURPOSE

To evaluate the performance of deep learning-based model in discriminating glioblastoma and single brain metastasis using conventional magnetic resonance images

METHOD AND MATERIALS

This retrospective study consecutively included 598 patients with magnetic resonance detected single brain mass, whom were pathologically confirmed as either glioblastoma (n=318) or metastasis (n=217). Among the total study group, 450 patients were randomly selected for model training (glioblastoma = 300, metastasis = 150) and 48 patients (glioblastoma = 32, metastasis=16) for model validation. Another 100 patients (glioblastoma =50, metastasis =50) were leaved out on patient-level as test dataset. Roughly placed rectangular regions of interest (ROIs) were drawn on every slice of which mass was visualized on preoperative axial T2 weighted images including the peritumoral T2 hyperintense area. Contrast-enhanced T1 weighted images were registered on the T2 weighted images and corresponding slides were also used for model training. A pretrained convolutional neural network (named ResNet50 model) was fine-tined to classify the lesions. Multi-channel representations of T1 and T2 weighted images were used for model training. Ensemble learning method was used with 5-fold cross validation. The diagnostic performance of deep learning-based model and two radiologists (with 14 and 4 years of experience) were evaluted using test dataset. Accuracy, precision, recall and F1-score were calculated for performance evaluation.

RESULTS

Te diagnostic performance of the ResNet50-based model was 89% in terms of average classification accuracy. The classifier's precision, recall and F1-score were 0.940, 0.855 and 0.893, respectively. The diagnostic accuracy, precision, recall and F1-Score of the two radiologists were 88%, 0.865, 0.9, 0.882 and 77%, 0.760, 0.745, 0.752, respectively.

CONCLUSION

Deep learning-based model can accurately discriminate glioblastoma and single brain metastasis using conventional magnetic resonance images

CLINICAL RELEVANCE/APPLICATION

Deep learning-based model may be used as a tool in preoperative decision making in cases with clinical suspicion of either glioblastoma and single brain metastasis.

SSK17-05 The Perfusion Characteristics of Dynamic Susceptibility Contrast Perfusion-Weighted Imaging in Patients' Malignant Brain Tumors Treated with Immunotherapy

Wednesday, Dec. 4 11:10AM - 11:20AM Room: S402AB

Xiang Liu, MD, Rochester, NY (*Presenter*) Nothing to Disclose Wei Tian, MD, PhD, Rochester, NY (*Abstract Co-Author*) Nothing to Disclose Ali H. Hussain, MD, FRCR, Pittsford, NY (*Abstract Co-Author*) Nothing to Disclose Henry Z. Wang, MD, PhD, Pittsford, NY (*Abstract Co-Author*) Nothing to Disclose

For information about this presentation, contact:

Xiang_Liu@URMC.Rochester.edu

PURPOSE

The immune checkpoint blockade therapy is a novel treatment in the malignant brain tumors. However, it is reported that dramatic imaging change on conventional MRI is common in such patients after immunotherapy, which is a dilemma for accurate evaluation of treatment response. The purpose of this study is to assess changes of relative cerebral blood volume (rCBV) derived from DSC-PWI in patients with malignant brain tumors treated with immunotherapy.

METHOD AND MATERIALS

MRI images of 45 patients with malignant brain tumors treated with immunotherapy were reviewed. , 25 patients with radiation necrosis or pseudoprogression without immunotherapy were enrolled in this study for comparison. Pathology result or serial followup MRI examinations were acquired to conform the final diagnosis. The rCBV maps with contrast leakage correction were generated using FDA-approved NordicICE program. Two neruoradiologists measured the maximal rCBV ratio of rCBV without and with contrast leakage correction, and compared the maximal rCBV ratio between the true tumor progression lesions and pseudoprogression after immunotherapy, and lesions of radiation necrosis/pseudo-progression changes without immunotherapy using Mann-Whitney U test.

RESULTS

There were 27 true tumor progression lesions and 9 pseudo-progression lesions after immunotherapy were evaluated. The mean maximal rCBV ratio of rCBV with contrast leakage correction of true tumor progression lesions (2.88 ± 1.357) was higher than rCBV without contrast leakage correction (1.27 ± 0.69 , p<0.001). The mean maximal rCBV ratio of rCBV without contrast leakage correction after immunotherapy was also higher than rCBV without contrast leakage correction of the patients with radiation necrosis or pseudoprogression without immunotherapy (0.83 ± 0.55 , p=0.013)

CONCLUSION

The MR imaging changes after immunotherapy in patients with malignant brain tumors are complex. The pseudoprogression lesion after immunotherapy may be mixed with necrosis/pseudo-progression and active inflammatory changes. The combination of rCBV without and with contrast leakage correction derived from MR DSC-PWI is useful in differentiating true tumor progression lesions with necrosis/pseudo-progression in such patients treated with immunotherapy.

CLINICAL RELEVANCE/APPLICATION

The rCBV changes are useful in differentiating true tumor progression lesions with necrosis/pseudo-progression in such patients treated with immunotherapy.

SSK17-07 Machine Learning Using Texture Analysis for Prediction of Glioma Grade Using Unenhanced Brain Computed Tomography

Wednesday, Dec. 4 11:30AM - 11:40AM Room: S402AB

Participants

Machiko Tateishi, Kumamoto , Japan (*Presenter*) Nothing to Disclose Takeshi Nakaura, MD, Amakusa, Japan (*Abstract Co-Author*) Nothing to Disclose Mika Kitajima, MD, Kumamoto, Japan (*Abstract Co-Author*) Nothing to Disclose Hiroyuki Uetani, Amakusa, Japan (*Abstract Co-Author*) Nothing to Disclose Jun-Ichiro Kuroda, Kumamoto, Japan (*Abstract Co-Author*) Nothing to Disclose Akitake Mukasa, Kumamoto, Japan (*Abstract Co-Author*) Nothing to Disclose Yasuyuki Yamashita, MD, Kumamoto, Japan (*Abstract Co-Author*) Consultant, DAIICHI SANKYO Group

PURPOSE

The purpose of this study was to determine whether machine learning methods based on unenhanced brain computed tomography (CT) features have adequate diagnostic ability to differentiate GBM from grade III glioma.

METHOD AND MATERIALS

We included 91 patients with pathologically confirmed high-grade glioma who underwent unenhanced brain CT for preoperative study. Of the 91 patients, 32 had grade III glioma and 59 had GB. Age, sex, tumor size, and 12 histogram and texture parameters (minimum; mean; standard deviation; and maximum normalized signal, skewness, kurtosis, homogeneity, energy, contrast, correlation, entropy, and dissimilarity) were assessed using unenhanced CT. We developed six prediction models with machine learning and calculated the area under the receiver operating characteristic curve (AUC) of the models using 5-fold cross validation; two board-certified radiologists, including one neuroradiologist and one general radiologist, compared the performances of these models.

RESULTS

The extreme gradient boosting produced the highest AUC (0.85), followed by random forest (0.79), multi-layer perceptron (0.76), support vector machine (0.75), k-nearest neighbor (0.74), and logistic regression (0.71). Age and kurtosis were the most important factors for differentiation, followed by minimum value (Gini index = 0.115, 0.115, and 0.105). AUC obtained from the extreme gradient boosting and that evaluated by the neuroradiologist were significantly higher than that evaluated by the general radiologist (0.85 vs. 0.85, 0.67, p = 0.01 and p < 0.01, respectively).

CONCLUSION

The performance of machine learning in the differentiation of GBM from grade III glioma was superior to that of an experienced general radiologist; this performance is highly dependent on the selection of the type of machine learning.

CLINICAL RELEVANCE/APPLICATION

Machine learning methods based on the assessment of unenhanced brain CT features may be a cost-effective imaging technique for differentiating GBM from grade III glioma.

SSK17-08 Prediction for Grading of Stereotactic Biopsy Glioma Targets Based on Preoperative MRI Textural Analysis

Wednesday, Dec. 4 11:40AM - 11:50AM Room: S402AB

Participants

Wenting Rui, Shanghai, China (*Abstract Co-Author*) Nothing to Disclose Haopeng Pang, Shanghai, China (*Abstract Co-Author*) Nothing to Disclose Qian Xie, Shanghai, China (*Abstract Co-Author*) Nothing to Disclose Yan Ren, MD, Shanghai, China (*Abstract Co-Author*) Nothing to Disclose Shiman Wu, Shanghai, China (*Presenter*) Nothing to Disclose Zhenwei Yao, Shanghai, China (*Abstract Co-Author*) Nothing to Disclose

For information about this presentation, contact:

wennyrui@126.com

PURPOSE

To explore the value of textural analysis based on T1 BRAVO+C images for grading of glioma targets by stereotactic biopsy (WHO grade II and III).

METHOD AND MATERIALS

A total of 36 diffuse glioma cases and 64 puncture targets were included in this study. All underwent preoperative MR scanning and intraoperative MR-guided stereotactic puncture biopsy. Histopathological diagnosis was WHO grade II or III diffuse glioma. By Omni Kinetics software, regions of interest (ROIs) which were consistent with the puncture target were delineated on 3D T1 BRAVO+C images, size of which was about 10×10 mm. Texture features of each ROI were automatically calculated by the software. Mann-Whitney rank sum test was used to analyze the texture differences between WHO grade II and III ROIs. Receiver operating characteristic curve (ROC) was used to evaluate the diagnostic value of textural analysis for grading glioma targets. Cutoff value was set according to Youden index, and sensitivity, specificity, positive predictive value (PPV), and negative predictive value (NPV) were all calculated.

RESULTS

Texture features Maxintensity (P=0.001), Quantile 95 (0.002), Range (< 0.001), Variance (< 0.001), Standard deviation (< 0.001), Sum variance (0.022) and Cluster prominence (< 0.001) were higher in WHO grade III gliomas than those of WHO grade II. While WHO grade II gliomas had higher Uniformity (P=0.001) and ShortRunLowGrayLevelEmphasis values (0.018) than WHO grade III ones. First-order features Maxintensity (area under the curve (AUC) = 0.751, sensitivity = 96.6%, NPV = 94.2%), Quantile 95 (0.737, 86.2%, 80.0%) and Range (0.801, 89.7%, 87.0%); AUC value was the highest in Variance and Standard deviation (0.826); Uniformity (AUC = 0.746, specificity = 82.8%, PPV = 76.2%). Second-order gray-level co-occurrence matrix features Cluster prominence (AUC = 0.784, specificity = 89.7%, PPV = 85.8%), and Sum variance (0.675, 96.6%, 91.0%). Diagnostic efficiency of high-order gray-level run-length matrix features was slightly lower than first-order and second-order features. AUC was 0.887 (95% confidence interval: 0.805-0.969, P<0.001) by combined ROC analysis with multiple texture features.

CONCLUSION

Textural analysis on T1 BRAVO+C images may be helpful in grading glioma targets by stereotactic biopsy (WHO II and III).

CLINICAL RELEVANCE/APPLICATION

This research is helpful for grading gliomas, and guiding precise selection of puncture targets preoperatively.

SSK17-09 Reduction of Intratumoral Perfusion in Brain Cancers Patients by Noninvasive Electrical Stimulation

Wednesday, Dec. 4 11:50AM - 12:00PM Room: S402AB

Participants

Giulia Sprugnoli, MD, Boston, MA (*Presenter*) Nothing to Disclose Lucia Monti, MD, Siena, Italy (*Abstract Co-Author*) Nothing to Disclose Laura Lippa, MD, Siena, Italy (*Abstract Co-Author*) Nothing to Disclose Francesco Neri, Siena , Italy (*Abstract Co-Author*) Nothing to Disclose Lucia Mencarelli, MS, Siena, Italy (*Abstract Co-Author*) Nothing to Disclose Giulio Ruffini, BA,PhD, Cambridge, MA (*Abstract Co-Author*) Founder, Neuroelectrics Ricardo Salvador, Barcelona, Spain (*Abstract Co-Author*) Engineer, Neuroelectrics Giuseppe Oliveri, MD, Siena , Italy (*Abstract Co-Author*) Nothing to Disclose Barbara Batani, MD, Siena , Italy (*Abstract Co-Author*) Nothing to Disclose Barbara Batani, MD, Siena , Italy (*Abstract Co-Author*) Nothing to Disclose Alfonso Cerase, MD, Siena, Italy (*Abstract Co-Author*) Nothing to Disclose Alvaro Pascual-Leone, MD,PhD, Boston, MA (*Abstract Co-Author*) Medical Advisory Board, Neuroelectrics Alessandro Rossi, Siena , Italy (*Abstract Co-Author*) Nothing to Disclose Simone Rossi, MD, Siena , Italy (*Abstract Co-Author*) Nothing to Disclose Emiliano Santarnecchi, Boston, MA (*Abstract Co-Author*) Nothing to Disclose

For information about this presentation, contact:

gsprugno@bidmc.harvard.edu

PURPOSE

Invasive electrical stimulation of bodily tumors has been shown to reduce tumor perfusion and even potentially induce necrosis.

Transcranial electrical stimulation (tES) is currently applied in psychiatric and neurological conditions to restore neuronal activity as well as modulate brain local perfusion. Our aim was to test the safety, feasibility and efficacy of applying tES in patients with brain cancers to reduce intratumoral perfusion.

METHOD AND MATERIALS

Six patients with glioblastoma and two with metastasis underwent a single tES session (20 minutes) inside the MRI scanner before their scheduled surgery, while perfusion was assessed using pulsed Arterial Spin Labelling (ASL) MRI. Multichannel tES was applied with an MRI-compatible device according to individualized biophysical models based on manually traced tumor masks of the (i) necrotic core, (ii) solid tumor and (iii) edema region as per the RANO criteria (using T1w and T2-w MRIs). Tissue electrical conductivity values were assigned to each mask as well as to the healthy brain tissue according to existing literature. The electrical field (E-field) distribution was calculated for multiple multi-electrode solutions in order to maximize E-field over the solid tumor mass. Normalized Cerebral Blood Flow (CBF) was calculated using previously described equations (Alsop et al. 2015). CBF values were extracted from the three masks (i.e. edema, solid tumor, necrotic core) as well as from healthy control regions in the ipsilateral and contralateral hemisphere not affected by the stimulation.

RESULTS

No adverse effects were reported. Significant CBF reduction was found in the solid tumor masks (-36%, p.=0.001), ranging from - 26% for glioblastoma to -45% in metastasis patients, while CBF changes for necrotic tumor core and the edema region were not significant (-8.9%, p.=0.294 and -5%, p.=0.328 respectively). Additionally, no significant CBF changes were detected in the control regions (i.e. ipsilateral regions: +5.7%, p.=0.194; contralateral ones: +5.4%, p.=0.502).

CONCLUSION

Pilot data demonstrate the safety and feasibility of using tES to noninvasively target and modulate intratumoral perfusion.

CLINICAL RELEVANCE/APPLICATION

If confirmed in larger samples, tES could be tested as a stand-alone therapy for selected brain tumor patients or as an adjuvant treatment in combination with chemo/radiotherapy.

Printed on: 10/29/20







SSK18

Physics (CT Protocols/Risk Reduction)

Wednesday, Dec. 4 10:30AM - 12:00PM Room: E353C



AMA PRA Category 1 Credits ™: 1.50 ARRT Category A+ Credit: 1.75

Participants

Frank N. Ranallo, PhD, Madison, WI (*Moderator*) Grant, General Electric Company Tinsu Pan, PhD, Waukesha, WI (*Moderator*) Consultant, Bracco Group

Sub-Events

SSK18-01 Total Risk Index: A Mathematical Model for Decision Making Based on Clinical and Radiation Risk Assessment in CT

Wednesday, Dec. 4 10:30AM - 10:40AM Room: E353C

Participants

Francesco Ria, DMP, Durham, NC (*Presenter*) Nothing to Disclose Taylor Smith, Durham, NC (*Abstract Co-Author*) Nothing to Disclose Jocelyn Hoye, Durham, NC (*Abstract Co-Author*) Nothing to Disclose Daniele Marin, MD, Durham, NC (*Abstract Co-Author*) Research support, General Electric Company Ehsan Samei, PhD, Durham, NC (*Abstract Co-Author*) Research Grant, General Electric Company Research Grant, Siemens AG Advisory Board, medInt Holdings, LLC License agreement, 12 Sigma Technologies License agreement, Gammex, Inc

For information about this presentation, contact:

francesco.ria@duke.edu

PURPOSE

Radiological risk is a combination of radiation and clinical risk (likelihood of not delivering a proper diagnosis), which together may be characterized as a total risk index (TRI). While many strategies have been developed to ascertain radiation risk, there has been a paucity of studies assessing the clinical risk. This knowledge gap makes impossible to determine the total radiological procedure risk and, thus, to perform a comprehensive optimization. The purpose of this study was to develop a mathematical model to ascertain TRI and to identify the minimum TRI (mTRI) in a clinical CT population.

METHOD AND MATERIALS

This IRB approved study included 21 adults abdomen exams performed on a dual-source single energy CT at two different dose levels (84 CT series). Virtual liver lesions were inserted into projection data to simulate localized stage liver cancer (LSLC). The detectability index (d') was calculated in each series and converted to percentage of correct observer answers (AUC) in a two-alternative forced-choice model. The AUC was converted into the loss of 5-year relative survival rate (SEER, NCI), considering an upper bound on patient's risk for a misdiagnosis of LSLC (false positive+false negative). Concerning radiation risk, organ doses were estimated using a Monte Carlo method and the Risk Index was calculated and converted in 5-year relative survival rate for cancer. Finally, the two risks were weighted equally into a combined TRI curve per each patient as a function of CTDIvol. The analytical minimum of each TRI curve provided the patient mTRI.

RESULTS

The mTRI for LSLC patients that underwent an abdominal CT exhibited a rapid rise at low radiation dose due to enhanced clinical risk of under-dosed examinations. Increasing dose offered less risk with mortality per 100 patients between 2.1 and 6.5 (mean 4.5) at CTDIvol=5mGy; between 1.1 and 5.9 (mean 3.5) at CTDIvol=10mGy; and between 0.5 and 5.4 (mean 3.0) at CTDIvol=20 mGy.

CONCLUSION

The clinical risk seems to play a more dominant factor in designing optimum CT protocols. The TRI may provide an objective and quantifiable metric of the interplay of radiation and clinical risks during the optimization of the CT technique for individual patients.

CLINICAL RELEVANCE/APPLICATION

CT risk-based Optimization can be made possible by first quantifying both radiation and clinical risk using comparable units, then calculating an overall risk, and finally minimizing the total risk.

SSK18-02 Repeated/Rejected Events in CT: A Study Quantifying their Frequency and Impact on Patient Dose

Wednesday, Dec. 4 10:40AM - 10:50AM Room: E353C

Participants

Sean Rose, PhD, Madison, WI (*Presenter*) Nothing to Disclose Ben Viggiano, Madison, WI (*Abstract Co-Author*) Nothing to Disclose Timothy P. Szczykutowicz, PhD, Madison, WI (*Abstract Co-Author*) Equipment support, General Electric Company; License agreement, General Electric Company; Founder, Protocolshare.org LLC; Medical Advisory Board, medInt Holdings, LLC; Consultant, General Electric Company; Consultant, Takeda Pharmaceutical Company Limited

For information about this presentation, contact:

sdrose3@wisc.edu

PURPOSE

We have developed and validated an algorithm for automated detection of repeat/reject CT scans. Here we use the method to identify high repeat rate protocols at two sites and estimate their associated excess dose. We additionally determine reference standard repeat rates for each protocol.

METHOD AND MATERIALS

The algorithm estimated repeat/reject rates from high-volume protocols at CT scanners from two sites using dose monitoring data collected over 3 years. The sites included a rural and an academic hospital, sites A and B, respectively. We only considered repeats consisting of additional overlapping helical/axial scans in this study. Effective doses were calculated from all exams performed with the ten highest repeat-rate protocols at each site. Site-wide reference repeat rates were identified for each protocol by pooling exams performed with similar protocols (e.g. abdomen/pelvis protocols for all patient sizes) at each site and taking the minimum aggregate repeat rate between the two sites. Reference repeat rates were used to identify protocols for which targeted training has the largest potential to reduce repeat rates.

RESULTS

Overall repeat rates were the same for both sites, 1.4% [1.2,1.6] and 1.4% [1.3,1.5] (95% confidence intervals shown in brackets). Among the ten highest repeat rate protocols, the median percent increase in mean effective dose between normal and repeat-containing exams was 107.5% (interquartile range [89.9,130.2]) for site A and 64.6% (interquartile range [44.4,88.8]) for site B. More multiphasic protocols were used at Site B relative to Site A, making the relative dose increase smaller. Using the site-wide reference repeat rate (i.e. best institution practice), we calculated Site A and B could have reduced their number of repeat exams by 55 and 42 respectively over a three year period.

CONCLUSION

Overall repeat rates at the two sites were similar, but the ten highest repeat rate protocols differed. Comparison to site-wide reference repeat rates suggests that protocol-specific intervention may be effective in reducing repeat rates at both sites.

CLINICAL RELEVANCE/APPLICATION

Our informatics based repeat/reject methodology for CT can be used to quantify excess dose delivered due to operator error and identify best practice scanning within an institution.

SSK18-03 One Size Does Not Fit All: Factors Associated With Increased Frequency Of Radiation Overexposure Alerts Based On Fixed Alert Thresholds

Wednesday, Dec. 4 10:50AM - 11:00AM Room: E353C

Participants

Vladimir Valtchinov, PhD, Brookline, MA (*Abstract Co-Author*) Nothing to Disclose Jenifer W. Siegelman, MD, MPH, Newton, MA (*Abstract Co-Author*) Employee, Takeda Pharmaceutical Company Limited Bingxue K. Zhai, ARRT,MSc, Waban, MA (*Abstract Co-Author*) Nothing to Disclose Ramin Khorasani, MD, Roxbury Crossing, MA (*Abstract Co-Author*) Nothing to Disclose Aaron D. Sodickson, MD,PhD, Boston, MA (*Presenter*) Institutional research agreement, Siemens AG; Speaker, Siemens AG; Speaker, General Electric Company

For information about this presentation, contact:

asodickson@bwh.harvard.edu

PURPOSE

To quantify the expected rate of CT radiation dose alerts for three body regions using accepted radiation benchmarks, and to assess key determinants of alert frequency.

METHOD AND MATERIALS

This IRB-approved retrospective cohort study evaluated 6 months of consecutive CT examinations performed within an academic medical system. CTDIvol x-ray tube output metrics were compared to the body-region-specific benchmark levels Achievable Doses (AD), Diagnostic Reference Levels (DRL), and Dose Notification Values (DNV), and simulated alerts were generated when benchmarks were exceeded. Frequency and proportion of events triggering alerts were calculated. A logistic regression model was fit for the outcome of simulated alert as a function of the independent predictors: scanner, body region, gender, weight, and age.

RESULTS

For 17,000 head, chest and abdomen exams, the proportion of events triggering alerts increased with weight for all scanners and body regions. Significant covariates were scanner, body region, patient weight, and age (all p<0.0001). Odds of alert generation for the AD, DRL, and DNV benchmarks increased by 3.3%, 3.0%, and 1.3% per pound, respectively, and by 0.8%, 1.1% and -2.7% per year of age (all p < 0.0001). Compared to the most highly optimized scanner, odds of alert generation varied by a factor of 595 for AD, 1126 for DRL, 13 for DNV.

CONCLUSION

Alert frequency was significantly correlated with weight, age, body region and scanner. Controllable factors include scanner functionality and associated protocol optimization. The patient factors driving alert frequency are predominantly weight, and to a lesser degree, age. Fixed dose threshold values can thus frequently produce false alerts in appropriately performed exams of large patients, while not triggering alerts in outlier scans of higher than expected dose in small patients.

CLINICAL RELEVANCE/APPLICATION

Factors influencing dose alert frequency were explored for a large cohort of CT scans in a multi-scanner environment. These have

implications to the utility of fixed dose threshold alert values.

SSK18-04 How to Use Lead Apron to Reduce Excess Radiation Dose Caused by Over-Scan in Computed Tomography Using 40mm Collimation: An Anthropomorphic Phantom Study

Wednesday, Dec. 4 11:00AM - 11:10AM Room: E353C

Participants Xinyu Li, Xian, China (*Presenter*) Nothing to Disclose Jianying Li, Beijing, China (*Abstract Co-Author*) Employee, General Electric Company Yun Shen, PhD, Beijing, China (*Abstract Co-Author*) Employee, General Electric Company Researcher, General Electric Company Jianxin Guo, Xian, China (*Abstract Co-Author*) Nothing to Disclose Xijun Jiao, Xian, China (*Abstract Co-Author*) Nothing to Disclose Xianghui Zhang, Xian, China (*Abstract Co-Author*) Nothing to Disclose Peiyun Li, Xian, China (*Abstract Co-Author*) Nothing to Disclose Jian Yang, Xian, China (*Abstract Co-Author*) Nothing to Disclose

For information about this presentation, contact:

2397990794@qq.com

PURPOSE

The typical over-scan range with 40mm collimation in helical scans was about 25x2mm resulting in dose penalty, but the use of lead apron may be used to reduce the dose penalty. The purpose of this study was to explore the optimal way of placing the lead apron to maximize dose reduction for the over-scans without negatively impact image quality with 40mm collimation.

METHOD AND MATERIALS

We used an anthropomorphic phantom containing a pig liver, kidney, meat and a femur head in a water box to evaluate image quality with the apron placed at different distances to the imaging boundary. A scout was taken first without lead apron to determine the desired imaging range and set up the automatic tube current modulation before putting on the lead apron. The helical scan groups were designed as follows: group 1, without apron as a reference and groups 2-22 with the apron first placed at the imaging boundary and in 0.5mm increment away from the it. The scan techniques were kept the same for all scans at 40mm collimation, 120kVp, 10-740mA for a noise index of 7HU. Images were reconstructed at 5mm slice thickness and the image nearest the imaging boundary was used for analysis and comparison. 10 regions of interest (ROI, 5mm*5mm in size) of different tissues in the images were selected to measure CT value. Measurements in group 1 (without apron) were as reference standards. The CT values of the 10 ROIs in each group from groups 2-22 were compared with group 1 using Paired t-test and the CT value difference (dCT(i)=CT(i)) for each ROI in matched location was calculated to evaluate objective imaging quality by a boxplot. Subjective image quality was also evaluated in terms of image noise and shading artifacts.

RESULTS

In the Paired t-test, the p values were continuously greater than 0.05 for groups 13-22 (apron 5.5-10mm from the boundary) with the average dCT values smaller than 3HU. There was no difference in subjective image quality between groups 13-22 and group 1.

CONCLUSION

Placing lead apron at least 5.5mm from the imaging boundary when using 40mm collimation is recommended, reducing the over-scan dose penalty by 78%.

CLINICAL RELEVANCE/APPLICATION

Lead apron may reduce the dose penalty for the over-scans without negatively impact image quality and placing lead apron at least 5.5mm from the imaging boundary in 40mm collimation is recommended.

SSK18-05 Effect of Gonad Shields on the Automatic Exposure Control in Computed Tomography: Influence on the Development of Standard Operating Procedures

Wednesday, Dec. 4 11:10AM - 11:20AM Room: E353C

Participants

Andrea Steuwe, Dusseldorf, Germany (*Presenter*) Nothing to Disclose Yan Klosterkemper, Dusseldorf, Germany (*Abstract Co-Author*) Nothing to Disclose Christoph K. Thomas, MD, Dusseldorf, Germany (*Abstract Co-Author*) Nothing to Disclose Elisabeth Appel, MD, Dusseldorf, Germany (*Abstract Co-Author*) Nothing to Disclose Gerald Antoch, MD, Dusseldorf, Germany (*Abstract Co-Author*) Nothing to Disclose Johannes Boos, MD, Dusseldorf, Germany (*Abstract Co-Author*) Nothing to Disclose

For information about this presentation, contact:

andrea.steuwe@med.uni-duesseldorf.de

PURPOSE

To analyze the influence of a lead gonad shield on the automatic exposure control (AEC) of three different computed tomography (CT) scanner models to develop in-house standard operating procedures (SOPs).

METHOD AND MATERIALS

An anthropomorphic male Alderson phantom was scanned thrice with the standard abdomen/pelvis protocol on three different CT scanners (Somatom Definition Edge (1), Somatom Definition Flash (2), Somatom Definition AS (3), all Siemens Healthineers, Germany) in cranio-caudal direction. Per scanner, the phantom was scanned (a) without shield, (b) with added shield after the scout (Mavig gonad shield, 1mm Pb) and (c) scout and scan with shield, covering the entire abdomen/pelvis. Subsequently, the scan range was shortened at the cranial side with the following distances to the shield: (d) 0cm (scan range adjacent to shield), (e) 1cm, (f) 2cm and (g) 3cm. Exposure [mAs] per reconstructed slice was determined and averaged over the three repetitions.

RESULTS

Compared to scans without shield (acquisition a), inclusion of the gonad shield on the scout resulted in increased x-ray exposure: For all scanners, exposure increased adjacent to the shield for approximately one detector width (up to 15%). Along the caudal part of the shield exposure increased by up to 85%. Modulation along the cranial part of the shield varied per scanner: Exposure increased for scanner 1 (+10%), stayed similar for scanner 2 and decreased for scanner 3 (-20%). For scans without gonad shield in the scan range (acquisitions d-g), exposure still increased adjacent to the shield (up to 15%). Placement of the shield after the scout (acquisition b) did not change exposure considerably for all evaluated scanners.

CONCLUSION

Our results indicate that the FOV range needs to be adapted to the scanner's detector width when using gonad shields with AEC, or ideally, placement of the shield needs to be performed after acquisition of the scout scan.

CLINICAL RELEVANCE/APPLICATION

Even for the same vendor, the influence of gonad shields on the AEC varies per scanner model and needs to be assessed prior to the development of scanner- and protocol-dependent SOPs.

SSK18-06 An Organ Dose Calculation Tool for Fetus at Various Ages Undergoing Computed Tomography

Wednesday, Dec. 4 11:20AM - 11:30AM Room: E353C

Participants

Choonsik Lee, PhD, Rockville, MD (*Presenter*) Nothing to Disclose Les R. Folio, MPH,DO, Bethesda, MD (*Abstract Co-Author*) Institutional research agreement, Carestream Health, Inc

For information about this presentation, contact:

choonsik.lee@nih.gov

PURPOSE

Pregnant patients may undergo CT in emergencies unrelated with pregnancy and potential risk to the developing fetus is of concern. It is critical to accurately estimate fetal organ doses in CT scans. We developed a fetal organ dose calculation tool using pregnancy-specific computational phantoms combined with Monte Carlo radiation transport techniques.

METHOD AND MATERIALS

We adopted a series of pregnancy computational phantoms developed at the University of Florida at the gestational ages of 8, 10, 15, 20, 25, 30, 35, and 38 weeks (Maynard et al. 2011). More than 30 organs and tissues and 20 skeletal sites are defined in each fetus model. We calculated fetal organ dose normalized by CTDIvol to derive organ dose conversion coefficients (mGy/mGy) for the eight fetuses for consequential slice locations ranging from the top to the bottom of the pregnancy phantoms with 1 cm slice thickness. Organ dose from helical scans were approximated by the summation of doses from multiple axial slices included in the given scan range of interest. We then compared dose conversion coefficients for major fetal organs in the abdominal-pelvis CT scan of pregnancy phantoms with the uterine dose of a non-pregnant adult female computational phantom.

RESULTS

A comprehensive library of organ conversion coefficients was established for the eight developing fetuses undergoing CT. They were implemented into an in-house graphical user interface-based computer program for convenient estimation of fetal organ doses by inputting CT technical parameters as well as the age of fetus. We found that the esophagus received the least dose whereas the kidneys received the greatest dose in all fetuses in AP scans of the pregnancy phantoms. We also found that when the uterine dose of a non-pregnant adult female phantom is used as a surrogate for fetal organ doses, root-mean-square-error ranged from 0.08 mGy (8 weeks) to 0.38 mGy (38 weeks). The uterine dose was up to 1.7-fold greater than the esophagus dose of the 38-week fetus model.

CONCLUSION

The calculation tool should be useful in cases requiring fetal organ dose in emergency CT scans as well as patient dose monitoring.

CLINICAL RELEVANCE/APPLICATION

The methods and tool we developed in this study should provide more accurate fetal organ dose estimations at various gestational ages, which should help radiologists and mothers to better understand the health impact of fetus undergoing CT.

SSK18-07 AEC- and Scan Time-Optimized Pediatric Body CT Protocols based on Size-Specific Dose Needs

Wednesday, Dec. 4 11:30AM - 11:40AM Room: E353C

Participants

Megan Lipford, PHD, Madison, WI (*Presenter*) Nothing to Disclose

Timothy P. Szczykutowicz, PhD, Madison, WI (*Abstract Co-Author*) Equipment support, General Electric Company; License agreement, General Electric Company; Founder, Protocolshare.org LLC; Medical Advisory Board, medInt Holdings, LLC; Consultant, General Electric Company; Consultant, Takeda Pharmaceutical Company Limited

For information about this presentation, contact:

tszczykutowicz@uwhealth.org

PURPOSE

We have developed a method for creating pediatric CT protocols. Currently, no methods exist for building a protocol that meets specific dose and scan time requirements for as a function of size/age.

METHOD AND MATERIALS

In our method, CT manuals and/or measurements define the maximum CTDIvol based on the tube limits and the range of available

collimations, pitches, rotation times, etc. Then, using aggregated clinical data from 210 pediatric CT body exams, we characterized the dose and scan length required as a function of patient size (AP+Lat). With these data, we created a spreadsheet having an input of acquisition parameters and scanner specific speed and dosimetry values. Combining the clinical data with the scanner input data, the spreadsheet output a maximum patient size and scan time. We demonstrate the method by building protocols for the GE Revolution and Siemens Force. For each, we build two sets of protocols: one optimized for scan speed but with limited patient size dynamic range (i.e. size bins spanning a couple years), and one clinically robust protocol that can span large size ranges with a single protocol (i.e. size bins spanning 5-10 years).

RESULTS

The speed optimized sets of protocols resulted in 5 protocols for the Force and 4 for the Revolution in order to span newborn to teenager. The clinically robust set only used 2 protocols to span newborn to teenager. Scan times for the speed optimized sets had a minimum of 0.26 s, but at that scan speed could only image to a patient size of 310 mm AP+Lat (i.e. 2 years). The clinically robust set of protocols allowed a minimum scan time of 0.48 seconds for newborns but with a dose dynamic range up to 430 mm AP+Lat (i.e. 12 years). Our results also show the scan times between these premium models were similar, with no scanner taking longer than 2 seconds to scan a pediatric abdomen.

CONCLUSION

With this method of creating protocols, it is easy to predict how parameter adjustments affect the scan time (i.e. breath hold) and range of appropriate patient sizes (i.e. ages). In our demonstration, running a scanner as fast as possible required more changes in rotation time and pitch as a function of patient size.

CLINICAL RELEVANCE/APPLICATION

Before our work, no method existed for predicting if a protocol will actually allow for enough dose or a short enough scan time on a patient size and indication basis.

SSK18-08 Diagnostic Reference Levels and Achievable Doses for Computed Tomography for EUCLID (European Study on Clinical DRLs) Defined Clinical Indications: Data from a Multinational Dose Registry

Wednesday, Dec. 4 11:40AM - 11:50AM Room: E353C

Participants

Denise Oldenburg, MD, Essen, Germany (*Presenter*) Nothing to Disclose Sophronia Yu, San Francisco, CA (*Abstract Co-Author*) Nothing to Disclose Jason K. Luong, San Francisco, CA (*Abstract Co-Author*) Nothing to Disclose Philip Chu, San Francisco, CA (*Abstract Co-Author*) Nothing to Disclose Yifei Wang, San Francisco, CA (*Abstract Co-Author*) Nothing to Disclose Axel Wetter, Essen, Germany (*Abstract Co-Author*) Nothing to Disclose Rebecca Smith-Bindman, MD, San Francisco, CA (*Abstract Co-Author*) Nothing to Disclose

PURPOSE

Radiation doses for Computed Tomography (CT) examinations between patients, institutions, and countries are highly variable. Diagnostic reference levels (DRLs), and achievable doses (ADs) are often created to help reduce unnecessary variation. The European Society of Radiology has identified common indications for CT named EUCLID (European Study on Clinical DRLs) in order to create benchmarks for these examination types. We generated DRLs and ADs for these examinations.

METHOD AND MATERIALS

Standardized data from > 2.3 million CT examinations in adults 18 years of age and older were collected between January 2016 and December 2018 from 155 institutions across 7 countries in a large, multinational CT Dose Registry. Two dose metrics were evaluated: CT-dose index (CTDIvol), and dose-length product (DLP).

RESULTS

AD (50% in dose distribution) and DRL (75% in dose distribution) are summarized as follows (CTDIvol (mGy)/ DLP (mGy-cm), sample size n): chronic sinusitis (15 and 21 / 250 and 373, n= 57070), stroke to detect and exclude hemorrhage (47 and 53/ 872 and 1076, n= 14040), cervical spine trauma (19 and 30/ 450 and 962, n= 111397), pulmonary embolism (10 and 15/ 372 and 558, n= 112784), coronary calcium scoring (4 and 7/ 66 and 102, n= 22579), coronary angiography (21 and 31/ 497 and 915, n= 3176), lung cancer first and follow-up (11 and 15/ 556 and 858, n= 7064), hepatocellular carcinoma (9 and 14/ 1304 and 2016, n= 4289), colic/abdominal pain (10 and 14/ 519 and 773, n= 64724), and appendicitis/routine abdomen (11 and 16/661 and 1059, n= 721263). Most CT scans for clinical indications showed large differences in radiation dose compared to routine CT scans, e.g. sinusitis scans were >60% lower in both CTDIvol and DLP compared to routine head CT scans. Further, there were large differences in the DRLs and ADs across facilities.

CONCLUSION

DRLs and ADs for the clinical indications of EUCLID were presented and showed differences to routine CT scans. Dose metrics from large multi-center studies can help create representative DRLs and ADs that can be used for dose optimization, institutional evaluation, and indication-specific dose-optimized protocols.

CLINICAL RELEVANCE/APPLICATION

DRLs and ADs for clinical indications are essential due to high variation of CT radiation doses and for dose optimization, institutional evaluation, and indication-specific dose-optimized protocols.

SSK18-09 Reference Dataset for Benchmarking Organ Doses Derived from Monte Carlo Simulations of CT Exams

Wednesday, Dec. 4 11:50AM - 12:00PM Room: E353C

Participants Anthony Hardy, MS, Los Angeles, CA (*Presenter*) Nothing to Disclose Maryam Bostani, PhD, Los Angeles, CA (*Abstract Co-Author*) Nothing to Disclose Erin Angel, PhD, Tustin, CA (*Abstract Co-Author*) Employee, Canon Medical Systems Corporation Christopher H. Cagnon, PhD, Los Angeles, CA (*Abstract Co-Author*) Nothing to Disclose Michael F. McNitt-Gray, PhD, Los Angeles, CA (*Abstract Co-Author*) Institutional research agreement, Siemens AG

PURPOSE

AAPM Report 195 contains reference datasets for the direct comparison of results between different Monte Carlo (MC) simulation tools but stops short of providing the necessary information for comparing organ doses. The purpose of this work was therefore to extend the efforts of AAPM Report 195 by providing a reference dataset for benchmarking absolute and normalized organ doses from MC simulations of CT exams.

METHOD AND MATERIALS

The reference dataset contains (1) scanner characteristics, (2) patient information, (3) exam specifications, and (4) organ dose results in tabular form. The scanner characteristics include descriptions of equivalent source spectrum, bowtie filtration profile, and scanner geometry information. Additionally, for MCNPX MC engines, normalization factors are provided to convert simulation results to units of absolute dose. The patient information was based on publicly available fetal dose models and includes de-identified image data; voxelized MC input files with fetus, uterus, and gestational sac identified; and patient size metrics in the form water equivalent diameter (Dw) distributions from the image data and from a simulated topogram. Exam characteristics include the scan length and imaging protocol specifications. For tube current modulation (TCM) simulations, an estimate of TCM is provided based on a validated method that accounts for patient attenuation and scanner tube current limitations. In this case, CTDIvol estimates were based on average tube current across the scan volume. Organ dose simulation results are given for each patient model and for TCM and fixed tube current (FTC) CT exam scenarios both in terms of absolute and CTDIvol-normalized fetal dose.

RESULTS

Results TCM and FTC simulations for absolute and normalized fetal dose are presented in tabular form with associated MC error estimates for benchmarking.

CONCLUSION

The reference dataset for MC benchmarking is now available. This will enable researchers to compare their simulations to a set of reference data.

CLINICAL RELEVANCE/APPLICATION

This dataset will for benchmarking dose management software results against MC simulations.

Printed on: 10/29/20





SSK19

Physics (Dark-Field/X-Ray Phase Contrast Imaging)

Wednesday, Dec. 4 10:30AM - 12:00PM Room: E353B

PH

AMA PRA Category 1 Credits ™: 1.50 ARRT Category A+ Credit: 1.75

FDA Discussions may include off-label uses.

Participants

Guang-Hong Chen, PhD, Madison, WI (*Moderator*) Research funded, General Electric Company Srinivasan Vedantham, PhD, Tucson, AZ (*Moderator*) Research collaboration, Koning Corporation; Research collaboration, General Electric Company

Sub-Events

SSK19-01 Fast Data Acquisition for a Human-Compatible Multi-Contrast Breast Imaging System

Wednesday, Dec. 4 10:30AM - 10:40AM Room: E353B

Participants

Ran Zhang, PhD, Madison, WI (*Presenter*) Nothing to Disclose Amy M. Fowler, MD,PhD, Madison, WI (*Abstract Co-Author*) Institutional research support, General Electric Company; Author with royalties, Reed Elsevier Lee G. Wilke, MD, Madison, WI (*Abstract Co-Author*) Nothing to Disclose Frederick Kelcz, MD, PhD, Madison, WI (*Abstract Co-Author*) Shareholder, Elucent Ringers, LLC John W. Garrett, PhD, Madison, WI (*Abstract Co-Author*) Nothing to Disclose Guang-Hong Chen, PhD, Madison, WI (*Abstract Co-Author*) Research funded, General Electric Company

Ke Li, PhD, Madison, WI (Abstract Co-Author) Nothing to Disclose

For information about this presentation, contact:

rzhang229@wisc.edu

PURPOSE

A major technical obstacle to bringing x-ray phase contrast and dark-field imaging to clinical use is the prolonged data acquisition time associated with the phase stepping procedure: the majority of the imaging time is spent accelerating-decelerating-stabilizing the x-ray grating instead of delivering the actual x-ray exposures. The purpose of this work was to introduce a fast data acquisition technique to a prototype multi-contrast breast imaging system so that the imaging time is identical to that of the clinical breast imaging procedure.

METHOD AND MATERIALS

The prototype system was constructed based on a Hologic Selenia Dimensions 3D Mammography system. During a multi-contrast image acquisition process, the diffraction grating traveled continuously along the direction parallel to the chest wall, and a train of 15 short x-ray pulses (42 ms each) was delivered by using the Zero-Degree Tomo mode (usually used for QC) offered by the Hologic system. Standard phase retrieval was applied to the 15 sub-images without spatial interpolation to avoid spatial resolution loss. The method was evaluated using both physical phantoms and a fresh mastectomy specimen (10 min post-surgery). For comparison, each object was also imaged by operating the same system under the conventional phase stepping mode.

RESULTS

The image acquisition time of the proposed method is 6 s and only limited by the scan time of the current version of the Zero-Degree Tomo mode. In comparison, conventional phase stepping took 106 s. Fringe visibility of both methods is 18±3%; spatial resolution of both methods is identical; mean glandular dose of both methods was matched at 1.9 mGy. No artifacts were observed in images produced by the proposed method.

CONCLUSION

The proposed continuous phase stepping acquisition method eliminated the overhead of imaging time imposed by the interleaved stepping motion in x-ray phase contrast imaging. A prototype multi-contrast breast imaging system equipped with this technique was developed; in this system, data acquisition, system geometry and radiation dose are all compatible with requirements of clinical breast imaging.

CLINICAL RELEVANCE/APPLICATION

The proposed fast phase stepping method eliminates the constraint on the imaging time of multi-contrast x-ray imaging, bringing this technology closer to clinical breast imaging applications.

SSK19-02 Scatter Artifact Reduction in Dark-Field X-Ray Imaging

Wednesday, Dec. 4 10:40AM - 10:50AM Room: E353B

Thomas Koehler, PhD, Hamburg, Germany (Abstract Co-Author) Employee, Koninklijke Philips NV Klaus J. Engel, Eindhoven, Netherlands (Abstract Co-Author) Employee, Koninklijke Philips NV Andre Yaroshenko, Hamburg, Germany (Abstract Co-Author) Employee, Koninklijke Philips NV Bernd Lundt, Hamburg, Germany (Abstract Co-Author) Employee, Koninklijke Philips NV Thomas Pralow, Hamburg, Germany (Abstract Co-Author) Nothing to Disclose Konstantin Willer, Garching, Germany (Abstract Co-Author) Nothing to Disclose Wolfgang Noichl, Garching, Germany (Abstract Co-Author) Nothing to Disclose Theresa Urban, MSc, Garching, Germany (Abstract Co-Author) Nothing to Disclose Manuela Frank, MSc, Garching, Germany (Abstract Co-Author) Nothing to Disclose Fabio De Marco, MSc, Garching, Germany (Abstract Co-Author) Nothing to Disclose Rafael Schick, Garching, Germany (Abstract Co-Author) Nothing to Disclose Bernhard Gleich, Munich, Germany (Abstract Co-Author) Nothing to Disclose Bernhard Renger, MSc, Munich, Germany (Abstract Co-Author) Nothing to Disclose Alexander A. Fingerle, MD, Munich, Germany (Abstract Co-Author) Nothing to Disclose Daniela Pfeiffer, MD, Munich, Germany (Abstract Co-Author) Nothing to Disclose Ernst J. Rummeny, MD, Muenchen, Germany (Abstract Co-Author) Nothing to Disclose Julia Herzen, Garching, Germany (Abstract Co-Author) Nothing to Disclose Franz Pfeiffer, Munich, Germany (Presenter) Nothing to Disclose Ingo Maack, MS, Hamburg, Germany (Abstract Co-Author) Nothing to Disclose Sven Prevrhal, PhD, San Francisco, CA (Abstract Co-Author) Research Grant, Koninklijke Philips NV

For information about this presentation, contact:

thomas.koehler@philips.com

PURPOSE

Dark-field X-ray imaging is a new technology to visualize the alveolar structure of lung tissue, which relies on coherent small-angle x-ray scattering. Incoherent Compton scatter overlaying the dark-field signal impedes image formation and thus hampers diagnostic interpretation. The purpose of this work was to develop and validate an algorithm to eliminate the contribution of Compton scatter to the dark-field signal.

METHOD AND MATERIALS

A slot-scanning gratings-based chest dark-field system was used to acquire raw data of phantoms and 10 human patients. Correction for Compton scattering was performed in a two-step approach. First, a conventional x-ray transmission and a dark-field image were generated by standard so-called phase-retrieval, which was implemented as a weighted least-squares fit. The conventional image was the input for a kernel-based scatter estimation method, which accounts for the system geometry, the slot width, the attenuation by the grating assembly, and the detector efficiency. Second, estimates for scattered intensity were calculated for each slot position and were accounted for as additional incoherent background radiation during a second-pass phase-retrieval.

RESULTS

The dark-field signal level is physically limited to the range from 0 to 100%. Dark-field images without scatter correction show artificial dark-field signal in areas with a large scatter fraction. This can be primarily observed in image areas of the backbone, heart, and abdomen. The developed scatter correction greatly reduces this artificial signal and allows for a better quantitative measurement of the true dark-field signal generated by lung tissue. Typically, the correction of the dark-field signal by application of the scatter correction algorithms is in the order of 20%-40% in areas of the backbone, 10% in the area of the heart, and 10-20% in the abdomen.

CONCLUSION

Quantitative dark-field signal processing is possible if the developed Compton scatter correction is applied during image processing.

CLINICAL RELEVANCE/APPLICATION

In previous preclinical small-animal studies, dark-field X-ray radiography has demonstrated the potential to detect early stages of various lung diseases. By using the proposed scatter correction method, more accurate dark-field images are obtained.

SSK19-03 Detection of Monosodium Urate Crystals in X-Ray Dark-Field Radiography

Wednesday, Dec. 4 10:50AM - 11:00AM Room: E353B

Participants

Eva Braig, Garching, Germany (*Abstract Co-Author*) Nothing to Disclose Nathalie Roiser, MSc, Munich, Germany (*Abstract Co-Author*) Nothing to Disclose Melanie Kimm, Munich, Germany (*Abstract Co-Author*) Nothing to Disclose Jana Andrejewski, Garching bei Munchen , Germany (*Presenter*) Nothing to Disclose Josef Scholz, BSC, MSc, Garching, Germany (*Abstract Co-Author*) Nothing to Disclose Christian Petrich, Garching, Germany (*Abstract Co-Author*) Nothing to Disclose Alex Gustschin, BSC, MSc, Garching, Germany (*Abstract Co-Author*) Nothing to Disclose Andreas Sauter, MD, Munich, Germany (*Abstract Co-Author*) Nothing to Disclose Jannis Bodden, Munich, Germany (*Abstract Co-Author*) Nothing to Disclose Felix Meurer, Munich, Germany (*Abstract Co-Author*) Nothing to Disclose Franz Pfeiffer, Munich, Germany (*Abstract Co-Author*) Nothing to Disclose Julia Herzen, Garching, Germany (*Abstract Co-Author*) Nothing to Disclose Daniela Pfeiffer, MD, Munich, Germany (*Abstract Co-Author*) Nothing to Disclose

For information about this presentation, contact:

eva.braig@mytum.de

PURPOSE

To detect gout crystals in radiography by employing the X-ray dark-field signal caused by refractive index fluctuations of the

amorphous crystal structure.

METHOD AND MATERIALS

Monosodium urate (MSU) crystals were injected into mouse legs post mortem to simulate gout crystal deposition and then imaged in a preclinical X-ray grating interferometer setup with a rotating molybdenum anode operated at 50 kVp acceleration voltage and a photon counting detector with an effective pixel size of 166µm. All animal procedures were performed with permission of the local regulatory authority. Every image acquisition provides the dark-field image together with the conventional attenuation image at the same time. In a reader study with 3 experienced radiologists, 7 image sets of dark-field and attenuation images have been evaluated first separately and then with both images available for the reader.

RESULTS

The contrast to noise ratio (CNR) of the MSU crystals in the dark-filed image is more than a factor of 5 higher than in the conventional radiography. All readers correctly identified all three cases with injected MSU crystals and rejected most of the images without crystal injection in the dark-field images (sensitivity = 100%, specificity = 92%) but could not give a reliable diagnose based on the conventional attenuation images (sensitivity = 11%, specificity = 92%). Sensitivity, specificity and confidence level have been maximized when attenuation and dark-field image where presented simultaneously to the reader (sensitivity = 100%, specificity = 100%, confidence level = high).

CONCLUSION

Our ex-vivo study demonstrates the potential of gout detection in radiography with a grating interferometer. The simultaneous accessibility of the conventional attenuation image and the dark-field image allowed a 100% specific and sensitive diagnose in a reader study with mouse legs.

CLINICAL RELEVANCE/APPLICATION

X-ray dark-field imaging enables the detection of MSU crystals in a radiographic projection and has the potential to supersede invasive joint puncture for gout diagnosis.

SSK19-04 Variation of Darkfield Chest X-Ray Signal Strength with Breathing State

Wednesday, Dec. 4 11:00AM - 11:10AM Room: E353B

Participants

Theresa Urban, MSc, Garching, Germany (Presenter) Nothing to Disclose Konstantin Willer, Garching, Germany (Abstract Co-Author) Nothing to Disclose Wolfgang Noichl, Garching, Germany (Abstract Co-Author) Nothing to Disclose Manuela Frank, MSc, Garching, Germany (Abstract Co-Author) Nothing to Disclose Fabio De Marco, MSc, Garching, Germany (Abstract Co-Author) Nothing to Disclose Rafael Schick, Garching, Germany (Abstract Co-Author) Nothing to Disclose Bernhard Gleich, Munich, Germany (Abstract Co-Author) Nothing to Disclose Kai Scherer, Munich, Germany (Abstract Co-Author) Nothing to Disclose Bernhard Renger, MSc, Munich, Germany (Abstract Co-Author) Nothing to Disclose Alexander A. Fingerle, MD, Munich, Germany (Abstract Co-Author) Nothing to Disclose Gregor Zimmermann, Munich, Germany (Abstract Co-Author) Nothing to Disclose Hubert Hautmann, Munich, Germany (Abstract Co-Author) Nothing to Disclose Bernhard Haller, Munich, Germany (Abstract Co-Author) Nothing to Disclose Pascal Meyer, Munich, Germany (Abstract Co-Author) Nothing to Disclose Juergen Mohr, Karlsruhe, Germany (Abstract Co-Author) Nothing to Disclose Thomas Koehler, PhD, Hamburg, Germany (Abstract Co-Author) Employee, Koninklijke Philips NV Roland Proksa, Hamburg, Germany (Abstract Co-Author) Employee, Koninklijke Philips NV Hanns-Ingo Maack, Hamburg, Germany (Abstract Co-Author) Nothing to Disclose Andre Yaroshenko, Hamburg, Germany (Abstract Co-Author) Employee, Koninklijke Philips NV Thomas Pralow, Hamburg, Germany (Abstract Co-Author) Nothing to Disclose Bernd Lundt, Hamburg, Germany (Abstract Co-Author) Employee, Koninklijke Philips NV Karsten Rindt, Hamburg, Germany (Abstract Co-Author) Employee, Koninklijke Philips NV Daniela Pfeiffer, MD, Munich, Germany (Abstract Co-Author) Nothing to Disclose Ernst J. Rummeny, MD, Muenchen, Germany (Abstract Co-Author) Nothing to Disclose Julia Herzen, Garching, Germany (Abstract Co-Author) Nothing to Disclose Franz Pfeiffer, Munich, Germany (Abstract Co-Author) Nothing to Disclose

PURPOSE

To evaluate the lung signal strength of the first human dark-field chest X-rays with respect to the breathing state of the patient.

METHOD AND MATERIALS

We constructed a clinical prototype for grating-based dark-field chest radiography with a field of view of 37 x 37 cm², suitable for human chest imaging. It employs a scanning image acquisition procedure with an acquisition time of 7 s and a tube voltage of 70 kVp. The average effective dose for one posterior-anterior thorax radiograph is 0.04 mSv. So far, more than 60 patients have been examined in an IRB approved study in posterior-anterior orientation in two different respiratory states, viz. inspiration and expiration. From these images, the variation of the dark-field signal due to the micromorphological changes in the lung is assessed.

RESULTS

While the attenuation signal shows anatomical changes, the dark-field signal varies in strength due to underlying structural changes in the lung. In inspiration, the dark-field signal is quite homogeneous over the lung, which can be attributed to a homogeneous distribution of alveolar size and density. In expiration, the alveoli size is reduced and their packing density is increased, particularly in the lower parts of the lung. This leads to more air-tissue interfaces in the beam path, which cause small-angle scattering and thus produce a stronger dark-field signal. The variation strength naturally depends on patient cooperation, but mainly on his or her pulmonary health and ability to breathe. The difference in dark-field signal between the two breathing states allows to spatially identify regions that change micromorphologically and thus participate in the ventilation of the lung.

CONCLUSION

With this technique, it is possible to obtain spatial information about microstructural changes in the lung and thus the physiological activity of different lung regions between inspiration and expiration. The change in signal strength illustrates the origin of the dark-field signal and its sensitivity to the microstructure of the lung, promising a distinct diagnostic value of dark-field images for the assessment of lung diseases.

CLINICAL RELEVANCE/APPLICATION

The variation of dark-field signal with respect to respiration state is strong and thus motivates future investigations on its potential clinical benefit with regard to improved diagnosis and staging of lung diseases, including COPD.

SSK19-05 Grating-Based Spectral X-Ray Dark-Field Imaging for Correlation with Structural Size Properties

Wednesday, Dec. 4 11:10AM - 11:20AM Room: E353B

Participants

Kirsten Taphorn, Garching, Germany (*Presenter*) Nothing to Disclose Fabio De Marco, MSc, Garching, Germany (*Abstract Co-Author*) Nothing to Disclose Jana Andrejewski, Garching bei Munchen, Germany (*Abstract Co-Author*) Nothing to Disclose Thorsten Sellerer, MSc, Garching Bei Munchen, Germany (*Abstract Co-Author*) Nothing to Disclose Franz Pfeiffer, Munich, Germany (*Abstract Co-Author*) Nothing to Disclose Julia Herzen, Garching, Germany (*Abstract Co-Author*) Nothing to Disclose

PURPOSE

Previous small-animal studies have revealed a decrease in X-ray dark-field signal for various structural lung pathologies (i.e. emphysema, fibrosis), which typically are characterized by destruction or densification of alveolar structure. In our studies we have characterized correlations between the structure size of complex samples closely resembling human lung tissue and spectral X-ray dark-field imaging with a polychromatic X-ray source.

METHOD AND MATERIALS

At a setup for grating-based X-ray dark-field imaging with a multi-threshold photon-counting detector (Direct Conversion AB, Danderyd, Sweden), various types of closed-cell foams and hollow glass microspheres were measured. By separating the incoming X-ray photons at the detector into energy intervals, two distinct correlations lengths were sampled and the according energy-dependent X-ray dark-field signal was recorded. A connection between both energy intervals was achieved by determination of the quotient of the resulting X-ray dark-field signals. The structure size of sample materials was defined using micro computed tomography scans and the subsequent calculation of mean chord length, a medically-approved measure for alveolar structure size, which is known to be affected by several structural lung diseases.

RESULTS

For increasing mean chord lengths of the sample materials, an increase of the quotient of energy-dependent X-ray dark-field signals was found. Our findings reveal the possibility to differentiate between objects based on varying structural properties in a single X-ray dark-field scan with a spectral detector. For future clinical X-ray dark-field lung imaging, this implies an increase of diagnostic power as information about destruction or densification of lung tissue are directly accessible.

CONCLUSION

A differentiation of objects with various structural properties is shown to be possible based on the approach of mean chord length and the use of spectral X-ray dark-field imaging, which forms a connection between a medical measure for alveolar structure and X-ray dark-field imaging.

CLINICAL RELEVANCE/APPLICATION

The demonstrated accessibility of information about structural properties using spectral X-ray dark-field imaging potentially increases the diagnostic power of future X-ray dark-field lung imaging.

SSK19-06 Motion Artifact Reduction in Dark-Field X-Ray Imaging

Wednesday, Dec. 4 11:20AM - 11:30AM Room: E353B

Participants

Thomas Koehler, PhD, Hamburg, Germany (Abstract Co-Author) Employee, Koninklijke Philips NV Andre Yaroshenko, Hamburg, Germany (Abstract Co-Author) Employee, Koninklijke Philips NV Sven Prevrhal, PhD, San Francisco, CA (Abstract Co-Author) Research Grant, Koninklijke Philips NV Bernd Lundt, Hamburg, Germany (Abstract Co-Author) Employee, Koninklijke Philips NV Thomas Pralow, Hamburg, Germany (Abstract Co-Author) Nothing to Disclose Ingo Maack, MS, Hamburg, Germany (Abstract Co-Author) Nothing to Disclose Konstantin Willer, Garching, Germany (Abstract Co-Author) Nothing to Disclose Wolfgang Noichl, Garching, Germany (Abstract Co-Author) Nothing to Disclose Theresa Urban, MSc, Garching, Germany (Abstract Co-Author) Nothing to Disclose Manuela Frank, MSc, Garching, Germany (Abstract Co-Author) Nothing to Disclose Fabio De Marco, MSc, Garching, Germany (Abstract Co-Author) Nothing to Disclose Rafael Schick, Garching, Germany (Presenter) Nothing to Disclose Bernhard Gleich, Munich, Germany (Abstract Co-Author) Nothing to Disclose Bernhard Renger, MSc, Munich, Germany (Abstract Co-Author) Nothing to Disclose Alexander A. Fingerle, MD, Munich, Germany (Abstract Co-Author) Nothing to Disclose Daniela Pfeiffer, MD, Munich, Germany (Abstract Co-Author) Nothing to Disclose Ernst J. Rummeny, MD, Muenchen, Germany (Abstract Co-Author) Nothing to Disclose Julia Herzen, Garching, Germany (Abstract Co-Author) Nothing to Disclose Franz Pfeiffer, Munich, Germany (Abstract Co-Author) Nothing to Disclose Hanns-Ingo Maack, Hamburg, Germany (Abstract Co-Author) Nothing to Disclose

For information about this presentation, contact:

thomas.koehler@philips.com

PURPOSE

Dark-field x-ray radiography is a new technology to visualize the alveolar structure of lung tissue. Dark-field images are generated from several x-ray exposures with a grating interferometer assembly in the beam. Motion between the exposures causes artifacts in the final dark-field image. The purpose of this work was to develop and validate an algorithm to reduce these motion artifacts.

METHOD AND MATERIALS

A slot-scanning grating interferometer was used to acquire dark-field images of 10 human study patients. Local illumination time was approximately 700 ms at total acquisition time of 7 seconds, which implies e.g. heart motion during exposure. In a first step, dark-field phase-retrieval processing based on a weighted least-squares fit was used to generate an x-ray transmission and a dark-field image. Motion artefact reduction processing relied on detection of motion-affected areas by analyzing the deviation of the weighted least-squares fit cost function from its expected value. For these areas, alternative dark-field images were generated by iteratively selecting a narrowed slot width and thus a shorter local illumination time. The selection criterion was to optimize the match of the cost function to its statistically expected value.

RESULTS

The dark-field signal level is physically limited to the range from 0 to 100%. Dark-field images generated with conventional processing revealed clearly visible motion artefacts, seen as horizontal stripes especially in the area of the heart, diaphragm, and aorta. The amplitude of these stripes reaches up to 50%. The newly developed processing achieved a substantial motion artifact reduction in dark-field images.

CONCLUSION

Local choice of a subset of exposures to generate a dark-field image can help to significantly reduce motion artefacts. Thus, the presented method enables a quantitative assessment of the dark-field signal strength in areas where lung tissue overlaps with moving objects like the heart.

CLINICAL RELEVANCE/APPLICATION

Motion artifact reduction is an important processing step if the dark-field image near moving objects like the heart is evaluated.

SSK19-07 Osteo-Articular X-Ray Phase Contrast Imaging Using Conventional Radiography Systems and a Random Modulator: Proof of Concepts on Human Fingers and Wrists

Wednesday, Dec. 4 11:30AM - 11:40AM Room: E353B

Participants

Helene Labriet, Grenoble , France (*Abstract Co-Author*) Nothing to Disclose Jean Noel Ravey, La Tronche, France (*Abstract Co-Author*) Nothing to Disclose Ludovic Broche, Grenoble , France (*Abstract Co-Author*) Nothing to Disclose Philippe Chaffanjon, la Tronche , France (*Abstract Co-Author*) Nothing to Disclose Barbara Fayard, Grenoble , France (*Abstract Co-Author*) Nothing to Disclose Sylvain Bohic, Grenoble , France (*Abstract Co-Author*) Nothing to Disclose Sebastien Berujon, PhD, Grenoble, France (*Abstract Co-Author*) Nothing to Disclose Emmanuel Brun, Grenoble, France (*Presenter*) Nothing to Disclose

For information about this presentation, contact:

helene.labriet@novitom.com

PURPOSE

X-ray Phase Contrast Imaging (PCI) has been introduced a few decades ago at synchrotrons. It has demonstrated an increased contrast that allows the visualization of all tissues in a single modality with high resolution. Applications of PCI on laboratory or clinical set-up often encounter various limitations due to the optics it requires. In this work we present medical results of a PCI approach on a conventional device with solely the addition of a random beam intensity modulator. We present a preliminary comparison of results between standard radiography and PCI at 80% of the conventional radiograph radiation dose.

METHOD AND MATERIALS

Phantoms and anatomical pieces (human finger and hands) were imaged. Two different X-ray commercially available devices were used: a C-arm Siemens ARCADIS Avantic and a radiography table Primax Clisis Exel. The samples were imaged using both the standard radiography and the PCI approaches at 60 kvp and with clinical compatible doses. For the PCI acquisitions, a single thin random modulator was included upstream of the samples. Before imaging the samples, a first radiograph of the modulator was taken. Then, by numerically processing the couples of images taken with and without the sample, we are able to map the phase shifts induced by the samples.

RESULTS

The phase maps of the samples were obtained using the conventional device. The image quality from X-ray PCI visually permits the visualization of features invisible to conventional X-ray imaging techniques such as Styrofoam ball, cartilage thickness, micro calcifications, bone microstructures.

CONCLUSION

The study shows that, with a simple beam modulator, phase maps can be retrieved on conventional devices. Here, the experimental complexity of PCI is translated in to the numerical processing side. Despite not yet being implemented in routine, the PCI improved visualization capabilities demonstrated so far suggests that healthcare could significantly benefit from a widespread application of PCI. These preliminary results combined with more recent technical developments let foresee the availability of the proposed PCI method on conventional sources in a close future.

CLINICAL RELEVANCE/APPLICATION

This study presents the results of medical PCI using conventional X-ray device modified with an additional simple random modulator. The results reveal some advantages of PCI over standard radiograph.

SSK19-08 Dosimetry for Combined Dark-Field and Attenuation Chest X-Ray Imaging on Patients

Wednesday, Dec. 4 11:40AM - 11:50AM Room: E353B

Participants

Manuela Frank, MSc, Garching, Germany (Presenter) Nothing to Disclose Theresa Urban, MSc, Garching, Germany (Abstract Co-Author) Nothing to Disclose Konstantin Willer, Garching, Germany (Abstract Co-Author) Nothing to Disclose Wolfgang Noichl, Garching, Germany (Abstract Co-Author) Nothing to Disclose Fabio De Marco, MSc, Garching, Germany (Abstract Co-Author) Nothing to Disclose Rafael Schick, Garching, Germany (Abstract Co-Author) Nothing to Disclose Bernhard Gleich, Munich, Germany (Abstract Co-Author) Nothing to Disclose Kai Scherer, Munich, Germany (Abstract Co-Author) Nothing to Disclose Bernhard Renger, MSc, Munich, Germany (Abstract Co-Author) Nothing to Disclose Peter B. Noel, PhD, Philadelphia, PA (Abstract Co-Author) Nothing to Disclose Alexander A. Fingerle, MD, Munich, Germany (Abstract Co-Author) Nothing to Disclose Alexander Schegerer, Neuherberg, Germany (Abstract Co-Author) Nothing to Disclose Ursula Lechel, Neuherberg, Germany (Abstract Co-Author) Nothing to Disclose Pascal Meyer, Munich, Germany (Abstract Co-Author) Nothing to Disclose Juergen Mohr, Karlsruhe, Germany (Abstract Co-Author) Nothing to Disclose Thomas Koehler, PhD, Hamburg, Germany (Abstract Co-Author) Employee, Koninklijke Philips NV Roland Proksa, Hamburg, Germany (Abstract Co-Author) Employee, Koninklijke Philips NV Hanns-Ingo Maack, Hamburg, Germany (Abstract Co-Author) Nothing to Disclose Andre Yaroshenko, Hamburg, Germany (Abstract Co-Author) Employee, Koninklijke Philips NV Thomas Pralow, Hamburg, Germany (Abstract Co-Author) Nothing to Disclose Bernd Lundt, Hamburg, Germany (Abstract Co-Author) Employee, Koninklijke Philips NV Karsten Rindt, Hamburg, Germany (Abstract Co-Author) Employee, Koninklijke Philips NV Daniela Pfeiffer, MD, Munich, Germany (Abstract Co-Author) Nothing to Disclose Ernst J. Rummeny, MD, Muenchen, Germany (Abstract Co-Author) Nothing to Disclose Julia Herzen, Garching, Germany (Abstract Co-Author) Nothing to Disclose Franz Pfeiffer, Munich, Germany (Abstract Co-Author) Nothing to Disclose

PURPOSE

To demonstrate that the applied effective dose for patient examinations at the first clinical X-ray dark-field chest radiography system is within a clinically acceptable dose range.

METHOD AND MATERIALS

A clinical setup for grating-based dark-field chest radiography was constructed which operates at an acceleration voltage of 70 kVp. The study was approved by the institutional review board and the national radiation protection agency. To obtain conversion coefficients relating effective dose to dose area product (DAP) at the dark-field system, thermoluminescent dosimeter (TLD) measurements were conducted using a phantom with approximately 200 TLDs, modeling the ICRP reference man with a body weight of 73.5 kg and a trunk length of 68 cm. The effective dose for the TLD measurements was calculated with weighting factors according to ICRP 103. For n = 53 patients, the DAP values for both posterior-anterior (pa) and lateral (lat) measurements were collected at the dark-field system and a conventional radiography system which is operated at 125 kVp. With the determined conversion coefficients, the respective effective dose was calculated.

RESULTS

The average effective dose for one measurement at the dark-field radiography system in pa orientation is determined to 44 μ Sv in the case of a typical patient as modeled by the anthropomorphic phantom. For the conventional system, an effective dose of 18 μ Sv was determined. For the examined patients, we obtain an average effective dose of pa: (40 ± 21) μ Sv (lat: (81 ± 34) μ Sv) at the dark-field system and pa: (13 ± 5) μ Sv (lat: (34 ± 31) μ Sv) for the conventional device. A strong variation in effective dose was observed, as patients of various weights and heights were imaged while targeting a fixed detector dose.

CONCLUSION

The effective dose at the clinical dark-field radiography system is about a factor of three higher compared to a conventional system. A potential diagnostic value provided by this novel contrast modality, which will be evaluated in further studies, could justify the higher dose.

CLINICAL RELEVANCE/APPLICATION

Dark-field chest radiography is compatible with clinical dose requirements, thus it qualifies as a potential mass screening tool for early detection of pulmonary disorders.

SSK19-09 Characterizing Cartilage Microarchitecture on Phase-Contrast X-Ray Computed Tomography - A Machine Learning Approach

Wednesday, Dec. 4 11:50AM - 12:00PM Room: E353B

Participants

Anas Ż. Abidin, MS, Rochester, NY (*Abstract Co-Author*) Nothing to Disclose Adora M. D'Souza, MSc, Rochester, NY (*Abstract Co-Author*) Nothing to Disclose Paola Coan, Grenoble, France (*Abstract Co-Author*) Nothing to Disclose Seyed Saman Saboksayr, Rochester, NY (*Abstract Co-Author*) Nothing to Disclose Axel Wismueller, MD, PhD, Munich, Germany (*Presenter*) Nothing to Disclose Phase-contrast x-ray computed tomography (PCI-CT) has been shown to achieve soft-tissue contrast with micrometer scale resolution for cartilage imaging. In this study, we investigate the ability of deep learning with convolutional neural networks (CNNs) to characterize and classify between chondrocyte patterns in healthy and osteoarthritic cartilage.

METHOD AND MATERIALS

A total of 842 regions of interest (ROI) were annotated from five osteochondral cylinders (7 mm diameter, 3 osteoarthritic, 2 healthy) extracted from post-mortem human patellae. Specimens were subject to high-resolution (voxel size 8 µm3, 26 keV, synchrotron source) phase-contrast x-ray CT imaging. ROIs were defined for capturing chondrocyte patterns in the radial zone of the cartilage matrix. The deep learning task was performed using a pre-trained CaffeNet neural network. We obtained representations from each of the eight layers of this network serving as input features for supervised machine learning. Random sub-sampling cross-validation was utilized in optimizing a support vector machine with a radial basis function kernel for classifying healthy and osteoarthritic cartilage. Additionally, ROIs from the same subject were not used for training as well as testing. Classification performance was evaluated by Area Under the Curve (AUC) for Receiver Operator Characteristics (ROC) analysis. Furthermore, we compared the results obtained with traditional first and second-level (measures from gray-level co-occurrence matrices) statistical features.

RESULTS

An AUC=0.81 was achieved for differentiating between healthy and osteoarthritic cartilage, when features were extracted from the first fully connected CNN layer. Interestingly, the best classification performance was observed for features extracted from the last fully connected as well as the last convolutional layer (AUC=0.91 for both). For comparison, conventional first and second order statistical features performed poorly (best AUC=0.78, p<0.05, Wilcoxon signed-rank test).

CONCLUSION

Features from internal layers of pre-trained CNNs achieve high classification performance and can serve as benchmarks for cartilage characterization, as they significantly outperform traditional statistical features.

CLINICAL RELEVANCE/APPLICATION

Deep learning approaches for cartilage pattern characterization on phase-contrast CT imaging can contribute to the development of diagnostic imaging biomarkers for osteoarthritis.

Printed on: 10/29/20





SSK20

Radiation Oncology (Genitourinary)

Wednesday, Dec. 4 10:30AM - 12:00PM Room: S102CD



AMA PRA Category 1 Credits ™: 1.50 ARRT Category A+ Credit: 1.75

FDA Discussions may include off-label uses.

Participants

Sanjay Aneja, MD, New Haven, CT (*Moderator*) Research Consultant, AG Mednet, Inc Marco A. Amendola, MD, Coral Gables, FL (*Moderator*) Speakers Bureau, Varian Medical Systems, Inc

Sub-Events

SSK20-01 A PSMA-PET-Radiomics Signature Model for Characterization of Gleason Score in Patients with Prostate Cancer

Wednesday, Dec. 4 10:30AM - 10:40AM Room: S102CD

Participants

Montserrat Carles, PhD, Freiburg, Germany (*Presenter*) Nothing to Disclose Constantinos Zamboglou, Freiburg, Germany (*Abstract Co-Author*) Nothing to Disclose Michael Mix, Freiburg, Germany (*Abstract Co-Author*) Nothing to Disclose Anca L. Grosu, MD, Freiburg, Germany (*Abstract Co-Author*) Nothing to Disclose

For information about this presentation, contact:

montserrat.carles@uniklinik-freiburg.de

PURPOSE

To evaluate the performance of PSMA-PET-radiomics modelling for non-invasive characterization of Gleason score (GS).

METHOD AND MATERIALS

Twenty prostate cancer (PCa) patients, who underwent [68Ga]-PSMA-PET/CT followed by radical prostatectomy, were prospectively enrolled. Two PCa segmentations were performed: the PCa manually contoured by experts (GTV-Exp) and the coregistered histopathological PCa (GTV-Histo). 133 PET image features (IF) were computed. The study involved: (i) the comparison of IF derived from PCa and non-PCa ; (ii) the comparison of IF derived from both segmentations (GTV-Histo vs GTV-Exp); (iiii) the evaluation of the IF correlations with GS and (iv) the development of a radiomics signature model for GS characterization. Comparisons were analysed in terms of two-tailed Mann-Whitney U test for non-pairwise testing (i) and Spearman's correlation test (ii and iii). The incorporation of features into multivariable models (iv) was performed using logistic regression. Model development involved imbalance-adjusted bootstrap resampling in the following processes: IF selection, prediction performance estimation and computation of model coefficients.

RESULTS

Most IF discriminated significantly between PCa and non-PCa tissue: 76% for GTV-Histo and 81% for GTV-Exp. 82% of the IF derived from GTV-Expert showed significant strong correlation (r>0.8) with respect to the IF derived from GTV-Histo. For GTV-Exp, the best performance in GS characterization was observed for the IF short-zones-high-gray-level emphasis-after-quantization-resampling (QSZHGE) with area-unde-the-curve (AUC) of 0.91. In addition, a radiomics signature (5 IF) discriminated between GS 7 and >=8 (AUC=0.93 and sensitivity=0.90). Preliminary validation with an internal cohort of 20 additional patients (GTV_Exp_val) confirmed the results.

CONCLUSION

From our results it could be proved the feasibility of model development based on PSMA-PET radiomics for GS characterization.

CLINICAL RELEVANCE/APPLICATION

GS characterization has an impact on clinical decision making as it defines intermediate- and high-risk PCa patients which influences for example the duration of androgen deprivation therapy during radiation therap. Because of the fact that GS before primary therapy is based on biopsy tissue, a model derived from PSMA-PET radiomics could serve as an alternative for non-invasive GS characterization in the future.

SSK20-02 Pre-Treatment Quantitative Multi-Parametric MRI Can Predict the Biochemical Outcome of Prostate Cancer Patients Undergoing Radiotherapy

Wednesday, Dec. 4 10:40AM - 10:50AM Room: S102CD

Participants Aritrick Chatterjee, PhD, Chicago, IL (*Presenter*) Nothing to Disclose Stanley L. Liauw, MD, Chicago, IL (*Abstract Co-Author*) Nothing to Disclose William T. Turchan, MD, Chicago, IL (*Abstract Co-Author*) Nothing to Disclose Xiaobing Fan, PhD, Chicago, IL (*Abstract Co-Author*) Nothing to Disclose Gregory S. Karczmar, PhD, Crete, IL (*Abstract Co-Author*) Nothing to Disclose Aytekin Oto, MD, Chicago, IL (*Abstract Co-Author*) Research Grant, Koninklijke Philips NV; Research Grant, Guerbet SA; Research Grant, Profound Medical Inc; Medical Advisory Board, Profound Medical Inc; Consultant, IBM Corporation; ; ; Alexander B. Griffin, MD, Chicago, IL (*Abstract Co-Author*) Nothing to Disclose Ambereen Yousuf, MBBS, Chicago, IL (*Abstract Co-Author*) Nothing to Disclose

For information about this presentation, contact:

aritrick@uchicago.edu

PURPOSE

Up to one-third of men treated with radiation therapy (RT) for prostate cancer may experience biochemical failure, often identified beyond 5 years of follow-up. An earlier diagnosis of recurrent prostate cancer can better inform prognosis and treatment. This study evaluates whether quantitative multiparametric MRI (mpMRI) can be used to predict the biochemical outcome of prostate cancer (PCa) patients.

METHOD AND MATERIALS

Fifty-one patients with biopsy confirmed PCa underwent prostate mpMRI on 3T Philips MR scanner prior to RT with a median dose of 78 Gy. 51% had concurrent hormonal therapy for a median of 16.5 months. The index lesion was outlined by a radiologist and quantitative ADC, T2 and DCE parameters (Tofts model) were measured. The biochemical failure based on Phoenix criteria was associated with these values.

RESULTS

After a median follow-up of 65 months, 6 patients had biochemical failure, and 3 had distant metastasis. ADC had an area under the ROC curve of 0.71 for predicting RT outcome with significantly (*t*-test) lower ADC ($0.78\pm0.17 vs 0.96\pm0.26 \mu m2/ms, p=0.04$) found in patients showing biochemical failure. Ideal ADC cutoff point (Youdens index) was 0.96 $\mu m2/ms$ which had a sensitivity of 47% and specificity of 100% for biochemical failure. Kaplan-Meier analysis showed that lower ADC values predicted for significantly lower freedom from biochemical failure (*p*=0.03, no failures out of 20 men if ADC >=0.96 $\mu m2/ms$; 7 of 31 with failures if ADC <0.96 $\mu m2/ms$). Quantitative T2 and DCE parameters were not associated with biochemical outcome.

CONCLUSION

This study demonstrates that quantitative mpMRI, and specifically ADC values, are associated with biochemical outcome in patients with PCa treated with RT. Lower ADC values were associated with biochemical failure.

CLINICAL RELEVANCE/APPLICATION

Quantitative MRI, specifically ADC values can predict biochemical outcomes in PCa patients undergoing RT, with lower ADC values associated with biochemical failure. mpMRI may improve risk stratification and help determine optimal treatment.

SSK20-03 Integrated Gene Expression Score in Circulating Tumor Cells to Predict Treatment Response in Muscle-Invasive Bladder Cancer

Wednesday, Dec. 4 10:50AM - 11:00AM Room: S102CD

Participants

William L. Hwang, MD, PhD, Boston, MA (Presenter) Nothing to Disclose Haley Pleskow, BA, Boston, MA (Abstract Co-Author) Nothing to Disclose Juliane A. Andrade Czapla, MS, Boston, MA (Abstract Co-Author) Nothing to Disclose Rebecca R. Fisher, Boston, MA (Abstract Co-Author) Nothing to Disclose Sophia C. Kamran, MD, Boston, MA (Abstract Co-Author) Nothing to Disclose Richard J. Lee, Boston, MA (Abstract Co-Author) Nothing to Disclose Philip J. Saylor, Boston, MA (Abstract Co-Author) Nothing to Disclose Dror Michaelson, Boston, MA (Abstract Co-Author) Nothing to Disclose Anthony L. Zietman, MD, Boston, MA (Abstract Co-Author) Editor, Reed Elsevier Brenda L. Silvia, Boston, MA (Abstract Co-Author) Nothing to Disclose David T. Ting, Boston, MA (Abstract Co-Author) Consultant, EMD Millipore Sigma; Founder, PanTher Therapeutics; Founder and Consultant, ROME Therapeutics Shyamala Maheswaran, Boston, MA (Abstract Co-Author) Nothing to Disclose Daniel A. Haber, Boston, MA (Abstract Co-Author) Nothing to Disclose Jason Efstathiou, Boston, MA (Abstract Co-Author) Consultant, Blue Earth Diagnostics Ltd Consultant, TARIS BioMedical, Inc. Consultant, Bayer AG Advisory Board, Merck KGaA

David T. Miyamoto, MD, PhD, Boston, MA (Abstract Co-Author) Nothing to Disclose

For information about this presentation, contact:

whwang1@mgh.harvard.edu

PURPOSE

Muscle-invasive bladder cancer (MIBC) is often treated with radical cystectomy, but select pts can be treated with bladder-sparing trimodality therapy (TMT) with comparable long-term survival. There is an urgent need for reliable biomarkers to optimize treatment selection and detect disease recurrence early. Circulating tumor cells (CTCs) in the blood have potential as non-invasive, serial "liquid biopsies" to predict and monitor therapeutic response. The purpose of this study is to develop a CTC gene expression score (CTC-GES) to monitor response to TMT using microfluidic CTC isolation coupled with droplet digital PCR.

METHOD AND MATERIALS

Candidate genes were identified by differential expression analysis comparing RNA-seq data from MIBC (TCGA; n=67) to normal bladder (GTEX; n=11) and leukocytes (n=20). Primer/probe sets for each gene were validated using bladder cancer cell lines (RT4: luminal, HT-1376: basal) spiked into healthy blood. Blood is being collected from a discovery cohort of MIBC pts undergoing TMT (n = 11 to date, median age 73 yr) at several time points (baseline, on-treatment, two-month follow-up). CTCs were isolated using

the microfluidic CTC-iChip and the CTC-GES was computed as log(?(positive droplets/mL blood)+1).

RESULTS

Eight candidate genes (PPARG, UPK1A, UPK2, KRT14, EGFR, KRT19, TMEM129, DSG2) were analytically validated and comprised the CTC-GES. The assay lower limit of detection was 3 CTCs per 10 mL blood. The assay predicted recurrences >2 months prior to clinical detection. At a median follow-up of 20.3 weeks for the 5 pts to date with all time points collected, development of metastatic disease was associated with an increase in CTC-GES from baseline to on-treatment (n = 3), whereas a decline in CTC-GES was seen in 2 pts with no evidence of disease (average Δ GESmet = +2.61 vs. Δ GESNED = -0.43; p=0.048).

CONCLUSION

We have developed a novel CTC gene expression score for MIBC pts undergoing TMT. Our preliminary data suggests this biomarker can predict cancer recurrence more than two months prior to clinical detection. In contrast to circulating tumor DNA, CTC-GES does not require interpatient customization based on prior knowledge of specific mutations.

CLINICAL RELEVANCE/APPLICATION

With continued refinement and substantiation, the CTC-GES has potential as a universal biomarker in MIBC to predict early failures after TMT and enable treatment modification/intensification at a lower disease burden.

SSK20-04 Radium 223 Therapy in Hormone Refractory Metastatic Prostate Cancer: Clinical and Quality of Life Outcomes

Wednesday, Dec. 4 11:00AM - 11:10AM Room: S102CD

Participants

Ashwatha B. Narayana, MD, Mount Kisco, NY (*Presenter*) Nothing to Disclose Judith Hasak, BSN,RN, Greenwich, CT (*Abstract Co-Author*) Nothing to Disclose Carolyn Troy, BSN,RN, Greenwich, CT (*Abstract Co-Author*) Nothing to Disclose Samuel Cotte, ARRT,RT, Grewnwich, CT (*Abstract Co-Author*) Nothing to Disclose Christopher Fey, Greenwich, CT (*Abstract Co-Author*) Nothing to Disclose

For information about this presentation, contact:

anarayana2@northwell.edu

PURPOSE

Radium 223 (Ra 223) has been shown to improve survival in hormone refractory metastatic prostate cancer. However, the optimal duration of therapy and its true benefit in improving quality of life is not clear in patients who have already undergone extensive systemic therapy. We present the outcomes from a single community institution with mature follow-up.

METHOD AND MATERIALS

Fifty four patients with refractory metastatic prostate cancer were treated between August 2013 and April 2019. The median age of the patients was 76 years (range 49-100). The median number of chemotherapy regimens used proir to starting Ra 223 was 3 (range 1-7). The treatment plan was to use 6 monthly injections of Ra 223 at a dose of 1.49 microcuries.kg. The patients were followed regularly in both radiation oncology and medical oncology clinics to assess pain control, quality of life and overall survival.

RESULTS

The median follow-up was 18 months (range 1-48). The median survival time was 8.3 months (range 1-48). Twenty six (48%) of the patient completed all planned 6 monthly injections. The median survival for the patient who completed all 6 cycles of therapy was 16 months (range 7-48) as compared to 5.2 months (range 1-22) who received less than planned 6 cycles (p<0.01). Adequate pain relief was noted in 70% and improved ambulation was observed in 64% of cases, in patients who finished all planned therapy. Disease progression was the cause of early stoppage of Ra 223 therapy in 86% of cases. Fatigue was the most common symptom at the end of therapy in 72% of cases.

CONCLUSION

Only half of the patients who receive Ra 223 completed all planned 6 monthly injections. Improved survival, adequate pain relief and better ambulation was seen in patients who completed planned therapy. Earlier use of therapy may result in better treatment outcome as compared to delayed use in this patient population.

CLINICAL RELEVANCE/APPLICATION

Completion of all planned six cycles is necessary to have an improved survival, pain relief and quality of life in hormone refractory metastatic patients receiving Ra 223 therapy.

SSK20-05 Patterns of Failure by Gallium-68 PSMA PET For Biochemically Recurrent Hormone Sensitive Prostate Cancer Following Prostatectomy and Salvage Radiotherapy

Wednesday, Dec. 4 11:10AM - 11:20AM Room: S102CD

Participants

Brandon S. Imber, MD, New York, NY (Presenter) Nothing to Disclose

Melissa Varghese, BA, New York, NY (Abstract Co-Author) Nothing to Disclose

Daniel Gorovets, MD, New York, NY (Abstract Co-Author) Nothing to Disclose

Sean M. McBride, MD, New York, NY (Abstract Co-Author) Research funded, Johnson & Johnson; Research funded, F. Hoffmann-La Roche Ltd;

Marisa A. Kollmeier, MD, Rockville Centre, NY (Abstract Co-Author) Nothing to Disclose

Neeta Pandit-Taskar, MD, New York, NY (*Abstract Co-Author*) Consultant, Actinium Pharmaceuticals, Inc; Consultant, Progenics Pharmaceuticals, Inc; Consultant, inviCRO, LLC; Consultant, AstraZeneca PLC; Advisory Board, Actinium Pharmaceuticals, Inc; Advisory Board, Progenics Pharmaceuticals, Inc; Advisory Board, InviCRO, LLC; Speaker, Actinium Pharmaceuticals, Inc; Speaker, Progenics Pharmaceuticals, Inc; Speaker, InviCRO, LLC; Speaker, InviCRO, LLC; Speaker, AstraZeneca PLC

Michael Morris, New York, NY (Abstract Co-Author) Consultant, Endocyte, Inc; Consultant, Bayer AG; Consultant, Advanced Accelerator Applications SA: Consultant, Blue Earth Diagnostics Ltd; Consultant, Tokai Pharmaceuticals; Consultant, Tolmar Pharmaceuticals; Consultant, Oric Pharmaceuticals; Institutional research support, Bayer AG; Institutional research support, sanofiaventis Group; Institutional research support, Endocyte, Inc; Institutional research support, Corcept Therapeutics Inc; Institutional research support, F. Hoffmann-La Roche Ltd; ;

Heiko Schoder, MD, New York, NY (Abstract Co-Author) Nothing to Disclose Michael J. Zelefsky, MD, New York, NY (Abstract Co-Author) Nothing to Disclose

For information about this presentation, contact:

imberb@mskcc.org

PURPOSE

Disease localization for patients who develop biochemical failure post radical prostatectomy (RP) and salvage radiotherapy (SRT) is critical for optimizing subsequent management strategies. The role of Gallium-68 PSMA PET is not established in this setting after SRT.

METHOD AND MATERIALS

We analyzed 70 non-castrate men with 71 total Gallium-PSMA PET scans obtained on a prospective imaging trial (NCT03204123) for PSA recurrence after prior RP+SRT. Men with known metastasis or castrate resistance were excluded. A PSMA scan was called positive if at least one avid site was interpreted as at least 'possibly' metastatic. For patterns of failure analyses, pelvic lymph nodes (PLN) included common iliac, internal/external iliac, obturator, perirectal and presacral.

RESULTS

Post RP, most had pT3/4 disease (73%), 26% had extracapsular extension, 30% had positive margins and 23% were pN1. Median time from RP to SRT was 1.6 years (IQR 0.6, 4.1). SRT fields included the prostate bed only (56%), prostate bed and PLN (41%) or unknown (3%) delivered to a median total prostate bed dose of 72 Gy (range 58-81). PSMA scans were performed a median of 4.4 years (interquartile range 2.3, 8.8) post SRT when median PSA was 1.1 ng/mL (IQR 0.4, 2.8). Overall, 51 scans (72%) were positive; positivity rates by pre-PSMA PSA levels of <0.5 (n=26), 0.5-2 (n=23) and >2 ng/mL (n=22) were 69%, 61% and 86%, respectively. Patterns of failure were heterogeneous (Figure). 9 scans (13%) had concern for prostate bed recurrence; with respect to SRT, 5 recurrences (7%) were in field, 3 (4%) were marginal and 2 (2%) were out of field. 27 scans (38%) had concern for PLN relapse, of these, SRT fields had included PLN in 9 (33%). Incidence of PLN relapse was not significantly lower (p=0.2) in men who received SRT to the pelvic nodes. 29 scans (41%) had at least one distant avid site. 20 (28%) had at least one PSMA avid site biopsied, of which 80% were positive.

CONCLUSION

There is predictive value in the use of PSMA PET for men with PSA recurrence after RP and SRT. Patterns of failure are heterogeneous but relapse in the irradiated prostate bed is rare. PSMA may be an important tool to identify men who remain salvageable post SRT.

CLINICAL RELEVANCE/APPLICATION

68Ga-PSMA PET identifies recurrence in the majority of men with PSA recurrence post prostatectomy and salvage radiotherapy and information regarding sites of residual disease would be critical for guiding further personalized treatment interventions.

SSK20-06 Assessment of Patterns of Failure with Gallium-68 PSMA PET for Early Biochemically Recurrent **Prostate Cancer following Primary Prostate Radiotherapy**

Wednesday, Dec. 4 11:20AM - 11:30AM Room: S102CD

Participants

Michael J. Zelefsky, MD, New York, NY (Presenter) Nothing to Disclose Brandon S. Imber, MD, New York, NY (Abstract Co-Author) Nothing to Disclose Melissa Varghese, BA, New York, NY (Abstract Co-Author) Nothing to Disclose Marisa A. Kollmeier, MD, Rockville Centre, NY (Abstract Co-Author) Nothing to Disclose Sean M. McBride, MD, New York, NY (Abstract Co-Author) Research funded, Johnson & Johnson; Research funded, F. Hoffmann-La Roche Itd: Daniel Gorovets, MD, New York, NY (Abstract Co-Author) Nothing to Disclose

Neeta Pandit-Taskar, MD, New York, NY (Abstract Co-Author) Consultant, Actinium Pharmaceuticals, Inc; Consultant, Progenics Pharmaceuticals, Inc; Consultant, inviCRO, LLC; Consultant, AstraZeneca PLC; Advisory Board, Actinium Pharmaceuticals, Inc; Advisory Board, Progenics Pharmaceuticals, Inc; Advisory Board, inviCRO, LLC; Advisory Board, AstraZeneca PLC; Speaker, Actinium Pharmaceuticals, Inc; Speaker, Progenics Pharmaceuticals, Inc; Speaker, inviCRO, LLC; Speaker, AstraZeneca PLC Michael Morris, New York, NY (Abstract Co-Author) Consultant, Endocyte, Inc; Consultant, Bayer AG; Consultant, Advanced Accelerator Applications SA; Consultant, Blue Earth Diagnostics Ltd; Consultant, Tokai Pharmaceuticals; Consultant, Tolmar Pharmaceuticals; Consultant, Oric Pharmaceuticals; Institutional research support, Bayer AG; Institutional research support, sanofiaventis Group; Institutional research support, Endocyte, Inc; Institutional research support, Corcept Therapeutics Inc; Institutional research support, F. Hoffmann-La Roche Ltd; ;

Heiko Schoder, MD, New York, NY (Abstract Co-Author) Nothing to Disclose

For information about this presentation, contact:

zelefskm@mskcc.org

PURPOSE

There is a lack of information regarding the value of PSMA PET scans for disease evaluation after definitive prostate radiotherapy (RT). Improved detection following RT will offer opportunities for targeted treatment and may improve disease-free survival outcomes.

METHOD AND MATERIALS

We analyzed 28 non-metastatic patients who underwent Gallium-68 PSMA PET scans after definitive prostate RT. All were enrolled

on an IRB-approved prospective imaging trial. Patients' initial PSA level was low (14%), intermediate (46%), and high (40%) and 4 (14%) had N1 disease. Definitive RT approaches were conventional EBRT (43%), brachytherapy-based regimens (46%), and hypofractionated EBRT (11%). Post RT, all had at least 2 consecutive PSA rises and 17 (60%) had nadir+2 relapse. A PSMA scan was considered positive if at least one avid site was noted as at least possibly metastatic. Pelvic lymph nodes (PLN) included common iliac, internal/external iliac, obturator, perirectal, and presacral. 22 (78%) had an available pelvic MRI for comparison to PSMA PET. Median time from RT to PSMA PET was 6 years.

RESULTS

Prior to PSMA PET, 4 (14%), 4 (14%) and 21 (75%) had PSA ranging between 0.5-1, 1-2, and >2 ng/mL, respectively. For these PSA ranges, the incidence of a positive PSMA scan was n=1 (25%), n=4 (100%), and n=18 (86%), respectively. Among the 23 patients with positive PSMA, local prostate/SV failure, PLN failure, and distant failure rates were n=14 (50%), n=7 (25%), and n=12 (48%), respectively. We observed prostate only, PLN only, and distant only failure in 8 (35%), 1 (4%), and 5 (22%) patients. 9 patients were initially treated with RT to the pelvis and only 1 (11%) of these patients failed in a PLN. Pelvic MRI revealed nodal recurrence in only 3 men (14%) but local recurrence in 11 men (50%). Discordant PSMA and MRI findings were noted in 22 (41%) cases. Based on PSMA results, 15 underwent further treatment, which included salvage RT to sites of PSMA avid disease (n=8).

CONCLUSION

PSMA PET provides information beyond other diagnostic studies routinely obtained for restaging. While MRI remains valuable for detecting intraprostatic relapses, PSMA was advantageous for detecting PLN and distant failures.

CLINICAL RELEVANCE/APPLICATION

PSMA PET identifies radiographic recurrence (mostly PLN) among patients whose PSAs demonstrate consistent rise after primary radiotherapy but prior to reaching nadir+2 biochemical relapse.

SSK20-07 SBRT Re-Irradiation Therapy for Locally Recurrent Prostate Cancer after External-Beam Radiation Therapy

Wednesday, Dec. 4 11:30AM - 11:40AM Room: S102CD

Participants

Gabriella Pastore, Empoli, Italy (*Presenter*) Nothing to Disclose Claudia Menichelli, Empoli, Italy (*Abstract Co-Author*) Nothing to Disclose Eleonora Paulicelli, Empoli, Italy (*Abstract Co-Author*) Nothing to Disclose Alessandro Fanelli, Empoli, Italy (*Abstract Co-Author*) Nothing to Disclose Ezio Lombardo, Empoli, Italy (*Abstract Co-Author*) Nothing to Disclose Franco Casamassima, Empoli, Italy (*Abstract Co-Author*) Nothing to Disclose

For information about this presentation, contact:

gabriella.pastore@ecomedica.it

PURPOSE

The aim of this study is to evaluate the toxicity of re-irradiation with stereotactic body radiotherapy (SBRT) in pts with recurrent prostate cancer after external beam radiotherapy (EBRT) in order to assess the potential risk predictors of rectal and urinary toxicity.

METHOD AND MATERIALS

From Apr 2011 to Feb 2019, SBRT was delivered to 11 pts for isolated local recurrence of prostate cancer. 10 pts were high risk while a patient was an intermediate risk. The pts were previously treated with 3DCRT to a median dose of 76,6Gy (68-78Gy). After a median time of 40 mos (13-84 mos), the pts had recurrences confirmed by multiparametric MRI and 18Ffluorocoline PET-CT. Median PSA at the time of SBRT was 4,38 (2.5-9.9). The prescribed dose was 30 Gy in 3fx to 80% isodose in 9 pts and 30Gy in 6fx to 80% isodose in 2 pts. The PTV delineation was performed on CT-MRI fusion to limit normal tissue toxicity. The VMAT treatment was delivered by 6MV Linac. CBCT was employed to control patient set-up before each fraction. Toxicity was evaluated according to CTCAE v.4.0 and the treatment response was assessed by PSA. Dose to rectum and bladder (Dmax of EBRT+SBRT plans) were evaluated using DVH converted into NTD2Gy (a/ß ratio=3Gy for rectum and a/ß ratio=5Gy for bladder) to determine factors that predict toxicity.

RESULTS

Median follow-up was 8 mos (range 1-18). LC, defined by PSA returned to zero, was achieved in all treated pts. Two pts (18%) had a biochemical failure due to metastatic progression without local recurrence. 4 pts (36%) showed grade<=2 urinary toxicity and no grade>2 acute gastrointestinal or late toxicities were reported. Dmax was predictive for toxicity of bladder (98 Gy) and rectum (130 Gy).

CONCLUSION

SBRT re-irradiation of prostatic recurrences after EBRT showed favorable results in terms of LC. In our experience only two relapses occurs outside of prostate gland. Acute and late toxicity was mild. In our study a threshold Dmax (98Gy) for bladder may be related to a greater probability of low toxicity and confirms data already published in literature (Dmax=130 Gy) for rectum. The results need to be confirmed with more pts and longer follow up.

CLINICAL RELEVANCE/APPLICATION

Prostate re-irradiation with SBRT

SSK20-08 Constraining Rectal Dose to Attain Higher Dose Coverage to Prostate Volumes in Robotic SBRT Using Perirectal Hydrogel Spacer for Low- and Intermediate-Risk Prostate Cancer

Wednesday, Dec. 4 11:40AM - 11:50AM Room: S102CD

Hong Xiang, PhD, Lancaster, PA (*Presenter*) Nothing to Disclose Hsiao-Ming Lu, Boston, MA (*Abstract Co-Author*) Nothing to Disclose Jason Efstathiou, Boston, MA (*Abstract Co-Author*) Consultant, Blue Earth Diagnostics Ltd Consultant, TARIS BioMedical, Inc Consultant, Bayer AG Advisory Board, Merck KGaA Kishor Singapuri, MD, Lancaster, PA (*Abstract Co-Author*) Nothing to Disclose Sujatha Pai, MS, Houston, TX (*Abstract Co-Author*) Nothing to Disclose Kenneth R. Blank, MD, Glen Ridge, NJ (*Abstract Co-Author*) Nothing to Disclose

PURPOSE

Avoiding or minimizing acute and delayed rectal toxicities is a critical objective for safe dose-escalation in prostate SBRT. This retrospective study aims at examining if there is a dosimetric benefit in using perirectal hydrogel spacers for patients eligible for SBRT treatment per PACE Trial for low- and intermediate-risk prostate cancer.

METHOD AND MATERIALS

The study included 16 prostate cancer patients, 8 were planned with perirectal hydrogel spacer and the other 8 with no spacer. CT and T2-weighted MRI (when available) scans were used with SBRT plans optimized with the Volo Optimizer in a PrecisionTM TPS (2.0) utilizing MLC-based delivery on a CyberKnife M6 system. CTVs include prostate and 1.5-2.0 cm proximal seminal vesicles under the intermediate-risk prostate cancer scenario. PTV margins were 3-5 mm per PACE protocol with 36.25 Gy to PTVs and 40 Gy to prostate volumes and a mandatory rectum constraint V36 <= 1.0 cc. Comparisons are made for the volume overlaps between rectum and PTV, dose coverage to the prostate (V40) and PTV (V36.25), and absolute prostate sub-volumes receiving < 40 Gy. In addition, to examine if placing the spacer may lead to consistent rectal dose reduction, rectum DVH profiles are compared by requiring both V40 >= 95% for prostate and V36.25 >= 95% for PTV and no overriding priority for rectum V36 <= 1.0 cc.

RESULTS

In planning under the intermediate-risk case scenario, the mean rectum overlap with PTV was 2.0 cc (range 0.8 to 3.9 cc) in the no-spacer group, and 0.2 cc (range 0.0 to 0.4 cc) in the spacer group. The mean prostate V40 is 93.2% (range: 78.4% to 99.3%), the mean PTV V36.25 is 94.3% (range: 90.7% to 97.4%), and the mean prostate sub-volume receiving <40 Gy is 3.8 cc (range: 0.3 to 10.7 cc) in the no-spacer group; The mean prostate V40 is 98.9% (range: 96.6% to 100%), the PTV mean V36.25 is 97.5% (range: 94.9% to 99.9%) and the mean prostate sub-volume receiving <40 Gy is 0.8 cc (range: 0.0 to 2.3 cc) in the spacer group. By requiring both prostate V40 >= 95% and PTV V36.25 >= 95%, the mean rectum V36 is 1.5 cc (range: 0.2 to 2.8 cc), the mean V18.125, V29, V32.625 and V36.25 are 31.0%, 11.0%, 6.3% and 1.9% in the no-spacer group; and the mean rectum V36 is 0.5 cc (range: 0.0 to 1.0 cc), the mean DVHs values are 35.9%, 8.6%, 3.7% and 0.6% in the spacer group. Similar trends were observed for planning the low-risk prostate cancer scenario.

CONCLUSION

Significantly lower rectum overlaps with PTV are achieved by using perirectal hydrogel spacer. Preliminary results reveal a promising way to consistently lower the dose to the rectum while attaining higher specified dose coverage to the prostate volumes for low-and intermediate-risk prostate cancer.

CLINICAL RELEVANCE/APPLICATION

This study provides a first report on the dosimetric benefits of consistent rectal dose reduction while safely escalating dose to the clinical target volumes by using perirectal hydrogel spacer for prostate cancer patients eligible for SBRT under the international randomized PACE trial for treating low- and intermediate-risk prostate cancer.

SSK20-09 TraceIT: A Prospective Pilot Study Evaluating the Role of a Temporary Intravesical Fiducial Marker for Bladder Cancer Image-Guided Radiation Therapy

Wednesday, Dec. 4 11:50AM - 12:00PM Room: S102CD

Participants

Stephanie K. Schaub, MD, Seattle, WA (*Presenter*) Nothing to Disclose Stephen R. Bowen, PhD, Seattle, WA (*Abstract Co-Author*) Nothing to Disclose Jay J. Liao, MD, Seattle, WA (*Abstract Co-Author*) Nothing to Disclose Kenneth J. Russell, MD, Seattle, WA (*Abstract Co-Author*) Nothing to Disclose George R. Schade, MD, Seattle, WA (*Abstract Co-Author*) Nothing to Disclose James T. Kearns, MD, Seattle, WA (*Abstract Co-Author*) Nothing to Disclose John L. Gore, MD, 98195, WA (*Abstract Co-Author*) Nothing to Disclose Jonathan Wright, MD, Seattle, WA (*Abstract Co-Author*) Nothing to Disclose Jing Zeng, MD, Seattle, WA (*Abstract Co-Author*) Nothing to Disclose

For information about this presentation, contact:

skschaub@uw.edu

PURPOSE

Daily anatomic variability of the bladder and challenging visualization of the bladder tumor bed limits the ability to offer imageguided radiotherapy (RT) for patients with muscle-invasive bladder cancer (MIBC). We hypothesized that TraceIT, an injectable biocompatible hydrogel, could offer a safe and feasible temporary bladder wall fiducial marker to guide RT planning and daily image guidance on cone-beam CT (CBCT) in patients undergoing definitive RT.

METHOD AND MATERIALS

We enrolled 12 patients in an IRB-approved prospective observational cohort study from 2017-2018. Eligibility included MIBC planned to receive definitive RT or chemoRT over at least 4 weeks of daily treatment. TraceIT hydrogel was injected around the circumference of the tumor bed during pre-treatment and/or midcourse transurethral resection of the bladder tumor. The primary endpoint was fiducial marker localization to assess interfraction motion on daily CBCTs. Van Herk (VH) margin equation was used to determine the planning target volume margin optimized for the clinical target volume receiving at least 95%-prescription dose in 90% of patients. Toxicities were measured by CTCAE v4.

12 MIBC patients underwent RT to a median total dose of 64.4 Gy [37.5-66.6]. Median TraceIT volume was 0.5cc [0.3-0.75] per site for a total of 4 [4-6] sites per patient with a total volume of 2cc [2-3]. All patients demonstrated 100% visibility of TraceIT on the initial simulation CT-scan and day 1 CBCT. Average visualization of TraceIT after the initial and boost phase of RT was 91.5% [40-100] and 82.5% [0-100%], respectively. For the initial phase, alignment to fiducials over bone anatomy allowed for reduced VH margins (0.95cm vs 1.57cm). This was due to decreased total systematic error from 0.64cm (bone) to 0.23cm (fiducial) (p=0.005). For the boost phase, the VH margin was similar between fiducial and bone alignment (1.06cm vs 0.95cm). No grade >=1 toxicity was observed related to TraceIT.

CONCLUSION

TraceIT serves as a feasible intravesical fiducial that can aid in target delineation for RT planning and daily image-guidance, which may allow for increasingly conformal margins to reduce toxicity and improve tumor control via dose escalation.

CLINICAL RELEVANCE/APPLICATION

For bladder cancer radiotherapy, TraceIT is a feasible intravesical fiducial marker for tumor bed visualization and image-guidance, allowing for reduced margins with the goal of decreased toxicity.

Printed on: 10/29/20





SSK21

Vascular/Interventional (Peripheral Arterial Disease)

Wednesday, Dec. 4 10:30AM - 12:00PM Room: E260



AMA PRA Category 1 Credits ™: 1.50 ARRT Category A+ Credit: 1.75

FDA Discussions may include off-label uses.

Participants

Dimitrios Filippiadis, MD, PhD, Athens, Greece (*Moderator*) Nothing to Disclose Bora Peynircioglu, MD, Ankara, Turkey (*Moderator*) Nothing to Disclose Ava Star, MD, Olympia, WA (*Moderator*) Nothing to Disclose

Sub-Events

SSK21-01 Inguinal Lymphadenopathy as a Negative Prognostic Factor for Clinical Success after Technically Successful Endovascular Treatment in Patients with Critical Limb Ischemia

Wednesday, Dec. 4 10:30AM - 10:40AM Room: E260

Participants

Daniel Raskin, Ramat - Gan, Israel (*Presenter*) Research Consultant, AIDOC Boris Khaitovich, Ramat Gan, Israel (*Abstract Co-Author*) Nothing to Disclose Shmuel Balan, Ramat Gan, Israel (*Abstract Co-Author*) Nothing to Disclose Daniel Silverberg, MD, Ramat Gan, Israel (*Abstract Co-Author*) Nothing to Disclose Moshe Halak, Ramat Gan, Israel (*Abstract Co-Author*) Nothing to Disclose Uri Rimon, MD, Tel-Hashomer, Israel (*Abstract Co-Author*) Nothing to Disclose

PURPOSE

To assess the correlation between inguinal lymph node characteristic and ipsilateral primary amputation rates in patients with ischemic foot ulcers who had a technically successful endovascular treatment.

METHOD AND MATERIALS

A retrospective review of patients who were endovascularly treated for ischemic foot ulcers between January 2015 and May 2017 was performed. Two hundred and two limbs in 202 patients (135 male, 67 female; median age 72.8; range, 42.2-93.7 y) were technically successfully treated. Technical success was defined as occluded artery recanalization with residual stenosis < 30%, and ABI improvement by at > 0.2 after 24 hours. Unilateral lymph node size, contrast enhancement, necrosis and perinodular fat infiltration were assessed on a preprocedural computer tomography angiography (CTA). Primary end points were amputation and sepsis within six months. Independent-samples t-tests and chi-square test of independence were conducted to examine relation between lymph node characteristics and amputation or septic shock.

RESULTS

Forty-two (20.8%) patients had undergone amputation. Sepsis occurred in 6 out of 202 patients (3%). There was a significant difference in the scores of lymph node sizes between amputated and non-amputated limbs (p = 0.000). Relations between lymph node characteristics and amputation was significant (p < 0.001). Patients with perinodular fat infiltration or increased node size were 5.940 and 1.109 times (respectively) more likely to undergo limb amputation than those without. The relation between lymph node characteristics and septic shock was significant (p < 0.05).

CONCLUSION

Unilateral lymph node size and characteristics are associated with limb amputation in technically successful endovascular treatment of patients with ischemic foot ulcers. Moreover, increased lymph node size and perinodular fat infiltration predicted limb amputation.

CLINICAL RELEVANCE/APPLICATION

Lymph node size and characteristics are associated with limb amputation in critical ischemia patients who were successfully treated endovascularly.

SSK21-02 Exosomes from Endothelial Progenitor Cells Facilitate Vascular Endothelial Cell Repair through Transferring miR-21-5p to Suppress THBS1 Expression

Wednesday, Dec. 4 10:40AM - 10:50AM Room: E260

Participants

Jungong Zhao, MD, Shanghai, China (*Abstract Co-Author*) Nothing to Disclose Hui Hu, Shanghai, China (*Presenter*) Nothing to Disclose Xiaohong Liu, Shanghai, China (*Abstract Co-Author*) Nothing to Disclose

For information about this presentation, contact:

zhaojungong@sjtu.edu.cnjshuhui2003@163.com

PURPOSE

we sought to investigate the mechanisms of exosomes released from endothelial progenitor cell(EPC) mediated endothelial cell (EC) repair by studying their miRNA content and uptake

METHOD AND MATERIALS

The efficacy of EPC derived exosome-mediated reendothelialization was examined by histological examinations and Evans blue dye in the balloon-induced carotid artery endothelial injury model of rats in vivo. The effects of EPC-exosomes on human vascular endothelial cells (HUVECs) were also studied by the evaluation of growth rates, migratory ability and tube-formation activity. To dissect the underlying mechanisms, RNA-sequencing assays were performed to determine miRNA abundancy in exosomes and mRNA profiling in exosome-treated HUVEC. Meanwhile, by using specific miRNA inhibitors or siRNAs, the roles of the candidate miRNA and its target genes in exosomes induced regulation of function of HUVEC were assessed.

RESULTS

Administration of EPC-derived exosomes accelerated the reendothelialization in the early phase after endothelial damage in the rat carotid artery. The uptake of exogenous EPC-exosomes intensified HUVEC cells in the proliferation rate, migratory and tube-forming ability. Integrative analyses of miRNA-mRNA profiles and the following functional studies revealed that miR-21-5p was highly enriched in EPC-exosomes, which specifically suppressed THBS1 expression in the recipient vascular endothelial cells and contributed to the pro-angiogenic activities of EPC derived exosome.

CONCLUSION

Our study indictated that EPC-exosome delivered miR-21-5p into vascular endothelial cells to inhibit the expression of THBS1, and therefore promoted endothelial cell repair.

CLINICAL RELEVANCE/APPLICATION

EPC derived exosome mediated reendothelialization after vascular injury

SSK21-03 Impact of Calcification Modeling and Planning Circles with Fusion Imaging for the Chronical Total Occlusion of Iliac and Femoral Arteries

Wednesday, Dec. 4 10:50AM - 11:00AM Room: E260

Participants Nicolas Louis, Nimes , France (*Presenter*) Research Consultant

For information about this presentation, contact:

drlouisnicolas@yahoo.fr

PURPOSE

To examine the contribution of calcification modeling and planning circles with fusion imaging for the chronical total occlusion (CTOs) of iliac and femoro-popliteal arteries.

METHOD AND MATERIALS

We analyzed a cohort of 180 patients who were treated by endovascular means for iliac and femoro-popliteal arteries CTOs during a period of 3 years. The procedures were performed in a hybrid room equipped with the IGS 530 system (GE Healthcare). The preoperative imaging fusion was edited on the dedicated workstation Advantage Windows 4.7 with vessel ASSIST. A centerline was manually adjusted inside the occluded artery. The planning circles were strategically positioned inside the calcifications edited by the centerline. The Workstation allows to combined in the the same volume the modeling of all the calcifications and the planning circles. The fusion technic was a fusion between 3D volume extracted from preoperative CT and 2D live fluoroscopy with bone registration. An arteriography was systematically achieved allowing to adjust if necessary the vascular ans calcifications volumes.

RESULTS

46 Iliac CTOs (mean length occlusion= 61.6 mm), and 84 femoro-popliteal CTOs (80.2 mm) were performed. The success of the recanalisation reach 94% (n=122/130). In 51.5% (n=67/130) the recanalisation have been directly in transluminal inside the planning circles. In 35.3% (n=46/130) the recanalization have been subintimal and have been redirected in transluminal between two circles. In 6.9% (n=9/130) the subintimal recanalisation can't be redirected transluminal and an IVUS-guided re-entry catheter have been used.

CONCLUSION

The CTOs under fusion imaging with calcification modeling and planning circles is a reliable and reproductible technic. It allows to redirect easily between two circles inside the calcification. It might have an economic impact by reducing the use of re-entry device, and might have an impact on the radiation exposure.

CLINICAL RELEVANCE/APPLICATION

This new technic allows to navigate step by step in an occluded artery by knowing constantly when the guide wire is positioning compared to the calcifications and the good lumen.

SSK21-04 Long-Term Outcome of Percutaneous Coronary Intervention in Prediabetes and Normoglycaemia Patients: A Systematic Review and Meta-Analysis

Wednesday, Dec. 4 11:00AM - 11:10AM Room: E260

Participants Rui Shi, Chengdu, China (*Presenter*) Nothing to Disclose Zhigang Yang, MD, Chengdu, China (*Abstract Co-Author*) Nothing to Disclose Kaiyue Diao, Chengdu, China (*Abstract Co-Author*) Nothing to Disclose Yue Gao, Chengdu, China (*Abstract Co-Author*) Nothing to Disclose

For information about this presentation, contact:

1184494754@qq.com

PURPOSE

Prediabetes, an abnormal glucose metabolism before onset diabetes, was proven to be risk factor for coronary artery disease (CAD) in previous studies. However, whether prediabete would impact the long-term prognosis for CAD patients after percutaneous coronary intervention (PCI) remains controversial. Thus, the purpose of this study was to summarize the previous studies and to demonstrate the difference of long term prognosis between CAD patients with and without prediabetes after PCI.

METHOD AND MATERIALS

Pubmed and EMBASE were systematically searched, supplemented with manual searches of the included reference lists. Studies reporting long-term (>/=1 year) cardiovascular outcomes including all-cause mortality, myocardial infarction (MI), revascularization and other mentioned major adverse cardiac events (MACE) in prediabetes patients were included. Odds ratio (OR) with 95% confidence interval (CI) was used to express the pooled effect on discontinuous variables and the pooled analyses were performed with Stata 15.1.

RESULTS

Nine cohort studies were finally included in this meta-analysis consisting of a total of 10266 patients (3112 prediabetes, 3783 diabetes and 5171 normoglycaemia). In CAD patients treated with PCI, prediabetes individuals were found to have significantly higher long-term mortality and more MACE than normoglycaemia patients (odds ratio (OR):1.85;95% confidence interval (CI): 1.25-2.74; P=0.002; $I^2 = 36.6\%$), (OR:1.43; 95% CI:1.05-1.94;P=0.022; $I^2=69.3\%$) respectively. No statistical difference was found on MI and revascularization between the two groups (MI: OR:1.06;95% CI:0.86-1.31; P=0.561; $I^2=0\%$) and (revascularization: OR:1.20; 95% CI: 0.88-1.63; P=0.242; $I^2=31\%$) respectively.

CONCLUSION

The present meta-analysis suggests that following PCI, long-term rates of death and MACE were significantly higher in prediabetes. However, there were no difference on MI and repeat revascularization between prediabetes and normoglycaemia patients.

CLINICAL RELEVANCE/APPLICATION

The present meta-analysis provide evidence that health care practitioners should put emphasize on screening and management of abnormal glucose metabolism before and after PCI to combat adverse cardiovascular outcomes.

SSK21-05 Micro-Channel Recanalization with Orbital Atherectomy as a Viable Method to Failed Standard Recanalization of TASC-II D Aorto-Iliac Occlusive Disease

Wednesday, Dec. 4 11:10AM - 11:20AM Room: E260

Participants

Roger T. Tomihama, MD, Loma Linda, CA (*Presenter*) Nothing to Disclose Yuki Miura, MD, Loma Linda, CA (*Abstract Co-Author*) Nothing to Disclose Ahmed Abou-Zamzam, MD, Loma Linda, CA (*Abstract Co-Author*) Nothing to Disclose Sharon C. Kiang, MD, Loma Linda, CA (*Abstract Co-Author*) Nothing to Disclose

PURPOSE

Endovascular treatment of TASC II D aorto-iliac lesions now an accepted form of revascularization. We sought to demonstrate that native micro-channel recanalization and orbital atherectomy is a successful recanalization method of TASC II D aorto-iliac lesions refractory to standard recanalization techniques.

METHOD AND MATERIALS

Four consecutive patients from 2016-2018 with symptomatic TASC-II D Aorto-Iliac Occlusive Disease (AIOD) prohibitive for open bypass and failed traditional prodding guidewire or device recanalization technique were identified and underwent advanced native micro-channel selection and subsequent orbital atherectomy. Native micro-channels were probed and traversed with a 0.014 wire. Orbital atherectomy is initiated with the 1.25 crown and continued until the micro-channel is sufficiently large to track a microcatheter. Lesion characteristics, survival, limb salvage, patency, and change in clinical symptoms were analyzed.

RESULTS

Four patients underwent successful native micro-channel recanalization and orbital atherectomy of the CIA. There were no intraoperative ruptures or dissections. Three patients presented with rest pain and 1 with CLTI. Average age was 68, average Rutherford class was 3 and 2 of the patients smoked. All 4 patients presented with unilateral CIA occlusion with contralateral CIA stenosis. Average occlusion lesion length of the R CIA was 5.8 cm and of the L CIA was 6.2 cm. Kissing stent technique was used in all patients for reconstruction of the aortic bifurcation. Two of the patients had outflow lesions (SFA stenosis or occlusion) but had patent profunda arteries. At 30 days, all patients had improvement in pain and primary patency of 100%. Long-term follow up at 21.6 months noted continued improvement in symptoms and primary patency of 75%. The fourth patient died at 4 mo from lung cancer with occluded iliac stents by imaging at that time.

CONCLUSION

Native micro-channel recanalization with subsequent orbital atherectomy is an option in high-risk patients with TASC II D aorto-iliac disease whom have failed traditional prodding recanalization. Further work in proper patient selection and safe utilization of atherectomy devices in the CIA is needed.

CLINICAL RELEVANCE/APPLICATION

Native micro-channel recanalization with subsequent orbital atherectomy is an option in high-risk patients with TASC II D aorto-iliac disease whom have failed traditional prodding recanalization.

SSK21-06 Evaluation of Collateral Circulations for Therapeutic Effects in Chronic Leriche's Syndrome: A Preliminary Case-Control Study between Bypass Grafting and Intraluminal Stent Implantation

Wednesday, Dec. 4 11:20AM - 11:30AM Room: E260

Participants Yang Peng, Guangzhou, China (*Presenter*) Nothing to Disclose Qiuxia Xie, Shenzhen, China (*Abstract Co-Author*) Nothing to Disclose Fan Zhang, Guangzhou, China (*Abstract Co-Author*) Nothing to Disclose Jian Guan, MD, Guangzhou, China (*Abstract Co-Author*) Nothing to Disclose

For information about this presentation, contact:

usefulkey0077@hotmail.com

PURPOSE

To investigate the changes in collateral arteries after bypass grafting or intraluminal stent implantation in chronic Leriche's syndrome, and to compare effects of the two operations.

METHOD AND MATERIALS

From January 2015 to December 2018, there were 26 patients diagnosed as chronic Leriche's syndrome. They were treated with bypass grafting (n=14, group A) or intraluminal stent implantation (n=12, group B). All the patients received aorta and common iliac CT angiography before and one month after the operations. CT angiography findings and clinical records were reviewed retrospectively. Sectional areas of the occlusive aorta before operation (a0), the systemic collateral pathways before (a1) and after (a2) operation, and the recanalization pathway (the grafts or the stent lumen) (ar) were manually measured at aortic bifurcation level by two experienced radiologists, and the mean values were admitted. The compensation rate before (C1) and after (C2) operation as well as the reduction rate of the systemic collateral pathways after operation (R) were defined as follow: C1=a1/a0; C2=(a2+ar)/a0; R=(a1-a2)/a1. The values of C1, C2 and R of both groups were calculated respectively, and independent sample *T*-test was performed.

RESULTS

C1 of bypass grafting group and intraluminal stent implantation group were $30.67\%\pm16.77\%$ and $31.35\%\pm23.70\%$ respectively, and there was no significant difference (*P*=0.933). C2 of bypass grafting group were significantly higher than those of intraluminal stent implantation group ($98.83\%\pm26.01\%$ vs. $44.44\%\pm7.62\%$, *P*<0.001), while R of both groups had no significant difference ($81.98\%\pm7.12\%$ vs. $85.81\%\pm5.95\%$, *P*=0.154).

CONCLUSION

According to the changes in collateral arteries after operation, intraluminal stent implantation was non-inferior to bypass grafting for patients with chronic Leriche's syndrome, although the recanalization pathway seemed much smaller.

CLINICAL RELEVANCE/APPLICATION

The changes in collateral circulation can reflect short-term effects of operation. And Intraluminal stent implantation could be the favorable treatment for patients with high risk of operation.

SSK21-07 To Evaluate the Role of FDG PET/CT in Assessing Disease Activity in Large Vessel Vasculitis

Wednesday, Dec. 4 11:30AM - 11:40AM Room: E260

Participants Sikandar M. Shaikh, DMRD, Hyderabad, India (*Presenter*) Nothing to Disclose

For information about this presentation, contact:

idrsikandar@gmail.com

PURPOSE

To evaluate the role of FDG PET-CT in the assessment of disease activity in large vessel vasculitis (LVV).

METHOD AND MATERIALS

54 PET/CT scans were performed in 19 pts with suspected and diagnosed LVV (giant cell arteritis, Takayasu arteritis or idiopatic aortitis). The amount of vascular uptake was graded using a 4-point scale (0=no uptake, 1=less than liver, 2=similar to liver, 3=higher than liver). Grade 0-1 was negative, 2 was moderately positive and 3 was markedly positive. This PET/CT was correlated with clinical indices of ITAS (Indian Takayasu Activity Score) and Kerr/National Institute of Health (Kerr/NIH), serum acute-phase reactants (ESR, C-reactive protein [CRP]) levels as well as interleukin-6 (IL-6) and the soluble IL-6 receptor (sIL-6R).

RESULTS

43% of 54 PET-CT were negative, 31% were moderately positive, and 26% were markedly positive. A significant correlation between the SUV uptake and both ESR and CRP levels was found and correlated. Significantly higher ESR values were observed in pts with markedly positive PET/CT (49.4 + 36.5 mm/1st h) compared with moderately positive (27 + 21 mm/1st h, p = 0.0001) and inactive scans (22.7 + 15.9 mm/1st h, p=0.0001). CRP levels were 0.8+1.0 mg/dL in pts with inactive scans, 1.3 + 2.2 mg/dL in pts with moderately positive (p=0.001) and 3.0 + 3.6 in patients with markedly positive scans (p = 0.0001). Higher levels of IL-6 resulted in patients with markedly positive scans (10.0 + 8.9 gg/ml) compared to those with inactive scans (8.1+18.5 gg/ml, p=0.013). We found no association between sIL-6R levels and vascular FDG uptake. There was a significant association between vascular FDG uptake and both ITAS and Kerr/NIH scores

CONCLUSION

The above findings of PET/CT is a very useful tool for evaluating disease activity in patients with LVV.

CLINICAL RELEVANCE/APPLICATION

The relevance of FDG PET-CT in evaluation of Large vessel vasculitis is having importnat and significant role.

SSK21-08 Spectral CT Imaging for the Assessment of Non-Calcified Plaque Compositions in Lower Extremity Atherosclerosis

Wednesday, Dec. 4 11:40AM - 11:50AM Room: E260

Participants

Tingting Qu, Xian, China (*Presenter*) Nothing to Disclose Jianxin Guo, Xian, China (*Abstract Co-Author*) Nothing to Disclose Jianying Li, Beijing, China (*Abstract Co-Author*) Employee, General Electric Company Ningning Ding, Xian, China (*Abstract Co-Author*) Nothing to Disclose Yun Shen, PhD, Beijing, China (*Abstract Co-Author*) Employee, General Electric Company Researcher, General Electric Company Jian Yang, Xian, China (*Abstract Co-Author*) Nothing to Disclose

PURPOSE

To assess the composition of non-calcified plaques in patients with lower extremity atherosclerosis using spectral CT imaging.

METHOD AND MATERIALS

Thirty-four patients with lower extremity atherosclerosis underwent CT angiography (CTA) with the dual-energy spectral imaging mode. Monochromatic images were reconstructed to measure CT values at 74keV and to generate spectral curve for calculating the slope: [(CT(40keV)-CT(110keV))/70] and the effective-Z for plaques; Material decomposition (MD) images of iodine-based and lipid-based were generated to measure the iodine and lipid density, respectively. Measurements for different plaque types were statistically compared.

RESULTS

A total of 116 non-calcified plaques were found in 34 patients, including 87 fibrous plaques, 21 plaques with intra-plaque hemorrhage and 8 plaques with lipid components with slopes of the spectral curve of 1.05 ± 0.54 , 0.36 ± 0.26 , and -0.20 ± 0.20 , and the effective-Z values of 8.21 ± 0.30 , 7.80 ± 0.18 and 7.40 ± 0.15 , respectively. The iodine contents (in 100ug/ml) were 9.99 ± 5.13 , 3.42 ± 2.60 , and -1.97 ± 1.95 , and lipid contents (in 1mg/ml) were -755.12 ± 387.89 , -258.05 ± 195.75 , and 148.95 ± 148.14 , respectively for the fibrous plaque, intra-plaque hemorrhage and lipid plaque. There were statistical differences in all measurements between any two types of plaques (all p<0.001). CT values at 74keV was $54.54\pm14.16HU$, $23.35\pm13.80HU$ and $28.88\pm11.69HU$ for these three groups. There was significant difference between fibrous plaque and the other two contents (p<0.001), but no significant difference between the intra-plaque hemorrhage and lipid plaque (p=0.652).

CONCLUSION

Fibrous plaque, plaque with intra-plaque hemorrhage and lipid components in non-calcified plaque have distinctive spectral imaging characteristics. The parameters of dual-energy spectral CT imaging can provide quantification information for the differentiation of fibrous, lipid and hemorrhage plaques.

CLINICAL RELEVANCE/APPLICATION

The use of imaging methods to distinguish stable plaques and unstable plaques can provide guidance for the selection of clinical pathways.

SSK21-09 Improving Diagnostic Accuracy for Inferior Genicular Arteries in Lower Extremity with Dual-Energy Spectral CT Imaging

Wednesday, Dec. 4 11:50AM - 12:00PM Room: E260

Participants

Xianghui Zhang, Xian, China (*Presenter*) Nothing to Disclose Jia Xiaoqian, Xian, China (*Abstract Co-Author*) Nothing to Disclose Jianying Li, Beijing, China (*Abstract Co-Author*) Employee, General Electric Company Jingtao Sun, Xian, China (*Abstract Co-Author*) Nothing to Disclose Shumeng Zhu, Xian, China (*Abstract Co-Author*) Nothing to Disclose Qian Tian, Xian, China (*Abstract Co-Author*) Nothing to Disclose Yue Yao, Xian, China (*Abstract Co-Author*) Nothing to Disclose Yun Shen, PhD, Beijing, China (*Abstract Co-Author*) Employee, General Electric Company Researcher, General Electric Company Jianxin Guo, Xian, China (*Abstract Co-Author*) Nothing to Disclose Jian Yang, Xian, China (*Abstract Co-Author*) Nothing to Disclose

PURPOSE

Investigate the clinical value of improving diagnostic accuracy for inferior genicular arteries in the lower extremity with low energy images in spectral CT imaging.

METHOD AND MATERIALS

110 (mean age 67±10 years) and 72 (mean age, 65±13 years) patients underwent CT angiography (CTA) in the lower extremities using spectral and conventional (at 120kVp) imaging mode, retrospectively with similar radiation dose and contrast dose. The 50keV monochromatic images were reconstructed in the spectral CT group. CT value and standard deviation of vessels and psoas major muscle was measured to calculate to the signal-to-noise ratio (SNR) and contrast-to-noise ratio (CNR) for vessels. Two independent observers assessed the subjective image quality of the lower extremities using a 4-point scale. The quantitative and qualitative image quality of the two groups were compared and the diagnostic accuracy for the degree of occlusion of the vessels (Each patient received one time DSA for 11 vessels) were also compared using DSA as the gold standard. Chi-square test, independent sample T test and Mann-Whitney test was used for counting data, quantitative measurement data and subjective image quality score, respectively.

The use of 50keV images in the spectral CT significantly increased the CT values in the abdominal iliac, femoral popliteal and lower knee segments (618.52 ± 100.78 vs. 371.10 ± 98.36 on average, p<0.001) and provided higher SNR (50.48 ± 12.47 vs. 45.97 ± 12.90 , P=0.014) and higher CNR (44.08 ± 11.45 vs. 38.86 ± 12.35 , P<0.01) compared with the conventional images. Mann-Whitney test showed that the subjective image quality of femoral popliteal in the spectral CT group was higher than in the conventional group (P=0.01), while there was no difference in the abdominal iliac segment (P=0.10) and lower knee segment (P=0.07). The spectral CT images also significantly improved the diagnostic accuracy for the vessels in the lower knee segment (92.05% vs. 84.03%, P<0.01).

CONCLUSION

The use of 50keV spectral CT images enhances the contrast in the lower extremity arteries and improves the diagnostic accuracy for the vessels in the lower knee segment, compared with the conventional CTA protocols.

CLINICAL RELEVANCE/APPLICATION

Low-energy images in spectral CT can improve the diagnostic accuracy of the lower knee arteries while achieving higher SNR and CNR.







ASRT@RSNA 2019: Mass Casualty Radiology 2019-From Traditional to Advanced Imaging

Wednesday, Dec. 4 10:40AM - 11:40AM Room: N230B

СТ

AMA PRA Category 1 Credit ™: 1.00 ARRT Category A+ Credit: 1.00

Participants

Barry D. Daly, MD, Baltimore, MD (Presenter) Nothing to Disclose

For information about this presentation, contact:

bdaly@umm.edu

LEARNING OBJECTIVES

1) To describe the role of radiology services in the management of mass casualty events. 2) To review the technological advances in high resolution 3D whole body CT imaging leading to the recent development of postmortem CT (PMCT) as a noninvasive 'Virtual Autopsy' tool. 3) To address the potential development of infrastructure and logistics that would allow PMCT to become a valuable tool in mass casualty situations.

ABSTRACT

Conventional and dental radiography are long established techniques with a valuable role in mass casualty and disaster management today. A more recent addition to forensic operations is the development of high resolution 3D whole body CT imaging that has led to the introduction of postmortem CT (PMCT) or "Virtual Autopsy" as a noninvasive tool in the investigation of death. The role of PMCT has become well-established over the last 20 years for the non-invasive investigation of many different causes of death including blunt force and projectile or blast injuries, burns, and drowning. It also has a role in deaths of undetermined cause and for evaluation of decomposed or unidentified bodies. In some cases PMCT may replace or curtail the extent of autopsy procedures, of great importance in mass casualty situations.







RCA43

Hands-on Introduction to Social Media: Advanced (Hands-on)

Wednesday, Dec. 4 12:30PM - 2:00PM Room: S401AB

IN

AMA PRA Category 1 Credits ™: 1.50 ARRT Category A+ Credit: 1.75

Participants

Amy K. Patel, MD, Liberty, MO (*Moderator*) Nothing to Disclose Amy K. Patel, MD, Liberty, MO (*Presenter*) Nothing to Disclose Courtney M. Tomblinson, MD, Nashville, TN (*Presenter*) Nothing to Disclose Darel E. Heitkamp, MD, Windermere, FL (*Presenter*) Nothing to Disclose Ryan B. Peterson, MD, Norcross, GA (*Presenter*) Nothing to Disclose

For information about this presentation, contact:

darelheitkamp@gmail.com

amykpatel64112@gmail.com

ryan.peterson@emory.edu

LEARNING OBJECTIVES

1) Develop image-rich, high yield radiology educational and promotional content. 2) Recognize important patient privacy considerations regarding use of medical images on Social Media. 3) Devise a social media strategy which best suits digital medium objectives. 4) Learn how to participate in a live tweet chat during the session.





RCC43

Regulatory Considerations for Hospital-based 3D Printing

Wednesday, Dec. 4 12:30PM - 2:00PM Room: E353B

IN

AMA PRA Category 1 Credits ™: 1.50 ARRT Category A+ Credit: 1.75

Participants

Andy Christensen, BS, Littleton, CO (*Moderator*) Consultant, Integrum AB; Board Member, Integrum AB; Stockholder, Somaden LLC Jane S. Matsumoto, MD, Rochester, MN (*Moderator*) Nothing to Disclose

Sub-Events

RCC43A Regulatory Considerations for Hospital-based 3D Printing

Participants

Andy Christensen, BS, Littleton, CO (Presenter) Consultant, Integrum AB; Board Member, Integrum AB; Stockholder, Somaden LLC

LEARNING OBJECTIVES

1) Understand the FDA's regulations for medical devices. 2) Review the types of products that the FDA regulates which are related to medical 3D printing. 3) Understand how to apply knowledge of the regulatory landscape for in-house, point of care 3D printing.

RCC43B FDA Current Practices and Regulations-3D Printed Patient-Specific Anatomic Models

Participants

Nooshin Kiarashi, PhD, Silver Spring, MD (Presenter) Nothing to Disclose

RCC43C Best Practices in Quality Control

Participants

Jane S. Matsumoto, MD, Rochester, MN (Presenter) Nothing to Disclose

RCC43D Manufacturing Quality Control for 3D Printing

Participants

Jayanthi Parthasarathy, BDS, PhD, Columbus, OH (Presenter) Nothing to Disclose

For information about this presentation, contact:

Jayanthi.Parthasarathy@Nationwidechildrens.org

LEARNING OBJECTIVES

1) Understand the need for quality control and quality assurance program in 3D printing of patient specific non implantable devices. 2) Understand concept of failure Model Effect Analysis (FMEA) as applied in 3D printing in a clinical setting. 3) Learn the process of setting up a quality assurance program in a clinical setting.

RCC43E Sterilization of 3D Printed Parts

Participants

William J. Weadock, MD, Ann Arbor, MI (Presenter) Owner, Weadock Software, LLC





MSRT44

ASRT@RSNA 2019: It's Complicated-Imaging and Diversity in Healthcare (Interactive Session)

Wednesday, Dec. 4 1:00PM - 2:00PM Room: N230B

ОТ

AMA PRA Category 1 Credit ™: 1.00 ARRT Category A+ Credit: 1.00

Participants

Timothy J. Blackburn, PhD, Dallas, TX (Presenter) Nothing to Disclose

For information about this presentation, contact:

timothy.blackbun@utsouthwestern.edu

LEARNING OBJECTIVES

1) Evaluate automated and manual technique considerations to improve image quality and dose optimization. 2) Differentiate sex, gender, gender identity and gender expression. 3) Describe the proper use of pronouns when working with gender and sexual minorities. 4) Identify communication barriers and health information qualifiers for improved healthcare outcomes in radiology.

ABSTRACT

Medical imaging continues to face ongoing challenges as the technologist is presented with an ever increasing diverse patient population. This presentation will review imaging fundamentals and techniques as they apply to radiography, fluoroscopy, mammography, and CT. Diversity in patient populations with respect to imaging technique span age, size, and composition (anatomy, physiology and pathology). Considerations will to be taken into account regarding patients with physical and mental disabilities. Information on gender and sexual minorities (GSM) will be presented to aid the technologist with imaging and communication awareness.

Active Handout: Timothy J. Blackburn

http://abstract.rsna.org/uploads/2019/19001233/Active MSRT44.pdf

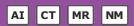




SPAI42

RSNA AI Deep Learning Lab: Generative Adversarial Networks (GANs)

Wednesday, Dec. 4 1:00PM - 2:30PM Room: AI Showcase, North Building, Level 2, Booth 10342



AMA PRA Category 1 Credits ™: 1.50 ARRT Category A+ Credit: 1.75

Participants

Bradley J. Erickson, MD, PhD, Rochester, MN (*Presenter*) Board of Directors, VoiceIt Technologies, LLC; Stockholder, VoiceIt Technologies, LLC; Board of Directors, FlowSigma, LLC; Officer, FlowSigma, LLC; Stockholder, FlowSigma, LLC

Special Information

In order to get the best experience for this session, it is highly recommended that attendees bring a laptop with a keyboard, a decent-sized screen, and the latest version of Google Chrome. Additionally, it is recommended that attendees have a basic knowledge of deep learning programming and some experience running a Google CoLab notebook. Having a Gmail account is also helpful. Here are instructions for creating and deleting a Gmail account.

ABSTRACT

This course describes a more recent advance in deep learning known as Generative Adversarial Networks (GANs). GANs are a deep learning technology in which a computer is trained to create images that look very 'real' even though they are completely synthetic. Getting 'large enough' data sets is a problem for most deep learning applications, and this is particularly true in medical imaging. This may be one way to address the 'data shortage' problem in medicine. GANs have also been created that can convert MRIs to CTs (e.g. for attenuation correction with MR/PET).

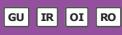




VSIO41

Interventional Oncology Series: Renal Ablation/Embolization

Wednesday, Dec. 4 1:00PM - 3:00PM Room: S405AB



AMA PRA Category 1 Credits ™: 2.00 ARRT Category A+ Credits: 2.25

FDA Discussions may include off-label uses.

Participants

Stephen J. Hunt, MD,PhD, Philadelphia, PA (*Moderator*) Consultant, Amgen Inc; Research Consultant, BTG International Ltd; Speakers Bureau, Galil Medical Ltd; Research Grant, BTG International Ltd; Research Grant, Geurbet SA Debra A. Gervais, MD, Boston, MA (*Moderator*) Nothing to Disclose

For information about this presentation, contact:

stephen.hunt@uphs.upenn.edu

LEARNING OBJECTIVES

1) Provide an overview of the current interventional oncology therapies utilized in the management of primary and metastic renal malignancies, their mechanisms of action, their indications for use, their published outcomes, and their modality specific complications. 2) Be able to provide examples of future interventional oncology therapies for renal malignancy currently in development.

ABSTRACT

This course provides an overview of interventional oncology techniques for the management of primary and metastatic renal malignancies. Treatment modalities that will be discussed include radiofrequency ablation, microwave ablation, cryoablation, embolization, and combined modalities. After participating in this course, participants will be able to provide an overview of the current interventional oncology therapies utilized in the management of primary and metastic renal malignancies, their mechanisms of action, their indications for use, their published outcomes, and their modality specific complications. Participants will also be able to provide examples of furture interventional oncology therapies for renal malignancy currently in development.

Sub-Events

VSI041-01 Historical Overview of Renal Ablation

Wednesday, Dec. 4 1:00PM - 1:15PM Room: S405AB

Participants

Susan Shamimi-Noori, MD, Philadelphia, PA (Presenter) Consultant, Sirtex Medical Ltd; Consultant, Boston Scientific Corporation

For information about this presentation, contact:

susan.shamimi-noori@pennmedicine.upenn.edu

LEARNING OBJECTIVES

1) To understand how ablation technology has evolved, particularly in relation to treatment of renal lesions.

VSI041-02 RF Ablation of Renal Masses

Wednesday, Dec. 4 1:15PM - 1:30PM Room: S405AB

Participants

Stephen J. Hunt, MD, PhD, Philadelphia, PA (*Presenter*) Consultant, Amgen Inc; Research Consultant, BTG International Ltd; Speakers Bureau, Galil Medical Ltd; Research Grant, BTG International Ltd; Research Grant, Geurbet SA

LEARNING OBJECTIVES

1) To understand the basic mechanism of radiofrequency ablation. 2) To identify the advantages and disadvantages of RF ablation in the kidney compared with other modalities. 3) To know when to use RF for treatment of RCC and how to perform the procedure safely.

VSI041-03 MWA of Renal Masses

Wednesday, Dec. 4 1:30PM - 1:45PM Room: S405AB

Participants

John J. Schmitz, MD, Rochester, MN (Presenter) Nothing to Disclose

LEARNING OBJECTIVES

1) Be able to articulate the basic principles behind microwave ablation. 2) Be able to identify strengths and potential shortcomings of microwave ablation in the kidney. 3) Understand how microwave ablation of renal masses fits into the larger picture of treatment

options available.

VSIO41-04 Safety and Oncologic Efficacy of Cryoablation in Small Renal Masses (SRMs) Using an Innovative Liquid Nitrogen-Based Device

Wednesday, Dec. 4 1:45PM - 1:55PM Room: S405AB

Participants

Tamar Gaspar, MD, Haifa, Israel (*Abstract Co-Author*) Nothing to Disclose Ilya Volovik, MD, Haifa, Israel (*Presenter*) Nothing to Disclose Simona Croitoru, Haifa, Israel (*Abstract Co-Author*) Nothing to Disclose Karina Dorfman, MD, Haifa, Israel (*Abstract Co-Author*) Nothing to Disclose Yair Halpern, MD, Haifa, Israel (*Abstract Co-Author*) Nothing to Disclose Sagi Shprits, MD, Haifa, Israel (*Abstract Co-Author*) Nothing to Disclose Ofir Avitan, MD, Haifa, Israel (*Abstract Co-Author*) Nothing to Disclose Zaher Bahouth, MD, Haifa, Israel (*Abstract Co-Author*) Nothing to Disclose Robert Sachner, MD, Haifa, Israel (*Abstract Co-Author*) Nothing to Disclose

PURPOSE

We assessed safety, efficacy, and oncologic outcomes of the new innovative Liquid Nitrogen device in patients with early-stage (T1a) SRMs.

METHOD AND MATERIALS

74 patients (mean age: 69y; 68% males) with 78 lesions (mean: 2.35 cm) smaller than 4 cm, were included; Mean R.E.N.A.L score was 6.53; 16% were endophytic. Percutaneous cryoablation using ProSense™ (10G/13G; IceCure Medical Ltd, Caesarea, Israel) was performed in all patients under CT guidance with sedation/light general anesthesia. It's extremely low temperatures (-1960C) produces larger lethal zone per needle. All procedures were done in two cycles of freezing with intervening passive thaw. Patients underwent imaging and clinical surveillance every 3 months during first year and annually thereafter. Oncologic success was indicated by a reduction in lesion size and lack of enhancement on follow-up CT or MRI. Safety was determined by monitoring Creatinine (Cr) and Hemoglobin (Hb) levels.

RESULTS

Ablation was oncologically successful in all 78 lesions. Average freezing cycles was 22 minutes. Average procedure time was 50.5 min. 45 lesions were followed in 42 patients for more than 12 months (mean: 18.2 m). 3 treatment failures occurred (6.6%): of them, one is a candidate for repeat procedure. One serious event was noted; a late-onset ipsilateral hydronephrosis in a patient treated for a complex medial lower pole lesion (1.2%). Mean Cr and Hb levels remained unchanged in all patients.

CONCLUSION

Cryoablation of SRMs with an innovative Liquid Nitrogen cryogenic device is feasible and safe procedure, with similar oncologic results as nephron spearing surgery and with low rate of serious adverse events.

CLINICAL RELEVANCE/APPLICATION

Cryoablation of SRMs with a new Nitrogen cryogenic device is feasible and safe procedure with low rate of serious adverse events.

VSI041-05 Cryoablation of Renal Masses

Wednesday, Dec. 4 1:55PM - 2:10PM Room: S405AB

Participants

Andrew J. Gunn, MD, Vestavia Hills, AL (*Presenter*) Consultant, BTG International Ltd; Speakers Bureau, BTG International Ltd; Research support, Penumbra Inc

LEARNING OBJECTIVES

1) Explain the technology underlying cryoablation. 2) List the advantages of cryoablation for renal masses. 3) List the disadvantages of cryoablation for renal masses. 4) Develop a safe approach in using cryoablation for renal masses.

VSI041-06 Outcomes for Ablation versus Resection of Small Renal Masses

Wednesday, Dec. 4 2:10PM - 2:25PM Room: S405AB

Participants

Nima Kokabi, MD, Atlanta, GA (Presenter) Research support, Sirtex Medical Ltd

LEARNING OBJECTIVES

1. Learn the most up-to-date guidelines regarding managment of small renal masses. 2. Learn the contemporary evidence regarding oncologic outcome of treating small renal masses with thermal ablation. 3. Learn the contemporary evidence regarding oncologic outcome of treating small renal masses with partial nephrectomy.

VSI041-07 Is There a Role for Combination Arterial Embolotherapy and Ablation for Renal Tumors?

Wednesday, Dec. 4 2:25PM - 2:40PM Room: S405AB

Participants

David C. Madoff, MD, New York, NY (*Presenter*) Advisory Board, RenovoRx Consultant, General Electric Company Consultant, Terumo Corporation Consultant, Argon Medical Devices, Inc Consultant, Abbott Laboratories Consultant, Embolx, Inc

VSIO41-08 Treatment Approach for Renal Cell Carcinoma Metastases

Matthew R. Callstrom, MD,PhD, Rochester, MN (*Presenter*) Research Grant, EDDA Technology, Inc Research Grant, Galil Medical Ltd Consultant, Medtronic plc Consultant, Endocare, Inc Consultant, Johnson & Johnson Consultant, Thermedical, Inc

For information about this presentation, contact:

callstrom.matthew@mayo.edu

LEARNING OBJECTIVES

1) Description of the clinical situations for patients with metastatic renal cell carcinoma that are appropriate for consideration of interventional oncology intervention. 2) Understand how interventional oncology has a role in the treatment of patients with metastatic renal cell carcinoma.

VSI041-09 Panel Discussion

Wednesday, Dec. 4 2:55PM - 3:00PM Room: S405AB







MSCT41

Case-based Review of Thoracic Radiology (Interactive Session)

Wednesday, Dec. 4 1:30PM - 3:00PM Room: S406A

СН

AMA PRA Category 1 Credits ™: 1.50 ARRT Category A+ Credit: 1.75

Participants

Diana Litmanovich, MD, Haifa, Israel (Director) Nothing to Disclose

For information about this presentation, contact:

dlitmano@bidmc.harvard.edu

LEARNING OBJECTIVES

1) Become familiarized with an overview of Pediatric Chest Disorders, including frequent and rare entities. 2) Understand a variety of mediastinal pathologies and new imaging techniques. 3) Become familiarized with the Physiology and imaging findings of Lung Manifestations of Cardiovascular Pathology. 4) Understand the current concepts of Chest Tuberculosis.

ABSTRACT

This course is designed to highlight the variety of thoracic pathology, including pediatric, cardiovascular, infectious and malignant etiology. Special attention would be fiven to the new understading of cardio-pulnmonary interaction in a varierty of pulmonary disorders, role of new imaging techniques in assessment of pediatric chest pathology and mediastinal disorders, as well as new understanding of Mycobartieria Tuberculosis infections. Our goal is to provide a broad update in the field while addressing new opportunities and challenges for everyday practice.

Sub-Events

MSCT41A Pediatric Chest Disorders: From Aunt Minnie to Zebra

Participants Edward Y. Lee, MD, Boston, MA (*Presenter*) Nothing to Disclose

MSCT41B Private Tour in the Mediastinal Maze

Participants

Isabel Oliva Cortopassi, MD, New Haven, CT (Presenter) Author, Reed Elsevier; Editor, Reed Elsevier

For information about this presentation, contact:

isabel.cortopassi@yale.edu

MSCT41C Many Faces of Lung Manifestations of Cardiovascular Pathology

Participants Michael K. Atalay, MD, PhD, Providence, RI (*Presenter*) Nothing to Disclose

MSCT41D Many Faces of Tuberculosis Involving Chest

Participants Lamia G. Jamjoom, MD, Jeddah, Saudi Arabia (*Presenter*) Nothing to Disclose

For information about this presentation, contact:

Lgjamjoom@gmail.com







MSCZ41

Case-based Review of CT (Interactive Session)

Wednesday, Dec. 4 1:30PM - 3:00PM Room: S402AB

СТ

AMA PRA Category 1 Credits ™: 1.50 ARRT Category A+ Credit: 1.75

Participants

Edward Y. Lee, MD, Boston, MA (Director) Nothing to Disclose

Sub-Events

MSCZ41A Pediatric Brain and Spine CT

Participants Thierry Huisman, MD, Houston, TX (*Presenter*) Nothing to Disclose

For information about this presentation, contact:

huisman@texaschildrens.org

MSCZ41B Adult Gastrointestinal CT

Participants Perry J. Pickhardt, MD, Madison, WI (*Presenter*) Stockholder, SHINE Medical Technologies, Inc; Stockholder, Elucent Medical; Advisor, Bracco Group;

LEARNING OBJECTIVES

1) Review CT imaging of GI disorders in a case-based format. 2) Highlight common GI pitfalls and differential diagnosis at CT.

MSCZ41C CT of Adult Small Airways Disease

Participants Theresa C. McLoud, MD, Boston, MA (*Presenter*) Nothing to Disclose

MSCZ41D Adult Large Airway CT

Participants Phillip M. Boiselle, MD, Boca Raton, FL (*Presenter*) Nothing to Disclose

For information about this presentation, contact:

pboiselle@health.fau.edu

LEARNING OBJECTIVES

1) Apply a pattern-based framework to accurately assess the large airways on axial CT images. 2) Recognize common patterns of disease in order to accurately diagnose acute and chronic airway disorders. 3) Identify normal variants and differentiate them from acute and chronic airway disorders.





MSES43

Essentials of Cardiac Imaging

Wednesday, Dec. 4 <u>1:30PM - 3:00PM Room: S100AB</u>

CA

AMA PRA Category 1 Credits ™: 1.50 ARRT Category A+ Credit: 1.75

Sub-Events

MSES43A Imaging of Non-traumatic Aortic Emergencies

Participants Stephen Ledbetter, MD, Boston, MA (*Presenter*) Nothing to Disclose

LEARNING OBJECTIVES

1) Understand common and differentiating features among the acute aortic syndromes. 2) Review prognostic features of acute aortic syndromes. 3) Determine what imaging features indicate aneurysm instability.

ABSTRACT

In this session, we will review the acute aortic syndromes in order to understand their common, differentiating and prognostic features. We will also review the imaging features indicating aneurysm instability.

MSES43B Cardiac MR in Non-ischemic Myocardial Inflammation

Participants

Iacopo Carbone, MD, Rome, Italy (Presenter) Nothing to Disclose

For information about this presentation, contact:

iacopo.carbone@uniroma1.it

LEARNING OBJECTIVES

1) To understand the diagnostic targets used by CMR for the identification of active myocardial inflammation. 2) To be able to recommend the MR protocol for patients with suspected myocarditis. 3) To learn the different clinical presentations of Acute Myocardial Inflammation. 4) To discuss the Consensus Recommendations for CMR in nonischemic myocardial inflammation in comparison with the original Lake Louise Criteria.

ABSTRACT

Acute myocarditis is a relatively common clinical entity but challenging to diagnose due to the low sensitivity of conventional diagnostic tools and to the variety of its clinical presentation.::Despite its invasiveness, the lack of standardized protocols and the high prevalence of sampling errors, endomyocardial biopsy still remains the gold standard diagnostic technique. Due to its ability of non-invasive tissue characterization, Cardiovascular Magnetic Resonance Imaging (CMR) represents an extremely powerful tool in this complex clinical setting. CMR is able to non invasively detect the 3 typical hallmarks of myocardial inflammation represented by edema, hyperemia, and necrosis or scar. These 3 diagnostic targets published in 2009 and well known as the Lake Louise Criteria (LLC) might be derived from signal intensity assessment in T2-weighted, early gadolinium enhancement (EGE) and late gadolinium enhancement (LGE) CMR images. The recent introduction of new promising mapping sequences have dramatically impacted the CMR protocols in patients with a clinical suspicion of acute myocarditis. The consequence is that LLC were recently updated, integrating mapping sequences in the recommended protocol.::The revised LLC also recommend a protocol free of intravenous injection of contrast, when contraindicated, which further expands CMR potentials in this clinical setting. In conclusion, acute myocarditis is a difficult diagnosis and CMR has now become a fundamental diagnostic tool allowing to avoid invasive procedures in the vast majority of clinical scenarios.

MSES43C Common and Uncommon Pacemakers and Implantable Cardiac Defibrillators

Participants Ahmed El-Sherief, MD, Redondo Beach, CA (*Presenter*) Nothing to Disclose

LEARNING OBJECTIVES

1) Identify the basic components of a pacemaker/ICD. 2) Use appropriate terminology for description of pacemakers/ICDs. 3) Identify complications post pacemaker/ICD implantation.

MSES43D Building a Transcatheter Aortic Valve Replacement (TAVR) Program

Participants Jeffrey S. Mueller, MD, Pittsburgh, PA (*Presenter*) Nothing to Disclose

For information about this presentation, contact:

jeffrey.mueller@ahn.org

1) Describe the importance of building a multispecialty TAVR program. 2) List strategies to improve patient care. 3) Learn how to overcome barriers.







MSRO43

BOOST: Protons vs. Photons: How Do Radiation Therapy Centers with Both Decide Which is Right for Their Patients?

Wednesday, Dec. 4 1:30PM - 2:30PM Room: S103CD



AMA PRA Category 1 Credit ™: 1.00 ARRT Category A+ Credit: 0

Participants

Ralph P. Ermoian, MD, Seattle, WA (*Presenter*) Nothing to Disclose

Chelsea C. Pinnix, MD, PhD, Houston, TX (*Presenter*) Research Grant, Merck & Co, Inc; Consultant, Global One Inc; Speaker, International Journal of Radiation Oncology, Biology & Physics

LEARNING OBJECTIVES

1) Describe the level of evidence supporting proton therapy for treating children with cancer and adults with lymphoma. 2) List three categories of considerations a radiation center with protons and photons may use when deciding which modality to use when treating a child or adult patient with lymphoma. 3) List one pediatric tumor with relatively favorable indications for use of proton therapy, and one pediatric tumor with relatively unfavorable indications for proton therapy.

ABSTRACT

Proton radiation therapy is increasingly available to patients, particularly in the United States where the number of centers continues to increase, sometimes with multiple proton center within large cities. There are dosimetric arguments for proton therapy with some additional studies supporting its efficacy and favorable toxicity. Most proton centers are part of radiation oncology departments that also treat with photon radiation. This session will explore how providers at centers with both modalities select the type of radiation that best fits two populations of patients: adults with lymphoma and children with tumors.







MSSR43

RSNA/ESR Sports Imaging Symposium: Musculoskeletal Interventional Procedures (Interactive Session)

Wednesday, Dec. 4 1:30PM - 3:00PM Room: E350



AMA PRA Category 1 Credits ™: 1.50 ARRT Category A+ Credit: 1.75

Participants

Andrew J. Grainger, MD, Leeds, United Kingdom (*Moderator*) Consultant, Levicept Ltd; Director, The LivingCare Group; Laura W. Bancroft, MD, Venice, FL (*Moderator*) Nothing to Disclose

For information about this presentation, contact:

laurabancroftmd@gmail.com

LEARNING OBJECTIVES

1) To learn the targeted approach to injecting joints, ligaments, tendons and tendon sheaths. 2) To appreciate pitfalls to avoid in MSK procedures for treatment of sports-related injuries. 3) To understand evidence-based data on various MSK procedures in order to give patients realistic expectations after treatment.

Sub-Events

MSSR43A Diagnostic and Therapeutic Injections in the Athlete: Pearls and Pitfalls

Participants

Philippe A. Peetrons, MD, Brussels, Belgium (Presenter) Research Consultant, Canon Medical Systems Corporation

For information about this presentation, contact:

ppeetrons@his-izz.be

LEARNING OBJECTIVES

1) To become familiar with the most common requests and indications for sports-related injuries. 2) The learn about technical considerations for performing MSK injections. 3) To understand reasons to delay injections or avoid certain injectables.

ABSTRACT

The main pitfall is from far an mistake in the diagnosis done before sending the patient to the ultrasound guided treatment. Good examination and looking carefully to the examinations done before is mandatory. Among pearls, some innovative technique for injecting will be shown, such as Trapezo-metacarpal joint, sternoclavicular joint, Morton's neuroma, subtalar joint, hip and shoulder joints, carpal tunnel and de Quervain tenosynovitis. Treatment of nerve injuries will also be depicted and illustrated. Some tips will be given for ganglia tretment

MSSR43B Injectables, Percutaneous Tendon Fenestration and Tenotomy: Clinical Outcomes and Current Evidence

Participants

Jon A. Jacobson, MD, Ann Arbor, MI (*Presenter*) Research Consultant, BioClinica, Inc; Advisory Board, Koninklijke Philips NV; Royalties, Reed Elsevier

For information about this presentation, contact:

jjacobsn@umich.edu

LEARNING OBJECTIVES

1) To be aware of the indications and benefits of available injectables used to treat sports-related injuries. 2) To learn about technical considerations for performing tendon fenestration and tenotomy. 3) To become familiar with current evidence on results of MSK procedures in the literature.

ABSTRACT

For joint abnormalities and tendinopathy, there exists many percutaneous treatment options. Anaesthetic agents are used, often combined with corticosteroids, to inject joints and bursae for diagnostic and therapeutic purposes. With regard to anaesthetic agents, all are cytotoxic to chondrocytes and synovial cells to some degree. Corticosteroids may be used to decrease inflammation within a synovial space. The use of corticosteroid to treat tendinopathy is counterintuitive, as inflammation is not present, injection into tendon causes tenocyte death, and the analgesic effect of corticosteroids is short lived, and therefore the underlying tendon pathology is not treated. A number of ultrasound-guided tendon treatments can be used for tendinopathy. One treatment is percutaneous tendon fenestration or tenotomy. With this procedure, a needle is passed through the abnormal tendon segment repeatedly to break up the degenerative process, induce bleeding and inflammation, and initiate the healing of the abnormal tendon. Other procedures include the injection of autologous whole blood during the fenestration process, as well as the injection of platelet-rich plasma during fenestration. With this latter technique, the autologous whole blood is centrifuged to concentrate the platelets for injection. All three of these percutaneous tendon treatments have been shown to be effective, although it is

controversial which technique is best. The cost of each procedure should also be considered. There exists newer and more controversial percutaneous tendon treatment, such as injection of mesenchymal stem cells, human amniotic membrane, and deer antler velvet. These procedures are largely considered experimental until research studies demonstrate their safety and efficacy.

MSSR43C Interactive Case Discussion

Participants

Jon A. Jacobson, MD, Ann Arbor, MI (*Presenter*) Research Consultant, BioClinica, Inc; Advisory Board, Koninklijke Philips NV; Royalties, Reed Elsevier

Philippe A. Peetrons, MD, Brussels, Belgium (Presenter) Research Consultant, Canon Medical Systems Corporation

For information about this presentation, contact:

ppeetrons@his-izz.be

jjacobsn@med.umich.edu

LEARNING OBJECTIVES

1) To learn the targeted approach to injecting joints, ligaments, tendons and tendon sheaths. 2) To appreciate pitfalls to avoid in MSK procedures for treatment of sports-related injuries. 3) To understand evidence-based data on various MSK procedures in order to give patients realistic expectations after treatment.





PS40

Wednesday Plenary Session

Wednesday, Dec. 4 1:30PM - 2:45PM Room: E450A

от

AMA PRA Category 1 Credits ™: 1.25 ARRT Category A+ Credit: .75

Participants

Valerie P. Jackson, MD, Tucson, AZ (Presenter) Nothing to Disclose

Sub-Events PS40A	Announcement of Education Exhibit Awards
PS40B	Announcement of Quality Improvement Report Awards
PS40C	Annual Oration in Radiation Oncology: Online Adaptive Radiation Therapy (OART): The True Intersection of Diagnostic Radiology and Radiation Oncology

Participants

Lisa A. Kachnic, MD, New York, NY (*Presenter*) Speaker, TRM Oncology; Royalties, Wolters Kluwer nv Anna Shapiro, MD, Syracuse, NY (*Presenter*) Nothing to Disclose

Abstract

Diagnostic radiology (DR) and radiation oncology (RO) were linked from their inceptions through the post-World War II era. In the 1970s and 80s, a progressive division occurred, with the creation of separate departments, training programs and stakeholder organizations. Despite this governmental and philosophical separation, the clinical practice of RO has become increasingly dependent on more sophisticated image guidance to precisely delineate target versus nontarget tissues in treatment planning, confirm daily patient set-up to accommodate continuous changes in motion and anatomy, and to determine response during and after therapy. Over the last decade, advances in oncologic imaging, including technologies such as multi-phase CT, PET, MRI and highly selective interventional radiology, have provided exciting new opportunities to develop personalized radiation oncology delivery. Initially, CT-based (and more recently MRI and PET-based) delineation of patient anatomy and treatment geometry was employed for radiation treatment planning. Over the past decade, we have adapted on-board cone or fan beam CT and MRI imaging acquisition systems to medical linacs to guide and verify pre-treatment patient positioning as well as to inform re-planning should changes in target anatomy (e.g., tumor shrinkage, normal organ deformation) or patient's physiology (e.g., weight loss) dictate. This rudimentary form of Adaptive Radiation is resource intensive and may be inconvenient to the patient and facility, as it often requires an entirely new CT-based planning session. Recently, the concept of Online Adaptive Radiation Therapy (OART) has emerged. This technique has the potential to develop daily, personalized radiation delivery in real time, without the patient ever leaving the treatment couch. Central to this novel approach is leveraging progress in machine learning. Through iterative modeling, radiation oncologists will be able to combine clinical patient and tumor data (e.g., age, gender, comorbidities and tumor grade, stage, histology, and site), with ongoing changes in physiological metrics (e.g., blood cell counts, pulse rates, breathing characteristics), tumor biology (e.g., hypoxia), radiation dosimetry of the target and normal structures, and most importantly imaging (e.g., tumor shrinkage, radiomics), for adaptive decision-making regarding the need to adjust radiation doses and/or distributions to the target as well as to the normal surrounding at-risk organs. The overarching goal of this OART framework is to improve tumor control and to minimize harm to uninvolved healthy tissues. The synthesis of this data may also allow for novel clinical trials testing true adaptive radiation approaches, as well as biomarkers of response. This presentation will review the advances of adaptive therapeutic radiation delivery, highlighting the significance of increasingly sophisticated image-guidance. Although diagnostic radiology and radiation oncology have evolved into separate disciplines, greater collaboration will be warranted in this exciting era of integrating machine learning and artificial intelligence into routine clinical practice.





SPHA41

Hospital Administrators Symposium

Wednesday, Dec. 4 1:30PM - 4:50PM Room: S503AB



AMA PRA Category 1 Credits ™: 3.25 ARRT Category A+ Credits: 4.00

Participants

Gregory N. Nicola, MD, River Edge, NJ (Moderator) Founder, N2 Health Insights; Consultant, CMO Neutigers

For information about this presentation, contact:

gnnicola@yahoo.com

Sub-Events

SPHA41A Achieving Operational Efficiency in a Radiology Department

Participants Daniel E. Wessell, MD, PhD, Ponte Vedra Beach, FL (*Presenter*) Nothing to Disclose

SPHA41B Contracts and Negotiations

Participants Lauren P. Golding, MD, Summerfield, NC (*Presenter*) Nothing to Disclose

For information about this presentation, contact:

laurengoldingmd@gmail.com

LEARNING OBJECTIVES

Identify different types of negotiations relevant to radiologists: employment contracts, hospital contracts, payer contracts, etc.
 Discuss strategies for successful negotiation. 3) Identify common pitfalls in evaluating contracts.

SPHA41C Using Best Practice Paradigms in Radiology

Participants

Ryan K. Lee, MD, Philadelphia, PA (*Presenter*) Consultant, Zebra Medical Vision Ltd; Speakers Bureau, Koninklijke Philips NV ; Speakers Bureau, Bayer AG; Speakers Bureau, NDSC

For information about this presentation, contact:

leeryan1@einstein.edu

LEARNING OBJECTIVES

1) Describe concepts.

SPHA41D Q&A

Participants Daniel E. Wessell, MD, PhD, Ponte Vedra Beach, FL (*Presenter*) Nothing to Disclose Lauren P. Golding, MD, Summerfield, NC (*Presenter*) Nothing to Disclose Ryan K. Lee, MD, Philadelphia, PA (*Presenter*) Consultant, Zebra Medical Vision Ltd; Speakers Bureau, Koninklijke Philips NV ; Speakers Bureau, Bayer AG; Speakers Bureau, NDSC

SPHA41E Price Transparency and Consumerism in Radiology

Participants Rebecca Farrington, Media, PA (*Presenter*) Nothing to Disclose

LEARNING OBJECTIVES

1) Compare the pros and cons of sharing pricing information with a patient prior to scheduling a test in an outpatient imaging environment. 2) Identify the areas that health systems and physician groups should focus on in order to manage the patient's experience and increase the patient's satisfaction before, during and after the imaging process. 3) Examine new policies aimed at ensuring patient satisfaction before, during and after the imaging process.

SPHA41F Effective Strategies of Navigating Hospital Consolidation: Radiology Steering Committee

Participants Mohit Naik, MD, River Edge, NJ (*Presenter*) Nothing to Disclose

LEARNING OBJECTIVES

1) Develop standardized quality metrics to benchmark performance across a healthcare network. 2) Recognize strategies to maximize savings by leveraging economies of scale. 3) Identify methods to gain alignment among disparate Radiology groups to forge a cohesive path forward.

SPHA41G Using Imaging Data to Optimize Radiology Department Operations

Participants

Kelly Denney, PHD, El Segundo, CA (Presenter) Nothing to Disclose

LEARNING OBJECTIVES

Recognizing ways that Data Science can be applied to increase operational efficiency and standardization of patient care that provide actionable intelligence and informed decision-making to your department.

SPHA41H Q&A

Participants Rebecca Farrington, Media, PA (*Presenter*) Nothing to Disclose Mohit Naik, MD, River Edge, NJ (*Presenter*) Nothing to Disclose Kelly Denney, PHD, El Segundo, CA (*Presenter*) Nothing to Disclose





MSRT45

ASRT@RSNA 2019: Professionalism in Everyday Practice

Wednesday, Dec. 4 2:20PM - 3:20PM Room: N230B

PR

AMA PRA Category 1 Credit ™: 1.00 ARRT Category A+ Credit: 1.00

Participants

Kevin R. Clark, RT, Houston, TX (Presenter) Nothing to Disclose

LEARNING OBJECTIVES

1) Describe what professionalism looks like in the medical imaging and radiation therapy profession. 2) Recognize and address inappropriate behavior in the health care environment. 3) Discuss the importance of using empathetic communication in health care settings. 4) Apply strategies to promote professionalism in the medical imaging and radiation therapy profession.

ABSTRACT

Health care professionals must understand the importance of professionalism and the need to act in a professional, ethical, legal, and competent manner. More than just having good conduct, professionalism involves establishing respectable relationships with patients, colleagues, supervisors, and the public. This presentation discusses professionalism in everyday practice and describes the personal and professional traits of medical imaging technologists and radiation therapists. This presentation also explores various unprofessional behaviors, such as workplace bullying and incivility, and provides strategies to eliminate those behaviors and promote professionalism in the health care environment.







RCA44

PowerPoint Tips (Hands-on)

Wednesday, Dec. 4 2:30PM - 4:00PM Room: S401AB

IN

AMA PRA Category 1 Credits ™: 1.50 ARRT Category A+ Credit: 1.75

Participants

William J. Weadock, MD, Ann Arbor, MI (*Moderator*) Owner, Weadock Software, LLC William J. Weadock, MD, Ann Arbor, MI (*Presenter*) Owner, Weadock Software, LLC Sarah C. Abate, BS, Ann Arbor, MI (*Presenter*) Nothing to Disclose

For information about this presentation, contact:

weadock@umich.edu

LEARNING OBJECTIVES

1) Understand the use of color, font size and backgrounds to optimize PowerPoint presentations. 2) Understand the use of PowerPoint templates, and how they can be used to save time and improve presentations. 3) Learn about optimization of textual content on slides.







RCC44

Clinical Decision Support: From Theory to Clinical Practice

Wednesday, Dec. <u>4</u> 2:30PM - 4:00PM Room: <u>S406B</u>



AMA PRA Category 1 Credits ™: 1.50 ARRT Category A+ Credit: 1.75

Participants

Emanuele Neri, MD, Pisa, Italy (Moderator) Nothing to Disclose

For information about this presentation, contact:

emanuele.neri@med.unipi.it

LEARNING OBJECTIVES

1) To explore the strategy of implementation of CDS in US and Europe. 2) To report the clinical implementation and impact of CDS in a real setting. 3) To preview the future implementation of artificial intelligence in CDS.

Sub-Events

RCC44A How Can Radiologists Implement Decision Support Systems in Clinical Routine: ACR View

Participants

Bibb Allen JR, MD, Mountain Brk, AL (Presenter) Nothing to Disclose

LEARNING OBJECTIVES

1) Apply lessons learned from the Medicare Demonstration project to implement effective Clinical Decision Support (CDS) programs. 2) Formulate strategies for compliance with current regulations requiring CDS.

RCC44B How Can Radiologists Implement Decision Support Systems in Clinical Routine: ESR View

Participants

Boris Brkljacic, MD, PhD, Zagreb, Croatia (Presenter) Advisory Board Member, contextflow GmbH

For information about this presentation, contact:

boris@brkljacic.com

LEARNING OBJECTIVES

1) To learn about the use of imaging referral guidelines in Europe. 2) To understand the challenges of implementing a CDS for heterogeneous European countries. 3) To describe the varying experiences of implementing CDS and imaging referral guidelines in different countries.

RCC44C Results and Lessons from Brigham and Women's Hospital

Participants Ramin Khorasani, MD, Roxbury Crossing, MA (*Presenter*) Nothing to Disclose

LEARNING OBJECTIVES

1) Briefly review existing federal regulations pertinent to imaging clinical decision support. 2) Discuss design, implementation and results of large scale imaging CDS intervention at Brigham and Women's Hospital. 3) Contrast results and discuss implications from CDS interventions that have and have not impacted ordering physician behavior. 4) Recommend strategies to optimize imaging CDS implementation to improve quality and enable and promote evidence-based practice.

RCC44D Application of Machine Learning in Clinical Decision Support Systems

Participants

Tarik K. Alkasab, MD, PhD, Boston, MA (Presenter) Consultant, Nuance Communications, Inc





MSRO44

BOOST: Advanced Techniques in Image-guided Therapy (Interactive Session)

Wednesday, Dec. 4 <u>3:00PM - 4:15PM Room: S103CD</u>



AMA PRA Category 1 Credits [™]: 1.25 ARRT Category A+ Credits: 1.50

Participants

Florence K. Keane, MD, Boston, MA (*Presenter*) Advisory Board, AstraZeneca PLC Susanna I. Lee, MD, PhD, Boston, MA (*Presenter*) Royalties, Wolters Kluwer nv; Royalties, Springer Nature Homer A. Macapinlac, MD, Houston, TX (*Presenter*) Nothing to Disclose Peter Balter, PhD, Houston, TX (*Presenter*) Research Grant, Varian Medical Systems, Inc; Research Grant, RaySearch Laboratories AB

For information about this presentation, contact:

slee0@mgh.harvard.edu

LEARNING OBJECTIVES

1) Explain and apply modern CT, MR, and PET technologies for treatment planning of solid malignancies in the chest, abdomen and pelvis. 2) Explain and apply the modern techniques in radiotherapy safely and effectively in the chest, abdomen and pelvis.

ABSTRACT

The last decade has seen emergence of important advances in locoregional cancer therapy. Use of functional imaging and advanced radiotherapy often integrated with targeted chemotherapy have improved patient outcomes. This course will present the underlying principles in diffusion MRI, novel MR contrast agents, ultrasound contrast agents and dual energy CT. PET tracers to be discussed are F-18 FDG, widely used for most solid tumors, C-11 choline/F-18 Fluciclovine for prostate cancer and Ga-68-DOTATATE for neuroendocrine tumors. Advances in PET detector instrumentation will be presented. Advanced radiotherapy techniques such as Image Guided Radiotherapy (IGRT), Intensity Modulated Radiation Therapy (IMRT), and Stereotactic Body Radiation Therapy (SBRT) using image guidance with X-ray, CT, MRI and PET will be described.







SPAI43

RSNA AI Deep Learning Lab: Beginner Class: Classification Task (Intro)

Wednesday, Dec. 4 3:00PM - 4:30PM Room: AI Showcase, North Building, Level 2, Booth 10342



Participants

Bradley J. Erickson, MD, PhD, Rochester, MN (Presenter) Board of Directors, VoiceIt Technologies, LLC; Stockholder, VoiceIt Technologies, LLC; Board of Directors, FlowSigma, LLC; Officer, FlowSigma, LLC; Stockholder, FlowSigma, LLC

Special Information

In order to get the best experience for this session, it is highly recommended that attendees bring a laptop with a keyboard, a decent-sized screen. Having a Gmail account will be helpful. Here are instructions for creating and deleting a Gmail account.

ABSTRACT

This class will focus on basic concepts of convolutional neural networks (CNNs) and walk the attendee through a working example. A popular training example is the MNIST data set which consists of hand-written digits. This course will use a data set we created, that we call 'MedNIST', and consists of images of 6 different classes: Chest X-ray, Chest CT, Abdomen CT, Head CT, Head MR and Breast MRI. The task is to identify the image class. This will be used to train attendees on the basic principles and some pitfalls in training a CNN. • Intro to CNNs • Data preparation: DICOM to jpeq, intensity normalization, train vs test • How do we choose the labels? Inconsistencies... Use Fast.AI routines to classify; Validation of results: Are the performance metrics reliable? 'Extra Credit': if there is time, explore data augmentation options, effect of batch size, training set size.







SSM01

Breast Imaging (Functional Imaging)

Wednesday, Dec. 4 3:00PM - 4:00PM Room: E451B

BR

AMA PRA Category 1 Credit ™: 1.00 ARRT Category A+ Credit: 1.00

Participants

Matthias Dietzel, MBA, MD, Erlangen, Germany (*Moderator*) Nothing to Disclose Mami Iima, MD, PhD, Kyoto, Japan (*Moderator*) Nothing to Disclose

Sub-Events

SSM01-01 Role of 18F-FDG Uptake on PET/CT in Identifying Androgen Receptor Expression and Prognostic Factors in Triple-Negative Breast Cancer

Wednesday, Dec. 4 3:00PM - 3:10PM Room: E451B

Participants

Hyo-jae Lee, Gwangju, Korea, Republic Of (*Presenter*) Nothing to Disclose So Yeon Ki, Jeollanam-do, Korea, Republic Of (*Abstract Co-Author*) Nothing to Disclose Hyo Soon Lim, MD, Gwangju, Korea, Republic Of (*Abstract Co-Author*) Nothing to Disclose Jong Eun Lee, Gwangju, Korea, Republic Of (*Abstract Co-Author*) Nothing to Disclose

For information about this presentation, contact:

N/C

PURPOSE

To investigate the relationship between 18F-FDG uptake and androgen receptor (AR) expression in triple-negative breast cancer (TNBC).

METHOD AND MATERIALS

Between May 2015 and May 2017, 110 patients (mean age, 53.5 years) with primary TNBC (mean, 25.7mm; range, 4-75 mm) were retrospectively categorized into AR+ (n = 25) and AR- (n = 85) groups by using immunohistochemical staining and underwent 18F-FDG PET/CT for staging. Maximum standardized uptake (SUVmax) value on PET/CT and clinicopathologic features including age, size of tumor, lymph node metastasis, histological grade of tumor, histological type, Ki-67, associated ductal carcinoma in situ (DCIS) component, p53 overexpression, and basal marker (CK5/6, CK14, EGFR) expression by immunohistochemical staining were compared between the two groups. In addition, the correlation between SUVmax and prognostic factors was assessed.

RESULTS

Mean SUVmax was significantly higher in AR- (9.9 ± 5.5) group than in AR+ (7.2 ± 4.8) group (P = .025). AR- group was significantly younger (P = .001) and showed significantly more histological grade 3 (P = .025) and Ki-67 proliferation rate (>14%) of TNBC (P < .001). There were positive correlations between SUVmax and Ki-67 (Spearman's rho = 0.240, P = .012), histological grade (Spearman's rho = 0.252, P = .008), and the size of tumor (Spearman's rho = 0.455, P < .001). There were negative correlations between SUVmax and AR (Spearman's rho = -0.215, P = .024) and associated DCIS component (Spearman's rho = -0.261, P = .006). In a multiple regression analysis, the size of tumor (P = .001) was significantly associated with SUVmax.

CONCLUSION

18F-FDG uptake was significantly higher in AR- group than in AR+ group and correlated with larger tumor size in TNBC.

CLINICAL RELEVANCE/APPLICATION

Suspected from SUVmax on PET/CT before biopsy in terms of androgen receptor status could help to expedite management of triple-negative breast cancer.

SSM01-02 Investigation of Breast Cancer Detectability Using Total Breast PET Imager

Wednesday, Dec. 4 3:10PM - 3:20PM Room: E451B

Participants

Suranjana Samanta, BEng,MS, St.Louis, MO (*Presenter*) Nothing to Disclose Jianyong Jiang, St. Louis, MO (*Abstract Co-Author*) Nothing to Disclose Alan Register, Durham, NC (*Abstract Co-Author*) Nothing to Disclose Timothy Turkington, PhD, Durham, NC (*Abstract Co-Author*) Consultant, Data Spectrum Corporation Sergei Dolinsky, PhD, Rockville, MD (*Abstract Co-Author*) Nothing to Disclose Joseph A. O'Sullivan, PhD, Saint Louis, MO (*Abstract Co-Author*) Nothing to Disclose Stan Majewski, MD, Morgantown, WV (*Abstract Co-Author*) Research Grant, General Electric Company Research Grant, ONCOVISION Mark B. Williams, PhD, Charlottesville, VA (*Abstract Co-Author*) Nothing to Disclose Martin P. Tornai, PhD, Durham, NC (*Abstract Co-Author*) Nothing to Disclose Yuan-Chuan Tai, PhD, Saint Louis, MO (*Abstract Co-Author*) Nothing to Disclose

For information about this presentation, contact:

ssamanta@wustl.edu

PURPOSE

Whole-body PET/CT has low sensitivity in the detection of small breast cancers due to its limited image resolution and system sensitivity which led to the development of positron emission mammography(PEM) systems. Most PEM systems employ a planar or a ring geometry to surround a breast. A ring geometry provides high resolution and high sensitivity, but is incapable of imaging the axilla. The planar geometry provides more flexibility in detector placement but has lower sensitivity and image quality. In both cases, the sensitivity of the system approaches zero for tissues near or beyond the chest wall. To overcome this limitation, we propose a novel geometry that can image both breasts with high resolution and sensitivity with an extended imaging field-of-view (FOV) that also includes the entire torso and axilla.

METHOD AND MATERIALS

The scanner consists of a racetrack-like geometry that surrounds two breasts along with a rectangular front panel and a curved back panel. The detectors in the racetrack and front panel consist of 2x2x6 mm3 (double layer DOI) LSO crystals while the back panel consists of 3.95x5.3x25 mm3 LSO crystals. We used GATE to simulate this system and a GPU-based list-mode reconstruction program to characterize the system performance with Time-of-Flight (ToF) information.

RESULTS

The sensitivity images of standard PET system, ring and flat-type PEM systems and our proposed geometry are compared. Body phantom with different tumor sizes and contrast are reconstructed for different systems. Results show superior sensitivity for the latter and demonstrate a large imaging FOV that can detect all lesions with good image quality.

CONCLUSION

The proposed system has high sensitivity and can significantly improve resolution as compared to whole-body PET system and achieve a larger imaging FOV, including the entire torso and axilla, than typical PEM systems. Detailed system design and characteristics will be presented.

CLINICAL RELEVANCE/APPLICATION

Radiotracer-based molecular imaging can complement conventional breast imaging technologies such as mammography and MRI to improve the overall diagnostic accuracy. Total Breast PET Imager offers the benefits of conventional PEM system (high resolution and high sensitivity) and whole-body PET scanner (large imaging FOV) for improved detectability of breast cancer.

SSM01-03 Evaluation of Contrast Enhanced Digital Mammography in the Preoperative Staging of Breast Cancer: Large-Scale Single-Center Experience

Wednesday, Dec. 4 3:20PM - 3:30PM Room: E451B

Participants

Giulia Bicchierai, Florence, Italy (*Presenter*) Nothing to Disclose Paolina Tonelli, MD, Florence, Italy (*Abstract Co-Author*) Nothing to Disclose Alba Piacenti, Florence, Italy (*Abstract Co-Author*) Nothing to Disclose Diego De Benedetto, Florence, Italy (*Abstract Co-Author*) Nothing to Disclose Federica Di Naro, Palermo, Italy (*Abstract Co-Author*) Nothing to Disclose Donatello Cirone, Florence, Italy (*Abstract Co-Author*) Nothing to Disclose Cecilia Boeri, Florence, Italy (*Abstract Co-Author*) Nothing to Disclose Ermanno Vanzi, MD, Florence, Italy (*Abstract Co-Author*) Nothing to Disclose Vittorio Miele, MD, Florence, Italy (*Abstract Co-Author*) Nothing to Disclose Jacopo Nori, Florence, Italy (*Abstract Co-Author*) Nothing to Disclose

PURPOSE

The aim of this retrospective study was to evaluate the diagnostic performance of Contrast-enhanced Digital Mammography (CEDM) in the preoperative staging of breast cancer and to evaluate the effects of this new technique on the surgical management of all patients and of the various subgroups.

METHOD AND MATERIALS

Data have been collected from a cohort of 326 patients affected by breast cancer who were diagnosed in our department between December 2016 and January 2019. All patients underwent CEDM and subsequent surgical excision (SE). The results of preoperative staging with CEDM and surgical management were correlated with histopathological results, considered as the gold standard. The diagnostic performance of CEDM in the identification of the index lesion and of additional homo and contralateral lesions was evaluated. The authors also analyzed any possible changes in surgical management of the patients due to CEDM findings and the diagnostic performance of CEDM in various subgroups i.e. women with age 50 or less and greater than 51; patients with dense breast (BI-RADS C and D) and non-dense (BI-RADS A and B), palpable index lesion or not.

RESULTS

CEDM sensivity in detecting index cancer was 98.8% (322/326). For detection of secondary cancer in the ipsilateral or contralateral breast CEDM sensivity, specificity, positive and negative predictive values and accuracy were 93%, 98%, 90%, 98% and 97% respectively. The ROC Curve comparing CEDM to the gold standard showed an area under the curve (AOU) of 0.955. CEDM changed type of surgery planned before the examination in 18.4% of the cases, 17,2% of these due to true-positive findings and 2,8% to false-positive findings. CEDM has led to 17,8% of additional biopsies, of these 53,5% proved to be malignant and 46,5% were benign.

CONCLUSION

Cedm has demonstrated a very high diagnostic performance in preoperative breast cancer staging and often leads to a more strict and appropriate surgical planning.

CLINICAL RELEVANCE/APPLICATION

This study supports the Cedm as a promising alternative to magnetic resonance imaging in the surgical planning of patients with breast cancer.

SSM01-04 Contrast-Enhanced Mammography: Does Acquisition Time Matter?

Wednesday, Dec. 4 3:30PM - 3:40PM Room: E451B

Participants Christina S. Konstantopoulos, MD, Boston, MA (*Presenter*) Nothing to Disclose Vandana M. Dialani, MD, Boston, MA (*Abstract Co-Author*) Nothing to Disclose Rashmi Mehta, MBA, Boston, MA (*Abstract Co-Author*) Nothing to Disclose Tejas S. Mehta, MD, MPH, Boston, MA (*Abstract Co-Author*) Nothing to Disclose Evguenia J. Karimova, MD, Memphis, TN (*Abstract Co-Author*) Research Consultant, Intrinsic Imaging LLC Parisa Lotfi, MD, Newton, MA (*Abstract Co-Author*) Nothing to Disclose Valerie J. Fein-Zachary, MD, Boston, MA (*Abstract Co-Author*) Nothing to Disclose Alexander Brook, PhD, Boston, MA (*Abstract Co-Author*) Nothing to Disclose Tarana K. Gill, MD, Boston, MA (*Abstract Co-Author*) Nothing to Disclose Jordana Phillips, MD, Newton Center, MA (*Abstract Co-Author*) Research Grant, General Electric Company Consultant, General Electric Company

For information about this presentation, contact:

ckonstan@bidmc.harvard.edu

PURPOSE

The technique for contrast enhanced mammography (CEM) was developed based on subtraction angiography and temporal subtraction techniques. Our purpose was to determine at what time points cancers are best visualized on CEM based on already acquired cases, to drive a future larger prospective study refining CEM technique.

METHOD AND MATERIALS

This HIPAA compliant IRB approved reader study included 40 consecutive cancer containing CEM exams from February 17th 2016 to November 8th 2018. Cases were included if cancer was seen on both CC and MLO views, cancer was not yet biopsied, and only up to two sites of cancer were present. Bilateral CC and MLO recombined images were presented side-by-side to 4 fellowship-trained breast imagers. Radiologists provided interpretations of background parenchymal enhancement (BPE) and rated CC and MLO projections for cancer visibility, confidence in margins, and conspicuity of the finding as compared with BPE using a 5-point Likert scale. Objective measure of cancer conspicuity was determined using region-of-interest calculations of cancer versus BPE to determine a contrast-to-noise ratio (CNR).

RESULTS

Data from one reader is available for this abstract. CC views were performed first in all cases. After contrast administration, the median times for the CC and MLO views were 2:20 and 4:25, respectively. 15 patients (37.5%) had low (minimal and mild) BPE and 25 (62.5%) had high (moderate and marked) BPE. Mean visibility difference for CC (4.4 ± 0.9) and MLO (4.1 ± 1.2) views was significantly significant (p=0.008). Mean confidence in margins for CC (4.2 ± 1.3) and MLO (4.0 ± 1.3) was not significantly different (p=0.14). Mean conspicuity of cancer relative to BPE for CC (4.3 ± 0.9) and MLO (3.9 ± 1.2) was significantly different (p=0.002). CNR on CC (mean 3.9, median 3.5) and MLO (mean 4.0, median 3.8) were not significantly different (p=0.89).

CONCLUSION

There is improved cancer visibility and conspicuity of cancer relative to BPE on earlier CC views. This suggests post-contrast images may be optimized by imaging earlier after contrast administration. However, additional reader results are necessary and will be included in this presentation.

CLINICAL RELEVANCE/APPLICATION

There is improved cancer visibility and conspicuity of cancer relative to BPE on earlier CC views. This suggests post-contrast images may be optimized by imaging earlier after contrast administration.

SSM01-05 Are There Differences in 18F-FDG PET-MRI Imaging Biomarkers of Contralateral Healthy Tissue between Patients with Benign and Malignant Breast Lesions?

Wednesday, Dec. 4 3:40PM - 3:50PM Room: E451B

Participants

Doris Leithner, MD, Frankfurt Am Main, Germany (*Presenter*) Nothing to Disclose Thomas H. Helbich, MD, Vienna, Austria (*Abstract Co-Author*) Research Grant, Medicor, Inc ; Research Grant, Siemens AG ; Research Grant, C. R. Bard, Inc; Research Grant, Guerbet SA; Research Grant, Novomed GmbH Blanca Bernard-Davila, MPH,MS, New York, NY (*Abstract Co-Author*) Nothing to Disclose Maria Adele Marino, MD, Messina, Italy (*Abstract Co-Author*) Nothing to Disclose Daly B. Avendano, MD, Monterrey, Mexico (*Abstract Co-Author*) Nothing to Disclose Dany F. Martinez, BSC,MSc, New York, NY (*Abstract Co-Author*) Nothing to Disclose Maxine S. Jochelson, MD, New York, NY (*Abstract Co-Author*) Nothing to Disclose Panagiotis Kapetas, Vienna, Austria (*Abstract Co-Author*) Nothing to Disclose Pascal A. Baltzer, MD, Vienna, Austria (*Abstract Co-Author*) Nothing to Disclose Elizabeth A. Morris, MD, New York, NY (*Abstract Co-Author*) Nothing to Disclose Katja Pinker-Domenig, MD, New York, NY (*Abstract Co-Author*) Nothing to Disclose Katja Pinker-Domenig, MD, New York, NY (*Abstract Co-Author*) Nothing to Disclose

For information about this presentation, contact:

doris.leithner@gmail.com

PURPOSE

To evaluate whether there are differences in multiparametric 18F-fluorodeoxyglucose positron emission tomography - magnetic resonance imaging (18F-FDG PET-MRI) biomarkers of contralateral healthy breast tissue between patients with benign and malignant breast tumors.

METHOD AND MATERIALS

In this IRB-approved HIPAA-compliant prospective single-institution study, 141 women with imaging abnormality on mammography or sonography (BI-RADS 4/5) were included and underwent combined 18F-FDG PET-MRI of the breast at 3T including dynamic contrast-enhanced MRI (DCE-MRI) and diffusion-weighted imaging (DWI). The following imaging biomarkers were recorded in all patients for the contralateral tumor-free breast: 18F-FDG breast parenchymal uptake (BPU), mean apparent diffusion coefficient (ADCmean), DCE-MRI background parenchymal enhancement (BPE) and amount of fibroglandular tissue (FGT), as well as BPU, BPE and FGT of the ipsilateral diseased breast. Appropriate statistical tests were used to assess differences in imaging biomarkers between patients with benign and malignant lesions.

RESULTS

There were 100 malignant and 41 benign lesions. BPE was minimal in 61, mild in 56, moderate in 19, and marked in 5 patients. BPE differed significantly (P<0.001) between patients with benign and malignant lesions, with patients with cancer showing decreased BPE in the contralateral tumor-free breast. A borderline significant difference was observed for FGT (P=0.055). BPU for patients with mild BPE was 1.5, for mild BPE 1.9, for moderate BPE 2.2, and for marked BPE 1.9. BPU differed significantly between patients with benign (mean, 1.9) and malignant lesions (mean, 1.8) (P<.001). ADCmean did not differ between groups (P=0.19). In both groups, no differences in imaging biomarkers between contralateral healthy and ipsilateral diseased breast were found, excluding a potential stealing phenomenon of the diseased breast with respect to vascularity and metabolic activity.

CONCLUSION

Differences in multiparametric 18F-FDG PET-MRI biomarkers, obtained from contralateral tumor-free breast tissue, exist between patients with benign and malignant breast tumors. Contralateral BPE, BPU, and FGT are decreased in breast cancer patients.

CLINICAL RELEVANCE/APPLICATION

BPE and BPU may potentially serve as imaging biomarkers for the presence and risk of malignancy.

SSM01-06 Evaluation of a Low-Dose Contrast-Enhanced Mammography System Compared to Contrast-Enhanced Breast MRI in the Assessment Setting

Wednesday, Dec. 4 3:50PM - 4:00PM Room: E451B

Participants

Paola Clauser, MD, Vienna, Austria (*Presenter*) Nothing to Disclose Pascal A. Baltzer, MD, Vienna, Austria (*Abstract Co-Author*) Nothing to Disclose Panagiotis Kapetas, Vienna, Austria (*Abstract Co-Author*) Nothing to Disclose Ramona Woitek, MD, Vienna, Austria (*Abstract Co-Author*) Nothing to Disclose Mathias D. Hoernig, DIPLPHYS, Forchheim, Germany (*Abstract Co-Author*) Employee, Siemens AG Michael Weber, Vienna, Austria (*Abstract Co-Author*) Nothing to Disclose Thomas H. Helbich, MD, Vienna, Austria (*Abstract Co-Author*) Nothing to Disclose Research Grant, C. R. Bard, Inc; Research Grant, Guerbet SA; Research Grant, Novomed GmbH

For information about this presentation, contact:

clauser.p@hotmail.it

PURPOSE

To evaluate the diagnostic performance of a low-dose contrast enhanced mammography (L-CEM) in women with suspicious findings on conventional imaging, and compare it to contrast-enhanced magnetic resonance imaging (CE-MRI) of the breast.

METHOD AND MATERIALS

The ethics committee approved this prospective, single center study and all patients gave written informed consent. Women with suspicious findings on conventional imaging (mammography, tomosynthesis and ultrasound) and no contraindications for L-CEM or CE-MRI were invited to participate in the study. The L-CEM system performs the acquisition without anti-scatter grid and a sowtware based scattered correction is than applied to the images. Three off-site, blinded readers evaluated the images according to BI-RADS lexicon in a randomized order, each in two separate reading sessions. Histology served as a gold standard. Lesion detection rate, sensitivity, specificity, negative and positive predictive values (NPV, PPV) were calculated and compared with multivariate statistics. Average glandular dose per view was measured (AGD).

RESULTS

Included were 80 patients (mean age 54.3 years, standard deviation 11.2) with 93 lesions (32 benign, 61 malignant). Sensitivity (L-CEM 65.6%-90.2%; CE-MRI 83.6%-93.4%, P=0.086) and NPV (L-CEM 59.6%-71.4%; CE-MRI 63.0%-76.5%, P=0.780) did not differ. Specificity (L-CEM 46.9%-96.9%; CE-MRI 37.5%-53.1, P=0.001) and PPV were significantly higher with L-CEM (L-CEM 76.4%-97.6%; CE-MRI 73.3%-77.3% P=0.007). Detection rate was significantly higher with CE-MRI (92.5%-94.6%) compared to L-CEM (79.6%-91.4%, P=0.014). Variations between readers were significant for sensitivity and NPV, but not for specificity. Accuracy of L-CEM was as good as for CE-MRI (75.3%-76.3% versus 72.0%-75.3%, P=0.514). AGD dose per view ranged according to the breast thickness from 1,074 mGy to 2,49 mGy.

CONCLUSION

L-CEM showed a high sensitivity and accuracy in women with suspicious findings on conventional imaging. Compared to CE-MRI, L-CEM has the potential to increase specificity and PPV. Based on our results, low-dose CEM might help reducing unnecessary follow up and false positive biopsies while increasing cancer detection comparably to CE-MRI.

CLINICAL RELEVANCE/APPLICATION

L-CEM could help reducing unnecessary follow up and false positive biopsies, while increasing cancer detection in an extent

comparable to CE-MRI, with a dose up to 70% less than a full dose CEM. Printed on: 10/29/20 $\,$





SSM02

Breast Imaging (Radiomics)

Wednesday, Dec. 4 3:00PM - 4:00PM Room: E451A



AMA PRA Category 1 Credit ™: 1.00 ARRT Category A+ Credit: 1.00

FDA Discussions may include off-label uses.

Participants

Christiane K. Kuhl, MD, Aachen, Germany (*Moderator*) Nothing to Disclose Despina Kontos, PhD, Philadelphia, PA (*Moderator*) Research Grant, Hologic, Inc

Sub-Events

SSM02-01 Radiomics Signatures of DCE-MRI Combined with Clinicopathologic Characteristics for Preoperative Prediction of Axillary Lymph Node Metastasis in Breast Cancer

Wednesday, Dec. 4 3:00PM - 3:10PM Room: E451A

Participants

Mei Xue, Beijing , China (*Presenter*) Nothing to Disclose Jing Li, MD, PhD, Beijing, China (*Abstract Co-Author*) Nothing to Disclose Shunan Che, MD, Beijing, China (*Abstract Co-Author*) Nothing to Disclose Yuan Tian, Beijing, China (*Abstract Co-Author*) Nothing to Disclose Xiaojun Luo, Beijing, China (*Abstract Co-Author*) Nothing to Disclose Li-Yun Zhao, Beijing, China (*Abstract Co-Author*) Nothing to Disclose Lizhi Xie, Dalian, China (*Abstract Co-Author*) Nothing to Disclose Bing Wu, Beijing, China (*Abstract Co-Author*) Nothing to Disclose Xiong Zhang, Beijing , China (*Abstract Co-Author*) Nothing to Disclose Yan Jia, Beijing, China (*Abstract Co-Author*) Nothing to Disclose Xiang-Fei Chai, Guangzhou, China (*Abstract Co-Author*) Nothing to Disclose

For information about this presentation, contact:

9476138@qq.com

PURPOSE

To explore the use of noninvasive dynamic contrast-enhanced magnetic resonance imaging (DCE-MRI) and clinicopathologic risk factors based on radiomics for preoperative prediction of axillary lymph node metastasis (ALN) in breast cancer.

METHOD AND MATERIALS

The prediction model was developed in a primary cohort that consisted of 215 patients who was diagnosed with breast cancer(ALN Metastasis (+): 54; ALN Metastasis (-): 161). Radiomic features were extracted from the early and late stage of DCE-MRI of breast cancer. The primary cohort was randomly divided into two independent subsets: a training set (80%, 171 patients with 43 positive SLN) and a validation set (20%, 44 patients with 11 positive SLN). A total of 2058 candidate radiomics features(1029 for each stage) that were extracted from DCE-MRI images of the above two stages. 9 radiomics features were selected from 2058 features using 10-fold cross-validation LASSO model. We incorporated the radiomics signature and independent clinicopathologic risk factors. A random forest classifier was also built using union features. The performance of the classifier was assessed with the area under the ROC curve (AUC), sensitivity, specificity and precision of training set and validation set.

RESULTS

The prediction model using DCE-MRI radiomics alone achieved a AUC of 0.846(95% CI [0.740-0.935]), and the sensitivity, specificity and precision respectively were 0.64, 0.88, and 0.64 in the independent validation set. While the combination of DCE-MRI radiomic features with clinicopathologic characteristics achieved a high AUC of 0.912 (95% CI [0.819-0.979]) in the independent validation set, and the sensitivity, specificity and precision were 0.91, 0.88, and 0.71, respectively, which outperformed the prediction model using DCE-MRI radiomics alone.

CONCLUSION

This study presents a radiomics analysis based on DCE-MRI that incorporates the radiomics signature could be conveniently used to facilitate the preoperative individualized prediction of ALN metastasis in patients with breast cancer, especially when it combines with clinicopathologic characteristics can improved the prediction performance.

CLINICAL RELEVANCE/APPLICATION

The subsequent analysis of radiomics features can provide potential noninvasive biomarkers for clinical-decision support, it may be used to predict the axillary lymph node metastasis of breast cancer before operation.

SSM02-02 Do Preoperative Dynamic Radiomic Features Based on Pharmacokinetic Modeling Dynamic Contrast-Enhanced Magnetic Resonance Imaging Correlate with Prognostic Factors in Breast Cancer?

Participants

Hong Bing Luo, MD, Cheng Du , China (*Presenter*) Nothing to Disclose Jing Ren, Cheng du, China (*Abstract Co-Author*) Nothing to Disclose Peng Zhou, Chengdu , China (*Abstract Co-Author*) Nothing to Disclose

For information about this presentation, contact:

rohbin@163.com

PURPOSE

To correlate preoperative dynamic radiomic features based on PK-DCE-MRI with prognostic factors of breast cancer.

METHOD AND MATERIALS

224 patients histopathologically proven breast cancer were retrospectively reviewed. 97 dynamic radiomic features including 22 pharmacokinetic quantitative parameters (Ktrans, Kep and Vp) with corresponding histogram features and 75 texture features were obtained. These features were compared using the Mann-Whitney U-test between every two groups defined of pathologic and immunohistochemical prognostic factors. Binary logistic regressions were applied to classify these prognostic factors, and ROCs were plotted to determine the performance.

RESULTS

4, 21, 4 of 97 radiomic features between DCIS versus IDC, LN metastasis negative versus positive, and histologic grade nonhigh versus high groups were statistically different respectively (p<0.05). The sensitivity and specificity of regression models for IDC, LN metastasis positive and histologic grade high identification were 55.2% and 84.2%, 77.5% and 45.9%, 64.7% and 58.7%. 22, 23, 33, 18, 6, 3 of 97 radiomic features were statistically different (p<0.05) between ER negative versus ER positive, PR negative versus PR positive, HER2 negative versus HER2 positive, Ki-67 low versus high, EGFR negative versus positive, and CK5/6 negative versus positive groups respectively. The sensitivity and specificity of comprehensive models for ER, PR, HER2, Ki-67, EGFR, CK5/6 identification were 39.9% and 84.8%, 46.1% and 71.1%, 57.8% and 82.1%, 59.6% and 71.7%, 92.3% and 68.2%, 51.5% and 72.2% respectively .

CONCLUSION

Dynamic radiomic features based on PK-DCE-MRI may serve as potential imaging biomarkers for prognosis prediction in breast cancer .

CLINICAL RELEVANCE/APPLICATION

(dealing with Radiomics based on DCE-MRI and breast cancer prognosis prediction) ' Preoperative dynamic radiomic features based on PK-DCE-MRI may serve as potential imaging biomarkers for prognosis prediction in breast cancer.

SSM02-03 Breast Cancer Molecular Subtype Prediction Using Radiomic Signature on Two-Dimensional Synthetic Mammography from Digital Breast Tomosynthesis

Wednesday, Dec. 4 3:20PM - 3:30PM Room: E451A

Participants

Jin Woo Son, MD, Seoul, Korea, Republic Of (*Presenter*) Nothing to Disclose Eun-Kyung Kim, MD, Seoul, Korea, Republic Of (*Abstract Co-Author*) Nothing to Disclose Sungwon Kim, MD, Seoul, Korea, Republic Of (*Abstract Co-Author*) Nothing to Disclose

PURPOSE

To predict molecular subtype of breast cancer using radiomic signature extracted from two-dimensional synthetic mammography reconstructed from digital breast tomosynthesis (DBT).

METHOD AND MATERIALS

From December 2015 to July 2016, 150 patients with newly diagnosed pathologically confirmed breast cancer who had undergone preoperative DBT were identified and assigned to the training set. Specifically, 50 consecutive patients were enrolled in the training set for each molecular subtype (luminal A+B, luminal; HER2-positive, HER2; triple negative, TN). A temporally independent validation cohort consisted of consecutive 71 patients with breast cancer between August 2016 and September 2016 (50 luminal, 9 HER2, and 12 TN). Total of 129 radiomic features was extracted from the craniocaudal (CC) and mediolateral oblique (MLO) view of the synthetic mammography. The performances of three binary radiomic classifications for each subtype were measured using the area under the receiver operating characteristic curve (AUC). The radiomic classification model was built using the elastic-net with tenfold cross-validation and validated in the independent validation cohort.

RESULTS

The three radiomic models were built from the selected 21 features for TN vs non-TN, 19 for HER2 vs non-HER2 and 67 for luminal vs non-luminal. In the training set, the radiomic models yielded an AUC of 0.834 for TN, 0.842 for HER2, and 0.941 for luminal subtypes. In the validation cohort, the radiomic models yielded an AUC of 0.838 for TN, 0.556 for HER2, and 0.645 for luminal subtypes. With the optimal cut-off value of radiomics signature, sensitivity, and specificity of the models in the validation cohort were 83.3% and 79.7% for TN, 11.1% and 79.0% for HER2, 44.0% and 66.7% for luminal subtypes, respectively.

CONCLUSION

The radiomic signature derived from the synthetic mammography from DBT showed high performance in distinguishing between TN and non-TN breast cancer. However, it showed poor performances in distinguishing the other subtypes.

CLINICAL RELEVANCE/APPLICATION

The radiomic signature from the synthetic 2D mammography of the DBT may serve as a biomarker to distinguish TN subtype of breast cancer and may affect the direction of treatment.

SSM02-04 Multiparametric MR Imaging Radiomics Predicts the Recurrence Risks Derived from Oncotype DX Gene Signatures in Estrogen Receptor Positive Breast Cancer

Wednesday, Dec. 4 3:30PM - 3:40PM Room: E451A

Participants

Wan-Chen Tsai, MD, Taipei, Taiwan (*Presenter*) Nothing to Disclose Tengfei Li, Chapel Hill, NC (*Abstract Co-Author*) Nothing to Disclose Bingxin Zhao, Chapel Hill, NC (*Abstract Co-Author*) Nothing to Disclose Cherie M. Kuzmiak, DO, Chapel Hill, NC (*Abstract Co-Author*) Research Grant, Delphinus Medical Technologies, Inc Kaiming Chang, Taipei, China (*Abstract Co-Author*) Nothing to Disclose Kuo-Jang Kao, Taipei, Taiwan (*Abstract Co-Author*) Nothing to Disclose Weili Lin, PhD, Chapel Hill, NC (*Abstract Co-Author*) Nothing to Disclose

For information about this presentation, contact:

wctsai@kfsyscc.org

PURPOSE

The Oncotype DX score (ODX) plays a pivotal role for risk stratification in Estrogen receptor (ER) positive breast cancer patients, where only high-risk patients exhibit significant benefit from adjuvant chemotherapy. This study assessed how multiparametric MR imaging radiomics can be used to stratify ER positive breast cancer patients in high versus low (Exp-1), high versus intermediate to low (Exp-2), and low versus intermediate to high (Exp-3) ODX risks, respectively.

METHOD AND MATERIALS

This study was approved by the local IRB and written consent were obtained from 124 ER positive breast cancer patients who underwent research MR imaging. ODX predictors of the primary tumors were obtained from RNA microarray gene assay. Radiomic features were extracted from multiparametric MR images including T1 weighted images (WIS), pharmacokinetic maps derived from a perfusion sequence (4.49sec/phase for 75 phases), T2 WIS (post contrast T2, T2c), and DCE images (90sec/phase for 4 phases). Extreme gradient boosting (XGBoost) was used for the three prediction tasks (Exp 1 - 3). Leave-one-out cross validation and area under the receiver operating characteristic curve (AUC) were conducted to access classification performance.

RESULTS

There were 51 low, 26 intermediate, and 47 high ODX risk patients. Among all different combinations of sequences, T2c+DCE achieves the highest AUC for Exp-1 (0.83, 95%CI: 0.75-0.91), and Exp-2 (0.78, 95%CI: 0.69-0.85), respectively, whereas T2c yields the highest AUC for Exp-3 (0.74, 95%CI: 0.65-0.83). These results underscore the importance of T2c+DCE for stratifying high-risk from either low or intermediate/low-risk patients. In contrast, T2c alone enables the best prediction of low-risk from intermediate to high risk patients. The identified important features for risk stratification include T2 max signal, early and delayed enhancement texture. Comparing to previously reported results where only DCE was employed, adding T2c features improve the prediction performance of AUC by 11-15% in risk prediction.

CONCLUSION

Multiparametric MR radiomics with T2c and DCE sequences shows promise for recurrence risk prediction in ER positive breast cancer patients.

CLINICAL RELEVANCE/APPLICATION

In addition to DCE features, the inclusion of features extracted from T2W images further improve recurrence risk prediction in ER positive breast cancer patients.

SSM02-05 Diagnosis of Benign and Malignant Breast Lesions on DCE-MRI Using Radiomics and Deep Learning with Peri-Tumor Tissue

Wednesday, Dec. 4 3:40PM - 3:50PM Room: E451A

Participants

Meihao Wang, MD, Wenzhou, China (*Presenter*) Nothing to Disclose Yang Zhang, Irvine, CA (*Abstract Co-Author*) Nothing to Disclose Jiejie Zhou, Wenzhou, China (*Abstract Co-Author*) Nothing to Disclose Kyoung Eun Lee, MD, Seoul, Korea, Republic Of (*Abstract Co-Author*) Nothing to Disclose Kai-Ting Chang, Irvine, CA (*Abstract Co-Author*) Nothing to Disclose Peter Chang, MD, San Francisco, CA (*Abstract Co-Author*) Nothing to Disclose Daniel S. Chow, MD, Orange, CA (*Abstract Co-Author*) Nothing to Disclose Ouchen Wang, Wenzhou, China (*Abstract Co-Author*) Nothing to Disclose Jiance Li, Wenzhou, China (*Abstract Co-Author*) Nothing to Disclose Min-Ying Su, PhD, Irvine, CA (*Abstract Co-Author*) Nothing to Disclose

For information about this presentation, contact:

wzwmh@wmu.edu.cn

PURPOSE

To evaluate the diagnostic accuracy of lesions detected on DCE-MRI using ROI-based, radiomics and deep learning methods considering peri-tumor tissues.

METHOD AND MATERIALS

Retrospective cases from 91 malignant and 62 benign lesions were used for training. Fuzzy-C-means clustering and region growing were applied for tumor segmentation, and from which the tumor volume and mean DCE parameters were measured. DCE contained 6 frames, and three parametric maps (F2-F1, F3-F1, and F6-F3) were generated. A total of 99 texture and histogram parameters were calculated for each case, and 15 were selected using random forest to build a radiomics model. Deep learning was

implemented using ResNet50, evaluated with 10-fold cross-validation in training set. The tumor alone, smallest bounding box, and 1.2, 1.5, 2.0 times enlarged boxes were used as inputs to investigate the diagnostic impact of peri-tumor tissue. ROC curve was generated based on the predicted per-slice malignancy probability. For per-lesion diagnosis, the highest probability among all slices of one lesion was used. The developed models from the training set were tested in prospective cases collected in recent 6 months (48 malignant, 26 benign). In addition, T2 was used to replace F3-F1 in ResNet to investigate its diagnostic role.

RESULTS

The diagnostic accuracy was 76% using ROI-based, 84% using radiomics, and 86% using ROI+radiomics models. In deep learning using per-slice basis, the AUC was comparable for tumor alone, smallest and 1.2 times box (0.97-0.99), significantly higher than 1.5 and 2.0 times box (0.86 and 0.71, p < 0.001). For per-lesion diagnosis, the highest accuracy of 91% was achieved when using the smallest bounding box. The accuracy in the testing dataset were worse in per-slice basis, but when the results were combined to give per-lesion diagnosis, the accuracy only decreased slightly to 89%. When replacing F3-F1 with T2, the specificity was improved from 81% to 85%, and accuracy to 91%.

CONCLUSION

Deep learning using ResNet50 achieved a high diagnostic accuracy. Including small amount of peri-tumor tissue adjacent to tumor led to a higher accuracy compared to using tumor alone or larger boxes.

CLINICAL RELEVANCE/APPLICATION

Deep learning using ResNet algorithm by including adjacent peri-tumor tissue as input yielded a high differential diagnostic accuracy around 90%, and when T2 was considered specificity was improved.

SSM02-06 Quantitative versus Qualitative Ultrasonographic Feature Analysis in Associating with Clinicopathological and Immunohistochemical Characteristics of Triple-Negative Invasive Breast Carcinomas

Wednesday, Dec. 4 3:50PM - 4:00PM Room: E451A

Participants

Jiawei Li, PhD,MD, Shanghai, China (*Presenter*) Nothing to Disclose Zhou Fang, Shanghai, China (*Abstract Co-Author*) Nothing to Disclose Jin Zhou, Shanghai, China (*Abstract Co-Author*) Nothing to Disclose Cai Chang, Shanghai, China (*Abstract Co-Author*) Nothing to Disclose Yi Guo, Shanghai, China (*Abstract Co-Author*) Nothing to Disclose Yuanyuan Wang, PhD, Shanghai, China (*Abstract Co-Author*) Nothing to Disclose

For information about this presentation, contact:

jiaweili2006@163.com

PURPOSE

Ultrasonographic features are associated with clinicopathological and immunohistochemical characteristics of triple-negative breast cancer (TNBC). To predict the biological property of TNBC, the performance using quantitative high-throughput sonographic feature analysis was compared with that using qualitative feature assessment.

METHOD AND MATERIALS

We retrospectively reviewed ultrasound images, clinical, pathological and immunohistochemical data of 156 patients who were pathologically diagnosed as TNBC. According to the histological grade, Ki67 expression level and human epidermal growth factor receptor 2 (HER-2) score, all patients were divided to two groups. The qualitative sonographic features assessment included shape, margin, posterior acoustic pattern and calcification based on the Breast Imaging Reporting and Data System (BI-RADS). Quantitative sonographic features were acquired based on the computer aided radiomics analysis. The breast cancer masses were automatically segmented from the surrounding breast tissues by deep convolution neural network. From each ultrasound image, 460 radiomics features in terms of intensity, morphology, texture and wavelet decomposition were extracted. As shown in Figure 1, sparse representation and support vector machine (SVM) were used to determine the high-throughput sonographic features that were highly correlated to clinicopathological and immunohistochemical data of TNBC. The performance using sonographic features to predict biological property of TNBC was represented by area under curve (AUC) of the receiver operating characteristic (ROC) curve.

RESULTS

In the qualitative assessment, regular tumor shape, no angular or spiculated margin, posterior acoustic enhancement and no calcification were used as the independent sonographic features for TNBC. Using the combination of these four features to predict the histological grade, Ki67, and HER2, the AUC was 0.678, 0.717 and 0.668, respectively. The number of high-throughput features that are highly associated with biological properties was 40 for histological grade (AUC 0.794), 60 for Ki67 level (AUC 0.882), and 125 for HER2 score (AUC 0.978).

CONCLUSION

High-throughput ultrasonographic features are superior to qualitative ultrasound features in predicting biological behavior of TNBC.

CLINICAL RELEVANCE/APPLICATION

High-throughput ultrasonographic features have the potential to differentiate TNBCs with aggressive biological property.





SSM03

Cardiac (Myocardial Disease)

Wednesday, Dec. 4 3:00PM - 4:00PM Room: S401CD



AMA PRA Category 1 Credit ™: 1.00 ARRT Category A+ Credit: 1.00

FDA Discussions may include off-label uses.

Participants

Hajime Sakuma, MD, Tsu, Japan (*Moderator*) Research Grant, EIZAI; Research Grant, DAIICHI SANKYO Group; Research Grant, FUJIFILM Holdings Corporation; Research Grant, Guerbet SA; Research Grant, Nihon Medi-Physics Co, Ltd; Borek Foldyna, MD, Boston, MA (*Moderator*) Nothing to Disclose Friedrich D. Knollmann, MD, PhD, Wynnewood, PA (*Moderator*) Nothing to Disclose

Sub-Events

SSM03-01 Role of Cardiac Magnetic Resonance (CMR) Imaging for Early Detection of Myocardial Involvement in Patients Affected by Anderson- Fabry Disease (AFD)

Wednesday, Dec. 4 3:00PM - 3:10PM Room: S401CD

Participants

Simona Coco, MD, Roma, Italy (*Presenter*) Nothing to Disclose Angelica Bracci, Rome, Italy (*Abstract Co-Author*) Nothing to Disclose Gianluca de Rubeis, Rome, Italy (*Abstract Co-Author*) Nothing to Disclose Nicola Galea, MD, Rome, Italy (*Abstract Co-Author*) Spouse, Employee, Merck & Co, Inc Marco Francone, MD,PhD, Rome, Italy (*Abstract Co-Author*) Nothing to Disclose Carlo Catalano, MD, Rome, Italy (*Abstract Co-Author*) Nothing to Disclose Francesco Cilia, MD, Rome, Italy (*Abstract Co-Author*) Nothing to Disclose Rosa Maria Ammendola, Rome, Italy (*Abstract Co-Author*) Nothing to Disclose

For information about this presentation, contact:

simona.coco@uniroma1.it

PURPOSE

Cardiomyopathy is a complication of Anderson-Fabry Disease (AFD) with dramatic impact on morbidity and mortality; medical therapy is recommended in patients with evidence of cardiac involvement. However, early identification of cardiac involvement in AFD patients may be arduous at pre-hypertrophic stage. Our aim was to evaluate the role of Cardiac Magnetic Resonance (CMR) in early detection of cardiac involvement in AFD at pre-hypertrophic stage.

METHOD AND MATERIALS

16 biopsyproven AFD patients with normal maximal wall thickness at echocardiography (<11mm) underwent to CMR (1.5 T, Avanto, Siemens, Erlangen, Germany) with following sequence protocol: STIR T2w, cineMR, late enhancement and T1 mapping with MOLLI technique before and 15 minutes after injection of 0.15 mmol/Kg gadolinium (GdDOTA, Guerbet, Paris, France). Indexed LV volumes and mass, native T1 (nT1), extracellular volume fraction (ECV) and tissue tracking parameters were analyzed. Results were compared with 16 healthy age and gendermatched volunteers.

RESULTS

No significative differences were found in myocardial mass (Mass/BSA:45,61vs51,24 g/m2,p:0,27), ventricular volumes (EF:58,9vs60,62%,p:0,62) and left ventricular myocardial strain (Global radial strain:46,11vs42,75,p:0,65; global circumferential strain:-20,4vs-18,8,p:0,26; global longitudinal strain:-20,9 vs-18,7,p:0,09) between AFD and healthy subjects. No subjects had shown edema or LGE; nT1 was significantly lower (p=0,01) in AFD patients (988+/-58 ms) than healthy volunteer cohort (1024+/-63 ms); no significative differences was noted between the two groups in ECV values (23%vs24,2%,p:0,23).

CONCLUSION

Native T1 value appears the only marker of early myocardial involvement in pre-hypertrophic AFD patients.

CLINICAL RELEVANCE/APPLICATION

AFD patients should be treated as soon as early signs of organ injury occur (kidney, heart and/or neurological signs). Enzyme replacement therapy is the only specific treatment for AFD but is very expensive and limited to patients with demonstrated organ involvement. Native T1 mapping appear to be reliable and accurate to detect early cardiac involvement before hypertrophic phenotype expression.

SSM03-02 Impact of Myocardial Fibrosis on Left Ventricular Function Evaluated by Feature Tracking Myocardial Strain CMR in Competitive Male Triathletes with Normal Ejection Fraction

Wednesday, Dec. 4 3:10PM - 3:20PM Room: S401CD

Participants

Enver G. Tahir, MD, Hamburg, Germany (*Presenter*) Nothing to Disclose Jitka Starekova, MD, Hamburg, Germany (*Abstract Co-Author*) Nothing to Disclose Kai Muellerleile, Hamburg, Germany (*Abstract Co-Author*) Nothing to Disclose Maxim Avanesov, MD, Hamburg, Germany (*Abstract Co-Author*) Nothing to Disclose Julius M. Weinrich, Hamburg, Germany (*Abstract Co-Author*) Nothing to Disclose Christian Stehning, Hamburg, Germany (*Abstract Co-Author*) Nothing to Disclose Christian Bohnen, Hamburg, Germany (*Abstract Co-Author*) Nothing to Disclose Ulf K. Radunski, Hamburg, Germany (*Abstract Co-Author*) Nothing to Disclose Gerhard B. Adam, MD, Hamburg, Germany (*Abstract Co-Author*) Nothing to Disclose Gunnar K. Lund, MD, Hamburg, Germany (*Abstract Co-Author*) Nothing to Disclose

For information about this presentation, contact:

e.tahir@uke.de

PURPOSE

To analyze the impact of myocardial fibrosis on left ventricular (LV) function evaluated by feature-tracking strain analysis using cine cardiac magnetic resonance (CMR) in competitive male triathletes with normal ejection fraction.

METHOD AND MATERIALS

78 asymptomatic male triathletes with >10 weekly training hours (43 ± 11 years) and 28 male age-matched controls were studied by late gadolinium enhancement (LGE) and cine CMR. Global and segmental radial, longitudinal and circumferential strains were analyzed using feature-tracking cine CMR. Focal non-ischemic LGE was observed in 15 of 78 triathletes (19%, LGE+) with predominance in basal inferolateral segments. LV ejection fraction was normal in LGE+ ($62\pm6\%$) and in LGE- triathletes ($62\pm5\%$, P=0.958). In contrast, global radial strain was lower in LGE+ triathletes with 40 $\pm7\%$ compared to LGE- triathletes ($45\pm7\%$, P<0.05). Reduced segmental radial strain occurred either in LGE+ segments or in directly adjacent segments. Strain analysis revealed regional differences in controls with highest radial and longitudinal strain in the inferolateral segments, which were typically affected by fibrosis in LGE+ triathletes.

RESULTS

Focal non-ischemic LGE was observed in 15 of 78 triathletes (19%, LGE+) with predominance of the basal inferolateral segments. LV ejection fraction was normal in LGE+ ($62 \pm 6\%$) and in LGE- triathletes ($62 \pm 5\%$, P=0.958). In contrast, global radial strain was lower in LGE+ triathletes with 40 $\pm 7\%$ compared to LGE- triathletes ($45 \pm 7\%$, P<0.05). Reduced segmental radial strain occurred either in LGE+ segments or in directly adjacent segments. Strain analysis revealed regional differences in controls with highest radial and longitudinal strain in the inferolateral segments, which were typically affected by fibrosis in LGE+ triathletes.

CONCLUSION

Reduced global and regional radial strain suggests a negative effect of myocardial fibrosis on LV function in LGE+ triathletes with normal ejection fraction. The observed regional differences in controls with highest radial and longitudinal strains in the inferolateral segments may explain the typical occurrence of fibrosis in this myocardial region in triathletes.

CLINICAL RELEVANCE/APPLICATION

Non-ischemic myocardial fibrosis might cause subclinical impairment of LV systolic function in athletes.

SSM03-03 Multiparametric Cardiac Magnetic Resonance Detects Extensive Subclinical Myocardial Disease in Patients with Advanced Liver Cirrhosis

Wednesday, Dec. 4 3:20PM - 3:30PM Room: S401CD

Participants

Alexander Isaak, Bonn, Germany (*Presenter*) Nothing to Disclose Michael Praktiknjo, Bonn, Germany (*Abstract Co-Author*) Nothing to Disclose Darius Dabir, Bonn, Germany (*Abstract Co-Author*) Nothing to Disclose Anton Faron, MD, Bonn, Germany (*Abstract Co-Author*) Nothing to Disclose Christian Jansen, Bonn, Germany (*Abstract Co-Author*) Nothing to Disclose Daniel Kuetting, MD, Bonn, Germany (*Abstract Co-Author*) Nothing to Disclose Daniel K. Thomas, MD, PhD, Bonn, Germany (*Abstract Co-Author*) Nothing to Disclose Julian A. Luetkens, MD, Bonn, Germany (*Abstract Co-Author*) Nothing to Disclose

For information about this presentation, contact:

alexander.isaak@ukbonn.de

PURPOSE

Liver cirrhosis is the end-stage of different chronic liver diseases and causes multi-systemic pathologies, leading to a high mortality level, especially in mid-age people. Cirrhotic cardiomyopathy (CCM) was defined as a cardiac involvement in patients suffering from cirrhosis, which can increase the risk for cardiac dysfunction and induce poor prognosis, especially in the context of other invasive procedures such as surgery, transjugular intrahepatic portosystemic shunt (TIPS) or liver transplantation. We aimed to determine the extent of cardiovascular involvement in patients with liver cirrhosis by a comprehensive cardiac magnetic resonance (CMR) approach.

METHOD AND MATERIALS

Patients with advanced cirrhosis (n=15; mean MELD-Score: 15±5), without known cardiac disease and preserved ejection fraction

as well as matched control subjects (n=15) underwent CMR. In the setting of a multiparamteric CMR protocol, cardiac function, T1 relaxation times, T2 relaxation times, visible myocardial edema, extracellular volume fraction (ECV) and late gadolinium enhancement (LGE) were determined.

RESULTS

Patients suffering from cirrhosis showed significant changes in myocardial tissue composition (native T1 relaxation times: 1018 ± 48 ms vs. 953 ± 32 ms, P<0.001; T2 relaxation times: 59 ± 3 ms vs. 53 ± 3 ms, P<0.001; ECV: 36.7 ± 6.4 % vs. 29.2 ± 5.7 %, P=0.002). Non-ischemic LGE indicating fibrosis was found in 6/15 (40%) patients (P<0.001). No differences in left ventricular ejection fraction were present between both groups ($65\pm6\%$ vs. 64 ± 3 %, P=0.100).

CONCLUSION

Comprehensive CMR showed extensive myocardial alterations in patients with cirrhosis without history for cardiac disease or symptoms. The elevated markers for focal and diffuse myocardial fibrosis and inflammation indicate a high prevalence of subclinical myocardial disease in cirrhotic patients. Subclinical myocardial disease might be a precursor of CCM in patients with advanced liver cirrhosis.

CLINICAL RELEVANCE/APPLICATION

Comprehensive CMR revealed a high burden of cardiovascular disease in patients with advanced liver cirrhosis and might serve as a potential new screening parameter for CCM.

SSM03-04 Circulating microRNAs as Biomarkers for Myocardial Fibrosis in Hypertrophic Cardiomyopathy

Wednesday, Dec. 4 3:30PM - 3:40PM Room: S401CD

Participants

Kate Hanneman, MD, FRCPC, Toronto, ON (*Presenter*) Medical Advisory Board, sanofi-aventis Group Filio Billia, Toronto, ON (*Abstract Co-Author*) Nothing to Disclose Shanna Stanley Hasnain, Toronto, ON (*Abstract Co-Author*) Nothing to Disclose Daniela Grothe, Toronto, ON (*Abstract Co-Author*) Nothing to Disclose Harry Rakowski, Toronto, ON (*Abstract Co-Author*) Nothing to Disclose Andrew M. Crean, MD, Cincinnati, OH (*Abstract Co-Author*) Research support, sanofi-aventis Group

PURPOSE

Circulating microRNAs (miRNAs) are important regulators of a range of cellular processes and may represent novel biomarkers for myocardial disease. The purpose of this study was to evaluate whether miRNAs are differentially expressed in the blood of patients with hypertrophic cardiomyopathy (HCM) and whether they correlate with cardiac magnetic resonance imaging (MRI) findings.

METHOD AND MATERIALS

Thirty HCM patients (51.4±11.6 years, 80.0% male) and 10 healthy controls (38.9±12.6 years, 70.0% male) were prospectively recruited. Peripheral plasma levels of 11 miRNAs were assessed by quantitative real-time polymerase chain reaction and compared between HCM patients and controls. Cardiac MRI was performed at 3T including late gadolinium enhancement (LGE) and T1 mapping using a modified inversion recovery Look-Locker (MOLLI) sequence.

RESULTS

Sixteen HCM patients demonstrated LGE (53.3%), quantified at $9.5\pm7.3\%$ of left ventricular (LV) mass. Native T1 values were significantly higher in HCM patients with LGE compared to those without (1281.5±62.4 ms vs. 1234.9±62.4 ms, p=0.017). Four miRNAs were significantly downregulated in all HCM patients (miRNA-10b, -17, -133, and -18a). Two miRNAs were significantly downregulated in HCM patients with LGE but not in those without LGE (miRNA-192, fold change -2.15, p=0.024 and miRNA-133, fold change -1.84, p=0.028) and one miRNA was significantly upregulated only in patients with extensive fibrosis (defined as LGE >15% of LV mass; miRNA-146, fold change 8.36, p=0.046), suggesting that these miRNAs may play a role in fibrotic HCM. miRNA-192 correlated significantly with quantitative LGE (r=0.328, p=0.047), whereas miRNA-146 and miRNA-193 correlated significantly with native T1 (r=-0.456, p=0.008 and r=-0.423, p=0.007, respectively).

CONCLUSION

Our data suggest that circulating levels of miRNAs are differentially expressed in the blood of patients with HCM. miRNA-192 is downregulated and miRNA-146 is upregulated in HCM patients with LGE. These miRNAs correlate with cardiac MRI markers of fibrosis, identifying them as potential non-invasive biomarkers for myocardial remodelling assessment in HCM.

CLINICAL RELEVANCE/APPLICATION

Circulating miRNAs are potential non-invasive biomarkers for myocardial fibrosis in HCM. These results support the necessity for future larger studies to confirm these findings and evaluate their prognostic significance.

SSM03-05 The Application Value of Multi-Modal MRI in Assessment of Myocardial Edema in Patients with End-Stage Renal Disease

Wednesday, Dec. 4 3:40PM - 3:50PM Room: S401CD

Participants

Wanlin Peng, MS, Chengdu, China (*Abstract Co-Author*) Nothing to Disclose Huayan Xu, Chengdu, China (*Abstract Co-Author*) Nothing to Disclose Chunchao Xia, Chengdu, China (*Abstract Co-Author*) Nothing to Disclose Zhenlin Li, MD, Chengdu, China (*Abstract Co-Author*) Nothing to Disclose Keling Liu, Chengdu, China (*Presenter*) Nothing to Disclose

PURPOSE

ESRD patients are highly prevalent cardiovascular risk. ME occurred in various cardiovascular disease and precipitate myocardial fibrosis and arrhythmia in ESRD patients, and ultimately lead to heart failure or cardiac death. The study is to compare the

effectiveness of native T1 mapping,T2 mapping and conventional T2-weighted imaging (T2WI) in the detection of myocardial edema in patients with end stage renal disease, and further explore clinical value of ME in early diagnosis of myocardial injury.

METHOD AND MATERIALS

Seventy hemodialysis ESRD patients and 16 age- gender-matched healthy volunteers were prospectively enrolled and underwent CMR. All the parameters from CMR, including native T1 values,T2 values, T2 SI ratio, were measured (cmr42; Circle Cardiovascular Imaging Inc.; Calgary; Canada) and compared. Receiver operating characteristic analysis was performed to determine whether T2 values could be used in discriminating myocardial edema between ESRD patients and normal subjects.

RESULTS

The global T2 and native T1 values of ERSD patients were higher than normal controls (all P<0.05). But there was nosignificant difference in T2 SI ratios between two groups (p=0.146). The myocardial native T1 and T2 values of ESRD patients with preserved and decreased LVEF were both higher than those of normal controls (p<0.05), but there was no significant difference between the two groups in native T1 and T2 values. There was no significant difference between the three groups in T2 SI values (p=0.366). Moreover, the global T2 values of patients with MF and without MF were higher than normal controls (43.69 \pm 3.62, 41.82 \pm 3.43 v.s 38.79 \pm 3.69ms, respectively, all P<0.05). The global T1 values of ERSD patients with MF was highest among three groups (1286.12 \pm 52.60 v.s 1321.02 \pm 56.65, 1356.79 \pm 40.08ms, respectively, all P<0.05),but no statistical difference were found between normals and patients without MF. There were no significant difference in T2 SI ratios among three groups (p=0.311). In ESRD with MF f, the proportion of left ventricular dysfunction (19, 52.8%) was higher than that in the ESRD without MF (8, 23.5%). By ROC analysis, T2 values exhibited a higher diagnostic accuracy for detecting ME than did native T1 or T2 SI values (0.83 vs. 0.67 and 0.63, all p<0.05). A cutoff value for global myocardial T2 of >= 41.94ms provided a sensitivity and specificity of 73.5% (52.0-85.8%) and 87.5% (61.7-98.4%) for ME in ESRD patients, respectively.

CONCLUSION

The myocardial pathological changes in patients with end stage renal disease were complex. The multiple cardiac magnetic resonance sequence demonstrated that myocardial edema exited in patients with ESRD patients. The CMR T2 mapping technique has a higher accuracy in quantifying the myocardial edema in patients with end stage renal disease compared with native T1 mapping and conventional T2WI.

CLINICAL RELEVANCE/APPLICATION

Early and accurate evaluation of ME in ESRD patients to evaluate the extent and scope of left ventricular myocardial tissue injury is greatly important for adjustment of clinical dialysis and medication intervention programs timely, combination of multiple sequence (includingT2 mapping, native T1 mapping, T2WI) will contribute to detection of diffused ME in ESRD patients.

SSM03-06 Multiparametric Cardiac Magnetic Resonance Imaging in Fabry's Disease Improves Diagnostic Accuracy Compared to T1 Mapping

Wednesday, Dec. 4 3:50PM - 4:00PM Room: S401CD

Participants

Tilman S. Emrich, MD, Mainz, Germany (*Presenter*) Nothing to Disclose Sebastian Benz, Mainz, Germany (*Abstract Co-Author*) Nothing to Disclose Moritz Halfmann, Mainz, Germany (*Abstract Co-Author*) Nothing to Disclose Sarah Lyschik, Mainz, Germany (*Abstract Co-Author*) Nothing to Disclose Christoph Dueber, MD, Mainz, Germany (*Abstract Co-Author*) Nothing to Disclose Julia B. Hennermann, PhD,MD, Mainz, Germany (*Abstract Co-Author*) Nothing to Disclose Christoph Kampmann, MD, Mainz, Germany (*Abstract Co-Author*) Nothing to Disclose Karl F. Kreitner, MD, Mainz, Germany (*Abstract Co-Author*) Nothing to Disclose

For information about this presentation, contact:

tilman.emrich@gmail.com

PURPOSE

Fabry's Disease (FD) is a hereditary, x-chromosomal linked storage disease that lead to accumulation of sphingolipids. Recently published work highlight the diagnostic potential of T1 Mapping in the detection of Fabry's disease. The aim of this study was to evaluate a combined diagnostic approach using basic cardiac parameters, T1 and T2 Mapping as well as left and right ventricular strain values.

METHOD AND MATERIALS

In this retrospective study, 61 patients in all phenotypic stages of Fabry's disease and 57 healthy volunteers were included. CMR was performed at 3T and incorporated CINE imaging, T1 and T2 Mapping as well as Late Gadolinium Enhancement imaging. In a post-processing manner, cvi42 (Circle, Calgary, Canada) was used to calculate global and septal T1 and T2 times as well as left and right ventricular function and Feature-tracking based strain parameters.

RESULTS

In univariate analysis, longitudinal strain parameters outperform conventional and mapping parameters in detection of Fabry's disease. Nevertheless, the combination of left and right ventricular global longitudinal strain (GLS) with T1 Mapping yielded the highest diagnostic accuracy with a sensitivity and specificity of 83.3 and 82.4% (Figure). The combined approach results in significant improvement of diagnostic accuracy compared to a univariate approach, demonstrated by increasing Youden's indexes (YI): YI (T1 Mapping) 0.468 vs YI (LV GLS) 0.623 vs YI (combination) 0.657.

CONCLUSION

A multi-parametric imaging approach incorporating FT strain parameters and T1 Mapping improved the diagnostic accuracy of CMR for detection of Fabry's disease in all stages of disease. Further research is needed to establish Strain imaging as a surrogate for prognosis and therapy.

CLINICAL RELEVANCE/APPLICATION

CMR with T1 Mapping is an important diagnostic method for diagnosis, initiation of therapy and estimation of prognosis in FD. Our work demonstrates the additive value of LV and RV FT strain imaging in FD.







Cardiac (Anatomy and Function)

Wednesday, Dec. 4 3:00PM - 4:00PM Room: S404AB



AMA PRA Category 1 Credit ™: 1.00 ARRT Category A+ Credit: 1.00

Participants

Hildo J. Lamb, MD, PhD, Leiden, Netherlands (*Moderator*) Nothing to Disclose Pamela K. Woodard, MD, Saint Louis, MO (*Moderator*) Researcher, Siemens AG; Research Grant, F. Hoffmann-La Roche Ltd; Consultant, Medtronic plc; ; ; ; ; ; Frandics P. Chan, MD, PhD, San Francisco, CA (*Moderator*) Nothing to Disclose

Sub-Events

SSM04-01 Overdiagnosis of Late Gadolinium Enhancement by Cardiovascular Magnetic Resonance

Wednesday, Dec. 4 3:00PM - 3:10PM Room: S404AB

Participants

Hui Zhou, MD, Changsha, China (*Presenter*) Nothing to Disclose Ping Hu, Changsha, China (*Abstract Co-Author*) Nothing to Disclose Zhenhua Chen, Changsha, China (*Abstract Co-Author*) Nothing to Disclose Moling Zhou, Changsha, China (*Abstract Co-Author*) Nothing to Disclose Yihua Huang, Shenzhen, China (*Abstract Co-Author*) Nothing to Disclose Rong Chen, Changsha, China (*Abstract Co-Author*) Nothing to Disclose

PURPOSE

To evaluate the rate of overdiagnosis of late gadolinium enhancement (LGE) by cardiac magnetic resonance (CMR) in a large-scale comprehensive university hospital.

METHOD AND MATERIALS

This study is a retrospective review of all cardiac magnetic resonance examinations performed in a comprehensive university hospital over a 18-month period. Studies originally reported as positive for myocardial LGE were retrospectively reinterpreted by three subspecialty cardiovascular radiologists with more than 5 years' experience. A CMR was considered negative for LGE when all three cardiovascular radiologists were in agreement that the CMR study was negative for LGE. The location and potential causes for LGE overdiagnosis were recorded.

RESULTS

A total of 523 CMR studies were performed over the study period. LGE was diagnosed in the initial report in 126 of these cases (24.1%). There was discordance between the cardiovascular radiologists and the original radiologist in 32 of 126 (25.4%) cases. Discordance occurred more often where there were partial volume effects (46.9%, 15/32): in interventricular septum caused by RV deep intertrabecular recesses were mistaken for stria LGE (40.0%, 6/15); in lateral wall caused by non-compacted myocardium were mistaken for subendocardial LGE (33.3%, 5/15); in RV insertion point caused by RV cavity were mistaken for patchy LGE (26.7%, 4/15). Crypt and diverticulum (18.8%, 6/32) were mistaken for indramyocardial (50.0%, 3/6) or subendocardial LGE (50.0%, 3/6). Pericardial fat were mistaken for epicardial LGE (15.6%, 5/32); False positive LGE (12.5%, 4/32) as detected by original observers due to a wrong inversion time (TI). Lipomatous metaplasia were mistaken for LGE (3.1%, 1/32). Congenital aneurysm in apical wall were mistaken for transmural LGE (3.1%, 1/32).

CONCLUSION

When compared with the consensus opinion of expert cardiovascular radiologists, we found a high rate of overdiagnosis of LGE by CMR In routine clinical practice. Improvements in the quality of CMR examination and increased recognition of potential diagnostic pitfalls in CMR are recommended to minimize misdiagnosis of LGE.

CLINICAL RELEVANCE/APPLICATION

LGEs diagnosed by CMR are frequently overdiagnosed, which appeared to be due to a lack of recognition of the false positive LGEs. Increased education among radiography technologists, radiologists, and clinicians regarding these imaging pitfalls should be encouraged.

SSM04-02 Single and Multiframe Super-Resolution: Feasibility for Cardiac MRI

Wednesday, Dec. 4 3:10PM - 3:20PM Room: S404AB

Awards

Trainee Research Prize - Medical Student

Participants

Evan Masutani, La Jolla, CA (*Presenter*) Nothing to Disclose Naeim Bahrami, PhD, MSc, San Diego, CA (*Abstract Co-Author*) Nothing to Disclose Albert Hsiao, MD,PhD, La Jolla, CA (*Abstract Co-Author*) Founder, Arterys, Inc; Consultant, Arterys, Inc; Shareholder, Arterys, Inc; Speaker, Bayer AG; Research Grant, Bayer AG; Speaker, General Electric Company; Research Grant, General Electric Company;

For information about this presentation, contact:

emasutan@ucsd.edu

PURPOSE

Cardiac MRI (cMRI) is the clinical reference standard for visual and quantitative assessment of heart function. However, MRI suffers from long acquisition times, averaging over multiple heart beats, and a tradeoff between spatial and temporal resolution. We investigated the use of convolutional neural networks (CNN) to recover spatial resolution of subsampled MR images with the goal of accelerating cMRI.

METHOD AND MATERIALS

With HIPAA compliance and IRB waiver of informed consent, we retrospectively collected 200 short axis (SAX) cine SSFP from cMRI examinations performed at our institution. Spatial-subsampling was simulated by zeroing outer k-space. We simulated downsampling factors ranging from 2-32x. We employed CNNs to perform single-frame and multi-frame superresolution, called k-SRNet and kt-SRNet respectively, to predict full-sampling from subsampled images. We used 70% of cases for training, 20% for validation, and 10% for testing. We compared SRNet and traditional methods of bicubic interpolation and Fourier-based zero-padding (Z-pad) by calculating the Structural Similarity Index (SSIM) between fully-sampled ground truth and each method of upscaling. We report the mean and standard deviation of SSIM and determine statistical significance using paired Student's t-test with type I error threshold of 0.05.

RESULTS

For single frame spatial superresolution (k-SRNet), mean SSIM was 0.943 ± 0.022 for 8x, 0.878 ± 0.036 for 16x, and 0.810 ± 0.052 for 32x upsampling. For multiframe spatiotemporal superresolution (kt-SRNet), mean SSIM was 0.941 ± 0.021 for 8x, 0.886 ± 0.035 for 16x, and 0.816 ± 0.052 for 32x upsampling. In comparison, bicubic interpolation yielded mean SSIM of 0.827 ± 0.054 for 8x and 0.723 ± 0.076 for 16x upsampling. Z-pad yielded mean SSIM of 0.924 ± 0.029 for 8x and 0.857 ± 0.047 for 16x upsampling. SRNet significantly outperformed traditional methods at all upscaling factors.

CONCLUSION

CNNs can recover spatial resolution from spatially subsampled MR images. Multiframe kt-SRNet yielded comparable results to k-SRNet in recovering image quality from spatial undersampling. Both k-SRNet and kt-SRNet appear to be superior to traditional methods of image upsampling, especially for higher upsampling factors.

CLINICAL RELEVANCE/APPLICATION

Convolutional neural networks have potential to reduce the sampling requirements for resolving cardiac structures in cardiac MRI, and may complement other techniques used to accelerate MRI.

SSM04-03 Biventricular and Left Atrial Myocardial Strain Assessment by MRI Feature Tracking in T2DM Patients with and without Hypertension

Wednesday, Dec. 4 3:20PM - 3:30PM Room: S404AB

Participants

Yukun Cao, Wuhan, China (*Presenter*) Nothing to Disclose Guozhu Shao, Wuhan, China (*Abstract Co-Author*) Nothing to Disclose Heshui Shi, MD, Wuhan, China (*Abstract Co-Author*) Nothing to Disclose

PURPOSE

The purpose of this study was to assess left atrium (LA), right ventricle (RV) and left ventricle(LV) strain in type 2 diabetes mellitus (T2DM) patients with and without hypertension using CMR feature tracking (FT) and their underlying relationships with clinical parameters.

METHOD AND MATERIALS

We recruited 20 T2DM patients without hypertension(T2DM-NHT) (mean age: 53 ± 7 years; 11 males), 20 T2DM patients with hypertension(T2DM-HT) and 40 controls matched for gender, age, and BMI to undergo CMR examinations. The LA , LV and RV myocardial strains were evaluated with using routine cine images based on feature-tracking software. The clinical baseline parameters were collected before the CMR examination.

RESULTS

The T2DM-NHT patients had significantly reduced LA global longitudinal (GLS), circumferential (GCS), radial strain (GRS), and RVGLS compared with those in the controls(LAGCS: 27.6 \pm 3.6% vs 33.9 \pm 8.7%; LAGRS: -29.2 \pm 4.7% vs -32.9 \pm 3.9%; LAGLS: 23.8 \pm 5.5% vs 30.9 \pm 6.0%; RVGLS: -22.1 \pm 3.3% vs -26.0 \pm 7.4%, p<0.05 for all). The T2DM-HT patients had significantly greater LAGCS, LAGRS and LAGLS compared with those in T2DM-NHT patients (LAGCS: 39.4 \pm 12.7% vs 27.6 \pm 3.6%; LAGRS: -34.8 \pm 7.3% vs -29.3 \pm 4.7%; LAGLS: 36.7 \pm 17.6% vs 23.8 \pm 5.5%, p<0.05 for all). However, the LA volume, the LV global systolic strain and routine cardiac function were similar between three groups. Moreover, in the diabetic patients, the LA GCS was independently associated with the microalbuminuria levels (standardized β =-0.56, p=0.023), and the LA GLS was independently correlated with diuretic treatment (standardized β =0.313, p=0.027).

CONCLUSION

T2DM-NHT patients with preserved LV function demonstrated impaired LAGRS, LAGLS, LAGCS and RVGLS compared with controls. Hypertension may compensatorily improve LA strain in T2DM patients, as opposed to the microalbuminuria levels. Diuretic treatment can help ameliorate LA function.

CLINICAL RELEVANCE/APPLICATION

In T2DM patients, the impact of hypertension, microalbuminuria levels and diuretic treatment on LA strain deserves further study.

SSM04-04 Association B-Type Natriuretic Peptide (BNP) of and Dialysis Vintage with CMRI- Derived Cardiac Indices in Stable Hemodialysis Patients with Preserved Left Ventricular Ejection Fraction

Wednesday, Dec. 4 3:30PM - 3:40PM Room: S404AB

Participants Xiaoyu Han, Wuhan, China (*Presenter*) Nothing to Disclose Heshui Shi, MD, Wuhan, China (*Abstract Co-Author*) Nothing to Disclose Yukun Cao, Wuhan, China (*Abstract Co-Author*) Nothing to Disclose

For information about this presentation, contact:

xiaoyuhan1123@163.com

PURPOSE

Cardiovascular disease (CVD) is a major cause of morbidity and mortality in (HD) patients. Native T1/T2 mapping and tissuetracking strain analysis by cardiac magnetic resonance imaging (CMRI) are proved to be useful as early quantitative techniques for evaluating myocardial tissue and mechanical alterations in HD patients. We aim to assess the left ventricular myocardial native T1/T2 values and systolic strains and the associations with B-type natriuretic peptide (BNP) and dialysis vintage in HD patients with a preserved left ventricular ejection fraction (LVEF).

METHOD AND MATERIALS

Forty-three stable HD patients (mean age: 59 ± 11 years; 28 males)with end-stage renal disease with a preserved LVEF (>=50%) and 28 healthy volunteers (mean age: 61 ± 7 years; 14 males)matched for sex, age, and body mass index. The native T1/T2 values of the left ventricular myocardium were measured on the T1 and T2 maps. The left ventricular global systolic strain was evaluated on routine cine images using prototype postprocessing software. BNP was measured at the time of CMR measurements.

RESULTS

Compared with controls, the global native T1 and T2 values were significantly higher in the HD patients than in the controls (native T1: $1056\pm32 \text{ ms vs.} 1006\pm25 \text{ ms}$, p<0.001; T2: $50\pm3 \text{ ms vs.} 46\pm2 \text{ ms}$, p<0.001). The mean peak global circumferential strain (GCS) and global longitudinal strain (GLS) were both significantly reduced in the HD patients compared with the controls (GCS: $-13\pm3 \text{ vs.} -16\pm3$, p<0.001; GLS: $-12\pm4 \text{ vs.} -15\pm3$, p=0.001). However, no significant difference was found between two groups regarding LVEF($61\pm8 \text{ vs } 64\pm8$, p=0.057). In HD patients, a significant positive correlation was found between T2 value and BNP levels (r=0.402,p<0.001). The GLS was independently correlated with the dialysis vintage in HD patients (standardized β =-0.321, p=0.044).

CONCLUSION

The HD patients with preserved LVEF have increased native T1/T2 value and decreased strain, while increased T2 values relates to high BNP. GLS may be improved in long-term HD patients.

CLINICAL RELEVANCE/APPLICATION

Multiple advanced CMR technologies, including native T1/T2 mapping and tissue-tracking analysis could detected early cardiomyopathy in HD patients without gadolinium-based contrast agents. The correlation of CMRI-derived cardiac indices with heart failure index BNP and dialysis vintage could help timely prevent cardiovascular disease and assess prognosis in HD patients.

SSM04-05 Preliminary Validation of Turbulent Kinetic Energy Measurement of HOCM by Using Multi-VENC 4D Flow MRI

Wednesday, Dec. 4 3:40PM - 3:50PM Room: S404AB

Participants

Kotomi Iwata, Tokyo, Japan (*Presenter*) Nothing to Disclose Tetsuro Sekine, MD, PhD, Tokyo, Japan (*Abstract Co-Author*) Nothing to Disclose Masaki Tachi, MD, PhD, Tokyo, Japan (*Abstract Co-Author*) Nothing to Disclose Yoichi Imori, Tokyo, Japan (*Abstract Co-Author*) Nothing to Disclose Junya Matsuda, Tokyo, Japan (*Abstract Co-Author*) Nothing to Disclose Yasuo Amano, MD, Tokyo, Japan (*Abstract Co-Author*) Nothing to Disclose Takahiro Ando, Tokyo, Japan (*Abstract Co-Author*) Nothing to Disclose Makoto Obara, Tokyo, Japan (*Abstract Co-Author*) Nothing to Disclose Makoto Obara, Tokyo, Japan (*Abstract Co-Author*) Nothing to Disclose Hitoshi Takano, Tokyo, Japan (*Abstract Co-Author*) Nothing to Disclose Shinichiro Kumita, MD, Tokyo, Japan (*Abstract Co-Author*) Nothing to Disclose

For information about this presentation, contact:

kotomi-iwata@nms.ac.jp

PURPOSE

In the patients with hypertrophic cardiomyopathy (HCM), the impairment of cardiac ejection efficiency due to the obstruction of left ventricle outflow tract (LVOT) relates to the HCM-related death. Recently, the turbulent kinetic energy (TKE) estimation based on 4D Flow MRI has been developed. Previous studies revealed that 4D Flow-based TKE measurement well correlates to the pressure drop at LVOT in the patients with aortic stenosis which has a similar physiological entity as HCM. The purpose of this study was to validate the clinical value of 4D Flow-based TKE measurement in the patients with HCM.

METHOD AND MATERIALS

From April 2018 to March 2019, we recruited consecutive 17 HCM patients. Based on echocardiography, they were assigned into obstructive HCM (HOCM) (9 patients, 67.0 ± 9.9 years old, 4 males) or non-obstructive HCM (HNCM) (8 patients, 68.9 ± 12.8 years old, 5 males). We also recruited 9 normal volunteers(30.9 ± 3.0 years old, 6 males). The parameters of 4D Flow MRI were as follows; resplution=1.7*1.7*2.0mm; Triple VENC acquisition = 50-150-450 cm/s; k-t PCA (acceleration factor, 5-7), free breath acquisition;

and acquisition time 8-15 min.). GT Flow (Gyrotools, Zurich, Switzerland) was used for analysis. The VOI from left ventricular to aortic arch was drawn semi-automatically. We defined TKEphase as the sum of entire VOI at each cardiac phase, and TKEpeak as the highest TKEphase in the all cardiac phase.

RESULTS

TKEpeak of HOCM is significantly higher than HNCM (p=0.008) or volunteers (p=0.002). TKEpeak correlated to max velocity (p=0.007, r=0.631) and maximum short dimeter of the valve orifice (p=0.006, r=-0.658). TKEpeak in the patients with systolic anterior movement (SAM) were significantly higher than without SAM (p=0.008). TKEpeak correlated to LV mass (p=0.035, r=0.514).

CONCLUSION

TKE measurement based on 4D Flow MRI can noninvasively detect the flow alteration induced not only by systolic flow jet but also by LVOT geometry such as SAM in the patients with HOCM. The elevated TKE correlates increasing LV mass. It may indicate that increasing cardiac load by the pressure loss due to turbulence induced the progression of LV mass. This physiology reaction is considered as the worse outcome.

CLINICAL RELEVANCE/APPLICATION

TKE measurement based on 4D Flow MRI can noninvasively detect the flow alteration in the patients with HOCM.

SSM04-06 T2 Mapping and Cardiac Stress Test to Detect and Monitor Myocardial Edema and Ischemia in Female Patients after Left-Sided Breast Cancer Radiation Therapy

Wednesday, Dec. 4 3:50PM - 4:00PM Room: S404AB

Participants

Enver G. Tahir, MD, Hamburg, Germany (Presenter) Nothing to Disclose Sahar Shihada, Hamburg, Germany (Abstract Co-Author) Nothing to Disclose Manuella Azar, Hamburg, Germany (Abstract Co-Author) Nothing to Disclose Jitka Starekova, Hamburg, Germany (Abstract Co-Author) Nothing to Disclose Malte L. Warncke, MD, Hamburg, Germany (Abstract Co-Author) Nothing to Disclose Yvonne Goy, Hamburg, Germany (Abstract Co-Author) Nothing to Disclose Cordula L. Petersen, Dresden, Germany (Abstract Co-Author) Nothing to Disclose Katharina Seiffert, Hamburg, Germany (Abstract Co-Author) Nothing to Disclose Volkmer Muller, Hamburg, Germany (Abstract Co-Author) Nothing to Disclose Isabell Witzel, Hamburg, Germany (Abstract Co-Author) Nothing to Disclose Ulf K. Radunski, Hamburg, Germany (Abstract Co-Author) Nothing to Disclose Sebastian Bohnen, Hamburg, Germany (Abstract Co-Author) Nothing to Disclose Jan Schneider, Hamburg, Germany (Abstract Co-Author) Nothing to Disclose Kai Muellerleile, Hamburg, Germany (Abstract Co-Author) Nothing to Disclose Gerhard B. Adam, MD, Hamburg, Germany (Abstract Co-Author) Nothing to Disclose Gunnar K. Lund, MD, Hamburg, Germany (Abstract Co-Author) Nothing to Disclose

For information about this presentation, contact:

e.tahir@uke.de

PURPOSE

To detect and monitor subclinical cardiomyopathy by cardiac magnetic resonance (CMR) in female patients with first-time diagnosis of left-sided breast cancer following radiation therapy.

METHOD AND MATERIALS

27 female patients (56 ±14 years) with newly diagnosed breast cancer underwent serial 3 Tesla CMR (Ingenia, Philips Medical Systems). Baseline (BL) CMR was performed 18 ±16 days before the start of a left-sided radiation. None of the patients received chemotherapy. First follow-up (FU1) CMR was 7 ±12 days and second follow-up (FU2) 12 ±1 months after completion of radiotherapy. A free-breathing, navigator-gated multi-echo sequence was used for short-axis T2 mapping. Cardiac stress test was performed at 400 μ g regadenoson stress on 3 representative short axis slices (basal, midventricular and apical) using an ultrafast gradient echo sequence.

RESULTS

A mean radiation dose of 47 ±4 Gy was applied with a calculated mean cardiac dose of 2.4 ±2.3 Gy. High sensitive Troponin T increased immediately after radiation therapy (5 ±2 vs. 6 ±3 pg/ml, P<0.05) and declined to baseline values on FU2 (6 ±3 vs. 5 ±2 pg/ml, P<0.05). NT-proBNP and creatine kinase remained unchanged throughout the observation period. LVEF was constant between BL and FU1 (62 ±5 vs. 64 ±6%, P=0.218) and FU1 and FU2 (64 ±6 vs. 62 ±5%, P=0.171). LVEDV declined on FU1 (78 ±10 vs. 75 ±11 ml/m2, P<0.05) and remained decreased on FU2 (72 ±11 ml/m2, P<0.05). RVEDV declined between BL and FU2 (81 ±12 vs. 75 ±13 ml/m2, P<0.05). T2 relaxation times increased on FU1 (47 ±2 vs. 48 ±4 ms, P<0.05) and declined on FU2 (47 ±2 ms, P=0.092). On visual evaluation cardiac stress test did not detect any myocardial ischemia after radiation therapy.

CONCLUSION

Radiation treatment of female left-sided breast cancer can lead to development of myocardial edema and troponin increase in the early phase following therapy, which subside within the first 12 months. Both ventricular volumes decrease after radiation therapy. There is no evidence of myocardial ischemia development within the first 12 months post-radiation.

CLINICAL RELEVANCE/APPLICATION

Development of myocardial edema and decreased of ventricular volumes might be used as indicators for subclinical cardiomyopathy in patients with left-sided breast cancer undergoing radiation therapy.





Chest (Dual-energy CT - Malignancy)

Wednesday, Dec. 4 3:00PM - 4:00PM Room: N226



AMA PRA Category 1 Credit ™: 1.00 ARRT Category A+ Credit: 1.00

FDA Discussions may include off-label uses.

Participants

Patricia J. Mergo, MD, Jacksonville, FL (*Moderator*) Nothing to Disclose Jeffrey B. Alpert, MD, New York, NY (*Moderator*) Nothing to Disclose

Sub-Events

SSM05-01 Improved Differentiation between Primary Lung Cancer and Pulmonary Metastases by Combining Dual-Energy CT Derived Iodine Concentration and Conventional CT Attenuation

Wednesday, Dec. 4 3:00PM - 3:10PM Room: N226

Participants

Dominik A. Deniffel, MD, Toronto, ON (*Presenter*) Nothing to Disclose Yucheng Zhang, Toronto, ON (*Abstract Co-Author*) Nothing to Disclose Andreas Sauter, MD, Munich, Germany (*Abstract Co-Author*) Nothing to Disclose Alexander A. Fingerle, MD, Munich, Germany (*Abstract Co-Author*) Nothing to Disclose Ernst J. Rummeny, MD, Muenchen, Germany (*Abstract Co-Author*) Nothing to Disclose Daniela Pfeiffer, MD, Munich, Germany (*Abstract Co-Author*) Nothing to Disclose

For information about this presentation, contact:

ddeniffel@lunenfeld.ca

PURPOSE

To assess the clinical utility of dual-energy CT (DECT) derived iodine concentration (IC) in addition to conventional CT attenuation (HU) for the discrimination between primary lung cancer and pulmonary metastases from different primary malignancies.

METHOD AND MATERIALS

In this retrospective research ethics board approved study, we analyzed contrast-enhanced DECT scans in 79 patients with primary lung cancer (adenocarcinoma, n=45; squamous cell carcinoma (SCC), n=16; small-cell lung cancer (SCLC), n=18) and 89 patients with pulmonary metastases from primary breast (invasive-ductal adenocarcinoma, n=17), colorectal (adenocarcinoma, n=27), head and neck (squamous cell carcinoma, n=17), kidney (RCC) (clear-cell renal cell carcinoma, n=10) and pancreato-biliary (PBC) (adenocarcinoma, n=18) malignancies. Quantitative IC and conventional HU values were extracted and normalized to the thoracic aorta. Differences between groups were assessed by Kruskal-Wallis test with Dunn's post-hoc correction. Multivariate logistic regression was used to generate a diagnostic model. Diagnostic accuracy was evaluated by the area under receiver operator characteristic (ROC) curve (AUC).

RESULTS

Significant differences in conventional HU values (p<0.001) were found only between SCLC and metastases from RCC, with median HU [IQR] values of 57 [18] and 100 [35], respectively. Significant differences in IC (p<0.05) were noted for SCC (1.3 [0.71] mg/ml) and SCLC (1.2 [0.68] mg/ml) versus pulmonary metastases from RCC (2.8 [1.7] mg/ml) and PBC (2.1 [1.2] mg/ml). In multivariate analysis, both IC (odds ratio 0.16, p<0.0001) and HU (odds ratio 1.06, p<0.0001) were independent diagnostic features for the discrimination of primary lung cancer from pulmonary metastases. The corresponding multivariate model (AUC=0.73) significantly outperformed both single parameters in diagnostic accuracy (IC: AUC=0.57, p<0.01; HU: AUC=0.55, p<0.001), achieving a sensitivity and specificity (at maximum Youden index) of 65.82% and 76.40%, respectively.

CONCLUSION

A combined diagnostic model incorporating both DECT derived IC, and conventional CT attenuation values significantly improves the differentiation between primary lung cancer and pulmonary metastases.

CLINICAL RELEVANCE/APPLICATION

A combination of dual-energy CT derived iodine concentration, and conventional CT attenuation provides improved discrimination between primary lung cancer and pulmonary metastases.

SSM05-02 Improving Diagnostic Accuracy for Pulmonary Nodules with the Combination of Morphological Characteristics and Spectral CT-Specific Multi-Parameters

Wednesday, Dec. 4 3:10PM - 3:20PM Room: N226

He Taiping, MMed, Xianyang, China (*Abstract Co-Author*) Nothing to Disclose Yong Yu, Xianyang City, China (*Abstract Co-Author*) Nothing to Disclose Nan Yu, MD, Xianyang, China (*Abstract Co-Author*) Nothing to Disclose Jianying Li, Beijing, China (*Abstract Co-Author*) Employee, General Electric Company Yun Shen, PhD, Beijing, China (*Abstract Co-Author*) Employee, General Electric Company Researcher, General Electric Company Haifeng Duan, Xianyang City, China (*Abstract Co-Author*) Nothing to Disclose Yongjun Jia, MMed, Xianyang, China (*Abstract Co-Author*) Nothing to Disclose Xirong Zhang, Xianyang, China (*Abstract Co-Author*) Nothing to Disclose Lei Yuxin, MMed, Xianyang City, China (*Abstract Co-Author*) Nothing to Disclose Xiaoxia Chen, MMed, Xianyang City, China (*Abstract Co-Author*) Nothing to Disclose Zhang Yanzi, Xianyang City, China (*Abstract Co-Author*) Nothing to Disclose

For information about this presentation, contact:

395654582@qq.com

PURPOSE

To demonstrate the value of improving pulmonary nodules (PN) diagnostic accuracy by combining the morphological characteristics and spectral CT-specific parameters.

METHOD AND MATERIALS

173 patients with pulmonary nodules (61 benign pulmonary nodules (BPN) and 112 malignant pulmonary nodules (MPN)) underwent dual-phase contrast-enhanced spectral CT. Monochromatic and material decomposition images were reconstructed. The morphological characteristics of PN were observed on 70keV images, including location, size, bronchial truncation, density, shape, lobulation, spiculation, spinous sign, vessel convergence sign, boundary, cavity, necrosis, lymph node, pleural invasion, pleural effusion, enhanced pattern and vascular invasion. The CT values from 40keV to 140keV, Effective-Z, blood concentration (BC), iodine concentration (IC), water concentration (WC) of PN and the aorta at the same level were measured to calculate the slope of spectral HU curve (λ), normalized blood concentration (NBC), normalized iodine concentration (NIC) and normalized water concentration (NWC). The receiver operating characteristic (ROC) curve was drawn to evaluate the diagnostic performance of differentiating BPN from MPN.

RESULTS

The two patient groups were similar demographically (P>0.05). The incidence of bronchial truncation, irregular shape, lobulation, pleural effusion and vascular invasion in MPN was significantly higher than those in BPN (P<0.05). The CT values from 40keV to 90keV, λ 40keV-90keV, λ 100keV-140keV, λ 40keV-140keV, BC, IC, NBC, NIC, Effective-Z values of BPN were significantly higher than those of MPN (P<0.05), while both lesions had similar CT values from 100keV to 140 keV, and WC and NWC values (P>0.05). The diagnostic accuracy in differentiating BPN and MPN (AUC 0.891) with combined morphological characteristics and spectral CT-specific parameters was significantly higher than that of only using morphological characteristics (AUC 0.726) or spectral multi-parameters (AUC 0.843).

CONCLUSION

Morphological characteristics with combination of spectral CT multi-parameters spectral CT can help to improve the diagnostic accuracy in differentiating pulmonary nodules.

CLINICAL RELEVANCE/APPLICATION

The morphological characteristics with combination of multi-parameters based on spectral CT can improve the diagnostic accuracy of pulmonary nodules.

SSM05-03 Comparison in Pulmonary Small Vessel Area and Association with Pulmonary Emphysema between Lower and Standard Energy Data Acquisition: Quantitative Assessment with Dual-Energy Computed Tomography

Wednesday, Dec. 4 3:20PM - 3:30PM Room: N226

Participants

Yukihiro Ichikawa, RT, Osaka,Osaka , Japan (*Presenter*) Nothing to Disclose Yukihiro Nagatani, MD, Otsu, Japan (*Abstract Co-Author*) Nothing to Disclose Tomohiro Hirose, MD, Osaka, Japan (*Abstract Co-Author*) Nothing to Disclose Kenji Furuichi, MD, Osaka, Japan (*Abstract Co-Author*) Nothing to Disclose Norihisa Nitta, MD, Kyoto, Japan (*Abstract Co-Author*) Nothing to Disclose Kie Shindo, MD, Osaka,Osaka, Japan (*Abstract Co-Author*) Nothing to Disclose Akikatsu Sakumoto, RT, Osaka, Japan (*Abstract Co-Author*) Nothing to Disclose Shinsuke Tsubouchi, RT, Suita, Japan (*Abstract Co-Author*) Nothing to Disclose Hao Zhong, Suita,Osaka, Japan (*Abstract Co-Author*) Nothing to Disclose

For information about this presentation, contact:

muff.fuzz.ukulele.guide2@gmail.com

PURPOSE

To investigate the merit of lower energy data acquisition on computed tomography(CT) for the quantification of pulmonary smaller vessels and emphysema

METHOD AND MATERIALS

The institutional review board approved this study and consents from patients were waived because of retrospective study design. A hundred and fifty patients underwent chest CT by using fast kVp switching dual-energy scanner (80/140 kVp) with scan parameters to secure target standard deviation(SD) 11 (Revolution GSI, General Electric Medical Systems, Milwaukee, WI, USA). Scan data were converted to virtual monochromatic images (VMI) at 3 tube voltages; 40, 55 and 70 KeV. Low attenuation area < -950 HU (% LAA-950) was quantified with dedicated software as emphysema extent. By using a free software Image J, percentage of cross-sectional area of pulmonary vessels < 5 mm2 to total lung field (%CSA<5) was calculated as pulmonary small vessel area at predefined 3 trans-axial levels; aortic arch, bronchial bifurcation and right pulmonary veins orifice, and SD in CT density in 10 mm-quadrangular region of interest inside descending aorta was measured as objective image noise (OIN) at the bronchial bifurcation level. %LAA-950 and %CSA<5 in total and each of the 3 levels were compared among the 3 tube voltages by using Friedman and Wilcoxon signed rank test. Spearman's rank correlation analyses were performed to assess the associations of the %LAA-950 and %CSA< 5, and analyses of covariance were performed to assess the similarity of slope of regression lines among the 3 tube voltages.

RESULTS

%CSA<5 on VMI at 40 KeV in total as well as the 3 levels was the largest (1.96 \pm 0.32), followed by that at 55 (1.34 \pm 0.30) and 70 KeV (0.85 \pm 0.27). %LAA-950 on VMI at 40 KeV was also the largest (14.6 \pm 8.9 %), followed by that at 55 (5.9 \pm 7.6 %) and 70 KeV (2.8 \pm 6.6 %). Negative correlation was found between %CSA<5 and %LAA-950 all in the 3 tube voltages (r = -0.529, p <0.001 at 40 KeV). Slope of regression line at 40 KeV was similar to that at 55 KeV irrespective of OIN increase.

CONCLUSION

Data acquisition at 40 KeV can be useful for quantification of pulmonary smaller vessels closely-associated with emphysema on CT.

CLINICAL RELEVANCE/APPLICATION

Data acquisition at 40KeV may be potential to play an important role for early detection of peripheral vessel impairment leading to pulmonary hypertension in combination with iterative reconstruction.

SSM05-04 Can Dual-Energy Derived Perfusion Parameters Provide Information on Tumor Hypoxia? Preliminary Experience in 49 Operable Non-Small Cell Lung Carcinomas

Wednesday, Dec. 4 3:30PM - 3:40PM Room: N226

Participants

Julie Dewaguet, Lille, France (*Abstract Co-Author*) Nothing to Disclose Marie-Christine Copin, MD, PhD, Lille, France (*Abstract Co-Author*) Nothing to Disclose Alain Duhamel, PhD, Lille, France (*Abstract Co-Author*) Nothing to Disclose Thomas G. Flohr, PhD, Forchheim, Germany (*Abstract Co-Author*) Employee, Siemens AG Jacques Remy, MD, Mouvaux, France (*Abstract Co-Author*) Research Consultant, Siemens AG Martine J. Remy-Jardin, MD, PhD, Lille, France (*Presenter*) Research Grant, Siemens AG; Speaker, Siemens AG

For information about this presentation, contact:

martine.remy@chru-lille.fr

PURPOSE

To investigate potential relationships between DECT perfusion characteristics and prognostic histopathologic features.

METHOD AND MATERIALS

A two-phase DECT scanning protocol was obtained in the presurgical evaluation of 49 tumors (squamous cell carcinomas: n=12; adenocarcinomas: n=37), including (a) an early phase over the entire thorax (i.e., intravascular phase of tumoral perfusion); (b) completed by a delayed acquisition over the tumor, 50 s later (i.e., interstitial phase of tumoral perfusion). The first-pass and delayed iodine concentration (IC; mg/mL) and the arterial enhancement fraction (AEF=first pass IC/delayed IC x 100) were calculated over the entire tumor and within the most peripheral 2-mm thick tumor layer, automatically segmented. The expression of the membranous carbonic anhydrase IX (mCAIX), an immunohistochemical marker of hypoxia, was assessed in tumor specimens.

RESULTS

33 tumors were mCAIX positive (Group 1) and 16 mCAIX negative (Group 2), the former showing a statistically significantly larger volume (p=0.04). At the level of the whole tumor, the delayed IC was significantly higher than that at first pass (median: 1.53 vs 1.4; p=0.04), suggestive of extravascular leakage within the interstitial space; there was no difference in DECT perfusion parameters between the two groups. Compared to Group 2, the outer layer of Group 1 tumors had significantly higher median values of IC (0.53 vs 0.21; p=0.02) and AEF (102.6 vs 65.6; p=0.02) with a trend toward higher delayed IC (0.48 vs 0.39; p=0.34). The distribution of neovessel profile was significantly different between Groups 1 & 2 with a greater proportion of functional neovessels in Group 1.

CONCLUSION

DECT can provide insight into perfusion characteristics at the level of the tumoral invasion front.

CLINICAL RELEVANCE/APPLICATION

Hypoxia-induced neovascularization may contribute to tumor progression and metastasis. DECT can provide information on perfusion characteristics at the level of the tumoral invasion front.

SSM05-05 The Predictive Value of Energy Spectrum CT Parameters for Ki67 Expression of Lung Cancer

Wednesday, Dec. 4 3:40PM - 3:50PM Room: N226

Participants

Pei P. Dou, Xuzhou , China (*Presenter*) Nothing to Disclose Zhongxiao Liu, Xuzhou, China (*Abstract Co-Author*) Nothing to Disclose Yankai Meng, Beijing , China (*Abstract Co-Author*) Nothing to Disclose Yingying Cui, Xuzhou , China (*Abstract Co-Author*) Nothing to Disclose Guangjun Cheng, Xuzhou, China (*Abstract Co-Author*) Nothing to Disclose Hongmei Zhang, MD, PhD, Beijing, China (*Abstract Co-Author*) Nothing to Disclose Kai Xu, MD, PhD, Xuzhou, China (*Abstract Co-Author*) Nothing to Disclose Chun-Wu Zhou, MD, Beijing, China (*Abstract Co-Author*) Nothing to Disclose

For information about this presentation, contact:

1062920760@qq.com

PURPOSE

To investigate the predictive value of energy spectrum CT parameters for lung cancer Ki67 expression.

METHOD AND MATERIALS

Between December 2018 and February 2019, 27 primary lung cancer patients confirmed by pathological examination enrolled this prospective cohort study. All patients underwent energy spectrum CT (ESCT) scan. ESCT parameters were derived from dualenergy virtual imaging in Siemens postprocessed workstation by a radiologist (M.Y.K.). All enrollment patients clinicopathological data derived from electronic record system. SPSS 19.0 were used for statistical analysis.Quantitive and qualitative data used X2, t and Rank test respectively.ROC curves were used for analysis predicting performance of the Ki67 expression. P<0.05 was considered statistically significant.

RESULTS

Tumor was larger in Ki67 high expression group than low group (P=0.046). The other demographic and clinicopathological characteristics of all enrollment patients showed no significant difference (Table 2). Venous phase iodine value (IV), iodine ratio (IR) and the slope of the 40-80 keV energy spectrum curve (SP) improved than arterial phase IV, IR and SP, respectively (Fig. 1). The arterial phase IV, IR, SP and venous phase IV are no significant difference in low and high Ki67 expression group (P value ranged from 0.105 to 0.182) (Table 3). There are significantly different in two groups for venous phase IR and SP (0.249 \pm 0.083, 0.360 \pm 0.162, P=0.033 in IR and 1.744 \pm 0.607, 2.562 \pm 1.236, P=0.037 in SP, respectively) (Table 3, Fig. 2). Venous phase IR ROC analysis showed boderline P value (P=0.056) with AUC, sensitivity (SE), specificity (SP) and cutoff value were 0.717, 92.86, 61.54 and <=0.347 respectively. The AUC, SE, SP and cutoff value were 0.698, 92.86, 53.85 and <=2.407 respectively (Table 4, Fig. 6).

CONCLUSION

Venous phase IR and SP based on single energy spectrum curve and iodine image may effectively stratify primary lung cancer Ki67 expression into low and high group. The efficacy of other energy spectrum parameters need further investigation.

CLINICAL RELEVANCE/APPLICATION

The baseline energy spectrum CT parameters may non-invasion predict Ki67 expression. And the results may use for stratification lung cancer patients and individulization treatment in some extent.

SSM05-06 The Application of Spectral CT Multi-Parameter in Differentiating Pathological Types of Lung Cancer

Wednesday, Dec. 4 3:50PM - 4:00PM Room: N226

Participants

Zhanli Ren, Xianyang, China (*Presenter*) Nothing to Disclose
He Taiping, MMed, Xianyang, China (*Abstract Co-Author*) Nothing to Disclose
Yong Yu, Xianyang City, China (*Abstract Co-Author*) Nothing to Disclose
Nan Yu, MD, Xianyang, China (*Abstract Co-Author*) Nothing to Disclose
Yun Shen, PhD, Beijing, China (*Abstract Co-Author*) Employee, General Electric Company Researcher, General Electric Company
Jianying Li, Beijing, China (*Abstract Co-Author*) Employee, General Electric Company
Yongjun Jia, MMed, Xianyang, China (*Abstract Co-Author*) Nothing to Disclose
Haifeng Duan, Xianyang City, China (*Abstract Co-Author*) Nothing to Disclose
Xirong Zhang, Xianyang, China (*Abstract Co-Author*) Nothing to Disclose
Sijin Dong, Xianyang, China (*Abstract Co-Author*) Nothing to Disclose

PURPOSE

To explore the application of spectral CT multi-parameter in differentiating pathological types of lung cancer.

METHOD AND MATERIALS

57 patients with lung cancer who underwent spectral CT imaging were collected, of which there were 24 cases with adenocarcinoma,18 cases with squamous cell carcinoma and 15 cases with small cell lung cancer. The dual-phase (aortic phase and pulmonary venous phase) enhanced scanning was used for all patients. The CT values of 40kev-90kev, iodine concentration(IC), water concentration(WC), effective-Z and the iodine concentration and water concentration of aorta at the same level were measured in the arterial phase, and the normalized iodine concentration(NIC) and the normalized water concentration(NWC) and the spectral curve slope were calculated. One-way ANOVA was used to compare the parameters.

RESULTS

The CT values of 40kev-60kev,iodine concentration,normalized iodine concentration,effective-Z and the spectral curve slope showed significant difference among three kinds of lung cancer(P<0.001).The CT values of 40kev-60kev,iodine concentration,normalized iodine concentration,effective-Z and the spectral curve slope in adenocarcinoma and squamous cell carcinoma were significantly different from small cell lung cancer(P<0.001).The CT values of 40kev-60kev,iodine concentration,normalized iodine concentration,effective-Z and the spectral curve slope in adenocarcinoma were higher than those in squamous cell carcinoma (P<0.001).

CONCLUSION

Spectral CT multi-parameter can be used to identify different pathological types of lung cancer, of which the iodine concentration, normalized iodine concentration, effective-Z, CT values of 40kev-60kev and spectral curve slope played a role in differential diagnosis.

CLINICAL RELEVANCE/APPLICATION

Spectral CT imaging can provide multi-parameter identification basis for the pathological types of lung cancer, which was helpful to determine the reasonable treatment plan and improve the prognosis.





Chest (Infection/Incidental Lung Nodule)

Wednesday, Dec. 4 3:00PM - 4:00PM Room: N227B



AMA PRA Category 1 Credit ™: 1.00 ARRT Category A+ Credit: 1.00

Participants

Jonathan H. Chung, MD, Chicago, IL (*Moderator*) Royalties, Reed Elsevier; Consultant, Boehringer Ingelheim GmbH; Speakers Bureau, Boehringer Ingelheim GmbH; Consultant, F. Hoffmann-La Roche Ltd; Speakers Bureau, F. Hoffmann-La Roche Ltd; Consultant, Veracyte, Inc;

Seth J. Kligerman, MD, Denver, CO (Moderator) Speakers Bureau, Boehringer Ingelheim GmbH; Author, Reed Elsevier; Consultant, IBM Corporation

Sub-Events

SSM06-01 Can Ultra-Low Dose Chest CT Accurately Detect Radiological Patterns of Fungal Infection in Immunocompromised Patients?

Wednesday, Dec. 4 3:00PM - 3:10PM Room: N227B

Participants

Anita Ghali, FRCR, Halifax, NS (*Abstract Co-Author*) Nothing to Disclose Luigia D'Errico, Toronto, ON (*Abstract Co-Author*) Nothing to Disclose Hatem Mehrez, Toronto, ON (*Abstract Co-Author*) Employee, Canon Medical Systems Corporation Mini V. Pakkal, FRCR,MBBS, Toronto, ON (*Abstract Co-Author*) Nothing to Disclose Micheal McInnis, MD, Toronto, ON (*Abstract Co-Author*) Nothing to Disclose Narinder S. Paul, MD, Toronto, ON (*Presenter*) Research Grant, Canon Medical Systems Corporation; Research Grant, Carestream Health, Inc

For information about this presentation, contact:

Narinder.Paul@lhsc.on.ca

PURPOSE

To compare the accuracy of ultralow dose (uLDCT) to low dose chest CT (LDCT) in detection of major and minor findings of fungal infection.

METHOD AND MATERIALS

IRB approved this prospective study and patient consent was obtained. 100 consecutive immunocompromised patient had 2 chest CT scans (135kV, 0.5s, 64x0.5mm) during a single breath-hold with LDCT (40mA, ~1mSv) and uLDCT (10mA, ~0.25mSv). Images were reconstructed using lung and mediastinal kernels at slice thickness/interval of 3.0/2.4mm. 3 board certified chest radiologists independently evaluated the studies in randomized and blinded setting, and qualitatively assessed 1) image quality, 2) diagnostic confidence for detecting fungal infection and 3) detection of EORTC major criteria (halo sign, cavitation, consolidation) and minor criteria (nodules: clustered or isolated nodules of 4-10mm diameter, GGO/atelectasis) for fungal disease using a 5-point Likert score. Discrepant findings were adjudicated by a senior thoracic radiologist. Patients were stratified by BMI (kg/m2): <=18.5, 18.5-25.0, 25.0-30.0 and >30.0. uLDCT results were compared to LDCT findings.

RESULTS

<u>Image quality and diagnostic confidence:</u> LDCT had median and mean scores >4.0. uLDCT had median and mean scores >3.4 for lung reconstructions; and the Wilcoxon-paired test demonstrated no statistical difference between LDCT and uLDCT scores (p>0.45). uLDCT mediastinum reconstruction images had median and mean scores >3.7 for diagnostic confidence in patients with BMI <25.0; but with BMI>25.0 there was suboptimal IQ and diagnostic confidence (p<0.05) compared to LDCT. <u>Evaluation of fungal disease:</u> uLDCT accuracy in detecting major radiological criteria: halo sign, cavitation, consolidation was 99, 100, and 98% respectively; and in detecting minor criteria: sub-cm nodules and GGO, was 88 and 86%, respectively. uLDCT had reduced accuracy for detection of small (4-6mm) nodules and small volume GGO due to increased image noise.

CONCLUSION

Thoracic uLDCT has high accuracy in detection of major radiological criteria for fungal disease and should be considered in immunocompromised patients with BMI <= 30.0 kg/m².

CLINICAL RELEVANCE/APPLICATION

Immunocompromised patients undergo multiple chest CT scans to rule out opportunistic infection. uLDCT has comparable diagnostic accuracy to LDCT for detecting major radiological criteria of fungal disease with 80% lower radiation dose and should be routinely used in these patients.

SSM06-02 Analysis of Alveolar Duct Network as Possible Collateral Ventilation and Spreading of Diseases by Magnified 3D Print of Lung Specimen by Micro CT

Participants Hiroshi Natori, MD, PhD, Sapporo, Japan (*Presenter*) Nothing to Disclose Hirotsugu Takabatake, MD,PhD, Sapporo, Japan (*Abstract Co-Author*) Nothing to Disclose Masaki Mori, MD,PhD, Sapporo, Japan (*Abstract Co-Author*) Nothing to Disclose Masahiro Oda, PhD, Nagoya, Japan (*Abstract Co-Author*) Nothing to Disclose Kensaku Mori, PhD, Nagoya, Japan (*Abstract Co-Author*) Nothing to Disclose Kensaku Mori, PhD, Nagoya, Japan (*Abstract Co-Author*) Developer, Olympus Corporation; Developer, Cybernet System Inc; Developer, Morita Mfg Inc Hiroyuki Koba, MD,PhD, Sapporo, Japan (*Abstract Co-Author*) Nothing to Disclose Hiroki Takahashi, MD,PhD, Sapporo, Japan (*Abstract Co-Author*) Nothing to Disclose

For information about this presentation, contact:

hnatori@sapmed.ac.jp

PURPOSE

Study on architecture of peripheral lung beyond respiratory bronchiole is important as pathway of collateral ventilation and disease extension in peripheral lung. However, it is difficult to get 3-D view of alveolar duct area by series of microscopic histological slides, Establishment of naked eye visible 3-D view analysis method was attempted by magnified print of virtual image of the micro focus CT of the lung specimen.

METHOD AND MATERIALS

Virtual image data based on micro CT of the inflated fixed lung specimen was used to make 40 times magnified peripheral lung model by 3D printer. Virtual lung tissue image was displayed on the flat screen by originally created application micro-NewVES. Two identical models were printed by 3D printer to confirm artifacts at the printing procedures. Internal structure of the magnified 3D print model was shown by virtual image by MDCT data of the 3D print model.

RESULTS

By virtual bronchoscopic view, beyond the respiratory bronchiole, alveolar ducts divide and reached to the blind end with one alveolus in the center surrounded by 6 alveoli. Numbers of surrounding alveoli were 5 to 7, but mainly 6. However most of alveolar ducts continuously divide and connect to adjacent duct to make alveolar duct network. The ducts connected loop back to initial respiratory bronchiole. Loop constructions of ducts were frequently found. Occasionally space surrounded by hundreds alveoli, that suggest destruction of alveolar duct unit. Alveoli revealed many shapes as semi-spherical or variety of semi-polygonal types on the 40 times magnified 3D print model. Sizes of the alveoli preliminary measured at 286 SD 27 micrometers, n=120, by this method. More measurements are necessary and also absolute sizes may considered according to, an official research policy statement of the ATS/ERS. The pores of Kohn as inter-alveolar communicating passes were found by naked eye view. Ten to thirty micrometer in diameter of small pores and various shapes of larger inter-alveolar communications were found.

CONCLUSION

Establishment of the method may apply for analysis of COPD, and that realized the development of new research field in respiratory radiology. Present method may also give us new insight in radiology of COPD, multi-cystic lung diseases, interstitial lung diseases, and other lung manifestations.

CLINICAL RELEVANCE/APPLICATION

That may give us new insight in radiology of COPD and other peripheral lung diseases.

SSM06-03 Anaplastic Lymphoma Kinase Inhibitor Induced Pneumonitis in Patients with Non-Small Cell Lung Cancer: Clinical and Radiologic Characteristics and Risk Factors

Wednesday, Dec. 4 3:20PM - 3:30PM Room: N227B

Participants

Hye Jeon Hwang, MD,PhD, Anyang, Korea, Republic Of (*Presenter*) Nothing to Disclose Mi Young Kim, MD, PhD, Seoul, Korea, Republic Of (*Abstract Co-Author*) Nothing to Disclose Hye-Young Choi, Seoul, Korea, Republic Of (*Abstract Co-Author*) Nothing to Disclose Chang-Min Choi, Seoul, Korea, Republic Of (*Abstract Co-Author*) Nothing to Disclose Jae Cheol Lee, Seoul, Korea, Republic Of (*Abstract Co-Author*) Nothing to Disclose

For information about this presentation, contact:

umttette@hanmail.net

PURPOSE

To investigate the clinical and radiologic characteristics and risk factors of anaplastic lymphoma kinase (ALK) inhibitor induced pneumonitis (ALK-IIP) in patients with non-small cell lung cancer (NSCLC).

METHOD AND MATERIALS

A total of 250 NSCLC patients who had been treated with ALK inhibitors from January 2015 to January 2018 were retrospectively enrolled. Clinical characteristics and clinical course were reviewed from the medical records. Chest CT of ALK-IIP was analyzed and classified into four CT patterns, i.e. organizing pneumonia (OP), hypersensitivity pneumonitis (HP), diffuse alveolar damage (DAD), and nonspecific interstitial pneumonia (NSIP), using the American Thoracic Society/European Respiratory Society classification of interstitial pneumonia. Clinical characteristics including toxicity grading according to the National Cancer Institute Common Terminology Criteria for Adverse Events and treatment course was analyzed in regarding to the classified CT patterns. Clinical characteristics with ALK-IIP and without ALK-IIP.

RESULTS

ALK-IIP was identified in 11 patients (4.4%). The most common CT pattern was the OP pattern (n = 7, 63.6%) and followed by the HP pattern (n = 2, 18.2%) and the DAD pattern (n = 2, 18.2%). ALK-IIP showed pneumonitis toxicity grade ranged from 1 to 3, and DAD pattern had the highest toxicity grade, followed by HP and OP patterns (median grade: 3.5, 2.5, 1). All of the patients with

the OP pattern were successfully treated, while half of patients with the DAD pattern died during treatment. The smoking history and extrathoracic metastasis were more frequent in patients with ALK-IIP (P < 0.005). The smoking history was associated with a higher incidence of ALK-IIP [odds ratio: 3.586, 95% confidence interval: 1.058-13.432, P = 0.049].

CONCLUSION

ALK-IIP showed a spectrum of chest CT patterns and various toxicity grades, and CT patterns reflected the toxicity grades of ALK-IIP. The OP pattern was the most common CT pattern of ALK-IIP, and patients with ALK-IIP of the OP pattern were successfully treated. The smoking history was a significant risk factor of ALK-IIP in NSCLC patients.

CLINICAL RELEVANCE/APPLICATION

A pattern approach in diagnosing ALK-IIP on chest CT is appropriate and effective in routine practice. ALK inhibitors should be used with caution in NSCLC patients with smoking history.

SSM06-04 Deep-Learning based Automated Detection Algorithm for Active Pulmonary Tuberculosis on Chest Radiographs: Diagnostic Performance in Systematic Screening of Asymptomatic Individuals

Wednesday, Dec. 4 3:30PM - 3:40PM Room: N227B

Participants

Jong Hyuk Lee, MD, Seoul, Korea, Republic Of (Presenter) Nothing to Disclose

Chang Min Park, MD, PhD, Seoul, Korea, Republic Of (Abstract Co-Author) Research funded, Lunit Inc

Sunggyun Park, Seoul, Korea, Republic Of (Abstract Co-Author) Employee, Lunit Inc

Eui Jin Hwang, Seoul, Korea, Republic Of (Abstract Co-Author) Nothing to Disclose

Jin Mo Goo, MD, PhD, Seoul, Korea, Republic Of (*Abstract Co-Author*) Research Grant, INFINITT Healthcare Co, Ltd; Research Grant, DONGKOOK Pharmaceutical Co, Ltd;

Hyungjin Kim, MD, Seoul, Korea, Republic Of (Abstract Co-Author) Research Grant, Lunit Inc

For information about this presentation, contact:

lee87jh@gmail.com

PURPOSE

To validate deep-learning based automated detection (DLAD) algorithm for detection of active pulmonary tuberculosis (TB) and any radiologically-identifiable relevant abnormality on chest radiographs (CRs) in systematic screening setting.

METHOD AND MATERIALS

We performed out-of-sample testing of a trained DLAD algorithm, using CRs from 19,686 asymptomatic individuals (male: 19,475, female: 211; mean \pm standard deviation: 21.3 \pm 1.9 years) as part of systematic screening for TB between January 2013 and July 2018. Area under the receiver operating characteristic curves (AUC) of DLAD for diagnosis of TB and any relevant abnormalities were measured. Accuracy measures including sensitivities, specificities, positive predictive values (PPVs), negative predictive values (NPVs) were calculated at pre-defined operating thresholds (high sensitivity threshold, 0.16; high specificity threshold, 0.46).

RESULTS

Four individuals with five CRs were confirmed with active pulmonary TB, and 28 CRs were judged as having radiologically-identifiable relevant abnormalities in 26 individuals. All five CRs with active pulmonary TB were correctly classified as having abnormal findings by DLAD with specificities of 0.959 and 0.997, PPVs of 0.006 and 0.068, and NPVs of both 1.000 at high sensitivity and high specificity thresholds, respectively. With high specificity thresholds, DLAD showed comparable diagnostic measures for tuberculosis to the pooled radiologists (P values > 0.005). For the detection of any radiologically-identifiable relevant abnormality, DLAD showed AUC value of 0.967 (95% confidence interval, 0.938-0.996) with sensitivities of 0.821 and 0.679, specificities of 0.960 and 0.997, PPVs of 0.028 and 0.257, and NPVs of both 1.000 at high sensitivity and high specificity thresholds, respectively.

CONCLUSION

In systematic screening for TB in a low-prevalence setting, DLAD algorithm demonstrated excellent diagnostic performance, comparable to the radiologists in the detection of active pulmonary TB.

CLINICAL RELEVANCE/APPLICATION

DLAD algorithm can help radiologists detect active pulmonary TB on CRs in a time-efficient manner, and identify individuals for further clinical and diagnostic evaluation for active TB. In a resource-constrained environment, it may be utilized as a standalone screening tool for individuals with active pulmonary TB.

SSM06-05 Comparison of Radiologist and Natural Language Processing-Based Image Annotation For Deep Learning System for Tuberculosis Screening on Chest X-Rays

Wednesday, Dec. 4 3:40PM - 3:50PM Room: N227B

Participants

Paul H. Yi, MD, Baltimore, MD (*Presenter*) Nothing to Disclose Tae Kyung Kim, Baltimore, MD (*Abstract Co-Author*) Nothing to Disclose Gregory D. Hager, PhD, MSc, Baltimore, MD (*Abstract Co-Author*) Co-founder, Clear Guide Medical LLC CEO, Clear Guide Medical LLC Cheng Ting Lin, MD, Baltimore, MD (*Abstract Co-Author*) Nothing to Disclose

For information about this presentation, contact:

pyi10@jhmi.edu

PURPOSE

To compare 1) agreement between natural language processing (NLP) and radiologist-curated labels for possible tuberculosis (TB) on chest radiographs (CXR) and 2) performance of deep convolutional neural networks (DCNN) trained on images using the two sets

METHOD AND MATERIALS

We obtained 10,951 de-identified CXRs from the NIH ChestX-ray14 database annotated for 14 thoracic conditions by NLP. Each CXR was labeled as positive for possible TB if they had any of the following: pneumonia, infiltrate, mass, nodule, or consolidation. A fellowship-trained thoracic radiologist blinded to image labels interpreted each image and labeled each as positive or negative for possible TB. Kappa coefficients were calculated to evaluate inter-rater agreement between radiologist- and NLP-curated labels. We created 5 datasets with progressively increasing numbers of images with roughly equal proportions of positive and negative cases based on NLP-curated labels: 996, 2994, 6033, 9955, and 10,951 images (Table 1). Each dataset was divided into training (80%) and validation (20%) splits. The ResNet-50 DCNN pretrained on ImageNet was trained and validated using each dataset and tested on an external dataset of 753 CXRs used to screen for TB in Montgomery County, MD (USA) [58 with TB, 80 normal) and Shenzhen, China (275 with TB, 340 normal). Receiver operating characteristic (ROC) curves with area under the curve (AUC) were used to evaluate the DCNNs; AUCs were compared between DCNNs using DeLong's parametric method.

RESULTS

There was poor agreement between NLP and radiologist-curated labels with regards to potential TB on CXRs (Kappa coefficient ranging from 0.33 to 0.37). DCNNs trained using radiologist-curated labels consistently had significantly higher performance than the algorithm trained using the NLP-labels, regardless of the number of the number of images used for training and validation (Table 1). The best-performing DCNN had an AUC of 0.88, which was trained on 11,000 images using the radiologist-annotated sets.

CONCLUSION

DCNNs trained on CXRs labeled by a radiologist outperformed those trained on the same CXRs labeled by NLP, highlighting the benefit of radiologists' determining groundtruth for machine learning dataset curation.

CLINICAL RELEVANCE/APPLICATION

DCNNs trained on CXRs labeled by a radiologist consistently outperformed those trained on the same CXRs labeled by NLP.

SSM06-06 Radiologists Improve Timeliness of CT Follow-Up for Incidental Lung Nodules with a Novel 'Tracker' System

Wednesday, Dec. 4 3:50PM - 4:00PM Room: N227B

Participants

Debra S. Dyer, MD, Greenwood Village, CO (*Presenter*) Nothing to Disclose Pearlanne Zelarney, Denver, CO (*Abstract Co-Author*) Nothing to Disclose Laurie Carr, MD, Denver, CO (*Abstract Co-Author*) Advisory Board, AstraZeneca PLC Elizabeth Kern, MD, MS, Denver, CO (*Abstract Co-Author*) Nothing to Disclose

For information about this presentation, contact:

DyerD@NJHealth.org

PURPOSE

Evaluate improvement in timeliness of follow-up chest CT for incidental lung nodules after implementation of a 'Tracker Phrase' system.

METHOD AND MATERIALS

In 2011, a system was implemented where dictating radiologists tagged chest CT reports with 'Tracker' phrases and text indicating the recommended follow-up for incidental nodules. An electronic registry for tracking patients with nodules was built using the Tracker phrases. The registry generated automated patient and provider reminders when scans were overdue. An EHR query found 41,692 chest CTs had been performed 2008 - 2016. A random sample of reports describing an incidental nodule were selected for retrospective review. Patient records before (n=448) and after (n=848) implementation of the Tracker system were examined for timeliness of follow-up. Timeliness was broadly defined as follow-up CT occurring within 13 months of the index CT. Patient age, gender, and risk of lung cancer were obtained. High risk was defined by a personal history of lung cancer, or diagnosed COPD, or at least two of the following: age>50 years, 20+ pack years of smoking, or first degree relative with lung cancer.

RESULTS

Age and gender did not differ significantly in the pre-Tracker vs. the post-Tracker groups. 58% of the pre-Tracker vs. 69% of the post-Tracker patients were high risk (p<.01). Fewer (42% vs. 54%) in the pre-Tracker group had timely follow-up compared to the post-Tracker group (p<.01). Adjusting for risk and age group, we found that patients whose CT report contained a Tracker phrase were 50% more likely to have a timely follow-up chest CT compared to those whose CT scans did not (OR = 1.55; 95% CI 1.23-1.96 p <.001). Being 'high risk' for lung cancer increased the likelihood of timely follow-up (OR = 1.89; 95% CI 1.50-2.40 p<.001), as did age of 65 years or older (OR = 1.39; 95% CI 1.11-1.74 p=.004) at the time of the index CT scan.

CONCLUSION

Timeliness of CT follow-up for incidental lung nodules significantly improved after the implementation of a Tracker phrase system. Older age and higher risk of lung cancer were also associated with more timely follow-up.

CLINICAL RELEVANCE/APPLICATION

A radiologist driven Tracker system can improve timeliness of CT surveillance for follow-up of incidental lung nodules.







Emergency Radiology (Acute Care Imaging Utilization)

Wednesday, Dec. 4 3:00PM - 4:00PM Room: N228

ER

AMA PRA Category 1 Credit ™: 1.00 ARRT Category A+ Credit: 1.00

Participants

Douglas S. Katz, MD, Mineola, NY (*Moderator*) Nothing to Disclose Felipe Munera, MD, Key Biscayne, FL (*Moderator*) Nothing to Disclose

Sub-Events

SSM07-01 Can AI Outperform a Junior Resident? Comparison of Deep Neural Network to First-Year Radiology Residents for Identification of Pneumothorax

Wednesday, Dec. 4 3:00PM - 3:10PM Room: N228

Awards

Trainee Research Prize - Resident

Participants

Paul H. Yi, MD, Baltimore, MD (*Presenter*) Nothing to Disclose Tae Kyung Kim, Baltimore, MD (*Abstract Co-Author*) Nothing to Disclose Alice Yu, MD, Baltimore, MD (*Abstract Co-Author*) Nothing to Disclose Bradford Bennett, MD, Baltimore, MD (*Abstract Co-Author*) Nothing to Disclose John Eng, MD, Cockeysville, MD (*Abstract Co-Author*) Nothing to Disclose Cheng Ting Lin, MD, Baltimore, MD (*Abstract Co-Author*) Nothing to Disclose

For information about this presentation, contact:

pyi10@jhmi.edu

PURPOSE

To develop a deep learning system for identification of pneumothorax and compare its performance to that of two 1st-year radiology residents.

METHOD AND MATERIALS

We obtained 112,120 frontal chest radiographs (CXRs) from the NIH ChestX-ray 14 database, of which 4360 cases (4%) had been labeled as pneumothorax by natural language processing. We utilized 111,494 CXRs to train and validate the ResNet-152 deep convolutional neural network (DCNN) pretrained on ImageNet to identify pneumothorax. DCNN testing was performed on a hold-out set of 602 CXRs (176 with pneumothorax and 426 without), whose groundtruth was determined by re-interpretation by a cardiothoracic radiologist with 5 years of post-fellowship experience; images were presented at 1024 x 1024 resolution and had a mix of both subtle and more obvious pneumothorax using a 6-point Likert scale to reflect levels of confidence ranging from low to intermediate to high. Receiver operating characteristic (ROC) curves were generated for the DCNN and 2 residents with area under the curve (AUC) calculated to evaluate test performance. AUCs were compared using the DeLong parametric method (significance defined as p<0.05).

RESULTS

The best-performing DCNN achieved AUC of 0.841 for identification of pneumothorax at a rate of 1980 images/minute. In contrast, both 1st-year residents achieved significantly higher AUCs of 0.942 and 0.905 (p<0.01 for both compared to DCNN; Figure 1), but at a slower rate of 2 images/minute.

CONCLUSION

Our DCNN for pneumothorax identification achieved significantly lower test AUC than two 1st-year radiology residents. However, the DCNN was able to interpret images >1000x as fast. Further work is warranted to compare the relative performance of AI to radiologists of varying levels, and the relative benefits of image interpretation speed to accuracy, particluarly for use in time-sensitive settings like the Emergency Department.

CLINICAL RELEVANCE/APPLICATION

1st-year radiology residents outperformed a deep learning system for pneumothorax detection, but the deep learning system interpreted images >1000x faster.

SSM07-02 New Diagnoses of Torso Cancer Based on CT Imaging is Low in the Emergency Department

Wednesday, Dec. 4 3:10PM - 3:20PM Room: N228

For information about this presentation, contact:

mscheinf@montefiore.org

PURPOSE

Emergency department torso (chest, abdomen and/or pelvis) CT occasionally demonstrates cancer. It is unknown what the rate of new cancer diagnosis is based on torso CT is in this setting. The purpose of this study is to determine this rate.

METHOD AND MATERIALS

All reports for ED CT studies involving the chest, abdomen or pelvis or combinations of these were selected for the 2017 calendar year. Each report impression was searched for the following keywords: mass, tumor or cancer. Each report with a keyword was manually checked whether the text was reporting a lesion, absence of a lesion (e.g. There is no mass effect), or hedge for a lesion (ie favored a non-cancer diagnosis but suggested that an underlying mass could not be excluded). Among reports describing a lesion, the electronic medical record was used to determine whether it was an old lesion, new lesion or was indeterminate based on lack of follow up or workup. Each lesion was also categorized as being related to the chief complaint or as an incidental finding.

RESULTS

During the 2017 calendar year, there were 339,593 ED visits, by 203,412 unique patients. 19,496 CT exams including a portion of the torso were performed. Of these, 1606 included one of the keyword: 621 were known cases of cancer, 490 were describing the abscess of a mass, 231 hedged the presence of cancer, 60 were of subcentimeter lung nodules, 21 were indeterminate (as there was no workup or follow up), and 180 were confirmed new diagnoses of cancer. The breakdown of cancer types is demonstrated in the figure. This yielded a CT-based new torso cancer diagnosis rate of 9 new diagnoses per 1000 torso CTs and 0.5 diagnoses per day (based on our average daily CT volume of 53 exams). Among the 180 new cases of cancer, 122 (68 %) were, 38 (21%) were not, and 20 (11%) were possibly related to the presenting symptoms.

CONCLUSION

CT-diagnosis of a new torso cancer is uncommon in the ED setting. The top three diagnose were, gastrointestinal tract (mostly colorectal cancer), lung and genitourinary (mostly renal cell carcinoma). Most CT based new torso cancers will be related to the patient's presenting symptoms.

CLINICAL RELEVANCE/APPLICATION

This data provides new insight into the diagnostic makeup of patients undergoing CT in the emergency department. This may also have implications for ED radiologist staffing.

SSM07-03 Assessing Prior Neuroimaging Utilization to Identify Recidivistic Patients with Psychosocial Maladies

Wednesday, Dec. 4 3:20PM - 3:30PM Room: N228

Participants

Daniel Braga, MD, Jacksonville, FL (*Presenter*) Nothing to Disclose Sukhwinder J. Sandhu, MD, Jacksonville, FL (*Abstract Co-Author*) Nothing to Disclose Dinesh Rao, MD, Jacksonville, FL (*Abstract Co-Author*) Nothing to Disclose Peter J. Fiester, MD, Jacksonville, FL (*Abstract Co-Author*) Nothing to Disclose Patrick Natter, MD, Jacksonville, FL (*Abstract Co-Author*) Nothing to Disclose Marie Crandall, MD,MPH, Jacksonville, FL (*Abstract Co-Author*) Nothing to Disclose Erik R. Soule, MD, Jacksonville, FL (*Abstract Co-Author*) Nothing to Disclose Victoria Villescas, MD, Jacksonville, FL (*Abstract Co-Author*) Nothing to Disclose

For information about this presentation, contact:

daniel.braga@jax.ufl.edu

PURPOSE

The purpose of this study is to determine if a correlation exists between patients who undergo repeat computed tomography (CT) imaging of the brain on multiple separate emergency department (ED) visits with the presence of psychosocial illness such as mental health illness, substance abuse, or interpersonal violence.

METHOD AND MATERIALS

An IRB-approved retrospective chart review was performed on 27,004 patients presenting to the adult ED or trauma center at our institution from 2013 to 2017. Patients who had at least one CT of the brain as part of their diagnostic workup met inclusion criteria. The number of head CT's on separate ED visits was counted. ICD-9 and 10 codes were analyzed from admission data to identify diagnoses of mental health illness, substance abuse, and/or interpersonal violence for each patient. Statistical analysis was then performed to explore the correlation between the number of head CT's per patient and the presence of these underlying psychosocial maladies.

RESULTS

Linear logistic regression was used to determine whether the number of CT scans is associated with psychosocial illness. We found that with each additional CT, the odds of psychosocial diagnosis increases by 1.93 (p <0.0001). The magnitude of the associations was described using odds ratio (OR), along with its 95% confidence intervals (CI). The level of significance was set at 5%. All analyses were done in SAS® for Windows Version 9.4.

CONCLUSION

Each additional unenhanced CT of the head performed on patients during separate distinct ED visits increases the likelihood of psychosocial illness with an odds ratio of 1.93. The presence of multiple head CT's in a patient's medical record may suggest the presence of mental health illness, substance abuse, or interpersonal violence.

CLINICAL RELEVANCE/APPLICATION

Assessment of prior neuroimaging in recidivistic patients with psychosocial illness could aid in diagnostic identification, prevent over-utilization of health care resources, and guide early interventions directed at this elusive patient population.

SSM07-04 Chest CT's During Immune Checkpoint Inhibitor Therapy in the Emergency Department: A Single Institute 9-Year Experience in 139 Patients

Wednesday, Dec. 4 3:30PM - 3:40PM Room: N228

Participants

Daniel A. Smith, MD, Cleveland, OH (*Presenter*) Nothing to Disclose Ethan Radzinsky, Cleveland, OH (*Abstract Co-Author*) Nothing to Disclose Kianoush Ansari-Gilani, MD, Cleveland, OH (*Abstract Co-Author*) Nothing to Disclose Amit Gupta, MBBS, Cleveland, OH (*Abstract Co-Author*) Nothing to Disclose Sreeharsha Tirumani, MBBS, MD, Beachwood, OH (*Abstract Co-Author*) Nothing to Disclose Christopher Hoimes, DO, Cleveland, OH (*Abstract Co-Author*) Nothing to Disclose Nikhil H. Ramaiya, MD, Shaker Heights, OH (*Abstract Co-Author*) Nothing to Disclose

PURPOSE

To assess chest CT findings of oncology patients on immune checkpoint inhibitor (ICI) therapy who present to the emergency department (ED) with acute chest symptoms.

METHOD AND MATERIALS

A retrospective review was performed of 139 adult oncology patients on ICIs who presented to the ED and received chest CT imaging. These patients included adults >=18 years old at a single institution from 2010-2018 who received treatment with >=1 ICI. Chest CT findings were reviewed to evaluate tumor burden and assess immune-related adverse events (irAEs).

RESULTS

The 139 patients included 55% males and 45% females with a mean age of 65. The most common cancer types included lung (63%), melanoma (11%), and bladder/kidney (9%). 163 chest CTs were acquired at unique ED visits, with a median time of 50 days between first dose of ICI and ED visit. Common imaging indications included dyspnea (64%), chest pain (28%), cough (14%), and hypoxia (10%). 85% of chest CTs were ordered as pulmonary embolism (PE) protocols, with new PE detected in 7% of cases. Worsening tumor burden was identified in 60% of ED chest CTs at a median of 37 days after ICI initiation. 21 (13%) of chest CTs demonstrated immunotherapy-induced pneumonitis with a median duration of 60 days between initiation of ICI and ED presentation. These cases of ICI-associated pneumonitis included 6 reflecting radiation recall pneumonitis, with the remainder reflecting patterns of HSP (4), AIP/ARDS (4), bronchiolitis (3), COP (2), and NSIP (2). All but two (90%) of the 21 patients presenting with ICI-associated pneumonitis received high-dose steroids. 79% of ED encounters resulted in hospital admission after chest imaging. 63% of patients demonstrated clinical or radiographic improvement during their ED/hospital visits, whereas 37% experienced no significant clinical improvement, were discharged to hospice, or died during their admission.

CONCLUSION

60% of oncology patients on ICI therapy who present to the ED demonstrate worsening tumor burden on chest CT, with a median time of 37 days from ICI initiation to disease progression on ED chest CT. Immunotherapy-induced pneumonitis is the second most common chest CT finding in the ED setting, occurring in 13% of patients.

CLINICAL RELEVANCE/APPLICATION

This study provides insight into the radiographic findings on chest CT associated with acute presentations to the ED among oncology patients on immune checkpoint inhibitor therapy.

SSM07-05 Evaluation of the Effectivity and Therapeutic Impact of CT in ICU Patients with Unknown Focus of Infection

Wednesday, Dec. 4 3:40PM - 3:50PM Room: N228

Participants

Daniel Kuetting, MD, Bonn, Germany (*Presenter*) Nothing to Disclose Julian A. Luetkens, MD, Bonn, Germany (*Abstract Co-Author*) Nothing to Disclose Anton Faron, MD, Bonn, Germany (*Abstract Co-Author*) Nothing to Disclose Daniel K. Thomas, MD, PhD, Bonn, Germany (*Abstract Co-Author*) Nothing to Disclose Ron Martin, Bonn, Germany (*Abstract Co-Author*) Nothing to Disclose

PURPOSE

To evaluate the impact of computerized tomography (CT) on diagnosis and change of therapy in ICU patients with fever, systemic inflammatory response syndrome (SIRS) or sepsis with unknown focus of infection

METHOD AND MATERIALS

Non-ECG-gated chest/abdominal CT examinations of ICU patients (internal medicine, surgery, heart surgery, neurology/ neurosurgery) were prospectively analyzed for inflammatory foci. Both confirmation of and changes in the diagnosis or therapy based on CT findings were analyzed. Prior CT, X-Ray, MRI, bronchioalveolar lavage, urine analysis and ultrasound examinations, performed during the same ICU treatment but prior to the CT, were cross-checked to verify whether foci were actually new.

RESULTS

In 99 out of 112 (88,4 %) consecutively evaluated patients (34,8% female, mean age 64,8 years), a total of 147 possible foci (thoracic: n=92; abdominal: n=55) were detected. Of the 147 foci (58,5% defined as definite, 41,5% as questionable), prior examinations had suspected inflammatory focus in 64 cases, confirmed focus in 20 cases. CT diagnosis lead to 77 changes in therapy regimen in 58 of 99 Patients (59%): change/initiation of antibiotics: 52,7%, CT guided thoracic/abdominal puncture: 21,6%, operation: 8,1%, change in patient positioning: 8,1%; other: 9,5%.

CONCLUSION

CT examinations in ICU patients with unknown focus of infection leads to diagnosis in most cases as well as to adaption in therapy regimen and thus should be considered in patients with obscure clinical infection.

CLINICAL RELEVANCE/APPLICATION

CT is an effective diagnostic tool for the evaluation of patients with unknown focus of infection. CT should be considered a routine procedure in the workup of septic patients when other diagnostic evidence of infection is absent.

SSM07-06 CNN-Based Regression Model Learning the Abbreviated Injury Scale Predicts Respiratory Distress Syndrome in Polytraumatized Patients at Admission

Wednesday, Dec. 4 3:50PM - 4:00PM Room: N228

Participants

Johannes Hofmanninger, Vienna, Austria (*Abstract Co-Author*) Siemens AG Boehringer Ingelheim GmbH Sebastian Roehrich, MD, Vienna, Austria (*Abstract Co-Author*) Consultant, contextflow GmbH Lukas Negrin, Vienna, Austria (*Abstract Co-Author*) Nothing to Disclose Georg Langs, Vienna, Austria (*Presenter*) Co-founder, contextflow GmbH; Shareholder, contextflow GmbH Helmut Prosch, MD, Vienna, Austria (*Abstract Co-Author*) Nothing to Disclose

For information about this presentation, contact:

johannes.hofmanninger@meduniwien.ac.at

PURPOSE

To automate lung-related risk stratification of polytraumatized patients based on chest computed tomography (CT) by training deep-learning models to predict abbreviated injury scale (AIS) scores for the thorax.

METHOD AND MATERIALS

The dataset used contains 123 polytraumatized patients, not younger than 18 years and with an assigned Injury Severity Score (ISS) of at least 15. Patients which died within 48 hours after admission, suffered burning injuries or had known oncologic or chronic inflammatory lung diseases were excluded. All scans were conducted on the same scanner and were conducted within one hour of the accident. We automatically extracted the lungs including pleural effusions via a U-Net convolutional neural network (CNN). After stripping of image areas outside the lung, we resampled the volumes to an isotropic voxel resolution of 1mm and cropped the images to the lung masks. Subsequently, we generated maximum intensity projections (MIP) in the axial and coronal direction and resampled the images to 200x200 pixels. We trained two independent CNNs (axial & coronal) to predict the AIS scores (thorax only) associated with the patients. Finally, the predictions of the two networks were averaged to receive the final risk score

RESULTS

To test whether the resulting risk scores have predictive power for lung complications, we used the score to predict acute respiratory distress syndrome (ARDS) according to the Berlin definition. Note, that the CNN was not trained to predict ARDS. However, after 5-fold cross-validation, using 99 patients for training and 24 for prediction, the resulting risk score yielded an area under the curve (AUC) of 0.76 for ARDS prediction compared to 0.68 and 0.66 when using the AIS score or ISS, respectively.

CONCLUSION

The AIS score encodes injuries with and without involvement of the lung and does not fully encode the lung specific extent of the injuries. By providing only image information of the lung and excluding the surrounding tissue, we forced the neural networks to learn lung related severity when predicting AIS scores. By this, we were able to disentangle the lung specific component of the AIS score and to learn an organ specific risk score without explicit training data available.

CLINICAL RELEVANCE/APPLICATION

By automatically extracting the organ specific component of overall scores such as AIS, risk stratification for complications related to the organ of interest can be optimized.







Gastrointestinal (Liver Diffuse Disease: Iron, Fat)

Wednesday, Dec. 4 3:00PM - 4:00PM Room: E450B



AMA PRA Category 1 Credit ™: 1.00 ARRT Category A+ Credit: 1.00

FDA Discussions may include off-label uses.

Participants

Jeong Min Lee, MD, Seoul, Korea, Republic Of (*Moderator*) Grant, Bayer AG; Speaker, Bayer AG; Grant, Canon Medical Systems Corporation; Grant, Koninklijke Philips NV; Grant, General Electric Company; Grant, Guerbet SA; Speaker, Guerbet SA; Grant, Samsung Electronics Co, Ltd; Speaker, Samsung Electronics Co, Ltd; Grant, Bracco Group; Speaker, Siemens AG Alice W. Fung, MD, Portland, OR (*Moderator*) Nothing to Disclose

Sub-Events

SSM08-01 Accuracy of Viscoelasticity Measurement Using Ultrasound Shear Wave Elastography for Assessing Histologic Parameters in Patients with Nonalcoholic Fatty Liver Disease

Wednesday, Dec. 4 3:00PM - 3:10PM Room: E450B

Participants

Katsutoshi Sugimoto, MD, PhD, Tokyo, Japan (*Presenter*) Nothing to Disclose Hirohito Takeuchi, Tokyo, Japan (*Abstract Co-Author*) Nothing to Disclose Takao Itoi, Tokyo, Japan (*Abstract Co-Author*) Nothing to Disclose

For information about this presentation, contact:

sugimoto@tokyo-med.ac.jp

PURPOSE

To investigate the accuracy of shear wave (SW) speed (related to viscoelasticity), dispersion slope (related to viscosity), and attenuation value (related to degree of steatosis) measurements obtained using a new ultrasound (US) elastography system in assessing steatosis, inflammation, and fibrosis in patients with suspected nonalcoholic fatty liver disease (NAFLD).

METHOD AND MATERIALS

Data was collected from 74 consecutive adults who underwent liver biopsy for suspected NAFLD from April 2017 through November 2018. A US-based SW imaging system (Aplio-i800; Canon Medical Systems) was used to measure three US parameters (SW speed [m/s], dispersion slope [(m/s)/kHz], and attenuation value [dB/cm/MHz]) immediately before biopsy. The biopsy specimens were scored by 1 blinded expert pathologist according to the Nonalcoholic Steatohepatitis Clinical Research Network criteria. Diagnostic accuracy was assessed using the area under the receiver operating characteristic curve (AUROC) for the categories of steatosis, inflammation, and fibrosis. The effects of these histologic parameters on attenuation value, dispersion slope, and SW speed were evaluated by multivariable analysis.

RESULTS

With biopsy results as the reference standard, attenuation value identified patients with steatosis with AUROCs of 0.8335 for S>=S2 and 0.8090 for S=S3. Dispersion slope identified patients with inflammation with AUROCs of 0.7677 for A>=F2 and 0.9179 for A=A3. SW speed identified patients with inflammation with AUROCs of 0.7907 for F>=F1, 0.8403 for F>=F2, 0.8694 for F>=F3, and 0.9625 for F=F4. Multivariable analysis showed that steatosis significantly affected attenuation value (P<.0001), fibrosis and inflammation significantly affected dispersion slope (P=.0026 and P=.0299, respectively), and fibrosis significantly affected SW speed (P<.0001).

CONCLUSION

Prospective analysis of patients with NAFLD showed that attenuation value, dispersion slope, and SW speed were useful for assessing liver steatosis, lobular inflammation, and fibrosis, respectively, with AUROCs ranging from 0.7677 to 0.9625. Both inflammation and fibrosis affected dispersion slope.

CLINICAL RELEVANCE/APPLICATION

Three US parameters (attenuation value, dispersion slope, and SW speed) can be used to noninvasively assess the histopathologic parameters steatosis, inflammation, and fibrosis in NAFLD patients.

SSM08-02 Precision Analysis of Fat and Iron Measures in the Liver and Pancreas: Repeatability and Reproducibility Analysis Using Different Quantification Methods

Wednesday, Dec. 4 3:10PM - 3:20PM Room: E450B

Participants Hilton M. Leao Filho, MD, Sao Paulo, Brazil (*Presenter*) Nothing to Disclose Manoel S. Rocha, MD, PhD, Sao Paulo, Brazil (*Abstract Co-Author*) Nothing to Disclose Claudia Oliveira, Sao Paulo, Brazil (*Abstract Co-Author*) Nothing to Disclose Wanida Wanida Chua-Anusorn, Perth , Australia (*Abstract Co-Author*) Director, MagnePath Pty Ltd; Paul Clark, Perth, Australia (*Abstract Co-Author*) Employee, MagnePath Pty Ltd Director, MagnePath Pty Ltd Stockholder, MagnePath Pty Ltd

PURPOSE

Robust methods to measure fat and R2* exist, using proton density fat fraction(PDFF)Although PDFF is accessible, there are various comercial techniques available, which may impair the longitudinal assessment of patientsThe study seeks to evaluate PDFF precision (R2* and fat) with distinct methods through examinations performed in volunteers on 3T and 1.5T scanners at different times, using the same parameters.

METHOD AND MATERIALS

30 volunteers were recruited. Participants underwent a 3TMRI exam and were re-scanned on the same scanner using the same protocol, less than 1 week apart. They were also examined at a 1.5T scanner.Protocols were the same across devices, using 3 multi-gradient echo distinct sequences (MGE) to calculate PDFF. Philips Achieva 3T and Ingenia 1.5T scanners were used with surface coils. Post-processing techniques were made by 4 different vendors in the 3T and 2 different vendors at 1.5T.All measures were performed by the same radiologist (13 years of experience), using a ROI that encompassed the whole liver and pancreas area in a single slice. The measures repeatability on the 3TMRI was assessed through the within-subject coefficient of variation and the repeatability coefficient(RC). The agreement between different methods assessment was evaluated by ICC.

RESULTS

Fat-Fraction(FF) results:LiverFF achieved excellent RC with values between 1.55-3.45%Pancreas showed good RC, albeit lower, ranging between 2.26-5.54%The ICC for 3T scans was 0.94(liver) and 0.69(pancreas) in the first scan and 0.94 and 0.6 respectively for the last.Agreement between 3T and 1,5T measures for liver was excellent with ICC of 0.94(CI95%:0.8-0.97)ICC for pancreas was good, but with wide variation, with mean of 0.86(CI95%:0.26-0.95)Results R2*:LiverR2* showed good results, with mean RC of 9.18-13.08s-1Pancreas showed a RC of 9.66-15.53ICC for 3T scans was 0.97(liver) and 0.46(pancreas) in the first acquisition and 0.96 and 0.22 respectively for the second.

CONCLUSION

The study showed excellent reproducibility and repeatability for fat and iron measures in liver, using different scanners and techniques. The performance of pancreas was lower

CLINICAL RELEVANCE/APPLICATION

The study showed excellent precision for liver deposits measure with different techniques/scanners.Pancreas assessment should be used with caution. The morphology of the gland and the ROI methodology may have contributed to this results

SSM08-03 Validation of Different Measurement Methods of Fat and R2* in the Liver: Focus on Reproducibility

Wednesday, Dec. 4 3:20PM - 3:30PM Room: E450B

Participants

Nathalia S. Mendonca, MD, Sao Paulo, Brazil (*Abstract Co-Author*) Nothing to Disclose Rafael M. Sachetin, Sao Paulo, Brazil (*Abstract Co-Author*) Nothing to Disclose Virginia d. Goncalves, MD, Sao Paulo, Brazil (*Abstract Co-Author*) Nothing to Disclose Abdalla Y. Skaf, MD, Sao Paulo, Brazil (*Abstract Co-Author*) Nothing to Disclose Beatriz M. Cunha, MD, Sao Paulo, Brazil (*Abstract Co-Author*) Nothing to Disclose Hilton M. Leao Filho, MD, Sao Paulo, Brazil (*Presenter*) Nothing to Disclose

For information about this presentation, contact:

hiltonmlf@gmail.com

PURPOSE

-The development of robust methods to measure liver fat and R2*, such as proton density fat fraction (PDFF) techniques, made them the standard of care in hepatic deposit assessment. -Although PDFF is increasingly accessible, there isn't a clear rule to measure disease for a good correlation with biopsy or an acceptable variation among readers.-The study objective was to compare the correlation between readers with different experiences in abdominal imaging, using two distinct methods of measuring liver deposits, by placing regions of interest (ROI's) in the parenchyma.

METHOD AND MATERIALS

-100 consecutive patients who underwent MRI of the liver to evaluate steatosis and/or iron deposition were selected, searched retrospectively in our PACS. We include the first 100 that had an acceptable image quality with the use of a PDFF technique.-The patients were anonymized and 4 readers with different experiences in abdominal image analyse the images.Readers reviewed all exams independently using the following ROI placement rule:a) 4 circular ROI's (CR) deposited in the anterior and posterior region of the right liver lobe in different slices. 1 CR on the left liver lobe. We record the average value.b) 1 geographic ROI (GR) involving the entire liver area in a slice above the gallbladder, excluding vessels and artifact areas.-We calculate the ICC for the readers and both methods for fat and R2*. Bland-Altman plots were acquired.

RESULTS

-97 patients were included in the final analysis.-Fat deposits ranges from 1.6%-42.8%(Mean:12.6%/SD: 9.1%)-R2* ranged from 27s-1-171s-1 (Mean:52s-1/SD: 26s-1).>The ICC was very high for all readers with both analyses with the average --ICC for fat with the CR method was 0.983 (95%CI:0.977-0.988) / the GR method achieved an ICC of 0.958(95%CI:0.943-0.97).--ICC for R2* with CR was 0.983(95%CI:0.977-0.988) / the R2* with GR achieved a mean value of 0.983(95% CI:0.977-0.988).>The ICC between CR and GR also showed an excellent agreement with a mean ICC of 0.994(95% CI:0.993-0.995) for fat / and 0.992(95%CI:0.990-0.993)

CONCLUSION

- We showed an excellent correlation for hepatic iron and fat measurement between readers of different experience levels using

two distinct ROI placement methods.

CLINICAL RELEVANCE/APPLICATION

-Using either method described, one can achieve an excellent agreement between readers with different expertise levels.

SSM08-04 MRI Based Liver Iron Content Determination with Gradient EchoR2* versus Spin-Echo R2 Relaxometry

Wednesday, Dec. 4 3:30PM - 3:40PM Room: E450B

Participants

Arthur P. Wunderlich, PhD, Ulm, Germany (*Presenter*) Nothing to Disclose Stephan Kannengiesser, Erlangen, Germany (*Abstract Co-Author*) Employee, Siemens AG Valeria Mauro, Ulm, Germany (*Abstract Co-Author*) Nothing to Disclose Lena Kneller, Ulm, Germany (*Abstract Co-Author*) Nothing to Disclose Berthold Kiefer, PhD, Erlangen, Germany (*Abstract Co-Author*) Employee, Siemens AG Meinrad J. Beer, MD, Ulm, Germany (*Abstract Co-Author*) Nothing to Disclose Stefan A. Schmidt, MD, Ulm, Germany (*Abstract Co-Author*) Nothing to Disclose Holger Cario, Ulm, Germany (*Abstract Co-Author*) Nothing to Disclose

For information about this presentation, contact:

arthur.wunderlich@uni-ulm.de

PURPOSE

To investigate correlation between liver iron content (LIC) determined with a reference method based on Spin-Echo (SE) vs. gradient-echo (GRE) R2*.

METHOD AND MATERIALS

117 patients suspected for liver iron overload were scanned between July 2014 and April 2018. 65 patients (25 f, 40 m, 24.5±13.1 years (mean±std.dev.), range 8.2 to 59.3 years) were assigned to the study group analyzed by two observers, the other 52 patients (26 f, 26 m, age 19.1±14.6 (mean±std.dev.), range 2 to 60.6 years) served as control group. All patients were examined on a 1.5 T MRI scanner (MAGNETOM Avanto, Siemens Healthcare, Erlangen, Germany). For the Ferriscan® method (Resonance Health, Burswood, Australia), transversal liver slices were acquired during free breathing using the appropriate protocol (five TEs ranging from 6 to 18 ms, single-echo acquisitions, eleven 5 mm thick slices, 100% gap, resolution 1.64x1.64 mm, acquisition time 16:20 min.). Results served as LIC reference values. With a prototype breath-hold GRE sequence, 40 partitions of 4 mm thickness at 2.5x2.5 mm voxel size were acquired in 18 sec. with parallel imaging in both phase and slice encoding direction, and in-line voxelwise R2* calculation considering fat/water signal modulation. To obtain liver mean R2* values, regions of interest were manually placed in tissue free of vessels and/or artifacts. R2* was linearly correlated to reference LIC values. Results of the study group were used to calculate LIC for control group patients, further referred to as GRE-LIC. GRE-LIC was compared to reference LIC values.

RESULTS

Study group LIC values ranged from 0.5 to 27.3 mg/g liver dry wt. Linear correlation to R2* was excellent with coefficient of determination (R2) of 0.9. Slope values were 0.039 ± 0.00016 mg*s/g and intercept was -0.85 ± 0.38 mg/g. Observer results were identical within the confidence interval. For the control group, GRE-LIC values showed near-ideal concordance to LIC reference values with regression line close to identity (slope 1.04 ± 0.05 , intercept -0.64 ± 0.83), R2 was 0.89.

CONCLUSION

Linear correlation of R2* to reference LIC in the study group and concordance of LIC values determined from GRE to reference LIC values in the control group were both excellent. Also, we found good inter-observer agreement.

CLINICAL RELEVANCE/APPLICATION

The volumetric single breath-hold GRE sequence studied is suitable for reliable MR-based LIC determination.

SSM08-05 Multi-Point Dixon PDFF MRI for Fat Quantification: Cross Vendor and Field Strength Assessment

Wednesday, Dec. 4 3:40PM - 3:50PM Room: E450B

Participants

Erika Schneider, PhD, Cleveland, OH (*Presenter*) Stockholder, General Electric Company Stockholder, Pfizer Inc Stockholder, NitroSci Pharmaceuticals, LLC

Erick M. Remer, MD, Beachwood, OH (Abstract Co-Author) Travel support, Bracco Group

Xiaobo Ding, MD, MD, Changchun , China (Abstract Co-Author) Nothing to Disclose

Bryan Addeman, Toronto, ON (Abstract Co-Author) Nothing to Disclose

Charles A. McKenzie, PhD, London, ON (Abstract Co-Author) Research Grant, General Electric Company

Sankar D. Navaneethan, MD, Houston, TX (Abstract Co-Author) Nothing to Disclose

Nancy A. Obuchowski, PhD, Cleveland, OH (*Abstract Co-Author*) Research Consultant, Siemens AG; Research Consultant, IBM Corporation; Research Consultant, Elucid Bioimaging Inc; Research Consultant, FUJIFILM Holdings Corporation

For information about this presentation, contact:

remere1@ccf.org

PURPOSE

To assess multi-point Dixon (PDFF) using multiple platforms for accuracy and reproducibility of fat quantification.

METHOD AND MATERIALS

Fat-water phantom sets (0, 10, 16, 35, 100 % fat) were evaluated using FDA-approved PDFF sequences, reconstruction and

analysis algorithms. Phantoms were imaged with subjects in the Visceral Adiposity and Physical Fitness in CKD study on 2 Siemens 3T Skyra, 1 Siemens 3T Prisma, 1 Siemens 1.5T Avanto, 1 GE Discovery 3T MR750, and 1 Philips 3T Ingenia systems. Technical performance metrics include cross-sectional bias (by weight), bias, linearity and reproducibility for the entire study, for each site, for each manufacturer and field strength.

RESULTS

392 subjects were scanned with phantoms on Siemens 1.5T (105), Siemens 3T (140), Philips 3T (68) and GE 3T (88). Overall, a linearity relationship was observed with negligible quadratic value and slope of 0.94 (95% CI: 0.938, 0.947). Mean bias was -3.8%, 1.5%, 1.8%, 0.3% and 2.4% for 100%, 35%, 16%, 10% and 0% fat fraction, with reproducibility standard deviation of 2.6%, 5.0%, 3.4%, 2.5% and 2.8% respectively. The mean bias differed significantly by vendor (p<0.001) and field strength (p<0.001). Siemens had the lowest overall bias and GE the highest. The bias was higher for field strength of 1.5T. Reproducibility differed by vendor (p=0.021) and field strength (p=0.015). Better precision (i.e. lower variance, thus higher reproducibility) was observed for GE, and worst precision (higher variance, thus poorer reproducibility) for Siemens. A field strength of 1.5T had better precision.

CONCLUSION

In general, PDFF is an excellent method of quantifying fat in vivo and is stable over time and across all fat fractions. However, the PDFF measurement is biased; slightly overestimated when the PDFF value is small and underestimated at higher PDFF values. The reproducibility coefficient (RDC) or %fat difference of 11.2% or larger, indicating a true difference when measured on different MR system vendors and field strengths and at different time points.

CLINICAL RELEVANCE/APPLICATION

Multi-point Dixon PDFF can quantify body fat accurately, however specific cutoffs for disease classification requires additional work and may depend upon vendor and field strength.

SSM08-06 Accuracy of Energy Spectrum CT Lipid Base Value in Quantitative Analysis of Non-Alcoholic Fatty Liver

Wednesday, Dec. 4 3:50PM - 4:00PM Room: E450B

Participants

Min Zhang, , China (*Presenter*) Nothing to Disclose Nan Yu, MD, Xianyang, China (*Abstract Co-Author*) Nothing to Disclose Jianying Li, Beijing, China (*Abstract Co-Author*) Employee, General Electric Company Ma Chunling, MMed, Xianyang City, China (*Abstract Co-Author*) Nothing to Disclose Lei Yuxin, MMed, Xianyang City, China (*Abstract Co-Author*) Nothing to Disclose Lihua Fan, Xian Yang, China (*Abstract Co-Author*) Nothing to Disclose Chuangbo Yang, MMed, Xianyang City, China (*Abstract Co-Author*) Nothing to Disclose Chuangbo Yang, MMed, Xianyang City, China (*Abstract Co-Author*) Nothing to Disclose Yongjun Jia, MMed, Xianyang, China (*Abstract Co-Author*) Nothing to Disclose Dong Han, MD, Xianyang, China (*Abstract Co-Author*) Nothing to Disclose Wanqiong Wang, Xianyang, China (*Abstract Co-Author*) Nothing to Disclose Mengting Yu, Shaanxi, China (*Abstract Co-Author*) Nothing to Disclose Yue Gao, Xianyang city, China (*Abstract Co-Author*) Nothing to Disclose

For information about this presentation, contact:

15596757635@163.com

PURPOSE

the accuracy of quantitative analysis and diagnosis of non-alcoholic fatty liver was assessed by comparing energy spectrum CT lipid matrix with magnetic resonance lipid matrix using magnetic resonance Q-dixon technique as a reference standard.

METHOD AND MATERIALS

Retrospective collection of patients who underwent both magnetic resonance quantitative Q-dixon sequence scan and energy spectrum CT scan within one week. After image acquisition, the average fat content of liver was quantitatively analyzed by placing region of interest (ROI). The method of sketching is to select ROI of two different hepatic lobes at the hepatic portal level, and one ROI from the hepatic portal level to the upper and lower levels, respectively, to record the liver fat fraction (FF) of each hepatic segment. Finally, the average fat fraction of the whole liver is obtained by the average method. Two doctors with rich experience in imaging diagnosis of liver diseases independently measured the lipid matrix and the corresponding ratio of liver to spleen on energy spectrum CT. The results were examined by a deputy director of imaging specialty. Finally, the differences among the groups were compared, and the correlation of MR fat fraction, fat matrix and liver-spleen ratio was analyzed. The diagnostic efficacy of energy spectrum CT fat matrix for mild fatty liver was tested by ROC curve.

RESULTS

This study total 80 cases. There was a positive correlation between FF on energy spectrum CT (r = 0.959, P = 0.000), and a negative correlation between liver-spleen ratio and fat fraction (r=-0.848, P = 0.000), as shown in Figures 1 and 2. ROC curve analysis showed that the sensitivity, specificity, cut-off point and area under curve were 95%, 100%, 351.19 and 0.990 respectively in the light fatty liver group, as shown in Figure 3.

CONCLUSION

Clinical evaluation of non-alcoholic fatty liver can refer to the fat content measured by CT fat matrix (the cut-off value is 351.19), and its correlation with the fat content measured by Q-dixon of 3.0T magnetic resonance is better than that measured by CT liver-spleen ratio. Energy spectrum CT lipid matrix can be used to quantitatively evaluate non-alcoholic fatty liver and has a good diagnostic effect for mild fatty liver.

CLINICAL RELEVANCE/APPLICATION

The fat concentration measurement in spectral CT can replace the Liver-Spleen CT Ratio as an imaging method for the diagnosis of fatty liver, and its accuracy is high.





Gastrointestinal (Pancreas Focal Disease)

Wednesday, Dec. <u>4 3:00PM - 4:00PM Room: E351</u>

GI

AMA PRA Category 1 Credit ™: 1.00 ARRT Category A+ Credit: 1.00

Participants

David M. Hough, MD, Rochester, MN (*Moderator*) Nothing to Disclose Hina Arif Tiwari, MD, Tucson, AZ (*Moderator*) Nothing to Disclose

Sub-Events

SSM09-01 Detection of Pancreatic Ductal Adenocarcinoma and Liver Metastases: Comparison of Contrast-Enhanced MR Imaging with Hepatobiliary versus Extracellular Contrast Materials

Wednesday, Dec. 4 3:00PM - 3:10PM Room: E351

Participants

Yoshifumi Noda, MD, PhD, Gifu, Japan (*Abstract Co-Author*) Nothing to Disclose Satoshi Goshima, MD, PhD, Hamamatsu City, Japan (*Abstract Co-Author*) Nothing to Disclose Yukiko Takai, Gifu, Japan (*Abstract Co-Author*) Nothing to Disclose Shoma Nagata, MD, Gifu, Japan (*Presenter*) Nothing to Disclose Nobuyuki Kawai, MD, Gifu, Japan (*Abstract Co-Author*) Nothing to Disclose Hiroshi Kawada, MD, Gifu, Japan (*Abstract Co-Author*) Nothing to Disclose Yukichi Tanahashi, MD, Gifu, Japan (*Abstract Co-Author*) Nothing to Disclose Masayuki Matsuo, MD, Gifu, Japan (*Abstract Co-Author*) Nothing to Disclose

PURPOSE

To compare the detectability of pancreatic ductal adenocarcinoma (PDAC) and liver metastases between contrast-enhcanced magnetic resonance (MR) imaging with hepatobiliary and extracellular contrast materials (ECCMs).

METHOD AND MATERIALS

Two hundred seventy-two patients with suspected of having a pancreatic disease underwent contrast-enhanced MR imaging with Gd-EOB-DTPA (EOB group, n = 79) or ECCMs (ECCM group, n = 193). The ECCMs included Gd-DTPA (n = 158), Gd-BT-DO3A (n = 28), Gd-DOTA (n = 5), and Gd-DTPA-BMA (n = 2). The signal intensities of pancreatic parenchyma, paraspinal muscle, PDAC if present, and background noise were measured, and then the signal intensity ratio (SIR) of the pancreas and tumor-to-pancreas contrast-to-noise ratio (CNR) were calculated. The conspicuity of PDAC was evaluated on the pancreatic parenchymal phase images, and that of liver metastases, if present, was also evaluated in all sequences. Qualitative and quantitative parameters were compared between EOB and ECCM groups.

RESULTS

The SIR of the pancreas (P = 0.30) and CNR (P = 0.46) were comparable between EOB and ECCM groups. The sensitivity (97.1% vs 93.5%, P = 0.42) and specificity (100.0% vs 99.2%, P = 1.00) for the detection of PDAC were comparable between EOB and ECCM groups. In the lesion-by-lesion analysis, EOB group showed significantly greater sensitivity for detecting liver metastases compared with ECCM group (95.0% vs 84.5%, P = 0.04).

CONCLUSION

Gd-EOB-DTPA-enhanced MR imaging with was comparable with ECCMs-enhanced MR imaging in detecting PDAC and demonstrated better sensitivity in detecting liver metastases.

CLINICAL RELEVANCE/APPLICATION

Gd-EOB-DTPA-enhanced MR imaging is all that is needed to examine patients with PDAC and contribute to the reduction of medical costs.

SSM09-02 The Stiffness as Obtained by Magnetic Resonance Elastography Correlates with the Stroma Proportion and Prognosis of Resectable Pancreatic Adenocarcinoma (PDAC)

Wednesday, Dec. 4 3:10PM - 3:20PM Room: E351

Participants

Shi Yu, MS, Shenyang, China (Presenter) Nothing to Disclose Xianyi Zhang, Shenyang , China (Abstract Co-Author) Nothing to Disclose Qiyong Guo, MD, Shenyang, China (Abstract Co-Author) Nothing to Disclose

For information about this presentation, contact:

18940259980@163.com

Abundant stroma is one of the most important features of PDAC that accounts for up to 90% of the tumor volume. The role of MRE in the prognostic prediction of PDAC remains unknown. Herein, our study was to investigate the value of the MRE-determined stiffness in evaluating the stroma proportion and the prognostic value of stiffness in resectable PDAC.

METHOD AND MATERIALS

A total of 146 resected PDAC patients were prospectively enrolled in this study from Jan 2016 to Dec 2018, all without preoperative chemotherapy or radiotherapy. Both sirius-red staining and H&E staining was used to evaluate the stromal proportion in PDAC. MRE examinations were performed on a 3.0T MR scanner (Signa HDX 3.0T system; GE Healthcare, Milwaukee). The imaging parameters were as follows: frequency=40Hz; TR/TE = 1375/38.8ms; phase offsets = 3; FOV = 40 cm; matrix = 96×96; number of signal averages = 1; frequency-encoding direction = RL; parallel imaging acceleration factor = 3; number of slices = 32; thickness = 3.5mm. Survival rates were calculated according to the Kaplan-Meier method and were compared using the log rank test. Multivariate analysis was performed with a Cox regression model.

RESULTS

PDAC showed significantly higher stiffness (3.11±0.61 kPa) than that of the non-tumor pancreatic parenchyma (1.22±0.24 kPa) (P<0.001). The average stromal proportion was 43.7±22.5%. The pancreatic stiffness was positively associated with the stromal proportion of resected PDAC (r= 0.811, P < 0.001). The pancreatic stiffness was also positively correlated with T stage and AJCC stage (AJCC 7th edition) (r= 0.713 and 0.692,both P < 0.001). High pancreatic stiffness (>3.19kPa) predicted unfavorable overall survival (OS) relative to low pancreatic stiffness (21.6 vs. 38.2 months, P= 0.011). The pancreatic stiffness was an independent prognostic factor for resected PDAC based on multivariate analysis (hazard ratio =5.174, 95%CI:2.41-11.07 P <0.001). Figure 1 showed 2 PDAC cases with 17% and 74% different stroma proportions as examples, respectively.

CONCLUSION

We demonstrated that the pancreatic stiffness obtained by MRE was positively associated with the stroma proportion in pancreatic cancer. Pancreatic stiffness can be a promising biomedical index for prognostic prediction in PDAC.

CLINICAL RELEVANCE/APPLICATION

MRE is a simple, fast and promising sequence that can be added in clinical routine pancreatic MR protocol, so as to help evaluate the stroma proportion of tumor and predict the prognosis of resectable PDAC for patients.

SSM09-03 Pancreatic Screening in High Risk Patients: Is Fast Non-Contrast MRI Protocol Feasible? A Proposal

Wednesday, Dec. 4 3:20PM - 3:30PM Room: E351

Participants Francesca Maio, MD, Napoli, Italy (Presenter) Nothing to Disclose Vincenzo Pasqualino, Padova, Italy (Abstract Co-Author) Nothing to Disclose Luca Bertana, MD, Rome, Italy (Abstract Co-Author) Nothing to Disclose Silvia Venturini, Treviso, Italy (Abstract Co-Author) Nothing to Disclose Valeria Cantoni, Napoli, Italy (Abstract Co-Author) Nothing to Disclose Michele C. Fusaro, Treviso, Italy (Abstract Co-Author) Nothing to Disclose Giovanni Morana, MD, Treviso, Italy (Abstract Co-Author) Speakers Bureau, Bracco Group

For information about this presentation, contact:

francescamaio9@gmail.com

PURPOSE

To validate a non-contrast fast MRI protocol for high risk patients as a screening tool to detect pancreatic cancer (PC) in its earliest phase, compatible with an R0 resection.

METHOD AND MATERIALS

200 patients (>40yo) were selected from our radiological database. 100 were negative for pancreatic lesions, 50 were positive for cystic lesions and 50 were positive for solid lesions; all lesions were smaller than 28mm. Three readers with a high, medium and low experience analysed selected MRI sequences (single-shot T2w breath-hold on axial and coronal plans, GE T1w FS on axial plan, DWI and 2D/3D MRCP) independently, randomly and anonymously. Readers identified or excluded the presence of pancreatic lesion. Results of reading session were compared with the final diagnosis and divided into five different classes of lesion: cystic, solid (all), adenocarcinoma, PNET and solid excluding PNET; Mcnemar's test was used to compare. Inter-observer agreement was determined according to the kappa statistic.

RESULTS

All readers showed high sensitivity and NPV in the identification of ADK (R1 100%-100%, R2 89%-98% and R3 83%-97%), with a good agreement to detect pancreatic lesions (k=0.52), especially ADK (k=0.82), PNET (>10mm) (k=0.70) and cystic lesions(k=0.87).

CONCLUSION

A non-contrast fast MRI protocol can be proposed as a screening tool in high risk patients for PC, reducing the time lapse between the controls, giving more chances for an early diagnosis with a better outcome.

CLINICAL RELEVANCE/APPLICATION

Fast MR protocol is able to detect small pancreatic lesions with high sensitivity and it can be used as a screening tool in high risk patients for pancreatic cancer, in order to achieve an early diagnosis and thus a better survival

SSM09-04 Relationship between Radiomics and Risk of Lymph Node Metastasis in Pancreatic Ductal Adenocarcinoma

For information about this presentation, contact:

bianyun2012@foxmail.com

PURPOSE

To explore the exact relationship between the arterial radiomics score (rad-score) and lymph node (LN) metastasis in pancreatic ductal adenocarcinoma (PDAC).

METHOD AND MATERIALS

A total of 225 patients with pathologically confirmed PDAC who underwent multislice computed tomography within one month of resection from December 2016 to August 2017 were retrospectively studied. For each patient, 1029 radiomics features of arterial phase were extracted, which were reduced using the least absolute shrinkage and selection operator (LASSO) logistic regression algorithm. Multivariate logistic regression models were utilized to analyze the association between the arterial rad-score and LN metastasis.

RESULTS

LN-negative and -positive patients accounted for 107 (47.56%) and 118 (52.44%) of the cohort, respectively. The rad-score, which consisted of 12 selected features of the arterial phase, was significantly associated with LN status (P<0.05). Univariate analysis revealed that the arterial rad-score and T stage were independently and positively associated with risk of LN metastasis (P<0.05). Stratified analysis showed that the impact of the arterial rad-score on LN metastasis was not affected by age, sex, BMI, CA19-9 level, tumor location, T stage, or grade of differentiation (P for interaction>0.05). The trend of increasing the arterial rad-score with higher likelihood of LN metastasis among age <59 years and >=66 years, sex, BMI, CA19-9 higher than 37ug/L, location, T2-4 stage and Well-moderately differentiation grade (P for trend <0.05). Multivariate analyses revealed a significant association between the arterial rad-score and the LN metastasis (p < 0.0001). Higher arterial rad-score was associated with LN metastasis (P for trend <0.0001).

CONCLUSION

The arterial rad-score is independently and positively associated with the risk of LN metastasis in PDAC.

CLINICAL RELEVANCE/APPLICATION

the arterial rad-score has significant association with the risk of LN metastasis in PDAC . A higher arterial rad-score is associated with a higher risk for LN metastasis. Thus, radiomics analysis may be a promising noninvasive method for assessment of LN metastasis.

SSM09-05 Time-intensity Curve Analysis of Endoscopic Contrast-Enhanced Ultrasound Can Help Discriminate Adenocarcinoma from Focal Pancreatitis

Wednesday, Dec. 4 3:40PM - 3:50PM Room: E351

Participants

Bino Á. Varghese, PhD, Los Angeles, CA (Abstract Co-Author) Nothing to Disclose James Buxbaum, MD, Los Angeles, CA (Abstract Co-Author) Nothing to Disclose Christopher Ko, Los Angeles, CA (Abstract Co-Author) Nothing to Disclose Kevin G. King, MD, La Crescenta , CA (Abstract Co-Author) Nothing to Disclose Ara Sahakian, Los Angeles, CA (Abstract Co-Author) Nothing to Disclose Jessica Serna, Los Angeles, CA (Abstract Co-Author) Nothing to Disclose Alice A. Lee, Los Angeles, CA (Abstract Co-Author) Nothing to Disclose Tanmay Deshmukh, Los Angeles, CA (Abstract Co-Author) Nothing to Disclose Shuchi Sehgal, Baltimore, MD (Abstract Co-Author) Nothing to Disclose Bhushan Desai, MBBS, MS, Los Angeles, CA (Abstract Co-Author) Nothing to Disclose Wilip M. Cheng, MD, MS, Culver City, CA (Abstract Co-Author) Nothing to Disclose Vinay A. Duddalwar, MD,FRCR, Los Angeles, CA (Presenter) Research Grant, Samsung Electronics Co, Ltd Advisory Board, DeepTek Consultant, Radmetrix

For information about this presentation, contact:

bino.varghese@med.usc.edu

PURPOSE

To evaluate the role of endoscopic contrast; enhanced ultrasound (CEUS) based time-intensity curve (TIC) analysis metrics in discriminating pancreatic ductal adenocarcinoma from focal pancreatitis.

METHOD AND MATERIALS

In this IRB approved study, we evaluated 13 patients with histopathology confirmed adenocarcinoma and 4 patients with focal pancreatitis. TIC were extracted from CEUS cine clips of focal pancreatic lesions following injection of 0.3 cc bolus of agitated perflutren lipid microspheres. The cine clips contained perfusion information for a minimum of 2mins post-injection and terminated once the characteristics enhancement patterns were obtained. 5mm circular ROI's were placed on the lesion by an experienced EUS expert and Intensity of contrast enhancement measured as an average were recorded from each image of the cine clip The ROIs were placed over homogenous regions of the lesion. In addition, surrounding normal tissue was used as a reference control). Using a customized MATLAB program, quantitative TIC analysis was performed on the extracted contrast-enhancement curves. Independent t-test was used to conduct exploratory univariate analysis of the TIC metrics to discriminate between lesion types and normal tissue and also to discriminate between lesion types. A significance threshold of 0.05 was used.

RESULTS

Among, the various TIC metrics, relative peak enhancement (PE) had the greatest utility to discriminate pancreatic ductal adenocarcinoma (PDAC) from focal pancreatitis. PDAC showed a significantly (p=0.003) lower PE of 0.46±0.22 compared to 0.99±0.27 for focal pancreatitis.

CONCLUSION

TIC analysis is a valuable evaluation tool for discriminating PDAC from focal pancreatitis which is a diagnostic dilemma.

CLINICAL RELEVANCE/APPLICATION

Improved differential diagnosis based on better discrimination of indeterminate solid pancreatic lesions will provide patient-specific care-management options.

SSM09-06 Incidental Multiple Intraductal Papillary Mucinous Neoplasms (IPMN): Imaging Findings that Predict Growth on Long-Term Follow-Up

Wednesday, Dec. 4 3:50PM - 4:00PM Room: E351

Participants

Roya Rezvani Habibabadi, Baltimore, MD (Presenter) Nothing to Disclose Mohammadreza Shaghaghi, MD, Baltimore, MD (Abstract Co-Author) Nothing to Disclose Maryam Ghadimi, MD, Baltimore, MD (Abstract Co-Author) Nothing to Disclose Pegah Khoshpouri, MD, Baltimore, MD (Abstract Co-Author) Nothing to Disclose Pallavi Pandey, MD, Baltimore, MD (Abstract Co-Author) Nothing to Disclose Sanaz Ameli, MD, Baltimore, MD (Abstract Co-Author) Nothing to Disclose Bita Hazhirkarzar, MD, Baltimore, MD (Abstract Co-Author) Nothing to Disclose Mounes Aliyari Ghasabeh, MD, Baltimore, MD (Abstract Co-Author) Nothing to Disclose Ankur Pandey, MD, Baltimore, MD (Abstract Co-Author) Nothing to Disclose Ihab R. Kamel, MD, PhD, Baltimore, MD (Abstract Co-Author) Research Grant, Siemens AG

For information about this presentation, contact:

rrezvan3@jhmi.edu

PURPOSE

To assess growth rate of incidental IPMNs on long-term imaging follow-up and to evaluate the association between baseline imaging features and rate of growth.

METHOD AND MATERIALS

This IRB-approved, retrospective study included incidental multiple IPMNs (diameter>=4mm); with baseline cross-sectional imaging between 2002-2015, and follow-up imaging performed at least 12 months apart. In each patient, up to five of the largest cysts were identified and measured at baseline and last follow-up. For IPMNs demonstrating size change, the estimated time to growth was determined by reviewing all the intermediate imaging. Cysts' growth was determined based on ACR criteria. For each cyst, location, cluster or solitary presentation, dominancy, and other characteristics of the background pancreas were determined. A cluster was defined as presence of >3 cysts in one anatomic location of pancreas. A cyst was defined as dominant when it was >50% larger than the second largest cyst in the pancreas. The association with growth was adjusted with time intervals using univariate Cox analysis.

RESULTS

95 cysts in 31 patients were followed for a median of 56 months (range, 12-170 months). The mean cyst growth rate was 0.46 mm/year. According to ACR-criteria, 22 cysts (24%) grew, 14 cysts (15%) decreased in size and 59 cysts (62%) remained stable on follow-up imaging. The median time to growth was 55 months (range, 12-133 months).13 cysts (14%) were identified as dominant. 44 cysts (46 %) were located in a cluster as compared to 51cysts (54%) with a solitary presentation. Clustered presentation was found to have significant association with occurrence and rate of growth in IPMNs (HR, 3.4; P= 0.035 & Coef, 0.59; p=0.002, respectively).

CONCLUSION

Clustered presentation was independently associated with growth in multiple IPMNs. This could be due to the presence of underlying pathology in a focal region of pancreas. Measuring the largest cyst may not be adequate in representing size change in all other cysts and other features of multiplicity need to be considered in multiple IPMNs surveillance.

CLINICAL RELEVANCE/APPLICATION

There is no specific recommendation regarding long-term follow-up in patients with multiple IPMNs. Our data might be useful for developing a more specific surveillance strategy for multiple IPMNs with regards to choosing the targeted cyst and identifying predictive parameters.





Gastrointestinal (DECT Technique)

Wednesday, Dec. <u>4</u> 3:00PM - 4:00PM Room: E352



AMA PRA Category 1 Credit ™: 1.00 ARRT Category A+ Credit: 1.00

FDA Discussions may include off-label uses.

Participants

Amir Borhani, MD, Chicago, IL (Moderator) Author, Reed Elsevier

Desiree E. Morgan, MD, Birmingham, AL (*Moderator*) Institutional Research Grant, General Electric Company; Consultant, General Electric Company

Huadan Xue, MD, Beijing, China (Moderator) Nothing to Disclose

Sub-Events

SSM10-01 Standardization of Dual-Energy CT Iodine Uptake of the Abdomen: Defining Reference Values in a Big Data Cohort

Wednesday, Dec. 4 3:00PM - 3:10PM Room: E352

Participants

Ibrahim Yel, MD, Frankfurt, Germany (*Presenter*) Nothing to Disclose Christian Booz, MD, Frankfurt am Main, Germany (*Abstract Co-Author*) Speaker, Siemens AG Simon S. Martin, MD, Charleston, SC (*Abstract Co-Author*) Institutional Research support, Siemens AG Lukas Lenga, Frankfurt, Germany (*Abstract Co-Author*) Nothing to Disclose Thomas J. Vogl, MD, PhD, Frankfurt, Germany (*Abstract Co-Author*) Nothing to Disclose Moritz H. Albrecht, MD, Charleston, SC (*Abstract Co-Author*) Speaker, Siemens AG Carlo N. De Cecco, MD, Atlanta, GA (*Abstract Co-Author*) Research Grant, Siemens AG Benjamin Kaltenbach, MD, Kelkheim, Germany (*Abstract Co-Author*) Nothing to Disclose

For information about this presentation, contact:

dr.ibrahimyel@gmail.com

PURPOSE

Despite a wealth of literature on dual-energy CT(DECT) iodine uptake in various pathologies, physiologic reference values for this technique for confident clinical application have not been defined to date. Therefore, we investigated the iodine uptake of healthy abdominal and pelvic organs in a big data cohort.

METHOD AND MATERIALS

Consecutive portal-venous abdominal DECTs were reviewed and unremarkable exams were included (n=520; white/asian=489; mean age= 59 ± 15 ,5 years; 265w/255m). ROI-measurements were performed in the following anatomical regions (number of ROIs): liver(9), pancreas(3), spleen(3), adrenal glands(2), kidneys(6), prostate(4), uterus(2), urinary bladder wall(1) and lymph nodes (3). Iodine uptake was compared among different organs and subgroup analysis was performed (young vs old/male vs female).

RESULTS

Overall mean iodine uptake values were as followed (mg/ml): liver= 1.93 ± 0.54 , pancreas= 2.06 ± 0.57 , spleen= 2.55 ± 0.65 , adrenal glands= 1.66 ± 0.43 , kidneys= 6.28 ± 1.36 , prostate= 1.11 ± 0.52 , uterus= 1.07 ± 0.74 , bladder= 0.69 ± 0.29 and lymph nodes= 0.75 ± 0.21 . Portal-venous iodine uptake was comparable between liver/pancreas and liver/adrenal glands (p>=0.119). Women showed higher iodine uptake for liver (2.07 ± 0.58 vs 1.79 ± 0.45 mg/ml), pancreas (2.29 ± 0.57 vs 1.83 ± 0.47 mg/ml), spleen (2.81 ± 0.65 vs 2.30 ± 0.53 mg/ml), adrenal glands (1.76 ± 0.49 vs 1.56 ± 0.33 mg/ml) and kidneys (6.74 ± 1.36 vs 5.83 ± 1.20 mg/ml) than men(p<0.001). In older patients, iodine uptake increased for liver (1.98 ± 0.52 vs 1.87 ± 0.54 mg/ml), spleen (2.48 ± 0.65 vs 2.63 ± 0.64 mg/ml) and kidneys (6.11 ± 1.24 vs 6.45 ± 1.45 mg/ml) compared to younger subjects (p<=0.040). Only the uterus showed lower values in older women (0.77 ± 0.45 vs 1.35 ± 0.84 mg/ml, p<0.001).

CONCLUSION

Physiologic iodine uptake values show age- and gender-related differences for the liver, spleen and kidneys. Pancreas and adrenal glands show higher iodine perfusion in women. While prostate parenchyma seems unaffected throughout lifetime, iodine supply of the uterus decreases in elderly women. Lymph nodes and bladder are unaffected by demographic influences.

CLINICAL RELEVANCE/APPLICATION

We defined physiologic reference values for static perfusion of abdominal organs, as indicated by DECT iodine uptake in a big data cohort and described the related differences regarding age and gender, in order to facilitate more reliable clinical application of this technique and ultimately, potential implementation in future guidelines.

SSM10-02 Texture Analysis of Split-Filter DECT Virtual Monoenergetic Images of Pancreas and Liver Tumors and Healthy Tissue

Participants

Lianna di Maso, Madison , WI (*Presenter*) Nothing to Disclose Jessie Huang, PHD, Madison, WI (*Abstract Co-Author*) Nothing to Disclose Michael Lawless, PHD, Madison, WI (*Abstract Co-Author*) Nothing to Disclose Larry A. Dewerd, PhD, Madison , WI (*Abstract Co-Author*) Stockholder, Standard Imaging, Inc Jessica Miller, PhD, Madison, WI (*Abstract Co-Author*) Research Grant, Siemens AG

For information about this presentation, contact:

dimaso@wisc.edu

PURPOSE

The purpose of this work is to investigate the effect of energy on CT texture analysis (CTTA) of pancreas and liver tumors and healthy tissue using virtual monoenergetic images (VMIs) generated from split-filter dual-energy CT (DECT).

METHOD AND MATERIALS

Split-filter DECT data was acquired for pancreatic and liver cancer patients using the Siemens SOMATOM Definition Edge CT scanner for radiation treatment planning with 100 ml of iodinated contrast medium. VMIs at energies ranging from 40-90 keV in 5 keV increments were reconstructed in Siemens' Syngo.via (VB30) software. Based on radiation oncologist reviewed contours of tumor and healthy tissue, first order CTTA parameters of the pancreas and liver tumor and healthy tissue were extracted from MIMvista including mean CT number (MCTN), standard deviation (SD), skewness, and kurtosis. Statistical analysis was performed using ANOVA.

RESULTS

Among the CTTA parameters investigated, MCTN and SD showed a statistically significant decrease with increasing energy of VMIs for pancreas and liver tumor and healthy tissue (p<0.0001). On the other hand, skewness and kurtosis did not change with energy of VMIs for pancreas and liver tumor and healthy tissue (p<0.7). There was a statistically significant difference in MCTN between pancreas and liver tumor and healthy tissue for low-energy VMIs (p<0.04). Although kurtosis did not change with energy, there was a statistically significant difference between the kurtosis of pancreas tumor and healthy tissue for all VMIs investigated (p<0.05). This trend was not apparent for liver tumor and healthy tissue for all VMIs investigated (p<0.05). This trend was not apparent for liver tumor and healthy tissue for all VMIs investigated (p<0.04). This trend was not apparent for tumor and healthy tissue for all VMIs investigated (p<0.04). This trend was not apparent for the liver cases (p>0.08).

CONCLUSION

The energy of split-filter VMIs has no impact on skewness or kurtosis of pancreas and liver tumor and healthy tissue. The difference in MCTN between pancreas tumor and healthy tissue is greatest for low-energy split-filter VMIs. Kurtosis determined from split-filter VMIs was different between pancreas tumor and healthy tissue.

CLINICAL RELEVANCE/APPLICATION

Skewness and kurtosis are reliable CTTA parameters that do not change as a function of energy. MCTN, SD and kurtosis have the potential to differentiate tumor and healthy tissue on split-filter VMIs. These results can be used as a baseline for higher-order CTTA of pancreas and liver tumor and healthy tissue.

SSM10-03 Quantification of the Liver-Fat Content Using Multimaterial Decomposition (MMD) Algorithm and Material Decomposition Technique: A Vitro Experiment Study

Wednesday, Dec. 4 3:20PM - 3:30PM Room: E352

Participants Tingting Xie JR, MD, Shenzhen, China (*Presenter*) Nothing to Disclose Guanxun Cheng, MD,PhD, Shenzhen, China (*Abstract Co-Author*) Nothing to Disclose Ying Guo, Guangzhou, China (*Abstract Co-Author*) Nothing to Disclose

For information about this presentation, contact:

ttxietinarsna@163.com

PURPOSE

Our first goal was to build in vitro liver-fat model to provide a phantom for fat content quantification in study. The second goal was to evaluate the difference of feasibility and accuracy of using MMD algorithm and dual energy CT material decomposition technique for fat content quantification to provide a basis for the precise fat quantification in clinical use.

METHOD AND MATERIALS

A total of 6 homogeneous liver-fat mixed samples with various fat volume contents from 0-50% (with an interval of 10%). Scanned by GE Revolution CT scanner using GSI mode with rapid tube voltage switching between 80-140 kVp. After the CT scan, reconstructed imaging data were processed with GSI imaging analysis software and MMD soft-ware currently not commercially available. Fat concentration (on fat-water bases) measured with consistent ROIs placed in the tube center. Each sample was recorded at 4 different regions for average and statistical analysis. A linear regression was performed using SPSS 19.0 software to analyze the relationship between the measured fat concentration and the actual fat concentration. P value less than 0.05 was considered to indicate a linear correlation.

RESULTS

(1) We had successfully developed the model in vitro for fat content quantification. With the designed concentration series, the gradient range covered clinical fat content in different body regions. And the model provided a novel way to investigate in vitro fat content. (2) Both algorithms showed good linear relationship between the measured fat concentration and actual concentration. MMD algorithm revealed a linear correlation equation of y=1.498x-73.5, $R^2 = 0.944$, P=0.001, F=84.748. For material decomposition technique, the linear correlation equation was y=0.079x+30.52, $R^2 = 0.983$, P=0.001, F=234.397.

CONCLUSION

Both of MMD algorithm and spectral CT material decomposition technique were demonstrated to provide accurate and reliable measurement of fat content for liver-fat model, which will contribute to the development of clinical fat content quantification assays.

CLINICAL RELEVANCE/APPLICATION

This study demonstrated the feasibility of using MMD algorithm and material decomposition techniques to precisely quantify the fat concentrations. The advantages of these quantification methods include reduced labor, high accuracy with no additional scanning required, which makes it attractive to be applied in future clinical tests and lipid metabolism studies.

SSM10-04 Virtual Non-Contrast Images from Contrast-Enhanced Dual-Layer Spectral CT for Pediatric Abdominal CT: Are They Different from Adults?

Wednesday, Dec. 4 3:30PM - 3:40PM Room: E352

Participants

Minako Azuma, Miyazaki, Japan (*Presenter*) Nothing to Disclose Toshinori Hirai, MD, PhD, Miyazaki, Japan (*Abstract Co-Author*) Research Grant, Bayer AG Youhei Hattori, Miyazaki, Japan (*Abstract Co-Author*) Nothing to Disclose Zaw Aung Khant, Miyazaki, Japan (*Abstract Co-Author*) Nothing to Disclose Hiroshi Nakada, MD, PhD, Miyazaki, Japan (*Abstract Co-Author*) Nothing to Disclose

PURPOSE

Virtual non-contrast (VNC) images from dual-layer spectral CT (DLSCT) might replace true unenhanced images for pediatric abdominal CT studies. We compared the accuracy of iodine subtraction in pediatric abdominal organs on VNC images obtained from contrast-enhanced DLSCT scans with that of true unenhanced (TU) images and assessed the difference between pediatric and adult patients.

METHOD AND MATERIALS

We included 10 child- (1-15 years, mean 8.7±4.4 year) and 40 adult patients (28-87 years, mean 56.4±17.6 year) who underwent unenhanced and contrast-enhanced DLSCT. Two radiologists assessed the image quality of all images on a 5-point scale. Venous-phase VNC images were generated and a region-of-interest (ROI) was placed on the liver, spleen, renal cortex, aorta, fat tissue, muscle and fiuid (gallbladder) on TU- and VNC images. The attenuation of each ROI in VNC image was subtracted from the corresponding attenuation of the TU image. The difference in attenuation between VNC- and TU images of children and adults was compared using the independent t-test and regression analysis.

RESULTS

In all 50 patients, there was no significant difference in the image quality of VNC- and TU scans (children: 4.8 \pm 0.4; adult: 4.5 \pm 0.5). The attenuation difference in the renal cortex between VNC- and TU images was significantly greater in adults than children (9.6 \pm 7.2 vs 1.2 \pm 8.2 HU, p=0.0046). The attenuation difference in the liver and spleen showed a similar tendency. With respect to fat tissue, attenuation was higher on VNC than TU images in almost all 50 patients. Scatter plots of the attenuation difference between VNC- and TU images versus the patient age showed a significant positive correlatoin only in the renal cortex (r=0.34, p=0.034).

CONCLUSION

VNC images derived from contrast-enhanced DLSCT showed iodine subtraction in abdominal organs more accurately on scans of children than adults.

CLINICAL RELEVANCE/APPLICATION

For the evaluation of abdominal contrast-enhanced CT scans, VNC imaging may be more useful in children than adults.

SSM10-05 Intra-individual Consistency of Spectral Detector CT-Enabled Iodine Quantification of the Intravascular and Renal Blood Pool

Wednesday, Dec. 4 3:40PM - 3:50PM Room: E352

Participants

Simon Lennartz, MD, Cologne, Germany (*Presenter*) Institutional Research Grant, Koninklijke Philips NV Nuran Abdullayev, MD, Cologne, Germany (*Abstract Co-Author*) Nothing to Disclose David Zopfs, MD, Cologne, Germany (*Abstract Co-Author*) Nothing to Disclose David C. Maintz, MD, Koln, Germany (*Abstract Co-Author*) Nothing to Disclose Stefan Haneder, MD, Cologne, Germany (*Abstract Co-Author*) Nothing to Disclose Thorsten Persigehl, MD, Koeln, Germany (*Abstract Co-Author*) Nothing to Disclose Nils Grosse Hokamp, MD, Koln, Germany (*Abstract Co-Author*) Speakers Bureau, Koninklijke Philips NV

For information about this presentation, contact:

Simon.Lennartz@uk-koeln.de

PURPOSE

Recent studies revealed high diagnostic accuracy of iodine maps from spectral detector CT (SDCT); however, little is known on reproducibility of iodine measurements in vivo which is crucial for oncologic follow-up imaging. Hence, the objective of this study was to analyze the intra-individual, longitudinal consistency in patients that underwent multiple SDCT examinations.

METHOD AND MATERIALS

79 patients with 2 (53 patients) or 3 (26 patients) clinically-indicated, biphasic (arterial/venous) abdominal SDCT scans were retrospectively identified for study inclusion. HU attenuation in conventional images and iodine concentration in iodine maps were measured by an experienced radiologist who placed circular regions of interest (ROI) in the following areas (two ROI each):

abdominal aorta, inferior caval vein, portal vein, renal cortices. To investigate intra-individual consistency of iodine and HU measurements, modified variation coefficients (MVC) were calculated.

RESULTS

Variability of HU attenuation and iodine concentration was significantly higher in arterial phase than in venous phase images (p <= 0.05). Regarding arterial phase attenuation measurements, median MVC was -1.8 (-20.5-21.3) % within the aorta and -6.5 (-44.0 - 48.7) % within the renal cortex while in the portal venous phase it was 0.62 (-11.1-11.7) % and -1.6 (-16.2-10.6) %, respectively. Regarding iodine quantification, MVC of arterial phase measurements was -2.5 (-22.9-28.4) % within the aorta and -5.8 (-55.9 - 29.6) % within the renal cortex. Referring MVCs of the portal venous phase were -0.7 (-17.9-16.9) % and -2.6 (-17.6-12.5) %.

CONCLUSION

Intra-individual iodine quantification of intravascular and renal blood pool is most consistent in venous-phase images (overall MVC: ± 15 %) whereas arterial phase measurements are subject to greater variability.

CLINICAL RELEVANCE/APPLICATION

For clinical application of SDCT-derived iodine quantification, a certain variability of venous phase images should be considered while particular care must be taken when calculating iodine thresholds from arterial phase images, e.g. in oncologic follow-up.

SSM10-06 Conventional versus Virtual Monoenergetic Images from Spectral Detector CT: Evaluation of Attenuation and Noise

Wednesday, Dec. 4 3:50PM - 4:00PM Room: E352

Participants

Nils Grosse Hokamp, MD, Koln, Germany (*Presenter*) Speakers Bureau, Koninklijke Philips NV Michelle K. Jordan, Beachwood, OH (*Abstract Co-Author*) Nothing to Disclose Kai Roman Laukamp, MD, Cleveland, OH (*Abstract Co-Author*) Nothing to Disclose Stefan Haneder, MD, Cologne, Germany (*Abstract Co-Author*) Nothing to Disclose David C. Maintz, MD, Koln, Germany (*Abstract Co-Author*) Nothing to Disclose Robert C. Gilkeson, MD, Cleveland, OH (*Abstract Co-Author*) Research Consultant, Riverain Technologies, LLC Research support, Koninklijke Philips NV Research support, Siemens AG Research support, General Electric Company Amit Gupta, MBBS, Cleveland, OH (*Abstract Co-Author*) Nothing to Disclose

For information about this presentation, contact:

nils.grosse-hokamp@uk-koeln.de

PURPOSE

The utilization of VMI in daily practice is limited as attenuation (HU) is quite different and extensive re-windowing may be required. We aimed to identify the VMI energy that closest represents conventional images (CI) in order to demonstrate that these images demonstrate improved image quality in terms of noise and Signal-to-noise ratio (SD/SNR) while attenuation values remain unaltered as compared to CI.

METHOD AND MATERIALS

60 and 30 patients with contrast-enhanced (CE) and non-enhanced (NCE) SDCT of the abdomen were included in this retrospective, IRB-approved study. CI and VMI of 66, 68, 70, 72 and 74keV as well as quantitative iodine maps were reconstructed (Q-IodMap). Two regions of interest were placed in each: aorta, liver, pancreas, renal cortex and psoas muscle. For each reconstruction, attenuation and standard deviation were averaged. Δ HU and Signal-to-noise ratio was computed (SNR=HU/SD) were calculated. Q-IodMap were considered as confounder for Δ HU.

RESULTS

In NCE studies, no significant differences for any region was found. In CE studies, VMI72keV images showed lowest Δ HU (HUliverCI/VMI72keV: 104±18/103±17, p>=0.05). Iodine containing voxels as indicated by Q-IodMap resulted in over- and underestimation of attenuation in lower and higher VMI energies. Image noise was lower in VMI images (e.g. muscle: CI/ VMI72keV: 15.3±3.3 / 12.3±2.9 HU, p<=0.05). Hence, SNR was significantly higher in VMI72keV compared to CI (e.g. liver 3.8±0.6 vs 3.0±0.8, p<=0.05).

CONCLUSION

VMI72keV show improved SD/SNR characteristics while the attenuation remains unaltered as compared to CI. These images possibly may be used as replacement for conventional images.

CLINICAL RELEVANCE/APPLICATION

The noise reduction enabled by VMI72keV may allow for a reduction of radiation dose. The CI-equivalent attenuation values may increase their clinical acceptance.





Gastrointestinal (CT Diagnosis)

Wednesday, Dec. 4 3:00PM - 4:00PM Room: E353A



AMA PRA Category 1 Credit ™: 1.00 ARRT Category A+ Credit: 1.00

Participants

Perry J. Pickhardt, MD, Madison, WI (*Moderator*) Stockholder, SHINE Medical Technologies, Inc; Stockholder, Elucent Medical; Advisor, Bracco Group;

Andrea S. Kierans, MD, New York, NY (Moderator) Nothing to Disclose

Sub-Events

SSM11-01 The Role of Dynamic Contrast-Enhanced CT in Diagnosis and Management of Patients with Sustained Bleeding After Liver Transplantation

Wednesday, Dec. 4 3:00PM - 3:10PM Room: E353A

Participants

Jieun Byun, MD, Seoul, Korea, Republic Of (*Presenter*) Nothing to Disclose Kyoung Won Kim, Seoul, Korea, Republic Of (*Abstract Co-Author*) Nothing to Disclose Ji Young Woo, Seoul, Korea, Republic Of (*Abstract Co-Author*) Nothing to Disclose Seongkeun Park, PhD, Asan, Korea, Republic Of (*Abstract Co-Author*) Nothing to Disclose Jae Hyun Kwon, Seoul, Korea, Republic Of (*Abstract Co-Author*) Nothing to Disclose Gi Won Song, Seoul, Korea, Republic Of (*Abstract Co-Author*) Nothing to Disclose Sung Gyu Lee, MD, Seoul, Korea, Republic Of (*Abstract Co-Author*) Nothing to Disclose

PURPOSE

To investigate the role of dynamic contrast-enhanced CT (DCE-CT) in the diagnosis and management of patients with sustained bleeding after liver transplantation (LT).

METHOD AND MATERIALS

Between November 2013 and December 2017, we retrospectively identified 270 patients (52.8±9.8 years; 18-76 years) who underwent DCE-CT after LT with clinically suspected postoperative bleeding. DCE-CT images were analyzed with emphasis on contrast media extravasation (CME): bleeding source, volume, rate, and morphologic pattern (type I, focal or stippled pattern; type II, jet-like pattern). Recipients were classified into two groups by primarily-chosen treatment method; nontherapeutic intervention (NTI) trial and primary therapeutic intervention (TI) groups. NTI trial group was further subdivided into NTI success and NTI failure groups according to results of NTI treatment. The differences of CME volume, rate, and pattern among the three groups and between the subgroups were evaluated. The concordances of bleeding source determined by DCE-CT to actual bleeding source were analyzed.

RESULTS

Of the 270 patients with clinically suspected postoperative bleeding, 134 CME sites were identified in 116 (43.0%) patients. While most (94.8%, 146/154) of patients without CME was successfully managed by NTI, the proportion decreased in the order particularly on portal venous phase with type I (48.5%, 16/33) and type II (16.9%, 14/83) CMEs. The mean CME volume on both arterial and portal venous phases and the mean CME rate significantly increased in order of NTI success, NTI failure, and primary TI groups (p<0.01, respectively). In subgroup analysis of NTI trial group, type II CME on portal venous phase was significantly higher in NTI failure group than in NTI success group (86.7% [13/15] versus 46.7% [14/30], p=0.01). There was substantial agreement in localization of bleeding source between DCE-CT and surgery or angiography (Cohen Kappa=0.78).

CONCLUSION

DCE-CT is helpful in the assessment for need of TI and to determine the treatment of choice in recipient with postoperative bleeding after LT.

CLINICAL RELEVANCE/APPLICATION

 $\mathsf{DCE-CT}$ is helpful in the assessment for need of the rapeuric intervention and in decision of treatment method in recipient with postoperative bleeding after LT.

SSM11-03 CT Evaluation of Bowel Perforation: Diagnostic Performance and Correlation of Imaging Features According to Sites and Causes

Wednesday, Dec. 4 3:20PM - 3:30PM Room: E353A

Participants

Keum-Nahn Jee, MD,PhD, Cheonan, Korea, Republic Of (*Abstract Co-Author*) Nothing to Disclose Yun Jin Lim, Cheonan, Korea, Republic Of (*Presenter*) Nothing to Disclose Mi Hyun Park, Cheonan, Korea, Republic Of (*Abstract Co-Author*) Nothing to Disclose

For information about this presentation, contact:

jkn1303@yahoo.com

PURPOSE

To evaluate diagnostic accuracy of CT and correlation of imaging features of bowel perforation, according to sites and causes

METHOD AND MATERIALS

239 patients (M; F = 190:49, mean age 56.2) confirmed as bowel perforation were included. We analyzed initial CT scan with 3-D reformation, and evaluated about pneumoperitoneum, ascites, bowel discontinuity, mechanical or paralytic ileus, active bleeding, hemoperitoneum, and localized peritoneal change like fecaloma, etc. according to sites and causes, by consensus of two abdominal radiologists, and reviewed medical record. Exclusion criteris were previous abdominal surgery or peritonitis or peritoneal carcinomatosis, liver cirrhosis, peritoneal dialysis, and more than 48 hours between CT scan and surgery.

RESULTS

97 patients were traumatic (gastro-duodenum [n=8], jejunum/ileum [n=67], colon/rectum [n=22]) and 142 non-traumatic (gastroduodenum [n=126], jejunum/ileum [n=8], colon/rectum [n=8]) causes. Overall CT accuracy was 84.1%; higher in traumatic and non-traumatic gastro-duodenum (100% and 96.8%) and non-traumatic colon/rectum (100%), and lowest in traumatic perforation of jejunum/ileum (61.5%). CT analysis results with statistical significant difference (p<.05) were as follows; pneumoperitoneum in gastro-duodenum and colon/rectum more than non-traumatic jejunum/ileum, ileus in traumatic gastro-duodenum and jejunum/ileum more than the others, bowel discontinuity in traumatic cuase more than non-traumatic, localized peritoneal change in traumatic gastro-duodenum and non-traumatic causes, regional lymphadenopathy in non-traumatic colon/rectum, active bleeding or hemoperitoneum only in traumatic causes, and increased morbidity and mortality in older age regardless of sites or causes.

CONCLUSION

Diagnostic accuracy is good, highest in gastro-duodenal and non-traumatic colo-rectal perforation, and lowest in traumatic perforation of jejunum and ileum shows low diagnostic accuracy due to lower frequency of bowel discontinuity, pneumoperitoneum, and localized peritoneal change. Bowel discontinuity is more frequent in traumatic cause. Localized peritonel abnormality is more frequent in non-traumatic cause.

CLINICAL RELEVANCE/APPLICATION

CT with 3-dimentional reformation could show good diagnostic performance for bowel perforation and various imaging features according to sites and causes of perforation.

SSM11-04 Relative Sarcopenia with Excess Adiposity is an Independent Predictor of Survival After Transjugular Intrahepatic Portosystemic Shunt (TIPS) Creation

Wednesday, Dec. 4 3:30PM - 3:40PM Room: E353A

Participants

Islam H. Zaki, MBBCh, Durham, NC (*Presenter*) Nothing to Disclose Erol Bozdogan, MD, Durham, NC (*Abstract Co-Author*) Nothing to Disclose Matthew K. Langman, MD, Durham, NC (*Abstract Co-Author*) Nothing to Disclose Matthew Kappus, MD, Durham, NC (*Abstract Co-Author*) Nothing to Disclose Steven S. Choi, MBBS, Durham, NC (*Abstract Co-Author*) Nothing to Disclose Jonathan Martin, MD, Durham, NC (*Abstract Co-Author*) Nothing to Disclose Jonathan Martin, MD, Durham, NC (*Abstract Co-Author*) Nothing to Disclose Tony P. Smith, MD, Durham, NC (*Abstract Co-Author*) Nothing to Disclose Charles Y. Kim, MD, Raleigh, NC (*Abstract Co-Author*) Nothing to Disclose Charles Y. Kim, MD, Raleigh, NC (*Abstract Co-Author*) Nothing to Disclose Charles Y. Kim, MD, Cary, NC (*Abstract Co-Author*) Research Grant, Siemens AG; Research Grant, NGM Biopharmaceuticals, Inc; Research Grant, Madrigal Pharmaceuticals, Inc; Research Grant, Metacrine, Inc; Research Grant, Pinnacle Clinical Research; Research Grant, ProSciento Inc; Research Grant, Carmot Therapeutics; Research Grant, 1Globe Health Institute; Research Consultant, ICON plc; James S. Ronald, MD, PhD, Durham, NC (*Abstract Co-Author*) Nothing to Disclose

For information about this presentation, contact:

Islam.Zaki@duke.edu

PURPOSE

To assess whether relative sarcopenia with excess adiposity is a risk factor for poor survival after TIPS.

METHOD AND MATERIALS

This single institution retrospective study included patients over 18 years of age who underwent TIPS creation and had abdominal CT scans performed within 100 days prior to or 30 days after TIPS. Subcutaneous fat, visceral fat and abdominal wall muscles were segmented at the inferior L3 endplate. Relative sarcopenia with excess adiposity was defined as the lowest gender specific quartile of muscle area divided by muscle plus fat area. Dates of death, liver transplantation, spontaneous occlusion or embolization of the TIPS, and post-TIPS hepatic encephalopathy (HE) were identified. Mortality was analyzed using competing risks survival analysis, and post-TIPS HE was analyzed using negative binomial regression and competing risks survival analysis

RESULTS

The cohort included 141 patients (mean age 56 years \pm 11, 91 men) who underwent CT an average of 17 days before TIPS (range 97 days prior to 26 days after). In univariate survival analyses, Model for End Stage Liver Disease (MELD) score (hazard ratio [HR]=1.09 per 1-point increase in MELD, 95% confidence interval [CI]=1.05-1.13, p<0.001) and relative sarcopenia with excess adiposity (HR=2.7, CI=1.55-4.69, p<0.001) were significant risk factors for shorter survival after TIPS. In a multivariate analysis both MELD score (HR=1.11, CI=1.06-1.16, p<0.001) and relative sarcopenia with excess adiposity (HR=2.46, CI=1.42-4.26, p=0.001) were significant predictors of survival. The C-index at 30 days was 0.71 for MELD, 0.72 for relative sarcopenia with excess adiposity, and 0.8 for a model including both. There was no association between relative sarcopenia with excess adiposity

and number of post-TIPS HE episodes (incidence rate ratio=1.08, CI=0.49-2.40, p=0.84) or time to first post-TIPS HE episode (HR=0.89, CI=0.51-1.54, p=0.67)

CONCLUSION

Relative sarcopenia with excess adiposity, defined as the lowest quartile of gender specific muscle area normalized to muscle plus fat measured by CT, is an independent risk factor for poor survival after TIPS and may supplement MELD score

CLINICAL RELEVANCE/APPLICATION

A deficiency in abdominal muscle mass relative to fat as assessed by CT is associated with poor survival after TIPS. This anthropometric index may improve the ability to predict outcomes in cirrhotic patients undergoing TIPS

SSM11-05 Value of Computed Tomography Finding in Evaluating the Acute Cellular Rejection of the Pancreas Allograft

Wednesday, Dec. 4 3:40PM - 3:50PM Room: E353A

Participants

Jeong A Yeom, Yangsan, Korea, Republic Of (*Abstract Co-Author*) Nothing to Disclose Hwaseong Ryu, Yangsan, Korea, Republic Of (*Presenter*) Nothing to Disclose Tae Un Kim, MD, Yangsan, Korea, Republic Of (*Abstract Co-Author*) Nothing to Disclose Jun Woo Lee, MD, Pusan, Korea, Republic Of (*Abstract Co-Author*) Nothing to Disclose

PURPOSE

To investigate computed tomography (CT) findings in patients with or without acute cellular rejection (ACR) after pancreas transplantation

METHOD AND MATERIALS

Twenty-two pancreas allograft recipients (pancreas transplantation alone: 17, pancreas transplantation after kidney transplantation: 3, pancreas transplantation after liver transplantation: 1, simultaneous pancreas and kidney transplantation: 1) that underwent at least one follow-up CT examination were included in this study. Among them, 8 patients were diagnosed as ACR by percutaneous biopsy within 3 day from CT examination. Two radiologists analyzed pre-biopsy CT images of patients with ACR and the latest CT images of patients without ACR compared with early follow-up CT for graft swelling, perivascular soft tissue infiltration of graft arteries, change from acute to obtuse angle between graft SMV and splenic vein, graft enhancement on the delayed phase, fat strands or fluid around graft, and graft duodenal wall thickening. Intra-class correlation (ICC) was used to analyze inter-observer agreement of CT findings.

RESULTS

Mean interval between transplantation and CT examination was not significantly different between patients with ACR and patients without ACR (467.5 ± 261.9 days vs 508.2 ±343.3 days, p = 0.838). Three patients with grade 1, and five patients with grade 2 ACR were noted by pathological analysis. Change from acute to obtuse angle between graft SMV and splenic vein (p = 0.001) and graft duodenal wall thickening (p < 0.001) were observed more frequently in patients with ACR. Other CT findings did not show significant difference between ACR and non-ACR group (p = 0.060-1.000). Inter-observer agreement for angle between graft SMV and splenic vein (ICC: 0.896), graft duodenal wall thickening (ICC: 0.945) were excellent, and fair to excellent agreements were noted for other CT findings (ICC: 0.456 - 1.000).

CONCLUSION

CT examination can be helpful to predict ACR in patients after pancreas transplantation using change of angle between graft SMV and splenic vein with excellent inter-observer agreement.

CLINICAL RELEVANCE/APPLICATION

CT findings including change of angle between graft SMV and splenic vein might be helpful for prediction of ACR as well as evaluation of postoperative complications in patients after pancreas transplantation.

SSM11-06 Diagnostic Accuracy of Multidetector CT in Detecting Juxta-Ampullary Duodenal Diverticulum in Symptomatic Patients

Wednesday, Dec. 4 3:50PM - 4:00PM Room: E353A

Participants

Daniel Fadaei Fouladi, MD, Baltimore, MD (*Presenter*) Nothing to Disclose Elham Eghbali, Tabriz, Iran (*Abstract Co-Author*) Nothing to Disclose Masoud Shirmohammadi, Tabriz, Iran (*Abstract Co-Author*) Nothing to Disclose Shadi Daghighi, San Diego, CA (*Abstract Co-Author*) Nothing to Disclose Shahab Shayesteh, MD, Baltimore, MD (*Abstract Co-Author*) Nothing to Disclose Saeed Ghandili, MD, Baltimore, MD (*Abstract Co-Author*) Nothing to Disclose Reza Javadrashid, MD, Tabriz, Iran (islamic Rep. Of) (*Abstract Co-Author*) Nothing to Disclose

PURPOSE

To determine the diagnostic accuracy of 64-slice multidetector computed tomography (MDCT) in detecting juxta-ampullary duodenal diverticulum (JADD) in symptomatic patients.

METHOD AND MATERIALS

After being approved by the Ethics Committee of our university, a total of 100 patients with endoscopic retrograde cholangiopancreatography (ERCP)-confirmed JADD and 20 patients with extrahepatic biliary obstruction due to other reasons were enrolled in this study. All patients were evaluated by MDCT, as well. Without knowing the result of ERCP, two experienced radiologists reviewed MDCT images and accordingly, the sensitivity, specificity, positive predictive value (PPV) and negative predictive value (NPV) of MDCT in detecting JADD, as the etiology of obstruction, were calculated.

RESULTS

The study group comprised 60 males and 60 females with the mean age of 68.83±12.71 years (range, 27-93) at the time of evaluation. The sensitivity, specificity, PPV and NPV of MDCT in detecting JADD were 76% (95% confidence interval, CI; 66%-84%), 100%, 100% and 45.5% (95%CI; 30%-61%), respectively. The only independent reason for missing a JADD on MDCT images was its small size (<10mm).

CONCLUSION

Abdominal MDCT is highly specific in detecting JADD as the underlying cause of obstruction in symptomatic patients. The accuracy increases when the diverticulum is larger than 10mm.

CLINICAL RELEVANCE/APPLICATION

64-slice MDCT is highly accurate in ruling in juxta-ampullary duodenal diverticula as the underlying cause of extrahepatic biliary obstruction.

Printed on: 10/29/20





SSM12

Genitourinary (Bi-Parametric versus Multi-Parametric Prostate MRI)

Wednesday, Dec. 4 3:00PM - 4:00PM Room: N229



AMA PRA Category 1 Credit ™: 1.00 ARRT Category A+ Credit: 1.00

FDA Discussions may include off-label uses.

Participants

Valeria Panebianco, MD, Rome, Italy (*Moderator*) Nothing to Disclose Temel Tirkes, MD, Indianapolis, IN (*Moderator*) Nothing to Disclose

Sub-Events

SSM12-01 The Added Value of Dynamic Contrast Enhanced Sequences for Detection of Clinically Significant Prostate Cancer: Results from the PROMIS Study

Wednesday, Dec. 4 3:00PM - 3:10PM Room: N229

Participants

Ahmed El-Shater Bosaily, PhD,MSc,MBBCh, London, United Kingdom (*Presenter*) Nothing to Disclose Elena Frangou, London, United Kingdom (*Abstract Co-Author*) Nothing to Disclose Hashim Ahmed, London, United Kingdom (*Abstract Co-Author*) Nothing to Disclose Mark Emberton, London, United Kingdom (*Abstract Co-Author*) Nothing to Disclose Richard Kaplan, London, United Kingdom (*Abstract Co-Author*) Nothing to Disclose Louise Brown, London, United Kingdom (*Abstract Co-Author*) Nothing to Disclose Alex P. Kirkham, MBChB, MD, London, United Kingdom (*Abstract Co-Author*) Nothing to Disclose

For information about this presentation, contact:

ashater@nhs.net

PURPOSE

Multiparametric MRI(MP-MRI) is now a well-established tool in the prostate cancer diagnostic pathway. Recently, the optimal combination of sequences has come into question with opposing views on the added value of dynamic contrast enhanced sequences (DCE). The main phase of the PROMIS (Prostate MRI Imaging Study) trial was adapted to provide a prospective analysis of the incremental value of diffusion (DWI) and DCE sequences in detection of significant cancer.

METHOD AND MATERIALS

497 biopsy naïve men underwent standardized MP-MRIs using T2, DWI (including a dedicated long b sequence) and DCE, followed by a detailed transperineal prostate mapping biopsy covering the whole prostate in 0.5cm intervals. In one sitting, the radiologist assigned a Likert score of 1-5 for the presence of significant tumour, in sequence, for the T2 images, then T2+DWI images , and finally T2+DWI+DCE images. For the primary analysis, a score of >/= 3 was considered positive for clinically significant cancer. Each combination was assessed against the primary PROMIS outcome measure of significance (>/= Gleason 4+3 tumour or >/=6mm maximum cancer core length) on biopsy.

RESULTS

The addition of DCE to T2+DWI resulted in a sensitivity of 95% vs 94%, specificity of 38% vs 37%, positive predictive value of 51% vs 51% and negative predictive value of 90% vs 91% respectively. Marginally more patients could avoid biopsy (score of 2/5 or less) with DCE (123/497 vs 121/497 patients). There was some evidence that contrast reduced the number of equivocal scores: 36% of positive patients were classified as equivocal (3/5) with addition of DCE compared to 42% on T2+DWI alone. The proportion of equivocal (3/5) and positive (4-5/5) cases showing significant tumour were similar (20% and 69 % with DCE, 23% and 71% with T2+DWI alone). None of these differences were statistically significant. No dominant Gleason pattern 4 disease or higher was missed with T2+DWI+DCE, compared to a single case with T2+DWI.

CONCLUSION

DCE did not significantly improve sensitivity or specificity. One dominant Gleason 4 tumour was missed using T2+DWI and none missed with DCE. Though not statistically significant, fewer cases were scored equivocal with the addition of DCE.

CLINICAL RELEVANCE/APPLICATION

The addition of DCE to T2+DWI in a prospective, multi centre study of prostate MRI did not result in convincing improvements in accuracy or a reduction in the number of men recommended for biopsy.

SSM12-02 Comparison of Biparametric and Multiparametric MRI in the Diagnosis of Prostate Cancer

Wednesday, Dec. 4 3:10PM - 3:20PM Room: N229

Gu Mu Yang Zhang, MD, Beijing, China (*Abstract Co-Author*) Nothing to Disclose Zhengyu Jin, Beijing, China (*Abstract Co-Author*) Nothing to Disclose Hao Sun, MD, Beijing, China (*Abstract Co-Author*) Nothing to Disclose

PURPOSE

To compare the diagnostic accuracy of biparametric MRI (bpMRI) and multiparametric MRI (mpMRI) for prostate cancer (PCa) and clinically significant prostate cancer (csPCa), and to explore the application value of dynamic contrast-enhanced (DCE) MRI in prostate imaging.

METHOD AND MATERIALS

This study retrospectively enrolled 235 patients with suspected PCa in our hospital from 2016 to 2017. The lesions were scored according to the Prostate Imaging Reporting and Data System version 2 (PI-RADS V2). The bpMRI and mpMRI scores were recorded to plot the receiver operating characteristic curve (ROC). Area under the curve (AUC), accuracy, sensitivity, specificity, negative predictive value (NPV), and positive predictive value (PPV) for each method were calculated and compared. The patients were further stratified according to bpMRI scores for the application value of DCE MRI.

RESULTS

The AUC values of bpMRI and mpMRI for PCa were comparable (0.790 and 0.791, respectively). The accuracy, sensitivity, specificity, PPV and NPV of bpMRI for PCa were 76.2%, 79.5%, 72.6%, 75.8%, and 76.6%; and the values for mpMRI were 77.4%, 84.4%, 69.9%, 75.2%, and 80.6%, respectively. For the diagnosis of csPCa, the AUC values of bpMRI and mpMRI were similar (0.781 and 0.779, respectively). The accuracy, sensitivity, specificity, PPV and NPV of bpMRI for csPCa were 74.0%, 83.8%, 66.9%, 64.8%, and 85.0%; and 73.6%, 87.9%, 63.2%, 63.2%, and 87.8% for mpMRI. For patients with bpMRI score >= 3, the difference in DCE between PCa and non-PCa, and between csPCa and non-csPCa were both statistically significant (both P = 0.001). Further stratification analysis showed that for patients with bpMRI score = 4, DCE had statistically significant difference between PCa and non-PCa, and between csPCa (P = 0.003, and P < 0.001, respectively).

CONCLUSION

The diagnostic accuracy of bpMRI is comparable with that of mpMRI in the detection of PCa and identification of csPCa. DCE is helpful in further identifying PCa and csPCa lesions in patients with bpMRI >= 3, especially bpMRI = 4, which may be conductive to achieve more accurate PCa risk stratification.

CLINICAL RELEVANCE/APPLICATION

For patients with suspected PCa, DCE may improve the tumor detection and aggressiveness classification. Rather than omitting DCE, we think further comprehensive studies are required for prostate MRI.

SSM12-03 Comparison of Bi-Parametric MRI Based Artificial Intelligence and Multi-Parametric MRI in Detection of Intraprostatic Lesions: A Multi-Reader Study

Wednesday, Dec. 4 3:20PM - 3:30PM Room: N229

Participants

Sherif Mehralivand, MD, Bethesda, MD (Presenter) Nothing to Disclose Stephanie A. Harmon, PhD , Bethesda, MD (Abstract Co-Author) Research funded, NCI Nathan S. Lay, PhD, Bethesda, MD (Abstract Co-Author) Nothing to Disclose Clayton P. Smith, BA, Bethesda, MD (Abstract Co-Author) Nothing to Disclose Thomas H. Sanford, Bethesda, MD (Abstract Co-Author) Research collaboration, NVIDIA Corporation Sonia Gaur, MD, Philadelphia, PA (Abstract Co-Author) Nothing to Disclose Jonathan J. Sackett, BS, Bethesda, MD (Abstract Co-Author) Research collaboration, NVIDIA Corporation Ronaldo H. Baroni, MD, Sao Paulo, Brazil (Abstract Co-Author) Nothing to Disclose Karabekir Ercan, Ankara, Turkey (Abstract Co-Author) Nothing to Disclose Peter Pinto, Bethesda, MD (Abstract Co-Author) Nothing to Disclose Andrei S. Purysko, MD, Westlake, OH (Abstract Co-Author) Nothing to Disclose Soroush Rais-Bahrami, MD, Birmingham, AL (Abstract Co-Author) Consultant, Koninklijke Philips NV; Consultant, Blue Earth Diagnostics Ltd; Consultant, Genomic Health, Inc Victor M. Tonso, MD, Sao Paulo, Brazil (Abstract Co-Author) Nothing to Disclose Bradford J. Wood, MD, Bethesda, MD (Abstract Co-Author) Researcher, Koninklijke Philips NV; Researcher, Celsion Corporation; Researcher, BTG International Ltd; Researcher, Siemens AG; Researcher, XAct Robotics; Researcher, NVIDIA Corporation; Intellectual property, Koninklijke Philips NV; Intellectual property, BTG International Ltd; Royalties, Invivo Corporation; Royalties, Koninklijke Philips NV; Equipment support, AngioDynamics, Inc; Researcher, Profound Medical Inc; Researcher, Canon Medical Systems Corporation; Researcher, AstraZeneca PLC; Researcher, Exact Imaging Inc Jennifer Gordetsky, MD, Birmingham, AL (Abstract Co-Author) Nothing to Disclose Maria Merino, MD, Bethesda, MD (Abstract Co-Author) Nothing to Disclose Tristan Barrett, MBBS, Cambridge, United Kingdom (Abstract Co-Author) Nothing to Disclose Leonardo K. Bittencourt, MD, PhD, Rio de Janeiro, Brazil (Abstract Co-Author) Nothing to Disclose Mehmet Coskun, MD, Ankara, Turkey (Abstract Co-Author) Nothing to Disclose Christopher M. Knaus, MD, Bethesda, MD (Abstract Co-Author) Nothing to Disclose Yan Mee Law, MBBS, Singapore, Singapore (Abstract Co-Author) Nothing to Disclose Ashkan A. Malayeri, MD, Andover, MA (Abstract Co-Author) Nothing to Disclose Daniel J. Margolis, MD, New York, NY (Abstract Co-Author) Consultant, Blue Earth Diagnostics Ltd Jamie Marko, MD, Bethesda, MD (Abstract Co-Author) Nothing to Disclose Derya Yakar, MD, PhD, Groningen, Netherlands (Abstract Co-Author) Nothing to Disclose Peter L. Choyke, MD, Rockville, MD (Abstract Co-Author) License agreement, Koninklijke Philips NV; Researcher, Koninklijke Philips NV; License agreement, ScanMed; License agreement, Rakuten Medical; Researcher, Rakuten Medical; Researcher, General Electric Company; Researcher, Progenics Pharmaceuticals, Inc; Researcher, Novartis AG; ; ; ; ; Ronald M. Summers, MD, PhD, Bethesda, MD (*Abstract Co-Author*) Royalties, iCAD, Inc; Royalties, Koninklijke Philips NV; Royalties, ScanMed, LLC; Royalties, Ping An Insurance Company of China, Ltd; Research support, Ping An Insurance Company of China, Ltd; Research support, NVIDIA Corporation; ; ; ; Baris Turkbey, MD, Bethesda, MD (Abstract Co-Author) Research support, Koninklijke Philips NV; Royalties, Invivo Corporation; Investigator, NVIDIA Corporation

For information about this presentation, contact:

turkbeyi.mail.nih.gov

PURPOSE

To compare a bi-parametric magnetic resonance imaging (bMRI) based artificial intelligence (AI) system which provides proposed regions of interests (ROI) overlaid on T2 weighted (T2W) with multi-parametric MRI (mpMRI) using PI-RADSv2 guided interpretation.

METHOD AND MATERIALS

Case and control patients were collected from 5 institutions and 9 radiologists from 9 different institutions participated as readers: 3 highly, 3 moderately, 3 less-experienced in reading prostate MRI. Patients were consecutive at each institution and underwent 3T mpMRI (T2W, ADC map, b-1500, DCE MRI). Case patients had subsequent radical prostatectomy with pathology mapping available, control patients had negative MRI and negative systematic biopsy. Two interpretation arms were executed with readers blinded to pathology: an mpMRI-alone arm utilizing PI-RADSv2 guidelines, then after 4-week washout, a first-reader AI-assisted arm. Lesion detection sensitivity was calculated for whole prostate. Per-lesion specificity was calculated on the AI-assisted arm on a per-ROI level.

RESULTS

153 case and 84 control patients were included across 5 institutions. For mpMRI-alone interpretation, lesion-based sensitivity was 62.2%, 63%, 65.3% and 58.2% for overall, high, moderate and low-experienced readers, respectively. For bMRI based AI system assisted interpretation, lesion-based sensitivity was 66.5%, 67.8%, 71.7% and 59.9% for overall, high, moderate and low-experienced readers, respectively. At threshold of PI-RADS >=3, specificity of AI assisted bMRI were 81.1%, 86.3%, 70.2% and 86.8% for overall, high, moderate and low-experienced readers, respectively.

CONCLUSION

AI-assisted bi-parametric MRI reads demonstrated higher sensitivities compared to multiparametric MRI reads at all experience categories for radiologists.

CLINICAL RELEVANCE/APPLICATION

AI-assisted MRI reads can standardize and improve prostate MRI reporting.

SSM12-04 Value of Dynamic Contrast Enhanced (DCE) MR Imaging for Patients in PI-RADS 4 Category

Wednesday, Dec. 4 3:30PM - 3:40PM Room: N229

Participants

Tim Ullrich, Duesseldorf, Germany (*Abstract Co-Author*) Nothing to Disclose Lars Schimmoeller, MD, Dusseldorf, Germany (*Abstract Co-Author*) Nothing to Disclose Farid Ziayee, Dusseldorf, Germany (*Presenter*) Nothing to Disclose Michael Quentin, MD, Duesseldorf, Germany (*Abstract Co-Author*) Nothing to Disclose Christian Arsov, MD, Duesseldorf, Germany (*Abstract Co-Author*) Nothing to Disclose Gerald Antoch, MD, Dusseldorf, Germany (*Abstract Co-Author*) Nothing to Disclose

PURPOSE

To assess the impact of dynamic contrast-enhanced imaging (DCE) in mp-MRI on prostate cancer (PCa) detection in a large patient cohort assigned to PI-RADS category 4.

METHOD AND MATERIALS

This prospective, single center cohort study includes 193 consecutive patients with PI-RADS assessment category 4 after mp-MRI (T2WI, DWI, DCE) at 3T with combined targeted plus systematic biopsy as reference standard. Prostate cancer detection with DCE and without inclusion of DCE upgraded lesions was compared.

RESULTS

Overall PCa detection rate in PI-RADS-4-patients was 62% (119/193) with DCE and 52% (101/193) without inclusion of DCE upgraded lesions; 48% (92/193) had clinically significant PCa (csPCa; Gleason score >=3+4=7) and 40% (78/193) without use of DCE. 38 of the 193 patients (20%) had peripheral lesions upgraded from PI-RADS category 3 to an overall PI-RADS category 4 due to focal positive DCE findings. Of these 38 patients 18 had PCa including 14 with a csPCa. Thus, 15% (18/119) of the patients with any prostate cancer and 15% (14/92) of the patients with csPCa were detected only based on additional DCE information.

CONCLUSION

DCE allows detection of a significant number of mostly csPCa in PI-RADS-4-patients and thus improves detection rates. The current PI-RADS decision rules regarding upgrading PI-RADS-3-lesions to overall category 4 due to positive DCE imaging are useful for PCa detection.

CLINICAL RELEVANCE/APPLICATION

Patients assigned to PI-RADS category 3 benefit from DCE for primary (early) tumor detection.

SSM12-05 Comparison of Standard Multiparametric and Unenhanced Biparametric MRI in Men with Elevated Prostate-Specific Antigen

Wednesday, Dec. 4 3:40PM - 3:50PM Room: N229

Participants Filippo Pesapane, MD, Milan, Italy (*Presenter*) Nothing to Disclose Giorgio Maria Agazzi, Brescia, Italy (*Abstract Co-Author*) Nothing to Disclose Marzia Acquasanta, Milan, Italy (*Abstract Co-Author*) Nothing to Disclose Priyan Tantrige, London, United Kingdom (*Abstract Co-Author*) Nothing to Disclose Chiara A. Mattiuz, MD, Milan, Italy (*Abstract Co-Author*) Nothing to Disclose Francesco Sardanelli, MD, San Donato Milanese, Italy (*Abstract Co-Author*) Speakers Bureau, Bracco Group Advisory Board, Bracco Group Research Grant, Bayer AG Advisory Board, General Electric Company Reserach Grant, General Electric Company Speakers Bureau, Siemens AG Reserach Grant, Real Imaging Ltd Marina Codari, MENG,PhD, San Donato Milanese, Italy (*Abstract Co-Author*) Nothing to Disclose Anastasia Esseridou, MD, San Donato Milanese, Italy (*Abstract Co-Author*) Nothing to Disclose

For information about this presentation, contact:

filippo.pesapane@unimi.it

PURPOSE

Multiparametric MRI (mpMRI) for prostate cancer (PCa) is usually composed of diffusion-weighted (DW), T2W and dynamic contrast enhancement (DCE) sequences. We compared biparametric MRI (bpMRI) composed of T2W and DW against mpMRI in patients with elevated prostate-specific antigen (PSA).

METHOD AND MATERIALS

1.5-T prostate MR was performed in 431 men (61.5+/-8.3 years) with PSA>4.0 ng/mL and included in a retrospective analysis. bpMRI and mpMRI were independently assessed in separate sessions >1 month apart in a random order by 2 readers with 5 (R1) and 3 years (R2) experience, using the PI-RADS2 criteria. Histopathology or >=2 years of follow-up served as a reference standard. PI-RADS score 3 was the threshold for a positive exam. Sensitivity and specificity were calculated with their 95% confidence interval (CI); McNemar and Cohen's K statistics were also used.

RESULTS

Population consisted in 195/431 (45,3%) histopathologically proven PCa, with 62/195 (31.8%) high-grade- (GS>=7b) and 133/195 (68.2%) low-grade-PCa. PCa could be excluded by histopathology in 58/431 (13.5%) patients and by follow-up in 178/431 (41.3%) patients. For bpMRI, sensitivity was 164/195 (84%, 95%CI 79-89%) for R1 and 156/195 (80%, 95%CI 74-86%) for R2; specificity was 182/236 (77%, 95%CI 72-82%) for R1 and 175/236 (74%, 95%CI 68-80%) for R2. For mpMRI, the sensitivity was 168/195 (86%, 95%CI 81-91%) for R1 and 160/195 (82%, 95%CI 77-87%) for R2; the specificity was 184/236 (78%, 95%CI 73-83%) for R1 and 177/236 (75%, 95%CI 69-81%) for R2. Omitting the DCE sequences (namely, using bpMRI) changed the PIRADS2 scores in 25/431 (5.8%) patients for R1 and in 35/431 (8.1%) patients for R2, when compared to mpMRI. PI-RADS score 3 increased by 5.3% for R1 and 7.4% for R2. bpMRI resulted in 4 more false negatives, compared to mpMRI, for both R1 and R2 and all of these were low-grade PCa. No high-grade PCa was missed with bpMRI. Not significant differences in accuracy were observed with both approaches by each readers (p>0.08). Interobserver agreement was substantial for both bpMRI (κ =0.802) and mpMRI (κ =0.787).

CONCLUSION

Diagnostic performance of bpMRI and mpMRI were similar, with no change in the detection of high-grade PCa

CLINICAL RELEVANCE/APPLICATION

bpMRI for PCa's detection could eliminate the adverse events and the retention of gadolinium, shorten time and reduce costs, possibly resulting in increased accessibility of MRI for men with elevated PSA

SSM12-06 Comparison of Measured Ultra-High b-Value ADC to Quantitative DCE for Enhancing Bi-Parametric (T2w and DWI) MRI Assessment of Clinically Significant Prostate Cancer

Wednesday, Dec. 4 3:50PM - 4:00PM Room: N229

Participants

Anoshirwan A. Tavakoli, MD, Heidelberg, Germany (*Presenter*) Nothing to Disclose Tristan A. Kuder, PhD, Heidelberg, Germany (*Abstract Co-Author*) Nothing to Disclose Jan P. Radtke, Heidelberg, Germany (*Abstract Co-Author*) Nothing to Disclose Viktoria Schutz, Heidelberg, Germany (*Abstract Co-Author*) Nothing to Disclose Magdalena Gortz, Heidelberg, Germany (*Abstract Co-Author*) Nothing to Disclose Markus Hohenfellner, MD, PhD, Heidelberg, Germany (*Abstract Co-Author*) Nothing to Disclose Heinz-Peter W. Schlemmer, MD, Heidelberg, Germany (*Abstract Co-Author*) Nothing to Disclose David Bonekamp, MD, PhD, Heidelberg, Germany (*Abstract Co-Author*) Speaker, Profound Medical Inc

For information about this presentation, contact:

s.tavakoli@gmx.de

PURPOSE

To compare the added diagnostic value of measured ultra-high b-value (UHB) - derived apparent diffusion coefficient (ADC) to quantitative normalized DCE assessment for the enhancement of bi-parametric (T2w and ADC) MRI for the prediction of clinically significant prostate cancer (sPC).

METHOD AND MATERIALS

73 consecutive patients (67.2 \pm 7.7 years, PSA 10.7 \pm 18.1 ng/dl) underwent prostate MRI at 3T (Magnetom Prisma) with EPI-DWI images acquired at b=50/500/1000/1500 s/mm2 as well as at b=100/500/1000/2250/3000/4000 s/mm2. Extended systematic and targeted MRI/TRUS fusion biopsies based on prospective clinical reads were matched to a second, retrospective blinded read and MR lesions segmented manually. ADC, UHB-ADC100,4000, early arterial DCE lesion contrast to surrounding parenchyma (nDCE) and T2w intensity normalized to pectineus muscle (nT2w) were extracted from each lesion. Three logistic regression models were created for prediction of sPC defined as Gleason Grade Group (GGG) >= 2: Model A (nT2w, ADC), model B (nT2w, ADC, nDCE) and model C (nT2w, ADC, UHB-ADC). For evaluation of the models AUC was calculated from ROC curves and Chi-square analysis of deviance or Vuong's test were used to compare the models.

RESULTS

In 73 patients 55 MRI-detected retrospectively validated MR-lesions revealed no cancer in 23 lesions (42%), GGG=1 in 10 lesions (18%), GGG=2 in 12 lesions (22%), GGG=3 in 4 lesions (7%), GGG=4 in 4 lesions (7%) and GGG=5 in 2 lesions (4%). Model A yielded

an AUC of 0.810 (sensitivity 80%, specificity 73%), model B yielded an AUC of 0.840 (sensitivity 80%, specificity 79%) and model C yielded an AUC of 0.806 (sensitivity 80%, specificity 73%), indicating a slightly higher AUC for model B when compared to model A and C (p=0.04 and p=0.13) and a comparable AUC between model A and C (p=0.76).

CONCLUSION

Measured UHB-ADC achieved no improvement in predictive performance over bi-parametric assessment with ADC and T2w, whereas added quantitative normalized DCE did improve predictive performance.

CLINICAL RELEVANCE/APPLICATION

Measured UHB-ADC does not provide a contrast-free alternative to DCE for the enhancement of bi-parametric prostate MRI.

Printed on: 10/29/20





SSM13

Science Session with Keynote: Health Service, Policy and Research (Patient and Family Centered Care)

Wednesday, Dec. 4 3:00PM - 4:00PM Room: S404CD

HP

AMA PRA Category 1 Credit ™: 1.00 ARRT Category A+ Credit: 1.00

Participants

Brian Haas, MD, San Francisco, CA (*Moderator*) Nothing to Disclose Martha G. Menchaca, MD, PhD, Brookfield, IL (*Moderator*) Nothing to Disclose

For information about this presentation, contact:

brian.haas@ucsf.edu

Sub-Events

SSM13-01 Health Service, Policy and Research Keynote Speaker: Surprise Billing: What You Don't Know Could Really Cost You

Wednesday, Dec. 4 3:00PM - 3:10PM Room: S404CD

Participants

Richard E. Heller III, MD, Chicago, IL (Presenter) Nothing to Disclose

SSM13-02 Financial Toxicity in Cancer Patients and their Caregivers: Correlation with Patient's Medication and Imaging Non-Adherence

Wednesday, Dec. 4 3:10PM - 3:20PM Room: S404CD

Participants

Deema Elchoufi, BS, Atlanta, GA (*Presenter*) Nothing to Disclose Ruth C. Carlos, MD, MS, Ann Arbor, MI (*Abstract Co-Author*) Editor, Journal of the American College of Radiology; Support, Harvey L. Neiman Health Policy Institute; In-kind support, Reed Elsevier; Debrua Coleman, Atlanta, GA (*Abstract Co-Author*) Nothing to Disclose Jane Meisel, Atlanta, GA (*Abstract Co-Author*) Nothing to Disclose Mehmet Asim Bilen, MD, Atlanta, GA (*Abstract Co-Author*) Nothing to Disclose David H. Lawson, MD, Atlanta, GA (*Abstract Co-Author*) Nothing to Disclose Soma Sengupta, Atlanta, GA (*Abstract Co-Author*) Nothing to Disclose Bassel El-Rayes, MD, Atlanta, GA (*Abstract Co-Author*) Nothing to Disclose Gelareh Sadigh, MD, Atlanta, GA (*Abstract Co-Author*) Nothing to Disclose

For information about this presentation, contact:

gsadigh@emory.edu

PURPOSE

To assess health-related financial toxicity in cancer patients and their caregivers and its correlation with financial coping strategies and care non-adherence.

METHOD AND MATERIALS

Dyads of adult cancer patients and their adult primary caregivers visiting outpatient oncology clinics were recruited. Financial toxicity at study entry was measured using the Comprehensive Score for Financial Toxicity (COST) score (ranging between 0-44, the lower the score, the worse the financial toxicity). Linear regression identified independent sociodemographic, clinical and insurance correlates of financial toxicity. Financial coping strategies, health-related quality of life (HRQOL) and care non-adherence were assessed.

RESULTS

34 dyads of cancer patients (57yo [95%CI,53-63]; 73% female; 79% White) and their caregivers (50yo [95%CI,43-67]; 60% female; 82% White) were recruited. 32% of patients had breast cancer, 32% genitourinary, 18% skin, and 18% other malignancies. Median months from diagnosis was 22(IQR,11-48). 53% of caregivers were spouses/partners; 26% parents and 14% children. Mean COST scores in patients and caregivers were 21(95%CI,17.5-25.3) and 23(95%CI,18.6-26.7) (Pearson coefficient 0.37;p<0.05). In response to financial burden, 41% of patients and 48% of caregivers used at least one financial coping strategy (see fig. 1). Medication and imaging non-adherence were reported by 15% and 3% of patients. In multivariable analyses, the key correlate of lower financial toxicity (e.g., higher COST score) in patients was higher financial self-efficacy (e.g., having more confidence in being able to manage money to last a lifetime) (coefficient 1.5 [95%CI,0.9-2.1];p<0.001). Key correlate of financial toxicity among caregivers was patient-caregiver relationship with spouses/partners reporting higher COST scores (coefficient 18 [95%CI,7.1-29]; p<0.05). Lower COST scores in caregivers correlated with lower caregiver HRQOL and higher patients' care non-adherence (p<0.05).

Spouses and partners experience lower financial toxicity as caregivers to cancer patients compared to parents or children. The degree of caregiver financial burden influences patient care non-adherence.

CLINICAL RELEVANCE/APPLICATION

Cancer impacts patient-caregiver dyads as a whole. The primary focus of interventions to improve health disparities resulting from financial burden should be shifted from the individual level to the dyadic level of patients and caregivers.

SSM13-03 Analysis of a Patient-Centered Ridesharing Program to Overcome Transportation Barriers in Access to Advanced Imaging Care

Wednesday, Dec. 4 3:20PM - 3:30PM Room: S404CD

Participants

Debra S. Whorms, MD, Boston, MA (*Presenter*) Nothing to Disclose Mckinley Glover IV, MD, Boston, MA (*Abstract Co-Author*) Nothing to Disclose Anand K. Narayan, MD,PhD, Boston, MA (*Abstract Co-Author*) Nothing to Disclose Jeremy Herrington, Boston, MA (*Abstract Co-Author*) Nothing to Disclose Wayne Marshall, Chelsea, AL (*Abstract Co-Author*) Nothing to Disclose Sanjay Saini, MD, Boston, MA (*Abstract Co-Author*) Nothing to Disclose Efren J. Flores, MD, Boston, MA (*Abstract Co-Author*) Nothing to Disclose Ali Pourvaziri, MD, MPH, Boston, MA (*Abstract Co-Author*) Nothing to Disclose

For information about this presentation, contact:

dswhorms@gmail.com

PURPOSE

Transportation difficulties are a known barrier to receiving appropriate, timely care for many patients. These barriers tend to affect patients from low socioeconomic status (SES) and underrepresented racial/ethnic minority communities. Patient-centered interventions can help address some of these barriers to care. The purpose of this study was to evaluate a rideshare program developed to address transportation barriers to MRI appointments at an outpatient imaging center affiliated with an academic medical center.

METHOD AND MATERIALS

Single-institution, HIPAA compliant, IRB approved study with waiver of informed consent was performed to evaluate a rideshare program, through Circulation © and Lyft ©, at an outpatient imaging site of a quaternary academic medical center during a 9-month period (June 2018- February 2019). Any patient who spontaneously expressed a desire to cancel their MRI appointment due to transportation issues was offered this program. Primary outcomes included 1) proportion of patient-related appointment cancellations and 2) exam timeliness. Logistic and linear regression analyses were used to compare outcomes in patients who used the ride share program with patients who did not use the ride share program, adjusted for potential confounders.

RESULTS

During the study period, 318 encounters out of 11,581 total encounters utilized ride shares (2.67%). Female patients (p = 0.042), Medicare (p = 0.008) and Medicaid (p = 0.042) patients were more likely to use the ride share service while employed (p < 0.001) and Hispanic (p = 0.001) patients were less likely to use the ride share service. No statistically significant differences were found in appointment cancellations comparing patients using the ride share service compared with patients who did not use the ride share service (Adjusted OR 0.86, 95% CI 0.66, 1.13, p = 0.286). Patients using the ride share service were more likely to be on time for their appointment compared with patients who did not use the ride share service (Adjusted Coefficient 8.53, 95% CI 3.19, 13.86, p = 0.002).

CONCLUSION

A patient-centered ridesharing program assisted patients that were older and from lower SES in overcoming transportation barriers to MRI care while improving timeliness to appointments.

CLINICAL RELEVANCE/APPLICATION

Providing patient-centered programs in radiology can assist in overcoming access barriers to advanced imaging care, while improving operational efficiency.

SSM13-04 Patient Preferences for Properties of Gadolinium-Based Contrast Media in the Setting of Breast MRI Screening

Wednesday, Dec. 4 3:30PM - 3:40PM Room: S404CD

Participants

Sean A. Woolen, MD, Ann Arbor, MI (*Presenter*) Nothing to Disclose Akshat C. Pujara, MD, Ann Arbor, MI (*Abstract Co-Author*) Institutional Grant, General Electric Healthcare Alana A. Lewin, MD, New York, NY (*Abstract Co-Author*) Nothing to Disclose Prasad R. Shankar, MD, Ann Arbor, MI (*Abstract Co-Author*) Nothing to Disclose Amy N. Melsaether, MD, New York, NY (*Abstract Co-Author*) Nothing to Disclose Ashley Nettles, Ann Arbor, MI (*Abstract Co-Author*) Nothing to Disclose Lisa Piccoli, New York, NY (*Abstract Co-Author*) Nothing to Disclose Matthew S. Davenport, MD, Ann Arbor, MI (*Abstract Co-Author*) Royalties, Wolters Kluwer nv

PURPOSE

To measure patient preferences toward individual properties of gadolinium-based contrast media (GBCM) when undergoing contrastenhanced screening Breast MRI.

METHOD AND MATERIALS

This is an interim analysis at 17% accrual of an IRB-approved prospective multicenter discrete choice conjoint experiment, administered to at-risk patients, undergoing screening MRI at 2 institutions (7/31/2018-present). Five GBCM attributes were studied: sensitivity for cancer (80-95%), degree of intracranial gadolinium retention (1-100 molecules per 100 million molecules administered), severe allergic-like reaction rate (1-19 per 100,000), mild allergic-like reaction rate (10-1,000 per 100,000), and out-of-pocket cost (\$25-\$100). Attribute levels were selected to include the range of marketed GBCM values. Quantitative patient preferences were derived using Bayesian hierarchical modeling.

RESULTS

One-hundred and fourteen subjects (17% of 670) have been accrued at the time of this interim analysis. The questionnaire response rate was 93% (120/129) and completion rate was 95% (114/120). Cancer sensitivity (utility: 13.59/percentage point increase) was valued more than contrast-related risks (gadolinium retention utility: -0.73/molecule retained per 100 million administered; severe reaction utility: -5.11/reaction of 100,000 administrations; mild reaction utility: -0.09/reaction of 100,000 administrations) or out-of-pocket cost (utility: -0.53/dollar).

CONCLUSION

Interim results indicate that patients undergoing annual breast MRI screening prioritize cancer detection over GBCM-related risks. Each percentage point increase in sensitivity is valued similarly to 19 molecules of retained gadolinium (of 100 million administered molecules), 3 severe reactions (of 100,000 administrations), 147 mild reactions (of 100,000 administrations), or \$25 in out-of-pocket cost.

CLINICAL RELEVANCE/APPLICATION

Gadolinium patient preference data has the potential to contribute to decision making for gadolinium formulary policies and guide industry creation of new gadolinium agents.

SSM13-05 Qualitative Analysis of Patient Perspectives and Priorities Regarding Artificial Intelligence in Radiology

Wednesday, Dec. 4 3:40PM - 3:50PM Room: S404CD

Participants Scott J. Adams, MD, Saskatoon, SK (*Presenter*) Nothing to Disclose Rachel Tang, BA, Saskatoon, SK (*Abstract Co-Author*) Nothing to Disclose Paul S. Babyn, MD, Saskatoon, SK (*Abstract Co-Author*) Nothing to Disclose

For information about this presentation, contact:

scott.adams@usask.ca

PURPOSE

To better understand patients' perceptions of artificial intelligence (AI) and patients' priorities for AI in radiology to inform the development and clinical implementation of AI in radiology.

METHOD AND MATERIALS

A patient engagement workshop was hosted with 17 participants from urban, rural, and remote communities. Facilitated roundtable discussions were conducted to better understand patients' perceptions of AI and patients' priorities for AI in radiology. Concepts from roundtable discussions were coded using NVivo 11 and analyzed using thematic analysis.

RESULTS

Patients' perceptions of AI were captured in the following three themes: fear of the unknown, trust (including uncertainty of what and whom to place trust in-AI or radiologists), and the importance of a human connection even when using AI. Enthusiasm and willingness for AI to be used in radiology were related to patient age, with greater enthusiasm among younger patients. Patients' priorities for improvements in radiology included improving communication, shortening time to diagnosis, reducing wait times, increasing diagnostic accuracy, empowering patients, and increasing access to diagnostic imaging and screening. Patients were comfortable with sharing de-identified imaging data for AI development as long as appropriate safeguards were in place. In addition to traditional diagnostic accuracy measures, participants wanted to ensure that downstream impacts of AI on patients' health and well-being were included in assessments of AI.

CONCLUSION

Patients' initial perceptions of AI-including fear of the unknown and uncertainty of what and whom to place trust in-may lead to patients' initial reluctance to accept AI in radiology, suggesting the need for patient education efforts. Patients identified numerous areas for improvement in radiology which could be enhanced through AI, potentially informing the prioritization of AI use cases.

CLINICAL RELEVANCE/APPLICATION

Patients' may initially be reluctant for AI to be used in their care due to a lack of familiarity; however, upon further education, patients identify numerous priorities for AI development which may inform prioritization of AI use cases.

SSM13-06 Patient Understanding of Abnormal Imaging Findings under Pennsylvania Act 112

Wednesday, Dec. 4 3:50PM - 4:00PM Room: S404CD

Participants

Gregory S. Mittl, MD, Philadelphia, PA (*Presenter*) Nothing to Disclose Tessa S. Cook, MD, PhD, Philadelphia, PA (*Abstract Co-Author*) Speaker, RadPartners AI; Speaker, AIMed Radiology Paul A. Hill, MD, MS, West Lebanon, NH (*Abstract Co-Author*) Nothing to Disclose Judy Shea, PhD, Philadelphia, PA (*Abstract Co-Author*) Nothing to Disclose Charles E. Kahn JR, MD, Philadelphia, PA (*Abstract Co-Author*) Nothing to Disclose Hanna M. Zafar, MD, Philadelphia, PA (*Abstract Co-Author*) Nothing to Disclose

For information about this presentation, contact:

PURPOSE

Pennsylvania Act 112 of 2018 requires diagnostic imaging facilities to directly notify patients in writing for test results warranting follow-up medical care within three months. The law specifies the patient notification wording written at a 12th-grade reading level. Our objective was to determine if patient understanding varied by the reading level and visual presentation of notification text (i.e. letter or image-rich infographic).

METHOD AND MATERIALS

Using the Amazon Turk crowdsourcing internet marketplace, we surveyed United States adult volunteers. The software cycled repetitively between four different versions of the notification: 12th-grade and 6th-grade reading level versions of both a letter and an image-rich infographic. Respondents who answered 12 questions related to notification comprehension and sociodemographic data were paid \$.10. Chi square analysis was used to compare differences in responses by question, reading level and visual presentation.

RESULTS

Among 340 survey respondents, most were female (61%), 26% self-identified as healthcare professionals and 59% had received at least a Bachelor's degree. There were no sociodemographic differences between the four notification groups. Respondents who viewed letters rather than infographics were more likely to correctly identify the notification subject as diagnostic imaging (90% and 81%, respectively) (p<.0001); no differences were observed between reading levels (p=.888). Respondents who viewed either notification type at a 6th-grade rather than a 12th-grade reading level were more likely to correctly identify the next best step as contacting the ordering provider as soon as possible (83% and 73%, respectively) (p=.032); no differences were observed by visual presentation (p=.0914). Reading level and visual presentation did not affect correct comprehension of the notification as abnormal. Most respondents strongly agreed (27%) or agreed (53%) that the notification text made them feel worried; no differences were observed by reading level or visual presentation (p=.920 both).

CONCLUSION

Notification reading level and visual presentation can impact patient understanding of abnormal imaging test results and follow-up, but do not address patient anxiety.

CLINICAL RELEVANCE/APPLICATION

Patient understanding of abnormal imaging test results and follow-up may be optimized through adjusting reading level and offering image-rich infographics rather than letters.

Printed on: 10/29/20





SSM14

Informatics (Artificial Intelligence: Generative Adversarial Networks)

Wednesday, Dec. 4 3:00PM - 4:00PM Room: E353C



AMA PRA Category 1 Credit ™: 1.00 ARRT Category A+ Credit: 1.00

FDA Discussions may include off-label uses.

Participants

Felipe C. Kitamura, MD, MSC, Sao Paulo, Brazil (*Moderator*) Consultant, MD.ai, Inc Srini Tridandapani, MD, PhD, Birmingham, AL (*Moderator*) Co-founder, CameRad Technologies, LLC; Spouse, Co-founder, CameRad Technologies, LLC; Officer, CameRad Technologies, LLC; Spouse, Officer, CameRad Technologies, LLC Kirti Magudia, MD,PhD, San Francisco, CA (*Moderator*) Nothing to Disclose George L. Shih, MD, New York, NY (*Moderator*) Consultant, MD.ai, Inc; Stockholder, MD.ai, Inc;

Sub-Events

SSM14-01 Multimodal CT Image Super-Resolution via Transfer Generative Adversarial Network

Wednesday, Dec. 4 3:00PM - 3:10PM Room: E353C

Participants

Yao Xiao, Gainesville, FL (*Abstract Co-Author*) Nothing to Disclose Manuel M. Arreola, PhD, Gainesville, FL (*Abstract Co-Author*) Nothing to Disclose Izabella Barreto, PhD, Gainesville, FL (*Abstract Co-Author*) Nothing to Disclose Christopher Fox, MD, Gainesville, FL (*Abstract Co-Author*) Nothing to Disclose Keith R. Peters, MD, Gainesville, FL (*Abstract Co-Author*) Nothing to Disclose Ruogu Fang, Gainesville, FL (*Presenter*) Nothing to Disclose

For information about this presentation, contact:

xiaoyao@ufl.edu

ruogu.fang@bme.ufl.edu

CONCLUSION

The experimental result indicates that transfer-GAN can effectively improve the resolution of multimodal CT images, thus, provides a practical solution for multimodal CT image quality enhancement.

Background

Multimodal CT scans including none-contrast CT (NCCT) and CT Perfusion (CTP) are widely used in acute stroke protocols. While each imaging modality has its own advantage in disease diagnosis, the varying image resolution of different modalities hinders the ability of the radiologist to discern subtle suspicious findings. Besides, higher image quality requires a high radiation dose, leading to increases in health risks such as cataract formation and cancer induction. Thus, it is highly crucial to develop an approach to improve multimodal image resolution and to lower radiation exposure. Based on the hypothesis that multimodal CT imaging of the same patient is highly correlated in structural features, the integration of the shared and complementary information from different modalities is beneficial for achieving high diagnostic image quality.

Evaluation

We present a novel transfer learning technique for the generative adversarial network (GAN) to improve the spatial resolution in multimodal medical imaging. Our method is evaluated on 4,111 images collected from nine patients, including 415 NCCT and 3,696 CTP slices. We down-sample the images into a quarter of the original size to generate the low-resolution images. We train the network for different modalities with and without transfer learning to compare the performance. The visual comparison and quantitative evaluation including peak-signal-to-noise-ratio (PSNR) and structural similarity (SSIM) index demonstrate the effectiveness and accuracy of the proposed method.

Discussion

We perform one-tailed paired t-tests with alpha = 0.05 to compare the performance improvements of PSNR and SSIM for CTP images. Through transfer learning of GAN, there is a significant improvement for both PSNR and SSIM for transferred from NCCT to CTP images than directly training for CTP images. We also compare our model with the model pre-trained on natural images, and our model achieves significantly higher results. Details are shown in Figure 1.

SSM14-02 Synthetic Training Data Augmentation for Assisting CT Liver Lesion Classification with Generative Adversarial Networks

Wednesday, Dec. 4 3:10PM - 3:20PM Room: E353C

Participants Hansang Lee, Daejeon, Korea, Republic Of (*Presenter*) Nothing to Disclose Helen Hong, PhD, Seoul, Korea, Republic Of (*Abstract Co-Author*) Nothing to Disclose Heejin Bae, Seoul, Korea, Republic Of (*Abstract Co-Author*) Nothing to Disclose Sungwon Kim, MD, Seoul, Korea, Republic Of (*Abstract Co-Author*) Nothing to Disclose Joonseok Lim, MD, Seoul, Korea, Republic Of (*Abstract Co-Author*) Nothing to Disclose Junmo Kim, Seoul, Korea, Republic Of (*Abstract Co-Author*) Nothing to Disclose

For information about this presentation, contact:

hlhong@swu.ac.kr

hlhong@swu.ac.kr

CONCLUSION

Our GAN-DA method has high potential to be applied to various medical image classification problems as well as liver lesion classification in CT images. (This work was supported by the NRF grant funded by the Korea government (MSIP) (2017R1D1A1B03029631))

Background

The small dataset problem due to the limited acquisition of medical images is one of the major challenges in deep learning-based medical image classification. Data augmentation (DA) through scaling and rotation of the training images have been performed to avoid the overfitting caused by the small dataset problem, but this conventional DA has limitations in diversifying data patterns and improving learning efficiency. Thus, we propose a generative adversarial network (GAN) based DA method and apply it to the deep learning classification of liver lesions in CT images to verify its performance.

Evaluation

Our method was evaluated on a dataset consisting of 502 abdominal CT scans including 676 cysts(C), 130 hemangiomas(H), and 484 metastases(M). Each lesion was contoured by the radiologist. To train a CNN classifier, the DA is performed to increase the amount of given training data to avoid overfitting. In classic DA, the augmented images were generated by randomly scaling or rotating an image patch. In GAN-DA, the augmented images were generated by training GAN on the given image patches to create synthetic training images. This GAN-DA can generate synthetic data with a novel pattern by combining the imaging characteristics of given images. The AlexNet CNN was then trained with the augmented training data to classify the unseen test data. In experiments, our method of combining two DA methods achieved the accuracy of 74.59% where the classic DA and GAN-DA each achieved the accuracies of 74.36% and 66.45%, respectively.

Discussion

In deep learning of small dataset, the classic DA plays a role in extending the amount of training data, but is limited to repeating the given pattern. The proposed GAN-DA can further complement the pattern distribution of given data by diversifying the data patterns. As a result, training CNN with combined two DA-generated data can achieve the most improved performance in liver lesion classification.

SSM14-03 Abnormal Chest X-Ray Identification with Generative Adversarial One-Class Classifier

Wednesday, Dec. 4 3:20PM - 3:30PM Room: E353C

Awards

Trainee Research Prize - Fellow

Participants

Yuxing Tang, Bethesda, MD (*Presenter*) Nothing to Disclose Youbao Tang, PhD, Bethesda, MD (*Abstract Co-Author*) Nothing to Disclose Mei Han, Palo Alto, CA (*Abstract Co-Author*) Nothing to Disclose Jing Xiao, Shenzhen, China (*Abstract Co-Author*) Nothing to Disclose Ronald M. Summers, MD,PhD, Bethesda, MD (*Abstract Co-Author*) Royalties, iCAD, Inc; Royalties, Koninklijke Philips NV; Royalties, ScanMed, LLC; Royalties, Ping An Insurance Company of China, Ltd; Research support, Ping An Insurance Company of China, Ltd; Research support, NVIDIA Corporation; ; ; ;

For information about this presentation, contact:

yuxing.tang@nih.gov

PURPOSE

To develop an automatic system of abnormality classification on chest radiographs that allows reporting focusing more on pathology analysis of abnormal CXRs, requiring only normal chest X-ray images as input in the training stage. The intuition of using only normal images for training is that it is not always possible to include or annotate all kinds of abnormalities for large scale training because some forms of anomaly are very rare.

METHOD AND MATERIALS

We propose an end-to-end architecture for abnormal chest X-ray identification using generative adversarial one-class learning, by training solely from normal CXRs. The proposed architecture is composed of three main modules: a U-Net autoencoder, a CNN discriminator and an encoder, which compete to learn while collaborating with each other for the target task. The adversarially trained generative model is capable of reconstructing the normal CXRs while performing poorly on reconstructing the abnormal ones, since only the normal CXRs are involved in training and those with various anomalies are unseen by the model. Such reconstruction differentiation enables the proposed model to identify abnormal CXRs. We design four different loss functions from pixel level to feature level, to joinlty optimize the whole network.

RESULTS

The proposed method is evaluated on two subsets of the NIH ChestX-ray14 dataset. For normal versus abnormal classification, our method achieves an AUC of 0.841, compared to 0.627 without using adversarial learning. For normal versus pneumonia classification, our method achieves an AUC of 0.802 (0.592 for non adversarial learning). Since the network has learned from distribution of normal images in the training stage, it knows the characteristics of normal distribution and it is able to reconstruct normal CXR of good quality in the testing stage. Since the abnormal CXRs are unseen in the training stage, the network is not able

to reconstruct abnormal CXRs of good quality in the testing stage.

CONCLUSION

The differentiation of reconstruction behaviors between normal and abnormal chest X-rays enables the model to distinguish abnormal CXRs from normal ones in this adversarial one-class setting. The proposed method could be extended and applied to other medical image modalities.

CLINICAL RELEVANCE/APPLICATION

This one-class learning may reduceing the need for manual annotations, thereby accelerating the development of automated CXR diagnosis software for radiologists.

SSM14-04 Generative Neural Networks: Synthesizing a Complete Tomographic Study from a Single Frontal Radiograph

Wednesday, Dec. 4 3:30PM - 3:40PM Room: E353C

Participants

Patrick Cole, Urbana, IL (*Presenter*) Nothing to Disclose Andrew Chen, Urbana, IL (*Abstract Co-Author*) Nothing to Disclose Sriram Sundararaman, Urbana, IL (*Abstract Co-Author*) Nothing to Disclose Avinash Kadimisetty, Urbana, IL (*Abstract Co-Author*) Nothing to Disclose Ayis T. Pyrros, MD, Hinsdale, IL (*Abstract Co-Author*) Research Consultant, Document Storage Systems, Inc Sanmi Koyejo, PhD, Urbana, IL (*Abstract Co-Author*) Nothing to Disclose Nasir A. Siddiqui, MD, Oak Brook, IL (*Abstract Co-Author*) Nothing to Disclose

For information about this presentation, contact:

ayis.pyrros@dupagemd.com

PURPOSE

Chest radiography encodes a three-dimensional image in a unique two-dimensional domain, which offers unique challenges even for the most experienced radiologists, as many critical findings are superimposed, often resulting in error or further imaging. In recent years, deep generative models have emerged as powerful models in generating realistic synthetic images. In this study a generative model was applied to synthesize tomographic views from a single frontal chest radiograph, which could improve diagnostic accuracy and potentially reduce the need for further unnecessary imaging.

METHOD AND MATERIALS

An anonymized noncontrast CT chest database, containing 20,000 (512x512) images, with orthogonal views for 229 patients in PNG format. Synthetic chest radiographs (input scout) were generated by taking the mean over the coronal CT slices per patient, which were then mapped to a three-dimensional volume, 128 x 128 x 128 pixels. An encoder-decoder approach with residual connections was utilized to synthesize the tomographic slices, which was inspired by the 3D-R2N2 model. The frontal view of the radiograph was encoded into a lower dimensional space, using a convolutional neural network, and later decoded into a 3D grid of CT slices. Training took approximately 5 hrs, with a batch size of 16, and 450 epochs, utilizing a p3.8x large instance. Images were reviewed by 3 board-certified radiologists.

RESULTS

Qualitative analysis of the initial results demonstrate the superstructure of the thorax, but lacking some of the details in the ground truth CT, such as the pulmonary vasculature (see figure). This is promising because shape is arguably one of the more difficult challenges due to the fact that a 2D shape may have many different 3D representations, i.e. a circle to a sphere, cylinder, etc.

CONCLUSION

The described method can synthesize a tomographic study from a frontal radiograph, using a generative neural network. The results retain the structural information from the ground truth CT, but lack some of the fine detail, due to hardware limitations and dataset size.

CLINICAL RELEVANCE/APPLICATION

In what we believe is groundbreaking work, we demonstrate the synthesis of a 3D tomographic study from a single radiographic view is technically feasible. This could significantly improve diagnostic accuracy and reduce unnecessary imaging, providing additional 3D information.

SSM14-05 pix2surv: A Generative Adversarial Network Model for Prediction of Survival in Patients with Interstitial Lung Diseases

Wednesday, Dec. 4 3:40PM - 3:50PM Room: E353C

Participants

Tomoki Uemura, MS,BA, Boston, MA (*Presenter*) Nothing to Disclose Chinatsu Watari, MD, Boston, MA (*Abstract Co-Author*) Nothing to Disclose Janne J. Nappi, PhD, Boston, MA (*Abstract Co-Author*) Royalties, Hologic, Inc Royalties, MEDIAN Technologies Toru Hironaka, Boston, MA (*Abstract Co-Author*) Nothing to Disclose Hyoungseop Kim, PhD, Kitakyushu, Japan (*Abstract Co-Author*) Nothing to Disclose Hiroyuki Yoshida, PhD, Boston, MA (*Abstract Co-Author*) Patent holder, Hologic, Inc; Patent holder, MEDIAN Technologies;

For information about this presentation, contact:

yoshida.hiro@mgh.harvard.edu

PURPOSE

To develop a novel survival analysis model for images, called pix2surv, based on a conditional generative adversarial network

(cGAN), and to evaluate its performance based on chest CT images of patients with idiopathic pulmonary fibrosis (IPF).

METHOD AND MATERIALS

The architecture of the pix2surv model has a generator network based on a U-net model which is trained to generate survival-time images from chest CT images of each patient, and a discriminator network based on a patch-based fully convolutional network which is trained to differentiate the "fake pair" of a chest CT image and a generated survival-time image from the "true pair" of an input CT image and the observed survival-time image of a patient. For evaluation, we retrospectively collected 171 IPF patients with high-resolution chest CT and pulmonary function tests from the Lung Tissue Research Consortium. The survival predictions of the pix2surv model on these patients were compared with those of an established clinical prognostic biomarker known as the gender, age, and physiology (GAP) index by use of a two-sided t-test with bootstrapping by 500 replications. Concordance index (C-index) and relative absolute error (RAE) were used as measures of the prediction performance.

RESULTS

Bootstrap evaluation yielded a C-index value of 57.4% [95% confidence interval (CI): 48.7, 66.2] and RAE value of 33.3% [95% CI: 28.7, 38.1] for the GAP index and C-index value of 87.4% [95% CI: 80.7, 94.0] and RAE value of 17.8% [95% CI: 13.3, 22.5] for the pix2surv model. The improvement in survival prediction by the pix2surv model was statistically significant (P<0.0001).

CONCLUSION

The pix2surv model yielded a significantly higher performance than GAP index in the prediction of the overall survival of IPF patients. Thus, it could be used to provide an effective imaging-based biomarker for the prediction of the overall survival of patients with IPF.

CLINICAL RELEVANCE/APPLICATION

There are few established imaging-based predictors for the survival of patients with IPF. Deep learning that can automatically predict survival from lung CT images could provide an effective prognostic imaging biomarker for precise management of patients with IPF.

SSM14-06 Reality of Body CT Images Generated by Generalized Adversarial Network (GAN): Classification Test of Real or Fake CT Images

Wednesday, Dec. 4 3:50PM - 4:00PM Room: E353C

Participants

Ho Young Park, MD, Seoul, Korea, Republic Of (*Presenter*) Nothing to Disclose Gil-Sun Hong, MD, Seoul, Korea, Republic Of (*Abstract Co-Author*) Nothing to Disclose Hyun-Jin Bae, PhD, Seoul, Korea, Republic Of (*Abstract Co-Author*) Co-founder, Promedius Inc; CEO, Promedius Inc Jihye Yun, Seoul, Korea, Republic Of (*Abstract Co-Author*) Nothing to Disclose Young Ji Song, Seoul, Korea, Republic Of (*Abstract Co-Author*) Nothing to Disclose Younghwa Byeon, Seoul, Korea, Republic Of (*Abstract Co-Author*) Nothing to Disclose Sung Won Park, Seoul, Korea, Republic Of (*Abstract Co-Author*) Nothing to Disclose Won-Jung Chung, Seoul, Korea, Republic Of (*Abstract Co-Author*) Nothing to Disclose Namkug Kim, PhD, Seoul, Korea, Republic Of (*Abstract Co-Author*) Nothing to Disclose

For information about this presentation, contact:

lyanhy@gmail.com

PURPOSE

This study aims to determine whether generalized adversarial network (GAN) can create far most realistic-looking body CT images or not.

METHOD AND MATERIALS

Using 11775 normal chest and/or abdominopelvic CT scans (172,249 chest slices and 301,584 abdominopelvic slices), we implemented a progressive growing of GAN (PGGAN) to create artificial images. Validation set consisted of total 300 axial body CT images (150 real and 150 fake images), which were composed of contrast-enhanced chest CT images with lung (Chest-L) and mediastinal window setting (Chest-M), and contrast-enhanced abdominopelvic CT images (AP-CT). Ten radiologists independently judged whether each CT images is real or not after analyzing images in visual manner without any time limits. Diagnostic accuracy, sensitivity, specificity and inter-reader agreement were calculated and compared among subgroups (thorax, thoracoabdominal junction, mid-abdomen and pelvis).

RESULTS

For total images, mean accuracy, sensitivity, specificity were 59.4%, 66.9%, 51.9%. There was no significant difference in accuracy between three image groups (Chest-L, 59.5%; Chest-M, 61.5%; and AP-CT, 57.1%, P = 0.33). Inter-reader agreements were poor for total images (k = 0.11) and poor for each three image group (k = 0.04 - 0.13). In subgroup analysis, thoracoabdominal junction level showed significantly higher accuracy (74.3%) than other subgroups (52.4% - 60.2%, P = 0.003), and had highest inter-reader agreement (k = 0.31).

CONCLUSION

GAN can generate realistic-looking body CT images, which cannot be easily distinguished from real images by radiologists. However, to increase the realism of body CT images, it is necessary to strengthen the learning of thoracoabdominal junction level.

CLINICAL RELEVANCE/APPLICATION

This is a first reported study to systematically evaluate reality of GAN-generated synthetic body CT images. Realistic images creation is the first step in applying GAN in various medical fields.





SSM15

Informatics (Image Sharing, Data, Security, Quality)

Wednesday, Dec. 4 3:00PM - 4:00PM Room: E353B



AMA PRA Category 1 Credit ™: 1.00 ARRT Category A+ Credit: 1.00

FDA Discussions may include off-label uses.

Participants

Seetharam C. Chadalavada, MD,MS, Cincinnati, OH (*Moderator*) Nothing to Disclose Christopher R. Deible, MD, PhD, Allison Park, PA (*Moderator*) Nothing to Disclose Kevin L. Junck, PhD, Birmingham, AL (*Moderator*) Nothing to Disclose Teresa Martin-Carreras, MD, Philadelphia, PA (*Moderator*) Nothing to Disclose Akshay Goel, MD, New York, NY (*Moderator*) Founder and CEO, Radlearn LLC

Sub-Events

SSM15-01 Development of Good Practice Compliant Clinical Trial Imaging Management System for Multi-Center Clinical Trials

Wednesday, Dec. 4 3:00PM - 3:10PM Room: E353B

Participants

Youngbin Shin, MS, Seoul, Korea, Republic Of (*Presenter*) Nothing to Disclose Junghyun A. Lee, Seoul, Korea, Republic Of (*Abstract Co-Author*) Nothing to Disclose Yu Sub Sung, Seoul, Korea, Republic Of (*Abstract Co-Author*) Nothing to Disclose Kyung Won Kim, MD, Seoul, Korea, Republic Of (*Abstract Co-Author*) Nothing to Disclose Seong Ho Park, MD, Seoul, Korea, Republic Of (*Abstract Co-Author*) Research Grant, Central Medical Service Co, Ltd Yousun Ko, MPH, Seongnam-si, Korea, Republic Of (*Abstract Co-Author*) Nothing to Disclose

PURPOSE

As utilization of imaging in multi-center clinical trials has rapidly increased, the amount of data and work flow complexity also increased, requiring a dedicated computerized system, a clinical trial imaging management system (CTIMS). Recently, the US FDA emphasizes the Good Clinical Practice compliance of the CTIMS. Thus, we aimed to develop a comprehensive CTIMS with intention to thoroughly meet the current regulatory guidelines and various functional requirements.

METHOD AND MATERIALS

Key regulatory and functional requirements of CTIMS were extracted thorough review of many related regulations/guidelines including ICH-GCP E6, FDA 21 CFR Part 11 and 820, Good Automated Manufacturing Practice (GAMP®), Clinical Data Interchange Standards Consortium (CDISC). Based on these requirements, the system architecture was designed by multidisciplinary team including radiologists, engineers, clinical trial specialists, regulatory medicine professionals. Computerized system validation of the developed CTIMS was performed internally and externally.

RESULTS

Our CTIMS was developed based on two-layer design composed of the server system and the client system, which is efficient to meet the regulatory/functional requirements. The server system manages system security, data archive, backup, audit trail, etc. The client system provides various functions including de-identification, image transfer, image viewer, image quality control, electronic record, etc. Computerized system validation internally using V-model and externally by global quality assurance company demonstrated that CTIMS meet all regulatory/functional requirements. Currently, our CTIMS system has been successfully implemented into more than 20 pharmaceutical multi-center clinical trials since 2017.

CONCLUSION

In the era of bigdata, the use of CTIMS is crucial in multi-center clinical trials to deal with the large amount of image data and complexity of imaging management process. CTIMS must meet the both regulatory and functional requirements of the clinical trial, enhancing work flow efficiency and more reliable data/outcomes.

CLINICAL RELEVANCE/APPLICATION

The Good Practice compliant CTIMS with comprehensive functions is an essential part of multi-center clinical trials to generate high quality data and minimize protocol violation.

SSM15-02 Tofu: For Stir-Fry and Ultrasound Procedural Training

Wednesday, Dec. 4 3:10PM - 3:20PM Room: E353B

Participants Maggie Chung, MD, San Francisco, CA (*Presenter*) Nothing to Disclose Eugene J. Huo, MD, San Francisco, CA (*Abstract Co-Author*) Nothing to Disclose

Eugene.huo@ucsf.edu

CONCLUSION

Firm tofu is a cheap US training medium that trainees at all reported improved their skills and confidence at minimal cost. Use of these blocks in a standard curriculum may be of benefit early on in resident education.

Background

Despite the availability of commercial simulations, training new residents in procedures has traditionally been on patients who present with a need for treatment. This "trial-by-fire" experience, can be stressful for supervising physicians and trainees, and often deleterious to patients. Commercial ultrasound (US) phantoms are extremely costly for limited utility. We postulated that a cheap non-anatomic simulation could still greatly improve procedural skills and trainee confidence at a low cost in time and money. Based on prior publications, the use of tofu was suggested as a tissue simulation due to similar propagation speed to soft tissue. Internal echogenicity was noted to be similar to some soft tissues.

Evaluation

Blocks of tofu were initially evaluated by both an attending interventional radiologist and a diagnostic radiologist to establish parameters. 11 trainees of varying levels of experience were asked to fill out a survey documenting their perceived experience, level of training and comfort with ultrasound guided procedures on a 10-point scale before completing testing. Trainees were randomized to initial testing on a tofu model or a commercially available phantom, and then completed a survey asking to evaluate change in the previously evaluated findings on a -5 to 5 point scale. Testing consisted of basic ultrasound guidance tasks including identification of target in multiple projections along with real-time needle guidance. Participants then underwent testing on the other model followed by a second survey.

Discussion

Although no statistically significant trend could be identified on pre-testing surveys, trainee confidence demonstrated an overall positive improvement after use of the tofu-based model by 3.4 points. Use of the commercial phantom resulted in an improvement of 2.2 points, with most of the trainee concerns raised by more experienced residents, including excessive stiffness and residual tracts from prior training.

SSM15-03 Protecting Patients from Cyber-Attacks on CT's Using Machine Learning Methods

Wednesday, Dec. 4 3:20PM - 3:30PM Room: E353B

Participants

Tom Mahler, Beer Sheva, Israel (*Presenter*) Nothing to Disclose Erez Shalom, PhD, Beer-Sheva, Israel (*Abstract Co-Author*) Nothing to Disclose Arnon Makori, MD, Tel Aviv, Israel (*Abstract Co-Author*) Medical Advisory Board, Carestream Health, Inc Ilan Shelef, MD, Beer-Sheva, Israel (*Abstract Co-Author*) Nothing to Disclose Yuval Elovici, PhD, Beer Sheva, Israel (*Abstract Co-Author*) Nothing to Disclose Yuval Shahar, PhD, Beer-Sheva, Israel, Israel (*Abstract Co-Author*) Nothing to Disclose

For information about this presentation, contact:

tom@mahler.tech

PURPOSE

Today, security methods for protecting medical imaging devices (MIDs) from cyber-attacks mainly focus on hospitals' network and endpoint security level; such methods are limited and are often breached (e.g., the WannaCry attack) as they rely on constantly installing regular security updates, a challenging task in a clinical setting with numerous devices. Moreover, cyber attacks that target internal components of MIDs ecosystem are harder to detect and protect; such attacks are potentially more dangerous and can potentially affect patients' health. For example, once the internal control unit of the MID is compromised, it is possible to manipulate its behavior and potentially jeopardize scans, device mechanics, and even patients safety.

METHOD AND MATERIALS

We recorded over 10,000 scan commands sent from a computed tomography (CT) scanner host control unit to the gantry. Each record contains various technical parameters of the scan, including lables such as the body part being scanned, the scan protocol, etc. Furthermore, we recorded, with the assistance of radiologists and technicians, potentially malicious commands on real CT device (while no patient was present). We then applied different machine learning methods (e.g., Random Forest) to create an anomality detection model that can distinguish between normal and malicious scans, with respect to the scan labels.

RESULTS

We were able to classify scan commands to the appropriate scan labels (i.e., body part, scan protocol, and study description) with 90-98% accuracy (depending on the specific scan label) and detect all synthesized malicious commands. Furthermore, our anomaly detection model can also help notify and protect anomalies resulting from human error.

CONCLUSION

Scan commands, often ignored or only used for maintenance purposes, contain important information about the scan process. By utilizing this information, we were able to study and define normal commands structure, and consequently detect scenarios in which anomalous commands where sent maliciously or by mistake.

CLINICAL RELEVANCE/APPLICATION

Using machine learning methods can help detect cyber-attacks, as well as other anomalies such as human error, and by that protect patients from potential harm and improves safety.

SSM15-04 Deploying Deep Learning for Quality Control: An AI-assisted Review of Chest X-Rays Reported as 'Normal' in Routine Clinical Practice

Participants

Vidur Mahajan, MBBS, New Delhi, India (*Abstract Co-Author*) Researcher, CARING; Associate Director, Mahajan Imaging; Research collaboration, General Electric Company; Research collaboration, Koninklijke Philips NV; Research collaboration, Qure.ai; Research collaboration, Predible Health; Research collaboration, Oxipit.ai; Research collaboration, Synapsica; Research collaboration, Quibim Vasanthakumar Venugopal, MD, New Delhi, India (*Presenter*) Consultant, CARING; Research collaboration, General Electric Company; Research collaboration, Qure.ai; Research collaboration, General Electric Company; Research collaboration, Carina (*Presenter*) Consultant, CARING; Research collaboration, General Electric Company; Research collaboration, Koninklijke Philips NV; Research collaboration, Qure.ai; Research collaboration, Predible Health; Research collaboration, Quibim

Salil Gupta, BEng, New Delhi, India (Abstract Co-Author) Nothing to Disclose

Murali Murugavel, PhD, New Delhi, India (Abstract Co-Author) Nothing to Disclose

Harsh Mahajan, MD, MBBS, New Delhi, India (*Abstract Co-Author*) Director, Mahajan Imaging Pvt Ltd; Research collaboration, General Electric Company; Research collaboration, Koninklijke Philips NV; Research collaboration, Qure.ai; Research collaboration, Predible Health

For information about this presentation, contact:

vidur@mahajanimaging.com

PURPOSE

Quality control in radiology has thus far been restricted to performing random double reads or collating information about clinical correlation - both tedious and expensive activities. We present a novel use-case for AI to double read Chest X-Rays (CXRs) and indicate a list of cases where the radiologist may have erred.

METHOD AND MATERIALS

This study on the feasibility of deploying deep learning algorithms for quality control was conducted on pooled data from four outpatient imaging departments. The radiology workflow included a 'report approval' station where a simple, high level, binary label -'normal' or 'abnormal' - was applied by radiologists. All adult CXRs marked 'normal' were prospectively analyzed through a deep learning algorithm (LUNIT Insight, S. Korea) tuned for automated normal vs abnormal classification. Note that the algorithm used was not trained on data from the institutes and country of testing. It provided an 'abnormality score' (range 0.00 - 1.00) and all images marked as 'abnormal' in high sensitivity setting (threshold = 0.16) were reviewed by a sub-specialist chest radiologist with 8 years' experience.

RESULTS

A total of 708 CXRs were marked 'normal' by radiologists during the one-month period of the study. 46 / 708 (6.49%) of CXRs were labelled 'abnormal' by the algorithm. Upon review of these 46 CXRs, 12 showed true abnormalities upon review. These 12 cases included four with lung opacities, three with significant blunting of costophrenic angles, two with apical fibrosis, one with a cavity, one with a nodule and one case with cardiomegaly. Appropriate corrective and preventive actions were taken, and feedback was provided to radiologists who reported these cases.

CONCLUSION

We demonstrate AI algorithms' ability to quickly parse through large datasets and help identify errors by radiologists. This is a fast and effective method to deploy AI algorithms in clinical practice with no risk (from AI) to patients, and clear measurable positive impact.

CLINICAL RELEVANCE/APPLICATION

Radiologists work flow supported by a parallel, second read AI would allow for faster reporting as it can help reduce errors in radiology reports, improving patient-care in the process. Importantly, this quality assurance study on CXR reporting, demonstrates the potential for AI to both personalize and prioritize training modules for radiologists.

SSM15-05 Informatics Challenges and Solutions to Host an Ultra-High Resolution Computed Tomography System

```
Wednesday, Dec. 4 3:40PM - 3:50PM Room: E353B
```

Participants

Sarah E. McKenney, PhD, Stanford, CA (*Presenter*) Nothing to Disclose
Thomas W. Loehfelm, MD, PhD, Atlanta, GA (*Abstract Co-Author*) Nothing to Disclose
John R. Hancock, Sacramento, CA (*Abstract Co-Author*) Nothing to Disclose
John R. Harrison, BA, Sacramento, CA (*Abstract Co-Author*) Nothing to Disclose
Erin Angel, PhD, Tustin, CA (*Abstract Co-Author*) Employee, Canon Medical Systems Corporation
John M. Boone, PhD, Sacramento, CA (*Abstract Co-Author*) Board of Directors and Shareholder, Izotropic Imaging Corporation; Co-author with royalties, Wolters Kluwer nv; Patent agreement, The Phantom Laboratory
J. Anthony Seibert, PhD, Sacramento, CA (*Abstract Co-Author*) Nothing to Disclose

For information about this presentation, contact:

jaseibert@ucdavis.edu

CONCLUSION

HRCT and other high-resolution imaging systems are now on the market and may test the limits of legacy informatics infrastructure for image transfer, storage, and display. Hospital IT must anticipate these future clinical needs and account for the large data challenges as imaging systems continue to advance.

Background

The acquisition of a high resolution CT (HRCT) scanner presents several challenges for data transfer & retrieval, storage and rendering. Unlike a conventional CT system with a standard image slice matrix of 512x512 and a minimum slice thickness of ~ 0.6 mm, the HRCT system acquires 1024 and 2048 matrix sizes with a minimum slice thickness of 0.25 mm. This results in CT acquisition

series 4 to 19 times larger than a conventional CT series.

Evaluation

Several aspects of the imaging informatics chain were evaluated in advance of installation and continued to be monitored once the system went live. 1. The timing of data transfer as a function of infrastructure lines and matrix size was examined to ensure that it met the requirements of the clinical workflow. 2. The adequacy of existing display hardware and software for image interpretation was assessed. 3. The data storage requirements were estimated and monitored.

Discussion

(1) Data transfer has proven to have a negligible workflow impact on a10 Gbps fiber (under 7 sec for a13 GB 2048x2048 study). However, transfer of the same study extended to 20 min on a shared 100 Mbps network. Data transfer times were under 10 sec for the 6GB 1024x1024 studies, demonstrating performance variability, particularly on shared networks. (2) A 5MP display is recommended to display a full 2048 image set at full resolution. Otherwise, clinicians must enable zoom and pan within the image slice. Anecdotally, the exams with 0.25 mm slice thicknesses are best navigated with a cine loop and a scout localizer to avoid excessive scrolling. Jerky scrolling became obstructive when viewing 2048 images on computers where caching or RAM was limited (e.g. <8 GB). (3) Within the first 2 weeks of installation, data storage remains stable despite the accelerated use of storage space due to a strategic contract with the PACS vendor.

SSM15-06 A Real-Time Gaze Tracking System to Analyze Spatial and Temporal Attention Characteristics of Radiologists

Wednesday, Dec. 4 3:50PM - 4:00PM Room: E353B

Participants

Oguz Akin, MD, New York, NY (*Abstract Co-Author*) Research Consultant, Ezra AI Yingli Tian, New York, NY (*Abstract Co-Author*) Nothing to Disclose Longlong Jing, New York, NY (*Abstract Co-Author*) Nothing to Disclose Benjamin Reichman, New York, NY (*Abstract Co-Author*) Nothing to Disclose Fuat Nurili, New York, NY (*Abstract Co-Author*) Nothing to Disclose Cihan Duzgol, MD, New York, NY (*Abstract Co-Author*) Nothing to Disclose Turan A. Ilica, New York, NY (*Abstract Co-Author*) Nothing to Disclose Omer Aras, MD, Edgewater, NJ (*Presenter*) Nothing to Disclose

For information about this presentation, contact:

akino@mskcc.org

PURPOSE

To develop a real-time attention tracking system that can handle dynamic back-and-forth scrolling through a series of images without any hardware or software intrusion while the radiologist interpreting a study.

METHOD AND MATERIALS

The system framework was built on the Open Health Imaging Foundation's open-source medical image viewer with integration of a Tobii 4C Eye Tracking camera. Spatial and temporal coordinates of the series of images are automatically recorded and the corresponding attention heapmaps are generated. For attention and search patent analysis, the commonly used eye-tracking metrics are analyzed including area of interest (AOI), time to first fixation, total fixation duration, fixation duration on AOI, number of fixations on AOI, dwell time ratio, and saccade length on each image. Furthermore, 3D dynamic analysis of attention characteristics are studied including total time of the scan, slice of interest (SOI), fixation duration on SOI, number of fixations on SOI, number of scrolling (scrolling back-and-forth while focusing on different areas), number of drilling (scrolling back-and-forth while focusing on one area). The system's performance was tested using the data from 4 radiologists while interpreting 30 CT studies from the LUNA16 dataset.

RESULTS

The system successfully captured the attention data in all interpretation sessions (n=120) without any software or hardware failure. The accuracy of the gaze tracking is 0.4° which is about 3.5-7 mm on the computer screen at a distance range of 0.5-1 m between the observer and the camera. The analysis of the attention heatmaps showed spatial and temporal variations in the 3D dynamic attention characteristics of 4 radiologists, indicating unique search patterns among different observers.

CONCLUSION

The proposed system can be used as an objective tool to study unique search patterns among human observers. These data can be further used to develop more interactive human-computer interfaces for artificial intelligence applications.

CLINICAL RELEVANCE/APPLICATION

As artificial intelligence applications advance, there is an increasing need to develop seamless human-computer interfaces that can capture the radiologists' attention. Such systems allowing artificial intelligence algorithms to operate more interactively with the human observers in real time could significantly expedite adoption of artificial intelligence in clinical practice.

Printed on: 10/29/20







SSM16

Molecular Imaging (Oncology)

Wednesday, Dec. 4 3:00PM - 4:00PM Room: S505AB



AMA PRA Category 1 Credit ™: 1.00 ARRT Category A+ Credit: 1.00

FDA Discussions may include off-label uses.

Participants

Pedram Heidari, MD, Charlestown, MA (Moderator) Nothing to Disclose

Benjamin Larimer, PhD, Charlestown, MA (Moderator) Co-founder, Cytosite Biopharma Inc; Consultant, Cytosite Biopharma Inc; Stockholder, Cytosite Biopharma Inc

Sub-Events

SSM16-01 Prospective Evaluation of the First Integrated PET/Dual-Energy CT System in Patients with Lung Cancer

Wednesday, Dec. 4 3:00PM - 3:10PM Room: S505AB

Awards

Trainee Research Prize - Resident

Participants

Simon S. Martin, MD, Charleston, SC (Presenter) Institutional Research support, Siemens AG Marly van Assen, MSc, Charleston, SC (Abstract Co-Author) Nothing to Disclose Philip Burchett, MSc, Charleston, SC (Abstract Co-Author) Nothing to Disclose James G. Ravenel, MD, Charleston, SC (*Abstract Co-Author*) Consultant, ImBio, LLC Leonie Gordon, MBChB, Charleston, SC (*Abstract Co-Author*) Nothing to Disclose Carlo N. De Cecco, MD, Atlanta , GA (Abstract Co-Author) Research Grant, Siemens AG Akos Varga-Szemes, MD, PhD, Charleston, SC (Abstract Co-Author) Research Grant and Travel Support, Siemens AG Research Consultant, Elucid Bioimaging Thomas J. Vogl, MD, PhD, Frankfurt , Germany (Abstract Co-Author) Nothing to Disclose U. Joseph Schoepf, MD, Charleston, SC (Abstract Co-Author) Research Grant, Astellas Group; Research Grant, Bayer AG; Research Grant, Bracco Group; Research Grant, Siemens AG; Research Grant, Heartflow, Inc; Research support, Bayer AG; Consultant, Elucid BioImaging Inc; Research Grant, Guerbet SA; Consultant, HeartFlow, Inc; Consultant, Bayer AG; Consultant, Siemens AG; ; ;

For information about this presentation, contact:

carlo.dececco@emory.edu

PURPOSE

The aim of this study was to prospectively evaluate the first integrated positron emission tomography (PET)/ dual-energy computed tomography (DECT) system in patients with small-cell lung cancer (SCLC) or non-small-cell lung cancer (NSCLC).

METHOD AND MATERIALS

In this single-center HIPAA compliant prospective trial, we included 25 patients (age range, 41-84 years; median age, 62 years) with NSCLC (n=21) or SCLC (n=4) who were referred for a PET/CT study between May 2017 and June 2018. All patients received contrast-enhanced imaging on a clinical PET/DECT system 70 min after the administration of 5MBq/kg of 18F-fluorodeoxyglucose (18F-FDG). Data analysis included PET-based standard uptake values (SUVmax) and DECT-based iodine densities of tumor masses and lymph nodes. Results between the different parameters were compared using Pearson correlation analysis and receiver operating characteristics (ROC) analysis.

RESULTS

SUVmax and iodine density parameters were measured in 33 malignant lung masses (15.0 and 2.3 mg/mL, respectively) and 56 enlarged mediastinal or hilar lymph nodes (8.4 and 2.2 mg/mL, respectively). A moderate correlation was found for SUVmax and iodine density values in tumor masses (r=0.53). SUVmax and iodine density values of lymph node metastases showed a weak correlation (r=0.36). Additionally, iodine quantification analysis provided no added value for the differentiation of malignant from benign lymph nodes with an area under the curve (AUC) of 0.52 using PET-based SUVmax analysis as the reference standard.

CONCLUSION

The integration of PET/DECT information in lung cancer staging can provide additional insights in the assessment of primary lung cancer and on the correlation between tumor vascularization and metabolic activity, offering an alternative for tumor characterization improvements. However, the weak correlation between SUVmax and iodine density in malignant lymph nodes suggest that iodine density alone has a limited value for lymph node characterization.

CLINICAL RELEVANCE/APPLICATION

This is the first clinical study on an integrated PET/DECT which provides additional insights in the assessment of lung cancer, offering an alternative for tumor characterization improvements.

SSM16-02 Deep Learning for Prostate Cancer Lymph Node Staging: Balance and Location Matter

Wednesday, Dec. 4 3:10PM - 3:20PM Room: S505AB

Participants

Alexander Hartenstein, Berlin, Germany (Abstract Co-Author) Nothing to Disclose

Falk Lubbe, Berlin, Germany (Abstract Co-Author) Nothing to Disclose

Bernd K. Hamm III, MD, Berlin, Germany (*Abstract Co-Author*) Research Consultant, Canon Medical Systems Corporation; Stockholder, Siemens AG; Stockholder, General Electric Company; Research Grant, Canon Medical Systems Corporation; Research Grant, Koninklijke Philips NV; Research Grant, Siemens AG; Research Grant, General Electric Company; Research Grant, Elbit Imaging Ltd; Research Grant, Bayer AG; Research Grant, Guerbet SA; Research Grant, Bracco Group; Research Grant, B. Braun Melsungen AG; Research Grant, KRAUTH Medical KG; Research Grant, Boston Scientific Corporation; Equipment support, Elbit Imaging Ltd; Investigator, CMC Contrast AB

Marcus R. Makowski, Berlin, Germany (Abstract Co-Author) Nothing to Disclose

Tobias Penzkofer, MD, Berlin, Germany (*Presenter*) Researcher, AGO; Researcher, Aprea AB; Researcher, Astellas Group; Researcher, AstraZeneca PLC; Researcher, Celgene Corporation; Researcher, Genmab A/S; Researcher, Incyte Coporation; Researcher, Lion Biotechnologies, Inc; Researcher, Takeda Pharmaceutical Company Limited; Researcher, Morphotec Inc; Researcher, Merck & Co, Inc; Researcher, Tesaro Inc; Researcher, F. Hoffmann-La Roche Ltd;

For information about this presentation, contact:

tobias.penzkofer@charite.de

PURPOSE

To evaluate if PSMA-PET lymph node status can be predicted using deep convolutional networks (CNN) from CT imaging alone and assess the influence of class balancing and anatomical context on classification results compared to radiologists' performance.

METHOD AND MATERIALS

549 patients, who had received 68Ga-PSMA PET/CT examination, were included. 2616 lymph nodes (LN) were segmented on CT, the corresponding status was determined from PSMA-PET/CT. Two training datasets were used: The first set ('naively balanced', NB) was created by balancing the infiltration status alone. The second set ('location balanced', LB), was created by additionally balancing within each anatomical region. 130 nodes were set aside for independent testing, leaving 732 (NB) and 548 nodes (LB) after balancing. Three CNNs were created, the first two trained with contrast-enhanced CT images and segmentations of either NB or LB test sets respectively, while the third received masked CT images of the NB set (xMask). All networks were analysed for their test set performance (vs. two radiologists) and heatmap patterns.

RESULTS

The NB trained CNN performed best, with an AUC of 0.955 (95% CI 0.923-0.987). The LB and xMask trained CNN performed comparably well, with AUCs of 0.858 (LB, 95% CI 0.793-0.922) and 0.863 (xMask, 95% CI 0.804 - 0.923). The radiologists achieved an average AUC, sensitivity, specificity and accuracy of 0.81, 65%, 96% and 81% respectively. Analyzing the heatmaps, activation patterns suggest, that CNNs learn features within the lymph nodes but also, and more troublingly, outside of the lymph nodes, which correlate to the infiltration status. It is critical to note that our best performing model appears to rely on features outside of the lymph node in question, such as the skin/air border often found in the inguinal region, which are rarely infiltrated.

CONCLUSION

Deep Learning systems are prone to learning unknown bias present in data, and efforts should be made to prove that classification systems perform as intended. Nevertheless, our results show that CNNs are capable of determining the 68Ga-PSMA PET/CT infiltration status from PCa on contrast-enhanced CT scans alone.

CLINICAL RELEVANCE/APPLICATION

Careful training of CNNs to predict the PSMA/PET lymph node status from CT alone could add value to non-PET staging examinations.

SSM16-03 18F-FMISO PET May Be Applicable in The Evaluation of Colorectal Cancer Liver Metastasis

Wednesday, Dec. 4 3:20PM - 3:30PM Room: S505AB

Participants Huijie Jiang, PhD, MS, Harbin, China (*Abstract Co-Author*) Nothing to Disclose Mingyu Zhang, PhD, harbin, China (*Presenter*) Nothing to Disclose

For information about this presentation, contact:

jhjemail@163.com

PURPOSE

Positron emission tomography (PET) imaging is a non-invasive functional imaging method used to reflect tumor spatial information, and to provide biological characteristics of tumor progression. The aim of this study was to focus on the application of 18F-fluoromisonidazole(FMISO) PET quantitative parameter of maximum standardized uptake value (SUVmax) ratio to detect the liver metastatic potential of human colorectal cancer in mice.

METHOD AND MATERIALS

Wound healing assays were performed to examine the ability of cell migration in vitro. 18F-FMISO uptake in CRC cell lines was measured by cellular uptake assay. 18F-FMISO-based micro-positron emission tomography imaging of colorectal liver metastasis and tumor-bearing mice was performed and quantified by tumor-to-liver SUVmax ratio. The correlation between the 18F-FMISO SUVmax ratio, liver metastases number, hypoxia-induced HIF-1a and serum starvation-induced GLUT-1 was evaluated using Pearson correlation analysis.

Compared with HT29 and HCT116, LoVo-CLM mice had significantly higher liver metastases ratio and shorter median survival time. LoVo cells exhibited stronger migration capacity and higher radiotracer uptake compared with HT29 and HCT116 in in vitro. Moreover, 18F-FMISO SUVmax ratio was significantly higher in both LoVo-CLM model and LoVo-bearing tumor model compared to models established using HT29 and HCT116. In addition, a linear regression analysis revealed a significant correlation between 18F-FMISO SUVmax ratio of CLM-mice and number of liver metastases larger than 0.5cm, as well as between 18F-FMISO SUVmax ratio and HIF-1a or GLUT-1 expression in tumor-bearing tissues.

CONCLUSION

18F-FMISO parameter of SUVmax ratio may provide useful tumor biological information in mice with CRC liver metastasis, thus allowing for better prediction of CRC liver metastasis and yielding useful radioactive markers for predicting liver metastasis potential in CRC.

CLINICAL RELEVANCE/APPLICATION

Better prediction of CRC liver metastasis and yielding useful radioactive markers for predicting liver metastasis potential in CRC.

SSM16-04 Comparison of 18F-DCFPyL-PSMA PET/CT and PET/MR for Detection of Prostate Cancer Biochemical Recurrence: Additive Value of PyL PET with Pelvic MRI for Salvage Radiation Therapy Planning

Wednesday, Dec. 4 3:30PM - 3:40PM Room: S505AB

Participants

Edward M. Lawrence, MD, PhD, Madison, WI (*Presenter*) Nothing to Disclose Minnie Kieler, Madison, WI (*Abstract Co-Author*) Nothing to Disclose Shane A. Wells, MD, Madison, WI (*Abstract Co-Author*) Consultant, Johnson & Johnson Greg Cooley, Madison, WI (*Abstract Co-Author*) Nothing to Disclose Steve Cho, MD, Madison, WI (*Abstract Co-Author*) Research Grant, General Electric Company; Consultant, Advanced Accelerator Applications SA;

For information about this presentation, contact:

scho@uwhealth.org

PURPOSE

To evaluate prostate specific membrane antigen (PSMA)-based 18F-DCFPyL(PyL) PET in prostate cancer (PC) biochemical recurrence (BCR) and benefit for salvage radiation therapy (RT) planning.

METHOD AND MATERIALS

Patients with PC history, prior prostatectomy, and planned RT for BCR were prospectively recruited. Three PyL PET studies were done - whole body PET/CT (wbPET/CT) on a Discovery 710, [pelvic PET/MR (pPET/MR) with multiparameteric pelvic MR (mpMRI), and whole body PET/MR (wbPET/MR) on a Discovery 710 and Signa scanner [GE, Waukesha, WI] respectively. Patients then underwent salvage RT. Two readers independently used two proposed PSMA PET evaluation methods (PSMA-RADS v1, PROMISE) for PET evaluation followed by third reader adjudication. Separately, the mpMRI was evaluated for local or pelvic lymph node (LN) recurrence and proposed post-PET treatment was compared to a standard plan using clinical risk and mpMRI. PET positive sites were evaluated in relation to the actual radiation field.

RESULTS

12 patients (mean age, 61.8 yrs; median pre-RT PSA, 0.92 ng/mL) had 29 PET sites of suspected recurrence. Eight of 12 patients (66%) had a positive PyL PET with suspected disease confined to the pelvis (n=5) or with distant disease (n=3). Positive sites had consensus PSMA-RADS scores of 5 (n=15), 4 (n=1), and 3 (n=12) as well as PROMISE miPSMA expression scores of 3 (n=5), 2 (n=12), and 1 (n=10). Median maximum standardized uptake value (SUVmax) was 9.5, 6.3, and 5.4 for reader 1 and 9.5, 5.9, and 6.1 for reader 2 on pPET/MR, wbPET/MR, and wbPET/CT respectively. pPET/MR detected all PET positive sites within the pelvis. Compared to PyL PET, mpMRI detected 2/4 sites of suspected local recurrences and 1/16 PET positive LNs. Five of 12 patients would have had a proposed treatment plan change based on PyL PET. One RADS-5 LN and 5 equivocal targets (LN, n=2; rib lesion, n=3) were outside the actual radiation field. Additionally, two RADS-5 LNs were at the edge of the field and would have resulted in extended coverage.

CONCLUSION

PSMA-based PyL PET detected suspicious sites in 66% of BCR patients with highest median SUVmax on pPET/MR. PyL PET results would have theoretically changed management in 42% (n=5) patients.

CLINICAL RELEVANCE/APPLICATION

PyL PET was positive in two-thirds of BCR after prostatectomy. PyL PET improves detection of suspected sites of PC recurrence and could impact patient management and RT treatment field planning.

SSM16-05 Real-Time 3D Thermography in a Liver Tumor Ablation Model Using Magnetic Particle Imaging

Wednesday, Dec. 4 3:40PM - 3:50PM Room: S505AB

Participants

Johannes M. Salamon, MD, Hamburg, Germany (*Presenter*) Nothing to Disclose Caroline Jung, Hamburg, Germany (*Abstract Co-Author*) Nothing to Disclose Michael G. Kaul, Hamburg, Germany (*Abstract Co-Author*) Nothing to Disclose Gerhard B. Adam, MD, Hamburg, Germany (*Abstract Co-Author*) Nothing to Disclose Tobias Knopp, DIPLENG, Hamburg, Germany (*Abstract Co-Author*) Nothing to Disclose Harald Ittrich, MD, Hamburg, Germany (*Abstract Co-Author*) Nothing to Disclose

For information about this presentation, contact:

j.salamon@uke.de

PURPOSE

Evaluation of the feasibility of visualizing the temperature course during a thermal ablation in an in vitro liver tumor phantom using MPI and different iron oxide tracers.

METHOD AND MATERIALS

In vitro liver tissue phantoms with different iron oxide tracers (L93, Bayer-Schering; LS008, Load Spin Labs; MM4, TOPASS GmbH, concentrations of 0.1-0.5 mg/ml) were generated in Eppendorf-Tubes using a 1:1 volume mixture of protein and water (Chicken White Protein, Sigma Aldrich). The phantoms were heated by means of an inserted copper wire (1 mm diameter) and MPI-induced eddy currents. The resulting signal changes of the phantom were simultaneously imaged by MPI. As an in vitro liver tumor ablation model, tracer-free protein (pseudotumor) was embedded in protein (pseudo-liver tissue) mixed with L93 (CFe = 0.356 mg/ml). The pseudotumors were heated by means of an inserted copper wire with simultaneous detection of the MPI signal of the surrounding pseudo-liver tissue. All experiments were carried out on a commercial MPI system (Philips/Bruker) using a FoV of 37.3 x 37.3 x 18.6 mm3 and a frame rate of 46 frames/s.

RESULTS

Corresponding to the heating, MPI signal increase could be detected in all tracers. L93 showed the highest temperature changes/sensitivity. In the liver tumor ablation model, the ablation of the pseudo-liver tissue was visualized in 3D in real time by MPI signal changes.

CONCLUSION

MPI is suitable for visualizing temperature distribution and changes in a liver tumor ablation model. The sensitivity depends decisively on the used tracer. A temperature monitoring of healthy tissue for optimized MPI-guided tumor ablation in real time and 3D is feasible.

CLINICAL RELEVANCE/APPLICATION

Real time temperature measurement using MPI in the course of an ablation procedure might emerge as a powerful tool for exact monitoring of ablation success.

SSM16-06 Study of Hypoxia in Pancreatic Cancer Patients Using Dynamic [18F]-FAZA PET

Wednesday, Dec. 4 3:50PM - 4:00PM Room: S505AB

Participants

Fiona Li, BS, London, ON (Abstract Co-Author) Nothing to Disclose

Edward Taylor, Toronto, ON (Abstract Co-Author) Nothing to Disclose

Ivan Yeung, PHD, Toronto, ON (Abstract Co-Author) Nothing to Disclose

David A. Jaffray, PhD, Toronto, ON (*Abstract Co-Author*) Research Grant, Koninklijke Philips Electronics NV Research Grant, Elekta AB Research Grant, Raysearch Laboratories AB Research Grant, IMRIS Inc Research Grant, Varian Medical Systems, Inc Research Grant, Modus Medical Devices Inc Royalties, Raysearch Laboratories AB Royalties, Modus Medical Devices Inc Royalties, Elekta AB Royalties, IMRIS Inc

David W. Hedley, MD, Toronto, ON (Abstract Co-Author) Nothing to Disclose

Ting-Yim Lee, MSc, PhD, London, ON (*Presenter*) License agreement, General Electric Company; License agreement, Neusoft Digital Medical Systems Co, Ltd

For information about this presentation, contact:

fli222@uwo.ca

PURPOSE

To estimate kinetic parameters of [18F]-FAZA in highly hypoxic pancreatic cancer and determine the sensitivity of these parameters in distinguishing normal tissue from hypoxic cancer.

METHOD AND MATERIALS

Twenty patients with pancreatic ductal adenocarcinoma underwent 55 min of dynamic [18F]-FAZA scan. The tissue time activity curve (TAC) was analysed using graphical methods - Patlak and Logan plot to determine the reversibility of binding and using standard two tissue compartment model (S2TCM) as well as our bespoke kinetic model, the flow modified two tissue compartment model (F2TCM) to estimate the kinetic parameters. F2TCM models mean transit time through blood vessels, which could significantly affect parameter estimations. Multivariate logistic regression was used to find the optimal parameter set for distinguishing normal tissue from hypoxia tumor.

RESULTS

Graphical analysis showed that the tracer was reversibly bound and distribution volume (DV) determined by S2TCM and F2TCM was correlated to that of Logan plot. F2TCM fitted TACs better than S2TCM according to the Akaike Information Criteria. Logistic regression determined that DV and dissociation rate constant (k4) classified normal tissue from hypoxic tumor with sensitivity, specificity and negative predictive value (NPV) of 57%, 95% and 92% respectively while it is lower - 43%, 79 % and 67% for Logan's DV.

CONCLUSION

Contrary to the accepted notion that [18F]-FAZA is irreversibly bound, both graphical and kinetic analysis showed that the binding is reversible. The proposed mechanism for the reversibility is that the reduced metabolite, amino-FAZA, is conjugated to glutathione (amino-FAZA-GS) which is usually trapped in cells due to its hydrophilicity, however, in the presence of elevated multidrug resistance protein (MRP-1) in pancreatic tumor, amino-FAZA-GS can be 'pumped' out of the cells leading to radioactivity washout or reversible binding. Besides distinguishing normal pancreatic tissue from hypoxic tumor, kinetic modeling allows evaluation of k4 which can be associated with MRP-1 activity, while the binding rate constant (k3) can be associated with nitroreductase and glutathione activity.

CLINICAL RELEVANCE/APPLICATION

A CONTRACTOR AND AND A CONTRACTOR AND A CONTRACTOR AND A CONTRACTOR AND AND AND AND A CONTRACTOR AND AND AND AND

Non-invasive monitoring of MRP-1 activity and hence drug resistance for hypoxic tumor with [18F]-FAZA could lead to personalization of cancer treatment.

Printed on: 10/29/20





=

SSM17

Musculoskeletal (Shoulder)

Wednesday, Dec. 4 3:00PM - 4:00PM Room: S105AB

МК

AMA PRA Category 1 Credit ™: 1.00 ARRT Category A+ Credit: 1.00

FDA Discussions may include off-label uses.

Participants

Christine B. Chung, MD, Solana Beach, CA (*Moderator*) Nothing to Disclose Jenny T. Bencardino, MD, Jericho, NY (*Moderator*) Nothing to Disclose

Sub-Events

SSM17-01 Saline versus Gadolinium Shoulder MR Arthrography: Contrast Agent or Joint Distention?

Wednesday, Dec. 4 3:00PM - 3:10PM Room: S105AB

Participants

Adam D. Singer, MD, Atlanta, GA (*Presenter*) Nothing to Disclose Samia K. Sayyid, Atlanta, GA (*Abstract Co-Author*) Nothing to Disclose Jeffrey Rosenthal, Atlanta, GA (*Abstract Co-Author*) Nothing to Disclose Monica B. Umpierrez, MD, Atlanta, GA (*Abstract Co-Author*) Nothing to Disclose Felix Gonzalez, MD, Atlanta, GA (*Abstract Co-Author*) Nothing to Disclose Gulshan B. Sharma, PhD,MBA, Calgary, AB (*Abstract Co-Author*) Nothing to Disclose Eric Wagner, MD, Atlanta, GA (*Abstract Co-Author*) Nothing to Disclose

For information about this presentation, contact:

adam.singer@emoryhealthcare.org

PURPOSE

Compare the diagnostic performance of saline and gadolinium shoulder MR arthrograms (MRA) in the detection of labral and rotator cuff injury with arthroscopic findings as a reference standard.

METHOD AND MATERIALS

In this IRB approved retrospective study, consecutive patients presenting over an 18 month period for a shoulder MRA who subsequently had shoulder arthroscopy were enrolled. No patients were excluded. An MSK radiologist reviewed each study to confirm whether saline or gadolinium was injected. The reports from the MRA and the surgery were reviewed. For the rotator cuff and the long head of the biceps tendon, status was designated as full thickness tear, partial thickness tear, tendinosis/low grade fraying or normal. For the labrum, status was designated as tear, fraying/blunting/degeneration or normal. A chi square analysis was performed to compare the correlation between the MRA and the surgical reference. Items were categorized in binary groups (no tear versus tear and normal versus abnormal) and the diagnostic performance of each contrast agent was calculated. Kappa values were calculated to correlate diagnosis of tear between MRA and arthroscopy.

RESULTS

There were a total of 34 gadolinium arthrograms and 24 saline arthrograms. When compared to the reference standard, saline was non-inferior to gadolinium in the diagnosis of tears of the supraspinatus (accuracy 0.88 vs 0.74, respectively) and infraspinatus (accuracy 0.88 vs 0.65, respectively) tendons. Regarding labral tears, saline was non-inferior in the diagnosis of anterior/anterior inferior, posterior and superior tears (accuracy 0.79 vs 0.76, 0.71 vs 0.62 and 0.58 vs 0.56, saline vs gadolinium, respectively). When superior labral fraying was considered a tear, gadolinium outperformed saline (accuracy 0.71 vs 0.54, respectively). In terms of agreement between MRA and the diagnosis of surgically reported tears, saline was non-inferior to gadolinium.

CONCLUSION

Saline performed at least as well as gadolinium for the diagnosis of surgically proven rotator cuff tears. Saline was non-inferior in the detection of anterior and posterior labral tears. If fraying was not considered a tear, saline was non-inferior to gadolinium in the diagnosis of superior labrum tears.

CLINICAL RELEVANCE/APPLICATION

In this series, saline was non-inferior to gadolinium shoulder MRA. This could translate to cost savings by reducing scan times and the need for gadolinium.

SSM17-02 Fully Automated MRI Bone Segmentation of the Glenoid and Humeral Head Using Deep Convolutional Neural Networks

Wednesday, Dec. 4 3:10PM - 3:20PM Room: S105AB

Cem M. Deniz, New York, NY (*Abstract Co-Author*) Nothing to Disclose Erin F. Alaia, MD, New York, NY (*Abstract Co-Author*) Nothing to Disclose Natalia Gorelik, MD, Montreal, QC (*Abstract Co-Author*) Nothing to Disclose James S. Babb, PhD, New York, NY (*Abstract Co-Author*) Nothing to Disclose Jared Dublin, New York, NY (*Abstract Co-Author*) Nothing to Disclose Soterios Gyftopoulos, MD, Scarsdale, NY (*Abstract Co-Author*) Nothing to Disclose

For information about this presentation, contact:

tcantarelli@gmail.com

PURPOSE

To present and evaluate a fully automated humeral head and glenoid segmentation using a deep learning method based based on two-dimensional deep convolutional neural networks (CNNs).

METHOD AND MATERIALS

The study received institutional review board approval. A retrospective dataset of MR images of the shoulder from 100 subjects for different clinical reasons, including 27 cases with history of previous dislocations, were manually segmented by experts. A 2D CNN architecture was trained with multiple initial feature maps and layers. Its segmentation performance was then tested against the ground truth of manual segmentation using a four-fold cross-validation scheme.

RESULTS

Automatic segmentation of the proximal humerus achieved a mean average precision for object detection of 0.99, a dice similarity score of 0.96, a segmentation precision of 0.96, and recall of 0.96. The Hausdorff distance was 23.8 mm, the mean surface distance of 0.5 mm, and the residual mean square distance of 1.3 mm. For the glenoid, automatic segmentation achieved a mean average precision for object detection of 0.92, a dice similarity score of 0.86, a segmentation precision of 0.88, and recall of 0.86. The Hausdorff distance was 20.7 mm, the mean surface distance of 0.8 mm, and the residual mean square distance of 1.8 mm. On average, the time for manual segmentation ranged between 90 to 120 minutes per imaging study. The time needed to train each epoch was around 14 minutes for the 2D CNN, and to calculate the segmentation masks using trained models takes around 4 seconds.

CONCLUSION

Using CNNs, we were able to accurately segment the humeral head and glenoid on MRI. Our results serve as an important initial step towards the automatic diagnosis and quantification of Hill-Sachs lesions and glenoid bone loss and determination of on/off track status. This, in turn, has the potential to provide consistently accurate imaging information that can be used to guide the selection of the most appropriate initial treatment for the anterior shoulder instability patient population.

CLINICAL RELEVANCE/APPLICATION

Using CNNs, we were able to accurately segment the humeral head and glenoid on MRI. Our results serve as an important initial step towards the automatic diagnosis and quantification of Hill-Sachs lesions and glenoid bone loss and determination of on/off track status.

SSM17-03 Identification of Glenoid Labral and Rotator Cuff Tears: Diagnostic Accuracy of Dual Energy CT versus Standard CT Arthrography of the Shoulder

Wednesday, Dec. 4 3:20PM - 3:30PM Room: S105AB

Participants

Giovanni Foti, MD, Negrar, Italy (*Abstract Co-Author*) Nothing to Disclose Fabio Lombardo, MD, Negrar, Italy (*Presenter*) Nothing to Disclose Luigi Romano, MD, Negrar, Italy (*Abstract Co-Author*) Nothing to Disclose Simone Caia, Negrar, Italy (*Abstract Co-Author*) Nothing to Disclose Alberto Beltramello, MD, Negrar, Italy (*Abstract Co-Author*) Nothing to Disclose Giovanni M. Carbognin, MD, Negrar, Italy (*Abstract Co-Author*) Nothing to Disclose

For information about this presentation, contact:

gfoti81@yahoo.it

PURPOSE

To compare the diagnostic accuracy of dual-energy Computed Tomography arthrography (DECTA) and standard computed tomography arthrography (CTA) of the shoulder in depicting glenoid labral tears (GLT) and rotator cuff tears (RCT).

METHOD AND MATERIALS

This prospective institutional review board-approved study included 32 consecutive patients (18 males and 14 females; mean age of 34.5, range 18-60 years) studied between January 2018 and January 2019. Articular cavity was distended with anterior approach by using a mixture of saline and iodinate contrast material before DECT exam (80 kV and tin filter 150 kV). DECT data were postprocessed on a dedicated offline workstation (SyngoVia®). Standard virtual blended 120 kVp images were obtained, representing CTA. Moreover a three-material decomposition algorithm was applied to generate DECT maps. Mono-energetic application was employed to choose the best kV values in order to enhance the vividness of contrast material and to reduce metal artifacts in previously operated shoulders. Two radiologists (26 and 12 years of experience, respectively), blinded to clinical data, evaluated the presence of GLT and RCT on CTA and DECTA images. Surgical findings served as standard of reference. Diagnostic accuracy values were calculated. Inter-observer and intra-observer agreement were calculated with k-statistics. A value of p<0.05 was considered statistically significant.

RESULTS

MRI revealed the presence of GLT in 24/32 patients (75.0%) and a RCT in 10/32 patients (31.2%). The sensitivity, specificity, PPV and NPV and accuracy of DECTA were 91.6, 100,100, 81.8 and 91.1%, and 100, 100, 100, 100, and 100%, as regards GLT and RCT, respectively. The sensitivity, specificity, PPV and NPV and accuracy of CTA were 91.6, 90.0, 95.6, 81.1 and 91.1%, and 90.0,

100, 90.0, 95.6, 85.7 and 96.8%, as regards GLT and RCT, respectively. By using McNemar test, the difference of accuracy between DECTA and CTA was not significant (p=0.23). The interobserver and intraobsever agreement were near perfect (k=0.82 and k=0.86, respectively).

CONCLUSION

DECTA can identify GLT and RCT with higher accuracy with respect to CTA.

CLINICAL RELEVANCE/APPLICATION

DECTA arthrography is an accurate imaging method for demonstration of glenoid labrum and rotator cuff tears. The increase of conspicuity of contrast material injected within the articular cavity may represent a key factor for the identification of subtle tears.

SSM17-04 Qualitative and Quantitative Analysis of Glenoid Bone Stock and Version: Inter-Reader Analysis and Correlation with Rotator Cuff Atrophy

Wednesday, Dec. 4 3:30PM - 3:40PM Room: S105AB

Participants

Matthew J. Siebert, BS, Dallas , TX (*Abstract Co-Author*) Nothing to Disclose Majid Chalian, MD, Dallas, TX (*Abstract Co-Author*) Nothing to Disclose Arghavan Sharifi, BS, Dallas, TX (*Abstract Co-Author*) Nothing to Disclose Parham Pezeshk, MD, Dallas, TX (*Abstract Co-Author*) Nothing to Disclose Yin Xi, PhD, Dallas, TX (*Abstract Co-Author*) Nothing to Disclose Parker Lawson, BA, Arlington, TX (*Abstract Co-Author*) Nothing to Disclose Michael Khazzam, MD, Dallas, TX (*Abstract Co-Author*) Nothing to Disclose Avneesh Chhabra, MD, Flowermound, TX (*Presenter*) Consultant, ICON plc; Consultant, Treace Medical Inc; Author with royalties, Wolters Kluwer nv; Author with royalties, Jaypee Brothers Medical Publishers Ltd

For information about this presentation, contact:

matt.siebert@utsouthwestern.edu

PURPOSE

Glenoid bone stock and morphology and rotator cuff muscle quality and tendon integrity affect the outcome of total shoulder arthroplasty. We hypothesized that glenoid bone loss severity correlates with rotator cuff tendinopathy and severity of rotator cuff muscle fatty infiltration (FI) and atrophy.

METHOD AND MATERIALS

Fourty-three 3-D CT scans and MRIs of 43 patients (mean age 62 years; SD 13 years; range 22 to 77 years) referred for primary shoulder pain without recent trauma or prior surgery were evaluated. Measurements of glenoid bone stock, version, and joint line medialization were assessed on an axial CT image reconstructed in the true scapular plane. Measurements utilized the Friedman line to approximate the pre-pathologic surface. Glenoid morphology was assigned by modified Walch classification. Rotator cuff FI, atrophy, and tendon integrity were assessed on corresponding MRIs.

RESULTS

Glenoid version, anterior and posterior bone loss among modified Walch subtypes was statistically significant (p<0.0001, <0.01 and <0.01 respectively). There was a very strong negative correlation between increasing glenoid version and posterior humeral subluxation index (HSI) (r=-0.908; p<0.0001). There was a moderately negative correlation between anterior bone loss and HSI (r=-0.562; p<0.0001) and a moderately positive correlation between posterior bone loss and HSI (r=-0.555; p<0.0001). Subscapularis muscle FI correlated moderately with increased anterior and central bone loss and increased humeral head medialization (r=0.512, p<0.05; r=0.479, p<0.05; r=0.494, p<0.05; respectively). Inter-observer reliability (intra-class correlation coefficient [ICC] and kappa) was good to excellent for all measurements and grading.

CONCLUSION

Glenoid anteversion, anterior and posterior bone loss are associated with humeral head subluxation. Subscapularis muscle FI, not the tendon integrity, correlates to anterior and central glenoid erosion. The study adds to the body of knowledge that neither rotator cuff tendinopathy, nor muscle atrophy showed a significant relationship to anterior or posterior humeral head subluxation. Anterior or central bone loss may indicate the need to strengthen the subscapularis muscle pre-operatively for potentially improved outcome.

CLINICAL RELEVANCE/APPLICATION

CT measurement of glenoid bone stock and MR measurement of rotator cuff pathology significantly impacts pre-operative planning of total shoulder arthroplasty.

SSM17-05 Addition of the RAVER View to Standard Shoulder Radiographs for Calculation of the Acromial Index and Prediction of Rotator Cuff Tears

Wednesday, Dec. 4 3:40PM - 3:50PM Room: S105AB

Participants

Adam C. Zoga, MD, MBA, Philadelphia, PA (*Presenter*) Nothing to Disclose Brian S. Gibbs, BA, Philadelphia, PA (*Abstract Co-Author*) Nothing to Disclose Vishal Desai, MD, Philadelphia, PA (*Abstract Co-Author*) Nothing to Disclose Alessandra J. Sax, MD, Philadelphia, PA (*Abstract Co-Author*) Nothing to Disclose William B. Morrison, MD, Philadelphia, PA (*Abstract Co-Author*) Consultant, AprioMed AB Patent agreement, AprioMed AB Consultant, Zimmer Biomet Holdings, Inc Consultant, Samsung Electronics Co, Ltd Consultant, Medical Metrics, Inc Christopher Aland, MD, Philadelphia, PA (*Abstract Co-Author*) Nothing to Disclose

For information about this presentation, contact:

PURPOSE

Rotator cuff disease is a common indication for subspecialty orthopaedics referral. MRI and US are definitive diagnosing rotator cuff tear (RCT), but patient selection for advanced imaging remains difficult. Arthroscopic studies have shown osseous hypertrophy at the anterosuperior humeral head is a frequent finding in patients with RCT. We sought to trial a novel radiographic view to allow for measurement of osseous features that predict RTC, and serve as a guide to direct patients appropriately for advanced imaging referral.

METHOD AND MATERIALS

Consecutive patients referred to a surgeon for RCT underwent a novel radiographic resting, abduction view in external rotation (RAVER), in conjunction with the standard shoulder series. Osseous prominence at the anterosuperior humerus was measured on the RAVER and an Acromial Index (AI), was calculated with the ratio of the prominence and distance between the acromion and the footprint. MRI, ordered based upon established practice protocol, was correlated the RAVER measurements. Non-parametric tests and logistic regression were used for data analysis.

RESULTS

113 subjects had a RAVER view and 48 (42.9%) subjects underwent MRI, of which 35 had rotator cuff tears. The mean AI in the RCT tear group was 1.15, whereas the mean AI in subjects without MRI or without tear at MRI was 2.53 and 1.82 respectively. The AI was significantly associated with RCT tear (p=0.003), independent of gender and age. 3 MSK trainees reviewed 18 cases independently to assess reliability of AI, and an intraclass correlation coefficient was 0.96 (95% CI: 0.92-0.98, p<0.001), showing high concordance and little variation in scoring.

CONCLUSION

The acromial Index is an easily reproducible, reliable radiographic predictor of rotator cuff tears and can be calculated with the addition of a single, novel RAVER radiographic view. The addition of this resting, abduction, external rotation view should be validated with larger scale implementation, particularly in shoulder clinics and in a patient population where suspected rotator cuff tears are prevalent.

CLINICAL RELEVANCE/APPLICATION

Once validated, tthe RAVER view and AI measurement can allow clinicians to more effectively select patients who would benefit from advanced imaging with MRI or US for rotator cuff tear, ultimately improving imaging efficiency, adding value, and expediting optimal outcomes.

SSM17-06 Imaging and Clinical Outcomes Following Superior Capsular Reconstruction for Massive Irreparable Rotator Cuff Tears

Wednesday, Dec. 4 3:50PM - 4:00PM Room: S105AB

Participants

Mohammad M. Samim, MD, MRCS, Yonkers, NY (*Presenter*) Nothing to Disclose Abigail Campbell, MD, New York, NY (*Abstract Co-Author*) Nothing to Disclose David Klein, New York, NY (*Abstract Co-Author*) Nothing to Disclose Soterios Gyftopoulos, MD, Scarsdale, NY (*Abstract Co-Author*) Nothing to Disclose Hank Ross, New York, NY (*Abstract Co-Author*) Nothing to Disclose Samuel Baron, New York, NY (*Abstract Co-Author*) Nothing to Disclose Robert Meislin, MD, New York, NY (*Abstract Co-Author*) Consultant, Arthrex, Inc

PURPOSE

Superior capsular reconstruction (SCR) has been recently developed as an arthroscopic treatment option for massive irreparable rotator cuff tears. The purpose of this study is to determine early imaging, clinical, and functional outcomes of SCR.

METHOD AND MATERIALS

Patients having undergone SCR at a single institution were included. Pre-operative and post-operative radiographs and MRIs were evaluated for acromiohumeral interval (AHI), superior subluxation distance (SSD), glenohumeral cartilage loss, cuff muscle atrophy, and graft integrity. Postoperative outcomes including range of motion (ROM), muscle strength and clinical outcomes scores were collected.

RESULTS

24 SCRs were included. Mean clinical follow-up was 21.3 months. MRI was obtained in all patients at mean 9.4 months postoperatively. There were 12 intact grafts (50%) and 12 grafts (50%) with tear at least at one location. The most common location of tear was from the glenoid attachment (50%), followed by the posterior side-to-side attachment (25%), the anterior attachment (18%), and greater tuberosity (7%). There was a significant improvement of American Shoulder and Elbow Surgeons (ASES) (p = 0.003) and visual analog scale (VAS) pain scores (p = 0.012). Significant improvement was observed in forward elevation ROM (p = 0.021). There was no significant difference in functional outcomes or range of motion between patients with torn graft and those with intact graft. The severity of preoperative cartilage loss or rotator cuff muscle fatty atrophy were not associated with graft tear. There was a significant difference in the SSD between patients with complete tear of the graft at least in one location and those without tear on postoperative MRI. SSD greater than 7.9 mm had a 79% sensitivity and 91% specificity for a complete tear of the graft.

CONCLUSION

SCR using human dermal allograft had a 50% tear rate mostly from the glenoid in the current series despite that it results in significant improvements in short term function and range of motion in patients with massive irreparable rotator cuff tears. The chronicity of this procedure's action to depress the humeral head remains in question, as well as the time this procedure provides to delay reverse total shoulder arthroplasty.

CLINICAL RELEVANCE/APPLICATION

SCR using human dermal allograft results in significant improvements in short term function and range of motion in patients with

massive irreparable rotator cuff tears.

Printed on: 10/29/20

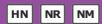




SSM18

Nuclear Medicine (Head and Neck/Thyroid Nuclear Medicine and PET)

Wednesday, Dec. 4 3:00PM - 4:00PM Room: S504CD



AMA PRA Category 1 Credit ™: 1.00 ARRT Category A+ Credit: 1.00

Participants

Robert R. Flavell, MD, PhD, San Francisco, CA (*Moderator*) Nothing to Disclose Amy M. Fowler, MD, PhD, Madison, WI (*Moderator*) Institutional research support, General Electric Company; Author with royalties, Reed Elsevier

Sub-Events

SSM18-01 What is the Incidence of Malignancy in Small Hypermetabolic Pulmonary Nodules?

Wednesday, Dec. 4 3:00PM - 3:10PM Room: S504CD

Participants

Charles M. Intenzo, MD, Philadelphia, PA (*Presenter*) Nothing to Disclose Paras Lakhani, MD, Media, PA (*Abstract Co-Author*) Nothing to Disclose Michael Unger, MD, Philadelphia, PA (*Abstract Co-Author*) Nothing to Disclose Achala Donuru, MD, Philadelphia, PA (*Abstract Co-Author*) Nothing to Disclose Boyd Hehn, Philadelphia, PA (*Abstract Co-Author*) Nothing to Disclose Gregory Kane, MD, Philadelphia, PA (*Abstract Co-Author*) Nothing to Disclose Nathaniel Evans, Philadelphia, PA (*Abstract Co-Author*) Nothing to Disclose Maansi R. Parekh, MBBS, Philadelphia, PA (*Abstract Co-Author*) Nothing to Disclose Scott Cowan, Philadelphia, PA (*Abstract Co-Author*) Nothing to Disclose Sung M. Kim, MD, Philadelphia, PA (*Abstract Co-Author*) Nothing to Disclose Julie Barta, MD, Philadelphia, PA (*Abstract Co-Author*) Nothing to Disclose

For information about this presentation, contact:

Charles.Intenzo@jefferson.edu

PURPOSE

FDG-PET/CT is often utilized to differentiate between benign and malignant indeterminate lung nodules. Throughout the literature, the sensitivity of FDG-PET/CT in this setting is quite high, however, the vast majority of studies focused on nodules generally larger than 1 to 2 cm in diameter. Our study focuses on the potential role of PET/CT imaging in small FDG-avid lung nodules. We define "small" nodules as those measuring 1 cm or smaller in greatest dimension.

METHOD AND MATERIALS

Our study is both prospective and retrospective. Over a four-year interval, we obtained histopathological follow-up of those patients whose PET/CT scans demonstrated a clearly visible FDG-avid lung nodule measuring up to 1 cm in greatest diameter, in whom there were final pathology results from wedge resection.

RESULTS

A total of 39 patients met the above criteria, 24 men and 15 women. One of these patients was proven to have a benign lung nodule, namely a granuloma measuring 9mm in greatest diameter with an SUV max of 0.94. Of the remaining 38 patients with proven malignant nodules, 23 had adenocarcinoma, 14 had squamous cell tumors, and one patient had Non-Hodgkins lymphoma. The least metabolically-active lung nodule, a squamous cell tumor, measured 5 mm in greatest diameter with an SUV max of 0.73 (background SUV max=0.38). The most active lung nodule, an adenocarcinoma, measured 1 cm with an SUV max of 2.60.

CONCLUSION

Thirty-eight of the 39 patients in our series had small FDG-avid lung nodules measuring up to 1 cm, that were subsequently proven to be malignant. This yields a positive-predictive value of 97.4%, despite the limitations imposed by the so-called partial volume effect, which potentially underestimates the SUV max. FDG-PET/CT is therefore highly sensitive and specific in diagnosing malignancy in such small lung nodules; perhaps this modality's potential has been overlooked in this subgroup of hypermetabolic lung nodules.

CLINICAL RELEVANCE/APPLICATION

Any lung nodule measuring up to 1 cm in greatest dimensions that is FDG-avid on PET/CT should be highly concerning for malignancy.

SSM18-02 FDG PET/CT May Predict Clinical Course in Radioiodine-Negative Lung Metastases from Differentiated Thyroid Cancer

Wednesday, Dec. 4 3:10PM - 3:20PM Room: S504CD

Kunihiro Nakada, Sapporo, Japan (*Presenter*) Nothing to Disclose Yasushi Furuta, Sapporo, Japan (*Abstract Co-Author*) Nothing to Disclose Hiromasa Takahashi, Sapporo, Japan (*Abstract Co-Author*) Nothing to Disclose Naoya Hattori, MD, PhD, Sapporo, Japan (*Abstract Co-Author*) Nothing to Disclose Hiroki Sugie, MD, Sapporo, Japan (*Abstract Co-Author*) Nothing to Disclose Noriyoshi Kato, MD, PhD, Sapporo, Japan (*Abstract Co-Author*) Nothing to Disclose Ichiro Sakuma, MD, PhD, Sapporo, Japan (*Abstract Co-Author*) Nothing to Disclose Masayuki Sakurai, Sapporo, Japan (*Abstract Co-Author*) Nothing to Disclose

For information about this presentation, contact:

metnakada@yahoo.co.jp

PURPOSE

There is a considerable variety in the clinical course of radioiodine negative Imetastasis from differentiated thyroid cancer (DTC). The aim of this study was to determine whether PET/CT with F-18 FDG was valuable in predicting prognosis of radioiodine-negative lung metastasis from DTC.

METHOD AND MATERIALS

This study included 39 patients who had lung metastases from DTC (PCA/FCA 35/4. age 33-86yrs.) that did not avid I-131 on the post therapy whole body scan and SPECT/CT after high-dose radioactive iodine therapy (RAI). Two out of 34 patients had bone metastasis and another 19 patients had lymph node metastasis in addition to lung metastasis. PET/CT imaging was performed 5-16 mos after the latest RAI using a dedicated scanner .Uptake of FDG in the metastatic tumor was visually evaluated by 2 independent radiologists. When a tumor showed FDG activity stronger than that in the mediastinum on the whole body MIP images, FDG uptake was defined as positive. Based upon FDG uptake, patients were classified into 2 subgroups: Positive FDG uptake (n=21), and negative FDG uptake (n=18) .Follow up period ranged from 45 to 147 mos(median:92mos.). Patents did not receive additional treatment for lung metastases except for TSH suppression, pleurodesis, or radiotherapy. Anatomical imaging and Tg measurement were performed at a regular interval to evaluate Tg-doubling time (TgDT) and longitudinal changes in tumor diameter (as a rule, based on RECIST1.1) during the follow- up period. Additionally, progression-free survival (PFS) was determined using Kaplan-Meier plot.

RESULTS

Short TgDT (< 1 yr) was more frequently seen in positive FDG uptake group than in negative FDG uptake group (67% vs 17%,p<0.005). The median PFS (mos.) in the positive FDG uptake group vs. the negative FDG uptake group was 40 vs. NA (p<0.001), respectively.

CONCLUSION

FDG positive lung metastases had a increased risk for shorter TgDT or shorter PFS than those with FDG negative ones , while FDG negative lung tumor were associated with stable clinical course. FDG uptake may be predictive of clinical core and prognosis of radioiodine negative lung metastasis from DTC.

CLINICAL RELEVANCE/APPLICATION

Early differentiation of patients with possible unfavorable prognosis from those with favorable prognosis should be helpful in planning an adjunctive treatment to RAI. FDG-PET/CT may be valuable in optimizing the management of radioiodine- negative lung metastases from DTC.

SSM18-03 Is 30mCi of I-131 Inadequate for Adjuvant Therapy for Postsurgical Thyroid Cancer?

Wednesday, Dec. 4 3:20PM - 3:30PM Room: S504CD

Participants

Kunihiro Nakada, Sapporo, Japan (*Presenter*) Nothing to Disclose Naoya Hattori, MD, PhD, Sapporo, Japan (*Abstract Co-Author*) Nothing to Disclose Hiroki Sugie, MD, Sapporo, Japan (*Abstract Co-Author*) Nothing to Disclose Yasushi Furuta, Sapporo, Japan (*Abstract Co-Author*) Nothing to Disclose Noriyoshi Kato, MD, PhD, Sapporo, Japan (*Abstract Co-Author*) Nothing to Disclose Ichiro Sakuma, MD, PhD, Sapporo, Japan (*Abstract Co-Author*) Nothing to Disclose Masayuki Sakurai, Sapporo, Japan (*Abstract Co-Author*) Nothing to Disclose

For information about this presentation, contact:

metnakada@yahoo.co.jp

PURPOSE

2015 ATA management guidelines recommend 100-150 mCi of I-131 for adjuvant therapy (AT) for postsurgical differentiated thyroid cancer. However, so far, number of patients in our country had been given 30mCi of I-131 for the purpose of AT. The aim of this study was to determine whether 30mCi of I-131 was inadequate for AT in patients with increased risk for recurrence.

METHOD AND MATERIALS

This study was retrospective analysis of 58 patients with thyroid cancer (M/F 19/39, PCA54/FCA4, age:59.8 \pm 13.7 yrs.), who underwent total thyroidectomy and were followed by rhTSH-aided RAI with 30mCi. Inclusion criteria were: a) clinicopathological finding by TNM 8th edition was either stage II of pT3 and pN positive (n=25), stage III (n= 24), or stage IVA (n=9), and b) there was no lymph node suspicious for metastasis on neck ultrasound (US) after surgery. Patients followed a low iodine diet (< 100µg/day) from 7 days before to 3 days after RAI. I.m. injection of rhTSH(0.9mg) was done for 2 consecutive days. Patients were given 30 mCi of I-131 on the day after 2nd rhTSH injection. Post therapy I-131 SPECT/CT was imaged 72- 96 hrs. after RAI. Response assessment was done 6-12 mos. after RAI by combination of diagnostic dose I-131 SPECT/CT, neck US, and stimulated Tg. Eleven patients with positive TgAb values were additionally underwent FDG-PET/CT. Fulfillment of negative I-131 uptake, no suspicious mass on anatomical imaging, and stimulated Tg value < 1.0 (ng/ml) was considered as complete response (CR). Patients were further followed up for 19-82mos. (median 44).

RESULTS

Seven patients were excluded from analysis because structural disease was depicted by post therapy imaging. In the remaining 51, CR was achieved in 35 (75%), while 16 showed incomplete response. Thirteen out of those 16 pts. underwent 2nd RAI with 30mCi. CR was additionally achieved in 7 (54%). Among 42 pts who attained CR, structural disease developed in 6 (14%) during the follow up period.

CONCLUSION

CR was achieved in more than 80% of patients after rhTSH-aided RAI with 30 mCi of I-131. Once CR was attained, prevalence for new structural disease was less than 15%. Although the impact on the long-term prognosis remains uncertain, 30 mCi of I-131 is not inadequate for AT in post-surgical thyroid cancer patients with increased risk for recurrence.

CLINICAL RELEVANCE/APPLICATION

30mCi of I-131 seems feasible for adjuvant therapy and thus, can be considered for selected patients.

SSM18-04 Defining Metabolic Heterogeneity Thresholds with FDG PET/CT for Head and Neck Tumors Can Help Predict Patient Risk of Death

Wednesday, Dec. 4 3:30PM - 3:40PM Room: S504CD

Participants James Cassuto, MD,PhD, Miami, FL (*Presenter*) Nothing to Disclose Juan Hinestroza, Medellin, Colombia (*Abstract Co-Author*) Nothing to Disclose Russ A. Kuker, MD, Miami, FL (*Abstract Co-Author*) Nothing to Disclose

For information about this presentation, contact:

james.cassuto@jhsmiami.org

PURPOSE

Disease risk stratification is a corner stone of precision oncology, with radiomic feature analysis being recognized as an important determinant of tumor behavior and overall prognosis. Accordingly, this study sought to quantify and define tumor metabolic heterogeneity thresholds predictive of patient mortality in the setting of head and neck cancer.

METHOD AND MATERIALS

This is a retrospective study examining 298 histologically proven head and neck cancer FDG PET/CT's (and associated clinical data) within the Cancer Imaging Archive data base from April 2006 to November 2014. Segmentation analysis of the most FDG avid lesion from each pre-treatment PET scan was performed. Tumor heterogeneity was defined by the standard deviation and skewness of the tumor pixel intensity distribution. These values were then segregated into ten equal groups (deciles) for further analysis. COX regression was used to model the relative risk (RR) of patient mortality with respect to tumor metabolic heterogeneity as defined by the standard deviation and skewness deciles. Patient age was also included in the regression model as a covariate - the only clinical variable independently associated with risk of death in univariate analysis.

RESULTS

Larger standard deviation and negative skewness define greater degrees of heterogeneity. Serial time dependent multivariable models identified head and neck tumors with PET data demonstrating pixel standard deviation above the eighth decile (27.39) and pixel skewness below the third decile (0.00) to be associated with increased risk of death (RR 2.4, P=0.022) compared to patients with tumor PET data not meeting any or only meeting one of these heterogeneity thresholds.

CONCLUSION

By defining standard deviation and skewness thresholds for head and neck cancer we have been able to identify a sub-set of patients with an increased risk of death based on analysis of pre-treatment FDG PET/CT scans. Inclusion of radiomic data in risk stratifying head and neck tumor patients may have important clinical implications, such as altering time to follow-up and the aggressiveness of treatment strategy.

CLINICAL RELEVANCE/APPLICATION

Quantitative analysis of pre-treatment head and neck cancer heterogeneity with FDG PET data (Radiomics) can be used to identify patients with increased risk of death.

SSM18-05 Interpretation of Response Assessment PET-CT in Head and Neck Carcinoma: Comparative Analysis of 4 Qualitative Interpretative Criteria in a Large Patient Cohort

Wednesday, Dec. 4 3:40PM - 3:50PM Room: S504CD

Participants

Jim Zhong, Leeds, United Kingdom (*Presenter*) Nothing to Disclose Moses Sundersingh, Leeds, United Kingdom (*Abstract Co-Author*) Nothing to Disclose Peter Brown, MBChB, BSc, Leeds, United Kingdom (*Abstract Co-Author*) Nothing to Disclose Karen Dyker, Leeds, United Kingdom (*Abstract Co-Author*) Nothing to Disclose Robin Prestwich, PhD, FRCR, Leeds, United Kingdom (*Abstract Co-Author*) Nothing to Disclose Stuart Currie, MBCHB, MRCS, Leeds, United Kingdom (*Abstract Co-Author*) Nothing to Disclose Sriram Vaidyanathan, MBBS, FRCR, Leeds, United Kingdom (*Abstract Co-Author*) Nothing to Disclose Andrew F. Scarsbrook, FRCR, York, United Kingdom (*Abstract Co-Author*) Nothing to Disclose

For information about this presentation, contact:

jim.zhong@nhs.net

PURPOSE

There is no clear concensus maarding the entired intermetive criteria (IC) for Elucrine 10 flueredeeverlucese (EDC) Desitron

Emission Tomography - Computed Tomography (PET-CT) response assessment following (chemo)radiotherapy (CRT) for head and neck squamous cell carcinoma (HNSCC). The aim of this study was to compare the accuracy of 4 IC (NI-RADS, Porceddu, Hopkins, Deauville) for predicting local control, regional control and progression free survival (PFS) in a large patient cohort.

METHOD AND MATERIALS

All patients with histologically-confirmed HNSCC treated at a specialist cancer center between August 2008 and May 2017 who underwent baseline and response assessment FDG PET-CT 4 months post CRT were included. Metabolic response was assessed using 4 different IC harmonised into 4-point scales (complete response, indeterminate, partial response, progressive disease). IC performance metrics (sensitivity, specificity, positive predictive value (PPV), negative predictive value (NPV), accuracy) were compared. The Kaplan-Meier method and Cox proportional hazards regression analyses were used for survival analysis.

RESULTS

562 patients were included (397 oropharynx, 53 hypopharynx, 48 larynx, 64 other/unknown primary). 420 patients (75%) received CRT and 142 (25%) had radiotherapy alone. Median follow-up was 26 months (range 3-148). 156 patients (28%) progressed during follow-up. All IC were accurate for prediction of local (primary tumor) outcome (mean NPV 85.0% (84.6-85.3), PPV 85.0% (82.5-92.3), Accuracy 84.9% (84.2-86.0)) and regional (nodal) outcome (mean NPV range 85.6% (84.1-86.6), PPV 94.7% (93.8-95.1), Accuracy 86.8% (85.6-88.0)). Number of indeterminate cases for NI-RADS, Porceddu, Deauville and Hopkins were 91, 25, 20 and 13. PPV was significantly reduced for indeterminate uptake across all IC (mean PPV primary tumor 36%, nodes 48%). Survival analyses showed significant differences in PFS and OS between response categories classified by each of the four IC (p < 0.001).

CONCLUSION

All four analysed IC had similar diagnostic performance characteristics although Porceddu and Deauville provided the best trade off minimising indeterminate scores whilst maintaining a high NPV.

CLINICAL RELEVANCE/APPLICATION

FDG PET-CT accurately predicts complete response or disease progression post-CRT in HNSCC. Porceddu and Deauville IC offer the best combination of high NPV and low indeterminate scores.

SSM18-06 Comparison Between 18F-FDG PET and DWI Data for Prediction of Therapy Response of Soft Tissues Sarcoma Under Neoadjuvant ILP

Wednesday, Dec. 4 3:50PM - 4:00PM Room: S504CD

Participants

Johannes Grueneisen, Essen, Germany (*Presenter*) Nothing to Disclose Benedikt M. Schaarschmidt, MD, Essen, Germany (*Abstract Co-Author*) Nothing to Disclose Michal Chodyla, Essen, Germany (*Abstract Co-Author*) Nothing to Disclose Ole Martin, Duesseldorf, Germany (*Abstract Co-Author*) Nothing to Disclose Aydin Demircioglu, Essen, Germany (*Abstract Co-Author*) Nothing to Disclose Axel Wetter, Essen, Germany (*Abstract Co-Author*) Nothing to Disclose Lars Podleska, MD, Essen, Germany (*Abstract Co-Author*) Nothing to Disclose Ken Herrmann, Essen, Germany (*Abstract Co-Author*) Nothing to Disclose Ken Herrmann, Essen, Germany (*Abstract Co-Author*) Co-founder, SurgicEye GmbH Stockholder, SurgicEye GmbH Consultant, Sofie Biosciences Consultant, Ipsen SA Consultant, Siemens AG Research Grant, Advanced Accelerator Applications SA Research Grant, Ipsen SA Michael Forsting, MD, Essen, Germany (*Abstract Co-Author*) Nothing to Disclose Lale Umutlu, MD, Essen, Germany (*Abstract Co-Author*) Consultant, Bayer AG For information about this presentation, contact:

Johannes.grueneisen@uk-essen.de

PURPOSE

To evaluate and compare the clinical utility of simultaneously obtained quantitative 18F-FDG PET and DWI datasets for the prediction of therapy response of soft tissue sarcomas (STS) under neoadjuvant isolated limb perfusion (ILP).

METHOD AND MATERIALS

A total of 39 patients with confirmation of a STS of the extremities underwent a 18F-FDG PET/MR examination before (1st scan) and after (2nd scan) ILP with melphalan and alpha-TNF. For each patient, the maximum tumor size, metabolic activity (SUVs) and diffusion-restriction (ADC-values) were measured in pre- and posttherapeutic examinations and percentage changes during treatment were calculated. A Mann-Whitney-U test was used and ROC analysis was performed to compare the results of the different quantitative parameters to predict therapy response. Histopathological results after subsequent tumor resection served as reference standard and patients were categorized as responders/non-responders based on the grading scale by Salzer-Kuntschik.

RESULTS

Histopathological analysis categorized 25 (64%) patients as therapy responders (Grade I-III) and 14 (36%) patients as nonresponders (Grade IV-VI). Tumors in the responder group showed a reduction in size of -8.6% and metabolic activity (SUVmax: -51.1%; SUVpeak: -56.3%) as well as an increase of the ADC values (ADCmin: +30.3% and ADCmean: +23.7%) under treatment. Percentage changes in the non-responder group amounted to: maximum tumor size -3.9%; SUVmax: -12.7%; SUVpeak: 13.3%; ADCmin: +11.8% and ADCmean: +10.5%. Differences of SUVs between histopathological responder and non-responders were significantly different (< 0.05), whereas differences in tumor size and the ADC values did not reach significance level (>0.01). The corresponding AUCs were 0.63 (tumor size), 0.83 (SUVmax), 0.81 (SUVpeak), 0.65 (ADCmin) and 0.68 (ADCmean), respectively.

CONCLUSION

Our study demonstrates the superiority of 18F-FDG PET data over MR-derived quantitative imaging parameters for response assessment of STS under neoadjuvant ILP.

CLINICAL RELEVANCE/APPLICATION

19E EDC DET data may be bishly yalyable when implemented into diagnostic algorithms for monitoring pasadiyyant treatment

strategies of STS. However, considering the importance of MRI data for presurgical evaluation, integrated PET/MRI could serve as a valuable tool for therapy planning and monitoring of neoadjuvant treatment strategies of STS.

Printed on: 10/29/20





SSM19

Neuroradiology/Head and Neck (General)

Wednesday, Dec. 4 3:00PM - 4:00PM Room: S501ABC



AMA PRA Category 1 Credit ™: 1.00 ARRT Category A+ Credit: 1.00

FDA Discussions may include off-label uses.

Participants

Greg D. Avey, MD, Madison, WI (*Moderator*) Research Consultant, General Electric Company Shinji Naganawa, MD, Nagoya, Japan (*Moderator*) Nothing to Disclose Alka Ashmita Singhal, MD,DMRD, New Delhi, India (*Moderator*) Nothing to Disclose

Sub-Events

SSM19-01 Analysis of Programmable Valve Setting Changes Due to Exposure to the MRI Environment

Wednesday, Dec. 4 3:00PM - 3:10PM Room: S501ABC

Participants Fehime E. Ucisik-Keser, MD, Houston, TX (*Presenter*) Nothing to Disclose Eliana E. Bonfante, MD, Houston, TX (*Abstract Co-Author*) Nothing to Disclose Alexander B. Simonetta, MD, Houston, TX (*Abstract Co-Author*) Nothing to Disclose

For information about this presentation, contact:

fehime.e.ucisikkeser@uth.tmc.edu

PURPOSE

Most patients with ventriculoperitoneal (VP) shunts undergo frequent magnetic resonance imaging (MRI) for various indications. It is a known fact that there may be unintentional valve setting changes due to interaction with the MRI magnetic field. Therefore, in many institutions, including ours, patients with a programmable VP shunt valve who undergo MRI receive skull radiographs before and after the MRI to check for any induced setting change. Based on empirical observation, we hypothesized that MRI related setting changes occur more frequently with some commercially available shunt valve types. This is a retrospective study to determine the rates of unintended, MRI related, programmable VP shunt valve setting changes for each commercially available programmable shunt valve type used at our institution.

METHOD AND MATERIALS

The study population consisted of patients with programmable shunt valves who underwent at least one MRI study with pre and post MRI radiographs in 2018. After IRB approval, the institutional radiology search tool 'Primordial' was used to extract the skull radiograph reports containing the words 'shunt' or 'setting', and the shuntogram reports containing the word 'setting'. Using the institutional electronic medical record system, a chart check was performed for each study to determine the ones that were performed following an MRI.

RESULTS

Our search revealed 89 post MRI radiographs from 73 patients, with an age range of 1 month to 88 years (Median: 40). For patients with more than one shunt valve, each valve was included separately in the analysis. Overall, setting change occurred in 45.2% of the studies. The setting change rates for individual valve types were as follows: 17 of 29 Strata NSC® (58.6%), 17 of 20 Strata II® (85%), 8 of 40 Codman-Hakim® (20%), 0 of 2 Codman Certas, and 0 of 2 Polaris Sophysa. Statistical analysis was performed on the most common three shunt valves. Student's T-test revealed a statistically significant difference between all three groups (p<0.05 for Strata NSC vs Codman-Hakim; and for Strata II vs Codman-Hakim; p=0.04 for Strata NSC vs Strata II).

CONCLUSION

VP shunt valves change settings occur frequently, especially for Strata NSC and Strata II.

CLINICAL RELEVANCE/APPLICATION

MRI related shunt valve setting changes are common. Post MRI manual reprograming of the commonly affected valves without obtaining radiographs could reduce radiation exposure and the cost to patients.

SSM19-02 Predictors of Positive Brain MR Imaging in Patients with New Daily Persistent Headache

Wednesday, Dec. 4 3:10PM - 3:20PM Room: S501ABC

Participants

George K. Vilanilam, MBBS, Jacksonville, FL (*Presenter*) Nothing to Disclose Neethu Gopal, MBBS, Jacksonville, FL (*Abstract Co-Author*) Nothing to Disclose Kaneez Zahra, MD, Jacksonville, FL (*Abstract Co-Author*) Nothing to Disclose Mohammed K. Badi, MBBS, Jacksonville, FL (*Abstract Co-Author*) Nothing to Disclose Bhavya Yarlagadda, MBBS, Jacksonville, FL (*Abstract Co-Author*) Nothing to Disclose

For information about this presentation, contact:

george.koshy.vilanilam@gmail.com

PURPOSE

The aim of our study is to evaluate the predictors of positive neuroimaging in patients with New Daily Persistent Headache (NDPH)

METHOD AND MATERIALS

All patients aged >=18 with documented NDPH were identified from a 10-year institutional database. Patient charts were reviewed using electronic medical records. NDPH characteristics, temporal profile, coexistent migraine, history of recognized trigger (eg. viral infection), and history of vascular comorbidities were included. Individual brain MRI and head CT at baseline evaluation were read. All tests were significant at P<0.05

RESULTS

Altogether 200 patients (mean age, 53.6 years+/-15.1) were diagnosed with NDPH (141 women and 58 men). Predominant headache locations included hemicranial in 21% (42/200), bilateral in 13% (26/200), holocranial in 9%(18/200), and side-changing in 7%(14/200). They were characterized by pressure-like stabbing pain in 37.5%(75/200) and throbbing in 11%(22/200) patients. Median baseline and median peak headache pain intensity were 5 (range, 2-8) and 8 (range, 2- 10) respectively. About 11.5% (23/200) had comorbid migraine with aura and 32.5% (65/200) did not have aura. About 59%(118/200) had positive history of a trigger prior to the onset of their headache. Additionally, 16%(32/200) patients with NDPH had history of a hypermobility disorder (Ehler-Danlos syndrome, Marfans syndrome, or isolated cervical hypermobility). Overall, a total of 59 patients had a positive MR brain imaging finding, with the majority of positive findings being dural meningiomas (15/59), subdural hemorrhages (13/59), and intracranial aneurysms (10/59). Patients with a positive history of trigger and comorbid dyslipidemia at baseline were associated with a positive brain MR imaging finding (P=0.02 and P=0.05 respectively). Other comorbidities including migraine, hypertension, vascular disorders, and thyroid disorders did not significantly predict MR brain imaging positivity. Data on brain CT imaging was insufficient

CONCLUSION

To date, this is the largest population study evaluating factors predicting positive neuroimaging finding in NDPH. Our results show that patients with a positive history of a trigger prior to NDPH and those with comorbid dyslipidemia are associated with a positive finding on brain MR

CLINICAL RELEVANCE/APPLICATION

Detecting predictors of positive neuroimaging will help triage a sub-cohort of NDPH patients with potentially reversible causes for early management

SSM19-03 An Observational Study to Evaluate the Management of Patients with Chronic Headache with Referral from Primary Care to Direct Access to Magnetic Resonance Imaging (MRI) Compared to Neurology Services

Wednesday, Dec. 4 3:20PM - 3:30PM Room: S501ABC

Participants

Tiago Rua, BSC, MSc, London, United Kingdom (*Abstract Co-Author*) Nothing to Disclose Shazia Afridi, London, United Kingdom (*Abstract Co-Author*) Nothing to Disclose Yvonne Akande, London, United Kingdom (*Abstract Co-Author*) Nothing to Disclose Charikleia Margariti, London, United Kingdom (*Abstract Co-Author*) Nothing to Disclose JoAnna Turville, London , United Kingdom (*Abstract Co-Author*) Nothing to Disclose Reza Razavi, MD, London, United Kingdom (*Abstract Co-Author*) Nothing to Disclose Janet Peacock, PhD, London, United Kingdom (*Abstract Co-Author*) Nothing to Disclose James Shearer, PhD, London, United Kingdom (*Abstract Co-Author*) Nothing to Disclose Vicky J. Goh, MBBCh, Chalfont St Giles, United Kingdom (*Abstract Co-Author*) Nothing to Disclose Paul McCrone, London, United Kingdom (*Abstract Co-Author*) Nothing to Disclose Asif Mazumder, MRCP, FRCR, London, United Kingdom (*Presenter*) Nothing to Disclose

For information about this presentation, contact:

tiago.rua@kcl.ac.uk

PURPOSE

To evaluate two existing clinical pathways used in the management of patients with chronic headache based on referral from General Practitioners (GPs) for a Neurologist appointment or direct access to Magnetic Resonance Imaging (MRI) brain scan.

METHOD AND MATERIALS

A pragmatic, non-randomised, prospective single-center study compared the two clinical pathways used in the management of chronic headache following referral from GPs that differed in the first appointment, either a Neurology appointment or a MRI brain scan. Subsequent participants' use of health care services and costs were estimated using primary and secondary care databases and questionnaires at baseline, 6 and 12 months post-recruitment. Cost analyses at 6 and 12 months were compared using generalized linear models (GLM). Secondary outcomes assessed access to care, headache burden and self-perceived quality of life using headache-specific (MIDAS, HIT-6) and general questionnaires (EQ-5D-5L).

RESULTS

The MRI group improved access to care (39.2 and 70.4 days from referral to MRI scan and report, respectively) compared to the Neurology group (110 days) (p<0.001). The Neurology group was associated with a trend (p>0.05) of better self-perceived quality of life using a generic questionnaire and an opposite trend from headache-specific questionnaires, exhibiting a trend (p>0.05) of

higher headache burden (HIT-6 score, MIDAS score and headache days). Mean (SD, n) cost up to 6 months post-recruitment per participant was £578 (£420, n=128) for the Neurology group and £245 (£172, n=95) for the MRI group, leading to an estimated cost difference of £333 (95% CI £253 to £413, p<0.001). The cost difference at 12 months increased to £518 (95% CI £401 to £637, p<0.001). This cost difference derives from the lower utilization of participants in the MRI group of both GP visits (1.8 vs 1.2, p=0.006) and hospital appointments (2.5 vs 0.3, p<0.001) and despite the higher utilization of MRI scans (0.6 vs 1.1, p<0.001).

CONCLUSION

Direct referral to brain MRI from Primary Care led to cost-savings and quicker access to care compared to the management of chronic headache with referral to Neurology services.

CLINICAL RELEVANCE/APPLICATION

Direct referral to MRI for the management of chronic headache should be incentivized for a subset of patient population more likely to be reassured by a negative brain scan.

SSM19-04 Oral Contraceptive Use Is Associated with Smaller Hypothalamic Volumes in Healthy Women

Wednesday, Dec. 4 3:30PM - 3:40PM Room: S501ABC

Participants

Ke Xun Chen, MD, Bronx, NY (*Presenter*) Nothing to Disclose Sandie Worley, BS, New York, NY (*Abstract Co-Author*) Nothing to Disclose Henry J. Foster, BS, Oakland, CA (*Abstract Co-Author*) Nothing to Disclose David Edasery, MD, New York, NY (*Abstract Co-Author*) Nothing to Disclose Shima Roknsharifi, MD, Bronx, NY (*Abstract Co-Author*) Nothing to Disclose Chloe Ifrah, Bronx, NY (*Abstract Co-Author*) Nothing to Disclose Michael L. Lipton, MD, PhD, Bronx, NY (*Abstract Co-Author*) Nothing to Disclose

PURPOSE

There is limited evidence on the structural and functional effects of hormonal contraceptives on the brain. In particular, these effects on the hypothalamus are not known. In this study, we aim to identify alteration of hypothalamic volume associated with oral contraceptive pill (OCP) use in healthy women.

METHOD AND MATERIALS

We acquired high-resolution MR images of the brain at 3T for a prospective cohort of 50 healthy women. Psychometric tests (Cogstate and PROMIS) were administered at the time of imaging. 21 participants took OCPs at the time of imaging while 29 did not. After training and validation, 5 raters independently performed manual segmentation of the hypothalamus using ITK-SNAP. Total intracranial volume (tICV) was determined using FreeSurfer. The intraclass correlation was calculated for a subset of 20 randomly-selected cases to assess inter-rater reliability. A general linear model was fit to test for the association of OCP use with hypothalamic volume, with tICV and birth control used as covariates. Additional exploratory analyses assessed associations with menstrual cycle phase and with cognitive and health measures.

RESULTS

The inter-rater ICC was 0.86. Total hypothalamic volume in participants taking OCPs was smaller than those not taking OCPs (b=- 63.4 ± 22.2 , p=0.006). There was a significant association of hypothalamic volume with greater anger (p=0.02) as well as a strong correlation with depression (p=0.09). However, no significant correlation was found between hypothalamic volume and cognitive testing results.

CONCLUSION

Our hypothalamic segmentation method is highly reliable. OCP use is associated with smaller total hypothalamic volume, which may be related to interference with known trophic effects of sex hormones and provide a structural mechanism for OCP-mediateed inhibition of folliculogenesis as well as potential functional effects.

CLINICAL RELEVANCE/APPLICATION

Characterizing effects of OCPs on the hypothalamus provides a bridge to understanding functional alterations associated with OCP use that may impact selection of contraceptive method.

SSM19-05 Blood-Brain Barrier Water Permeability Disruption in Major Depressive Disorder

Wednesday, Dec. 4 3:40PM - 3:50PM Room: S501ABC

Participants

Kenneth T. Wengler, MS, Stony Brook, NY (*Abstract Co-Author*) Nothing to Disclose Kwan Y. Chen, MD, Nesconset, NY (*Presenter*) Nothing to Disclose Christine DeLorenzo, PhD, Stony Brook, NY (*Abstract Co-Author*) Nothing to Disclose Mark E. Schweitzer, MD, Stony Brook, NY (*Abstract Co-Author*) Consultant, MMI Medical Metrics; Consultant, MCRA; Data Safety Monitoring Board, Histogenics Corporation; Data Safety Monitoring Board, Genae Americas Inc; Data Safety Monitoring Board, Premia Spine; Data Safety Monitoring Board, NeoCart; Turhan Canli, Stony Brook, NY (*Abstract Co-Author*) Nothing to Disclose Xiang He, PhD, Stony Brook, NY (*Abstract Co-Author*) Consultant, Endo International plc

For information about this presentation, contact:

kenneth.wengler@stonybrook.edu

PURPOSE

Major depressive disorder (MDD) is the most prevalent and disabling form of depression. Blood-brain barrier (BBB) disruption has been implicated in the development and progression of MDD. The purpose of this study was to investigate differences in BBB integrity between patients with MDD and healthy subjects using the recently developed Intrinsic Diffusivity Encoding of Arterial

Labeled Spins (IDEALS) MRI technique.

METHOD AND MATERIALS

14 healthy subjects and 14 MDD patients were recruited with IRB approval and informed consent. Depression symptom severity was assessed with the Beck's Depression Index (demographics in Table 1). All studies were performed on a Siemens 3T Prisma MRI with 64-channel head/neck coil. IDEALS images were acquired according to (Wengler et al. NeuroImage, 2019) for mapping of cerebral blood flow (*CBF*), water extraction fraction (*Ew*), and water permeability (*PSw*). High resolution T1w images were acquired for segmentation and spatial normalization. Four regions of interest (ROIs) implicated in MDD were evaluated: anterior cingulate cortex (ACC), amygdala, dorsolateral prefrontal cortex (DLPFC), and hippocampus. ROIs were selected using WFU Pickatlas. Analysis of covariance (ANCOVA) was used to evaluate group differences between BBB water permeability parameters within the 4 ROIs while controlling for age and gender; p < 0.05 was considered significant.

RESULTS

Figure 1 displays the group averaged IDEALS parameter maps. Box plots with individual data points for *PSw*, *Ew*, and *CBF* within ROIs are shown in Figure 2. Figure 3 displays the mean values after adjusting for age and gender. No significant differences in *CBF* between healthy subjects and MDD patients were. Significantly lower *Ew* was observed in the amygdala, ACC, DLPFC, and hippocampus of MDD patients compared to healthy subjects. Significantly lower *PSw* was observed in the amygdala and hippocampus of MDD patients compared to healthy subjects.

CONCLUSION

With active trans-membrane water cycling pathways, such as NaK-ATPase, accounting for a large fraction of water exchange, the lower BBB water permeability observed in MDD patients suggests BBB disruption and cerebral metabolic deficits.

CLINICAL RELEVANCE/APPLICATION

Despite its societal impact, the mechanisms underlying major depressive disorder (MDD) are not well understood. This study uses the IDEALS MRI method to probe BBB water permeability disruption in MDD.

SSM19-06 Redundant Neurovascular Imaging: Who's to Blame and What's the Value?

Wednesday, Dec. 4 3:50PM - 4:00PM Room: S501ABC

Participants

Elham Beheshtian, MD, Baltimore, MD (*Presenter*) Nothing to Disclose Sahra Emamzadehfard, MD, MPH, San Antonio, TX (*Abstract Co-Author*) Nothing to Disclose Sadaf Sahraian, Baltimore, MD (*Abstract Co-Author*) Nothing to Disclose Rozita Jalilianhasanpour, MD, Baltimore, MD (*Abstract Co-Author*) Nothing to Disclose David M. Yousem, MD, Owings Mills, MD (*Abstract Co-Author*) Royalties, Reed Elsevier; Employee, Medicolegal Consultation; Royalties, Analytical Informatics, Inc; Speaker, MRIOnline; ; ;

For information about this presentation, contact:

elhambeheshtian65@gmail.com

PURPOSE

Redundant neurovascular imaging (RNI) studies such as Doppler ultrasound (DUS), CTA, MRA, and DSA add cost to the evaluation of patients with new neurologic deficits. We sought to determine to what extent such redundant studies are generated by radiologists' recommendations and the agreement rates between modalities in this setting.

METHOD AND MATERIALS

The radiology reports of 200 consecutive patients admitted for acute stroke were reviewed to determine how often 1) there was a recommendation for another study, 2) it was suggested by the radiologist, not the clinician, and 3) the agreement rates between these RNI studies.

RESULTS

Among 89/200 (44.5%) patients with RNI there were 116 redundant studies. These included 45/116 RNI studies after CTA, 64/116 after MRA and 7/116 after DUS. The radiologist recommended another vascular study in 19/89 (21.3%) patients, the rest by clinicians. When radiologists recommended additional radiological studies, 15/19 (78.9%) occurred following an MRA and 4/19 (21.1%) occurred after CTA. There was a significant difference between the number of second imaging ordered by radiologists after MRA ad CTA (P-value: 0.049). The second study agreed with the first in 52.6% of cases recommended by radiologists and 74.2% recommended by clinicians (P-value: 0.06). CTA agreed with MRA, Carotid DUS, and DSA in 67.1%, 90%, and 77.8% respectively. MRA agreed with DUS and DSA in 65% and 71.4% respectively.

CONCLUSION

Of cases with RNI, the majority were generated by clinicians, but radiologists recommended RNI in 21.3% of patients; 78.9% occurred following the MRA. Most second studies (70.7%) confirmed the first study's findings. Such low-value-same-result RNIs were more common when clinicians ordered them (74.2%) than radiologists (52.6%). Such redundancy should be discouraged. Some combinations (CTA/DUS) had 90% concordance, while the greatest discrepancy rate across modalities resided between MRA and DUS (35%).

CLINICAL RELEVANCE/APPLICATION

Neurovascular redundant imaging should be addressed at a national level to reduce healthcare costs and could benefit from order entry feedback loops.







SSM20

Neuroradiology (Vascular, Non-Stroke)

Wednesday, Dec. 4 3:00PM - 4:00PM Room: S502AB



AMA PRA Category 1 Credit ™: 1.00 ARRT Category A+ Credit: 1.00

Participants

Alexander M. McKinney IV, MD, Minneapolis, MN (*Moderator*) CEO, VEEV, Inc Daniel M. Mandell, MD, PhD, Toronto, ON (*Moderator*) Nothing to Disclose Luca Saba, MD, Cagliari, Italy (*Moderator*) Nothing to Disclose

Sub-Events

SSM20-01 Intracranial Aneurysms In Hereditary Hemorrhagic Telangiectasia

Wednesday, Dec. 4 3:00PM - 3:10PM Room: S502AB

Participants

Matias J. Rodriguez, MD, CABA, Argentina (*Presenter*) Nothing to Disclose Manuel S. Perez Akly, Buenos Aires, Argentina (*Abstract Co-Author*) Nothing to Disclose Florencia Conde, MD, Ciudad Autonoma de Buenos Aires, Argentina (*Abstract Co-Author*) Nothing to Disclose Dan Dardik, MD, Buenos Aires, Argentina (*Abstract Co-Author*) Nothing to Disclose Cristina H. Besada SR, MD, PhD, Buenos Aires, Argentina (*Abstract Co-Author*) Nothing to Disclose

For information about this presentation, contact:

matiasj.rodriguez@hospitalitaliano.org.ar

PURPOSE

Hereditary hemorrhagic telangiectasia (HHT) is an autosomal dominant disease induced by mutation of genes involved in angiogenesis' regulation, around 10-20% of patients may have cerebral vascular malformations. Intracranial aneurysms (ICA) are acquired vascular lesions, with prevalence of 3-5% in general population. HHT has not been specifically linked to ICA. Our purpose is to describe the frequency of ICA in population with HHT diagnosis in a reference center.

METHOD AND MATERIALS

We performed a cross sectional study. We included patients with HHT who had performed an angiographic study: MR angiography, CT angiography or digital angiography from 2010 to 2018, with available images for interpretation. We recorded the location, the geometric characteristics and the presence of other cerebral vascular malformations. We evaluated the result of genetic test when available and it's association with ICA.

RESULTS

We included 151 patients with an angiographic studies, 96 female and 55 male. The average age was 47,7 years old (SD 18,3). We found 24 ICA in 22 (14,5%) patients. The location of aneurysms were: middle cerebral artery 7/24 (29,2%) ophthalmic artery 5/24 (26,1%), intracavernous carotid artery 3/24 (12,5%), posterior communicating artery 3/24 (12,5%), anterior communicating artery 2/24 (8,3%), 1/24 (4,2%) in basilar tip and 1/24 (4,2%) anterior cerebral artery. The mean diameter of ICA was 3,4mm (SD 1.18mm). Genetic test was available in 65 patients, we found ICA in 9 of them. No statistical association was found between the presence of ICA and genetic mutations. We found cerebral AVMs in 43 patients (28,5%), in this subgroup 12 patients also had ICA, (association between both vascular malformations p=0,004). The odds ratio of having both ICA and cerebral AVMs was 4,2 (CI 95%=1,6-11,4)

CONCLUSION

We found a frequency of ICA in HHT (14,5%). This finding may be related to arterial wall disorders induced by known genetic mutations in this disease. According to this findings, the risk of having an ICA increases approximately 3 to 5 times in patients with HHT compared to general population and its presence is associated with cerebral AVMs.

CLINICAL RELEVANCE/APPLICATION

There is an increased risk of having an intracranial aneurysm in patients diagnosed with HHT. This is important because it requires increasing suspicion in this patients for the diagnosis and treatment of the aneurysms.

SSM20-02 Readmission and Retreatment after Elective Treatment of Unruptured Cerebral Aneurysm: A Nationwide Readmission Database Analysis

Wednesday, Dec. 4 3:10PM - 3:20PM Room: S502AB

Participants Pedram Golnari, MD, Chicago, IL (*Presenter*) Nothing to Disclose Pouya Nazari, MD, Chicago, IL (*Abstract Co-Author*) Nothing to Disclose Roxanna M. Garcia, Chicago, IL (*Abstract Co-Author*) Nothing to Disclose Hannah K. Weiss, Chicago, IL (*Abstract Co-Author*) Nothing to Disclose Sameer A. Ansari, MD,PhD, Chicago, IL (*Abstract Co-Author*) Nothing to Disclose Ali Shaibani, MD, Chicago, IL (*Abstract Co-Author*) Nothing to Disclose Matthew B. Potts, MD, Chicago, IL (*Abstract Co-Author*) Nothing to Disclose Michael C. Hurley, MBBCh, Chicago, IL (*Abstract Co-Author*) Nothing to Disclose Babak S. Jahromi, MD,PhD, Chicago, IL (*Abstract Co-Author*) Nothing to Disclose

PURPOSE

Mortality rates following treatment of unruptured cerebral aneurysm (UA) have decreased over the past decades, which may be due to use of modern microsurgical and endovascular techniques as well as overall increased volumes of UA treatment. However, treatment of UA harbors a small but finite risk, and resulting readmission and retreatment rates have not been well described.

METHOD AND MATERIALS

Adult patients who underwent elective coiling or clipping of UA were extracted from the Nationwide Readmission Database spanning 2010 to 2015. Primary diagnosis for non-elective readmission within 30 and 90 days were identified and readmission and retreatment rates for coiling vs clipping were compared. To calculate 30 and 90-day readmission and retreatment rates, we included patients within the first 11 and 9 months of each year, respectively. Poisson regression was performed using generalized estimating equations and adjusted risk ratio (aRR)s were obtained for factors associated with 30 and 90 day readmission and retreatment. The adjusted model included terms for patient- and hospital-specific factors, comorbidity scores and disease severity.

RESULTS

Of 61,894 UA patients treated and discharged alive, 5.98% and 8.99% patients were readmitted and 0.14% and 0.33% patients were retreated within 30 and 90 days, respectively. The most common primary diagnoses for readmission within 30 and 90 days, respectively, was ischemic or hemorrhagic stroke (16.13%, 21.82%). The 30 and 90-day readmission rate for coiling vs clipping was 4.87% vs 8.68% (p<0.001) and 7.82% vs 11.87% (p<0.001), respectively (figure). The 30 and 90-day retreatment rates for coiling vs clipping were 0.18% vs 0.04% (p<0.001) and 0.37% vs 0.22% (p=0.007), respectively. Patients undergoing clipping had a higher adjusted risk of 30 and 90 day retreatment (aRR=0.33; 95%CI, 1.49-1.90; p<0.001) and aRR=1.40; 95%CI, 1.27-1.54; p<0.001) but a lower adjusted risk of 30 day retreatment (aRR=0.33; 95%CI, 0.12-0.89; p=0.029) than patients having coiling.

CONCLUSION

The most common primary diagnoses for 30 and 90 day non-elective readmission after treatment of UA is stroke. Readmission rates are higher for clipping, but retreatment rates are higher for coiling.

CLINICAL RELEVANCE/APPLICATION

Patients undergoing clipping of UA have higher readmission rates but lower retreatment rates. These data may help patients and clinicians in selection of treatment modality for UA.

SSM20-03 Management of Tiny Unruptured Intracranial Aneurysms: A Cost-Effectiveness Analysis

Wednesday, Dec. 4 3:20PM - 3:30PM Room: S502AB

Participants

Xiao Wu, New Haven, CT (*Presenter*) Nothing to Disclose Ichiro Ikuta, MD,MMedSc, Milford, CT (*Abstract Co-Author*) Nothing to Disclose Dheeraj Gandhi, MBBS, MD, Baltimore, MD (*Abstract Co-Author*) Research Grant, Stryker Corporation Research Grant, Medtronic plc Pina C. Sanelli, MD,MPH, Manhasset, NY (*Abstract Co-Author*) Nothing to Disclose Ajay Malhotra, MD, Stamford, CT (*Abstract Co-Author*) Nothing to Disclose

For information about this presentation, contact:

ajay.malhotra@yale.edu

PURPOSE

To evaluate the effectiveness, costs and incremental cost of routine treatment (aneurysm coiling) versus 3 different strategies for imaging surveillance in relation to no preventive treatment or routine follow-up of tiny UIAs.

METHOD AND MATERIALS

A decision-analytic model-based cost-effectiveness analysis was constructed using inputs from the medical literature. Five different management strategies for tiny unruptured intracranial aneurysms (UIAs) were evaluated - annual magnetic resonance angiography (MRA) screening, biennial MRA screening, MRA screening every 5 years, coiling and follow-up and, no treatment or preventive follow-up. Markov decision model for lifetime rupture was constructed from a societal perspective per 10,000 patients with incidental, tiny UIAs. Outcomes were assessed both in terms of cost and quality-adjusted life years (QALYs). Incremental cost-effectiveness ratio (ICER) and net monetary benefit (NMB) for each strategy were evaluated. Probabilistic, one-way, and two-way sensitivity analyses were performed.

RESULTS

The base-case calculation shows no treatment or preventive follow-up to be the most cost-effective strategy. Among the imaging follow-ups, MRA every 5 years is the best strategy with the next highest effectiveness. The conclusion remains robust in probabilistic and one-way sensitivity analyses. No routine follow-up remains the optimal strategy when the annual growth rate and rupture risk of growing aneurysms are varied. When the annual rupture risk of non-growing UIAs is <2.1%, no follow-up is the optimal strategy. If annual rupture risk is >2.1%, coiling should be performed directly.

CONCLUSION

Given the current literature, no preventive treatment or imaging follow-up is the cost-effective strategy in patients with aneurysms <=3 mm, resulting in better health outcomes and lower healthcare spending. More aggressive imaging surveillance for aneurysm growth or preventive treatment should be reserved for patients with high risk of rupture.

CLINICAL RELEVANCE/APPLICATION

Civen our findings we need to critically evaluate the annronriateness of our current clinical practices and potentially determine

specific guidelines to reflect the most effective management strategy for patients with incidental, tiny UIAs.

SSM20-04 Multi-Modal Convolutional Neural Networks with 2D and 3D Information Can Improve It's Sensitivity and Specificity for Detecting Cerebral Aneurysms in MR Angiography

Wednesday, Dec. 4 3:30PM - 3:40PM Room: S502AB

Participants

Yuki Terasaki, Chiba, Japan (*Presenter*) Nothing to Disclose Hajime Yokota, MD, Chiba, Japan (*Abstract Co-Author*) Nothing to Disclose Ryuna Kurosawa, Chiba, Japan (*Abstract Co-Author*) Nothing to Disclose Hiroki Mukai, Chiba, Japan (*Abstract Co-Author*) Nothing to Disclose Shoma Yamauchi, Chiba, Japan (*Abstract Co-Author*) Nothing to Disclose Joji Ota, Chiba, Japan (*Abstract Co-Author*) Nothing to Disclose Takuro Horikoshi, MD, Chiba, Japan (*Abstract Co-Author*) Nothing to Disclose Takashi Uno, Chiba, Japan (*Abstract Co-Author*) Nothing to Disclose Yasukuni Mori, Chiba, Japan (*Abstract Co-Author*) Nothing to Disclose Hiroki Suyari, Chiba, Japan (*Abstract Co-Author*) Nothing to Disclose

For information about this presentation, contact:

y_terasaki138@chiba-u.jp

PURPOSE

Convolutional neural networks (CNN) with two-dimensional inputs for detecting cerebral aneurysm in magnetic resonance angiography (MRA) images have been proposed. The CNN can archive high sensitivity, although its outputs contain a large number of false positives. Various efforts for reducing false positives were implemented so far, but techniques applying three-dimensional information have not been reported. The purpose of this study was to develop multi-modal CNN taking advantage of both 2D and 3D information, and to investigate the performance improvement of aneurysms detection. As the 2D and 3D streams extract different features from inputs, we hypothesized multi-modal CNN could obtain new feature representations different from CNN with 2D input only.

METHOD AND MATERIALS

This study included 142 aneurysms (mean size, 4.1 mm \pm 1.7 [standard deviation]; range, 1.3 - 9.7 mm) in 125 patients (76 men and 49 women; mean age, 67.6 years; range, 13 - 86 years). MRA were acquired with 81 1.5-T and 44 3.0-T MRI units, respectively. Two radiologists delineated volumes of interests (VOI) of each aneurysm on MRA with consensus. Multi-modal CNN with two streams, 2D and 3D CNNs was developed. Maximum intensity projection (MIP) images around VOI were input into 2D CNN, and a box containing VOI was directly used as the input voxel of 3D CNN. 4-fold cross validation was performed to calibrate generalization ability of the model. The new model was compared with conventional CNN with only 2D input using free-response receiver operating characteristic (FROC) analysis.

RESULTS

The average sensitivities of the 2D CNN and multi-modal CNN to detect aneurysms were 92.4% and 95.2% in eight positive candidates. Although the best sensitivity of 2D CNN was 92.4% at 6.7 false positives per image (FPI), multi-modal CNN achieved the same sensitivity as above at 5.7 FPI. In particular, the number of true positives increased at the middle cerebral artery using the proposed model.

CONCLUSION

Multi-modal CNN using 3D appearance information in addition to conventional 2D shape information improved sensitivity and specificity for detecting cerebral aneurysms compared with conventional CNN with 2D input only.

CLINICAL RELEVANCE/APPLICATION

Adding an auxiliary three-dimensional information can improve sensitivity and specificity of convolutional neural networks-based system for detecting cerebral aneurysms in MR angiography.

SSM20-05 Increased Diagnostic Accuracy of Giant Cell Arteritis Using Three-Dimensional Fat-saturated Contrast-Enhanced Vessel-Wall Magnetic Resonance Imaging at 3 Tesla

Wednesday, Dec. 4 3:40PM - 3:50PM Room: S502AB

Participants

Guillaume Poillon, MD, Paris, France (*Presenter*) Nothing to Disclose Adrien Collin, Paris, France (*Abstract Co-Author*) Nothing to Disclose Cecile Pinson, MD, Rouen, France (*Abstract Co-Author*) Nothing to Disclose Ygal Benhamou, Paris, France (*Abstract Co-Author*) Nothing to Disclose Gaelle Clavel, Paris, France (*Abstract Co-Author*) Nothing to Disclose Frederique Charbonneau, Paris, France (*Abstract Co-Author*) Nothing to Disclose Catherine Vignal, Paris , France (*Abstract Co-Author*) Nothing to Disclose Thomas Sene, Paris, France (*Abstract Co-Author*) Nothing to Disclose Julien Savatovsky, MD, Saint Mande, France (*Abstract Co-Author*) Nothing to Disclose Emmanuel Gerardin, MD, Rouen Cedex, France (*Abstract Co-Author*) Nothing to Disclose Augustin Lecler, MD, Paris, France (*Abstract Co-Author*) Nothing to Disclose

For information about this presentation, contact:

gpoillon@for.paris

PURPOSE

To compare the diagnostic accuracy of 3D versus 2D Contrast-Enhanced Vessel-Wall (CE-VW) MRI in the diagnosis of GCA.

METHOD AND MATERIALS

This prospective two-center study was approved by a national research ethics board and included 79 patients (51 GCA and 28 non-GCA) from December 2014 to October 2017. Two neuroradiologists, blinded to clinical data, individually analyzed 2D and 3D CE-VW MRIs separately and in random order. Discrepancies were resolved by consensus by a third neuroradiologist. The primary judgment criterion was the presence of GCA-related inflammatory changes, determined by arterial wall thickening and mural enhancement of extracranial arteries. Secondary judgment criteria included inflammatory changes of intracranial arteries and the presence of artifacts. A McNemar's test was used to compare 2D to 3D CE-VW MRIs.

RESULTS

3D CE-VW was significantly more sensitive and specific than 2D CE-VW when showing inflammatory change of extracranial arteries: 80% versus 70% (p= 0.03) and 100% versus 85% (p= 0.04), respectively. 3D CE-VW showed higher sensitivity when detecting inflammatory changes of intracranial arteries: 20% versus 8% (p=0.01).Interobserver agreement was excellent for both 2D and 3D CE-VW MRI: K = 0.84 and 0.82 respectively. There was a negative correlation between CE-VW MR diagnostic accuracy and a longer corticosteroids-MRI delay with an optimal threshold of 3 and 5 days for 2D and 3D CE-VW respectively.

CONCLUSION

3D CE-VW MRI supported more accurate diagnoses of GCA than 2D CE-VW. MRI should be performed as soon as possible, ideally before or within the first five days after corticosteroid therapy.

CLINICAL RELEVANCE/APPLICATION

3D Contrast-enhanced Vessel-wall Magnetic Resonance Imaging is a highly precise non-invasive tool that might compete for time to complete a temporal artery biopsy when Giant Cell Arteritis is suspected.

SSM20-06 Diagnostic Accuracy of Routine Non-Contrast MRI Sequences for Dural Venous Sinus Thrombosis

Wednesday, Dec. 4 3:50PM - 4:00PM Room: S502AB

Participants

Minako Azuma, Miyazaki, Japan (*Abstract Submitter*) Nothing to Disclose Yoshiyuki Watanabe, MD, PhD, Suita, Japan (*Abstract Co-Author*) Research Grant, Canon Medical Systems Corporation; Research Grant, Dai Nippon Printing Co, Ltd; Speakers Bureau, General Electric Company Yoshihito Kadota, Miyazaki, Japan (*Abstract Co-Author*) Nothing to Disclose Zaw Aung Khant, Miyazaki, Japan (*Abstract Co-Author*) Nothing to Disclose Youhei Hattori, Miyazaki, Japan (*Abstract Co-Author*) Nothing to Disclose Toshinori Hirai, MD, PhD, Miyazaki, Japan (*Presenter*) Research Grant, Bayer AG

PURPOSE

To determine what routine non-contrast MR imaging (MRI) sequence or combination of MRI sequences is most useful for the diagnosis of dural venous sinus thrombosis (DVST).

METHOD AND MATERIALS

This multicenter study included 81 DVST patients (39 men, 42 women; age range 20-91 years; mean age 50 years) who underwent routine non-contrast 1.5- or 3T MRI within 14 days of digital subtraction angiography (DSA), contrast-enhanced MR venography, and/or CT venography. The controls were 243 age- and sex-matched individuals without DVST. They also underwent routine 1.5- or 3T MRI before- or within one month after DSA. The DVSTs were located in the transverse-, sigmoid-, and/or superior sagittal sinus. Three independent, blinded observers separately evaluated T1-, T2-, diffusion-, T2*-, and susceptibility-weighed images (T1WI, T2WI, DWI, T2*WI, and SWI) and FLAIR images for the presence or absence of DVST. The area under the receiver operating characteristics curve (AUC) was calculated for each MRI sequence. Fleiss κ statistics were applied to assess interobserver agreement. Univariate and multivariate analyses were performed to evaluate the predictive value of the sequences.

RESULTS

The overall accuracy for the diagnosis of DVST was 0.592 for T1WI, 0.914 for T2WI, 0.874 for FLAIR, 0.871 for DWI, 0.792 for T2*WI, and 0.673 for SWI. T2WI and DWI were most predictive of DVST [odds ratio (OR): 41.0; 95% confidence interval (CI) 7.8 - 216.3 and OR 75.1; 95% CI 15.6 - 361.6, respectively]. The combined use of T2WI and DWI yielded significantly better diagnostic performance than each sequence alone (p<0.05); the AUC was 0.802 (95% CI, 0.749 - 0.856). Interobserver agreement was good for T1WI (κ =0.681), T2WI (κ = 0.795), FLAIR (κ =0.719), and T2*WI (κ =0.745). It was moderate for DWI (κ = 0.600) and fair for SWI (κ = 0.351).

CONCLUSION

Among the examined routine non-contrast brain MRI sequences, the combined use of T2WI and DWI was the most predictive of DVST.

CLINICAL RELEVANCE/APPLICATION

Routine non-contrast brain MRI sequences, especially T2WI and DWI, were useful for evaluating DVST.





SSM21

Neuroradiology/Head and Neck (Gadolinium)

Wednesday, Dec. 4 3:00PM - 4:00PM Room: S504AB



AMA PRA Category 1 Credit ™: 1.00 ARRT Category A+ Credit: 1.00

FDA Discussions may include off-label uses.

Participants

Robert J. McDonald, MD, PhD, Rochester, MN (*Moderator*) Consultant, General Electric Company Research Grant, General Electric Company Consultant, Bracco Group

Emanuel Kanal, MD, Pittsburgh, PA (*Moderator*) Consultant, Medtronic plc; Consultant, Bracco Group; Consultant, General Electric Company;

Sub-Events

SSM21-01 Analysis of Retention of Gadolinium by Brain, Bone and Blood Following Linear Gadolinium-Based Contrast Administration in Rats with Gram-Negative Endotoxin-Induced Experimental Sepsis

Wednesday, Dec. 4 3:00PM - 3:10PM Room: S504AB

Participants

Nik Damme, MD, Salt Lake City, UT (*Abstract Co-Author*) Nothing to Disclose Rheal A. Towner, PhD, Oklahoma City, OK (*Abstract Co-Author*) Nothing to Disclose John M. Hoffman, MD, Salt Lake Cty, UT (*Abstract Co-Author*) Nothing to Disclose Kathryn A. Morton, MD, Salt Lake City, UT (*Presenter*) Nothing to Disclose

For information about this presentation, contact:

kathryn.morton@hsc.utah.edu

PURPOSE

Linear gadolinium-based contrast agents (GBCA) used for MR imaging may undergo dechelation, leading to deposition of Gd3+ in the brain. This could be theoretically worsened by blood brain barrier (BBB) disruption. In a lipopolysaccharide (LPS) sepsis model in rats, we have previously demonstrated secondary neuroinflammation and sustained blood brain barrier permeability (to 6 weeks). In LPS treated and control rats, brain, blood and bone levels of Gd were compared at 24h, and at 1, 3 and 6 weeks post linear GBCA injection.

METHOD AND MATERIALS

Male Sprague Dawley rats (250 g) were injected intraperioneally with 10 mg/kg LPS. Control animals received no injection. 24h later, 0.2 mmol/kg of gadobenate dimeglumine (MultiHance®) MRI contrast medium was injected by tail vein. The brain, blood and bone were harvested at 24 h, 1 week, 3 weeks and 6 weeks post GBCA administration. Gd content was measured by inductively coupled plasma mass spectroscopy (ICP-MS).

RESULTS

There was a rapid decrease in Gd in the blood between 24h and 1 week, and thereafter was undetectable. There was no significant difference in Gd content in the blood of LPS vs control rats. Brain levels of Gd were significantly higher in LPS than control rats at all time points (4.3-fold at 24h, 2.4-fold at 1 week, 2.9-fold at 3 weeks and 3.2-fold at 6 weeks) with significant retention over time (~40% of 24h levels at 6 weeks). Bone levels of Gd were 10-fold higher than brain levels at 24 h (per kg), slightly but significantly higher in LPS than control rats (~1.3 fold), with significant retention over time (~60% of 24h levels at 6 weeks).

CONCLUSION

When GBCA was administered intravenously to rats under LPS-induced septic conditions, there was a significantly higher deposition of Gd in the brain compared to control rats. In both LPS and control rats, the brain retained substantial Gd even at 6 weeks post GBCA injection. The magnitude of findings could not be explained by differences in blood or bone levels, suggesting that BBB disruption may play a role. However, even in control rats, significant and sustained Gd occurred in the brain following linear GBCA. Comparisons to macrocyclic GBCA are warranted.

CLINICAL RELEVANCE/APPLICATION

Consideration should be given for avoidance of linear GBCA in septic patients, possibly because of enhanced vulnerability to Gd deposition due to blood brain disruption.

SSM21-02 Long-Term Retention of Gadolinium in the Cerebellum: Comparison of a Gadopiclenol, a New High-Relaxivity Macrocyclic Gadolinium-Based Contrast Agent, with Gadobutrol and Gadodiamide in a Rodent Model (Total Gd Quantification and Speciation)

Wednesday, Dec. 4 3:10PM - 3:20PM Room: S504AB

Philippe Robert, Roissy CDG Cedex, France (*Presenter*) Employee, Guerbet SA Anne-laure Grindel, Roissy CDG Cedex, France (*Abstract Co-Author*) Employee, Guerbet SA Cecile Factor, Roissy CDG Cedex, France (*Abstract Co-Author*) Employee, Guerbet SA Emilie Laveissiere, Roissy CDG, France (*Abstract Co-Author*) Employee, Guerbet SA Izabela Strzeminska, Roissy CDG, France (*Abstract Co-Author*) Employee, Guerbet SA Gaelle Jestin-Mayer, Roissy CDG, France (*Abstract Co-Author*) Employee, Guerbet SA Claire Wallon, Roissy CDG, France (*Abstract Co-Author*) Employee, Guerbet SA Robin Santus, Roissy CDG, French And Southern Antarctic Lands (*Abstract Co-Author*) Employee, Guerbet SA Marlene Rasschaert, Roissy CDG, France (*Abstract Co-Author*) Employee, Guerbet SA Aymeric Seron, Roissy CDG, France (*Abstract Co-Author*) Employee, Guerbet SA Claire Corot, PhD, Roissy, France (*Abstract Co-Author*) Employee, Guerbet SA

PURPOSE

To evaluate the long-term brain elimination kinetics and gadolinium species in healthy rats after repeated injections of gadopiclenol, a new high relaxivity gadolinium-based contrast agent (macrocyclic GBCA, currently under clinical trials) or gadobutrol (macrocyclic GBCA) as compared to gadodiamide (linear GBCA).

METHOD AND MATERIALS

N=80 healthy rats received five doses of 2.4 mmol/kg of gadopiclenol, gadobutrol or gadodiamide over 5 weeks (total dose of 12 mmol/kg), or the equivalent volume of saline. Animals were sacrificed at 1 or 5 months (M1, M5) after the last injection (n=10/group). Cerebellum was sampled to determine the total gadolinium concentration by using inductively coupled plasma mass spectrometry (ICP-MS, lower limit of quantification LLOQ=0.02 nmol/g). For the M5 group, gadolinium speciation analysis was performed after mild extraction using size exclusion chromatography coupled to ICP-MS. Elementary Gd concentrations are expressed as the remaining % of Gd per gram of wet tissue (%ID/g). Differences were evaluated with a Student t-test (significance for p<0.05).

RESULTS

Gadolinium content was stably retained in the cerebellum 1 and 5 months after the last injection of the linear GBCA gadodiamide $(0.691\pm0.121 \text{ and } 0.683\pm0.077 \text{ } \text{MD/g}10^{-6} \text{ respectively})$, with binding of water soluble gadolinium to macromolecules at M5, as shown in previous published studies. For the macrocyclics GBCAs gadopiclenol and gadobutrol, level of Gd were 27-fold lower than after gadodiamide at M5 (0.025 ± 0.007 and $0.026\pm0.021 \text{ } \text{MD/g}10^{-6}$ respectively, NS except p<0.0001 as compared to gadodiamide group), with a 73% and 66% decrease from M1 to M5 (0.094 ± 0.027 and $0.078\pm0.016 \text{ } \text{MD/g}10^{-6}$ at M1 for gadopiclenol and gadobutrol respectively, NS): see Figure. For macrocyclic GBCAs, only intact chelate is detected in the soluble fraction. No Gd was detected in the saline group at both delays (below the LLOQ).

CONCLUSION

After repeated administration of gadodiamide, a large portion of gadolinium was retained in the brain, with binding of soluble gadolinium to macromolecules. After repeated injections of gadopiclenol or gadobutrol, only traces of the intact chelated gadolinium were observed after 5 months, as expected for macrocyclic GBCA.

CLINICAL RELEVANCE/APPLICATION

In cerebellum, gadopiclenol, a new macrocyclic GBCA currently in clinical trials, shows massive clearance of the intact chelate, as for macrocyclic GBCA gadobutrol.

SSM21-03 Dose Finding Study of Gadopiclenol - A New Macrocyclic Gadolinium-Based Contrast Agent (GBCA) -In MRI of Central Nervous System

Wednesday, Dec. 4 3:20PM - 3:30PM Room: S504AB

Participants

Benjamin P. Liu, MD, Chicago, IL (Presenter) Speakers Bureau, Guerbet SA Research Grant, Guerbet SA Research Grant, Bayer AG

PURPOSE

To determine a safe and effective dose of gadopiclenol, a new high relaxivity macrocyclic GBCA, based on the Contrast to Noise Ratio (CNR) as compared to gadobenate dimeglumine at 0.1 mmol/kg body weight.

METHOD AND MATERIALS

This double-blind, randomized, dose-parallel group and cross-over study included patients with known or highly suspected focal areas of disrupted blood brain barrier. Patients were randomized to one of four doses of gadopiclenol (0.025, 0.05, 0.1, 0.2 mmol/kg) and to one series of two MRIs: gadopiclenol and then gadobenate dimeglumine or vice versa, separated by a wash out period ranging from 2 to 14 days. Three independent off-site blinded readers performed the signal intensity measurements. Adverse events were collected up to one day post second MRI.

RESULTS

The study population included 272 patients (58.5% females) with a mean (SD) age of 53.8 (13.6) years. The superiority of gadopiclenol over gadobenate dimeglumine was statistically demonstrated at 0.2 and 0.1 mmol/kg for all three readers with an increase in CNR>30%. At 0.05 mmol/kg, gadopiclenol showed a similar CNR as gadobenate dimeglumine (Figure 1). The relationship between CNR and doses of gadopiclenol was linear for all three readers. Similar results were observed for lesion to brain ratio (LBR) and contrast enhancement percentage. Rates of adverse reactions were comparable with gadopiclenol (11.7%) and gadobenate dimeglumine (12.1%).

CONCLUSION

Gadopiclenol at 0.1 mmol/kg led to significant higher CNR, and at 0.05mmol/kg showed similar CNR magnitude as compared to gadobenate dimeglumine at 0.1 mmol/kg. A good safety profile was observed for both doses.

CLINICAL RELEVANCE/APPLICATION

Gadopiclenol, as macrocyclic GBCA with very high relaxivity, is a valuable contrast agent, owing to its improved diagnostic

performance and less concerns about potential free gadolinium toxicity.

SSM21-04 The Use of Artificial Intelligence to Evaluate Differences in Contrast Enhancement between Two Macrocyclic Gadolinium Agents in Patients with Glioblastoma Multiforme

Wednesday, Dec. 4 3:30PM - 3:40PM Room: S504AB

Participants

Matthew J. Kuhn, MD, Peoria, IL (*Presenter*) Chief Medical Officer, AI Analysis, Inc Julia W. Patriarche, PhD, Bellevue, WA (*Abstract Co-Author*) CEO, A.I. Analysis, Inc Douglas H. Patriarche, BSC, Bellevue, WA (*Abstract Co-Author*) President, A.I. Analysis, Inc Gianpaolo Pirovano, MD, Princeton, NJ (*Abstract Co-Author*) Employee, Bracco Group Massimo Bona, San Donato, Italy (*Abstract Co-Author*) Employee, Bracco Group

For information about this presentation, contact:

matt@aianalysis.com

PURPOSE

The use of gadolinium based contrast agents for MRI in patients with glioblastoma multiforme (GBM) is well known. Interest in the use of macrocyclic agents is increasing due to greater awareness of gadolinium retention issues. Macrocyclic agents vary in concentration and there has been controversy related to the efficacy of using traditional concentration (0.5 mmol/ml) versus higher concentration (1 mmol/ml) agents. We have employed the use of advanced artificial intelligence/machine learning techniques to better evaluate contrast enhanced brain MRI for patients with GBM, each of whom received both gadoteridol and gadobutrol.

METHOD AND MATERIALS

32 patients with pathologically proven GBM qualified for this study. Each patient received 0.1 mmol/kg of both gadoteridol and gadobutrol within a 2-10 day time period using a double-blind, randomized crossover technique. The images were evaluated in a blinded fashion using artificial intelligence change detection software. Enhancement characteristics for both agents were processed and the differences for each set of image pairs were calculated and analyzed. A 90% confidence interval of the mean of the difference in enhancement was calculated with a zone of equivalence defined to be from -0.2 to +0.2.

RESULTS

27 of the patients with GBM were evaluable. Five patients were excluded because of the absence of enhancement on both of their studies. The artificial intellience/machine learning software demonstrated no statistically significant difference in enhancement characteristics between the traditional concentration gadoteridol and the higher concentration gadobutrol. The p-value from paired t-test was p=0.3126. The Pearson correlation coefficient between the normalized gadoteridol and gadobutrol was 0.958 (p<0.0001). For all 27 image pairs, the 90% confidence intervals were within the zone of equivalence.

CONCLUSION

Artificial intelligence/machine learning software demonstrates no statistically significant difference in the evaluation of GBM when using equal doses of gadoteridol or gadobutrol. Both agents were determined to be equivalent.

CLINICAL RELEVANCE/APPLICATION

The use of artificial intelligence processes support the hypothesis that despite concentration differences, 0.1 mmol/kg of gadoteridol and gadobutrol demonstrate equivalent contrast enhancement and are equally efficacious in the evaluation of patients with GBM.

SSM21-05 Where is Retained Gadolinium Localized in the Dentate Nucleus? Simultaneous Detection of Gd and Structural Proteins by Using Metal-Tagged Antibodies and LA-ICP-MS

Wednesday, Dec. 4 3:40PM - 3:50PM Room: S504AB

Participants

Janina Boyken, Berlin, Germany (*Abstract Co-Author*) Employee, Bayer AG Thomas Frenzel, PhD, Berlin, Germany (*Abstract Co-Author*) Employee, Bayer AG Gregor Jost, PhD, Berlin, Germany (*Abstract Co-Author*) Employee, Bayer AG Jessica Lohrke, PhD, Berlin, Germany (*Abstract Co-Author*) Employee, Bayer AG Hubertus Pietsch, PhD, Berlin, Germany (*Presenter*) Employee, Bayer AG

For information about this presentation, contact:

janina.boyken@bayer.com

PURPOSE

The precise localization of gadolinium (Gd) within the deep cerebellar nuclei (DCN) is not fully understood. This study aims to colocalize Gd with the cellular environment such as blood vessels or astrocytes by combining high-resolution laser ablation inductively coupled plasma mass spectrometry (LA-ICP-MS) with metal-tagged immunohistochemistry in the rat brain after repeated exposure to gadolinium-based contrast agents (GBCA).

METHOD AND MATERIALS

Rats received 8 intravenous injections of gadodiamide or gadobutrol at a dose of 1.8 mmol Gd/kg body weight and were sacrificed 35 days post injection. The spatial Gd distribution in brain sections was quantified and analyzed simultaneously with the endothelial marker von-Willebrand-factor (vWF) and the astrocytic marker GFAP detected by metal-tagged antibodies using LA-ICP-MS.

RESULTS

The immunohistological LA-ICP-MS approach was validated by comparison to classical immunofluorescence imaging. A spatial resolution of $2x2 \ \mu m2$ was achieved, which enabled the co-visualization of Gd with the cellular environment. In animals treated with gadodiamide, the Gd distribution pattern was not altered after the washing and staining procedures and the DCN contained Gd

concentrations up to 10nmol/g. The Gd pattern in the DCN only partially overlapped with the endothelial marker vWF while most Gd spots did not co-localize with vWF and GFAP. In gadobutrol animals, we observed an almost complete wash out of the residual Gd during the staining procedure with the Gd present after staining being localized only in blood vessels.

CONCLUSION

An immunohistological LA-ICP-MS approach was used to reveal the spatial context of Gd in the rat brain following GBCA administration. We observed differences between linear gadodiamide and macrocyclic gadobutrol. Whereas in gadobutrol animals, the remaining Gd traces were located in the vasculature, this was only a minor fraction of Gd in gadodiamide animals. It needs to be elucidated whether the major fraction of Gd co-localizes with other histological markers.

CLINICAL RELEVANCE/APPLICATION

In stained rat brain sections, Gd from linear gadodiamide but not macrocyclic gadobutrol was found outside of the vascular system.

SSM21-06 Gadolinium-induced Hypophosphatemia Does Not Correlate with Gadolinium Deposition in the Brain in Multiple Sclerosis Patients Undergoing Monthly Triple-Dose Gadopentetate Dimeglumine CE-MRI

Wednesday, Dec. 4 3:50PM - 4:00PM Room: S504AB

Participants

John J. Debevits IV, MD, Farmington, CT (*Presenter*) Nothing to Disclose Devin Bageac, Farmington, CT (*Abstract Co-Author*) Research funded, Guerbet SA Leo J. Wolansky, MD, Farmington, CT (*Abstract Co-Author*) Nothing to Disclose Paul A. DiCamillo, MD, PhD, Potomac , MD (*Abstract Co-Author*) Nothing to Disclose Reshma Munbodh, PHD, New Haven, CT (*Abstract Co-Author*) Research support, Guerbet SA Lihong Wang, Farmington, CT (*Abstract Co-Author*) Institutional Grant, Quberbet Rong Wu, PhD,MS, Farmington, CT (*Abstract Co-Author*) Nothing to Disclose Yanlin Wang, MD,PhD, Farmington, CT (*Abstract Co-Author*) Nothing to Disclose Chaoran Hu, MSc, Storrs, CT (*Abstract Co-Author*) Nothing to Disclose David S. Karimeddini, MD, Farmington, CT (*Abstract Co-Author*) Institutional Grant, Guerbet SA Suhayl Dhib-Jalbut, New Brunswick, NJ (*Abstract Co-Author*) Nothing to Disclose

For information about this presentation, contact:

debevits@uchc.edu

PURPOSE

The researchers have previously shown hypophosphatemia and increased T1 signal intensity (SI) after serial gadolinium administration. Transmetallation of gadolinium and co-precipitation with phosphate, with subsequent deposition as an insoluble gadolinium species, could help to explain these abnormalities. This would be a first-of-its-kind correlation of abnormal SI changes in the brain due to gadolinium deposition manifesting contemporaneously with a metabolic abnormality that could serve as a pathophysiologic link and/or inexpensive biomarker of this recently discovered phenomenon.

METHOD AND MATERIALS

The study cohort consisted of 75 patients with MS or Clinically Isolated Syndromes typical of MS who were randomized \sim 1:1 to Betaseron or Copaxone as part of the BECOME trial. Monthly follow-up MRI using off-label triple-dose gadopentetate dimeglumine (0.3mmol/kg) for up to 24 months included pre-MRI blood and urine samples for maintenance of protocol safety. ROI creation using a boundary approximation manual segmentation technique was performed from the MRI data to establish potential SI changes due to gadolinium deposition as represented by increased T1 SI. C/N ratios established average SI change over the first 12 months of the study, defined as: C/N = [Gray Matter Structure - White Matter Reference Structure] / Air. Phosphate levels were analyzed using the general estimation equation; type 3 test of fixed effects was performed to correlate phosphate and SI changes.

RESULTS

Increased T1 SI changes were seen in all grey matter structures analyzed: caudate head: C/N = 0.037 (S.E. 0.0037, p<0.0001); putamen: C/N = 0.031 (S.E. 0.0034, p<0.0001); globus pallidus: C/N = 0.046 (S.E. 0.0035, p<0.0001); thalamic pulvinar: C/N = 0.026 (S.E. 0.0027, p<0.0001); dentate nucleus: C/N = 0.098 (S.E. 0.0070, p<0.0001). Incidence of hypophosphatemia (<2.5 mg/dl) increased significantly over the course of the study in both treatment arms with an odds ratio of 1.267 (1.198, 1.344, p<0.001). No significant difference for any grey matter structure was seen between hypophosphatemic and normophosphatemic groups.

CONCLUSION

There is no correlation between hypophosphatemia and increased T1 signal of grey matter due to gadolinium deposition.

CLINICAL RELEVANCE/APPLICATION

Hypophosphatemia should be monitored and corrected in any patient undergoing serial CE-MRI, but its role in the pathophysiology of gadolinium deposition in the brain appears equivocal.



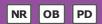




SSM22

Pediatrics (Neuroradiology and Fetal Neuroimaging)

Wednesday, Dec. 4 3:00PM - 4:00PM Room: S103AB



AMA PRA Category 1 Credit ™: 1.00 ARRT Category A+ Credit: 1.00

FDA Discussions may include off-label uses.

Participants

Beth M. Kline-Fath, MD, Cincinnati, OH (*Moderator*) Nothing to Disclose Bernadette L. Koch, MD, Cincinnati, OH (*Moderator*) Nothing to Disclose

Sub-Events

SSM22-01 Assessment of Normal Fetal Brain Development with No Biased-Apparent Diffusion Coefficient Values: A Prenatal MR Study

Wednesday, Dec. 4 3:00PM - 3:10PM Room: S103AB

Participants

Lucia Manganaro, MD, Roma, Italy (*Abstract Co-Author*) Nothing to Disclose Amanda Antonelli, MD, Rome, Italy (*Presenter*) Nothing to Disclose Maria Giovanna Di Trani, Rome, Italy (*Abstract Co-Author*) Nothing to Disclose Roberta Petrillo, MD, Rome, Italy (*Abstract Co-Author*) Nothing to Disclose Giada Ercolani, MD, Rome, Italy (*Abstract Co-Author*) Nothing to Disclose Carlo Catalano, MD, Rome, Italy (*Abstract Co-Author*) Nothing to Disclose Silvia Bernardo, MD, Roma, Italy (*Abstract Co-Author*) Nothing to Disclose Silvia Capuani, Rome, Italy (*Abstract Co-Author*) Nothing to Disclose Silvia Capuani, Rome, Italy (*Abstract Co-Author*) Nothing to Disclose Serena Satta, Rome, Italy (*Abstract Co-Author*) Nothing to Disclose

For information about this presentation, contact:

amanda.antonelli@uniroma1.it

PURPOSE

Fetal imaging is often perturbed by artifacts affecting the quality of Diffusion Weighted Imaging (DWI), with biased ADC measurements. In this context, the purpose of our study was to investigate the potential of denoising DWI to ameliorate the reliability of ADC values in the study of normal fetal brain maturation.

METHOD AND MATERIALS

36 normal pregnancies underwent fetal MR at 1.5T, using a normal fetal brain protocol including DW-Spin Echo EPI with three bvalues (50, 200, 700 s/mm²). Seven ROIs were manually placed in Frontal White Matter (FWM), Occipital WM (OWM), Thalamus (TH), Basal Ganglia (BG), Cerebellum (CH), Pons and Cerebral Spinal Fluid (CSF). Raw data were denoised and DWI were segmented to eliminate CSF. Differences of ADC values occuring in II and III trimester with and without DWI denoising were calculated. Signalto-Noise Ratio (SNR) was obtained with and without denoising correction. The correlation between ADC in different ROIs and GA was obtained.

RESULTS

SNR considerably increased with denoising correction. Significant differences in ADC mean values of CH, Pons, FWM and TH calculated in II and III trimester were found (p<0.01). ADC values of TH, CH and Pons show a progressive decline in mean diffusivity (p<0.001), depicting a decrease of anisotropy. Positive correlations were found between ADC and GA in FWM ROI (p<0.05). In particular, a bi-quadratic fashion in FWM ROI was found: during the II trimester the ADC increase, with a descending trend during the III trimester.

CONCLUSION

Due to the high amount of imaging artifacts in fetal imaging, denoising DWI is desireable to obtain reliable ADC values and charachterize normal fetal brain development. In our sample, no biased ADC parameters showed statistically significant changes in mean values of different fetal brain ROIs: this highlights the physiological heterogeneous microstructural changes occurring during normal fetal brain development, in terms of proliferation, migration and myelination processess.

CLINICAL RELEVANCE/APPLICATION

The study of denoised DW imaging of normal fetal brain is relevant in clinical practice since it allows the measurement of no biased ADC values of physiological brain maturation. The knowledge of normal ADC parameters represent a non-pathological comparison base and a helpful prenatal diagnostic tool to improve the complicated prenatal diagnosis of suspected fetal brain anomalies.

SSM22-02 Asymmetry of Superior Longitudinal Fasciculus Microstructure in Preterm Human Brain Revealed by Diffusion Tensor Imaging

Participants Hong Zhu, Philadelphia, PA (*Abstract Co-Author*) Nothing to Disclose Chenying Zhao, Philadelphia, PA (*Abstract Co-Author*) Nothing to Disclose Minhui Ouyang, Philadelphia, PA (*Abstract Co-Author*) Nothing to Disclose Junfeng Sun, Shanghai, China (*Abstract Co-Author*) Nothing to Disclose Hao Huang, PhD, Philadelphia, PA (*Abstract Co-Author*) Nothing to Disclose Qiang Zheng, Philadelphia, PA (*Presenter*) Nothing to Disclose

For information about this presentation, contact:

ZHUH2@email.chop.edu

PURPOSE

Language laterization in the human was one of the earliest observations of brain asymmetry. The influence of age on language laterization is unknown during the 3rd trimester. We employed diffusion tensor imaging (DTI) to investigate the white matter (WM) microstructure of language associated tract, superior longitudinal fasciculus (SLF), in preterm- and term-born neonates. We hypothesized that there is an age-related increase of asymmetry of SLF microstructure during 3rd trimester.

METHOD AND MATERIALS

High resolution (1.5x1.5x1.6 mm3) diffusion weighted imaging data with b values of 1000 s/mm2 were acquired from 61 neonates with ages of 31-42 postmenstrual weeks (PMW). Correction for eddy current distortion, tensor fitting, and deterministic diffusion tractography of SLF were conducted in DTIStudio. Specifically, the fiber tracing was terminated when the fractional anisotropy (FA) value was below 0.15 or the turning angle was greater than 50 degrees. An asymmetry index of FA in SLF was calculated as (Left FA - Right FA) / (Left FA + Right FA). A positive value indicated a leftward asymmetry.

RESULTS

Dramatically morphological changes of SLF from 31 to 42 PMW were observed. In addition, FA values in both left (r=0.794, p<0.001) and right (r=0.758, p<0.001) SLF significantly increased with age, suggesting WM microstructural maturation in SLF. Compared right SLF, left SLF was characterized with lower initial FA values and faster FA increase. Age-related growth trend lines of FA for left and right SLF intersected around 36 PWM. Interestingly, the asymmetry index of FA in SLF significantly increased with age (r=0.330, p<0.01), reflecting a transition toward a leftward structural asymmetry. All neonates were categorized into 3 age groups based on their scan ages to further explore the development of language lateralization. The asymmetry index of FA in SLF from groups aged 34-38 PMW and 38-42 PMW were significantly larger (p<0.05) than that of the youngest group (30-34 PMW) (p<0.05).

CONCLUSION

During the 3rd trimester, we observed age-related increase of leftward asymmetry in the WM microstructural maturation in language associated tract SLF.

CLINICAL RELEVANCE/APPLICATION

Age-related increase of leftward-laterization in language associated tract during 3rd trimester was found. This may serve as an anatomical substrate that enables the following language production.

ssM22-03 Early Fetal Brain Sulcation: Reassessing Initial Detection Age in Fetal MRI

Wednesday, Dec. 4 3:20PM - 3:30PM Room: S103AB

Participants Sepideh Sefidbakht, MD, Powel, OH (*Abstract Co-Author*) Nothing to Disclose Setareh Hemmati, Shiraz, Iran (islamic Rep. Of) (*Abstract Co-Author*) Nothing to Disclose Pooya Iranpour, MD, Houston, TX (*Abstract Co-Author*) Nothing to Disclose Fariba Zarei, MD, Shiraz, Iran (*Abstract Co-Author*) Nothing to Disclose Reza Jalli, Shiraz, Iran (*Abstract Co-Author*) Nothing to Disclose Bijan Bijan, MD, Sacramento, CA (*Presenter*) Nothing to Disclose

For information about this presentation, contact:

dr.sefid@gmail.com

PURPOSE

To re-evaluate early brain sulcation patterns in MRI, focusing on early midline sulci

METHOD AND MATERIALS

Out of the 658 fetal MRI's performed in our referral hospital over two years, 321 cases were performed before 20weeks. In 67 fetuses normal brain MRI was confirmed with normal post-delivery outcome as assessed with ASQ questionnaires. The sylvian sulcus (SS), also the calcarine (cal), and parietooccipital (POF) fissures were assessed subjectively by two radiologists with 9 and 8 years of experience in neuro and fetal imaging. The sulci were evaluated in standard orthogonal planes, but also in non-orthogonal nonstandard planes. We also included the axial view of proximal calcarine sulcus previously described in a previous study on postmortem fetal MRI at 7T and also postmortem pathology studies. The SS was graded based on the grading by Pretorius et al (0-5).

RESULTS

The mean scores for SS was 1, 1, 1, and 1.14 in fetuses with GA's of 16, 17, 18 and 19 respectively. The right POF mean scores was 0.66, 0.50, 0.22 ,and 0.97 in fetuses with GA's of 16, 17, 18 and 19 respectively. The left POF mean scores were 0, 0.50, 0.27, and 0.76 in GA's of 16,17,18 and 19 respectively. The mean scores for right Cal in the standard coronal plane was 0, 0,0.27, and 0.15 in GA's of 16,17, 18 and19 weeks respectively. While the mean scores for the proximal Cal in axial images was1, 0.5, 0.44, and 1.36. The mean scores for the proximal Cal in the standard coronal plane was 0, 0, 0.16, and 0.10 in GA's of 16,17,18 and 19 weeks respectively while mean scores for the proximal Cal in axial images was1, 0.5, 0.44, and 1.36. The mean scores for the proximal Cal in axial images was 0, 0, 0.16, and 0.10 in GA's of 16,17,18 and 19 weeks respectively while mean scores for the proximal Cal in axial images was 0.66, 0.25, 0.44, and 1.33. The axial and oblique axial images could detect a higher number of Cal's comparing to the standard coronal view.

CONCLUSION

Early midline sulci may be consistently visible in fetal MRI earlier than previously believed. For earlier detection these sulci should be sought not only in the standard orthogonal views, but also in non-orthogonal views.

CLINICAL RELEVANCE/APPLICATION

With more frequent and earlier use of fetal MRI, also with time restrictions imposed by legal abortion dates in many countries, a better understanding of the appearance of the early brain development has become necessary. Without a thorough understanding of the normal appearance, abnormal patterns cannot be recognized accurately.

SSM22-05 In-Utero Diffusion Weighted Imaging with Denoising Correction in the Study of Fetal Brain Microstructure in Isolated Ventriculomegaly

Wednesday, Dec. 4 3:40PM - 3:50PM Room: S103AB

Participants

Amanda Antonelli, MD, Rome, Italy (*Presenter*) Nothing to Disclose Lucia Manganaro, MD, Roma, Italy (*Abstract Co-Author*) Nothing to Disclose Maria Giovanna Di Trani, Rome, Italy (*Abstract Co-Author*) Nothing to Disclose Giada Ercolani, MD, Rome, Italy (*Abstract Co-Author*) Nothing to Disclose Roberta Petrillo, MD, Rome, Italy (*Abstract Co-Author*) Nothing to Disclose Carlo Catalano, MD, Rome, Italy (*Abstract Co-Author*) Nothing to Disclose Silvia Capuani, Rome, Italy (*Abstract Co-Author*) Nothing to Disclose Miriam Dolciami, MD, Rome, Italy (*Abstract Co-Author*) Nothing to Disclose Veronica Celli, MD, Roma, Italy (*Abstract Co-Author*) Nothing to Disclose

For information about this presentation, contact:

amanda.antonelli@uniroma1.it

PURPOSE

To investigate the potential of denoised DW imaging to study fetal brain affected by Venticulomegaly (VM) and to obtain improved ADC values for the characterization of fetal brain microstructure impairment.

METHOD AND MATERIALS

Fetal MR with Diffusion-weighted imaging (DWI) was performed in 48 fetuses at 1.5 T. The fetal brain MR protocol included a DW-Spin Echo EPI with three b-values (50, 200, 700 s/mm²). Dwidenoise tool and Unring software were used to denoise and correct diffusion imaging. Eight ROIs were manually placed in both normal and VM fetal brains in Centrum Semiovale (CSO), Frontal White Matter (FWM), Occipital WM (OWM), Thalamus (TH), Basal Ganglia (BG) Cerebellum (CH), Pons and Cerebral Spinal Fluid (CSF). In some VM cases, ROIs could not be placed in FWM, BG, TH, OWM, CH due to the severity of VM. ADC values were measured voxelby-voxel with a MATLAB fitting procedure. Differences in ADC measurements of normal and VM fetal brains and their correlation with Gestational Age (GA) were calculated.

RESULTS

In VM fetuses, ADC measurements were statistically significant different than normal brain, especially in CSO, TH and CSF ROIs (p<0.02), with different ADC values in II and III trimester of normal (p<0.001) and VM fetuses (p<0.05). In VM fetal brains, ADC values in CSO in the III trimester were higher than normal and in TH ROI statistically significant lower ADC values were found in the II trimester. Negative correlation were found between ADC values and GA in CSO, TH, CH and Pons ROIs, both VM and normal brains, showing a progressive decline in diffusivity.

CONCLUSION

The knowledge of reliable ADC values through denoising correction is a helpful tool able to better discriminate microstructural impairment occurring in fetal brain tissue during prenatal life. Our results showed differences in ADC measurement obtained in VM and normal fetal brains, in particular the increasing of ADC values in CSO may reflect the increment of anisotropy occurring in an impaired and non-ordered white matter affected by VM.

CLINICAL RELEVANCE/APPLICATION

In clinical practice, fetal DWI is often complicated by low imaging quality due to fetal motion artifacts. Denoising correction is crucial to allow a proper ADC measurement, providing a correct in vivo characterization of microstructural brain impairment in fetuses affected by VM, being helpful in the prenatal management of those pregnancies.

SSM22-06 Fetal Optic Structures: A Postmortem MRI Study

Wednesday, Dec. 4 3:50PM - 4:00PM Room: S103AB

Participants

Florian Prayer, MD, Vienna, Austria (*Presenter*) Institutional affiliation, Siemens AG; Research Grant, Boehringer Ingelheim GmbH Daniela Prayer, MD, Vienna, Austria (*Abstract Co-Author*) Nothing to Disclose Christiane Seitz, Vienna, Austria (*Abstract Co-Author*) Nothing to Disclose Peter C. Brugger, MD, PhD, Vienna, Austria (*Abstract Co-Author*) Nothing to Disclose Gerlinde Gruber, Vienna, Austria (*Abstract Co-Author*) Nothing to Disclose

PURPOSE

To establish normal values for fetal MRI of optic structures and to identify pathologies in order to supply basic information for future in vivo studies.

METHOD AND MATERIALS

Fifty-eight cases (16 - 42 gestational weeks), consisting of 33 fetuses with normal development of the optical structures and 25 fetuses with pathologies, were included. The pathological group was composed of: complex malformations (15), premature rupture

of membranes (4), twin-associated problems (3), intrauterine growth restriction (2), and stillbirth (1). Postmortem MRI was obtained within 24 hours of fetal demise using a 3T MR scanner (Siemens Trio) and an eight channel knee coil. Measurements were performed on axial T2-weighted images (TR 300ms, TE 140ms, isovoxel 0.4mm CISS 3D sequence) using Image J software. The following measurements were taken and correlated with gestational age: optic nerves: maximum diameter at retrobulbar and intracranial location; total length; angle between optic nerves; and optic chiasm: minimum transverse diameter.

RESULTS

Total optic nerve length increased from 10.5 mm to 29.4 mm within 26 weeks and correlated significantly with GA (r=0.885, p<0.001). Retrobulbar optic nerve diameter increased from 0.83 to 2.13 mm (right side) and 0.860 to 2.108 mm (left side) within 25 weeks, and correlated significantly with gestational age (right: r=0.852, p<0.001; left: r=0.843, p=<0.001). The angle of the optic nerves in front of the optic chiasm became considerably more acute with increasing age (111.49 - 75.04 degrees from 16 to 36 gestation weeks, correlation with gestational age r=-0.741, p<0.001). The course of the optic nerves altered with gestation. In young fetuses, the optic nerves had a U- evolving to a V-shape with higher gestational age. Fetuses in the pathologic group showed significant aberrations in one to three of the above-described parameters.

CONCLUSION

As sizes of fetal optic structures correlate with gestational age, and the shape of the optic chiasm changes from a U- to a V-form from early to late gestation, developmental deviations of the optic nerves and chiasm that may be part of malformative or acquired conditions, can be detected sensitively in postmortem MRI.

CLINICAL RELEVANCE/APPLICATION

Normal values of optic fetal structures obtained in this study allow the sensitive detection of developmental deviations that may be part of malformative or acquired conditions.





SSM23

Physics (Radiation Therapy/Outcome Modeling/Image Processing)

Wednesday, Dec. 4 3:00PM - 4:00PM Room: S102CD



AMA PRA Category 1 Credit ™: 1.00 ARRT Category A+ Credit: 1.00

FDA Discussions may include off-label uses.

Participants

Carri Glide-Hurst, PHD, Detroit, MI (*Moderator*) Researcher, ViewRay, Inc; Research Consultant, Koninklijke Philips NV; Researcher, Koninklijke Philips NV; Researcher, Modus Medical Devices Inc; Equipment support, Medspira, LLC; Equipment support, QFix Cem Altunbas, PhD, Aurora, CO (*Moderator*) Nothing to Disclose

Sub-Events

SSM23-01 Normalizing the Response of a Fixed Geometry EPID Using a Flattening Phantom on a Ring Gantry Linear Accelerator

Wednesday, Dec. 4 3:00PM - 3:10PM Room: S102CD

Participants

John Chapman, Baton Rouge, LA (*Presenter*) Research funded, Varian Medical Systems, Inc Eric Laugeman, MS, Wildwood, MO (*Abstract Co-Author*) Nothing to Disclose Baozhou Sun, Saint Louis, MO (*Abstract Co-Author*) Nothing to Disclose Nels Knutson, MS, New York, NY (*Abstract Co-Author*) Nothing to Disclose Sreekrishna Murty Goddu, PhD, Saint Louis, MO (*Abstract Co-Author*) Nothing to Disclose Geoffrey Hugo, PhD, Saint Louis, MO (*Abstract Co-Author*) Research Grant, ViewRay, Inc; Research Grant, Varian Medical Systems, Inc; Research Grant, Siemens AG Sasa Mutic, PhD, Saint Louis, MO (*Abstract Co-Author*) Stockholder, ViewRay, Inc Stockholder, Radialogica, LLC Bin Cai, PHD, St. Louis, MO (*Abstract Co-Author*) Nothing to Disclose

CONCLUSION

Based on our results, it is possible to characterize pixel variations by designing a phantom that flattens the beam at the EPID. In the near future, this phantom will be milled to validate the flatness of the beam at the level of the EPID. Finally, the EPID response under this flattening phantom can be directly used as the new "flood field" to correct the pixel response variations.

Background

Previous solutions that calibrated the variations of pixel response for the EPIDs on-board C-arm linacs used either a flat beam or a movable EPID panel. However, the Halcyon (Varian Medical Systems, Palo Alto, CA) is a ring gantry linac with a 6 MV flattening-filter-free (FFF) beam and an EPID rigidly fixed to the gantry. Therefore, this study introduces a strategy to design a beam flattening phantom, which is intended to calibrate the variations of pixel response while preserving the beam dosimetry features on EPID images derived from the Halcyon linac.

Evaluation

EPID images were acquired by irradiating a set of rectilinear solid water phantoms with various thicknesses (0-15 cm). Each solid water phantom was placed at the same position on the couch with a fixed source-to-couch distance (100 cm) and an open field set at the maximum size of 28 cm x 28 cm. Based on the EPID response as a function of solid water thickness, a quadratic form of the attenuation equation was fit with 2D parameter maps, a(x,y) and $\beta(x,y)$, which represent the first- and second- order attenuation of a poly-energetic beam. With the 2D attenuation coefficient maps and the ratio of ideal EPID response of the 6FFF beam to a flattened beam, a 2D phantom thickness map was derived.

Discussion

On the central-axis, the beam required 66% attenuation for the flattening phantom. The final flattening phantom design had an overall conical shape with a maximum thickness of 5.6 cm, making it economical and lightweight. Regression values for the linear fits used in our approach ranged between 94% and 95% with a maximum absolute fit error of 0.0083.

SSM23-02 Proton-Induced Acoustic Computed Tomography for Online Proton Beam Range Verification

Wednesday, Dec. 4 3:10PM - 3:20PM Room: S102CD

Participants

Yue Zhao, Norman , OK (*Abstract Co-Author*) Nothing to Disclose Yong Chen, Oklahoma City, OK (*Abstract Co-Author*) Nothing to Disclose Pratik Samant, BSC, Norman, OK (*Abstract Co-Author*) Nothing to Disclose Siqi Wang, Norman, OK (*Abstract Co-Author*) Nothing to Disclose John Merrill, Norman, OK (*Abstract Co-Author*) Nothing to Disclose Jesus Arellano, Norman, OK (*Abstract Co-Author*) Nothing to Disclose Salahuddin Ahmad, PhD, Oklahoma City, OK (*Abstract Co-Author*) Nothing to Disclose Terence Herman, Oklahoma City, OK (*Abstract Co-Author*) Nothing to Disclose

For information about this presentation, contact:

xianglzh@ou.edu

PURPOSE

To localize the proton Bragg Peak by measuring the acoustic emissions generated by a pulsed proton spill from a clinical synchrocyclotron, ideally in real-time and noninvasively during patient treatment.

METHOD AND MATERIALS

A proton-induced acoustic computed tomography system based on 1MHz two-dimensional matrix array ultrasound probe with 256elements, a 256-32ch switch and a parallel data acquisition system has been developed. The matrix array will now be placed in a water tank in front of the proton nozzle which enables rendering of the proton-induced acoustic images without mechanical scanning. The data acquisition will be synchronized by a trigger signal provided by the MEVION S250i Hyperscan proton therapy system. The digitized data will then be sent to the computer for real-time processing to generate proton-induced acoustic images with a full-field 3D filtered back-projection algorithm.

RESULTS

Hyperscan system has pulse width modulation from 0.5 to 20 us. On average, a full energy (230 MeV) pulse of 6.5 us produces 8 pC (~5x 10^7 protons) and deposits 3.2 cGy under Bragg peak. The total dose distribution of scanned proton pencil beams was simulated. The maximum spatial resolution of the proton-induced acoustic computed tomography was calculated to be about 1 mm, which is much better than the current range verification techniques proposed, for example, positron emission tomography and prompt gamma imaging. In addition, the proton-induced acoustic computed tomography system can obtain 50 frames of images per second without scanning, which means real-time in vivo images could be obtained during treatment to ensure the delivered dose distribution is as expected.

CONCLUSION

These results highlight the excellent prospect of the proton-induced acoustic computed tomography in clinical transformation providing the Bragg peak location, and monitoring proton dose distribution during radiation therapy.

CLINICAL RELEVANCE/APPLICATION

Proton-induced acoustic computed tomography provides real-time feedback with the possibility of adjustment during the treatment which reduces proton range uncertainty and improves the treatment output.

SSM23-03 Improving CBCT Quality to CT Level for Adaptive Radiation Therapy Using Deep-Learning with Generative Adversarial Network

Wednesday, Dec. 4 3:20PM - 3:30PM Room: S102CD

Participants

Yang Zhang, Irvine, CA (*Presenter*) Nothing to Disclose Ning J. Yue, PhD, New Brunswick, NJ (*Abstract Co-Author*) Nothing to Disclose Min-Ying Su, PhD, Irvine, CA (*Abstract Co-Author*) Nothing to Disclose Bo Liu, New Brunswick, NJ (*Abstract Co-Author*) Nothing to Disclose Yi Ding, New Brunswick, NJ (*Abstract Co-Author*) Nothing to Disclose Yin Zhang, PHD, New Brunswick, NJ (*Abstract Co-Author*) Nothing to Disclose Yongkang Zhou, New Brunswick, NJ (*Abstract Co-Author*) Nothing to Disclose Ke Nie, New Brunswick, NJ (*Abstract Co-Author*) Nothing to Disclose

For information about this presentation, contact:

yangz17@uci.edu

PURPOSE

To apply a deep-learning based algorithm to improve CBCT image quality and HU accuracy for extended clinical applications, especially for adaptive radiotherapy for proton and photon treatments.

METHOD AND MATERIALS

Data from 150 pelvic patients with paired planning CT and CBCT were used in this study. All CT images were collected in GE LightSpeed VCT scanner and CBCT images were acquired with Varian Truebeam. A 2.5D pixel to pixel generative adversarial network (2.5D GAN) model with feature matching (FM) loss was trained to translate from a source domain (CBCT) to a target domain (dCBCT). Image pre-processing including denoising and suppressing non-uniformity by a non-local means method. Registration was applied to map the planning CT to CBCT using Velocity and worked as the ground-truth CT. A total of 10800 slices were used for training and validating the GAN-based model, while 1200 slices of CT and CBCT were used for testing. The obtained deep-learning based CBCT were compared to ground-truth CT in terms of mean absolute error (MAE) in Hounsfield Unit (HU) and peak signal-to-noise ratio (PSNR), and compared with other deep learning methods, including U-net, 2D GAN without FM, 2.5D GAN without FM, 2D GAN with FM.

RESULTS

A 10-fold cross-validation was used to evaluate the deep-learning algorithm. The mean MAE improved from 26.1 ± 9.9 HU (CBCT vs. CT) to 8.1 ± 1.3 HU (dCBCT vs. CT) for all 1200 test slices and the PSNR also increased from 16.7 ± 10.2 (CBCT vs. CT) to 24.0 ± 7.5 (dCBCT vs. CT). The experiments were performed on a GPU-optimized workstation with a single NVIDIA GeForce GTX Titan X (12GB, Maxwell architecture) and written in Python 3.5. After training the model, each slice took 11-12 ms to process and a 3D-volume of the dCBCT (80 slices) could be generated in less than one second.

CONCLUSION

We presented a deep-learning based algorithm to improve CBCT image quality close to the level of CT in a time efficient manner

which opens up the possibility for online CBCT-based adaptive radiotherapy.

CLINICAL RELEVANCE/APPLICATION

The presented method is also promising as the improved quality CBCT scan can achieve close HU density to CT, thus have the potential to be used for adaptive planning.

SSM23-04 Evaluating the Complimentary Role of Pseudo-STIR in Assessment of Hyperintense Marrow Lesions as Compared to T2-STIR

Wednesday, Dec. 4 3:30PM - 3:40PM Room: S102CD

Participants

Sriram Rajan, MD, New Delhi, India (Presenter) Nothing to Disclose

Geetanjali Tomar, MD, Ahmedabad, India (Abstract Co-Author) Nothing to Disclose

Harsh Mahajan, MD, MBBS, New Delhi, India (*Abstract Co-Author*) Director, Mahajan Imaging Pvt Ltd; Research collaboration, General Electric Company; Research collaboration, Koninklijke Philips NV; Research collaboration, Qure.ai; Research collaboration, Predible Health

Murali Murugavel, PhD, New Delhi, India (Abstract Co-Author) Nothing to Disclose

Madhuri Barnwal, New Delhi, India (Abstract Co-Author) Nothing to Disclose

Salil Gupta, BEng, New Delhi, India (Abstract Co-Author) Nothing to Disclose

Vidur Mahajan, MBBS, New Delhi, India (*Abstract Co-Author*) Researcher, CARING; Associate Director, Mahajan Imaging; Research collaboration, General Electric Company; Research collaboration, Koninklijke Philips NV; Research collaboration, Qure.ai; Research collaboration, Predible Health; Research collaboration, Oxipit.ai; Research collaboration, Synapsica; Research collaboration, Quibim Vasanthakumar Venugopal, MD, New Delhi, India (*Abstract Co-Author*) Consultant, CARING; Research collaboration, General Electric Company; Research collaboration, Synapsica; Research collaboration, General Electric Company; Research collaboration, Koninklijke Philips NV; Research collaboration, Qure.ai; Research collaboration, General Electric Company; Research collaboration, Koninklijke Philips NV; Research collaboration, Qure.ai; Research collaboration, Predible Health; Research collaboration, Synapsica; Research collaboration, Predible Health; Research collaboration, Oxipit.ai; Research collaboration, Synapsica; Research collaboration, Quibim

For information about this presentation, contact:

vasanthdrv@gmail.com

PURPOSE

T2W weighted images contain inherent T1W weighted contrast. Pseudo-STIR images are generated by a simple post processing technique of subtracting T1W images from the T2W images. In this study we probe the diagnostic value of Pseudo-STIR to identify hyperintense marrow lesions in comparison with T2 STIR sequences.

METHOD AND MATERIALS

117 spine MR cases with sagittal T1FSE (n=85) or T1 FLAIR (n=32), T2W and STIR images from studies performed on 1.5T and 3.0T machines were extracted from PACS. The Pseudo-STIR images were created on an Osirix workstation by using the subtraction tool. The resulting 234 sets of STIR and Pseudo-STIR images were anonymized and blindly read by three independent Radiologists (R1, R2, R3 with 13 years, 16 years and 32 years of experience) with respect to the number of hyperintense lesions seen. The quality of study, and the confidence level of the observer in rating the lesions were also encoded. Accuracy for each Pseudo-STIR case was determined based on the observers' ability to match their independently reported count of the corresponding STIR Image.

RESULTS

The accuracy of the observers in reporting the count of hyper intense lesions in the Pseudo-STIR cases was reasonably good (R1: 69 %, R2: 78 %, R3: 64 %). The accuracy increased when the observers reported on cases where they assigned the highest image quality rating of three. All three reporters were more accurate while reporting cases that they gave the highest confidence rating of three (R1: 75 %, R2: 80 %, R3: 69%). It was observed that only two out of 117 cases (both T1 FLAIR derived Pseudo-STIR) were incorrectly marked by all three observers. Additionally, there was no significant bias in quality rating (at the highest rating of three) with respect to the Pseudo-STIR origin, with R1 (76% / 24%), R2 (77% / 23%) and R3 (69% / 31%) scoring in line with the data distribution (73% / 27%). Finally, statistical testing for difference in accuracy based on Pseudo-STIR origin (T1FSE / T1 FLAIR), revealed no difference in each of the three observers.

CONCLUSION

These results point to the value offered by including STIR sequence in an MSK protocol. In the absence of a specific view plane, a Pseudo-STIR provides supporting evidence.

CLINICAL RELEVANCE/APPLICATION

In this study, we demonstrate potential complimentary value offered by a simple post processing technique especially in situations where the STIR sequence is not obtained prospectively

SSM23-05 Prediction of Cervical Nodal Metastasis Using Primary Head and Neck Cancer Tumor Deep Features Extracted from Dual-Energy CT Color Iodine Maps

Wednesday, Dec. 4 3:40PM - 3:50PM Room: S102CD

Participants

Avishek Chatterjee, Montreal, QC (*Presenter*) Nothing to Disclose Martin Vallieres, PHD, Montreal, QC (*Abstract Co-Author*) Nothing to Disclose Jan Seuntjens, PHD, Montreal, QC (*Abstract Co-Author*) Nothing to Disclose Reza Forghani, MD,PhD, Cote Saint-Luc, QC (*Abstract Co-Author*) Researcher, General Electric Company; Institutional research collaboration, General Electric Company; Consultant, General Electric Company; Speaker, General Electric Company ; Founder, 4intelligent Inc; Stockholder, 4intelligent Inc; Stockholder, Real-Time Medical, Inc

PURPOSE

Establish whether convolutional neural networks (CNNs) pre-trained on everyday color images can be repurposed for prediction of lymphadenopathy based on primary tumor characteristics alone, using dual-energy CT color iodine maps.

METHOD AND MATERIALS

The dataset comprised 84 patients with head-and-neck squamous-cell-carcinoma. DICOM images of the central tumor slice (8 bits in each RGB channel) were converted to PNG format. The part of each image outside the tumor was made black. Images were cropped to the sizes appropriate for use with pre-trained CNNs. Three feature extraction methods (a method being defined by a CNN and a layer within it) were used: Alexnet 'fc6', Alexnet 'fc7', and Resnet18 'pool5'. This produced 4096, 4096, and 512 features, respectively. In all 3 cases, LASSO (variable selection and model building using L1 regularization) was used to choose a minimal set of features that are combined linearly to build a prediction model. The chosen λ parameter minimized the mean-squared-error (MSE). Performance metrics based on 4-fold cross validation were obtained. The reduced feature was fed to the t-distributed Stochastic Neighbor Embedding (t-SNE) algorithm to reduce dimensionality to 2 and illustrate the patients with positive and negative outcomes using a scatter plot.

RESULTS

LASSO chose 3 features for Alexnet 'fc6', 11 features for Alexnet 'fc7', and 7 features for Resnet18 'pool5'. Alexnet 'fc6' had accuracy = 0.76, sensitivity = 0.74, specificity = 0.79, and AUC = 0.86. We report the performance of the most parsimonious model (3 features) as it is least likely to suffer from over-fitting. The left figure shows how the λ parameter was chosen. The right figure shows the 2D representation of the cohort as obtained using the t-SNE algorithm. The hand-drawn line shows a separation accuracy consistent with what was reported.

CONCLUSION

To the best of our knowledge, this is the first demonstration that color iodine maps can be analyzed using pre-trained CNNs to for tumor characterization beyond what is currently done in clinical practice. The results need to be corroborated with external validation.

CLINICAL RELEVANCE/APPLICATION

This first successful demonstration of using iodine maps as color images to produce a quantitative biomarker using deep learning could lead to superior utilization of these maps.

SSM23-06 Imaging-Based Survival Prediction of Liver Cancer Patients Using Cox Proportional Hazard Models with Quantitative Texture and Shape Features

Wednesday, Dec. 4 3:50PM - 4:00PM Room: S102CD

Participants

Hansang Lee, Daejeon, Korea, Republic Of (*Presenter*) Nothing to Disclose Helen Hong, PhD, Seoul, Korea, Republic Of (*Abstract Co-Author*) Nothing to Disclose Hyun J. Kim, Seoul, Korea, Republic Of (*Abstract Co-Author*) Nothing to Disclose Hwa Kyung Byun, Seoul, Korea, Republic Of (*Abstract Co-Author*) Nothing to Disclose Jinsil Seong, MD, PhD, Seoul, Korea, Republic Of (*Abstract Co-Author*) Nothing to Disclose Jin Sung Kim, PhD, Seoul, Korea, Republic Of (*Abstract Co-Author*) Nothing to Disclose Junmo Kim, Seoul, Korea, Republic Of (*Abstract Co-Author*) Nothing to Disclose

For information about this presentation, contact:

hlhong@swu.ac.kr

hlhong@swu.ac.kr

CONCLUSION

Our method can be applied to construct the imaging feature-based staging system which can predict the survival rate more accurately than the conventional TNM staging. (*This work was supported by Radiation Technology R&D program through the NRF of Korea (NRF-2017M2A2A7A02070427)*)

Background

Prediction of survival period of liver cancer patients is an important task for treatment and therapy planning of patients. However, most of the current survival prediction depends on clinical information such as tumor size and metastasis. In this work, we propose a survival prediction system for liver cancer patients using quantitative imaging features including texture and shape features of tumors. In addition to the validation of the feasibility of imaging features for survival prediction, we analyze the key imaging features significantly affecting the survival of patients.

Evaluation

Our method was evaluated on a CT dataset acquired from 171 liver cancer patients with survival period recordings. All tumors were manually segmented by the clinical expert. From the tumor ROI images, the quantitative imaging features of 128-dimensions consisting of 119 texture features and 9 shape features. The Cox proportional hazard function was then fitted with those imaging features and survival periods. From the fitted Cox model, the features with the highest exponent weights were considered as key features for the survival. In experiments, the survival function was marginally fitted with the imaging-feature-based Cox model, which indicates the imaging features have a potential for survival prediction. In addition, the texture features including LBP and GLRLM low run features and the shape features including solidity and eccentricity were selected as the key features for the patient survival.

Discussion

The proposed method investigates the usefulness of quantitative imaging features instead of conventional patient information to predict time-variant survival in liver cancer patients. Throughout the Cox model fitting with imaging features, it was observed that the entropy-related texture features and size-related shape features have a significant effect on the prediction of the survival period.





SSM24

Radiation Oncology (Head and Neck, Skin)

Wednesday, Dec. 4 3:00PM - 4:00PM Room: S104A



AMA PRA Category 1 Credit ™: 1.00 ARRT Category A+ Credit: 1.00

FDA Discussions may include off-label uses.

Participants

Mauricio E. Gamez-Haro, MD, Columbus, OH (*Moderator*) Nothing to Disclose Stuart E. Samuels, MD, Miami, FL (*Moderator*) Nothing to Disclose

Sub-Events

SSM24-01 Merkel Cell Carcinoma Recurrence Risk Increases with Delay of Post-Operative Radiation Therapy

Wednesday, Dec. 4 3:00PM - 3:10PM Room: S104A

Participants

Nora A. Alexander, BS, Seattle, WA (*Presenter*) Nothing to Disclose Stephanie K. Schaub, MD, Seattle, WA (*Abstract Co-Author*) Nothing to Disclose Daniel S. Hippe, MS, Seattle, WA (*Abstract Co-Author*) Research Grant, Koninklijke Philips NV; Research Grant, General Electric Company; Research Grant, Canon Medical Systems Corporation; Research Grant, Siemens AG Kristina Lachance, MS, Seattle, WA (*Abstract Co-Author*) Nothing to Disclose Jay J. Liao, MD, Seattle, WA (*Abstract Co-Author*) Nothing to Disclose Smith Apisarnthanarax, MD, Seattle, WA (*Abstract Co-Author*) Nothing to Disclose Shailender Bhatia, MD, Seattle, WA (*Abstract Co-Author*) Nothing to Disclose Yolanda D. Tseng, MD, Seattle, WA (*Abstract Co-Author*) Nothing to Disclose Paul Nghiem, MD, PhD, Seattle, WA (*Abstract Co-Author*) Nothing to Disclose Upendra Parvathaneni, MBBS,FRANZCR, Seattle, WA (*Abstract Co-Author*) Nothing to Disclose

For information about this presentation, contact:

noraalex@uw.edu

PURPOSE

Merkel cell carcinoma (MCC) is a rare, aggressive skin cancer often treated with surgery followed by post-operative radiation therapy (PORT). Many factors affect the time interval between definitive surgery and initiation of PORT. The importance of minimizing this interval in MCC is unclear. We therefore evaluated the relationship of local-regional recurrences (LRRs) with the time interval between definitive surgery and initiation of PORT (time to PORT, TTP).

METHOD AND MATERIALS

We used an IRB-approved, prospective MCC registry to evaluate 125 patients with stage I/II (AJCC 8th edition) MCC. All patients had received definitive surgery and PORT that was initiated within 6 months of diagnosis. LRRs were defined as local, in-transit, and/or regional recurrences. Fine & Gray competing risk regression models were used to evaluate associations between the TTP and LRR, with distant recurrences and death treated as competing risks.

RESULTS

The cohort consisted of 125 patients with a median TTP of 41 days [8-125 days]. All were node negative (84% pN0, 16% cN0) and 14% had positive margins following definitive surgery. Median total dose and fractionation of PORT was 50 Gy [42-67 Gy] in 25 fractions [20-37 fractions]. 14% of patients experienced LRR, with a median follow-up of 1622 days [34-4703]. LRR at 5 years was markedly increased for TTP >=8 weeks (25% LRR) as compared to TTP <8 weeks (10% LRR; p=0.049). There was a significant increasing trend toward higher risk of LRR with longer time delays to PORT, with a hazard ratio of 1.17 per 1-week increase in TTP (p=0.003). Importantly, 15 of 17 LRRs (88%) occurred outside the radiation field (specifically, 2 of 3 locally, 5 of 6 in-transit, and 8 of 8 in regional lymph nodes).

CONCLUSION

In this cohort, TTP of >=8 weeks correlated with increased LRRs compared to <8 weeks in patients with stage I/II MCC. In the 4 to 10 week range of TTP, each subsequent week was associated with a 17% increase in LRRs. The majority of LRRs occurred outside the radiation field, suggesting that delay in PORT may allow MCC cells within the surgical bed to spread.

CLINICAL RELEVANCE/APPLICATION

Our data suggest that minimizing time delay to post-operative radiation therapy in patients with localized Merkel cell carcinoma reduces the risk of local-regional recurrence.

SSM24-02 High Dose Rate Brachytherapy in Elderly Patients with Non-Melanoma Skin Cancer - Clinical and Cosmetic Outcome

Participants Ashwatha B. Narayana, MD, Mount Kisco, NY (*Presenter*) Nothing to Disclose Carolyn Troy, BSN,RN, Greenwich, CT (*Abstract Co-Author*) Nothing to Disclose Judith Hasak, BSN,RN, Greenwich, CT (*Abstract Co-Author*) Nothing to Disclose Samuel Cotte, ARRT,RT, Grewnwich, CT (*Abstract Co-Author*) Nothing to Disclose Christopher Fey, Greenwich, CT (*Abstract Co-Author*) Nothing to Disclose

For information about this presentation, contact:

anarayana2@northwell.edu

PURPOSE

High dose rate brachytherapy (HDRBT) is a well-recognonized, but little used form of therapy for early stage non-melanoma skin cancer of the head and neck region. It offers a shorter course of therapy in the elderly population making it an attractive alternative to conventional electron therapy or surgical resection. We present a large series of patients treated with HDRBT using superficial molds with mature follow-up at a single community institution.

METHOD AND MATERIALS

Seventy patients with 81 lesions of either Basal cell carcinoma (BCC, n=53) or Squamous cell carcinoma (SCC, n=28) were treated between August 2013 and April 2019. The sites included nose (n=37), face (n=11), forehead/scalp (n=9), ear (n=8), neck (n=2), and legs (n=14). The median age of the patients was 85 years (range 70-100). The mean size of the lesion was 10 mm (range 3-26mm). Customized Liepzig applicators were used to treat the lesion with a 4 mm margin. A fractionation regimen of 700 cGy per fraction for 6 sessions over two weeks was used. The dose was prescribed at 3 mm depth. The patients were followed regularly in both radiation oncology and dermatology clinics.

RESULTS

The median follow-up was 24 months (range 1-48). The local control was 98% for BCC and 96% for SCC respectively. Two patients, 1 each with SCC and BCC recurred at 3 and 6 months from the time of therapy respectively. Both the recurrences were >2cm in size and involved lower extremity. The cosmetic outlook was excellent in 90% of all cases. Minor late effects in 6 patients included Hypopigmentation (n=3), Hyperpigmentation (n=2), telangiectasia (n=2) and atrophy of the skin (n=1). Two patients experienced wound breakdown 12 and 14 months after completion of therapy. No cases of cartilage necrosis was seen.

CONCLUSION

HDRBT using customized mold applicators offer an alternative option to Mohs surgery in elderly patients with early stage nonmelanoma skin cancers with excellent local control and cosmetic outcome.

CLINICAL RELEVANCE/APPLICATION

High dose rate brachytherapy using customized superficial mold applicators offer an alternative strategy to Mohs surgical resection for elderly patients presenting with early stage basal and squamous cell carcinoma of the skin in the head and neck region.

SSM24-03 Prior Attentions Constrained Convolutional Neural Network-Based Organs Segmentation for Nasopharyngeal Carcinoma Radiotherapy

Wednesday, Dec. 4 3:20PM - 3:30PM Room: S104A

Participants Haibin Chen, Guangzhou , China (*Abstract Co-Author*) Nothing to Disclose Mengqiu Tian, Guangzhou , China (*Abstract Co-Author*) Nothing to Disclose Ying Sun, Guangzhou, China (*Abstract Co-Author*) Nothing to Disclose Yao Lu, Guangzhou, China (*Presenter*) Nothing to Disclose

For information about this presentation, contact:

haibinc@hotmail.com

PURPOSE

To develop a spatially prior attention constrained convolutional neural network for the accurate organs at risk (OARs) segmentation in nasopharyngeal carcinoma (NPC) radiotherapy.

METHOD AND MATERIALS

To achieve OARs segmentation for NPC radiotherapy, a stepwise segmentation refinement(SSR) framework is proposed, which includes three segmentation steps: OARs groups, large/easy OARs and small/difficult OARs segmentation. 41 OARs are included in this segmentation task. Firstly, all OARs are divided as four groups, and segmented on the down sampled image via 3D ResUNet (UNet with residual shortcut connections). With the segmented mask of each OAR group, a smaller region of interest (ROI) is obtained for the large volume or easy OARs segmentation. Considering the previous rough segmentation as a spatial prior, we developed a prior attention constrained UNet (termed as PAUNet), in which, the feature maps extracted by double convolution is multiplied with the spatial attention combined from the prior and channel averaged feature map. The small/difficult OARs group is also regarded as one target and segmented in this step. Similarly, the small OARs(such as optical nerve, pituitary, etc.) are also segmentation refinement framework is evaluated on 139 CT images from NPC patients. 112 patients are used for training, and the rest are for testing. The segmentation accuracy is quantitatively evaluated by the Dice's coefficient (DSC). Higher DSC indicates more accurate OAR segmentation.

RESULTS

With the SSR framework, the PAUNet achieved superior performance than UNet with mean DSC improved from $50.3\% \sim 91.7\%$ to $55.9\% \sim 93.7\%$ for all OARs. For the OARs with small volume or low contrast, the proposed method improves the mean DSC from $65.9(\pm 9.9)\%$, $66.4(\pm 9.3)\%$, $52.5(\pm 13.7)$ and $50.3(\pm 35.8)\%$ to $76.3(\pm 7.7)\%$, $75.9(\pm 5.4)\%$, $60.3(\pm 14.2)$ and $55.9(\pm 33.2)\%$ for right optical nerve, left optical nerve, chiasm and pituitary, respectively. Figure 1 illustrates the segmentation result of a test case.

CONCLUSION

41 OARs are segmentated accurately based on the proposed PAUNet based SSR framwork, which is superior over the UNet.

CLINICAL RELEVANCE/APPLICATION

The accurate quantitative evaluation results demonstrate the PAUNet based SSR framework is effective in OARs segmentation for NPC radiotherapy, which is also suitable for H&N radiotherapy.

SSM24-04 The Prognostic Significance of Post-Treatment FDG-PET/CT after Definitive Chemoradiation Therapy in Oropharyngeal Squamous Cell Carcinoma

Wednesday, Dec. 4 3:30PM - 3:40PM Room: S104A

Awards

Trainee Research Prize - Medical Student

Participants

Hetal Patel, BS, St. Louis, MO (*Presenter*) Nothing to Disclose Prashant Gabani, MD, Saint Louis, MO (*Abstract Co-Author*) Nothing to Disclose Re-I Chin, St. Louis, MO (*Abstract Co-Author*) Nothing to Disclose Douglas Adkins, Saint Louis, MO (*Abstract Co-Author*) Nothing to Disclose Farrokh Dehdashti, MD, Saint Louis, MO (*Abstract Co-Author*) Nothing to Disclose Mackenzie Daly, St. Louis , MO (*Abstract Co-Author*) Nothing to Disclose Hiram A. Gay, MD, Saint Louis, MO (*Abstract Co-Author*) Nothing to Disclose Wade L. Thorstad, MD, Saint Louis, MO (*Abstract Co-Author*) Nothing to Disclose

PURPOSE

To determine if 3-month post-therapy PET/CT with F-18 fluorodeoxyglucose (FDG) can predict clinical outcomes in patients with oropharyngeal squamous cell carcinoma (OPSCC) treated with definitive chemo-radiation therapy (CRT).

METHOD AND MATERIALS

An IRB-approved retrospective database was used to identify patients with OPSCC treated with definitive CRT between 2004 - 2016. Patients receiving any surgery and RT alone were excluded. The 3-month post-CRT FDG-PET/CT studies were reviewed for complete response (CR), presence of residual FDG uptake (RD), and increase in FDG uptake and/or new areas of FDG uptake (i.e. progressive disease, PD). Patient- and treatment-specific factors including age, race, stage, HPV/p16 status, smoking status, type of chemotherapy, RT dose, and treatment response by post-CRT PET/CT were analyzed using multivariable cox proportional hazards method to evaluate factors associated with locoregional control (LRC), distant control (DC), and overall survival (OS). Kaplan-Meier method and log-rank statistics were used to compare LRC, DC, and OS between patients with CR, RD, and PD.

RESULTS

A total of 96 patients were included. The median follow-up was 44.7 months. The median age at diagnosis was 57.7 (range: 38.5-87.2) years. HPV/p16 status was positive in 34.4%, negative in 18.8%, and not assessed in 46.9% patients. Concurrent cisplatin chemotherapy was used in 76% patients. On multivariate analysis, HPV/p16 positivity was associated with an improved OS (HR 0.19, 95% CI 0.06 - 0.63, P = 0.01). Patients who had RD (HR 5.20, 95% CI 2.25 - 12.02, P<0.001) and PD (HR 12.25, 95% CI 4.48 - 33.48, P<0.001) on post-CRT PET/CT had a worse OS compared to patients with CR. Smoking history, T- and N- Stage, and gender were not associated with OS. The 4-year OS was 87.0% in patients with CR, 32.8% in patients with RD, and 0.0% in patient with PD (P<0.001) on post-CRT PET/CT (Fig 1). Similarly, the 4-year LRC and DC was 93.3% and 97.8% in patients with CR, 65.6% and 71.3% in patients with RD, and 41.7% and 12.5% in patients with PD (P<0.001).

CONCLUSION

Patients with CR on 3-month post-CRT FDG-PET/CT have improved clinical outcomes compared to those with RD or PD.

CLINICAL RELEVANCE/APPLICATION

Three-month post-treatment PET/CT can help predict clinical outcomes and is recommended after definitive chemoradiation therapy of oropharyngeal squamous cell carcinoma to guide further treatment.

SSM24-05 NBTXR3 Hafnium Oxide Nanoparticles Activated by IMRT for the Treatment of Locally-Advanced HNSCC in Frail and/or Elderly Patients: A Phase I/II Study

Wednesday, Dec. 4 3:40PM - 3:50PM Room: S104A

Participants

Christophe Le Tourneau, Paris, France (Presenter) Advisory Board, DSD; Advisory Board, BDS; Advisory Board, GSK ; Advisory Board, F. Hoffmann-La Roche Ltd; Advisory Board, Nanobiotix; Advisory Board, Celgene Corporation; Advisory Board, Mvaitis Valentin Calugaru, Paris, France (Abstract Co-Author) Speaker, Nanobiotix Victor Moreno Garcia, Madrid, Spain (Abstract Co-Author) Speaker, Nanobiotix Xavier Mirabel, Lille, France (Abstract Co-Author) Speaker, Nanobiotix Bernard Doger, Madrid, Spain (Abstract Co-Author) Speaker, Nanobiotix Emiliano Calvo, Madrid, Spain (Abstract Co-Author) Speaker, Nanobiotix Jacek Fijuth, Lodz, Poland (Abstract Co-Author) Speaker, Nanobiotix Tomasz Rutkowski, Gliwice, Poland (Abstract Co-Author) Speaker, Nanobiotix Nicolas Magne, Saint-priest-en-Jarez, France (Abstract Co-Author) Speaker, Nanobiotix Miren Sanz Taberna, Barcelona, Spain (Abstract Co-Author) Speaker, Nanobiotix Jorge Contreras, Malaga, Spain (Abstract Co-Author) Speaker, Nanobiotix Irene Brana, Barcelona, Spain (Abstract Co-Author) Speaker, Nanobiotix Zsuzsanna Papai, Budapest, Hungary (Abstract Co-Author) Speaker, Nanobiotix Zoltan Takacsi-Nagy, MD, Budapest, Hungary (Abstract Co-Author) Speaker, Nanobiotix Xavier Liem, Lille, France (Abstract Co-Author) Speaker, Nanobiotix Sebastien Salas, Marseille, France (Abstract Co-Author) Speaker, Nanobiotix

Stephanie Wong, Marseille, France (*Abstract Co-Author*) Speaker, Nanobiotix; Carmen Florescu, Caen, France (*Abstract Co-Author*) Speaker, Nanobiotix Juliette Thariat, Caen, France (*Abstract Co-Author*) Speaker, Nanobiotix Caroline Hoffmann, Paris, France (*Abstract Co-Author*) Speaker, Nanobiotix

PURPOSE

Elderly head and neck squamous cell carcinoma (HSNCC) patients (pts) ineligible for standard of care treatment require new therapeutic approaches. NBTXR3, hafnium oxide nanoparticles, may represent such an option. NBTXR3 is activated by radiotherapy, enhancing its effects, leading to physical destruction of cancer cells. A Phase I/II trial [NCT01946867] is underway to evaluate NBTXR3 in elderly (>=70 years) or frail pts with HNSCC of the oral cavity and oropharynx ineligible for cisplatin or intolerant to cetuximab.

METHOD AND MATERIALS

Pts received a single intratumoral injection of NBTXR3 and intensity modulated radiation therapy (IMRT; 70 Gy/35 fractions/7 weeks). The study was a 3 + 3 dose escalation to test the NBTXR3 dose equivalent to 5, 10, 15, and 22% of baseline tumor volume, followed by a dose expansion. Primary endpoints include Recommended Phase 2 Dose (RP2D) determination and early dose limiting toxicities (DLT). Presence of NBTXR3 in surrounding healthy tissues and efficacy (RECIST 1.1 principles) were also evaluated.

RESULTS

Enrollment for the dose escalation phase was completed at all dose levels: 5% (3 pts), 10% (3 pts), 15% (5 pts), and 22% (8 pts). No early DLT or SAE related to NBTXR3 or injection were observed. One G1 AE (asthenia; 22%) related to NBTXR3 and four AEs (G2 oral pain, G1 tumor hemorrhage, G1 asthenia, and G1 injection site hemorrhage) related to injection were reported. RT-related toxicity was as expected. The RP2D has been determined to be 22%. CT-scan assessment demonstrated absence of NBTXR3 in surrounding tissues. Among 13 evaluable pts treated at doses >=10%, 9 achieved complete response of the injected lesion. The final dose escalation safety results will be presented herein.

CONCLUSION

NBTXR3 was well tolerated at all tested doses and demonstrated a good safety profile. A dose expansion phase has started with the identified RP2D. NBTXR3 is currently being evaluated in a phase II/III trial in soft tissue sarcoma [NCT02379845] and phase I/II trials in prostate [NCT02805894], liver [NCT02721056] and rectal [NCT02465593] cancers.

CLINICAL RELEVANCE/APPLICATION

The results of this study highlight the potential of NBTXR3 as a novel treatment option for elderly and/or frail pts with locally advanced HNSCC and address an unmet medical need.

SSM24-06 Image-Guided Radiotherapy with Multimodal Gold Nanoconstructs Improves the Radiation Response of Head and Neck Tumor Xenografts

Wednesday, Dec. 4 3:50PM - 4:00PM Room: S104A

Participants

Gayatri Sharma, PhD, Milwaukee, WI (*Presenter*) Nothing to Disclose Abdul K. Parchur, PhD, Milwaukee, WI (*Abstract Co-Author*) Nothing to Disclose Jaidip Jagtap, PhD, Milwaukee, WI (*Abstract Co-Author*) Nothing to Disclose Brian Fish, Milwaukee, WI (*Abstract Co-Author*) Nothing to Disclose Carmen R. Bergom, MD, PhD, Okauchee, WI (*Abstract Co-Author*) Nothing to Disclose Meetha Medhora, Milwaukee, WI (*Abstract Co-Author*) Nothing to Disclose Michael H. Flister, Milwaukee, WI (*Abstract Co-Author*) Nothing to Disclose Amit Joshi, Milwaukee, WI (*Abstract Co-Author*) Nothing to Disclose

PURPOSE

Image-guided radiotherapy (IGRT) is the state of the art treatment for Head and Neck Cancer (HNC) patients. MRI and CT are the preferred imaging modalities for planning IGRT. Here, we report the use of 100nm theranostic nanoparticles (TNPs) with combined X-ray and MR contrast that can enable pre-procedure radiotherapy planning, as well as enhance radiation treatment efficacy.

METHOD AND MATERIALS

TNPs were synthesized on Au nanorods core by depositing epilayers of Gd2O3:Yb/Er, resulting in particles with optical, X-ray, and MR contrast. X-ray contrast was calibrated at 60kV on a Pxinc's X-RAD SmART scanner, and MR contrast was determined on a Brukur 9.4T small animal and GE 7T human scanners. Human HNC cell (OSC-19-luc) were orthotopically implanted in the tongue of immune compromised rats. The efficacy of TNPs in enhancing radiation therapy response was tested via both intra-tumoral (1*1014 TNPs) and systemic (tail vein) delivery (1 μ L/g of 1*1013 TNPs). Rats bearing tumors were randomized to saline+radiation (n=4) or TNP+radiation (n=7) groups. 8-Gy single dose radiation under CT or MRI guidance was provided immediately for intratumoral delivery, and 4h post tail vein injection for systemic delivery. Rats were followed via bioluminescence imaging for 4 weeks.

RESULTS

TNP demonstrated both X-ray and MR contrast in a dose linearly dependent manner. Tumors were clearly delineated in MRI images after i.v. injection of TNPs (Fig. 1A). MRI images showed optimal tumor-to-background ratio at 4h post injection (Fig. 1B). CT images also clearly identified the enhancement post-intratumoral injection of TNPs (Fig 1C). Following IGRT treatment, tumors in both intravenous and intratumoral TNP treated rats' responded superior to radiation therapy controls (Fig. 1D). Rats treated with TNPs and radiation experienced reduced tumor growth (Fig. 1E and F) and lung metastasis while rats treated with radiation alone increased tumor growth. These results indicate the therapeutic efficacy of TNPs in combination with IGRT.

CONCLUSION

TNPs allow an accurate demarcation of the tumor and also increase efficiency of radiation treatment.

CLINICAL RELEVANCE/APPLICATION

Theranostic nanoparticles with combined X-ray and MR contrast can enable pre-procedure radiotherapy planning, as well as enhance radiation treatment efficacy.





SSM25

Vascular/Interventional (Mixed Oncology/Embolization Science)

Wednesday, Dec. 4 3:00PM - 4:00PM Room: S403B



AMA PRA Category 1 Credit ™: 1.00 ARRT Category A+ Credit: 1.00

Participants

Paul M. Haste, MD, Indianapolis, IN (*Moderator*) Research support, Boston Scientific; Consultant, Boston Scientific Claire Kaufman, MD, Salt Lake City, UT (*Moderator*) Nothing to Disclose

Sub-Events

SSM25-01 Novel Performance Descriptor for Contrast-Free Ultrasound Microvascular Imaging Based on Spatio-Temporal Correlation of the Doppler Ensemble

Wednesday, Dec. 4 3:00PM - 3:10PM Room: S403B

Participants Rohit Nayak, PhD, Rochester, MN (*Presenter*) Nothing to Disclose Mostafa Fatemi, PhD, Rochester, MN (*Abstract Co-Author*) Nothing to Disclose Azra Alizad, MD, Rochester, MN (*Abstract Co-Author*) Nothing to Disclose

For information about this presentation, contact:

nayak.rohit@mayo.edu

PURPOSE

Despite effective clutter filtering, presence of motion in ultrasound microvascular imaging (USMI) can lead to incoherent integration of the Doppler ensemble (DE), resulting in poor blood flow visualization. A motion corrupted DE can lead to over- or underestimation of blood vessels [1], resulting in misleading diagnosis without any indication or forewarning. We hypothesize that the proposed spatiotemporal correlation matrix as a reliable indicator of coherency of the DE to (1) determine in real-time if the acquired DE is corrupted by motion, (2) identify frames in the DE that needs motion correction (MC) or rejection, and (3) determine the efficacy of MC of *in vivo* patient data, where ground truth is unavailable.

METHOD AND MATERIALS

We conducted in vivo USMI on 10 thyroid nodules -- prone to motion due to its proximity to the pulsating carotid artery. Thyroid displacements were estimated using normalized 2D cross-correlation and were motion corrected [1]. The pixels associated with the thyroid nodule in the DE were rearranged in the Casorati form and their correlation matrices were estimated [2]. [1] Non-contrast agent based small vessel imaging of human thyroid using motion corrected power Doppler imaging. Scientific Reports, 2018. [2] Non-invasive Small Vessel Imaging of Human Thyroid Using Motion-Corrected Spatiotemporal Clutter Filtering. UMB, 2019.

RESULTS

Visualization of the blood vessel substantially improved upon MC (Fig.1a-d). Correspondingly, the mean correlation of the DE (e,f) increased by 33 % upon MC, which is important for coherent integration of the DE [2]. Further, the frames 1580 - 1848 displayed relatively lower correlation even after MC, which indicated out-of-plane motion that cannot be motion corrected, and thus should be rejected prior to integration of the DE. Further, a mean-correlation-image estimated using overlapping 3x3 kernels was useful in assessing the quality of USMI, and in identifying regions that lacked visualization of the blood flow signal due to incoherency of the DE.

CONCLUSION

These preliminary results were encouraging for large-scale in vivo validation.

CLINICAL RELEVANCE/APPLICATION

Non-invasive, contrast-free USMI could be invaluable in detection and monitoring of diseases and cancerous masses. This technology addresses a key issue of obtaining robust, real-time feedback on if the absence of microflow signal in USMI is accurate and quantifies its degree of trustworthiness.

SSM25-02 Comparison of High-Resolution Cone-Beam CT and Multi-Detector Computed Tomography for Abdominal Post-Embolization Imaging: Effect on Image Quality, Workflow, Radiation Dose, and Accuracy of Lesion Volumetry

Wednesday, Dec. 4 3:10PM - 3:20PM Room: S403B

Participants

Leona Alizadeh, Frankfurt, Germany (*Abstract Co-Author*) Nothing to Disclose Thomas J. Vogl, MD, PhD, Frankfurt, Germany (*Presenter*) Nothing to Disclose Moritz H. Albrecht, MD, Charleston, SC (*Abstract Co-Author*) Speaker, Siemens AG Richard D. Maeder, Frankfurt, Germany (*Abstract Co-Author*) Nothing to Disclose

PURPOSE

To assess latest-generation intraprocedural cone-beam computed tomography (CBCT) versus multi-detector computed tomography (MDCT) after conventional transarterial chemoembolization (cTACE), regarding visualization of ethiodized oil distribution, imagequality, effective-dose, and tumor volumetry in patients with hepatic malignant tumors.

METHOD AND MATERIALS

114 patients (64 female, mean age 57 \pm 14 years) who had undergone TACE followed by CBCT and MDCT of the upper abdomen were included. Image quality scores were compared for both efficacy and complications and overall image quality between CBCT and MDCT images by two blinded readers using 4-point Likert-scales. Lesion volume was measured in both modalities and compared to values from pre-interventional T2-weighted MRI. In addition, we performed effective dose measurements for CBCT and two MDCT protocols using an anthropomorphous phantom.

RESULTS

CBCT outperformed MDCT in terms of efficacy and complications (mean score, 3.2 ± 0.7 versus 2.6 ± 0.4 , p=0.01X). Overall image quality was inferior for CBCT (mean score, 2.8 ± 0.7 versus 3.1 ± 0.4 for MDCT, p<0.001). The 4-second CBCT protocol showed a higher mean effective dose of 4.7 mSv compared to MDCT, we measured 2.5 mSv with a scan-length of 22.6 cm and 2.1 mSv for a shorter length of 17.3 cm, corresponding to the shorter CBCT field-of-view. No significant differences were found regarding volumetry of malignant lesions compared to MRI (mean volume on CBCT, 26.98 ± 17.43 mm2 and on MDCT: 26.75 ± 16.00 mm2, p=0.661).

CONCLUSION

Latest-generation CBCT facilitate sufficient image quality levels for the performance of this procedure in the post-interventional assessment in patients undergoing TACE at higher, yet acceptable effective dose levels compared to MDCT, while potentially improving the patient safety and clinical workflow. Both CBCT and MDCT can be robustly used for volumetric measurements.

CLINICAL RELEVANCE/APPLICATION

Latest CBCT may be preferentially chosen to MDCT for post lipiodol TACE evaluation as image quality, worklfow and treatment safety benefit from having an intraprocedural feedback, while giving the ability to immediately adjust therapy and react to complications if necessary.

SSM25-03 Survival after Local Therapies for Stage IA/B Renal Cancer: Subgroup Analysis Based on Tumor Histology

Wednesday, Dec. 4 3:20PM - 3:30PM Room: S403B

Participants

Johannes Uhlig, Goettingen, Germany (*Presenter*) Nothing to Disclose Hyun S. Kim, MD, New Haven, CT (*Abstract Co-Author*) Boston Scientific Corporation; Galil Medical Ltd ; Sirtex Medical Ltd

For information about this presentation, contact:

johannes.uhlig@yale.edu

PURPOSE

To assess the effectiveness of local ablation techniques and surgical resection for treatment of stage IA/B renal cell cancer (RCC).

METHOD AND MATERIALS

The 2004-2015 National Cancer Database was searched for stage IA/B RCC. Inclusion criteria were clear cell or papillary RCC, surgical resection (partial or radical nephrectomy), radiofrequency/microwave ablation (RFA/MWA) or cryoablation (CRA), age > 18yo, and complete follow up. RFA/MWA, CRA and surgical resection patients were 1:1:1 propensity score matched to account for confounders, separately for each histology. Overall survival (OS) was compared in the matched cohorts using Kaplan-Meier plots, log-rank tests, and Cox proportional hazards models.

RESULTS

162,640 patients met inclusion criteria: n=153,729 receiving surgical resection (94.5%), n=5,574CRA (3.4%) and n=3,337 receiving RFA/MWA (2.1%). Ablation patients were older, had more comorbidities and were more likely treated at academic centers for smaller diameter papillary RCCs. After multivariable adjustment, overall survival was comparable for papillary RCC and clear cell RCC (HR=0.97, 95% CI: 0.93-1.01, p=0.13). After propensity score matching, two separate cohorts with balanced distribution of patient- and tumor-related confounders were obtained (ccRCC n=6,168; papillary RCC n=1,899). For papillary RCC, OS was comparable for CRA and surgical resection (survival difference p=0.86; 1-year OS: 98 vs 98%; 3-year OS: 91 vs 90%; 5-year OS: 83 vs 83%), but inferior for RFA/MWA (p=0.024; 1-year OS: 97%: 3-year OS: 84%; 5-year OS: 76%). For ccRCC, OS was superior following surgical resection compared to both CRA and RFA/MWA (p<0.001). No statistically significant OS difference was evident comparing CRA and RFA/MWA in ccRCC patients (p=0.523).

CONCLUSION

Utilization of ablation versus resection for stage IA/B RCC varies with patient and tumor characteristics. There is evidence that tumor histology may affect ablation effectiveness, with higher survivals observed for CRA in papillary RCCs.

CLINICAL RELEVANCE/APPLICATION

In stage IA/B papillary RCC, CRA shows comparable survival to surgical resection and superior outcomes over RFA/MWA. CRA may be considered as preferential ablation technique in these cases.

SSM25-04 Image-Guided Percutaneous Thermal Ablation of Gynecologic Cancer Metastasis: A 10-Year Experience of Patient Survival, Technique Efficacy, and Safety Profile

Wednesday, Dec. 4 3:30PM - 3:40PM Room: S403B

Participants

Frank Yuan, MD, Alhambra, CA (*Presenter*) Nothing to Disclose Sindy Wei, MD, PhD, Los Angeles, CA (*Abstract Co-Author*) Nothing to Disclose Gottfried Konecny, MD, Los Angeles, CA (*Abstract Co-Author*) Nothing to Disclose Sanaz Memarzadeh, Los Angeles, CA (*Abstract Co-Author*) Nothing to Disclose Robert D. Suh, MD, Los Angeles, CA (*Abstract Co-Author*) Nothing to Disclose David S. Lu, MD, Los Angeles, CA (*Abstract Co-Author*) Nothing to Disclose David S. Lu, MD, Los Angeles, CA (*Abstract Co-Author*) Consultant, Medtronic plc Speaker, Medtronic plc Consultant, Johnson & Johnson Research Grant, Johnson & Johnson Consultant, Bayer AG Research Grant, Bayer AG Speaker, Bayer AG Steven S. Raman, MD, Santa Monica, CA (*Abstract Co-Author*) Consultant, Johnson & Johnson; Consultant, Bayer AG; Consultant, Merck & Co, Inc; Consultant, Amgen Inc; Consultant, Profound Medical Inc

For information about this presentation, contact:

frankyuanmd@gmail.com

PURPOSE

To assess the safety and efficacy of percutaneous thermal ablation treatment of metastatic GYN cancers.

METHOD AND MATERIALS

With IRB exemption and HIPAA compliance, we derived a study cohort of 42 consecutive women with metastatic GYN cancers treated with radiofrequency or cryogenic ablation from over 2800 ablations performed from 1/30/2001-1/11/2019. All efficacy parameters were reported according to the 2014 International Working Group on Image-guided Tumor Ablation. The technical success rate was defined as complete ablation of the targeted tumor on post-intervention imaging. Primary effectiveness was defined as the percentage of tumors successfully eradicated during the initial course of treatment. Secondary effectiveness was defined as successful eradication by repeated ablation of local tumor progression after complete necrosis was achieved. Major complications were defined as those necessitating unplanned hospitalization, prolonging hospital stay, or additional interventions.

RESULTS

In our study cohort of 42 women (mean age 59.3) with 126 metastatic lesions, the median follow-up was 9 months (range 1- 4022 days). The primary tumor types that were treated are ovarian (stage I-IV), endometrial (stage I, III, IV), uterine (stage II-IV), cervical (stage IB), and vaginal (stage II-III) cancers. Liver, lungs, kidney, peritoneum, lymph nodes, and abdominal soft tissues were targeted sites of metastasis. After the initial ablation session, 92.1% (n= 116/126) of the patients achieved complete tumor necrosis confirmed by contrast-enhanced MRI or CT. On follow-up scans, 7.9% (n= 8) of the previously ablated lesions developed local progression, which resulted in the primary treatment effectiveness of 94.7% (n= 107/113). Five lesions underwent repeated ablation due to local tumor progression with a mean size of 2.78 (SEM +/- 1.16; range 1.5 - 7.4 cm). Of these lesions, 4/5 achieved complete tumor eradication ensuing secondary effectiveness of 80%. Overall technique effectiveness was 94.1% (111/118). The median overall survival from first ablation was 22 months (49 - 4240 days) and the 1, 3, 5, & 10-year survival were 62.9%, 35.7%, 5.7% & 2.9%. The major complication rate was 4.8%.

CONCLUSION

In the largest reported series, thermal ablation was safe and effective for local control of metastatic GYN cancers.

CLINICAL RELEVANCE/APPLICATION

Image guided thermal ablation achieved excellent local control of metastatic GYN lesions.

SSM25-05 Adaptive Suppression of Time Gain Compensated (TGC) Noise Bias for Contrast-Free Ultrasound Microvascular Imaging

Wednesday, Dec. 4 3:40PM - 3:50PM Room: S403B

Participants

Rohit Nayak, PhD, Rochester, MN (*Presenter*) Nothing to Disclose Mostafa Fatemi, PhD, Rochester, MN (*Abstract Co-Author*) Nothing to Disclose Azra Alizad, MD, Rochester, MN (*Abstract Co-Author*) Nothing to Disclose

For information about this presentation, contact:

nayak.rohit@mayo.edu

PURPOSE

Recent advances in contrast-free ultrasound microvascular imaging (USMI) has considerably improved the sensitivity of detecting blood flow. However, suppression of tissue clutter exposes the ramp-shaped time-gain-compensated (TGC) noise bias that noticeably degrades the visualization of the flow signal [1]. We hypothesize that background equalization of USM images based on the noise bias estimated from the entire clutter-filtered singular value (SV) spectrum can considerably improve the visualization of blood vessels, compared to currently existing techniques [1].

METHOD AND MATERIALS

We conducted *in vivo* experiments on 20 patients with suspicious breast lesions. Its efficacy in imaging deeper organs (6-10 cm) was tested through imaging of hepatic and renal microvasculature in 4 healthy volunteers. All USM images were acquired using a clinical ultrasound scanner, implemented with ultrafast imaging, and singular value decomposition (SVD) based spatio-temporal clutter filtering. The TGC-based noise bias was estimated from the clutter filtered Doppler ensemble based on its local spatio-temporal correlation combined with low rank matrix estimation, which was subsequently used for background suppression of USM images.

RESULTS

USM images obtained after clutter filtering were corrupted with ramp-shaped TGC noise bias that increased with depth. The noise bias signal was visible in both superficial breast lesions (<3.5 cm) and deep-seated hepatic and renal (4-9 cm) USM images. The noise equalized USM images obtained using the proposed technique substantially improved the visualization of the blood flow signal [Fig. 1]. The noise bias in the background equalized USM images (b,d,f) were ~ 0dB, invariant of depth, which otherwise varied over 14 dB (a,c,e), respectively.

CONCLUSION

The preliminary results demonstrate the ability of using the proposed technique to improve the visualization of small vessel blood flow in contrast-free USMI. 1.Song, Noise Equalization for Ultrafast Plane Wave Microvessel Imaging.TUFFC 2017.

CLINICAL RELEVANCE/APPLICATION

Non-invasive, contrast-free ultrasound microvascular imaging can be clinically invaluable in early detection and monitoring of angiogenesis in cancerous masses. This technology addresses a key issue of improving the detection of the blood flow signal in USMI, which are poorly visualized at increased depth due to signal attenuation and TGC based amplification of channel noise.

SSM25-06 The Clinical Outcome of Utilizing Prophylactic Covered Stent in Patients with Sentinel Hemorrhage After Pancreaticoduodenectomy

Wednesday, Dec. 4 3:50PM - 4:00PM Room: S403B

Participants Yuan-Mao Lin, MD, Taipei, Taiwan (*Presenter*) Nothing to Disclose Ethan Y. Lin, MD, Sugar Land, TX (*Abstract Co-Author*) Nothing to Disclose Rheun-Chuan Lee, MD, Taipei, Taiwan (*Abstract Co-Author*) Nothing to Disclose

For information about this presentation, contact:

garbato@gmail.com

PURPOSE

To evaluate the clinical outcomes of prophylactic covered stent placement of common hepatic artery (CHA) in patients with sentinel hemorrhage (SH) after pancreaticoduodenectomy (PD) without positive image finding.

METHOD AND MATERIALS

Between July 2006 and September 2018, 27 patients (mean age, 61.3 y) with SH after PD underwent prophylactic covered stent placement of CHA (n = 18) or conservative treatment (n = 9) without positive image finding were enrolled in this retrospective study. All patients received CT angiography (n = 11) or digital subtraction angiography (n = 25) before the treatment. Overall survival, clinical outcome and complications were compared between the groups. Clinical success was defined as sustained cessation of hemorrhage; failure was defined as requiring additional management. Chi-square analysis and Kaplan-Mayer curve were used to analyze each group's result.

RESULTS

The clinical success rates were 55.5 % (5/9), and 88.8% (16/18) (p < .05) in conservative treatment and covered stent groups, respectively. The covered stent group had superior overall survival than conservative group (p < .05). In conservative group, delayed massive hemorrhage occurred in four patients: two died of recurrent bleeding with gastroduodenal artery pseudoaneurysm within sixteen days, and two had intraluminal hemorrhage within five days. In the covered stent group, one had inferior pancreaticoduodenal artery pseudoaneurysm one day after the placement of covered stent, and one patient had recurrent bleeding due to duodenal ulcer within 14 days. A late complication of stent related pseudoaneurysm was observed in one patient eight months after the procedure. There was no stent thrombosis, bile duct necrosis, or intrahepatic artery injury observed on follow-up CT.

CONCLUSION

The prophylactic covered stent placement of CHA can be performed safely and reduced delayed massive hemorrhage and mortality in most patients with SH after PD without positive image finding.

CLINICAL RELEVANCE/APPLICATION

The prophylactic covered stent placement of CHA can be performed safely and reduced delayed massive hemorrhage and mortality in most patients with SH after PD without positive image finding.





SSM26

Vascular/Interventional (Liver Cancer Basic Science)

Wednesday, Dec. 4 3:00PM - 4:00PM Room: S403A



AMA PRA Category 1 Credit ™: 1.00 ARRT Category A+ Credit: 1.00

FDA Discussions may include off-label uses.

Participants

Nadine Abi-Jaoudeh, MD, Orange, CA (*Moderator*) Research collaboration, Koninklijke Philips NV; Research collaboration, Teclison Cherry Pharma Inc; Research support, SillaJen, Inc; Intellectual property and Owner, Bruin Biosciences Inc D. T. Johnson, MD, PhD, South San Francisco, CA (*Moderator*) Inventor, Thunar Medical, Inc

Sub-Events

SSM26-01 Comparison Between HSV-TK Gene Therapy and Oncolytic Virotherapy for Radiofrequency Hyperthermia-Enhanced Treatment of Orthotopic Hepatic Cancer

Wednesday, Dec. 4 3:00PM - 3:10PM Room: S403A

Awards

Trainee Research Prize - Fellow

Participants Shanshan Gao, Seattle, WA (*Presenter*) Nothing to Disclose Jingjing Song Jr, Seattle, WA (*Abstract Co-Author*) Nothing to Disclose Xiaolin Wang, MD, Shanghai, China (*Abstract Co-Author*) Nothing to Disclose Fu Xiong, PhD, MD, Seattle, WA (*Abstract Co-Author*) Nothing to Disclose Spencer M. Cheng, Woodinville, WA (*Abstract Co-Author*) Nothing to Disclose Feng Zhang, MD, Seattle, WA (*Abstract Co-Author*) Nothing to Disclose Xiaoming Yang, MD, PhD, Mercer Island, WA (*Abstract Co-Author*) Nothing to Disclose

For information about this presentation, contact:

17111320002@fudan.edu.cn

PURPOSE

To compare the efficacies between intratumoral herpes simplex virus-thymidine kinase (HSV-TK)/ganciclovir (GCV) gene therapy and oncolytic virotherapy for image-guided radiofrequency hyperthermia (RFH)-enhanced treatment of orthotopic liver cancer.

METHOD AND MATERIALS

Luciferase-labeled rat hepatocellular carcinoma (HCC) cells and 36 rats with orthotopic HCCs were treated in 6 groups: (1) combination therapy with oncolytic viruses (T-VEC) plus RFH; (2) T-VEC alone; (3) HSV-TK/GCV gene therapy plus RFH; (4) gene therapy alone; (5) RFH alone; and (6) saline. For in-vitro experiments, confocal microscopy, MTS assay and bioluminescence optical imaging were used to evaluate cell viabilities and proliferation. For in-vivo validation, HSV-TK or T-VEC were directly infused into HCC masses through a multi-modal perfusion-thermal RF electrode under imaging guidance, followed by RFH at 42 °C for 30 minutes. For gene therapy groups, GCV was intraperitonially administrated daily for 14 days. Optical imaging and ultrasound imaging were used to follow up bioluminescence signal and size changes of tumors, followed by pathology confirmation.

RESULTS

Confocal microscopy showed the significant decreases of cell viabilities and bioluminescence signal intensities in the combination therapy of HSV-TK with RFH or T-VEC with RFH, compared to other monotherapy groups (n=6/group, P <.05). Ultrasound and optical imaging showed that both combination therapies of HSV-TK or T-VEC with RFH caused decreases of average tumor volume and bioluminescence signal intensity, compared to groups with monotherapy (n=6/group, P <.05). However, no statistically significant differences were found between the two combination therapy groups. Pathology examination with apoptosis analysis further confirmed these imaging findings.

CONCLUSION

Both intratumoral HSV-TK/GCV gene therapy and oncolytic virotherapy combined with RFH have the synergistic therapeutic effect on hepatic cancers, but no efficacy difference was found between these two combination therapies, which indicates RFH-enhanced oncolytic virotherapy is favorable for managing hepatic cancers, since the oncolytic virus, T-VEC, has been approved by FDA for human cancer treatment.

CLINICAL RELEVANCE/APPLICATION

RFH-enhanced oncolytic virotherapy is favarable for hepatic cancers, since the oncolytic virus, T-VEC, has been approved by FDA for human cancer treatment.

SSM26-02 Yttrium-90 Radioembolization as a New Treatment for Brain Cancer: Proof of Concept in a Canine Spontaneous Brain Tumor Model

Participants

Alexander S. Pasciak, PHD, Laurel, MD (*Presenter*) Research Grant, BTG International Ltd
Sasicha Manupipatpong, Baltimore, MD (*Abstract Co-Author*) Nothing to Disclose
Ferdinand K. Hui, MD, Richmond, VA (*Abstract Co-Author*) Speakers Bureau, Terumo Corporation Speakers Bureau, Penumbra, Inc
Stockholder, Blockade Medical Inc
Rebecca Krimins, DVM,MS, Baltimore, MD (*Abstract Co-Author*) Nothing to Disclose
Larry Gainsburg, Baltimore , MD (*Abstract Co-Author*) Nothing to Disclose
Matthew R. Dreher, PhD, Rockville, MD (*Abstract Co-Author*) Technical Director, Biocompatibles International plc
Dara L. Kraitchman, DVM, PhD, Baltimore, MD (*Abstract Co-Author*) Research Grant, Galil Medical
Clifford R. Weiss, MD, Baltimore, MD (*Abstract Co-Author*) Research Grant, Siemens AG Research Grant, Merit Medical Systems, Inc
Research Grant, BTG International Ltd Medical Advisory Board, Clear Guide Medical LLC Founder, Avasys, LLC Officer, Avasys, LLC

For information about this presentation, contact:

Alexander.pasciak@icloud.com

PURPOSE

To evaluate Yttrum-90 (Y90) radioembolization (RE) as a minimally invasive treatment for brain cancer in a canine model.

METHOD AND MATERIALS

Three healthy research dogs (R1-R3) and two patient dogs with spontaneous intra-axial brain tumors (T1-T2) underwent transarterial RE with Y90 glass microspheres. Both tumors enhanced on pre-treatment MRI and were compatible with high-grade glioma. Y90RE was performed on research dogs from unilateral MCA, PCA or ICA while both dogs with tumors were treated from the ICA. Post-treatment Y90 PET/CT was performed along with serial, weekly neurological exam by a veterinary neurologist. One month after treatment, a post-treatment MRI was obtained on all animals.

RESULTS

Average absorbed-dose for dogs R1-R3 calculated from Y90 PET/CT were: 20.2±2.8 Gy to the whole treated hemisphere, 52.5±23.5 Gy to the perfused tissue region and doses to the basal ganglia/thalamus ranging from 10.2-67.2 Gy depending on the treated territory. Dog T1 received 8.4 Gy to uninvolved brain and 35.0 Gy to tumor, while dog T2 received 13.2 Gy to uninvolved brain and 115.2 Gy to tumor. Transient changes in neurological exam lasting between 1-3 weeks before resolution were found in dogs R1, R2 and T1 and included unilateral delayed proprioception, postural reaction, decreased facial sensation and vision. Post-treatment MRI on dogs R1-R3 demonstrated absence of cortical atrophy or microinfarction. At 1-month post-therapy, MRI of dog T1 showed an 83% reduction in tumor volume, resolution of perilesional edema and falx shift as well as absence of cortical atrophy was not appreciated in either tumor bearing animal. T1 and T2 are currently clinically asymptomatic with an unremarkable neurologic exam and are scheduled for repeat MRI imaging at 3 months post-therapy.

CONCLUSION

Y90RE is technically feasible in a canine model. Critical normal brain structures tolerated up to 67.2Gy with complete resolution of symptoms. A favorable dosimetric distribution with increased uptake in tumor is possible even with hemispheric (ICA) treatment. Initial clinical outcomes are positive, however, additional data on safety and efficacy is required.

CLINICAL RELEVANCE/APPLICATION

Y90 radioembolization has shown initial promise in the treatment of spontaneous brain tumors in a canine model.

SSM26-03 Prognostic Significance of Pretreatment Inflammatory Markers in Uveal Melanoma Liver Metastases Undergoing Hepatic Chemoperfusion

Wednesday, Dec. 4 3:20PM - 3:30PM Room: S403A

Participants

Johannes M. Ludwig, MD, Dusseldorf, Germany (*Presenter*) Nothing to Disclose Nicola Spieker, MD, Essen, Germany (*Abstract Co-Author*) Nothing to Disclose Axel Wetter, Essen, Germany (*Abstract Co-Author*) Nothing to Disclose Benedikt M. Schaarschmidt, MD, Essen, Germany (*Abstract Co-Author*) Nothing to Disclose Johannes Haubold, MD, Essen, Germany (*Abstract Co-Author*) Nothing to Disclose Michael Forsting, MD, Essen, Germany (*Abstract Co-Author*) Nothing to Disclose Jens M. Theysohn, MD, Essen, Germany (*Abstract Co-Author*) Nothing to Disclose Jens M. Theysohn, MD, Essen, Germany (*Abstract Co-Author*) Nothing to Disclose Jens M. Theysohn, MD, Essen, Germany (*Abstract Co-Author*) Nothing to Disclose Ophelia 4. Drescher, Essen, Germany (*Abstract Co-Author*) Nothing to Disclose Heike Richly, Essen, Germany (*Abstract Co-Author*) Nothing to Disclose

For information about this presentation, contact:

Johannes-maximilian.ludwig@uk-essen.de

PURPOSE

To evaluate inflammatory markers (CRP, neutrophil to lymphocyte ratio (NLR), platelet to lymphocyte ratio (PLR) and systemic inflammatory index (SII)) as a pretreatment prognostic factors in patients with unresectable uveal melanoma liver metastases undergoing a structured transarterial hepatic chemoperfusion (THC) protocol.

METHOD AND MATERIALS

56 patients (median age: 61 years, 44% male) were retrospectively assessed. A median of 3 (range: 1-11) THC sessions were performed with melphalan replaced by Fotemustin when progressing. Inflammatory markers were calculated as follows: SII: (platelets/nl \times neutrophils/nl)/ (lymphocytes/nl), PLR: (platelets/nl)/(lymphocytes/nl), NLR: (neutrophils/nl)/(lymphocytes/nl).

Kaplan-Meier for median overall survival in months (OS;95%CI) and Cox Proportional Hazard Model for uni- (UVA) & multivariate (MVA) analyses (Hazard ratio;95%CI) were performed.

RESULTS

Median OS of the study cohort was 7.7 (6.3-10.9) months. Overall survival was prolonged for lower values of CRP (non-elevated: 13.5; 7.2-20,6 vs. elevated: 5.2; 3.9-7.7; p=.0003), PLR (<150: 15.8; 6.4-. versus >150: 7; 4.7-8.2, p=.003), SII (<1000: 11; 7.2-20.6 versus >1000: 5.6; 3.9-7.8, p=.0005) and NLR (<3.5: 11.1; 7,1-20.6, vs.>3.5: 6.3; 3.5-7.8, p=.004). MVA confirmed non-elevated CRP (0.37; 0.17-0.78; p=.008) and PLR <150 (0.39; 0.13-0.95p=.038) as independent predictors for longer overall survival. Combining significant values from in MVA improves survival prediction: Patients with non-elevated CRP and low PLR survived the longest (median not reached) vs. patients with either CRP or PLR elevation (11,1; 7-13.5) vs. elevated CRP and PLR (4.8; 3.4-7.5), p<.0001. Difference between each group was statistically significant in UVA.

CONCLUSION

Pretreatment inflammatory markers (CRP, NLR, PLR, SII) play a prognostic role in patient survival with uveal melanoma liver metastases treated with THC. Utilizing pretreatment CRP and PLR as independent predictors may help to identify patients potentially profiting from therapy.

CLINICAL RELEVANCE/APPLICATION

Inflammatory markers play a pivotal role in predicting overall survival and may provide information on treatment effectiveness and to estimate life expectancy. This can help informed clinical treatment decision making and is of great value for patients and their relatives to set expectations regarding transarterial hepatic chemoperfusion as treatment option for patients with uveal melanoma liver metastases.

SSM26-04 Comparison of Parallel and Crossed Placement of Multiple Radiofrequency Electrode in the Treatment of Liver Tumor: An Animal Experiment

Wednesday, Dec. 4 3:30PM - 3:40PM Room: S403A

Participants

Kun Zhao, Beijing, China (*Abstract Co-Author*) Nothing to Disclose An-Na Jiang, Beijing, China (*Abstract Co-Author*) Nothing to Disclose Wei Yang, Beijing, China (*Abstract Co-Author*) Nothing to Disclose Song Wang, Beijing, China (*Presenter*) Nothing to Disclose Zhong-Yi Zhang, PhD, Beijing, China (*Abstract Co-Author*) Nothing to Disclose Kun Yan, BS, Beijing, China (*Abstract Co-Author*) Nothing to Disclose

PURPOSE

The purpose of this study was to investigate the effect of parallel and crossed needle placement with radiofrequency ablation in liver.

METHOD AND MATERIALS

The experiment was performed in ex vivo bovine liver with the radiofrequency generator (Celon) and two electrode needles (200T30). Parallel and crossed needle placements were designed in our experiment. The electrode needles were placed in the shape of '=' in the parallel group and in the shape of 'x' in the crossed group. The ablation zones were compared when the shortest distances of the electrodes (2cm, 2.5cm, 3cm) or the output powers (20W, 25W, 30W) were different.(n=6 for each group). At 2 hours after ablation, the gross pathological specimens were stained with TTC. The long-axis diameter and the short-axis diameter were measured and the coagulation area of ablation zones were compared.

RESULTS

When 25W power was applied and the shortest distances of the electrodes were 2cm, 2.5cm and 3cm, the ablation zones in the two groups were quasi-circular and increased with distance. When the shortest distances were fixed, there was no significant difference in the coagulation area between the two groups (2cm: 4.6x3.7cm vs. 4.8x3.9cm, P=0.369; 2.5cm: 4.8x4.3cm vs.5.0x4.5cm, P=0.661; 3cm: 5.0x4.5cm vs. 5.3x4.6cm, P= 0.339). When the shortest distance was 3.5cm, the coagulation zone could not be fused and was lobulate-shaped. When the shortest distance was 2.5cm and the outputs were 25W and 30W, the coagulation areas were quasi-circular and did not increase with higher power. There was no significant difference. (25W: 4.8x4.3cm vs. 5.0x4.5cm, P=0.452; 30W: 5.1x4.5cm vs. 5.1x4.7cm, P= 0.894). When the output was 20W, the coagulation zone could not be fused in parallel group, while an effective coagulation area was produced in the crossed group (4.4x3.9cm).

CONCLUSION

The traditional opinion is that the crossed placement of electrodes was limited in coagulation area. Our study showed that the ablation zone of the two groups were similar when the shortest distance was the same and the maximum distance no more than 3cm. When the output was reduced, the fusion effect of coagulation area in crossed group was better than that in parallel group. These data provided helpful information for the design of needle placement in radiofrequency ablation of liver tumors.

CLINICAL RELEVANCE/APPLICATION

Radiofrequency ablation is one of the most widely used techniques in tumor ablation.

SSM26-05 A Novel Approach to Liver-Directed Therapy for Metastatic Well-Differentiated Neuroendocrine Tumor: Efficacy of Concurrent Everolimus with Hepatic Transarterial Bland Embolization (EveroEmbo)

Wednesday, Dec. 4 3:40PM - 3:50PM Room: S403A

Participants

Riham H. El Khouli, MD,PhD, Nicholasville, KY (*Abstract Co-Author*) Nothing to Disclose Gaby E. Gabriel, MD, Lexington, KY (*Presenter*) Nothing to Disclose Harit Kapoor, MD, Lexington, KY (*Abstract Co-Author*) Nothing to Disclose Ahmed H. Ragab, MBBCh, Alexandria , Egypt (*Abstract Co-Author*) Nothing to Disclose

```
M. Elizabeth Oates, MD, Lexington, KY (Abstract Co-Author) Nothing to Disclose
Aman Chauhan, Lexington, KY (Abstract Co-Author) Nothing to Disclose
Lowell B. Anthony, MD, Lexington, KY (Abstract Co-Author) Nothing to Disclose
```

PURPOSE

Liver-directed embolization have been the mainstay for locoregional metastatic tumor control. There continues to be considerable controversy around the optimal protocol. Recent studies suggested long-term hepatotoxicity of transarterial radioembolization (TARE). RADIANT-3 and -4 reported Everolimus resulting in median progression-free survival (PFS) of 11 months, while TAE resulted in median hepatic PFS (hPFS) of 15 months. TAE induces ischemic cell injury, yet ischemia- induced activation of vascular endothelial growth factor (VEGF) leads to neovascularization, a known cause of resistance. Everolimus is an mTOR kinase inhibitor shown to inhibit the response of vascular endothelial cells to stimulation by VEGF. Everolimus is typically held 2-4 weeks before and after embolization to minimize toxicity. We hypothesize that the concurrent use of Everolimus with TAE (EveroEmbo) would result in prolonged local liver tumor control compared to either therapy alone.

METHOD AND MATERIALS

Review of all consecutive patients who underwent EveroEmbo between 9/2016 and 12/2018 at the ------. Inclusion criteria included systemic Everolimus for >= 1 month before embolization. For median hPFS analysis, only patients with > 12 months post-TAE imaging were included. An independent radiologist reviewed all baseline and subsequent post-therapy imaging and assessed liver-specific treatment response according to RECIST 1.1 criteria

RESULTS

63 EveroEmbo procedures in 38 consecutive patients were performed. 58% (22/38) were females while 42% (16/38) were males, with mean age of 57.8 ± 12.8 years. Only 40 procedures had sufficient post-procedural imaging to apply RECIST 1.1. Imaging showed 82.5% with partial response and 17.5% with stable disease; no patient had disease progression. The percentage change in liver tumor burden was -46.3% + 18.3%. Among the 63 EveroEmbo procedures, 21 had > 12 months follow-up imaging; no patients progressed to date and their median hPFS was 17 months.

CONCLUSION

Concurrent EveroEmbo is a promising approach for local hepatic disease control with a median hPFS of 17 months. Longer follow-up is needed to assess the true median hPFS in metastatic well-differentiated NETs.

CLINICAL RELEVANCE/APPLICATION

Concurrent EveroEmbo resulted in partial response in 82.5% of patients with a mean of 46% reduction in tumor burden and 17 months median hPFS. To date, none of our patients have evidence of disease progression

SSM26-06 The Inhibiting Effect of All-Trans Retinoic Acid on Liver Cancer Stem-Like Cells after Insufficient RF Ablation

Wednesday, Dec. 4 3:50PM - 4:00PM Room: S403A

Participants

Song Wang, Beijing, China (*Presenter*) Nothing to Disclose Jing-tao Liu, Beijing, China (*Abstract Co-Author*) Nothing to Disclose Hao Wu, Beijing, China (*Abstract Co-Author*) Nothing to Disclose Wei Yang, Beijing, China (*Abstract Co-Author*) Nothing to Disclose Hai-bo Han, PhD, Beijing, China (*Abstract Co-Author*) Nothing to Disclose An-Na Jiang, Beijing, China (*Abstract Co-Author*) Nothing to Disclose Xiu-mei Bai, MD, Beijing, China (*Abstract Co-Author*) Nothing to Disclose Kun Yan, BS, Beijing, China (*Abstract Co-Author*) Nothing to Disclose Yan-hua Zhang, Beijing, China (*Abstract Co-Author*) Nothing to Disclose

For information about this presentation, contact:

worsonwang@163.com

PURPOSE

To investigate the role of tumor stem-like cells (TSCs) in recurrent HCC after insufficient RFA and the effect of combination treatment with all-trans retinoic acid (ATRA) in human HCC models.

METHOD AND MATERIALS

Methods: First, the self-renew ability of HepG2 cells was assessed in vitro at 37°C or 42°C. Second, mice bearing HepG2 liver adenocarcinomas were randomized into two groups: (a) no treatment, (b) treatment with insufficient RFA. Tumor size were monitored every 2 days and mice was sacrificed when the tumor was 2cm in diameter. Flow cytometry was used to analyze the percentage of CD133+ and CD326+ cells from the tissue samples of the two groups. Third, HepG2 mice were randomized into four groups: (a) RFA followed by IP ATRA (10mg/kg), (b) RFA followed by IP ATRA (20mg/kg), (c) RFA followed by IP ATRA (40mg/kg), (d) RFA alone. The tumor sizes at day 20 were compared among different groups by analysis of variance. Additionally, pathological staining, western blot and flow cytometry were used for analysing the TSCs and tumor apoptosis. Fourth, the subsequently transplanted formation rate of TSCs was evaluated.

RESULTS

First, in vitro, HepG2 cells which incubated at 42°C water bath displayed significantly higher sphere-forming efficiency compared with the cells incubated at 37°C (43±6% vs 8.7±3%, p<0.01). In vivo, the HepG2 tumor model after insufficient ablation grew up faster compare with no treatment group(p=0.021), and the percentage of CD133+ cells (39.3%) and CD326+ cells (42.7%) was higher than no treatment group (17.1%, 18.4%). The combination of ATRA and RFA decreased the tumor sizes at day 20 with different doses (0mg/kg: 774.2±158.6mm3 vs 10mg/kg: 369.7±106.5mm3 vs 20mg/kg: 152.8±113.7mm3 vs 40mg/kg:143.3±94.8mm3, Overall P<0.001). The combination of RFA and ATRA had the best survival outcome compare with RFA group. In addition, the combined treatment with ATRA showed less TSCs and more intensive cell apoptosis compared to RFA alone. The transplanted formation rate of TSCs after combination treatment was lower than no treatment group(P<0.001).

CONCLUSION

TSCs might had close relationship to the recurrent HCC after RFA. ATRA could significantly improve the effect of RFA, partially attributed to ATRA effectively induced differentiation of TSCs.

CLINICAL RELEVANCE/APPLICATION

Combining with ATRA could enhance the effects of RFA and reduce a part of promention of recurrent HCC involved in the TSCs after insufficient RFA.





VSIO42

Interventional Oncology Series: Clinical Trials in Interventional Oncology

Wednesday, Dec. 4 3:15PM - 5:15PM Room: S405AB



AMA PRA Category 1 Credits ™: 2.00 ARRT Category A+ Credits: 2.25

Participants

Riad Salem, MD, MBA, Chicago, IL (*Moderator*) Research Consultant, BTG International Ltd Research Grant, BTG International Ltd Consultant, Eisai Co, Ltd Consultant, Exelixis, Inc Consultant, Bristol-Myers Squibb Company Consultant, Dove

LEARNING OBJECTIVES

1) Learn about clinical trial design. 2) Discuss strengths and weaknesses of IO therapies.

Sub-Events

VSI042-01 Educating the Next Generation of Interventional Oncology Doctors and Researchers

Wednesday, Dec. 4 3:15PM - 3:35PM Room: S405AB

Participants

Michael C. Soulen, MD, Lafayette Hill, PA (*Presenter*) Consultant, F. Hoffmann-La Roche Ltd; Consultant, Guerbet SA; Research support, Guerbet SA; Research support, BTG International Ltd; Proctor, Sirtex Medical Ltd;

For information about this presentation, contact:

Michael.soulen@uphs.upenn.edu

LEARNING OBJECTIVES

1) Identify the gaps in necessary knowledge of oncology present in existing radiology training schemes and opportunities to close these gaps. 2) Identify the expected standards for clinical research in oncology and what interventional oncologists need to do to meet them. 3) Outline unique challenges in clinical trial design in IO and strategies to overcome them.

VSI042-02 Liver Transplantation after Y90 Radioembolization of Hepatocellular Carcinoma Patients Presenting Beyond Milan Criteria

Wednesday, Dec. 4 3:35PM - 3:45PM Room: S405AB

Participants

Ahmed Gabr, MD, MBBCh, Chicago, IL (*Presenter*) Nothing to Disclose Ahsun Riaz, MD, Chicago, IL (*Abstract Co-Author*) Nothing to Disclose Samdeep Mouli, MD, Chicago, IL (*Abstract Co-Author*) Nothing to Disclose Rehan Ali, MBBS, Staten Island, NY (*Abstract Co-Author*) Nothing to Disclose Ronald A. Mora, MD, Chicago, IL (*Abstract Co-Author*) Nothing to Disclose Kush R. Desai, MD, Chicago, IL (*Abstract Co-Author*) Speakers Bureau, Cook Group Incorporated; Consultant, Cook Group Incorporated; Consultant, Koninklijke Philips NV; Consultant, The Spectranetics Corporation; Consultant, AngioDynamics, Inc; Consultant, Boston Scientific Corporation; Consultant, W. L. Gore & Associates, Inc Kent T. Sato, MD, Chicago, IL (*Abstract Co-Author*) Nothing to Disclose Bartley Thornburg, MD, Chicago, IL (*Abstract Co-Author*) Nothing to Disclose Riad Salem, MD, MBA, Chicago, IL (*Abstract Co-Author*) Nothing to Disclose Riad Salem, MD, Chicago, IL (*Abstract Co-Author*) Research Consultant, BrG International Ltd Research Grant, BTG International Ltd Consultant, Eisai Co, Ltd Consultant, Exelixis, Inc Consultant, Bristol-Myers Squibb Company Consultant, Dove Robert J. Lewandowski, MD, Chicago, IL (*Abstract Co-Author*) Consultant, BTG International Ltd; Advisory Board, Boston Scientific Corporation; Consultant, Cook Group Incorporated; Advisory Board, ABK Biomedical Inc; Advisory Board, Accurate Medical; Consultant, C. R. Bard, Inc;

For information about this presentation, contact:

ahmed.gabr@northwestern.edu

PURPOSE

To report outcomes of radioembolization (TARE) of hepatocellular carcinoma (HCC) patients successfully downstaged to liver transplantation (LT) despite presenting with tumor stage beyond Milan Transplant Criteria.

METHOD AND MATERIALS

With IRB approval, we conducted a retrospective chart review (2005-2018) for HCC patients who presented with tumors beyond Milan criteria and were successfully downstaged to LT with TARE. Baseline (pre-TARE) and imaging immediately prior to LT were assessed to confirm and compare UNOS tumor stage. All explants underwent histopathologic assessment to evaluate degree of tumor necrosis and presence of vascular invasion (PVT). Overall survival (OS) and recurrence free survival (RFS) rates were estimated using Kaplan-Meier method. 38 (30 males; mean age 60 years) patients underwent LT after TARE as a downstaging therapy. Prior to TARE, 22 (58%) patients had T3 tumors, 12 (32%) had T4a tumors and 4 (10%) had T4b tumors with PVT. Patients were listed for LT after achieving good response to TARE at a median of 3.8 (CI: 2-6) months. 29 (76%) patients received cadaveric organs while 9 (24%) received living donor organs. At time of LT, 18 (47%) were downstaged to T2 (14 from T3, 2 from T4a, 2 from T4b). 20 (53%) patients did not achieve downstaging by size, but they achieved necrosis (mRECIST) response allowing LT. 16 (42%) displayed complete tumor necrosis at explant, 15 (39%) and 7 (18%) had extensive (>50%) and partial (<50%) necrosis, respectively. Median OS of entire cohort was 12.5 (CI: 4.6-12.5) years from LT. There was no difference in OS between patients who were downstaged by size to T2 vs patients who were >T2 at LT (p = 0.8). Median RFS was 6.5 (3.1-12.5) years, not significantly different for T2 vs >T2 tumors at LT.

CONCLUSION

TARE is effective in downstaging HCC patients beyond Milan Criteria, facilitating long-term survival outcomes following LT in these patients. This is evident not only in patients with T3 tumors but also for those with T4a and T4b disease. The results are consistent for both those downstaged based on size and necrosis criteria.

CLINICAL RELEVANCE/APPLICATION

Outcomes of Liver transplantation of HCC patients beyond Milan Criteria are satisfactory provided that they underwent downstaging treatment with Y90 radioembolization which can be achieved by inducing mRECIST response and tumor necrosis.

VSI042-03 Statistics in Image-guided Therapy: The Basics

Wednesday, Dec. 4 3:45PM - 4:05PM Room: S405AB

Participants

Jeffrey D. Blume, Nashville, TN (Presenter) Nothing to Disclose

For information about this presentation, contact:

j.blume@vanderbilt.edu

LEARNING OBJECTIVES

1) To explain the role of p-values and their proper usage. 2) To understand why confidence intervals are essential for proper interpretation of results. 3) To introduce modern assessment tools, such as second-generation p-values and false discovery rates.

ABSTRACT

In March of 2016, the American Statistical Association (ASA) released a statement on statistical significance and p-values. The statement detailed a vision for a reduced role of p-values in science, with greater emphasis on estimation, confidence intervals, and alternative assessments that account for clinical significance. In this talk, I will review the origins of p-value based inference and discuss the main thrust of the ASA's statement. I will also introduce more modern tools (second-generation p-values, false discovery rates, interval estimation) that provide a more nuanced statistical assessment, which is often more appropriate for science.

VSI042-04 Imaging Following Locoregional Therapies: Challenges

Wednesday, Dec. 4 4:05PM - 4:25PM Room: S405AB

Participants Mishal Mendiratta-Lala, MD, Ann Arbor, MI (*Presenter*) Nothing to Disclose

For information about this presentation, contact:

mmendira@med.umich.edu

LEARNING OBJECTIVES

1) Become familiar with the various types of locoregional therapy, using hepatocellular carcinoma as a prototype. 2) Evaluate imaging post-locoregional therapy to assess treatment response. 3) Identify imaging challenges when assessing tumor response after various forms of locoregional therapy. 4) Become familiar with existing tumor response criteria, such as mRECIST, EASL and LIRADS while also understanding pitfalls in treatment response assessment based on the type of locoregional treatment.

VSI042-05 The Use of Augmented Reality Guidance and Navigation for Percutaneous Ablation of Liver Tumors

Wednesday, Dec. 4 4:25PM - 4:35PM Room: S405AB

Participants

Charles Martin III, MD, Pepper Pike, OH (*Presenter*) Scientific Advisory Board, Boston Scientific Corporation Scientific Advisory Board, BTG International Ltd Consultant, Terumo Corporation

Jeffrey H. Yanof, PhD, Solon, OH (*Abstract Co-Author*) Patent pending, Co-inventor on System and Method for Holographic Imageguided Non-vascular Percutaneous Procedures, MediView XR Licensee

Sara Al-Nimer, MENG, Cleveland, OH (*Abstract Co-Author*) Patent pending, System & Method for Holographic Image-Guided Non-vascular Percutaneous Procedures, MediView XR Licensee; Inventor, System & Method for Holographic Image-Guided Non-vascular Percutaneous Procedures, MediView XR Licensee

Crew J. Weunski, Cleveland, OH (*Abstract Co-Author*) Nothing to Disclose Karl West, MSc, Cleveland, OH (*Abstract Co-Author*) Nothing to Disclose Aydan Hanlon, BS, Cleveland, OH (*Abstract Co-Author*) Nothing to Disclose Gaurav Gadodia, MD, Cleveland, OH (*Abstract Co-Author*) Nothing to Disclose

For information about this presentation, contact:

martinc7@ccf.org

PURPOSE

To describe our use of true 3D holographic guidance for PTA (3D HPA) in our first five first-in-human clinical evaluations, leading to increased ablation accuracy and usability of this technilogy.

METHOD AND MATERIALS

3D Holograms of the ablation probe and the liver and its target tumors, based on fused CT and real-time ultrasound images, are created using Unity software and then superimposed directly onto the operative site for more accurate probe placement relative to the preoperative plan. More accurate delivery of heat to target tumors with less to adjacent healthy tissue will yield fewer post-procedure complications and is key for treating tumors (<3 cm diameter) and complex anatomy. The resulting accuracy and usability provided by real-time, fused holographic visualization is of growing significance, as the use of PTA is increasing.

RESULTS

We demonstrate in our first five cases that this novel technique can be used to accurately target liver tumors and effectively ablate the lesions of concern in the liver.

CONCLUSION

New augmented reality (AR) headsets such as HoloLens have potential to benefit percutaneous intervention by overcoming limitations of 2D monitors presently used in standard-of-care image-guidance. Through these first five procedures our plan is to demonstrate the benefits of the unique platform relative to the use of 2D-monitors alone including improved tumor targeting (3), lower x-ray radiation dose (4), decreased procedure time (2), and improved overall outcomes for tumor ablation and a broad range of minimally invasive applications.

CLINICAL RELEVANCE/APPLICATION

This technique improves the safety and effectiveness of tumor ablation, and possibly other percutaneous procedures, by enhancing spatial and depth perception in comparison with 2D displays.

VSI042-06 Pivotal Trials in HCC: Contemporary Update

Wednesday, Dec. 4 4:35PM - 4:55PM Room: S405AB

Participants

Aparna Kalyan, MD, Chicago, IL (*Presenter*) Advisory Board, Eisai Co, Ltd; Advisory Board, Bristol-Myers Squibb Company; Advisory Board, Exelis; Advisory Board, Ipsen SA; Advisory Board, BTG International Ltd; Research funded, Bristol-Myers Squibb Company

VSI042-07 Patient-reported Outcomes in Interventional Oncology

Wednesday, Dec. 4 4:55PM - 5:15PM Room: S405AB

Participants

Sharon W. Kwan, MD, Seattle, WA (Presenter) Nothing to Disclose

LEARNING OBJECTIVES

1) Define what constitutes patient reported outcomes. 2) Describe the main types of patient reported outcome instruments. 3) Understand why patient reported outcomes are important in interventional oncology.







MSCT42

Case-based Review of Thoracic Radiology (Interactive Session)

Wednesday, Dec. 4 3:30PM - 5:00PM Room: S406A

СН

AMA PRA Category 1 Credits ™: 1.50 ARRT Category A+ Credit: 1.75

Participants

Diana Litmanovich, MD, Haifa, Israel (Director) Nothing to Disclose

For information about this presentation, contact:

dlitmano@bidmc.harvard.edu

LEARNING OBJECTIVES

1) Identify thoracic pathologies often missed on chest radiographs. 2) Differentiate patterns of radiation induced pneumonitis from complications/ recurrence and Identify pulmonary complications associated with chemotherapy and stem cell transplantation. 3) Identify and differentiate between multiple HIV-related cardiothoracic manifestations. 4) Identify the common Interstitial lung disease patterns and classify them best on the most recent classification.

ABSTRACT

This course is designed to highlight the variety of thoracic pathology, including lung cancer treatment related pathology, HIV - related infectious and malignant pathology, and updated classification of interstitial lung disease. Special attention would be fiven to the frequently missed patholgies on chest radiographs, new imaging modalities and understanding of post-treatment changes in patients with lung cancer. Our goal is to provide a broad update in the field while addressing new opportunities and challenges for everyday practice.

Sub-Events

MSCT42A What Do We Miss on Chest Radiographs?

Participants

Gerald F. Abbott, MD, Boston, MA (Presenter) Nothing to Disclose

For information about this presentation, contact:

gerald.abbott@gmail.com

LEARNING OBJECTIVES

1) To learn the most common location, imaging features, and etiologies of missed lesions on chest radiography.

MSCT42B The Many Faces of Pulmonary Changes Following Cancer Treatment

Participants

Edith M. Marom, MD, Tel Aviv, Israel (*Presenter*) Speaker, Bristol-Myers Squibb Company; Speaker, Boehringer Ingelheim GmbH; Speaker, Merck & Co, Inc; Officer, Voxellence ; ; ; ;

For information about this presentation, contact:

edith.marom@gmail.com

LEARNING OBJECTIVES

1) Differentiate patterns of radiation induced pneumonitis from complications/ recurrence. 2) Identify pulmonary complications associated with chemotherapy and stem cell transplantation.

MSCT42C Many Faces of HIV Chest Manifestations

Participants Ann N. Leung, MD, Stanford, CA (*Presenter*) Nothing to Disclose

MSCT42D Interstitial Lung Disease: Guide for the Perplexed

Participants Andetta R. Hunsaker, MD, Sudbury, MA (*Presenter*) Nothing to Disclose







MSCZ42

Case-based Review of CT (Interactive Session)

Wednesday, Dec. 4 3:30PM - 5:00PM Room: S402AB

СТ

AMA PRA Category 1 Credits ™: 1.50 ARRT Category A+ Credit: 1.75

Participants

Edward Y. Lee, MD, Boston, MA (Director) Nothing to Disclose

LEARNING OBJECTIVES

1) Review clinical presentations of congenital and acquired disorders. 2) Discuss optimal CT imaging techniques for assessing congenital and acquired disorders. 3) Learn characteristic CT findings of congenital and acquired disorders.

Sub-Events

MSCZ42A Adult Head and Neck CT

Participants Amy F. Juliano, MD, Boston, MA (*Presenter*) Nothing to Disclose

For information about this presentation, contact:

amy_juliano@meei.harvard.edu

LEARNING OBJECTIVES

1) Recognize an imaging abnormality and place it in the correct location/space of the neck. 2) Generate a differential diagnosis, and narrow it down by incorporating clinical history and pertinent positives and negatives on the available images. 3) Identify common entities in the head and neck, as well as some rare entities that have classic imaging findings.

MSCZ42B Adult Hepatobiliary CT

Participants Koenraad J. Mortele, MD, Boston, MA (*Presenter*) Nothing to Disclose

MSCZ42C Adult Genitourinary CT

Participants Hero K. Hussain, MD, Ann Arbor, MI (*Presenter*) Nothing to Disclose

For information about this presentation, contact:

hh141@aub.edu.lb

LEARNING OBJECTIVES

1) To discuss features of common and uncommon cystic and solid renal and perirenal lesions on CT, and identify features that help narrow the differential diagnosis.

MSCZ42D Adult Trauma CT

Participants Jorge A. Soto, MD, Boston, MA (*Presenter*) Royalties, Reed Elsevier

For information about this presentation, contact:

jorge.soto@bmc.org

LEARNING OBJECTIVES

1) Develop a search pattern that minimizes risk of missing subtle organ injuries. 2) Highlight key imaging features that are critical for determining need of operative or interventional repair of abdominal injuries. 3) Increase confidence in the interpretation of complex multi-trauma CT examinations.





MSES44

Essentials of Pediatric Imaging

Wednesday, Dec. 4_3:30PM - 5:00PM Room: S100AB

PD

AMA PRA Category 1 Credits ™: 1.50 ARRT Category A+ Credit: 1.75

Sub-Events

MSES44A Common Pediatric Abdominal Emergencies

Participants

Ting Y. Tao, MD, PhD, Saint Louis, MO (Presenter) Nothing to Disclose

LEARNING OBJECTIVES

1) Identify the most common abdominal emergencies in infants and children. 2) Develop an imaging approach for diagnosis. 3) Recognize normal variants, pitfalls, and mimics.

MSES44B Interventional (IR) Procedures to Diagnose and Treat Pediatric Liver Tumors

Participants

Richard B. Towbin, MD, Paradise Vly, AZ (Presenter) Nothing to Disclose

LEARNING OBJECTIVES

1) Briefly discuss the technical approach to the diagnosis and therapy of children with liver tumors. 2) Present the potential risks of these minimally invasive procedures. 3) Liberally Illustrate using imaging examples of the procedures, their outcomes and complications, when pertinent.

ABSTRACT

The current state of the art of Pediatric Intervention will be presented to illustrate the range of procedures available to diagnose and treat children with liver tumors. The technical aspects of the procedures will be lightly covered. Case illustrations and associated problems and complications will be discussed.

MSES44C Pediatric Liver Tumors

Participants

Alex Towbin, MD, Cincinnati, OH (*Presenter*) Author, Reed Elsevier; Grant, Guerbet SA; Grant, Cystic Fibrosis Foundation; Consultant, Reed Elsevier; Advisory Board, IBM Corporation; Advisory Board, KLAS Enterprises LLC;

For information about this presentation, contact:

alexander.towbin@cchmc.org

LEARNING OBJECTIVES

1) List the 3 most common benign and malignant pediatric liver tumors. 2) Utilize clinical information and imaging findings to diagnose the most common pediatric liver tumors. 3) Describe how and when to employ the PRETEXT classification system for pediatric liver tumors.

ABSTRACT

Liver tumors represent a dilemma in many pediatric radiology practices. The purpose of this lecture is to identify the most common pediatric liver tumors, to describe the clinical characteristics and imaging patterns associated with each lesion, and for malignant lesions, to define the PRETEXT classification system used to describe the liver involvement.

MSES44D Key Concepts in Pediatric Neuroimaging

Participants

Bruno P. Soares, MD, Burlington, VT (Presenter) Nothing to Disclose

For information about this presentation, contact:

bruno.soares@uvmhealth.org

LEARNING OBJECTIVES

1) Describe normal progression of myelination. 2) Describe common pediatric brain findings and their significance. 3) Apply practical imaging criteria to classify pediatric cystic posterior fossa anomalies.





MSSR44

RSNA/ESR Sports Imaging Symposium: Postoperative Imaging of Sports Injuries (Interactive Session)

Wednesday, Dec. 4 3:30PM - 5:00PM Room: E350



AMA PRA Category 1 Credits ™: 1.50 ARRT Category A+ Credit: 1.75

Participants

Andrew J. Grainger, MD, Leeds, United Kingdom (*Moderator*) Consultant, Levicept Ltd; Director, The LivingCare Group; Laura W. Bancroft, MD, Venice, FL (*Moderator*) Nothing to Disclose

For information about this presentation, contact:

laurabancroftmd@gmail.com

LEARNING OBJECTIVES

1) To review MRI findings of ACL reconstruction and cartilage repair. 2) To review the expected and abnormal MR imaging findings after labral repair, capsular shift/capsulorrhaphy and Laterjet/Bristow procedures. 3) To consolidate the knowledge gained from the session with interactive cases of postoperative sports imaging.

Sub-Events

MSSR44A Postoperative Shoulder MRI after Instability Surgery

Participants

Laura W. Bancroft, MD, Venice, FL (Presenter) Nothing to Disclose

For information about this presentation, contact:

laurabancroftmd@gmail.com

LEARNING OBJECTIVES

1) To become familiar with the expected and abnormal MR imaging findings after labral repair. 2) To learn about the postoperative imaging features after capsular shift/capsulorrhaphy. 3) To appreciate normal imaging and complications after remplissage and Laterjet/Bristow procedures.

ABSTRACT

Purpose: To become familiar with the expected and abnormal MR imaging findings after labral repair, capsular shift/capsulorrhaphy, remplissage and Latarjet/Bristow procedures. Methods and Materials: MR imaging will be used to demonstrate the various normal and abnormal imaging appearances after shoulder instability surgery. Results/Conclusion: Labral re-tear will be evident as contrast or joint fluid extension into linear or complex tear cleft, absent/truncated/fragmented labrum, or labral displacement from anatomic location. Capsular shift results in smaller capacity joint and sometimes irregular capsular nodularity. Complications of capsulorrhaphy include capsular tears and subluxation of humeral head. Postoperative MR imaging can evaluate healing after combined remplissage and Bankart repair for moderate size, engaging Hill-Sachs lesions. Laterjet and Bristow procedures may be performed in patients with recurrent dislocations and glenoid deficiency. Incorporated bone will yield non-anatomic glenoid configuration, and complications include non-union, fatty degeneration of subscapularis muscle, and osteoarthrosis.

MSSR44B ACL Reconstruction and Cartilage Repair

Participants

Claudia Weidekamm, MD, Auckland, New Zealand (Presenter) Nothing to Disclose

For information about this presentation, contact:

claudia.weidekamm@meduniwien.ac.at

LEARNING OBJECTIVES

1) To review the common and uncommon ACL reconstruction techniques. 2) To appreciate the expected and abnormal MR imaging findings after ACL reconstruction. 3) To understand common cartilage repair techniques, and corresponding normal and abnormal postoperative MRIs.

ABSTRACT

The aim of ACL reconstruction is to stabilize the knee and prevent chondral and meniscal injuries, which are sequelae of anteroposterior translation and are associated with early osteoarthritis. The idea of the double-bundle ACL graft was to restore normal joint kinematics by anatomic reconstruction of the anteromedial and the posterolateral bundle of the original ACL. This was expected to improve clinical outcomes and restore anterior and rotational knee stability. The single-bundle technique, however, causes less osseous defects and is still a popular technique. Complications, such as ACL graft failure, impingement, cyclops lesion, arthrofibrosis, and patellar inferior syndrome, are discussed. The second part of this presentation will illustrate cartilage repair techniques and imaging findings. The radiologist must be familiar with the different cartilage repair procedures and characteristics in cartilage imaging to evaluate long-term progression or failure. Abnormal postoperative findings include hypertrophic filling, incomplete integration of the transplant into the surrounding cartilage, or subchondral defects, osteophytes, cysts, and persistent

bone marrow edema and joint effusion.

MSSR44C Interactive Case Discussion

Participants Laura W. Bancroft, MD, Venice, FL (*Presenter*) Nothing to Disclose Claudia Weidekamm, MD, Auckland, New Zealand (*Presenter*) Nothing to Disclose

For information about this presentation, contact:

laurabancroftmd@gmail.com

LEARNING OBJECTIVES

1) To review the expected and abnormal MR imaging findings after labral repair, capsular shift/capsulorrhaphy and Laterjet/Bristow procedures in a case-based format. 2) To become familiar with the diagnosis features of failed ACL reconstructions, intact and failed cartilage repair. 3) To consolidate the knowledge gained from the session with interactive cases of postoperative sports imaging.





MSRT46

ASRT@RSNA 2019: The Impact of Radiographer-led Research-A Case Study from the UK (Interactive Session)

Wednesday, Dec. 4 3:40PM - 4:40PM Room: N230B

RS

AMA PRA Category 1 Credit ™: 1.00 ARRT Category A+ Credit: 1.00

Participants

Louise Harding, Warrington, United Kingdom (*Presenter*) Nothing to Disclose Paula Park, Warrington, United Kingdom (*Presenter*) Travel support, MIS Healthcare

For information about this presentation, contact:

paula.park@nhs.net

LEARNING OBJECTIVES

1) To understand the value of radiographer led research within clinical imaging services. 2) To understand the steps required in developing a local research strategy. 3) To understand how to examine opportunities and barriers within your clinical environment to help support effective research.

ABSTRACT

As Health Care Professionals, radiographers and technologists are encouraged to put the patient at the centre of everything they do. In the UK, the Society and College of radiographers (SCoR) states that this level of care should be based on up to date evidence that is of a high quality, using research to meet the needs of the patient. This drive to encourage research is also mirrored by the Allied Health Professions Federation (AHPF) who have published a strategy with one of its key goals focused on the impact of research methods and evaluation on population outcome. Historically, research undertaken by radiographers in the UK has been minimal. In 2015, a review of contributors to the journal for The European Federation of Radiographer Societies found that of 239 contributing affiliations, only 22 were represented by UK Trusts. Factors restricting engagement with research could be due to a lack of research experience and confidence among radiography practitioners and technologists, and a culture where research is not seen as a priority. In busy departments; time, lack of role models, difficulties in back filling roles and resistance to change, along with ever increasing imaging demands have led to further barriers in undertaking research. The question remains as to how we bridge the gap between embedding research at all levels of radiographic practice and current clinical research activity? The purpose of this presentation will be to focus on our research journey within a UK radiology department. We will share how we overcame barriers through collaboration, establishing a local research strategy to facilitate our research ideas. As a result, we will demonstrate how this led to achieving successes regarding the positive impact of research, both on our patients and staff.





MSRO49

BOOST: Lung Stereotactic Body Radiotherapy (SBRT)-eContouring

Wednesday, Dec. 4 4:30PM - 5:30PM Room: S103CD



AMA PRA Category 1 Credit ™: 1.00 ARRT Category A+ Credit: 1.00

Participants

Subba R. Digumarthy, MD, Boston, MA (*Presenter*) Speaker, Siemens AG; Research Grant, Lunit Inc; Researcher, Merck & Co, Inc; Researcher, Pfizer Inc; Researcher, Bristol-Myers Squibb Company; Researcher, Novartis AG; Researcher, F. Hoffmann-La Roche Ltd; Researcher, Polaris Pharmaceuticals, Inc; Researcher, Cascadia Healthcare, LLC; Researcher, AbbVie Inc; Researcher, Gradalis, Inc; Researcher, Zai Lab

Stephen Chun, MD, Houston, TX (Presenter) Nothing to Disclose

Florence K. Keane, MD, Boston, MA (Presenter) Advisory Board, AstraZeneca PLC

Special Information

The e-contouring sessions may be used by participating radiation oncologists to fulfill a PQI (practice quality improvement) requirement for ABR (American Board of Radiology) MOC (Maintenance of Certification). Interested radiation oncologist can download a e-contouring PQI template here: https://academy.astro.org/content/econtouring-pqi-template and handouts directing users to the same website will be available at the actual session.

LEARNING OBJECTIVES

1) Understand strategies to optimize tumor target delineation and motion management. 2) Differentiate between gross tumor and atelectasis. 3) Identify and contour cardiac/great vessel anatomy on CT-imaging. 4) Identify brachial plexus on CT-imaging. 5) Define the central airways and the central 'no fly zone'. 6) Learn appropriate normal tissue constraints for SBRT.

ABSTRACT

Stereotactic body radiation therapy (SBRT) has is a non-invasive therapeutic option that can deliver ablative radiation doses to both primary thoracic malignancies and lung metastases. The effectiveness and toxicity profile of SBRT is highly dependent upon accurately targeting the tumor as well as precise delineation of non-target organs at risk. With highly conformal SBRT plans, accurate tumor targeting is important to prevent marginal failure and also to minimize radiation delivered to normal tissues. As ablative doses pose substantial risk of injury, it is critical to accurately identify normal tissue structures such as the brachial plexus, central airways, heart, and great vessels to prevent catastrophic injury. This session will focus on strategies for tumor targeting through diagnostic evaluations, optimizing motion management and reconciling tumor anatomy in 4 dimensions. The session will also review the anatomy of critical thoracic anatomic structures at risk for injury with SBRT with appropriate radiation dose constraints. Information from the session is expected to facilitate safe treatment of thoracic malignancies with SBRT in light of potentially increasing indications such as oligometastases.





RCC45

Imaging in Proteogenomics Research

Wednesday, Dec. 4 4:30PM - 6:00PM Room: E353B

IN

AMA PRA Category 1 Credits ™: 1.50 ARRT Category A+ Credit: 1.75

Participants

Janet F. Eary, MD, Bethesda, MD (*Moderator*) Nothing to Disclose Evis Sala, MD, PhD, Cambridge, United Kingdom (*Presenter*) Co-founder, Cambridge AI Health; Speakers Bureau, GlaxoSmithKline plc Erich Huang, PhD, Rockville, MD (*Presenter*) Nothing to Disclose Luis E. Selva, PhD, Boston, MA (*Presenter*) Nothing to Disclose Olivier Gevaert, PhD, Stanford, CA (*Presenter*) Nothing to Disclose John B. Freymann, Rockville, MD (*Presenter*) Nothing to Disclose

For information about this presentation, contact:

erich.huang@nih.gov

Luis.Selva@va.gov

LEARNING OBJECTIVES

Learning Objectives:Learn about major NIH programs producing imaging correlated with proteogenomic dataLearn basics of proteomic data, levels of granularity and imaging correlationLearn examples of analytical and statistical approaches used in imaging-proteogenomic analysisLearn how medical studies are aggregated within the Veterans Administration domain for the purpose of conducting medical research including proteogenomics

ABSTRACT

Abstract: Major new research initiatives aim to systematically identify proteins that derive from alterations in cancer genomes and related biological processes, in order to understand the molecular basis of cancer that is not fully elucidated or not possible through genomics and to accelerate the translation of molecular findings into the clinic. Clinical imaging data collected with proteomics data can provide additional signal and information about spatial and temporal context that has the potential of improving and validating proteogenomic biomarkers.







SPDL41

Neuro and MSK (Case-based Competition)

Wednesday, Dec. 4 4:30PM - 6:00PM Room: E451B



AMA PRA Category 1 Credits ™: 1.50 ARRT Category A+ Credit: 0

Participants

Paul J. Chang, MD, Chicago, IL (*Presenter*) Co-founder, Koninklijke Philips NV; Researcher, Koninklijke Philips NV; Researcher, Bayer AG; Advisory Board, Bayer AG; Advisory Board, Aidoc Ltd; Advisory Board, EnvoyAI; Advisory Board, Inference Analytics; Advisory Board, Subtle Medical

Neety Panu, MD, FRCPC, Ottawa , ON (*Presenter*) Nothing to Disclose Omer A. Awan, MD, Baltimore, MD (*Presenter*) Nothing to Disclose Carina W. Yang, MD, Chicago, IL (*Presenter*) Nothing to Disclose

For information about this presentation, contact:

cyang@radiology.bsd.uchicago.edu

pchang@radiology.bsd.uchicago.edu

Special Information

This interactive session will use RSNA Diagnosis Live[™]. Please bring your charged mobile wireless device (phone, tablet or laptop) to participate.

LEARNING OBJECTIVES

1) Be introduced to a series of neuroradiology and musculoskeletal radiology case studies via an interactive team game approach designed to encourage 'active' consumption of educational content. 2) Use their mobile wireless device (tablet, phone, laptop) to electronically respond to various imaging case challenges; participants will be able to monitor their individual and team performance in real time. 3) Receive a personalized self-assessment report via email that will review the case material presented during the session, along with individual and team performance.

ABSTRACT

The extremely popular audience participation educational experience, Diagnosis Live!, is an expert-moderated session featuring a series of interactive case studies that will challenge radiologists' diagnostic skills and knowledge. The session features a lively, fast-paced game format: participants will be automatically assigned to teams who will then use their personal mobile devices to test their knowledge in a fast-paced session that will be both educational and entertaining. After the session, attendees will receive a personalized self-assessment report via email that will review the case material presented during the session, along with individual and team performance.





Controversy Session: Contrast Agent Controversies

Wednesday, Dec. 4 4:30PM - 6:00PM Room: N228



AMA PRA Category 1 Credits ™: 1.50 ARRT Category A+ Credit: 1.75

Participants

Douglas S. Katz, MD, Mineola, NY (*Moderator*) Nothing to Disclose Andrew B. Rosenkrantz, MD, New York, NY (*Moderator*) Nothing to Disclose

For information about this presentation, contact:

Andrew.Rosenkrantz@nyumc.org

douglasscottkatzmd@gmail.com

LEARNING OBJECTIVES

1) To discuss the pros and cons based on the current literature and clinical experience of the use of oral contrast for abdominal and pelvic CT in the emergency setting. 2) To review the current role of gadoxetate for hepatobiliary MR imaging, including the advantages and disadvantages, current protocols, and its role compared with the use of extracellular gadolinium-based MR contrast agents. 3) To review the current role of intravenous ultrasound contrast agents for abdominal and pelvic imaging, including a brief review of the current literature, clinical experience, barriers to its use, and geographic variability of its use.

Sub-Events

SPSC41A Pro and Con: Use of Oral Contrast for Emergency Abdominal and Pelvic CT

Participants

Perry J. Pickhardt, MD, Madison, WI (*Presenter*) Stockholder, SHINE Medical Technologies, Inc; Stockholder, Elucent Medical; Advisor, Bracco Group;

Ania Z. Kielar, MD, Shanty Bay, ON (Presenter) Nothing to Disclose

SPSC41B Cheerleader versus Realist: Use of Gadoxetate for Liver MRI

Participants

Bachir Taouli, MD, New York, NY (*Presenter*) Research Grant, Bayer AG; Research Grant, Takeda Pharmaceutical Company Limited; Research Grant, Regeneron Pharmaceuticals, Inc; Consultant, Alexion Pharmaceuticals, Inc; Consultant, Bayer AG; ; Victoria Chernyak, MD,MS, Bronx, NY (*Presenter*) Consultant, Bayer AG

For information about this presentation, contact:

vichka17@hotmail.com

LEARNING OBJECTIVES

1) To understand the effect of gadoxetate use on the quality of the hepatic arterial phase. 2) To review limitations of the hepatobiliary phase in patients with and without parenchymal liver disease. 3) To review challenges that gadoxetate use presents in diagnosis of hemangioma. 4) To review challenges of gadoxetate use in diagnosis of HCC and application of LI-RADS.

SPSC41C Use of IV Contrast for Abdominal US: Barriers/Issues and Current Literature Summary/Experience

Participants

Sheila Sheth, MD, Baltimore, MD (Presenter) Nothing to Disclose

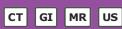
Aya Kamaya, MD, Stanford, CA (Presenter) Royalties, Reed Elsevier; Researcher, Koninklijke Philips NV; Researcher, Siemens AG





Controversy Session: Hepatocellular Carcinoma: Should We Use CT, MR, or US?

Wednesday, Dec. 4 4:30PM - 6:00PM Room: N227B



AMA PRA Category 1 Credits ™: 1.50 ARRT Category A+ Credit: 1.75

Participants

Claude B. Sirlin, MD, San Diego, CA (*Moderator*) Research Grant, Gilead Sciences, Inc; Research Grant, General Electric Company; Research Grant, Siemens AG; Research Grant, Bayer AG; Research Grant, Koninklijke Philips NV; Consultant, AMRA AB; Consultant, Fulcrum; Consultant, IBM Corporation; Consultant, Exact Sciences Corporation; Consultant, Boehringer Ingelheim GmbH; Consultant, Arterys Inc; Consultant, Epigenomics; Author, Medscape, LLC; Lab service agreement, Gilead Sciences, Inc; Lab service agreement, ICON plc; Lab service agreement, Intercept Pharmaceuticals, Inc; Lab service agreement, Shire plc; Lab service agreement, Enanta; Lab service agreement, Takeda Pharmaceutical Company Limited; Lab service agreement, Alexion Pharmaceuticals, Inc; Lab service agreement, NuSirt Biopharma, Inc

R. Brooke Jeffrey Jr, MD, Stanford, CA (Moderator) Nothing to Disclose

LEARNING OBJECTIVES

1) To understand the need for screening and surveillance for HCC in cirrhosis. 2) To understand that ultrasound is currently recommended as the primary modality for this purpose by all national and international guidelines. 3) To understand the advantages and disadvantages of ultrasound, CT, and MRI for HCC screening and surveillance in cirrhosis.

Sub-Events

SPSC42A Overview of HCC Screening and Surveillance: Definitions, Rationale, Basic Concepts, Current Guidelines, USA Landscape, Worldwide Landscape

Participants

Aya Kamaya, MD, Stanford, CA (Presenter) Royalties, Reed Elsevier; Researcher, Koninklijke Philips NV; Researcher, Siemens AG

SPSC42B Why Ultrasound Should Be Used for HCC Screening/Surveillance

Participants

Shuchi K. Rodgers, MD, Philadelphia, PA (Presenter) Nothing to Disclose

SPSC42C Why CT Should Be Used for HCC Screening/Surveillance

Participants

Avinash R. Kambadakone, MD, Boston, MA (*Presenter*) Research Grant, General Electric Company; Research Grant, Koninklijke Philips NV

For information about this presentation, contact:

akambadakone@mgh.harvard.edu

LEARNING OBJECTIVES

1) Understand the role of CT in the diagnosis of HCC. 2) Learn the limitations of CT in HCC screening including radiation dose and strategies to diminish the risk. 3) Review innovations in CT and its impact on screening of HCC.

SPSC42D Why MRI Should Be Used for HCC Screening/Surveillance

Participants Takeshi Yokoo, MD, PhD, Dallas, TX (*Presenter*) Nothing to Disclose

For information about this presentation, contact:

Takeshi.Yokoo@UTSouthwestern.EDU





Controversy Session: Radiology Practice Standards

Wednesday, Dec. <u>4</u> 4:30PM - 6:00PM Room: N226

HP

AMA PRA Category 1 Credits ™: 1.50 ARRT Category A+ Credit: 1.75

Participants

Erik K. Paulson, MD, Durham, NC (*Moderator*) Nothing to Disclose Pari V. Pandharipande, MD, MPH, Chestnut Hill, MA (*Moderator*) Research Grant, Medical Imaging & Technology Alliance

LEARNING OBJECTIVES

1) Discuss controversial considerations of patient portals. 2) Review patient navigators (a system to report unexpected findings and ensure clinical follow-up). 3) Describe controversies associated with 24/7 attending coverage.

Sub-Events

SPSC43A Benefits versus Challenges in Implementing 24/7 Subspecialty Imaging Coverage

Participants

Michael P. Recht, MD, New York, NY (*Presenter*) Nothing to Disclose Cheri L. Canon, MD, Birmingham, AL (*Presenter*) Royalties, The McGraw-Hill Companies; Consultant, Bracco Group

For information about this presentation, contact:

ccanon@uabmc.edu

SPSC43B Benefits versus Challenges in Implementing Closed-loop Communication for Non-urgent Imaging Recommendations

Participants

Tracy A. Jaffe, MD, Durham, NC (*Presenter*) Nothing to Disclose Mark M. Hammer, MD, Saint Louis, MO (*Presenter*) Nothing to Disclose

For information about this presentation, contact:

mmhammer@bwh.harvard.edu

LEARNING OBJECTIVES

1) Learn differences in expectations around closed loop communications. 2) Review some of the possible approaches to closed loop communications of unexpected/actionable findings. 3) Identify the potential logistical obstacles to address in the development of a closed loop communication program.

ABSTRACT

Creating a closed loop communication program for unexpected/actionable findings found in imaging studies requires collaboration between radiology departments and referring providers. There are many different approaches to developing process include those that use the electronic medical record and those that use a navigator. Consensus amongst radiologists and referring providers to goals and expectations is essential for a successful process.

SPSC43C Benefits versus Risks of Rapid Release of Imaging Reports and Data to Patients

Participants Marta E. Heilbrun, MD, Salt Lake City, UT (*Presenter*) Nothing to Disclose Jonathan B. Kruskal, MD,PhD, Boston, MA (*Presenter*) Author, Wolters Kluwer nv

For information about this presentation, contact:

marta.heilbrun@emory.edu





Controversy Session: Proton Therapy: Hope or Hype?

Wednesday, Dec. 4 4:30PM - 6:00PM Room: E353C

RO

AMA PRA Category 1 Credits ™: 1.50 ARRT Category A+ Credit: 1.75

Participants

Nina A. Mayr, MD, Seattle, WA (Moderator) Nothing to Disclose Michelle M. Miller-Thomas, MD, Kirkwood, MO (Moderator) Nothing to Disclose

LEARNING OBJECTIVES

1) Understand the clinical advantages of proton and particle therapy in the major disease sites with respect to tumor control and toxicity outcomes over conventional photon radiation therapy. 2) Understand the challenges and pitfalls of proton and particle radiation therapy and future directions. 3) Will obtain a balanced view on the clinical use of proton and particle therapy. 4) Will understand the expected evolution of imaging changes in the brain after proton therapy and differentiate between transient proton-related treatment changes and radiation necrosis.

Sub-Events

SPSC44A **Case for Proton Therapy**

Participants Jing Zeng, MD, Seattle, WA (Presenter) Nothing to Disclose

For information about this presentation, contact:

jzeng13@uw.edu

LEARNING OBJECTIVES

1) Understand rationale for proton therapy compared to photon radiation. 2) Understand common clinical scenarios where proton therapy may be advantageous over other modalities.

SPSC44B Equipoise

Participants

Tony J. Wang, MD, New York, NY (Presenter) Personal fees and Non-financial support, AbbVie Inc; Personal fees and Non-financial support, NovoCure Ltd; Personal fees and Non-financial support, Elekta AB; Personal fees and Non-financial support, Merck & Co, Inc; Personal fees and Non-financial support, RTOG Foundation; Personal fees, Doximity, Inc; Personal fees, Wolters Kluwer nv; Personal fees, AstraZeneca PLC; Personal fees, Cancer Panels

James S. Welsh, MD, Hines, IL (Presenter) Speaker, Varian Medical Systems, Inc

SPSC44C The Radiologist's Perspective: Imaging after Proton Therapy

Participants Michelle M. Miller-Thomas, MD, Kirkwood, MO (Presenter) Nothing to Disclose

For information about this presentation, contact:

miller-thomasm@wustl.edu





Controversy Session: Radiologist Burnout: How Should We Help Mitigate?

Wednesday, Dec. 4 4:30PM - 6:00PM Room: E353A

ОТ

AMA PRA Category 1 Credits ™: 1.50 ARRT Category A+ Credit: 1.75

Participants

Claire E. Bender, MD, Rochester, MN (*Moderator*) Nothing to Disclose Donald J. Flemming, MD, Hershey, PA (*Moderator*) Nothing to Disclose Jonathan B. Kruskal, MD, PhD, Boston, MA (*Presenter*) Author, Wolters Kluwer nv Marc H. Willis, DO, MMM, Palo Alto, CA (*Presenter*) Investor, Resonea, Inc Jay R. Parikh, MD, Houston, TX (*Presenter*) Nothing to Disclose James C. Anderson, MD, Portland, OR (*Presenter*) Nothing to Disclose

For information about this presentation, contact:

mwillis@bcm.edu

LEARNING OBJECTIVES

1) Define the different levels of responsibility for mitigation (from CEO/Chair to individual; this will be about who owns the problem. The importance of culture will be included here.) 2) Present individual radiologist mitigation strategies (what works, what does not work.). 3) Present leadership (CEO/institution/Chair) mitigation strategies (what works, what does not work.) 4) Provide special strategies for radiology residents/trainee (include recent ACGME mandate for establishment of well-being programs.)

ABSTRACT

RSNA 2019 Panel Presentation: 'Radiologist Burnout: How should we Help Mitigate?' Controversy Session Moderators: Don Flemming, MD and Claire Bender, MD ABSTRACT 'You know you or your colleague is burned out. What do you do about it? Where do you go for help? This session will share the different levels of responsibilities for mitigation of burnout which include the leadership or your organization, your department chair and the individual. It will stress the importance of organizational culture in the understanding of burnout issues as well as the implementation of successful programs to reduce this epidemic. Strategies used for mitigation for the individual radiologist and by radiology leaders will be shared-those that work and those which have failed. Special strategies utilized for radiology residents/fellows will also be discussed.'